Progress Toward the Total Synthesis of the Lomaiviticins and a Biomimetic Unified Strategy for the Synthesis of 7-Membered Ring-Containing Lycopodium Alkaloids

Progress Toward the Total Synthesis of the Lomaiviticins and a Biomimetic Unified Strategy for the Synthesis of 7-Membered Ring-Containing *Lycopodium* Alkaloids

A dissertation presented

by

Amy S. Lee

to

The Department of Chemistry and Chemical Biology

in partial fulfillment of the requirements

for the degree of

Doctor of Philosophy

in the subject of

Chemistry

Harvard University

Cambridge, Massachusetts

July, 2014

Dissertation Advisor: Professor Matthew D. Shair Amy S. Lee

Progress Toward the Total Synthesis of the Lomaiviticins and a Biomimetic Unified Strategy for the Synthesis of 7-Membered Ring-Containing *Lycopodium* Alkaloids

Abstract

Lomaiviticin A (**1**) and B (**2**) are natural products with remarkably complex C_2-symmetric structures and potent antiproliferative properties. Achieving total syntheses of **1** and **2** has been a long-standing project in the Shair group and part one of this thesis describes our first successful synthesis of the C4-*epi*-lomaiviticin A and B core structures. A key stereoselective oxidative enolate dimerization of an oxanorbornanone system was employed to establish the highly hindered C2–C2' bond. Crucial to our completion of the lomaiviticin core structures was the discovery of subtle yet far-reaching stereoelectronic effects imparted by the C4/C4'-stereocenters.

The *Lycopodium* alkaloids are a family of complex polycyclic alkaloid natural products that have long served as popular targets for developing synthetic chemistry. More recently, select members have been reported to exhibit neurological effects. Part two of this thesis presents the development of a biomimetic, unified strategy for the synthesis of 7-membered ring-containing *Lycopodium* alkaloids and its successful application toward the first total syntheses of the proposed structure of (–)-himeradine A (**38**), (–)-lycopecurine (**39**), and (–)-dehydrolycopecurine (**199**), and the syntheses of (+)-lyconadin A (**31**) and (–)-lyconadin B (**32**). A biosynthetically inspired one-pot cascade reaction sequence was developed to construct the strained polycyclic core structure shared amongst these alkaloids. Additionally, the syntheses of **38**, **39**, and **199** featured a biomimetic intramolecular Mannich reaction to furnish the tetracyclic ring system. The successful application of our unifying strategy toward the synthesis of a diverse set of alkaloids lends support to our biosynthetic hypothesis that 7-membered ring-containing *Lycopodium* alkaloids arise from a

common precursor. Our synthetic approach can potentially provide access to all such natural products.

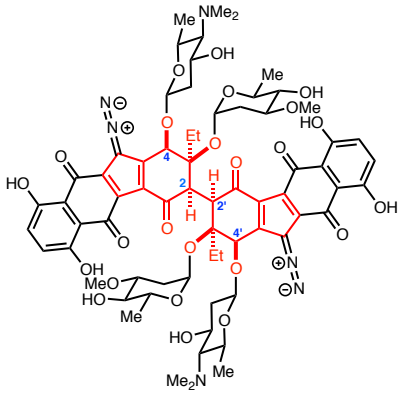

Lomaiviticin A (1)

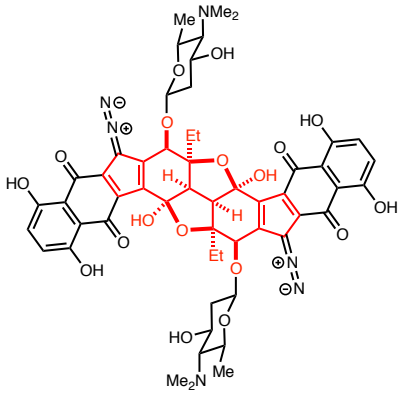

Lomaiviticin B (2)

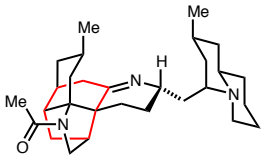

(–)-Himeradine A (38)

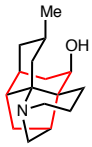

Lycopecurine (39)

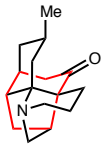

Dehydro-Lycopecurine (199)

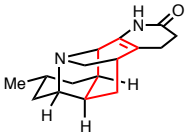

(–)-Lyconadin B (32)

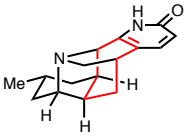

(+)-Lyconadin A (31)

Table of Contents

Acknowledgements

I would like to thank Professor Matthew D. Shair for the guidance and advice he has offered me throughout my graduate studies. Not only was I provided with the opportunity to pursue exciting and challenging research projects, I was also allowed to explore my own proposals with great freedom and flexibility, which helped me grow as a scientist. I would also like to thank Professors Yoshito Kishi and Tobias Ritter for serving on my thesis defense committee and for engaging in stimulating discussions about my research throughout my graduate career.

I would also like to express my deep gratitude to Professor Richmond Sarpong, my undergraduate research advisor at UC Berkeley. I first became excited about organic synthesis when I joined his lab as a sophomore student. During my three years in the Sarpong group and even throughout my graduate studies at Harvard, Richmond has provided me with unwavering support and I am forever grateful for his encouragement and enthusiasm about chemistry.

I would also like to thank all of my friends who have supported me through the years and offered me invaluable advice. In particular, I am very grateful for my friendships with Sharon Lee, Sarah House, Allen Hong, Justin Kim, Lauren Zarzar, Aaron Garner, Andrew Marcus, and Eric Bunnelle. Not only are they incredible scientists and will no doubt continue to make great achievements in the scientific field, but also wonderful friends. I also want to acknowledge members of the Shair group that I have worked with during my six years at Harvard. Not only have I learned a lot from everyone I overlapped with, but I have also enjoyed their friendship.

I would also like to thank my family for their devoted support and guidance throughout my entire life. The love and support from my dad, mom, and brother have shaped me into the person I am today. Lastly, and most importantly, I would like to thank my husband, best friend, and former baymate, Brian Liau, for his advice, guidance, support, and love. Thanks for helping me through the ups and downs that come naturally with graduate school. I would not be the scientist or person now without you. I am eternally grateful for your love and support and look forward to our future together.

List of Abbreviations

Å	angstrom
A(1,3)	1,3-allylic strain
Ac	acetyl
Bn	benzyl
Boc	*tert*-butyloxycarbonyl
BOM	benzyloxymethyl
brsm	based on recovered starting material
Bu	butyl
c	concentration (g/100 mL)
°C	degree celsius
cat.	catalytic
Cbz	carbobenzyloxy
cis	*L.,* on the same side
COSY	correlation spectroscopy
Cp	cyclopentadienyl
CSA	camphorsulfonic acid
D	dimensional
DBU	1,8-diazabicyclo[5.4.0]undec-7-ene
DCE	1,2-dichloroethane
DDQ	2,3-dichloro-5,6-dicyano-*p*-benzoquinone
DIBAL-H	diisobutylaluminum hydride
δ	chemical shift
DMAP	4-dimethylaminopyridine
DMF	*N,N*-dimethylformamide
DMP	Dess-Martin periodinane
DMSO	dimethyl sulfoxide
dr	diastereomeric ratio

E	*Ger.,* entgegen
ee	enantiomeric excess
endo	*Gr.,* within
ent	enantiomer
Eq.	equation
equiv	equivalent
ESI	electrospray ionization
Et	ethyl
exo	*Gk.,* external
FABMS	fast atom bombardment mass spectrometry
FTIR	Fourier transform infrared
g	gram
Grubbs II	Grubbs second-generation catalyst
h	hour
HMBC	heteronuclear multiple bond correlation
HMDS	hexamethyldisilazane
HMPA	hexamethylphosphoramide
HMQC	hetereonuclear multiple quantum coherence
HPLC	High-performance liquid chromatography
HRMS	high-resolution mass spectrometry
HSQC	heteronuclear single quantum coherence
Hz	hertz
Imid	imidazole
IR	infrared
J	coupling constant (in Hz)
KHMDS	potassium hexamethyldisilazide
LDA	lithium diisopropylamide
LiHMDS	lithium hexamethyldisilazide

LiTMP	lithium 2,2,6,6-tetramethylipiperidide
2,6-lut	2,6-lutidine
M	molar (mols/liter)
µ	micro
µm	micron
m-CPBA	*meta*-chloroperoxybenzoic acid
Me	methyl
mg	milligram
MHz	megahertz
min	minutes
min	minimize
mL	milliliter
mmol	millimole
mol	mole
MOM	methoxymethylether
MS	mass spectrometry
MsCl	methanesulfonyl chloride
NBS	*N*-bromosuccinimide
NIS	*N*-iodosuccinimide
NMO	4-methylmorpholine *N*-oxide
NMR	nuclear magnetic resonance
nOe	nuclear Overhauser effect
NOESY	nuclear Overhauser effect spectroscopy
Ns	2-nitrobenzenesulfonyl
NsCl	2-nitrobenzenesulfonyl chloride
Ox.	oxidation
OTf	trifluoromethanesulfonate
P	protecting group

pent	pentane
pH	hydrogen ion concentration
Ph	phenyl
Phth	phthalimide
PIFA	[bis(trifluoroacetoxy)iodo]benzene
Piv	pivaloyl
pKa	acid dissociation constant
ppm	parts per million
PPTS	pyridinium *p*-toluenesulfonic acid
^{n}Pr	*n*-propyl
PS	polymer supported
PTLC	preparatory thin-layer chromatography
Py	pyridine
R	general substituent
R	rectus (Cahn–Ingold–Prelog system)
R_f	retention factor
ROESY	rotating frame nuclear Overhauser effect spectroscopy
RT	room temperature
RXN	reaction
S	sinister (Cahn–Ingold–Prelog system)
sec	seconds
taut.	tautomerization
TASF(Et)	tris(diethylamino)sulfonium trimethyldifluorosilicate
TBAF	tetrabutylammonium fluoride
TBHP	*tert*-butyl hydroperoxide
TBS	*tert*-butyldimethylsilyl
TES	triethylsilyl
Tf	trifluoromethanesulfonyl

TFA	trifluoroacetic acid
TFE	2,2,2-trifluoroethanol
THF	tetrahydrofuran
TIPS	triisopropylsilyl
TLC	thin-layer chromatography
TMEDA	*N,N,N′,N′*-tetramethylethylenediamine
TMP	2,2,6,6-tetramethylpiperidine
TMS	trimethylsilyl
TMSE	2-trimethylsilylethyl
TOCSY	total correlation spectroscopy
TPAP	tetrapropylammonium perruthenate
trans	*L.,* across
trig	trigonal
TsCl	*p*-toluenesulfonyl chloride
TsOH	*p*-toluenesulfonic acid
UV	ultraviolet
vis	visible
X	general substituent
Z	*Ger.,* zusammen

I. Progress Toward the Total Synthesis of Lomaiviticin A and B

Chapter 1

Introduction to Lomaiviticin A and B

Introduction

The lomaiviticins comprise a family of type-II polyketide natural products with remarkable C_2-symmetric structures (**1** and **2**, Figure 1.1). The lomaiviticins were first isolated by He and coworkers in 2001[1] from a strain of actinomycetes originally classified as *Micromonospora lomaivitiensis* (reclassified as *Salinispora pacifica*),[2] and exhibit an array of biological activity. Lomaiviticin A (**1**) is potently cytotoxic toward 24 human cancer cell lines with IC_{50} values ranging from 0.007 to 72 nM. Furthermore, both **1** and lomaiviticin B (**2**) are antibiotics against Gram-positive bacteria, including *Staphylococcus aureus* and *Enterococcus faecium*.

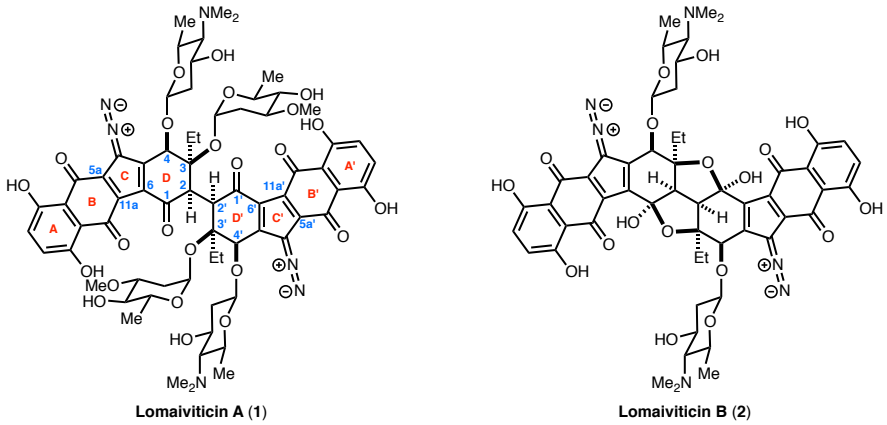

Figure 1.1. Lomaiviticin A (**1**) and B (**2**).

Elucidating the biological mechanism of action of the lomaiviticins (**1** and **2**) has been an area of active research. In the original isolation report, He and coworkers discovered that lomaiviticin A (**1**) cleaves double-stranded DNA (dsDNA) in vitro under reductive conditions; the details of these experiments have not been published. The biological activity of the lomaiviticins is postulated to arise from the diazobenzofluorene system, in analogy to the kinamycins[2] (Figure 1.2), which are

---

[1] He, H.; Ding, W.; Bernan, V. S.; Richardson, A. D.; Ireland, C. M.; Greenstein, M.; Ellestad, G. A.; Carter, G. T. *J. Am. Chem. Soc.* **2001**, *123*, 5362–5363.

[2] (a) Woo, C. M.; Beizer, N. E.; Janso, J. E.; Herzon, S. B. *J. Am. Chem. Soc.* **2012**, *134*, 15285–15288. (b) Herzon, S. B.; Woo, C. M. *Nat. Prod. Rep.* **2012**, *29*, 87–118.

closely related monomeric natural products. The kinamycins also display anticancer properties; (–)-kinamycin C is cytotoxic against the NCI-60 cell line panel[3] with an average GI_{50} = 340 nM.

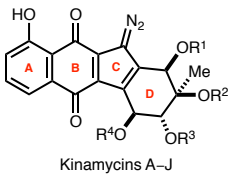

Kinamycins A–J

A: R^1 = H, R^2 = Ac, R^3 = Ac, R^4 = Ac
B: R^1 = H, R^2 = Ac, R^3 = H, R^4 = H
C: R^1 = Ac, R^2 = H, R^3 = Ac, R^4 = Ac
D: R^1 = Ac, R^2 = H, R^3 = H, R^4 = H
E: R^1 = Ac, R^2 = H, R^3 = H, R^4 = H
F: R^1 = H, R^2 = H, R^3 = H, R^4 = H
G: R^1 = Ac, R^2 = C(O)*i*-Pr, R^3 = Ac, R^4 = Ac
H: R^1 = C(O)*i*-Pr, R^2 = H, R^3 = Ac, R^4 = Ac
I: R^1 = C(O)*i*-Pr, R^2 = H, R^3 = Ac, R^4 = Ac
J: R^1 = Ac, R^2 = Ac, R^3 = Ac, R^4 = Ac

Figure 1.2. Kinamycins A–J.

Melander and coworkers have demonstrated that the kinamycins cleave dsDNA in the presence of a reducing cofactor, such as glutathione (GSH),[4] at relevant intracellular concentrations. Two possible mechanisms for kinamycin-mediated dsDNA cleavage are proposed (Figure 1.3). First, an initial $2e^-$ reduction of kinamycin leads to the corresponding hydroquinone, such as **3** or **4**. In the first proposed mechanism, subsequent expulsion of nitrogen may then afford the reactive *ortho*-quinone methide **5**, which can alkylate DNA and induce subsequent DNA cleavage. Alternatively, an exogenous nucleophile could add to the terminal nitrogen of the electrophilic diazo group of **3**, forming adduct **6**, which could then undergo C–N bond homolysis to form sp^2-radical **7**, leading to DNA damage. The lack of sequence specificity in the observed dsDNA cleavage products supports the latter radical-based mechanism.

---

[3] (a) Shoemaker, R. H. *Nat. Rev. Cancer* **2006**, *6*, 813–823. (b) Data at http://dtp.nci.nih.gov/.

[4] (a) Ballard, T. E.; Melander, C. *Tetrahedron Lett.* **2008**, *49*, 3157–3161. (b) Heinecke, C. L.; Melander, C. *Tetrahedron Lett.* **2010**, *51*, 1455–1458.

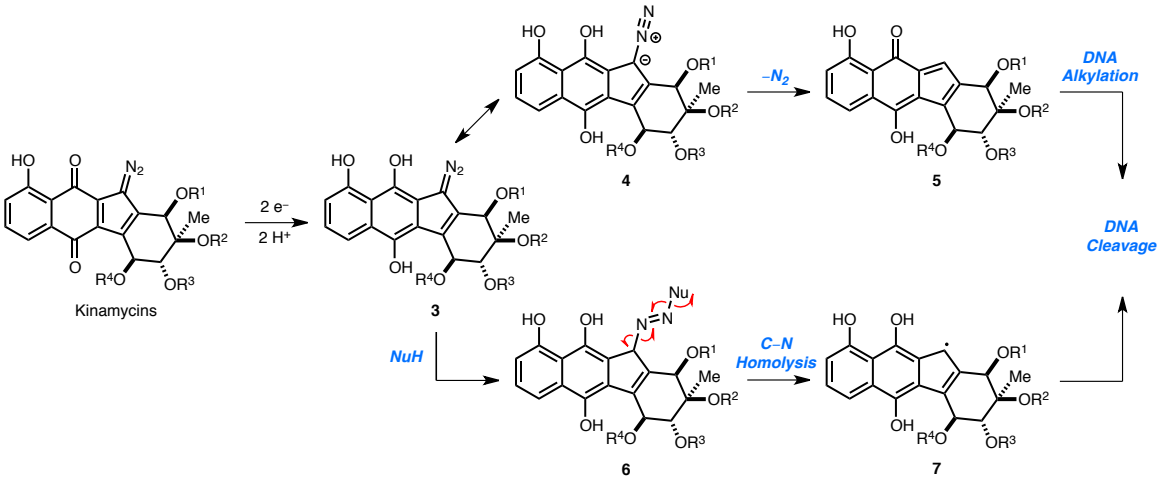

Figure 1.3. Proposed biological mechanism of action for the kinamycins.

More recently,[5] Herzon and coworkers have demonstrated that lomaiviticin A (**1**) induces dsDNA breaks in the presence of dithiothreitol (DTT) in a plasmid cleavage assay. Labelling studies seemed to suggest that DNA cleavage occurred via a radical pathway, supporting the formation of carbon-centered radical species **7**. The anti-proliferative properties of the lomaiviticins are believed to be due to an analogous biological mechanism of action involving the diazobenzofluorene system (Figure 1.4). Vinyl radical species **9** could lead to DNA damage and the formation of *ortho*-quinone methide **10**. Next, expulsion of the aminosugar residues at C4/C4' would generate the corresponding vinylogous *ortho*-quinone methide intermediate, whereupon DNA could act as a nucleophile and add to the C4/C4'-positions to afford alkylated species **11**. However, despite structural similarities with the kinamycins, the lomaiviticins exhibit enhanced cytotoxicity, which can likely be attributed to other structural elements. This includes the C_2-symmetric structure and the sugar residues, which may potentially serve as recognition elements for bringing the lomaiviticins to their biological target. In order to elucidate the biological mechanism of action, a synthesis of the lomaiviticins is necessary due to the low abundance of natural sources.

---

[5] (a) Colis, L. C.; Woo, C. M.; Hegan, D. C.; Li, Z.; Glazer, P. M.; Herzon, S. B. *Nature Chem.* **2014**, *6*, 504–510. (b) Mulcahy, S. P.; Woo, C. M.; Ding, W.; Ellestad, G. A.; Herzon, S. B. *Chem. Sci.* **2012**, *3*, 1070–1074.

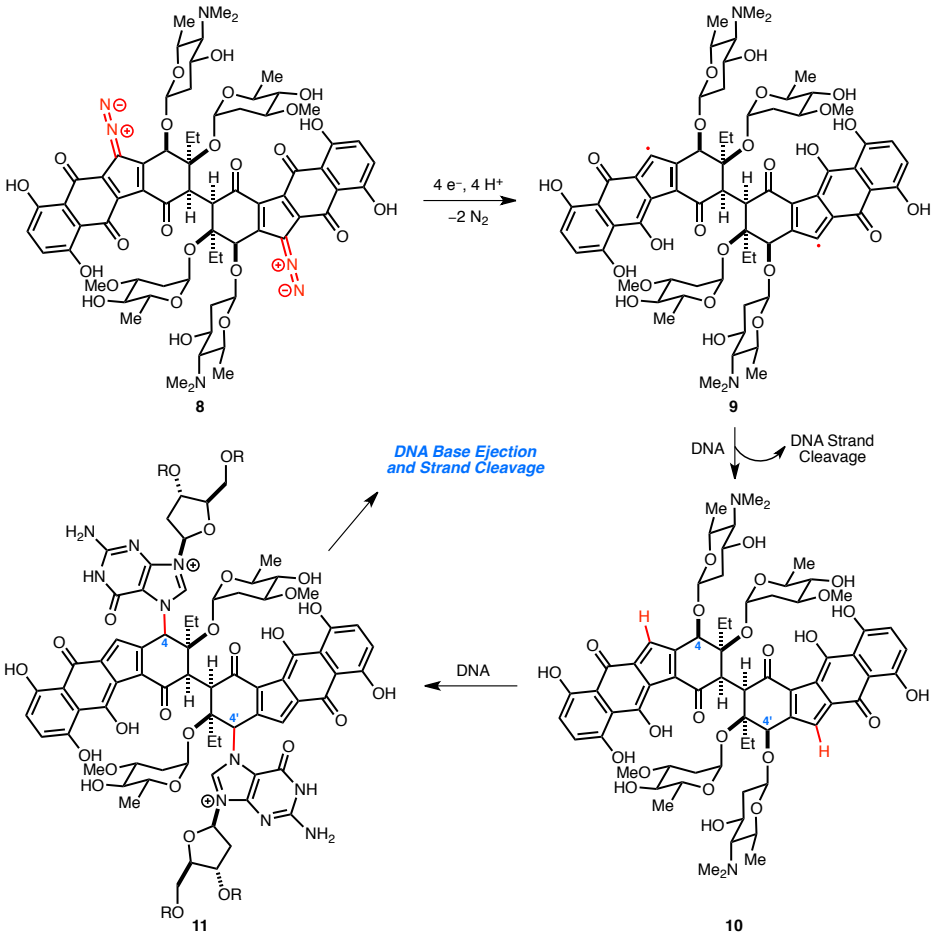

Figure 1.4. Proposed biological mechanism of action for the lomaiviticins.

The biosynthesis of the kinamycins has been extensively studied[6] and the kinamycin carbon skeleton has been demonstrated to be entirely polyketide-derived (10 equivalents of acetylcoenzyme A). Due to structural similarities with the kinamycins, the biosynthesis of the lomaiviticins is proposed to occur via a similar pathway, with key additional steps including two phenolic oxidations (Figure 1.5). An oxidation of the A-ring phenol in the kinamycins to the corresponding hydroquinone is required. Furthermore, a phenolic oxidative coupling is likely involved in the key dimerization

---

[6] (a) Gould, S. J. *Chem. Rev.* **1997**, *97*, 2499–2510. (b) Sato, Y.; Gould, S. J. *Tetrahedron Lett.* **1985**, *26*, 4023–4026. (c) Seaton, P. J.; Gould, S. J. *J. Am. Chem. Soc.* **1987**, *109*, 5282–5284. (d) Seaton, P. J.; Gould, S. J. *J. Antibiot.* **1989**, *42*, 189–197. (e) Gould, S. J.; Melville, C. R. *Bioorg. Med. Chem. Lett.* **1995**, *5*, 51–54. (f) Gould, S. J.; Melville, C. R.; Cone, M. C.; Chen, J.; Carney, J. R. *J. Org. Chem.* **1997**, *62*, 320–324.

reaction.[7] Subsequently, the lomaiviticin biosynthetic pathway could then follow the biosynthesis of the kinamycins, concluding with glycosylations of the C4/C4'- and C3/C3'-hydroxyl groups.

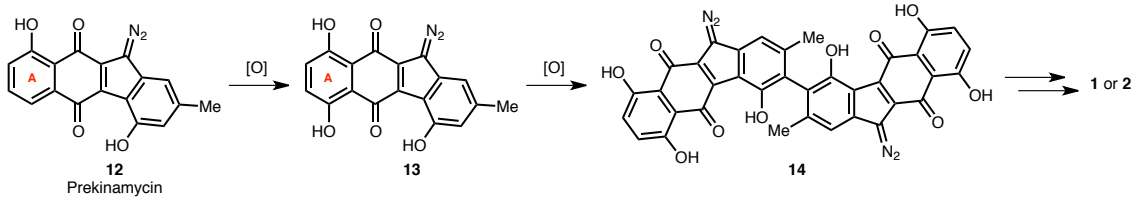

Figure 1.5. Proposed phenolic oxidative dimerization during the biosynthesis of the lomaiviticins.[8]

[7] (a) Huettel, W.; Mueller, M. *ChemBioChem* **2007**, *8*, 521–529. (b) Zhao, B.; Guengerich, F. P.; Bellamine A.; Lamb, D. C.; Izumikawa, M.; Lei, L.; Podust, L. M.; Sundaramoorthy, M.; Kalaitzis, J. A.; Reddy, L. M.; Kelly, S. L.; Moore, B. S.; Stec, D.; Voehler, M.; Falck, J. R.; Shimada, T.; Waterman, M. R. *J. Biol. Chem.* **2005**, *280*, 11599–11607. (c) Dewick, P. R. *Medicinal Natural Products*; 2nd ed.; John Wiley & Sons, LTC: West Sussex, 1995.

[8] Prekinamycin **12** is an intermediate identified in the biosynthetic pathway of the kinamycins.

First Total Synthesis and Selected Synthetic Studies of the Lomaiviticin Aglycon

The lomaiviticin family of natural products have long attracted synthetic interest due to their remarkable C_2-symmetric structures and complex architecture. The structural complexity of **1** and **2** poses several synthetic challenges (Figure 1.1). The highly oxidized carbon skeleton includes up to four 2-deoxyglycosides, and the central C2–C2' bond links two densely functionalized halves to generate up to eight contiguous stereocenters. Each monomeric half possesses an unusual diazofluorene system, a naphthazarin, and a β-alkoxyenone subunit.

Arguably, the stereoselective construction of the key C2–C2' bond presents the most formidable obstacle in achieving a synthesis of the lomaiviticins (Figure 1.6). Constructing the C2–C2' bond via a dimerization strategy is complicated by two critical challenges: (1) a high potential for β-elimination of the C3-alkoxy group by a C1–C2 enolate and (2) difficulty in achieving stereoselective formation of the C2/C2'-stereocenters.

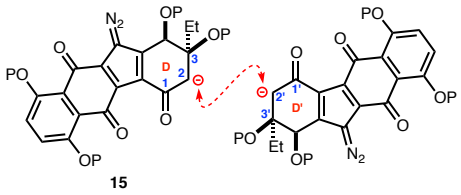

Figure 1.6. Potential problems for an oxidative dimerization strategy.

Altogether, these features render the lomaiviticins challenging synthetic targets. Indeed, despite efforts by various groups,[9] only one synthesis of the aglycon **35** has been accomplished to

---

[9] (a) Nicolaou, K. C.; Denton, R. M.; Lenzen, A.; Edmonds, D. J.; Li, A.; Milburn, R. R.; Harrison, S. T. *Angew. Chem. Int. Ed.* **2006**, *45*, 2076–2081. (b) Nicolaou, K. C.; Nold, A. L.; Li, H. *Angew. Chem. Int. Ed.* **2009**, *48*, 5860–5863. (c) Zhang, W.; Baranczak, A.; Sulikowski, G. A. *Org. Lett.* **2008**, *10*, 1939–1941. (d) Feldman, K. S.; Selfridge, B. R. *Org. Lett.* **2012**, *14*, 5484–5487.

date[10] and a total synthesis of the natural product has yet to be achieved. Selected synthetic studies toward the lomaiviticin aglycon, including the first synthesis, will be discussed.

The first approach to the core structures of lomaiviticin A (**1**) and B (**2**) utilizing a bridged tricyclic scaffold to control the stereochemistry of the model system by Nicolaou and coworkers will be discussed (Scheme 1.1).[9a] It was envisioned that core structures **16** or **17** could arise from tricycle **18**, where X would serve as a tethering group to provide a conformationally locked system that could subsequently be converted to the corresponding 1,4-dicarbonyl function (**17**). Due to the locked framework in 1,4-dicarbonyl **19**, organometallic double addition to the carbonyl groups should occur stereoselectively. **19** could arise from bis(cyclohexenone) **20**.

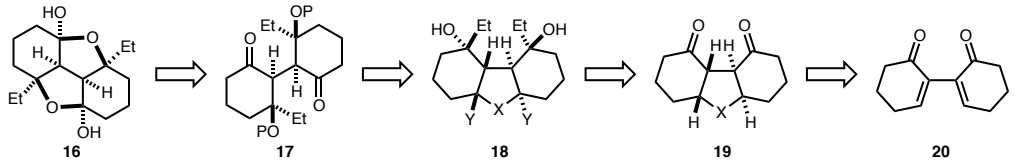

Scheme 1.1 Nicolaou's retrosynthetic analysis of the lomaiviticin core structure featuring a bridged tricyclic scaffold to control the stereoselective synthesis of the model system (**16**).

The synthesis commenced with the conjugate addition of dimethyl malonate to bisenone **20**, affording the double Michael-addition product **21** as a single diastereomer (Scheme 1.2). Exposure of **21** to ethyl cerium reagent generated in situ provided adduct **23** via proposed intermediate lactone **22**. **23** was converted to ketone **24** in 7 steps in 68% overall yield. Double α-oxygenation of **24** upon treatment with KHMDS and $P(OEt)_3$ yielded C_2-symmetric ketone **25** as a single diastereomer. Reduction of the ketone in **25** with $LiAlH_4$ afforded triol **26**. Finally, hydrogenolysis of the BOM ethers furnished pentaol **27**.

---

[10] (a) Herzon, S. B.; Lu, L.; Woo, C. M.; Gholap, S. L. *J. Am. Chem. Soc.* **2011**, *133*, 7260–7263. (b) Woo, C. M.; Gholap, S. L.; Lu, L.; Kaneko, M.; Li, Z.; Ravikumar, P. C.; Herzon, S. B. *J. Am. Chem. Soc.* **2012**, *134*, 17262–17273.

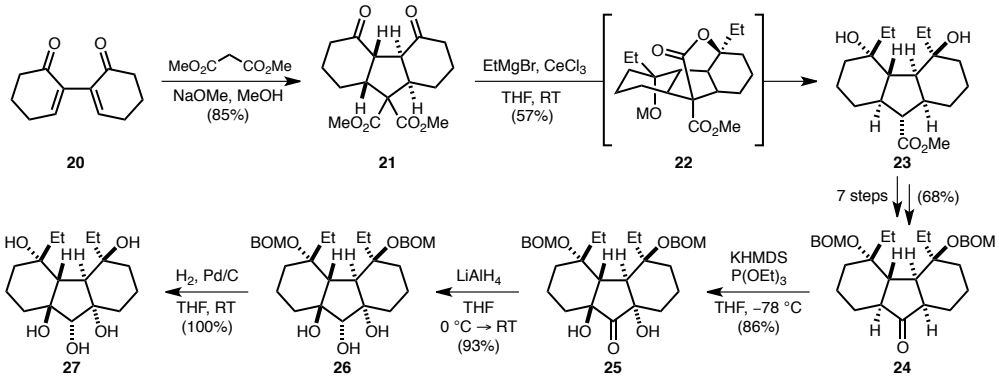

Scheme 1.2. Synthesis of tricycle **27**.

Exposure of triol **26** to $Pb(OAc)_4$ resulted in the formation of tetracyclic acetal **28**, which underwent reduction upon treatment with $LiBH_4$ and subsequent oxidative cleavage with $Pb(OAc)_4$ to afford hemiketal **29** as a 3:1 mixture of diastereomers (Scheme 1.3). Oxidation of the major diastereomer with TPAP and NMO then yielded the model core system of lomaiviticin A (**30**).

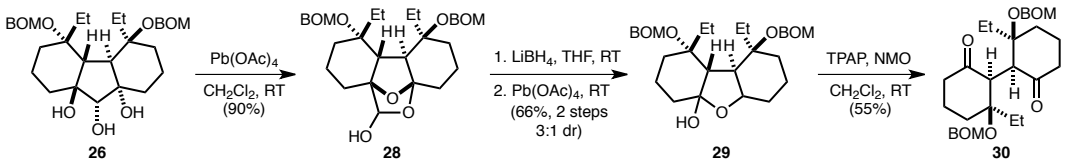

Scheme 1.3. Synthesis of the model core system **30** of lomaiviticin A (**1**).

The synthesis of the lomaiviticin B core model system (Scheme 1.4) was accomplished from intermediate **27** by initial exposure of **27** to $Pb(OAc)_4$ to furnish formate **33** via: (1) cleavage of the *cis*-1,2-diol to afford keto-aldehyde **31** and (2) oxidative cleavage of intermediate hemiacetal **32**. Finally, cleavage of the formate ester in **33** in the presence of methanolic ammonia provided the desired lomaiviticin B core **34**. In conclusion, Nicolaou and coworkers achieved the first stereoselective synthesis of the lomaiviticin A and B core systems using a bridged tricyclic scaffold strategy.

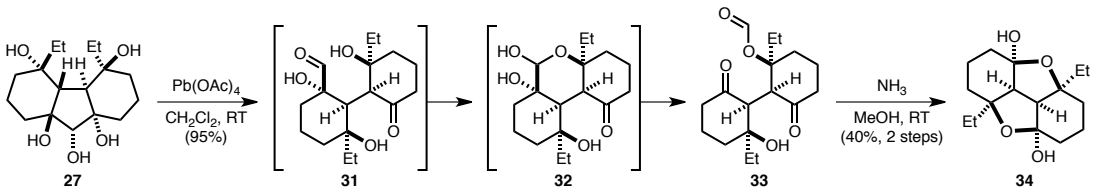

Scheme 1.4. Synthesis of the model core system **34** of lomaiviticin B (**2**).

In 2011, Herzon and coworkers accomplished the first synthesis of the lomaiviticin aglycon (**35**, Scheme 1.5).[10] Remarkably, an efficient enantioselective synthesis was realized in 13 steps from commercial starting material. Despite potential challenges associated with a synthetic strategy relying on late-stage dimerization of a monomer resembling kinamycin, including β-elimination of the C3-hydroxy or alkoxy group and uncertainty regarding the stereochemical outcome, a late-stage oxidative coupling was pursued.

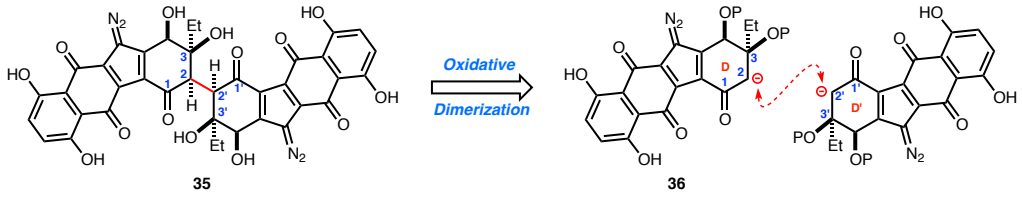

Scheme 1.5. Herzon's retrosynthesis of the lomaiviticin aglycon **35** featuring a late-stage oxidative dimerization to establish the key C2–C2' bond.

A 1:1 diastereomeric mixture of mesitylaldehyde acetals **37** was synthesized in five steps from 3-ethylphenol (Scheme 1.6). 1,4-Conjugate addition of trimethylsilylmethylmagnesium chloride to enone **37** in the presence of CuI, followed by enolate trapping with TMSCl and subsequent Saegusa oxidation, afforded enone **38**. **38** and naphthoquinone **39** were efficiently coupled together upon treatment with TASF(Et) to furnish tricycle **40**. Heck cyclization mediated by $Pd(OAc)_2$ in the presence of polymer-supported (PS) PPh_3 provided cyclized product **41**. Diazo transfer with TfN_3 then afforded diazofluorenes **42** and **43**, which were readily separable at this stage. Finally, formation of silyl enol ether **44** from ketone **43** occurred readily, yielding the dimerization substrate.

An extensive screen of oxidants was next conducted to effect the oxidative dimerization of either **43** or **44** (Scheme 1.7). It was eventually discovered that $Mn(hfacac)_3$ was capable of accomplishing the oxidative coupling of silyl enol ether **44**, albeit in low yield (26% desired diastereomer) and diastereoselectivity (~2:1 dr).

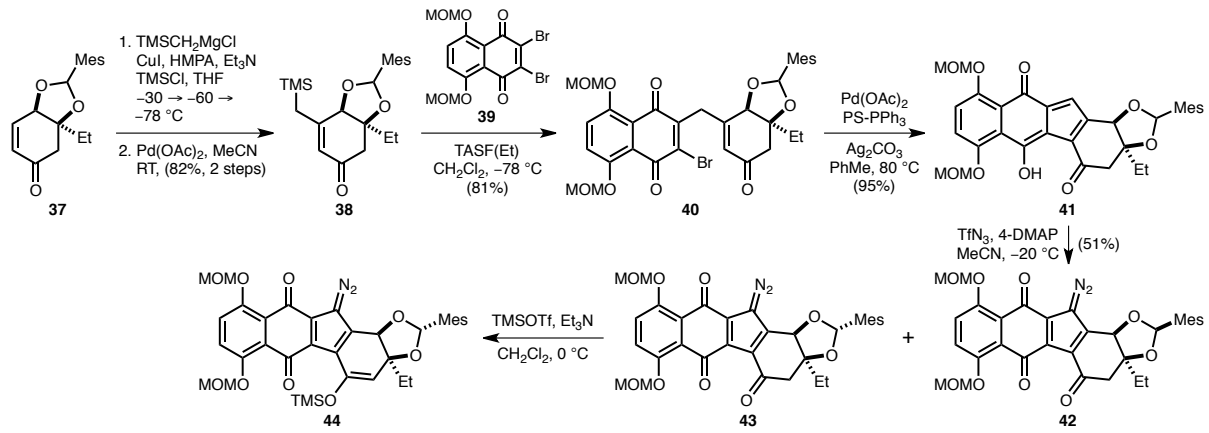

Scheme 1.6. Synthesis of diazofluorene dimerization substrate **44**.

Finally, deprotection of **45** occurred upon exposure to TFA and TBHP to afford the desired lomaiviticin B aglycon **47** after purification. Prior to silica gel preparative thin-layer chromatography, the initial product isolated from the deprotection reaction exists in the form of the open-chain ketone isomer lomaiviticin A (see **35**) aglycon, which could also be readily converted to **47** upon standing in MeOH. In conclusion, Herzon and coworkes have accomplished the first synthesis of the lomaiviticin aglycon by utilizing a late-stage oxidative silyl enol ether dimerization strategy.

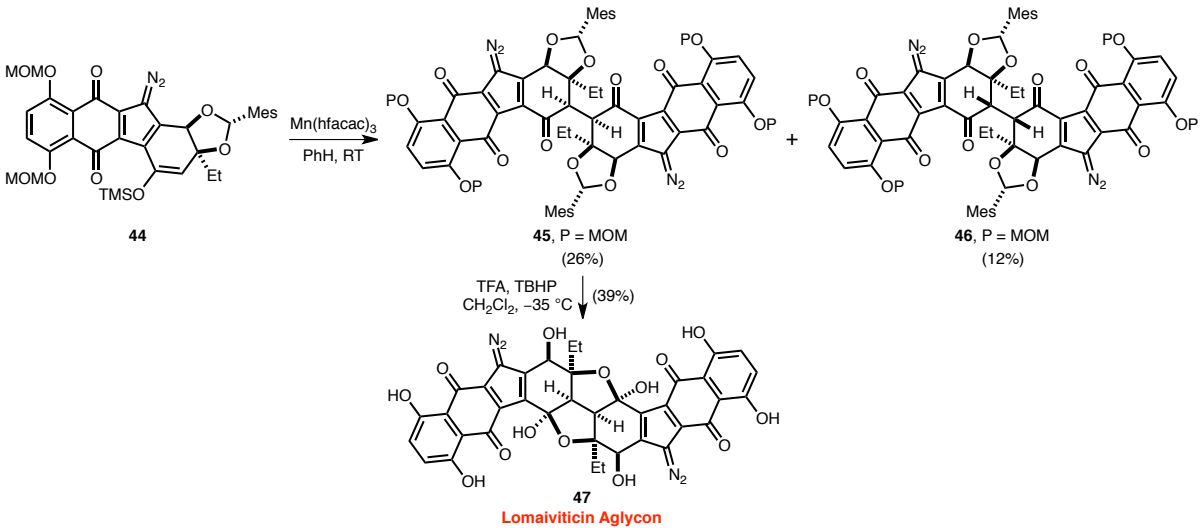

Scheme 1.7. Completed synthesis of the lomaiviticin aglycon **47**.

To summarize this chapter, a brief introduction and background for the lomaiviticin family of natural products was presented. Two selected key syntheses, Nicolaou's synthesis of the model core systems of lomaiviticin A and B and Herzon's enantioselective synthesis of the lomaiviticin aglycon, were discussed.

I. Progress Toward the Total Synthesis of Lomaiviticin A and B

Chapter 2

Progress Toward the Total Synthesis of Lomaiviticin A and B

Introduction

Achieving a synthesis of lomaiviticin A (**1**) and B (**2**) has been a long-standing project in the Shair group.[11] We were first attracted to the lomaiviticins not only because of their interesting biological activity, but also because of their fascinating and complex architecture. The structural composition and relative stereochemistry of the aglycon and carbohydrate residues were elucidated by extensive ^{1}H, ^{13}C, COSY, TOCSY, HMQC, HMBC, and ROESY NMR experiments, as well as IR and FTICR mass spectrometry. At the outset of the project, the absolute stereochemistry of the aglycon and the carbohydrate residues was ambiguous; however, this was subsequently determined by Herzon and coworkers in 2012.[2]

Selected routes pursued by the Shair group toward the synthesis of the lomaiviticin aglycon **47** will be discussed in detail.[11] We envisioned constructing the central C2–C2' bond in **1** and **2** via a late-stage oxidative enolate dimerization reaction[12] in order to minimize double processing (e.g., Scheme 1.5). A variety of oxidants[13] reported in the literature are capable of performing such an oxidative enolate dimerization to afford the corresponding 1,4-diketone product. Examples of such oxidants include $CuCl_2$, $Cu(OTf)_2$, Cu(2-ethylhexanoate)$_2$, $FeCl_3$, $Fe(acac)_3$, ferrocenium salts, I_2, hypervalent iodine, and $TiCl_4$.

---

[11] (a) More than 10 different generations of routes have been pursued. Only the most relevant routes will be discussed. (b) Krygowski, E. S. Ph.D. Thesis, Harvard University, 2008. (c) Lee, H. G. Ph.D. Thesis, Harvard University, 2012.

[12] (a) Ivanoff, D.; Spassof, A. *Bull. Soc. Chim. Fr.* **1935**, *2*, 76–78. (b) Ito, Y.; Konoike, T.; Saegusa, T. *J. Am. Chem. Soc.* **1975**, *97*, 2912–2914.

[13] (a) For review, see: Guo, F.; Clift, M. D.; Thomson, R. J. *Eur. J. Org. Chem.* **2012**, 4881–4896. (b) Kobayashi, Y.; Taguchi, T.; Tokuno, E. *Tetrahedron Lett.* **1977**, *42*, 3741–3742. (c) Baran, P. S.; Richter, J. M. *J. Am. Chem. Soc.* **2004**, *126*, 7450–7451. (d) Frazier, R. H.; Harlow, R. L. *J. Org. Chem.* **1980**, *45*, 5408–5411. (e) Baran, P. S.; Guerrero, C. A.; Ambhaikar, N. B.; Hafensteiner, B. D. *Angew. Chem. Int. Ed.* **2005**, *44*, 606–609. (f) Nguyen, P. Q.; Schaefer, H. J. *Org. Lett.* **2001**, *3*, 2993–2995. (g) Zhdankin, V. V.; Tykwinski, R.; Capple, R.; Berglund, B.; Koz′min, A. S.; Zefirov, S. *Tetrahedron Lett.* **1988**, *29*, 3717–3720. (h) Ojima, I.; Brandstadter, S. M.; Donovan, R. J. *Chem. Lett.* **1992**, *21*, 1591–1594.

While the exact mechanism for oxidative enolate dimerization is not completely understood, it is generally accepted that single electron transfers are involved. Three plausible mechanisms are shown in Scheme 2.1. In the first mechanism (Eq. 1), two equivalents of enoxy radical **50**, generated by single electron oxidation of the enolate **49**, can combine together to form 1,4-diketone **51**. In the second mechanism[14] (Eq. 2), the electrophilic enoxy radical **50** undergoes nucleophilic attack by one enolate equivalent **49**, forming ketyl radical anion **52**. A subsequent single electron oxidation of **52** then affords **51**. Thirdly (Eq. 3), another possibility is the involvement of a metal chelated intermediate (**53**). Depending on the oxidant and conditions utilized, these mechanisms may be differentially operative in individual contexts.

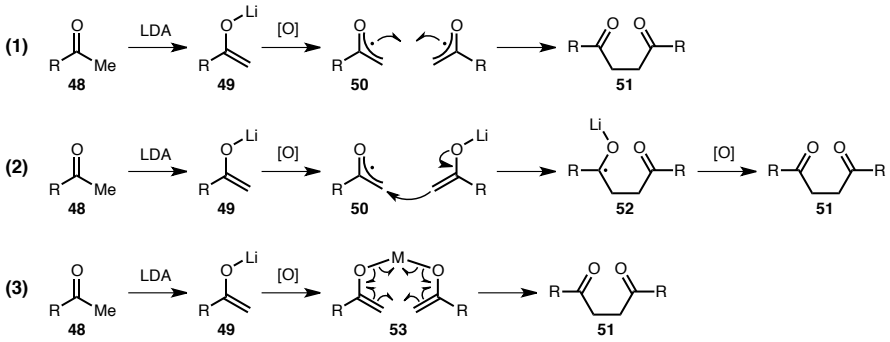

Scheme 2.1. Possible mechanisms for oxidative enolate dimerizations.

While there was precedence supporting our proposed oxidative enolate dimerization[15] reaction, several critical challenges existed. Not only does the central C2–C2' bond link two densely functionalized and sterically hindered halves, but two key concerns needed to be addressed: (1) controlling the stereoselective formation of the C2–C2' bond and (2) preventing β-elimination of the C3- and C3'-alkoxy groups.

---

[14] Schmittel, M.; Haeuseler, A. *J. Organomet. Chem.* **2002**, *661*, 169–179.

[15] At the outset of this project, a strategy utilizing an oxidative enolate dimerization for constructing the key C2–C2' bond in the lomaiviticins had not been reported in the literature.

A solution to both of these problems was discovered in the form of the oxanorbornanone[16] system, or specifically, an oxygen bridge between C3 and C6 (Figure 2.1). Stereoselective formation of the C2- and C2'-stereocenters is controlled by dimerization of the endocyclic enolate **54** from the less hindered convex *exo* face of the oxanorbornanone.[17] Furthermore, in oxanorbornanone system **54**, β-elimination is prevented due to the nearly orthogonal orientation of the endocyclic C1–C2 enolate π-system with the antibonding σ^*-orbital of the bridging C–O bond.[18] An exocyclic enolate (C5–C4a, see **55**), however, would have greater conformational flexibility and can thus achieve requisite orbital overlap for β-elimination.[19] We planned to exploit this stereoelectronic dichotomy of the oxanorbornanone system to achieve stereoselective oxidative endocyclic enolate dimerization without β-elimination, and at a subsequent stage, conduct regioselective fragmentation of the oxygen bridge via an exocyclic enolate.

---

[16] Vogel, P.; Cossy, J.; Plumet, J.; Arjona, O. *Tetrahedron* **1999**, *55*, 13521–13642.

[17] (a) Mosimann, H.; Vogel, P.; Pinkerton, A. A.; Kirschbaum, K. *J. Org. Chem.* **1997**, *62*, 3002–3007. (b) Marchionni, C.; Vogel, P.; Roversi, P. *Tetrahedron Lett.* **1996**, *37*, 4149–4152. (c) Arjona, O.; Menchaca, R.; Plumet, J. *Org. Lett.* **2001**, *3*, 107–109.

[18] (a) Tojo, S.; Isobe, M. *Synthesis* **2005**, 1237–1244. (b) Jackson, S. R.; Johnson, M. G.; Mikami, M.; Shiokawa, S.; Carreira, E. M. *Angew. Chem. Int. Ed.* **2001**, *40*, 2694–2697.

[19] (a) McMorris, T. C.; Staake, M. D.; Kelner, M. J. *J. Org. Chem.* **2004**, *69*, 619–623. (b) Jung, M. E.; Min, S. J. *Tetrahedron* **2007**, *63*, 3682–3701.

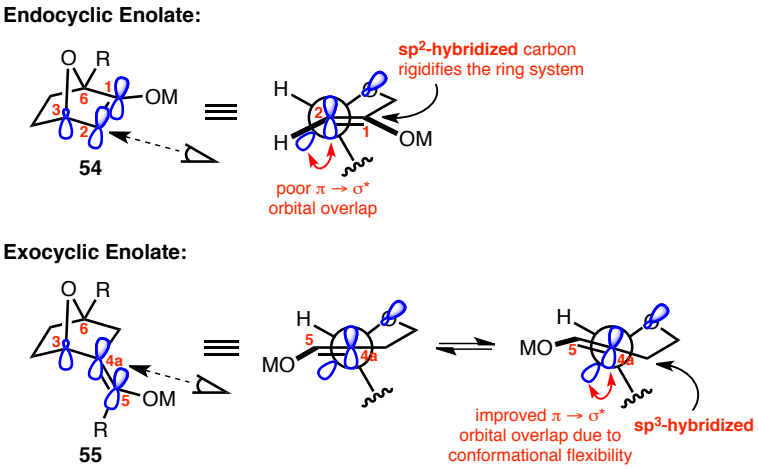

Figure 2.1. Reactivity of endocyclic vs. exocyclic oxanorbornanone enolates.

Due to the fascinating structural complexity of lomaiviticin A (**1**) and B (**2**) and their interesting biological activity, we embarked on a total synthesis of these two natural products. Specifically, we wished to address whether an oxidative oxanorbornanone enolate dimerization reaction to construct the key C2–C2' bond could be accomplished stereoselectively and without β-elimination of the C3-alkoxy group. At the outset of our project, a synthesis of the lomaiviticin aglycon had not yet been published.

Previous Approaches in the Shair Group

A simple model system was devised by Dr. Evan S. Krygowski and Dr. Kerry Murphy-Benenato in order to test the feasibility of an oxidative dimerization of an oxanorbornanone enolate or silyl enol ether (Scheme 2.2).[20] Gratifyingly, they discovered that treatment of silyl enol ether **57** with Ag_2O in DMSO at 100 °C afforded the desired dimerization product as a 7:1 mixture of C_2-symmetric **58** and meso **59** diastereomers.[21] Both products arise from exclusive *exo-exo* dimerization of **57** and no β-elimination products were observed.

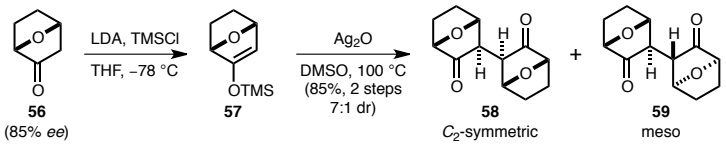

Scheme 2.2. Stereoselective dimerization of an oxanorbornanone model system.

A second model system was synthesized in order to study the β-elimination of the oxygen bridge via an exocyclic enolate (Scheme 2.3). Surprisingly, exposure of oxanorbornanone **60** to K_2CO_3 in MeOH at 0 °C not only resulted in β-elimination of the oxygen bridge, but also displacement of the phenylsulfone group with methoxide (vide infra).[22]

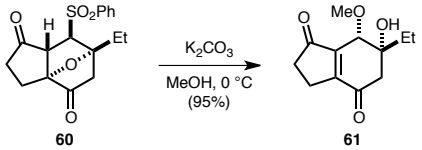

Scheme 2.3. Successful β-elimination of the oxygen bridge and displacement of the phenylsulfone.

---

[20] Krygowski, E. S.; Murphy-Benenato, K.; Shair, M. D. *Angew. Chem. Int. Ed.* **2008**, *47*, 1680–1684.

[21] A diastereomeric mixture of products was obtained because **57** was not a single enantiomer.

[22] We originally hypothesized that **61** resulted from initial β-elimination of the phenylsulfone group, followed by 1,4-conjugate addition of methoxide and generation of the corresponding exocyclic enolate. β-Elimination of the oxygen bridge from this enolate intermediate would then furnish **61**. This mechanism was subsequently revised.

In summary, we demonstrated that (1) an oxanorbornanone system can be dimerized stereoselectively and (2) subsequent β-elimination of the oxygen bridge via an exocyclic enolate can be achieved with displacement of the phenylsulfone group by a suitable nucleophile. With the success of these two model systems in hand, we embarked on a synthesis of the lomaiviticin aglycon. Initial efforts were focused on synthesizing the central CD/C'D'-ring system, which we believed would allow us to study our key strategy in detail and could potentially be elaborated to the full carbon skeleton. However, our ultimate goal was to perform a late-stage oxidative enolate dimerization of a tetracyclic precursor in order to minimize double processing.

To this end, oxanorbornanone tricycle **62** was synthesized[20] and our key oxidative enolate dimerization reaction was investigated (Scheme 2.4). Unfortunately, the conditions utilized in our model system (Ag_2O, DMSO, 100 °C) did not translate to the trimethylsilyl enol ether derived from **62**.[23] Other oxidants, including $Cu(OTf)_2$ and CAN did not afford any desired dimerization product. We next turned our attention to the oxidative dimerization of the enolate generated from **62**.

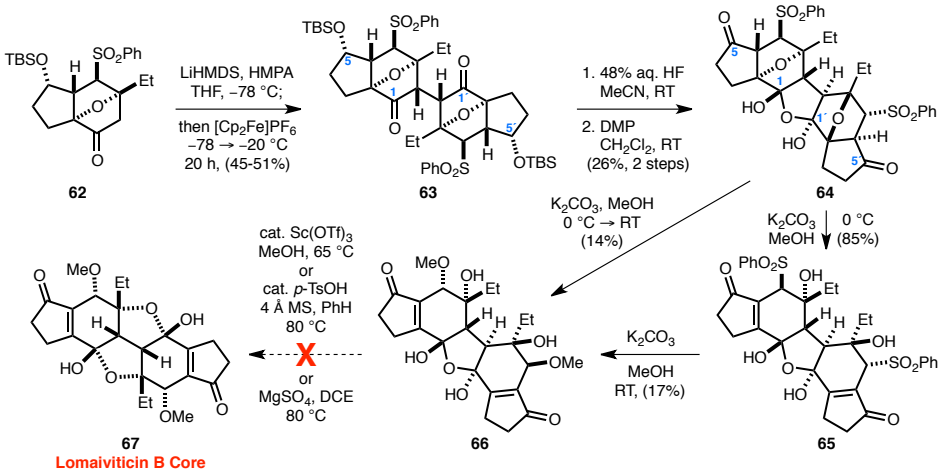

Scheme 2.4. Synthesis of the lomaiviticin core in the form of a stable cyclic hydrate.

---

[23] In all cases the TMS group was compromised and starting ketone **62** was recovered.

A screen[11b] of oxidants ($CuCl_2$, $Cu(OTf)_2$, Cu(2-ethylhexanoate)$_2$, $FeCl_3$, $Fe(acac)_3$, AgCl, $PhI(OAc)_2$, and I_2) for the dimerization of the enolate derived from **62** was next conducted. In all cases, no desired dimer **63** was obtained. One common problem of the aforementioned oxidants is that they all require temperatures of 0 °C or higher for enolate oxidation to occur. Unfortunately, however, the enolate generated from **62** was not stable above –20 °C and would undergo undesired β-elimination of the oxygen bridge. We rationalized that an oxidant capable of conducting single electron transfer at temperatures below –20 °C was necessary in order to achieve successful dimerization.

We next turned our attention to $[Cp_2Fe]PF_6$, a powerful outer-sphere, single-electron oxidant. There was precedence[24] in the literature that $[Cp_2Fe]PF_6$ was capable of oxidizing enolates at –78 °C. Gratifyingly, exposure of the lithium enolate of **62**, generated from deprotonation by LiHMDS, to $[Cp_2Fe]PF_6$ in the presence of HMPA at –78 °C, followed by subsequent warming to –20 °C and stirring for an additional 20 h, yielded the desired dimerization product **63** as a single diastereomer in 45-51% yield. Unfortunately, dimer **63** was only moderately stable to silica gel chromatography,[25] which likely accounted for the diminished yield of **63**.

With dimer **63** in hand, we next focused our attention on β-elimination of the oxygen bridge. To this end, global silyl deprotection, followed by DMP oxidation of the corresponding secondary carbinols, afforded cyclic hydrate **64**, where a single molecule of H_2O had added to the C1- and C1'-ketones. We hypothesized that a possible explanation for cyclic hydrate formation is the relief of ring strain introduced into the system by the newly formed sp^2 carbon after DMP oxidation. Another possible rationale is that the C5- and C5'-ketones may inductively make the C1- and C1'-ketones

---

[24] (a) Jahn, U. *J. Org. Chem.* **1998**, *63*, 7130–7131. (b) Jahn, U.; Hartmann, P. *Chem. Commun.* **1998**, 209–210. (c) Jahn, U.; Hartmann, P.; Kaasalainen, E. *Org. Lett.* **2004**, *6*, 257–260.

[25] Re-exposure of pure isolated dimer product **63** to a silica gel column resulted in loss of one-third of the material.

more electron deficient, thus promoting cyclic hydrate formation. Exposure of **64** to K_2CO_3 in MeOH at 0 °C furnished bisenone **65** in good yield (85%). Re-exposure of **65** to K_2CO_3 in MeOH at room temperature resulted in displacement of the allylic phenylsulfone groups with methoxide with inversion of configuration, albeit in low yield (17%), to provide bisenone **66**. Both transformations could be combined into a single one-pot operation (K_2CO_3, MeOH, 0 °C → RT) to afford **66** in 14% yield. Attempts to dehydrate **66** to the lomaiviticin B core system under acidic conditions proved unsuccessful and either resulted in recovery or decomposition of starting material.

In summary, we have demonstrated that the key C2–C2' bond could be stereoselectively constructed via an oxidative enolate dimerization of an oxanorbornanone system without undesired β-elimination of the oxygen bridge. Specifically, we discovered that $[Cp_2Fe]PF_6$ promoted oxidative dimerization at sufficiently low temperatures at which oxygen bridge fragmentation did not occur. Furthermore, we were able to subsequently β-eliminate the oxygen bridge via an exocyclic enolate to reveal the lomaiviticin core system in the form of a cyclic hydrate. With the success of these discoveries in hand, we next embarked on a synthesis of the full carbon skeleton of the lomaiviticin aglycon.

In order to minimize double-processing, the optimal strategy was to utilize a late-stage oxidative dimerization of a tetracyclic enolate intermediate such as **69** (Scheme 2.5).[26] Tetracycle **70** could be prepared from enone **71** and a phthalide derivative, such as **72** or **73**, via an anionic annulation reaction.[27] Enone **71** could be synthesized from a common intermediate utilized in our original model studies.

---

[26] Lee, H. G.; Ahn, J. Y.; Lee, A. S.; Shair, M. D. *Chem. Eur. J.* **2010**, *16*, 13058–13062.

[27] (a) Mal, D.; Pahari, P. *Chem. Rev.* **2007**, *107*, 1892–1918. (b) Rathwell, K.; Brimble, M. A. *Synthesis* **2007**, 643–662.

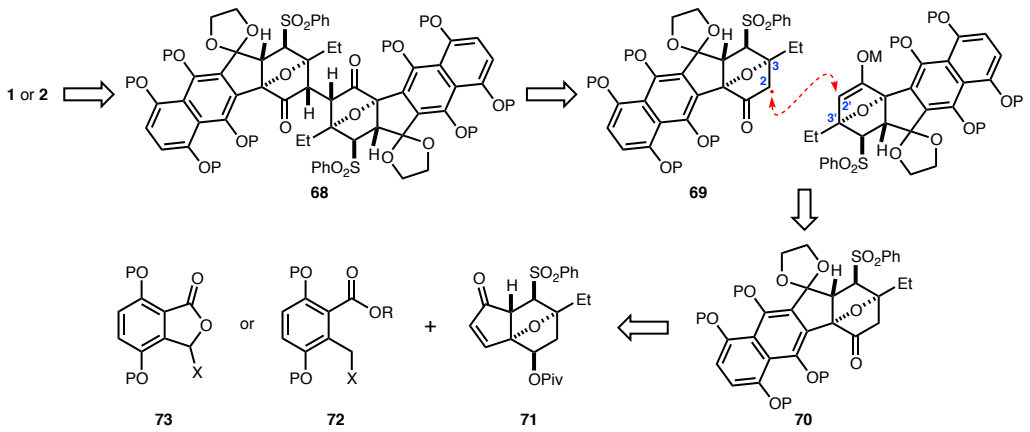

Scheme 2.5. Second-generation retrosynthesis of the lomaiviticin aglycon.

In work by Dr. Hong Geun Lee, enone **71**[28] and cyanophthalide **74** underwent efficient Kraus annulation[29] to afford hydroquinone **75** in 85% yield. Ketal-protection of the C5-ketone using Noyori[30] conditions, followed by allyl-protection of the hydroquinone phenols, furnished allylated product **77**. Finally, cleavage of the pivaloyl group and subsequent Ley oxidation of the resulting secondary carbinol yielded dimerization precursor **78**. **78** was subjected to our optimized oxidative dimerization conditions.[31] Quite surprisingly, the enolate of **78** did not undergo oxidative dimerization to provide the lomaiviticin full carbon skeleton **79**. Indeed, only starting material was recovered (>80%). Other permutations of oxidants and solvents were investigated but yielded no desired product.

---

[28] The synthesis of enone **71** will not be discussed here for brevity. Please see ref. 26 for details.

[29] Kraus, G. A.; Sugimoto, H. *Tetrahedron Lett.* **1978**, *19*, 2263–2266.

[30] Isunoda, T.; Suzuki, M.; Noyori, R. *Tetrahedron Lett.* **1980**, *21*, 1357–1358.

[31] The enolate of **78** was not stable above −60 °C and would undergo undesired oxygen bridge fragmentation.

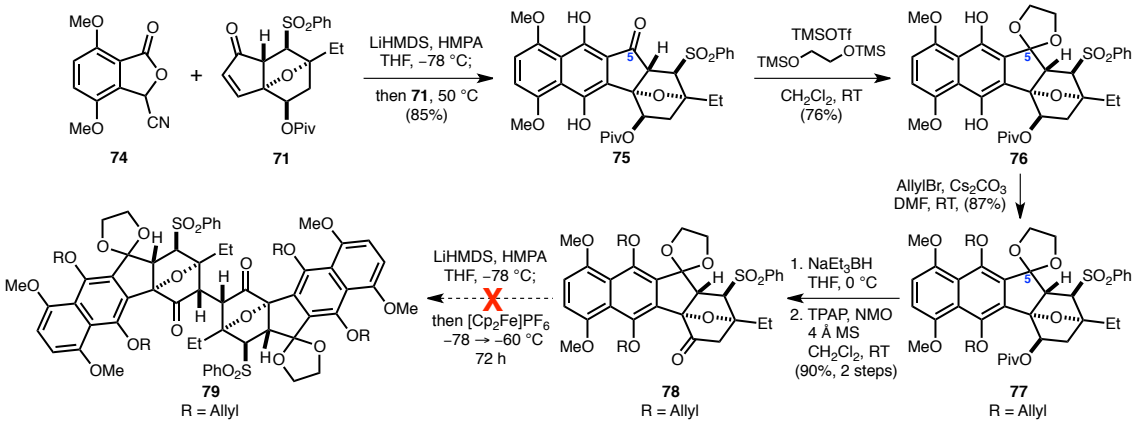

Scheme 2.6. Attempted oxidative dimerization of tetracycle **78**.

We speculated that non-bonding interactions could be disfavoring dimerization by preventing favorable approach of the two reacting partners in the transition state (Figure 2.2). In model **80**, we postulated that non-bonding interactions between the C3 and C11', and C3' and C11, ethyl and allyloxy groups, respectively, may be disfavoring dimerization. In the approach depicted in **81**, severe steric interactions between the C3- and C3'-ethyl groups and the C11- and C11'-allyloxy groups exist. Thus, we rationalized that a smaller C11/C11'-alkoxy group may remedy this problem. Instead of protecting the hydroquinone phenols in **76** as the allyl ethers, the corresponding methyl ether derivative was synthesized. Unfortunately, however, only trace quantities of the desired dimerization product were isolated. Predicated on these results, we believed that replacing the C11/C11'-alkoxy groups with the smallest substituent possible—a hydrogen atom—may circumvent these problems and facilitate dimerization.

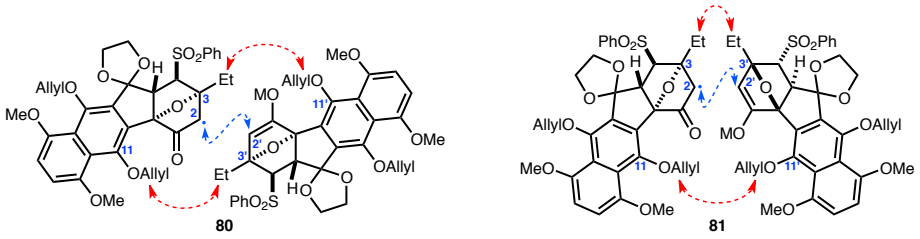

Figure 2.2. Postulated steric interactions during the dimerization event.

To this end, a modified Hauser annulation[32] using a sulfoxide donor (**82**) was employed in order to access tetracycle **83** (Scheme 2.7). Deprotonation of sulfoxide donor **82** with LiHMDS, followed by addition of enone **71**, furnished tetracycle **83** in 79% yield via: (1) initial 1,4-conjugate addition of the sulfoxide anion to the enone, (2) subsequent Claisen condensation, (3) sulfoxide *syn* elimination, and (4) tautomerization to the corresponding phenol. Utilizing the same sequence for the synthesis of **78**, tetracycle **83** was converted to our targeted dimerization substrate **86** in four straightforward steps.

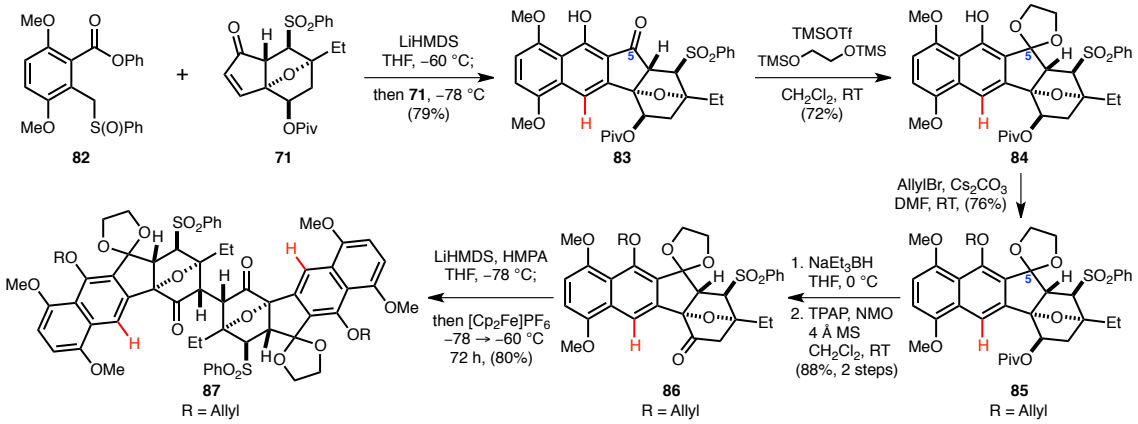

Scheme 2.7. Successful oxidative dimerization of tetracycle **86**.

Gratifyingly, tetracycle **86** underwent successful dimerization utilizing our optimal oxidative enolate coupling protocol to afford dimerization product **87** in 80% yield as a single diastereomer.

---

[32] Hauser, F. M.; Rhee, R. P. *J. Org. Chem.* **1978**, *43*, 178–180.

Single crystal X-ray diffraction analysis of derivative **88** (Figure 2.3), obtained from cleavage of the allyl ethers in **87**, unequivocally established the structure of **88**. Interestingly, the C1–C2–C2'–C1' dihedral angle in crystal **88** is 29° and the C11-hydrogen atom and C1'-ketone oxygen (and analogously, C11'-hydrogen atom and C1-ketone oxygen) were in very close proximity, which could potentially disfavor the dimerization reaction if the C11/C11'-substituent was larger than a hydrogen atom.

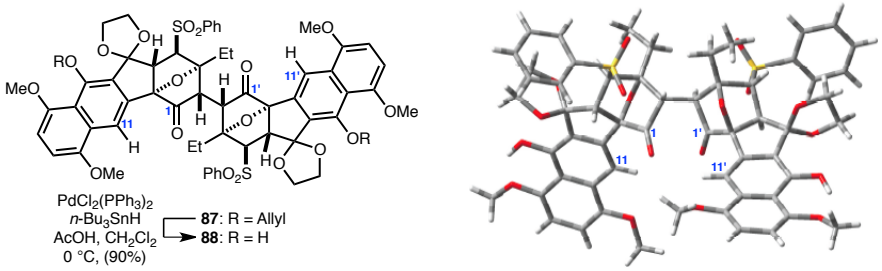

Figure 2.3. Single crystal X-ray diffraction analysis confirmed the structure of **88**.

Finally, with the desired dimerization product **87** in hand, we were ready to test the next crucial step in our strategy—fragmentation of the oxygen bridge. As expected, treatment of **87** with TfOH (Scheme 2.8) provided diketone dimer **89** in the form of a cyclic hydrate. Unfortunately, despite a wide screen of conditions by Dr. Hong Geun Lee, **89** did not undergo oxygen bridge fragmentation. Investigation of a variety of bases in protic solvents, including MeOH, EtOH, *t*-BuOH, and H_2O, only resulted in decomposition of starting material **89**. Similar results were obtained when stronger bases such as LDA, LiHMDS, and *t*-BuOK were used. At the time, it was believed that one possible explanation for unsuccessful oxygen bridge fragmentation of **89** was due to the base-sensitivity of the cyclic hydrate.

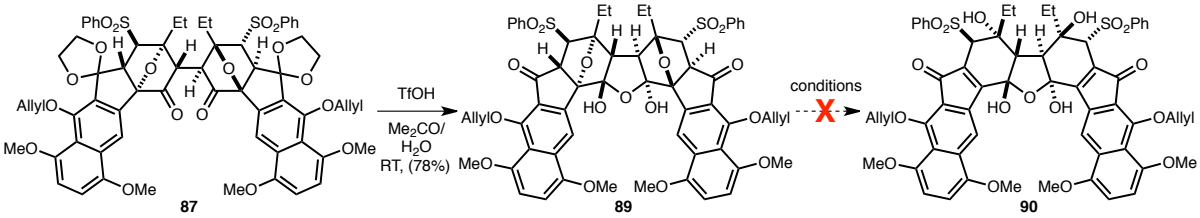

Scheme 2.8. Attempted oxygen bridge fragmentation of cyclic hydrate **89**.

Protection of the cyclic hydrate hydroxyl groups as the corresponding methyl ethers afforded cyclic hydrate **91** (Scheme 2.9). Exposure of **91** to KOH in THF/H_2O did not provide the desired oxygen bridge fragmentation product, but instead diol **92,** which was formed by initial β-elimination of the C4/C4'-phenylsulfone groups followed by addition of hydroxide to the resultant enone, was isolated. Resubjection of **92** to a variety of basic conditions did not result in oxygen bridge β-elimination but only in recovered starting material or decomposition under more forcing conditions. Even 1,3-diketone dimer **93**, synthesized from **92** via a Swern oxidation, did not undergo oxygen bridge fragmentation.

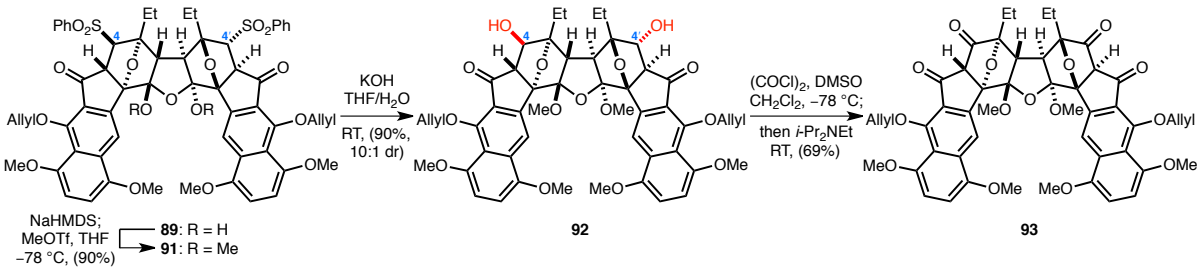

Scheme 2.9. Attempted oxygen bridge fragmentation of cyclic hydrates **92** and **93**.

We next turned our attention towards a reductive approach for oxygen bridge fragmentation via α-elimination[33] from the C1/C1'-ketones (Scheme 2.10). However, instead of the desired

[33] (a) De Schrijver, J.; De Clercq, P. J. *Tetrahedron Lett.* **1993**, *34*, 4369–4372. (b) Padwa, A.; Sandanayaka, V. P.; Curtis, E. A. *J. Am. Chem. Soc.* **1994**, *116*, 2667–2668.

diketone product **94**, only cyclobutanediol **96**,[34] the result of an intramolecular pinacol coupling between the proximal C1 and C1' ketones, was isolated. This was not surprising, since the crystal structure of **88** suggested that the dimer preferentially adopts a conformation that places the C1/C1'-ketones in close proximity to each other.

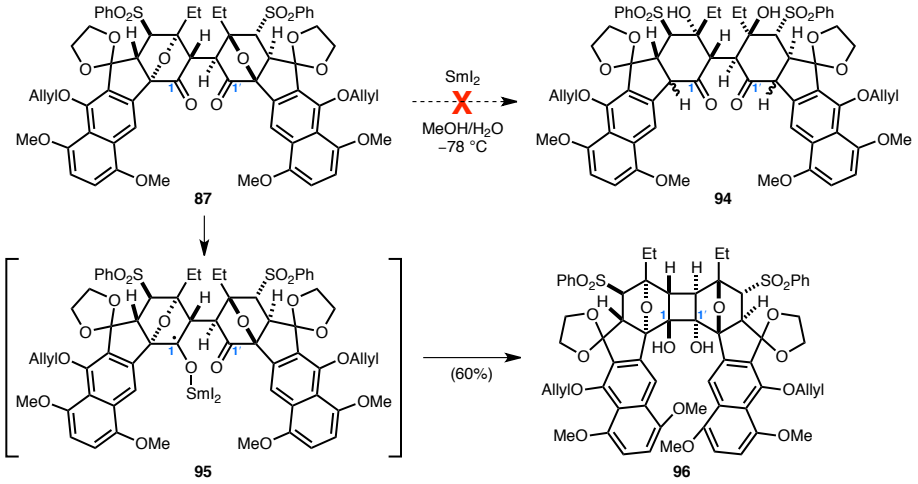

Scheme 2.10. Attempted reductive oxygen bridge fragmentation.

We next decided to pursue a strategy that would utilize the electron-rich nature of the AB/A'B'-naphthalene systems to facilitate oxygen bridge fragmentation (Scheme 2.11). This strategy would first involve oxidation of the B/B'-rings in **87** to the corresponding hydroquinones in **97**. Electron donation from the electron-rich AB/A'B'-naphthalene systems (specifically, the C11- and C11'-phenol groups), should assist in oxygen bridge fragmentation to provide intermediate **98**, which can undergo tautomerization to afford the desired product **99**.

---

[34] The pinacol product was also isolated in an analogous reaction on the model system by Dr. Evan S. Krygowski. See ref. 11b.

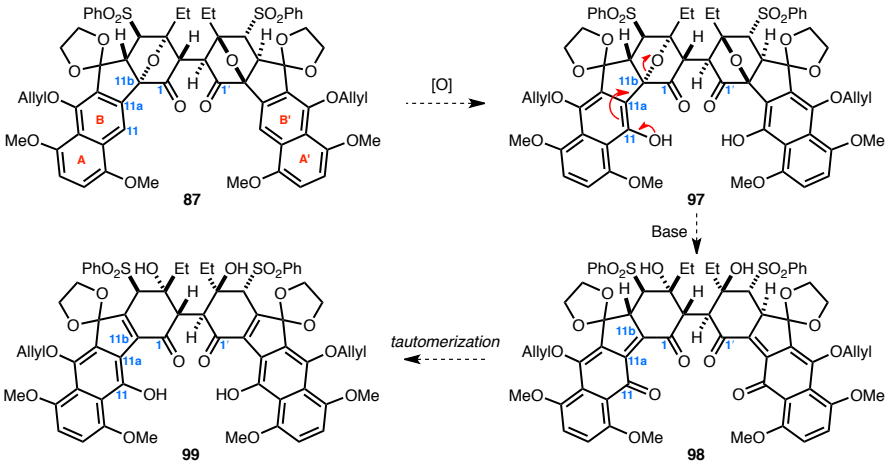

Scheme 2.11. Proposed oxygen bridge fragmentation via the electron-rich AB/A'B'-naphthalene systems.

Oxidation of the B/B'-rings proved to be challenging. After extensive experimentation,[35] it was eventually discovered that substrate **101**, where the C5- and C5'-carbonyl groups have been removed, could be oxidized to quinone dimer **106** (Scheme 2.12). Diketone **102** was synthesized from diol **92** via: (1) $LiEt_3BH$ reduction of the C5- and C5'-carbonyl groups, (2) acetylation of the resulting tetraol to provide the corresponding tetra-acetate, (3) ionic reduction in the presence of Et_3SiH and TfOH, (4) cleavage of the C4- and C4'-acetate groups, and (5) Ley oxidation of the C4- and C4'-secondary carbinol groups to the corresponding ketones. Diastereoselective reduction of the C4- and C4'-ketones in **102**[36] afforded diol **103** with the correct stereochemistry found in the natural product. As expected, hydride delivery occurred from the convex face of the molecule, *anti* to the oxygen bridge.

---

[35] In compounds where C5 existed as a ketone, ketal, or hydrazone, the B- and B'-rings could not be oxidized to the corresponding quinone. An electron-withdrawing group at C5 and C5' is likely responsible for suppressing oxidation of the B- and B'-rings. See ref. [11c].

[36] Attempted oxygen bridge fragmentation via the C4- and C4'-ketones under basic or acidic conditions proved unsuccessful.

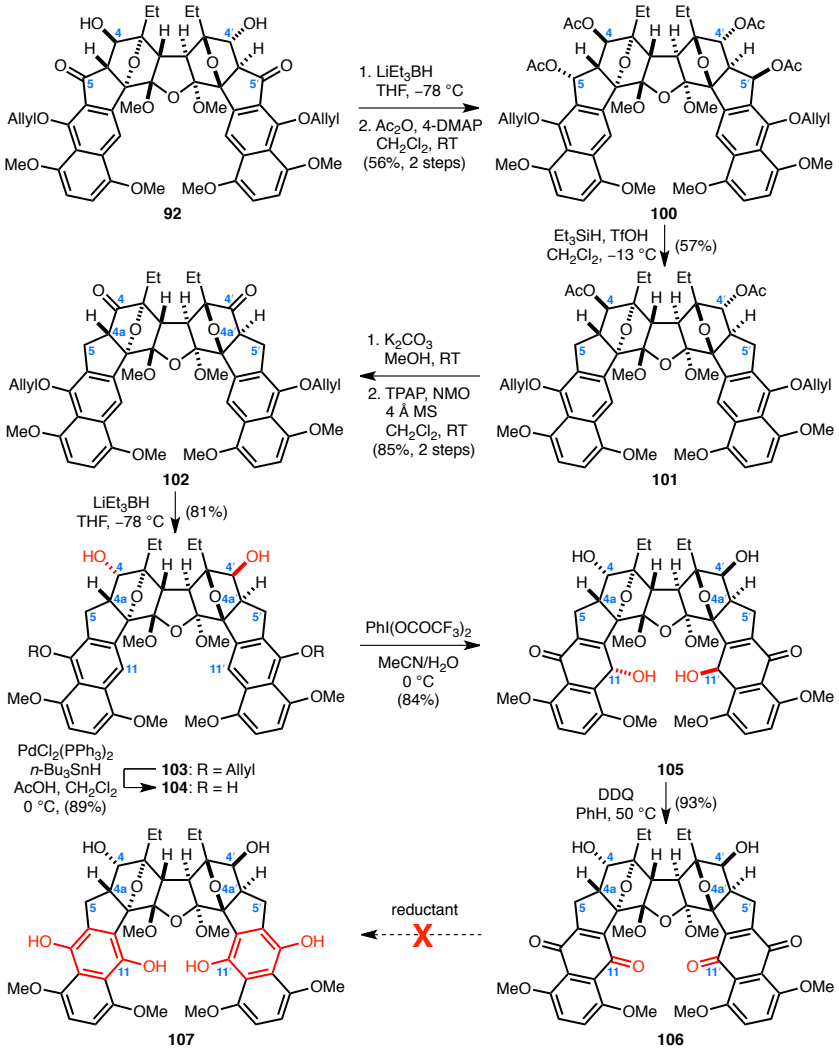

Scheme 2.12. Attempted synthesis of hydroquinone dimer **107**.

Cleavage of the allyl ethers in **103** occurred smoothly to provide naphthol dimer **104**. Surprisingly, treatment of **104** with $PhI(OCOCF_3)_2$, afforded the unaromatized hydroquinone tautomer **105**.[37] Exposure of **105** to a second oxidant, DDQ, then afforded the desired quinone dimer **106**. In order to test our proposed strategy for fragmentation of the oxygen bridge via the electron-rich naphthalene systems, the quinone functions in **106** must be reduced to the corresponding

[37] For an example where the unaromatized hydroquinone tautomer was isolated, see: Chikashita, H.; Porco, J. A.; Stout, T. J.; Clardy, J.; Schreiber, S. L. *J. Org. Chem.* **1991**, *56*, 1692–1694.

hydroquinone. Unfortunately, quinone reduction proved to be challenging and we were never able to isolate hydroquinone **107**.

At this point, Dr. Hong Geun Lee decided to no longer pursue this route due to our inability to β-eliminate the oxygen bridge. Both the model systems investigated by Dr. Evan S. Krygowski and Dr. Kerry-Murphy Benenato and the full carbon skeleton of the aglycon studied by Dr. Hong Geun Lee have provided valuable insight into designing a new route to circumvent the previously observed challenges. A summary of our previous discussion is provided below (Scheme 2.13).

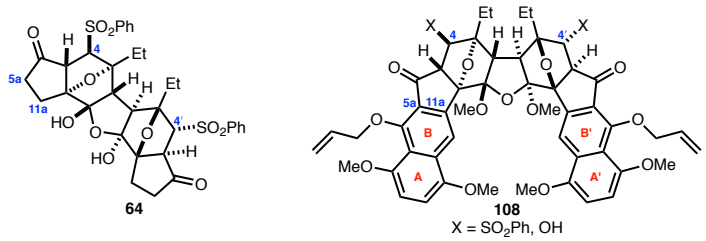

Scheme 2.13. Summary of previous work in the Shair group.

To summarize, in model system **64**, we demonstrated that stereoselective oxidative enolate dimerization of an oxanorbornanone system could be achieved without undesired β-elimination. Furthermore, we were able to subsequently fragment the oxygen bridge in **64** at the appropriate time. However, displacement of the C4-phenylsulfone with various oxygen nucleophiles was extremely low-yielding and the resulting product could not be converted to the lomaiviticin core from the cyclic hydrate. Unexpectedly, in our most advanced system containing the full aglycon carbon skeleton, we were unable to fragment the oxygen bridge. I attributed the unsuccessful fragmentation to the additional strain and rigidity that the AB/A'B'-naphthalenes introduce to the system. In **64**, C5a and C11a are both sp^3-hybridized, whereas in the case of **108** they are sp^2-hybridized. The sp^2-hybridization introduces more strain into an already strained and rigid system and may thus prevent attainment of the requisite orbital overlap for β-elimination of the oxygen bridge.

Predicated on the aforementioned observations, I embarked on a new route to synthesize a substrate with the correct C4- and C4'-stereochemistry in order to obviate the need for a late-stage

allylic phenylsulfone displacement. Additionally, I planned to introduce the AB/A'B'-naphthalene systems after β-elimination of the oxygen bridge because of the aforementioned discussion.

Development of a New Route to the Core of Lomaiviticin A and B

Based on the observations and results discussed in the previous section by my predecessors, I embarked on a new route to the lomaiviticin core system. My first-generation retrosynthesis of the lomaiviticin aglycon (**47**) is outlined in Scheme 2.14.[38] We envisioned that the AB/A'B'-naphthalenes of **109** could be constructed from lomaiviticin B core **110** via a late-stage double annulation reaction, such as a cyclopentadienyl anion bisannulation.[39] **110** could arise from oxanorbornanone dimer **111**, where the key C2–C2' bond would be established by a stereoselective oxidative enolate dimerization of monomer **112**. The oxanorbornanone system could be constructed from an intramolecular *exo*-selective furan Diels–Alder reaction of a suitable precursor such as furanone **114** or related derivative. **114** can be readily assembled from commercially available (*S*)-malic acid and furan **115**.[40]

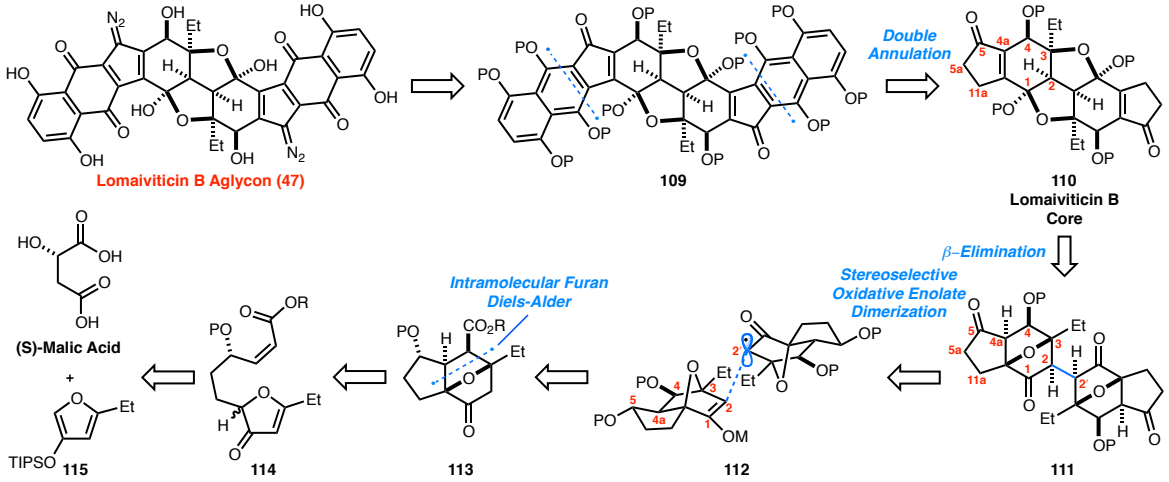

Scheme 2.14. First-generation retrosynthesis of the lomaiviticin aglycon.

---

[38] Lee, A. S.; Shair, M. D. *Org. Lett.* **2013**, *15*, 2390–2393.

[39] Birman, V. B.; Zhao, Z.; Guo, L. *Org. Lett.* **2007**, *9*, 1223–1225.

[40] For a synthesis of furan **115**, see ref. 11b.

Two key differences between the new proposed route and the previous systems investigated by Dr. Evan S. Krygowski and Dr. Hong Geun Lee are: (1) a substrate with the correct C4 and C4'-stereochemistry and oxygenation (**111**) would be utilized, obviating the need for displacement of a C4- and C4'-phenylsulfone group and (2) the AB/A'B'-naphthalene systems would be introduced after β-elimination of the oxygen bridge due to the aforementioned challenges faced by Dr. Hong Geun Lee in his studies when C5a and C11a were sp^2-hybridized.

The synthesis commenced with the formation of the dimethyl ester of commercially available (*S*)-malic acid (Scheme 2.15). Selective monoreduction with BH_3•SMe_2 in the presence of catalytic $NaBH_4$,[41] followed by protection of the resultant 1,2-diol afforded acetal **116**. Reduction of the methyl ester in **116** with $LiBH_4$, followed by formation of the corresponding iodide, occurred smoothly to yield alkyl iodide **117**. Lithiation of furan **115**, followed by alkylation with **117**, afforded coupled product **118**. DIBAL-H regioselective opening of the acetal afforded primary alcohol **119** in 46% yield (66% brsm). Attempts to oxidize primary alcohol **119** were met with surprising difficulty. Standard DMP, Swern, and Ley oxidation conditions resulted in decomposition. In all cases, the siloxy furan was most likely compromised, possibly via an intramolecular or intermolecular aldol reaction with the putative aldehyde intermediate.

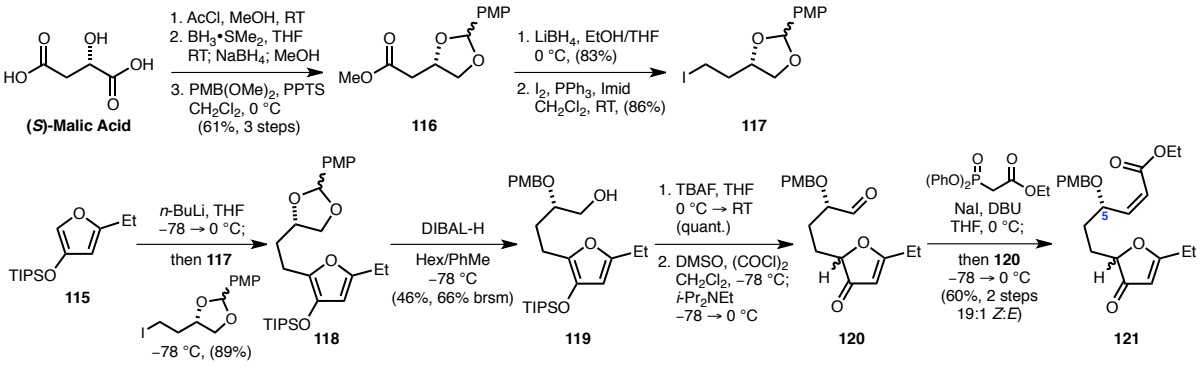

Scheme 2.15. Synthesis of furan Diels–Alder substrate **121**.

---

[41] (a) Gaunt, M. J.; Jessiman, A. S.; Orsini, P.; Tanner, H. R.; Hook, D. F.; Ley, S. V. *Org. Lett.* **2003**, *5*, 4819–4822. (b) Saito, S.; Ishikawa, T.; Kuroda, A.; Koga, K.; Moriwake, T. *Tetrahedron* **1992**, *48*, 4067–4086.

To circumvent this problem, the TIPS ether was cleaved upon treatment with TBAF to provide the corresponding furanone alcohol, which underwent subsequent Swern oxidation to provide furanone aldehyde **120**. Aldehyde **120** was then converted to (*Z*)-enoate **121** (19:1 *Z*/*E*), the desired Diels–Alder substrate, via the Ando variant of the Still modification of the Horner-Wadsworth-Emmons olefination with Masamune and Roush's adapted mild conditions.[42] With **121** in hand, we were ready to test our key intramolecular *exo*-selective furan Diels–Alder reaction.

We anticipated that the stereoselectivity of the *exo*-selective[43] intramolecular furan Diels–Alder reaction would be controlled by the single C5-stereocenter, which enforced a conformation where 1,3-allylic strain was minimized (Scheme 2.16). The *exo* transition state (**122**), which results in *cis*-5,5-fusion product **123**, should be favored over the *endo* transition state (**124**), which would result in highly strained *trans*-5,5-fusion product **125**.

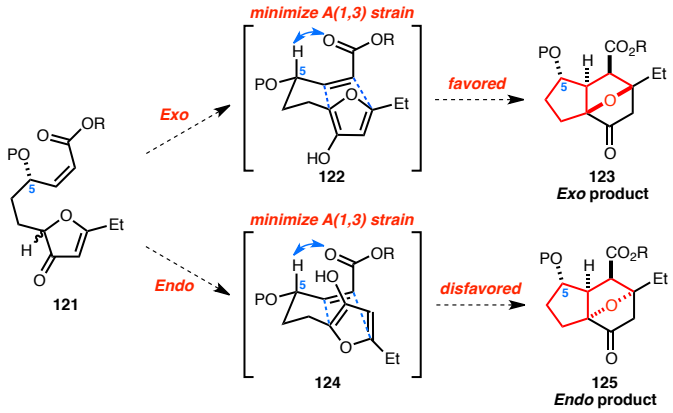

Scheme 2.16. Rationale for the stereoselectivity of the intramolecular furan Diels–Alder reaction.

Initial attempts to promote the Diels–Alder reaction by conventional thermal (PhMe, 50 →

---

[42] Ando, K.; Oishi, T.; Hirama, M.; Ohno, H.; Ibuka, T. *J. Org. Chem.* **2000**, *65*, 4745–4749.

[43] Kappe, C. O.; Murphree, S. S.; Padwa, A. *Tetrahedron* **1997**, *53*, 14179–14233.

100 °C)[44] and Lewis acidic conditions (e.g., $MeAlCl_2$) failed to provide the desired cycloadduct in synthetically useful yields (<25%). We rationalized that tautomerization of the furanone to the requisite furan may be slow and that basic conditions may therefore promote the desired transformation. Addition of DBU to promote enolization resulted in complete conversion of **121** to two new compounds (Scheme 2.17), determined to be the desired product **126** and Michael adduct **127**, in a 1.2:1 ratio, respectively. Both products were each isolated as single diastereomers.

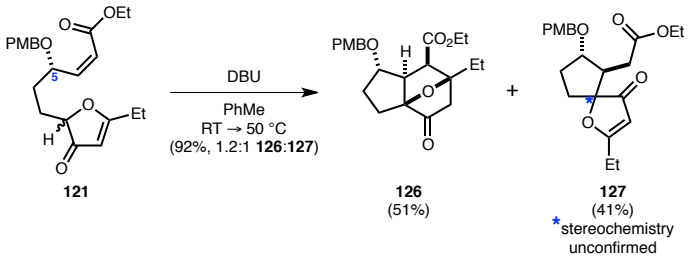

Scheme 2.17. Formal intramolecular furan Diels–Alder reaction.

These results suggested a stepwise Diels–Alder mechanism, i.e., a Michael–Michael sequence (Scheme 2.18). A stepwise "*exo*" mechanism (**128** and **129**) would lead to formation of the desired Diels–Alder product **126**. A stepwise "*endo*" mechanism should result in initial Michael adduct intermediate **130**, which cannot undergo a second Michael reaction to provide the highly strained, *trans*-5,5-fused *endo* product **125** due to poor orbital overlap, thus resulting in isolation of Michael adduct **127**.[45] Separate resubjection of pure **126** and **127** to the reaction conditions resulted in complete recovery of starting material **126** or **127**, respectively, suggesting that formation of Diels–Alder product **126** and Michael adduct **127** is irreversible under the given reaction conditions. In order to drive the reaction to Diels–Alder product **126** formation and prevent isolation of Michael adduct **127**, conditions under which formation of **127** was *reversible* were required. We hypothesized

---

[44] See ref. 20.

[45] The stereochemistry of **127**, postulated as depicted, was not verified.

that a stronger base such that the ester enolate of **127** could be regenerated may provide such a solution.

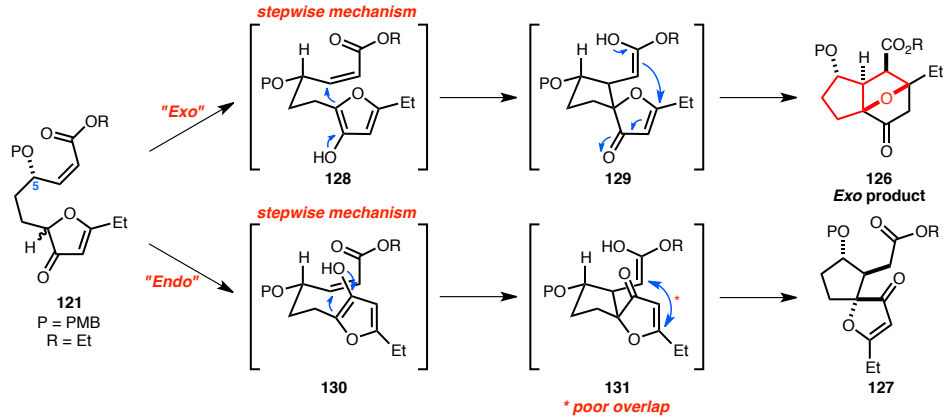

Scheme 2.18. Rationale for formation of Diels–Alder product **126** and Michael adduct **127**.

Gratifyingly, we discovered that treatment of **121** with LDA[46] (Scheme 2.19) provided the Diels–Alder product **126** as a 10:1 mixture of separable diastereomers, favoring the expected *cis*-5,5-fusion product (64% isolated yield). This process presumably occurs via a stepwise Michael–Michael reaction sequence. No Michael adduct **127** was observed under these conditions.

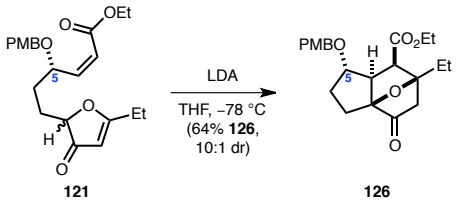

Scheme 2.19. Successful formal intramolecular *exo*-selective furan Diels–Alder reaction.

For reasons that will not be discussed in detail here, we revised our protecting group strategy due to challenges associated with removal of the PMB protecting group in **126** and cleavage of the ethyl ester to the corresponding carboxylic acid (Scheme 2.20). Instead of protecting the 1,2-diol as

---

[46] Caine, D. S.; Paige, M. A. *Synlett* **1999**, *9*, 1391–1394.

the corresponding PMP acetal, the two hydroxyl groups were differentially protected. Selective TBS-protection of the primary hydroxyl, followed by benzyl protection of the secondary hydroxyl group, reduction of the methyl ester in **133**, and formation of the corresponding iodide occurred smoothly to yield alkyl iodide **134**. Following the same sequence of operations utilized previously, lithiation of furan **115**, followed by alkylation with **134**, afforded coupled product **135**. Global silyl deprotection with TBAF provided the corresponding furanone alcohol, which upon Swern oxidation[47] cleanly delivered aldehyde **136**. A (*Z*)-selective modified Horner-Emmons reaction then delivered (*Z*)-enoate **137**. Treatment of **137** with LDA provided the Diels–Alder product **138** as a 10:1 mixture of diastereomers, once again favoring the desired *cis*-5,5-fusion product (64% isolated yield of **138**). We were able to prepare over 10 g of **138** using this protocol. It was imperative to conduct this reaction under extremely dilute conditions (0.02 M) in order to suppress undesired intermolecular pathways.

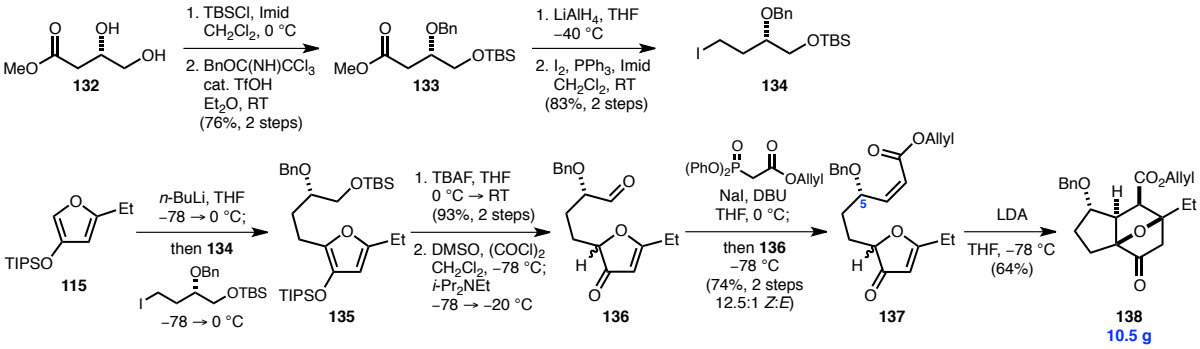

Scheme 2.20. Revised protecting group scheme and synthesis of oxanorbornanone **138**.

With oxanorbornanone **138** in hand, an oxidative "carboxy-inversion" sequence for converting the C4-ester to a hydroxyl group with retention of configuration was required (Scheme

---

[47] It was imperative to remove all *i*-Pr_2NEt during workup of the reaction. Residual *i*-Pr_2NEt promoted **136** to undergo undesired intra-and intermolecular pathways via addition of the furanone moiety to the newly formed aldehyde.

2.21).[48] First, the allyl ester of Diels–Alder product **138** was deprotected to carboxylic acid **139**. Next, *m*-chloroperbenzoic acid (*m*-CPBA) was coupled to carboxylic acid **139** via the acid chloride intermediate to afford diacyl peroxide **140**, which underwent ionic rearrangement ("carboxy-inversion") upon heating in benzene to afford the corresponding acyl carbonate species **141**. Methanolysis of this crude intermediate provided the desired secondary carbinol **142** as a single diastereomer. Attempted optimization of the carboxy-inversion sequence proved to be extremely challenging and the optimal yield obtained (33%, 4 steps) was irreproducible, especially on larger scale. Lewis acids (e.g., $ZnCl_2$, $Sc(OTf)_3$, $MgBr_2$), Brönsted acids (e.g., trichloroacetic acid), and more polar solvents (e.g., CCl_4, $PhCF_3$), all factors which are known to accelerate this ionic process, did not improve the yield.[49] Indeed, in most cases, lower yields were observed.

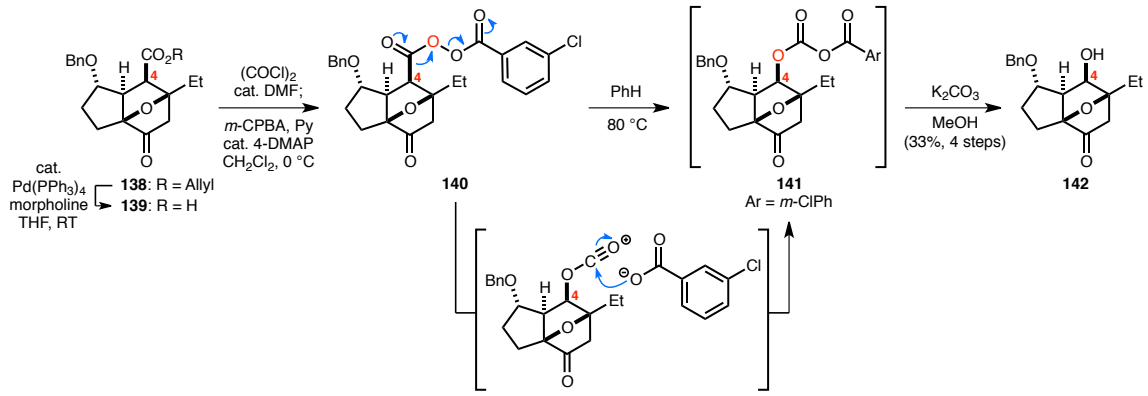

Scheme 2.21. Carboxy-inversion reaction to install the C4-oxygenation with retention of stereochemistry.

Eventually, it was discovered that heating *p*-nitrobenzoyl peroxide **143** (Scheme 2.22),

---

[48] (a) Denney, D. B.; Sherman, N. *J. Org. Chem.* **1965**, *30*, 3760–3761. (b) Fujimori, K.; Shigeru, O. *J. Chem. Soc., Perkin Trans. 2* **1989**, 1335–1348. (c) Meng, Z.; Danishefsky, S. J. *Angew. Chem. Int. Ed.* **2005**, *44*, 1511–1513.

[49] Numerous minor byproducts resulted from the carboxy-inversion reaction, although none were present in significant quantities for characterization.

synthesized via coupling of *p*-nitroperbenzoic acid (*p*-NPBA)[50] with carboxylic acid **139**, afforded desired alcohol **142** in 38% yield (4 steps). While this reaction did not significantly improve the yield, it was reproducible on scale. Furthermore, while *m*-chlorobenzoyl peroxide **140** required silica gel column chromatography, *p*-nitrobenzoyl peroxide **143** did not, obviating the need for an additional purification step. Protection of the hydroxyl group in **142** as a TBS ether yielded the dimerization precursor, oxanorbornanone **144**.

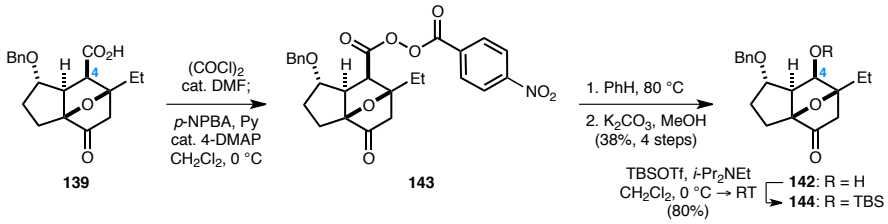

Scheme 2.22. Use of *p*-nitrobenzoyl peroxide **143** in the carboxy-inversion reaction.

Utilizing the optimal oxidative enolate dimerization conditions developed in our group (Scheme 2.23), ketone **144** was added to LiHMDS and HMPA in THF at −78 °C to generate the corresponding lithium enolate, which was then exposed to $[Cp_2Fe]PF_6$ and allowed to stir at −55 °C for 4 days. Contrary to our prior studies where only *exo-exo* dimerization was observed, unsymmetrical *exo-endo* dimer **145** was obtained exclusively (44%). The structure of **145** was further confirmed by the nOe's depicted in Scheme 2.23.

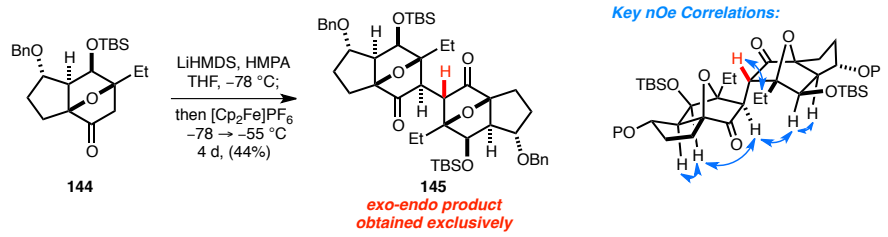

Scheme 2.23. Stereoselective oxidative enolate dimerization affords the *exo-endo* dimer exclusively.

---

[50] Vilkas, M. *Bull. Soc. Chim. Fr.* **1959**, 1401.

It appeared that although dimerization occurred with complete *exo* facial selectivity in the absence of any substitution on the oxanorbornanone carbon framework (Eq. 2, Scheme 2.24), the C4-substituent (pseudoaxial phenylsulfone) played a crucial role in reinforcing *exo-exo* selectivity (Eq. 3 and Eq. 4) in our prior more complex polycyclic systems.

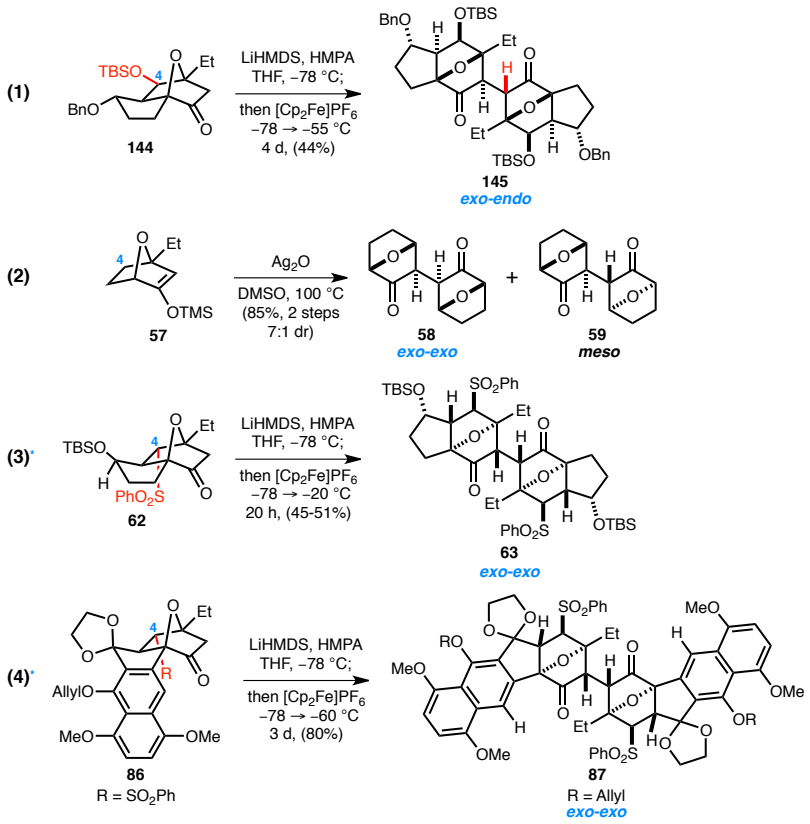

Scheme 2.24. Effect of the relative stereochemisty at C4 on the stereoselectivity of the oxidative dimerization reaction. *The opposite enantiomer to that which is shown was synthesized, but is drawn as such for ease of comparison.

In the current system (Eq. 1), the C4-substituent was a sterically large pseudoequatorial TBS ether group, which likely disfavors *exo-exo* dimerization due to steric interactions, which may cause the ethyl groups to gear towards each other in the transition state. Use of a sterically smaller MOM protecting group on the C4-hydroxyl resulted in a 1:1 *exo-endo*:*exo-exo* mixture of diastereomers, suggesting that not only does the relative stereochemistry at C4 play an important role in the trajectory of the dimerization, but also the size of the substituent.

Attempts to improve the yield of dimerization product **145** above 44% proved to be challenging. Typically 10-15% of starting ketone **144** was recovered from the dimerization reactions. Increasing the reaction temperature (up to −40 °C), varying the concentration (0.05 M−0.20 M), varying the amount of LiHMDS used (1.2−2.2 equiv) or the use of LDA, and allowing the reaction to proceed longer (up to 5 days) did not result in increased yields. Byproducts were not present in sufficient quantities for characterization.

Fortunately, *exo-endo* dimer **145** could be selectively epimerized to the desired and thermodynamically favored *exo-exo* dimer **146** by treatment with 2-*t*-butyl-1,1,3,3-tetramethylguanidine (Barton's base) (Scheme 2.25). With *exo-exo* dimer **146** in hand, the benzyl ethers were cleaved and the corresponding diol **147** was oxidized to 1,4-diketone dimer **148**. Surprisingly, and quite fortuitously, **148** did not exist as a cyclic hydrate if silica gel column chromatography was avoided; this is in contrast to our previously discussed systems where the analogous C5-ketone substrates (Scheme 2.13) existed exclusively as the cyclic hydrates. One possible explanation was that the sterically large pseudoequatorial C4- and C4'-TBS ethers may cause the ethyl groups to orient towards each other such that the cyclic hydrate, where the ethyl groups are in close proximity, would be disfavored. Regardless, the C4-stereochemistry has subtle yet far-reaching stereoelectronic consequences on the system.

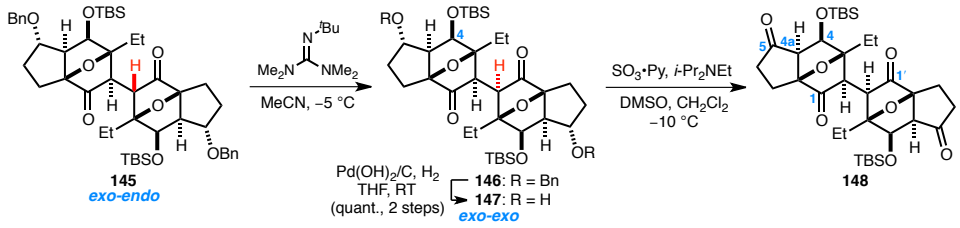

Scheme 2.25. Selective epimerization of *exo-endo* dimer **145** to the desired *exo-exo* dimer **146**.

With a successful synthesis of 1,4-diketone dimer **148** completed, the key oxygen bridge fragmentation was next investigated (Scheme 2.26). Quite surprisingly, all attempts to fragment the oxygen bridge of **148** or the cyclic hydrate form of **148** were unsuccessful. Exposure of **148** to acidic

(e.g., PPTS, BF_3•OEt_2, BCl_3) and basic (e.g., K_2CO_3/MeOH, DBU, Barton's base, KHMDS, KOH/THF/H_2O) conditions either resulted in nonspecific decomposition or no reaction. These results were especially surprising when compared to the model system studied by Dr. Evan S. Krygowski (Scheme 2.4). The only difference, aside from the absolute stereochemistry, between the current system and the previous model system is the stereochemistry and substituent at C4 (pseudoaxial phenylsulfone vs. pseudoequatorial TBS ether). Interestingly, deuterium incorporation studies (KOD in THF) revealed 100% deuterium incorporation at C4a/C4a' of **150** and **151**.

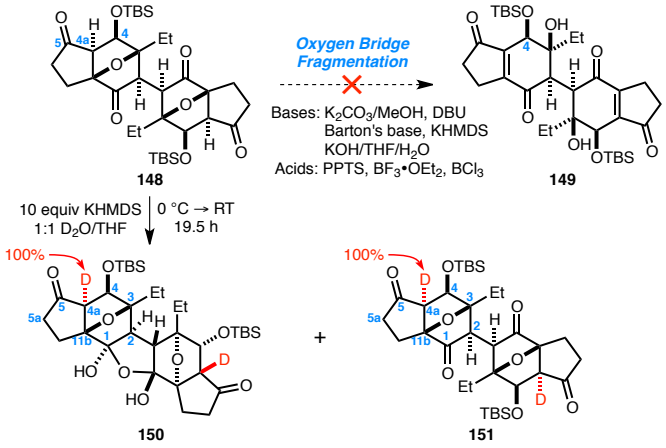

Scheme 2.26. Attempted oxygen bridge fragmentation.

Unlike the original successful model studies where the dimer contained a pseudoaxial C4-phenylsulfone (Scheme 2.4), we rationalized that fragmentation is disfavored due to a 1,3-allylic interaction (Scheme 2.27) between the enolate (C5–C4a) oxygen of **152** and the pseudoequatorial C4-TBS-ether that must occur during the transition state in order to achieve proper orbital overlap for fragmentation to occur. Unfortunately, moving to a sterically smaller protecting group (MOM) or even the free hydroxyl did not remedy this problem. In line with our hypothesis, we predicted that the C4-epimer of **148** would not suffer from an unfavorable 1,3-allylic-type interaction during oxygen bridge fragmentation. However, before we discuss a synthesis of the C4-epimer of **148**, other strategies we explored for β-eliminating the oxygen bridge in **148** will first be presented.

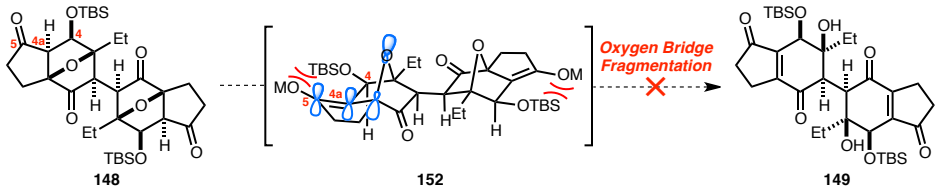

Scheme 2.27. Rationale for unsuccessful oxygen bridge fragmentation.

One strategy we considered was utilizing the electron-rich naphthalene system to facilitate oxygen bridge fragmentation (Scheme 2.28). This strategy was conceived prior to Dr. Hong Geun Lee's discovery that reduction of the B-ring quinone to the corresponding hydroquinone was extremely challenging (Scheme 2.12).

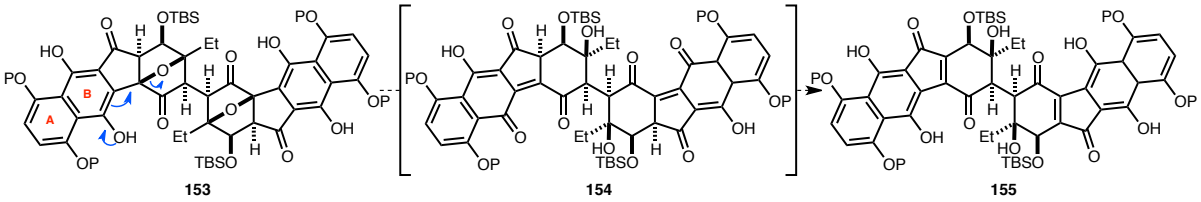

Scheme 2.28. Proposed oxygen bridge fragmentation via the electron-rich AB/A'B'-naphthalene systems.

To this end, 1,4-diketone dimer **148** was converted to bisenone **156** via formation of the bis-trimethylsilyl enol ether followed by Saegusa oxidation (Scheme 2.29). A double Hauser or Kraus annulation should then deliver hydroquinone dimer **158**. Several annulation donors were synthesized, including the cyanophthalide (**157**, X = CN), phenylsulfonylphthalide (**157**, X = SO_2Ph) and phenylsulfenylphthalide (**157**, X = SPh). Unfortunately, however, treatment of these annulation donors with base (e.g., *t*-BuOLi, LiHMDS), followed by addition of enone **156** under a variety of conditions, including the use of additives (e.g., $ZnCl_2$, HMPA), were unsuccessful.[51] We hypothesized that the C1- and C1'-ketones and the C2- and C2'-protons may not be compatible with

[51] We also attempted to stop the reaction at just the initial Michael addition, but this unfortunately also yielded complex product mixtures.

the basic reaction conditions and that the use of "neutral" annulation conditions may potentially circumvent this problem. We generated the corresponding siloxyisobenzofuran[52] intermediate in situ from **157** by treating **157** with base, followed by trapping with TMSCl. Unfortunately, addition of enone **156** to this intermediate also afforded a complex product mixture. We did not attempt bisannulation of the cyclic hydrate form of **156** because this would result in a product that is highly similar to the system extensively studied by Dr. Hong Geun Lee (**89**, Scheme 2.8), which did not undergo oxygen bridge fragmentation.

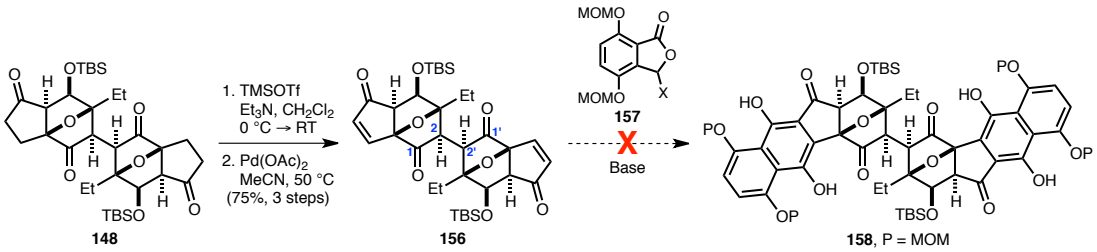

Scheme 2.29. Attempted bisannulation reactions to construct the naphthalene system.

We next turned our attention to reductively fragmenting the oxygen bridge from bisenone **156** and **159** (Scheme 2.30). Treatment of enone **156** or **159** with SmI_2 resulted in complete decomposition. No reaction was observed when **156** was treated with freshly activated Zn in AcOH,[53] even at high temperatures. Exposure of a derivative of cyclic hydrate **159**, where the hydroxyl groups were protected as the corresponding TMS ethers, to Birch reduction conditions (Li(0) or Na(0) in NH_3, THF, −78 °C) also resulted in decomposition.

---

[52] (a) Evans, J. C.; Klix, R. C.; Bach, R. D. *J. Org. Chem.* **1988**, *53*, 5519–5527. (b) Sutherland, H. S.; Souza, F. E. S.; Rodrigo, R. G. A. *J. Org. Chem.* **2001**, *66*, 3639–3641.

[53] Bao, G.; Liu, C.; Burnell, D. J. *J. Chem. Soc., Perkin Trans. 1* **2001**, 2657–2668.

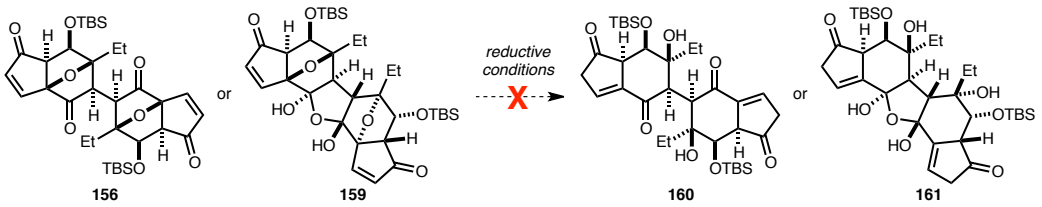

Scheme 2.30. Attempted reductive fragmentation of the oxygen bridge in bisenone **156** and **159**.

At this juncture, we decided to no longer pursue strategies for β-eliminating the oxygen bridge of **148**, **156**, and derivatives thereof. In summary, a highly efficient and scaleable route, featuring a "carboxy-inversion" sequence for installing the C4-oxygenation and an intramolecular *exo*-selective furan Diels–Alder reaction, to oxanorbornanone **144** was developed. Furthermore, a stereoselective oxidative dimerization of the enolate derived from **144** was achieved. Unfortunately, attempts to fragment the oxygen bridge to reveal the lomaiviticin core were unsuccessful.

The main obstacle preventing us from achieving a synthesis of the lomaiviticin core was β-elimination of the oxygen bridge. As discussed previously, we postulated that the C4-epimer of **148** would not suffer from the 1,3-allylic-type interaction during oxygen bridge fragmentation depicted in Scheme 2.27. Hence, we next turned our focus toward the development of a synthesis of the C4-epimer of **148**.

Synthesis of the C4-*Epi*-Lomaiviticin A and B Cores and Studies Toward the Aglycon

Due to our unsuccessful attempts to achieve β-elimination of the oxygen bridge in **148**, we decided to embark on a synthesis of the C4-epimer of **148**. Based on our previous observation that reagents approach from the convex face of the *cis*-5,5-fused system (Scheme 2.9, **92**), *anti* to the oxygen bridge, we believed that a Barton radical decarboxylation–oxidation reaction may afford the C4-epimer of **148**. To this end, the Barton ester was formed from carboxylic acid **139** by using *S*-(1-oxido-2-pyridinyl) 1,1,3,3-tetramethylthiouronium hexafluorophosphate (HOTT) (Scheme 2.31).[54] Upon complete formation of the Barton ester, the reaction was saturated with O_2 and $Sb(SPh)_3$ was added.[55] This one-pot protocol afforded alcohol **162** as a 2:1 mixture of diastereomers, favoring the desired epimer in 46% isolated yield. The HOTT reagent was very effective in facilitating the formation of hindered carboxylic acids, as was the case in **139**.[56] Use of the more conventional Barton radical decarboxylation–oxidation conditions (Barton ester formation, followed by exposure to O_2, *t*-BuSH, and a sunlamp, then reduction with PPh_3)[57] afforded the alcohol product in higher diastereoselectivity (4:1 dr) but in lower isolated yields of the desired diastereomer (37–40%). While the use of O_2 and $Sb(SPh)_3$ did not significantly improve the yield (46%), it permitted easier purification of the desired alcohol **162**.

Alcohol **162** was protected as the corresponding TBS-ether, affording oxanorbornanone **163**, the dimerization substrate. **163** underwent successful oxidative enolate dimerization to provide *exo-exo* dimer **164** exclusively. Benzyl ether cleavage and subsequent Parikh-Doering oxidation afforded

---

[54] Garner, P.; Anderson, J. T.; Dey, S. *J. Org. Chem.* **1998**, *63*, 5732–5733.

[55] (a) Barton, D. H. R.; Bridon, D.; Zard, S. Z. *Tetrahedron* **1989**, *45*, 2615–2626. (b) Zhu, J.; Klunder, A. J. H.; Zwanenburg, B. *Tetrahedron* **1995**, *51*, 5099–5116.

[56] We experienced difficulty in driving the Barton ester formation to completion via addition of the sodium salt of 2-mercaptopyridine *N*-oxide to the acid chloride derived from carboxylic acid **139**.

[57] Corey, E. J.; Hong, B. *J. Am. Chem. Soc.* **1994**, *116*, 3149–3150.

cyclic hydrate **166** in 47–57% yield over 3 steps. Due to the instability of dimeric intermediates **164** and **165** to silica gel column chromatography, purification could only be conducted on cyclic hydrate **166** after the 3-step sequence.[58] Optimization efforts to improve the yield beyond 57% were unsuccessful. Varying the concentration (0.07–0.16 M), varying the amount of HMPA used (0–5.0 equiv), purifying the $[Cp_2Fe]PF_6$, and carefully deoxygenating the THF solvent, were all investigated. The diminished yield likely reflected the instability of dimeric products **164** and **165**. With a successful synthesis of cyclic hydrate **166** completed, the key oxygen bridge fragmentation reaction was next investigated. Gratifyingly, a screen of basic conditions revealed that cyclic hydrate **166** underwent successful oxygen bridge fragmentation upon treatment with KOH in THF/H_2O at 0 °C, confirming our suspicion that the C4-stereocenter has far-reaching stereoelectronic effects.

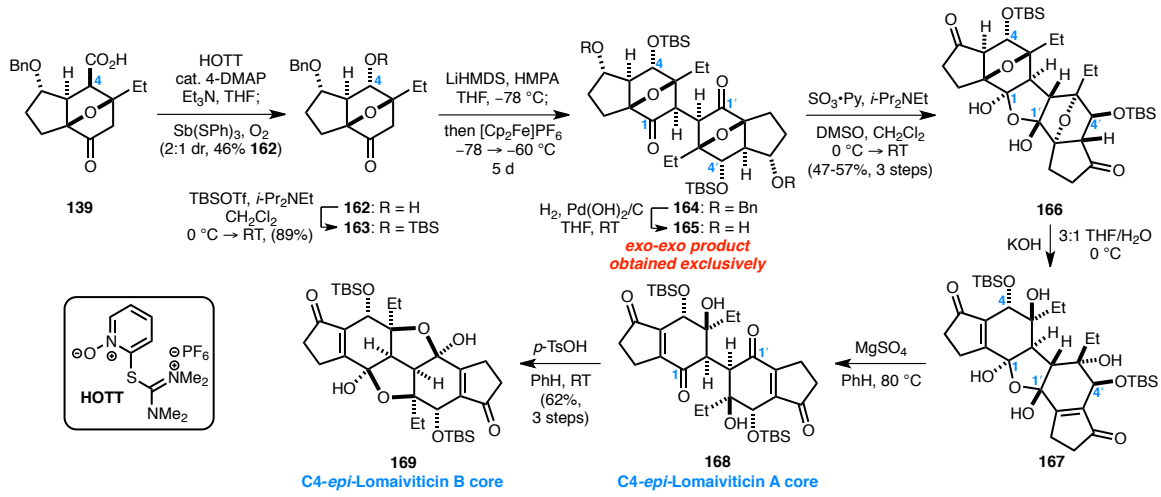

Scheme 2.31. Successful oxygen bridge fragmentation and conversion to C4-*epi*-lomaiviticin A (**168**) and B (**169**) cores.

[58] A very quick silica gel plug after the dimerization reaction to remove as much $[Cp_2Fe]PF_6$ and ferrocene byproduct as possible was conducted.

Bisenone product **167** was then converted to C4-*epi*-lomaiviticin B core **169** in two steps, involving (1) dehydration of cyclic hydrate **167** in the presence of $MgSO_4$[59] to yield C4-*epi*-lomaiviticin A core **168** and (2) stirring **168** with catalytic *p*-TsOH to provide C4-*epi*-lomaiviticin B core **169** (62%, 3 steps). The latter step required extensive optimization and use of various acidic (e.g., PPTS, CSA, $Sc(OTf)_3$, HCl, $MgBr_2 \bullet OEt_2$) and basic (e.g., K_2CO_3/MeOH, Et_3N, Barton's base) conditions resulted in either low conversion or decomposition. Some byproducts isolated appeared to be the result of D-ring aromatization. With a successful synthesis of lomaiviticin B core **169**, the stage was set for testing our key bisannulation strategy to install the AB/A'B'-naphthalene systems.

Despite the challenging aspects of double processing, our initial strategy was to pursue a cyclopentadienyl anion bisannulation (Scheme 2.32). We envisioned that a cyclopentadiene derivative (**170**) could be synthesized from **169**. Exposure of cyclopentadiene **170** to excess base should result in formation of the cyclopentadienyl anion dimer **172**, which upon treatment with two equivalents of an electrophilic phthalate derivative **171** should result in double addition to afford adduct **173** or **174**. A second nucleophilic addition of the anion to the remaining ester of the electrophile should then afford the desired hydroquinone dimer **175**. The closest literature precedence in support for such a transformation was a methodology developed by Birman and coworkers for the synthesis of benzofluorenes via an indanone dianion annulation,[39] which was applied to a synthesis of prekinamycin.

---

[59] In addition to serving as a dehydrating agent, $MgSO_4$ likely also facilitated the reaction by acting as a mild Lewis acid. Furthermore, Dr. Evan S. Krygowski attempted a very similar set of reaction conditions to dehydrate his model system **66** ($MgSO_4$, DCE, Scheme 2.4), but did not observe any desired product.

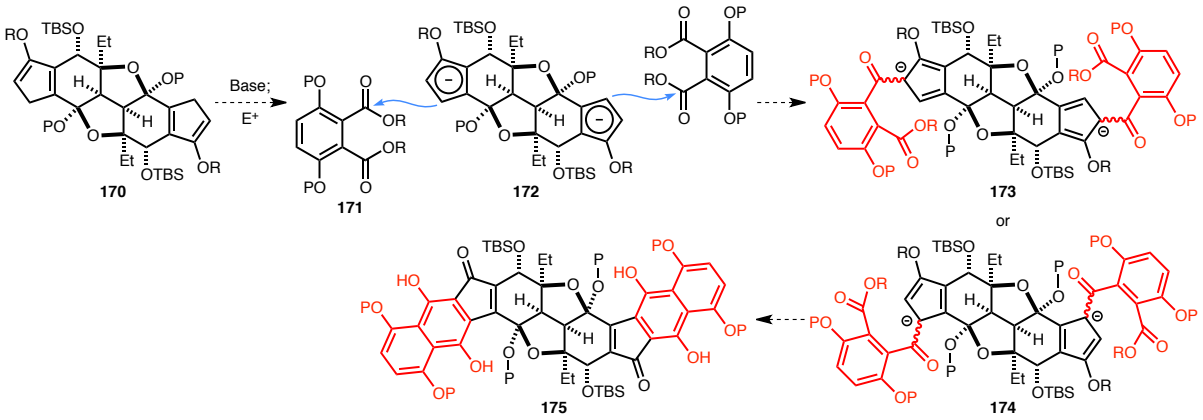

Scheme 2.32. Proposed cyclopentadienyl anion bisannulation strategy.

In preparation for our key annulation, lomaiviticin B core **169** was treated with TMSOTf and Et_3N (Scheme 2.33), which resulted in both silyl enol ether formation and protection of the bis-hemiketal core to furnish cyclopentadiene dimer **176**. In the event that **176** did not undergo cyclopentadienyl anion bisannulation, protected lomaiviticin B core **177** was synthesized from **169** by heating in neat TMSCN.

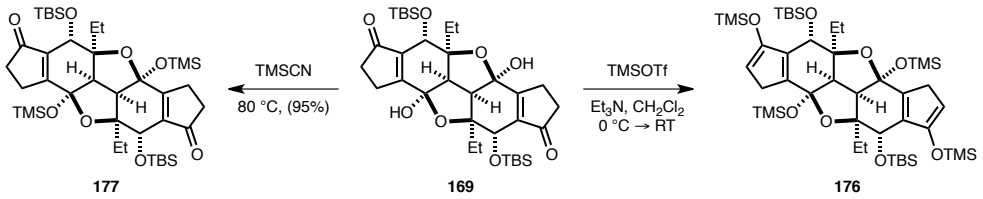

Scheme 2.33. Protection of the C4-*epi*-lomaiviticin B core **169**.

A variety of phthalate derivatives were synthesized (Figure 2.4) as potential annulation electrophiles. We originally anticipated that 2,2,2-trifluoroethanol (TFE) diester **179** would be the optimal electrophile for the bisannulation reaction, since it was most similar to the diester electrophile utilized in the indanone dianion annulation developed by Birman and coworkers.[39] A control experiment where **179** was utilized as the electrophile in the presence of the dianion generated from indanone was performed and complete conversion to the hydroquinone product was observed. In the event that **179** was not a sufficiently reactive electrophile due to electronic

deactivation of the esters by the electron-donating MOM-protected phenols on the aryl ring, we attempted to synthesize phthalate derivatives dialdehyde **184**, diacyl chloride **185**, and diacyl fluoride **186**. Unfortunately, however, dialdehyde **184** was prone to rapid polymerization and a synthesis of **185** and **186** was not realized due to insolubility problems encountered with the corresponding dicarboxylic acid precursor. Regardless, we believed TFE diester **179** was a promising electrophile with which to commence our cyclopentadienyl anion bisannulation studies.

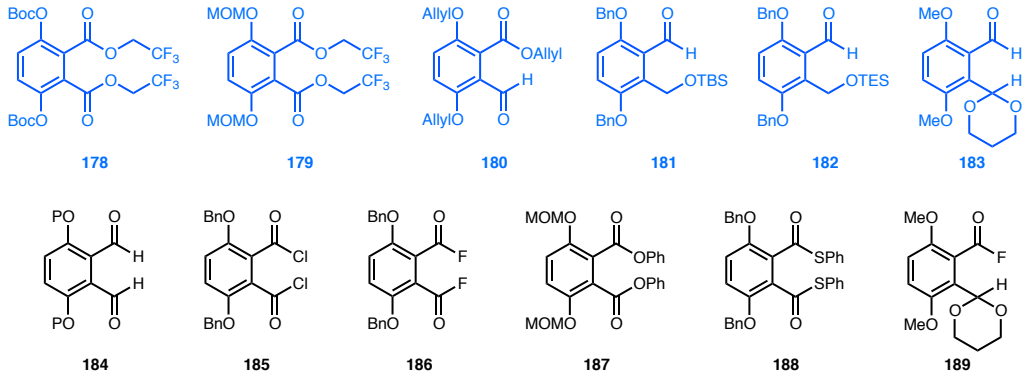

Figure 2.4. Successful (highlighted in blue) and attempted (in black) syntheses of annulation electrophiles.

The typical procedure employed involved premixing cyclopentadiene **176** and electrophile **179** (Scheme 2.34), followed by addition of base (e.g., KHMDS, LDA) and slow warming of the reaction to room temperature or higher (up to 50 °C). However, only unreacted starting material was recovered. Exposure of **177** to the described procedures also resulted in complete recovery of starting material. These results were not altogether surprising, as nucleophile **176** and **177** were extremely hindered and diester **179** was not very electrophilic. We rationalized that phthalate **178** (Figure 2.4), in which the phenol groups of the aryl ring are Boc-protected, would be a more reactive electrophile than **179**. Another electrophile we considered was **180**, where we believed initial cyclopentadienyl anion addition would occur on the aldehyde. Unfortunately, however, use of either electrophile **178** or **180** in the indanone annulation control system failed to produce any hydroquinone product.

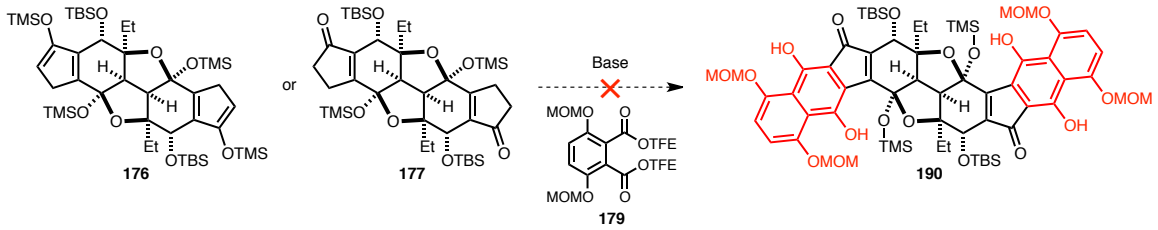

Scheme 2.34. Attempted cyclopentadienyl anion annulation to synthesize hydroquinone **190**.

Eventually, we discovered that deprotonation of cyclopentadiene **176**, followed by addition of aldehyde **183** (Scheme 2.35), afforded a mixture of monoaddition products, the regiochemistry of which were unverified, in low conversion. Efforts to obtain the double addition product and improve the conversion of the reaction proved unsuccessful. We suspected that the low conversion was due to incomplete deprotonation of **176**. However, warming of **176** with base (e.g., LiHMDS, LDA, LiTMP, *n*-BuLi) to higher temperatures resulted in decomposition of starting material.

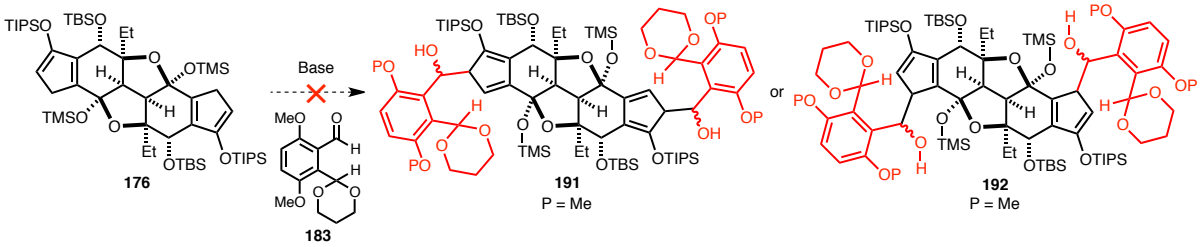

Scheme 2.35. Attempted cyclopentadienyl anion addition to aldehyde **183**.

We discovered that we could perform a double aldol reaction (Scheme 2.36) with the enolate dimer generated from **177** and either aldehyde **183** or **181**, furnishing the full carbon skeleton of the lomaiviticin aglycon (**193** and **194**). Next, we attempted to oxidize the newly generated β-hydroxy[60] groups in **193** and **194** to afford the corresponding 1,3-dicarbonyl function. Unfortunately, however, use of conventional oxidation conditions (e.g., Swern, DMP, Parikh-Doering) resulted in either decomposition or recovery of starting material. While we were excited at having finally obtained the

[60] The β-hydroxy groups were prone to β-elimination, especially under basic conditions.

full lomaiviticin aglycon carbon skeleton, it was difficult to envision a straightforward strategy for converting **193** or **194** to the desired hydroquinone **175**. Hence, we decided to embark on a new strategy where instead of utilizing **177** as the nucleophile, it would instead serve as the electrophilic component.

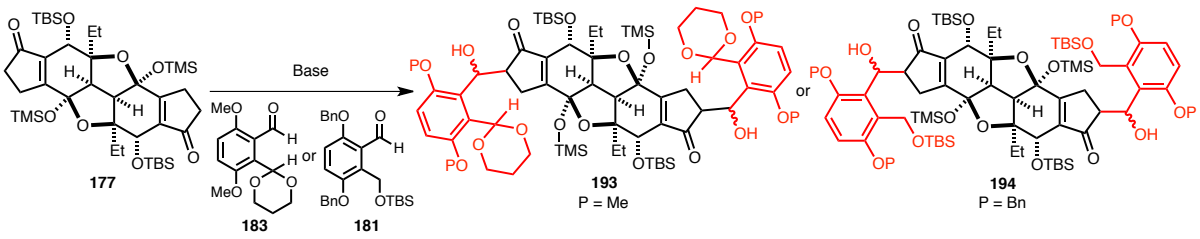

Scheme 2.36. Successful double aldol reaction to yield the full lomaiviticin aglycon carbon skeleton.

Due to their anti-aromatic nature, cyclopentadienones are highly reactive and tend to self-dimerize rapidly in a [4+2] pathway.[61,62] Although unprecedented, we hoped to exploit the reactivity of cyclopentadienones[63] to our advantage (**197**) by generating cyclopentadienone intermediate **197** in situ (Scheme 2.37) in the presence of a suitable nucleophile such as cyanophthalide anion **196** to immediately trap this reactive species, affording double Michael adduct **198**. A Claisen condensation, followed by elimination of cyanide and tautomerization, could then furnish desired hydroquinone dimer **200**. Furthermore, we hypothesized that since **197** was relatively hindered, it may be less prone to self-dimerization.

---

[61] For review, see: Ogliaruso, M. A.; Romanelli, M. G.; Becker, E. I. *Chem. Rev.* **1965**, *65*, 261–367.

[62] West, F. G.; Gunawardena, G. U. *J. Org. Chem.* **1993**, *58*, 5043–5044.

[63] For examples of 1,4-conjugate additions of Grignard reagents to cyclopentadienones, see: Pearson, A. J.; Kim, J. B. *Org. Lett.* **2003**, *5*, 2457–2459.

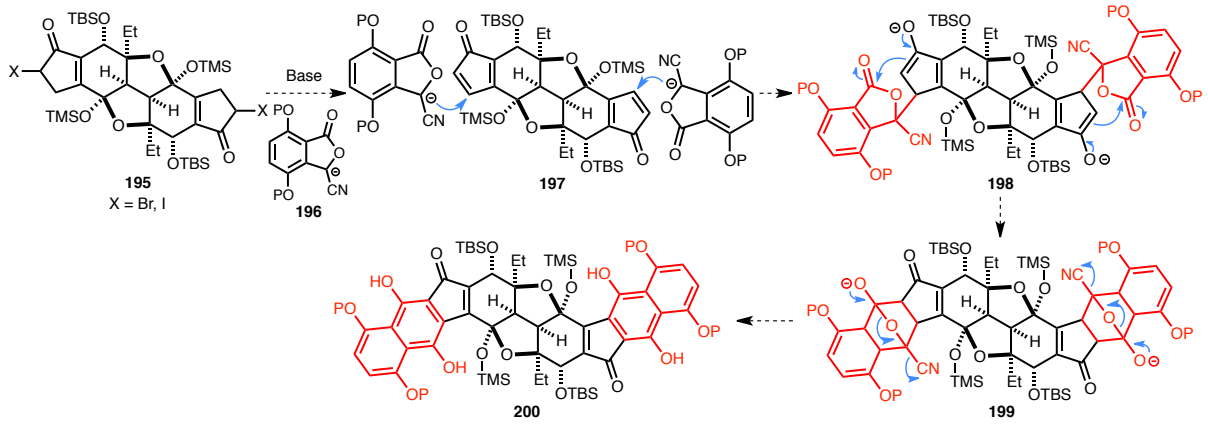

Scheme 2.37. Proposed cyclopentadienone bisannulation strategy.

To this end, several potential cyclopentadienone precursors were synthesized (Scheme 2.38). Treatment of cyclopentadiene **201** with NBS afforded α-bromide dimer **202** (Eq.1).[64] However, exposure of **202** to basic conditions resulted in only α-epimerization and no cyclopentadienone was observed. Next, we attempted to synthesize tetrabromide **204** from **177** by treatment with LiHMDS, followed by addition of NBS (Eq.2). Tetrabromide **204** was obtained only in minor quantities, with dibromide **203** being the major product. For reasons not entirely clear, efforts to drive the bromination reaction to completion were unsuccessful. Lastly, β-bromide dimer **205** was synthesized from **177** via a modified Wohl–Ziegler radical bromination with 1,3-dibromo-5,5-dimethylhydantoin (Eq.3). The major diastereomer obtained was unsymmetrical, an observation which will become important later (vide infra).

[64] Reaction was conducted on small-scale and yield was not determined.

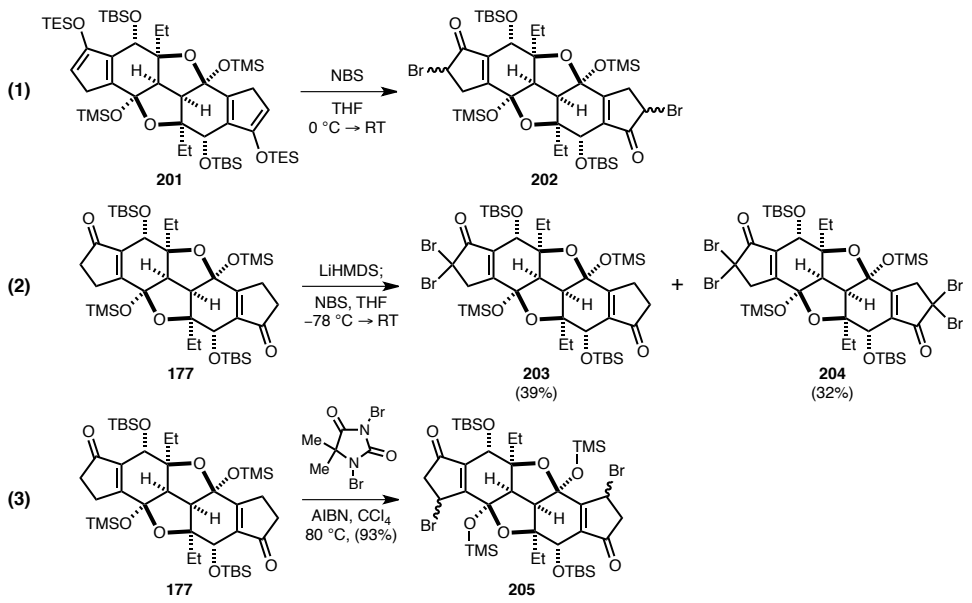

Scheme 2.38. Synthesis of several cyclopentadienone precursors.

For ease of analysis, a ^{1}H NMR experiment with dibromide **203** was conducted in order to determine whether a cyclopentadienone intermediate could be accessed from such a precursor (Scheme 2.39). Addition of DBU to dibromide **203** in CD_2Cl_2 resulted in formation of putative cyclopentadienone intermediate **206**, with the diagnostic cyclopentadienone proton at δ = 7.00 ppm.

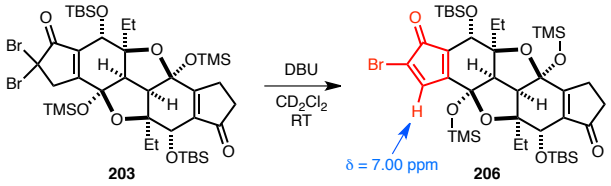

Scheme 2.39. Observation of cyclopentadienone intermediate in ^{1}H NMR experiment.

Encouraged by this result, but with only very limited quantities of tetrabromide **204** in hand, we decided to explore a Diels–Alder reaction of a suitable diene with the cyclopentadienone intermediate generated from **204** (Scheme 2.40), since cyclopentadienones are often utilized in the

literature[65] in Diels–Alder reactions. Although unprecedented, we decided to add tetrabromide **204** to the siloxyisobenzofuran generated from phthalide **207**[66] in the presence of DBU. All starting material was consumed and a new compound, where no nucleophile had been incorporated, was isolated. Unfortunately, we were unable to determine the structure of this new compound,[67] which was no longer C_2-symmetric and appeared to have undergone a skeletal rearrangement. The decision was made that pursuing this strategy was ultimately impractical due to the low yield and lack of scaleability in the synthesis of tetrabromide **204**.

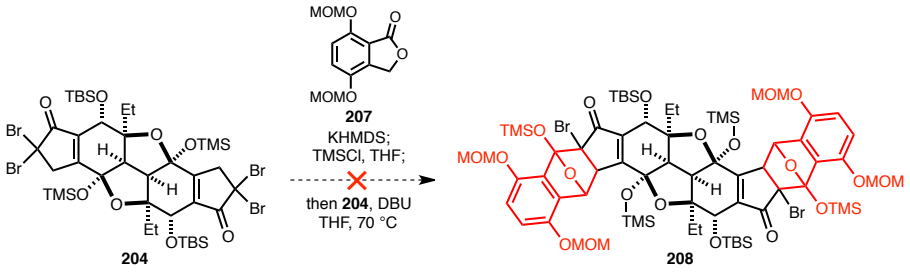

Scheme 2.40. Attempted cyclopentadienone annulation to access double Diels–Alder adduct **208**.

Next, we investigated generation of cyclopentadienone from β-bromide dimer **205** (Scheme 2.41). Cyanophthalide anion was preformed by stirring 15.0 equivalents of cyanophthalide **209** with 17.0 equivalents of LiHMDS (note two equivalents excess base). β-bromide dimer **205** was subsequently added, under the hypothesis that the two extra equivalents of LiHMDS would generate the corresponding cyclopentadienone intermediate in situ. Unfortunately, a new compound, no longer C_2-symmetric, was isolated. No nucleophile was incorporated and once again, the molecule appeared to have undergone a skeletal rearrangement. It became apparent that a common observation

---

[65] (a) Harmata, M.; Gomes, M. G. *Eur. J. Org. Chem.* **2006**, 2273–2277. (b) Ranier, J. D.; Imbriglio, J. E. *Org. Lett.* **1999**, *1*, 2037–2039.

[66] Myers, A. G.; Tom, N. J.; Fraley, M. K.; Cohen, S. B.; Madar, D. J. *J. Am. Chem. Soc.* **1997**, *119*, 6072–6094.

[67] This new compound was not the result of self-dimerization.

was that when excess base was used in an attempt to generate the cyclopentadienone intermediate, the molecule would undergo a skeletal rearrangement without incorporation of nucleophile (see also Scheme 2.40). In consideration of this observation, another experiment in which cyanophthalide anion was preformed by stirring 12.0 equivalents of **209** with 11.8 equivalents of LiHMDS was conducted. Gratifyingly, monoadduct **230** was isolated in 45% yield and no rearranged byproducts were observed.

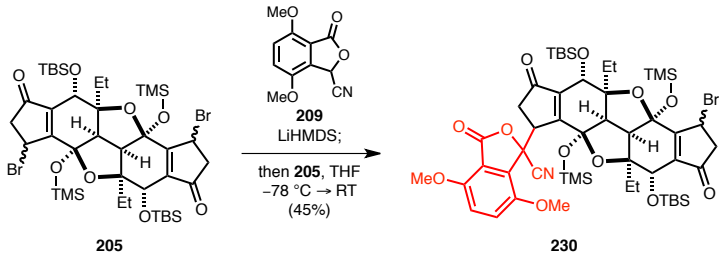

Scheme 2.41. Attempted cyclopentadienone bisannulation with cyanophthalide **209**.

Efforts to obtain the corresponding double addition product by resubjecting monoadduct **230** to the reaction conditions and using more polar solvents (e.g., DMF) and various additives (e.g., TBAI) were unsuccessful.[68] When DBU was used as an additive to discretely generate the cyclopentadienone from monoadduct **230**, a new compound was isolated in which a second equivalent of nucleophile was not incorporated and the molecule appeared to have undergone a skeletal rearrangement, in line with our previous observations when excess base was used. We hypothesized that under the given reaction conditions, it was unlikely that the cyclopentadienone intermediate was generated, since the cyanophthalide anion is not very basic (pK_a ~14). Rather, we believed that monoadduct **230** was the result of S_N2 displacement of the allylic bromide in **205** by the cyanophthalide anion. This notion appeared to be supported by two observations: (1) when DBU was used to discretely generate the cyclopentadienone intermediate, no nucleophile was incorporated

[68] Cyanophthalide anion was not stable under these conditions and rapidly decomposed.

and (2) only the monoaddition product was obtained. Recall the aforementioned observation that the major diastereomer of **205** was unsymmetrical. The shape of the lomaiviticin core exists in the form of a deep bowl, indicating that in the unsymmetrical β-bromide dimer **205**, one bromide is on the convex face and one bromide is on the concave face. If the formation of **230** occurs via an S_N2 mechanism, only the concave bromide could be displaced via convex approach of the cyanophthalide anion. Displacement of the convex bromide would require concave approach by the nucleophile, which is highly disfavored, resulting in the isolation of only monoadduct **230**. Predicated on the aforementioned hypothesis, we attempted to displace the allylic bromide in **230** with NaI and KI but without success. At this point, we decided to revise our strategy for introducing the AB/A'B'-naphthalene systems.

One of the main challenges involved in constructing the naphthalene system is the presence of the C5–C6 and C5'–C6' internal double bonds in **177** (Scheme 2.42, highlighted in red), which prevented us from employing conventional Hauser, Kraus, and related annulations. We therefore next planned on reductively removing the C5–C6 and C5'–C6' double bonds in **177** and subsequently oxidizing the resultant ketone **231** to enone **232**, the desired annulation substrate. Unfortunately, **177** was completely inert to the hydrogenation conditions we screened (H_2, from 1 to 20 atm, and Pd/C, PtO_2, Rh/C, and Crabtree's catalyst). These results were not surprising, as the internal double bonds in **177** are extremely hindered.

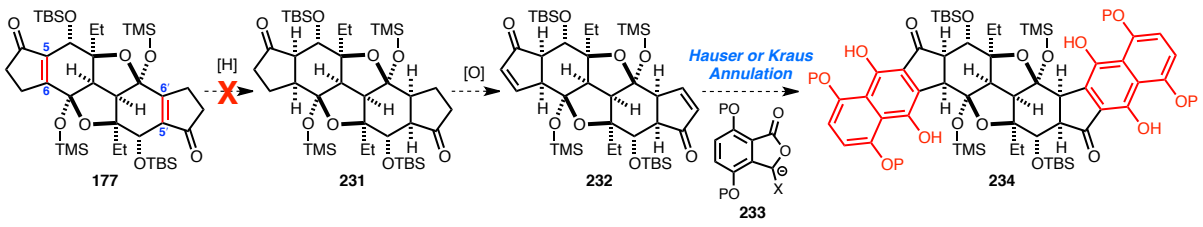

Scheme 2.42. Attempted reductive removal of the C5–C6 and C5'–C6' internal double bonds in **177**.

Interestingly, exposure of **177** to Birch reduction conditions cleanly afforded ketone **235** (Scheme 2.43), the result of C5–C6 (or C5'–C6') enone reduction followed by intramolecular 1,4-

conjugate addition of the resultant anion at the C6 (or C6') position to the C5'–C6' (or C5–C6) enone on the other half of the molecule. Closer examination of a 3D hand-held molecular model of **177** revealed that C6 and C6' are in very close proximity due to the bowl-shaped structure of the lomaiviticin B core **177**. While disappointing, this result further highlighted the unique reactivity of the lomaiviticin system.

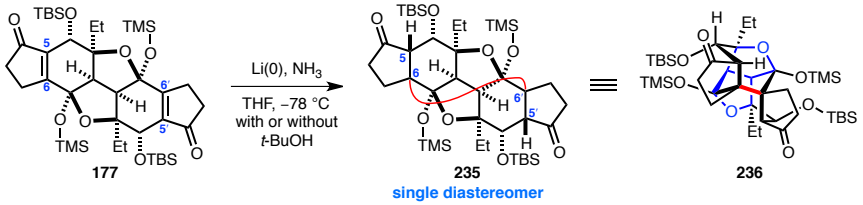

Scheme 2.43. Birch reduction of **177**.

Due to our unsuccessful attempts to reductively remove the C5–C6 and C5'–C6' double bonds, we next focused our attention on introducing nucleophiles to the C6 and C6' positions of **177** or **169** via 1,4-conjugate addition to the enone. However, our endeavors to add nucleophiles such as Et_2AlCN, Stryker's reagent, TBHP, PhSH, and EtSH under a variety of conditions resulted in no reaction. Eventually, we discovered that **169** underwent double nucleophilic epoxidation when treated with H_2O_2 and NaOH, providing bisepoxide **237** (Scheme 2.44). The bis-hemiketal core was protected as the TMS ethers, providing diketone substrate **238**. For reasons not entirely clear, attempts to oxidize bisepoxide **238**, including Saegusa oxidation of the corresponding TMS enol ether of **238** and α-selenation-elimination of the ketone in **238**, to enone dimer **239** were unsuccessful.

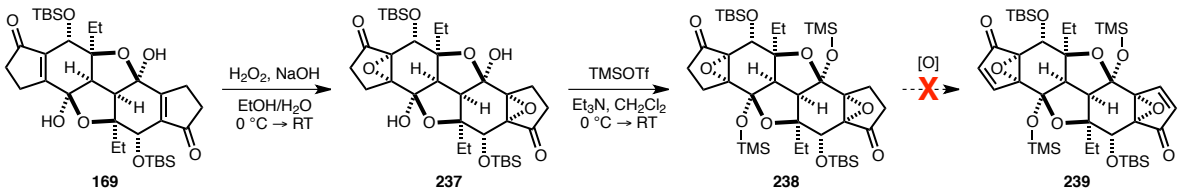

Scheme 2.44. Synthesis of bisepoxide **237** via a double nucleophilic epoxidation.

At this point, a reevaluation of our strategy was necessary. Based on our unsuccessful bisannulation studies, it was evident that a new approach to installing the AB/A'B'-naphthalene systems was required. From our investigation, it was apparent that the main challenge was forming the C11a–C11 and C11a'–C11' bonds after β-elimination of the oxygen bridge. Thus, in our revised strategy we envisioned preforming the C11a–C11 and C11a'–C11' bonds *prior* to the dimerization event (Scheme 2.45). Not only does this minimize double processing, but also provides a handle for introduction of the naphthalene system after oxygen bridge fragmentation.

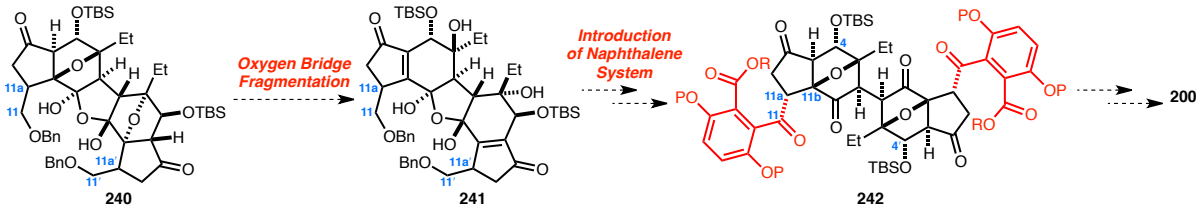

Scheme 2.45. Revised strategy involving preforming the C11a–C11 and C11a'–C11' bonds *prior* to the dimerization event.

In order to address the pressing question of whether a system such as oxanorbornanone **240** can undergo oxygen bridge fragmentation with a pendant substituent at C11a, enone **246** was synthesized from oxanorbonanone **163** in a few straightforward steps (Scheme 2.46). Reduction of ketone **163** with $NaBH_4$, followed by pivaloyl protection of the resultant secondary hydroxyl group, afforded pivaloyl ester **244**. Hydrogenolysis of the benzyl ether group and subsequent Parikh-Doering oxidation of the secondary carbinol provided ketone **245**. Saegusa oxidation of the TMS enol ether of **245** afforded enone **246**. Transmetallation of the (α-benzyloxymethyl)stannane **247** upon treatment with *n*-butyllithium, followed by addition of CuBr•SMe_2, resulted in formation of the corresponding ((benzyloxy)methyl)copper reagent. [69] Exposure of enone **246** to this

---

[69] (a) Hutchinson, D. K.; Fuchs, P. L. *J. Am. Chem. Soc.* **1987**, *109*, 4930–4939. (b) Yamamoto, Y.; Maruyama, K. *J. Am. Chem. Soc.* **1978**, *100*, 3240–3241.

((benzyloxy)methyl)copper reagent, followed by addition of BF_3•OEt_2, resulted in successful 1,4-conjugate addition to afford adduct **248** as a single diastereomer.

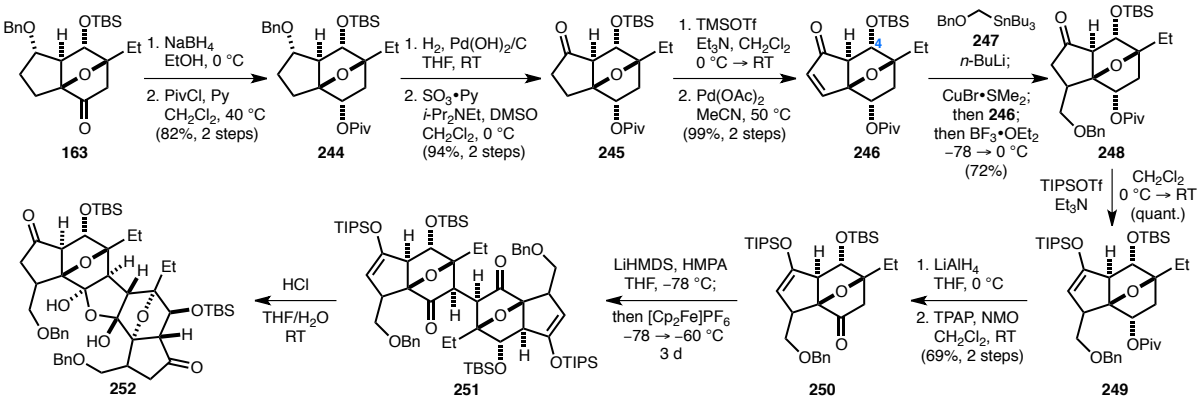

Scheme 2.46. Synthesis of oxygen bridge fragmentation substrate **252**.

Formation of the TIPS enol ether of **248**, reductive cleavage of the pivaloyl ester with $LiAlH_4$, and oxidation of the resultant secondary carbinol with TPAP and NMO yielded the desired dimerization substrate **250**. Exposure of monomer **250** to the optimal oxidative enolate dimerization conditions developed in our lab yielded dimer **251**.[70] Cleavage of the TIPS enol ether groups then cleanly afforded cyclic hydrate **252**.

The key oxygen bridge fragmentation reaction was next tested (Scheme 2.47). Quite surprisingly, exposure of cyclic hydrate **252** to the optimal β-elimination conditions (KOH, THF/H_2O) discovered earlier for a highly similar substrate (**166**), resulted in nonspecific decomposition. The only difference between **252** and **166**, which underwent successful oxygen bridge fragmentation, was the presence of a substituent at C11a and C11a'. Disappointingly, this result further highlighted the idiosyncratic nature of the oxanorbornanone system and the highly case-dependent success of β-elimination of the oxygen bridge.

---

[70] Due to the small-scale nature of the dimerization reaction, an accurate yield was not determined.

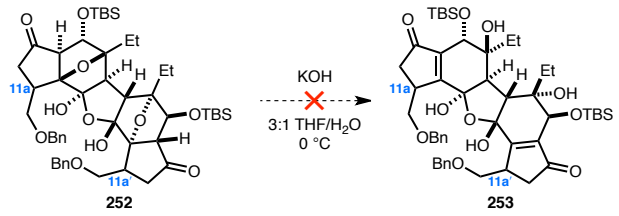

Scheme 2.47. Unsuccessful oxygen bridge fragmentation of cyclic hydrate **252**.

At this point, one last strategy involving an intermediate synthesized by Jae Young Ahn from the original model system was investigated (Scheme 2.48). Due to readily accessible material and the highly successful oxygen bridge fragmentation of **64** in Dr. Evan S. Krygowski's model system, we decided to explore the possibility of whether **257**, in which the C11–C11a bond was preformed, could undergo β-elimination of the oxygen bridge. Although downstream manipulations would be necessary in order to construct the B- and B'-ring systems in the correct oxidation state, we believed this strategy was superior to that illustrated in Scheme 2.45 because the aryl ring has already been introduced, obviating the need to install the naphthalene system *de novo* via late-stage double-processing.

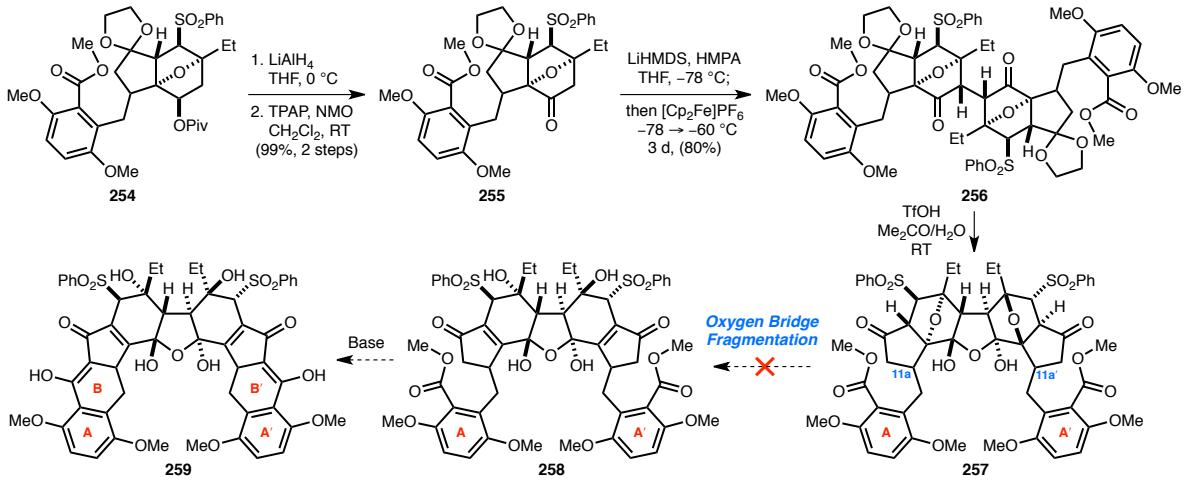

Scheme 2.48. Unsuccessful oxygen bridge fragmentation of cyclic hydrate **257**.

Reductive cleavage of the pivaloyl ester of **254**[71] and subsequent Ley oxidation of the resultant secondary carbinol afforded ketone **255**, the dimerization precursor. Oxanorbornanone **255** underwent successful oxidative enolate dimerization to furnish dimer **256**, which contained the full carbon skeleton of the lomaiviticin aglycon, in 80% yield. Ketal cleavage occurred smoothly upon exposure of **256** to TfOH in acetone/H_2O to provide cyclic hydrate **257**. Treatment of **257** with a variety of basic conditions (KOH/THF/H_2O, DBU/THF, K_2CO_3/MeOH) in an attempt to fragment the oxygen bridge resulted in nonspecific decomposition of **257**. These results were quite unexpected, given the highly successful oxygen bridge β-elimination (85%) of **64** to **65** (Scheme 2.4) in Dr. Evan Krygowski's original model system.

Due to the highly unpredictable and extremely case-dependent nature of β-elimination of the oxygen bridge, coupled with the lack of success in introducing the AB/A'B'-naphthalene systems, the difficult decision was made to cease pursuing a synthesis of the lomaiviticin aglycon. Although we successfully achieved a synthesis of the lomaiviticin core, which necessitated oxygen bridge fragmentation prior to installation of the naphthalene system, we were forced to utilize exotic and unprecedented bisannulation strategies, which not only involved challenging double-processing but were ultimately unsuccessful. Furthermore, installation of functionality at C11a and C11a' pre-dimerization, which would help enable subsequent introduction of the naphthalene ring systems after β-elimination of the oxygen bridge, again prevented oxygen bridge fragmentation. In fact, β-elimination could only be achieved in substrates containing the unnatural C4/C4'-stereochemistry and which lacked the C11a/C11a' substitution. Two important take-home lessons were realized from working on the lomaiviticin project: (1) the success of model systems rarely translate to the real system in a complex molecule setting and (2) double-processing is extremely challenging and when possible, should be avoided.

---

[71] Courtesy of Jae Young Ahn. **254** was synthesized from intermediate **71**.

Concluding Remarks

In conclusion, a synthesis of the C4-*epi*-lomaiviticin A and B cores was accomplished. A first-generation synthetic route featuring an intramolecular *exo*-selective furan Diels–Alder reaction to construct the oxanorbornanone system, a "carboxy-inversion" sequence for installing the correct C4-stereochemistry, and a stereoselective oxidative enolate dimerization reaction to establish the key C2–C2' bond, allowed us to access an oxygen bridge fragmentation precursor substrate. However, the discovery of subtle stereoelectronic effects imparted by the C4/C4'-stereocenters necessitated a second-generation synthesis of a substrate with the opposite C4-stereochemistry to that found in the natural product, which ultimately resulted in successful β-elimination of the oxygen bridge, an accomplishment which had eluded our lab for more than four years. This constituted the first time a synthesis of the lomaiviticin A and B cores had been achieved in our lab since we first began pursuing a total synthesis of the lomaiviticin aglycon more than ten years ago.

Unfortunately, efforts to elaborate the lomaiviticin B core to the full carbon skeleton of the lomaiviticin aglycon proved extremely challenging and were ultimately unsuccessful. Because the success of oxygen bridge β-elimination hinged on fragmenting the oxygen bridge *prior* to installation of the naphthalenes, we were forced to explore unprecedented bisannulation strategies. A variety of approaches for introducing the naphthalene ring systems were pursued, including a cyclopentadienyl anion bisannulation, double aldol reaction, and cyclopentadienone bisannulation. Introduction of a handle in order to simplify installation of the naphthalene system after oxygen bridge fragmentation was also investigated. All of the strategies investigated, which involved challenging late-stage double-processing, ultimately did not provide the desired hydroquinone dimer product.

At this stage in the lomaiviticin project, the difficult decision was made to no longer pursue a total synthesis of the lomaiviticin aglycon due to the highly unpredictable and idiosyncratic oxygen bridge fragmentation and inability to introduce the AB/A'B'-naphthalene ring systems. In retrospect,

the oxanorbornanone system was an elegant strategy for stereoselectively establishing the key C2–C2' central bond without undesired β-elimination of the oxygen bridge during the dimerization event. However, unexpected downstream complications were encountered when attempting to fragment the oxygen bridge at the appropriate time. In most systems investigated by our lab during the course of the past four years, we were unable to β-eliminate the oxygen bridge.

However, we are still optimistic that a successful synthesis of the aglycon can be achieved with our oxanorbornanone dimerization strategy from the knowledge we have obtained from our combined synthetic effort during the past ten years. We believe that the challenges associated with β-elimination of the oxygen bridge arise from the 5-membered C-ring (see **1**, Figure 1.1), which significantly restricts the conformational flexibility of the oxanorbornanone system. We speculate, however, that if the C5a–C11a bond was not preformed prior to β-elimination of the oxygen bridge, we could potentially overcome the challenges we encountered and achieve a synthesis of the aglycon.

Experimental Section

General Procedures. All reactions were performed in flame-dried glassware under a positive pressure of argon unless otherwise noted. Flash column chromatography was performed as described by Still et al. employing silica gel 60 (40-63 μm, Whatman).[72] Analytical thin-layer chromatography (TLC) was performed using 0.25 mm silica gel 60 F_{254} plates purchased from EMD Chemicals. Where necessary (so noted), silica gel was neutralized by treatment of the silica gel prior to chromatography with the eluent containing triethylamine (Et_3N) or 30% (w/v) ammonium hydroxide (NH_4OH). TLC plates were visualized by exposure to ultraviolet light (UV) and/or exposure to an acidic solution of *p*-anisaldehyde (Anis) or an aqueous solution of potassium permanganate ($KMnO_4$), followed by heating on a hot plate.

Materials. Commercial reagents and solvents were used as received with the following exceptions: tetrahydrofuran (THF), diethyl ether (Et_2O), dichloromethane (CH_2Cl_2), acetonitrile (MeCN), hexamethyldisilazane (HMDS), toluene (PhMe), benzene (PhH), and *N,N*-dimethylformamide (DMF) were degassed with argon and passed through a solvent purification system (designed by J. C. Meyer of Glass Contour) utilizing alumina columns as described by Grubbs et al.[73] Triethylamine, diisopropylethylamine, pyridine, and hexamethylphosphoramide were distilled over calcium hydride before use. TMSOTf was also distilled prior to use. The celite used was Celite® 545, purchased from J.T. Baker. The molarities of *n*-butyllithium solutions were determined by titration using 1,10-phenanthroline as an indicator (average of three determinations).

Instrumentation. ^1H NMR spectra were recorded with a Varian INOVA-600 or Varian

---

[72] Still, W. C.; Kahn, M.; Mitra, A. *J. Org. Chem.* **1978**, *43*, 2923–2925.

[73] Pangborn, A. B.; Giardello, M. A.; Grubbs, R. H.; Rosen, R. K.; Timmers, F. J. *Organometallics* **1996**, *15*, 1518–1520.

INOVA-500 spectrometer. Proton chemical shifts are reported in parts per million (δ scale) and are calibrated using residual undeuterated solvent as an internal reference ($CDCl_3$: δ 7.26 ($CHCl_3$), C_6D_6: δ 7.15 (C_6D_5H)). Data for ^1H NMR spectra are reported as follows: chemical shift (δ ppm) (multiplicity, coupling constant (Hz), integration). Multiplicities are reported as follows: s = singlet, d = doublet, t = triplet, q = quartet, m = multiplet, br = broad, app = apparent, or combinations thereof. ^{13}C NMR spectra were recorded with a Varian INOVA-500 spectrometer. Carbon chemical shifts are reported in parts per million (δ scale) and are referenced from the carbon resonances of the solvent ($CDCl_3$: δ 77.00, C_6D_6: δ 128.39). Infrared (FTIR) spectra were recorded on a Bruker Alpha FT-IR spectrophotometer referenced to a polystyrene standard. FTIR data is reported in frequency of absorption (cm^{-1}). High-resolution mass spectra (HRMS) were obtained from the Harvard University Mass Spectrometry Laboratory where electrospray ionization (ESI) mass spectroscopy (MS) experiments were performed on an Agilent 6210 TOF LC/MS instrument. Optical rotations were measured on a Jasco P-2000 digital polarimeter with a sodium lamp. Reported readings are the average of three measurements for each sample.

*(For clarity, intermediates that have not been assigned numbers in the text are numbered sequentially in the experimental section beginning with **S1**).*

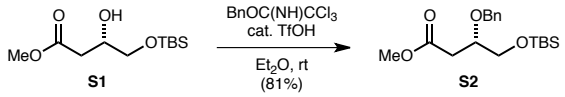

(*S*)-Methyl 3-benzyloxy-4-(*tert*-butyl)dimethylsilyloxybutanoate (S2):

To a round-bottom flask was added (*S*)-Methyl 4-[(*tert*-butyl)dimethylsilyloxy]-3-hydroxybutanoate (**S1**)[74] (1.00 g, 4.03 mmol, 1.00 equiv) and Et_2O (40 mL). Benzyl 2,2,2-trichloroacetimidate (1.12 mL, 6.04 mmol, 1.50 equiv) was then added via syringe and the solution was cooled to 0 °C. Catalytic trifluoromethanesulfonic acid (18.0 μL, 0.201 mmol, 0.05 equiv) was then added dropwise via syringe to the reaction mixture. Vigorous bubbling was observed. After 30 min, the reaction was allowed to warm to room temperature. After an additional 20 h, saturated aqueous $NaHCO_3$ solution (30 mL) and Et_2O (30 mL) were added to the stirred reaction mixture. The layers were separated and the organic layer was washed with brine. The aqueous layers were combined and further extracted with Et_2O (3 × 30 mL). The organic layers were combined, dried over anhydrous $MgSO_4$, and concentrated under reduced pressure. The resulting oil was then purified by flash column chromatography (silica gel, eluent: gradient, 12:1 → 7:1 hexanes:EtOAc) to afford (*S*)-methyl 3-benzyloxy-4-(*tert*-butyl)dimethylsilyloxybutanoate **S2** (1.10 g, 81%) as a colorless oil.

^{1}H NMR (500 MHz, $CDCl_3$) δ: 7.35–7.30 (m, 4H), 7.29–7.27 (m, 1H), 4.66 (d, *J* = 11.7 Hz, 1H), 4.61 (d, *J* = 11.7 Hz, 1H), 4.01–3.93 (m, 1H), 3.72 (dd, *J* = 5.4, 10.3 Hz, 1H), 3.67 (s, 3H), 3.59 (dd, *J* = 6.0, 10.4 Hz, 1H), 2.64 (dd, *J* = 5.1, 15.9 Hz, 1H), 2.53 (dd, *J* = 8.3, 15.6 Hz, 1H), 0.89 (s, 9H), 0.05 (s, 6 H). **^{13}C NMR** (126 MHz, $CDCl_3$) δ: 172.1, 138.5, 128.3, 127.8, 127.6, 76.7, 72.6, 64.7, 51.6, 37.3, 25.9, 18.3, –5.4, –5.5. **FTIR** (thin film) cm^{-1}: 2953, 2928, 2857, 1741, 1437, 1254, 1113, 1086, 836, 778. **HRMS** (ESI) (*m/z*) calc'd for $C_{18}H_{30}NaO_4Si$ $[M+Na]^+$: 361.1806, found 361.1815. **TLC** (4:1 hexanes:EtOAc), R_f: 0.63 (UV, $KMnO_4$).

---

[74] (a) Szpilman, A. M.; Cereghetti, D. M.; Wurtz, N. R.; Manthorpe, J. M.; Carreira, E. M. *Angew. Chem. Int. Ed.* **2008**, *47*, 4335-4338. (b) Gaunt, M. J.; Jessiman, A. S.; Orsini, P.; Tanner, H. R.; Hook, D. F.; Ley, S. *Org. Lett.* **2003**, *5*, 4819-4822.

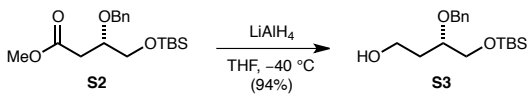

(*S*)-3-Benzyloxy-4-(*tert*-butyl)dimethylsilyloxybutan-1-ol (S3):

A suspension of $LiAlH_4$ (2.36 g, 59.0 mmol, 1.10 equiv) in THF (170 mL) was cooled to –40 °C. A solution of (*S*)-methyl 3-benzyloxy-4-(*tert*-butyl)dimethylsilyloxybutanoate **S2** (18.2 g, 53.6 mmol, 1.00 equiv) in THF (240 mL) was then added dropwise via syringe to the stirred suspension. After 40 min, a saturated aqueous NH_4Cl solution (250 mL) and EtOAc (200 mL) were added to the reaction mixture. The layers were separated and the aqueous layer was extracted with EtOAc (3 × 150 mL). The organic layers were combined, washed with brine (200 mL), dried over anhydrous $MgSO_4$, and concentrated under reduced pressure. The resulting oil was then purified by flash column chromatography (silica gel plug, eluent: 2:1 hexanes:EtOAc) to afford alcohol **S3** (15.6 g, 94%) as a colorless oil.

^{1}H NMR (500 MHz, $CDCl_3$) δ: 7.39–7.32 (m, 4H), 7.32–7.27 (m, 1H), 4.73 (d, *J* = 11.7 Hz, 1H), 4.59 (d, *J* = 11.7 Hz, 1H), 3.81–3.71 (m, 3H), 3.71–3.63 (m, 2H), 2.46 (t, *J* = 5.6 Hz, 1H), 1.92–1.71 (m, 2H), 0.91 (s, 9H), 0.07 (s, 6H). **^{13}C NMR** (126 MHz, $CDCl_3$) δ: 138.4, 128.4, 127.8, 127.7, 78.9, 72.2, 65.4, 60.3, 34.4, 25.9, 18.2, –5.4, –5.5. **FTIR** (thin film) cm^{-1}: 3403, 2954, 2928, 2857, 1472, 1255, 1091, 836, 776, 697. **HRMS** (ESI) (*m/z*) calc'd for $C_{17}H_{30}NaO_3Si$ $[M+Na]^+$: 333.1856, found 333.1858. **TLC** (2:1 hexanes:EtOAc), R_f: 0.57 ($KMnO_4$).

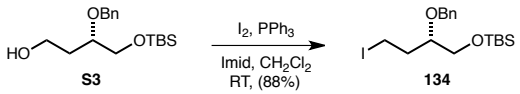

Iodide 134:

Triphenylphosphine (4.69 g, 17.7 mmol, 1.10 equiv) and iodine (5.32 g, 20.9 mmol, 1.30 equiv) were added sequentially in single portions to a stirred solution of imidazole (1.66 g, 24.2 mmol, 1.50 equiv) in CH_2Cl_2 (35 mL). After 20 min, a solution of alcohol **S3** (5.00 g, 16.1 mmol, 1.00 equiv) in CH_2Cl_2 (35 mL) was added dropwise via cannula to the reaction mixture. After 1 h, saturated aqueous Na_2SO_3 solution (50 mL) and EtOAc (20 mL) were sequentially added to the reaction. The layers were separated and the aqueous layer was extracted with EtOAc (3 × 50 mL). The organic layers were combined, washed with brine (50 mL), dried over anhydrous $MgSO_4$, and concentrated under reduced pressure. The residue was dissolved in Et_2O and triphenylphosphine oxide precipitated upon standing. The suspension was then filtered through a thin pad of silica gel and all volatiles were removed *in vacuo*. The resulting oil was then purified by flash column chromatography (silica gel, eluent: gradient, 20:1 → 15:1 hexanes:EtOAc) to afford iodide **134** (5.93 g, 88%) as a colorless oil.

^{1}H NMR (600 MHz, $CDCl_3$) δ: 7.40–7.32 (m, 4H), 7.32–7.27 (m, 1H), 4.74 (d, J = 11.4 Hz, 1H), 4.58 (d, J = 11.4 Hz, 1H), 3.72 (q, J = 5.3 Hz, 1H), 3.64–3.56 (m, 2H), 3.34–3.25 (m, 2H), 2.14–1.94 (m, 2H), 0.91 (s, 9H), 0.06 (s, 6H). **^{13}C NMR** (126 MHz, $CDCl_3$) δ: 138.6, 128.4, 127.9, 127.7, 79.5, 72.7, 64.9, 36.1, 25.9, 18.3, 3.1, –5.37, –5.40. **FTIR** (thin film) cm^{-1}: 2953, 2928, 2856, 1471, 1256, 1116, 837, 777, 734, 697. **HRMS** (ESI) (*m/z*) calc'd for $C_{17}H_{29}INaO_2Si$ $[M+Na]^+$: 443.0874, found 443.0830. **TLC** (7:1 hexanes:EtOAc), R_f: 0.71 (UV, Anis).

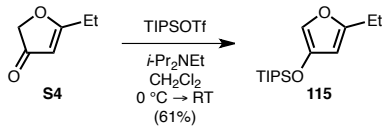

TIPS furan 115:

A solution of furanone **S4**[75] (309 mg, 2.76 mmol, 1.00 equiv) in CH_2Cl_2 (5.5 mL) was cooled to 0 °C. *i*-Pr_2NEt (1.06 mL, 6.06 mmol, 2.20 equiv) and TIPSOTf (815 μL, 3.03 mmol, 1.10 equiv) were then added dropwise sequentially via syringe to the stirred reaction mixture, which was subsequently allowed to warm slowly to room temperature. After 2 h, saturated aqueous NH_4Cl solution (5 mL) and CH_2Cl_2 (5 mL) were added sequentially to the reaction. The layers were separated and the aqueous layer was extracted with CH_2Cl_2 (3 × 3 mL). The organic layers were combined, washed with brine (5 mL), dried over anhydrous $MgSO_4$, and concentrated under reduced pressure. The resulting oil was then purified by flash column chromatography (silica gel, eluent: hexanes, 1% Et_3N) to afford TIPS furan **115** (455 mg, 61%) as a yellow oil.

^{1}H NMR (500 MHz, $CDCl_3$) δ: 7.08–6.86 (m, 1H), 5.78 (q, *J* = 1.0 Hz, 1H), 2.53 (dq, *J* = 1.0, 7.6 Hz, 2H), 1.24–1.15 (m, 6H), 1.09 (d, *J* = 6.8 Hz, 18H). **^{13}C NMR** (126 MHz, $CDCl_3$) δ: 156.3, 144.4, 126.1, 101.8, 21.8, 17.8, 12.3, 11.9. **FTIR** (thin film) cm^{-1}: 2944, 2867, 1617, 1463, 1384, 1149, 999, 882, 859, 683. **HRMS** (ESI) (*m/z*) calc'd for $C_{15}H_{29}O_2Si$ $[M+H]^+$: 269.1931, found 269.1934. **TLC** (2:1 hexanes:EtOAc), R_f: 0.95 (UV, Anis).

---

[75] Wasserman, H. H.; Lee, G. M. *Tet. Lett.* **1994**, *35*, 9783-9786.

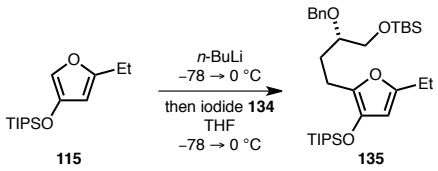

Alkylated furan 135:

A solution of TIPS furan **115** (5.40 g, 20.1 mmol, 1.30 equiv), which was azeotropically dried with benzene (3 × 10 mL), in THF (26 mL) was cooled to −78 °C. A solution of *n*-butyllithium in hexanes (2.62 M, 7.08 mL, 18.6 mmol, 1.20 equiv) was then added dropwise. After 10 min, the reaction mixture was allowed to warm to 0 °C. After an additional 75 min, the reaction was cooled to −78 °C and a solution of alkyl iodide **134** (6.50 g, 15.5 mmol, 1.00 equiv) in THF (26 mL) was added dropwise via syringe over 10 min. The reaction mixture was then allowed to warm slowly to 0 °C over 4 h, at which point brine (50 mL) and Et_2O (30 mL) were sequentially added. The organic and aqueous layers were separated and the aqueous layer was extracted with EtOAc (3 × 30 mL). The organic layers were combined, washed with brine (50 mL), dried over anhydrous $MgSO_4$, and concentrated under reduced pressure. The resulting oil was then purified by flash column chromatography (silica gel, eluent: 80:1 → 50:1 → 20:1 hexanes:EtOAc, 1% Et_3N) to afford alkylated furan **135** (8.84 g) as a yellow oil. Due to difficulties in removing trace TIPS furan **115** from product **135**, an accurate yield was determined after the next step.

^{1}H NMR (600 MHz, $CDCl_3$) δ: 7.36 (d, *J* = 6.7 Hz, 2H), 7.31 (t, *J* = 7.3 Hz, 2H), 7.26–7.23 (m, 1H), 5.67 (s, 1H), 4.69 (d, *J* = 11.7 Hz, 1H), 4.60 (d, *J* = 11.4 Hz, 1H), 3.71 (dd, *J* = 6.2, 10.5 Hz, 1H), 3.61 (dd, *J* = 5.0, 10.5 Hz, 1H), 3.52–3.46 (m, 1H), 2.74–2.67 (m, 1H), 2.61 (ddd, *J* = 6.6, 8.9, 15.2 Hz, 1H), 2.49 (q, *J* = 7.6 Hz, 2H), 1.91–1.81 (m, 1H), 1.81–1.70 (m, 1H), 1.22–1.13 (m, 6H), 1.08 (d, *J* = 7.3 Hz, 18H), 0.89 (s, 9H), 0.05 (s, 3H), 0.04 (s, 3H). **^{13}C NMR** (126 MHz, $CDCl_3$) δ: 153.1, 139.2, 138.1, 138.0, 128.2, 127.7, 127.3, 101.2, 79.5, 72.3, 65.9, 30.0, 25.9, 21.8, 21.0, 18.3, 17.9, 12.5, 12.1, –5.35, –5.41. **FTIR** (thin film) cm^{-1}: 2944, 2866, 1641, 1463, 1409, 1251, 1072, 997, 883,

836, 776, 684. **HRMS** (ESI) (*m/z*) calc'd for $C_{32}H_{56}NaO_4Si_2$ $[M+Na]^+$: 583.3609, found 583.3611. **TLC** (12:1 hexanes:EtOAc), R_f: 0.57 (UV, Anis).

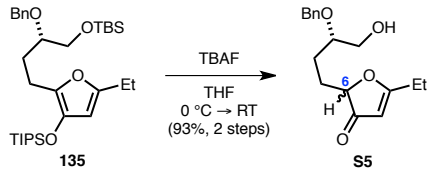

Furanone alcohol S5:

A solution of furan **135** (8.84 g, 15.8 mmol, 1.00 equiv) in THF (79 mL) was cooled to 0 °C. A solution of TBAF in THF (1.00 M, 39.4 mL, 39.4 mmol, 2.50 equiv) was then added dropwise via syringe to the solution. After 2 h, the reaction mixture was allowed to warm to room temperature. After an additional 10 min, brine (50 mL) and Et_2O (50 mL) were added sequentially to the reaction. The layers were separated and the aqueous layer was extracted with EtOAc (3 × 40 mL). The organic layers were combined, washed with brine (50 mL), dried over anhydrous $MgSO_4$, and concentrated under reduced pressure. The resulting oil was then purified by flash column chromatography (silica gel, eluent: gradient, 1:1 → 2:1 → 4:1 → 8:1 → 1:0 EtOAc:hexanes) to afford an inseparable 1:1 mixture of C6-diastereomers of furanone alcohol **S5** (4.16 g, 93% over 2 steps) as a yellow oil.

^{1}H NMR (600 MHz, $CDCl_3$) δ: 7.38–7.28 (m, 10H), 5.44 (s, 2H), 4.61 (d, J = 11.4 Hz, 2H), 4.56 (m, 2H), 4.47–4.39 (m, 2H), 3.76–3.68 (m, 2H), 3.60–3.51 (m, 4H), 2.52 (m, 4H), 2.12–2.04 (m, 1H), 2.03–1.94 (m, 1H), 1.88–1.61 (m, 6H), 1.24 (t, J = 7.5 Hz, 3H), 1.23 (t, J = 7.5 Hz, 3H). **^{13}C NMR** (126 MHz, $CDCl_3$) δ: 204.75, 204.72, 195.4, 195.3, 138.1, 128.5, 128.3, 127.83, 127.80, 126.9, 102.78, 102.76, 85.9, 85.8, 79.0, 78.8, 71.63, 71.60, 63.9, 63.8, 27.0, 26.9, 25.8, 25.7, 24.2, 10.2. **FTIR** (thin film) cm^{-1}: 3435, 2939, 2878, 1693, 1590, 1390, 1108, 1059, 740, 699. **HRMS** (ESI) (*m/z*) calc'd for $C_{17}H_{22}NaO_4$ $[M+Na]^+$: 313.1410, found 313.1418. **TLC** (2:1 EtOAc:hexanes), R_f: 0.25 (UV, Anis).

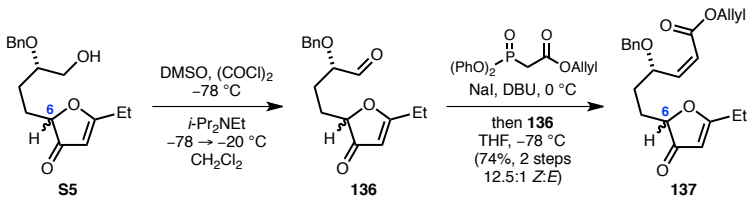

Furanone (*Z*)-enoate 137:

A solution of oxalyl chloride (6.86 mL, 79.5 mmol, 2.00 equiv) in CH_2Cl_2 (397 mL) was cooled to −78 °C. DMSO (11.3 mL, 159 mmol, 4.00 equiv) was then added dropwise. After 1.5 h, a solution of furanone alcohol **S5** (11.5 g, 39.8 mmol, 1.00 equiv) in CH_2Cl_2 (173 mL) at −78 °C was added dropwise via a dry-ice wrapped cannula to the stirred reaction. After 1 h, *i*-Pr_2NEt (41.5 mL, 239 mmol, 6.00 equiv) was added dropwise via syringe to the reaction mixture. After 15 min, the reaction was allowed to warm slowly to −20 °C over 30 min. After an additional 40 min, saturated aqueous NH_4Cl solution (500 mL) was added to the reaction, and the resultant mixture was allowed to warm to room temperature. EtOAc (1 L) was then added and the layers were separated. The aqueous layer was extracted with EtOAc (3 × 300 mL). The organic layers were combined, washed with saturated aqueous NH_4Cl solution (8 × 700 mL), then brine (500 mL), and dried over anhydrous $MgSO_4$ and concentrated under reduced pressure. The crude aldehyde **136** was carried forward to the next step without further purification.

A solution of allyl diphenylphosphonoacetate[76] (14.5 g, 43.7 mmol, 1.10 equiv) in THF (300 mL) was cooled to 0 °C. NaI (7.29 g, 47.7 mmol, 1.20 equiv) and DBU (6.54 mL, 43.7 mmol, 1.10 equiv) were then added sequentially to the solution. After 20 min, the reaction was cooled to −78 °C before a solution of crude aldehyde **136** in THF (100 mL) was added dropwise via cannula. After 2.5 h, saturated aqueous NH_4Cl solution (300 mL) was added to the stirred reaction mixture, which was then allowed to warm to room temperature. The mixture was diluted with EtOAc (600 mL) and the layers were separated. The aqueous layer was extracted with EtOAc (3 × 300 mL) and the organic

[76] Ando, K. *J. Org. Chem.* **1999**, *64*, 8406-8408.

layers were combined, washed with saturated aqueous NH_4Cl solution (5 × 300 mL), then brine (300 mL), and dried over anhydrous $MgSO_4$ and concentrated. The resulting oil was then purified by flash column chromatography twice using different eluent conditions (silica gel, eluent: (a) gradient, 20:1 → 15:1 → 10:1 → 7:1 → 5:1 → 2:1 CH_2Cl_2:EtOAc (removes unreacted allyl diphenylphosphonoacetate), (b) gradient, 6:1 → 4:1 → 2:1 hexanes:EtOAc) to afford an inseparable 1:1 mixture of C6-diastereomers of furanone (*Z*)-enoate **137** (11.0 g, 74% over 2 steps) as a pale yellow oil.

^{1}H NMR (600 MHz, $CDCl_3$) δ: 7.36–7.24 (m, 10H), 6.21 (dd, *J* = 2.3, 8.5 Hz, 1H), 6.19 (dd, *J* = 2.3, 8.5 Hz, 1H), 5.98–5.88 (m, 4H), 5.41 (m, 2H), 5.33 (m, 2H), 5.26 (m, 2H), 5.11–5.05 (m, 2H), 4.64–4.57 (m, 4H), 4.52 (m, 2H), 4.46 (dd, *J* = 4.1, 7.9 Hz, 1H), 4.44–4.39 (m, 3H), 2.50 (q, *J* = 7.6 Hz, 4H), 2.20–2.09 (m, 1H), 2.06–1.96 (m, 1H), 1.92–1.78 (m, 3H), 1.78–1.64 (m, 3H), 1.22 (t, *J* = 7.6 Hz, 6H). **^{13}C NMR** (126 MHz, $CDCl_3$) δ: 204.68, 204.65, 195.13, 195.09, 165.29, 165.26, 150.81, 150.79, 138.23, 138.19, 132.0, 128.3, 127.8, 127.7, 127.62, 127.60, 121.5, 121.4, 118.5, 102.6, 86.0, 85.8, 74.5, 74.3, 71.4, 71.3, 65.1, 65.0, 30.0, 29.9, 27.1, 27.0, 24.1, 10.2. **FTIR** (thin film) cm^{-1}: 2981, 2942, 1718, 1698, 1595, 1389, 1181, 1071, 986, 824, 698. **HRMS** (ESI) (*m/z*) calc'd for $C_{22}H_{26}NaO_5$ $[M+Na]^+$: 393.1673, found 393.1676. **TLC** (1:1 hexanes:EtOAc), R_f: 0.41 (UV, Anis).

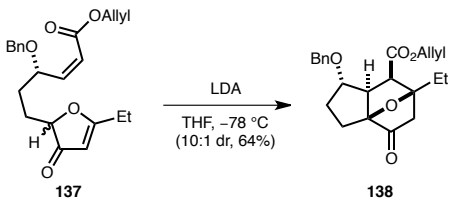

Oxanorbornanone allyl ester 138:

A solution of diisopropylamine (1.85 mL, 13.2 mmol, 1.40 equiv) in THF (140 mL) was cooled to −78 °C. A solution of *n*-butyllithium in hexanes (2.56 M, 4.78 mL, 12.3 mmol, 1.30 equiv) was then added dropwise via syringe to the solution. After 15 min, the reaction was allowed to warm to 0 °C for 20 min before recooling to −78 °C. Additional THF (210 mL) was added to the reaction at −78 °C. A solution of furanone (*Z*)-enoate **137** (3.49 g, 9.42 mmol, 1.00 equiv) in THF (120 mL) at −78 °C was added dropwise via a dry-ice wrapped cannula to the solution of LDA. After an additional 8.5 h, a solution of AcOH (3.5 mL) in THF (70 mL) was added via cannula to the stirred reaction. After an additional 15 min, saturated aqueous NH_4Cl solution (400 mL) was added to the mixture, which was then allowed to warm to room temperature. The resultant mixture was diluted with EtOAc (400 mL) and the layers were separated. The aqueous layer was extracted with EtOAc (3 × 300 mL) and the organic layers were combined, washed with saturated aqueous $NaHCO_3$ solution (3 × 200 mL) and brine (300 mL). The organic layers were then dried over anhydrous $MgSO_4$ and concentrated under reduced pressure. The resulting oil was then purified by flash column chromatography (silica gel, eluent: gradient, 9:1 → 8:1 → 7:1 → 5:1 hexanes:EtOAc) to afford oxanorbornanone allyl ester **138** (2.24 g, 64%) as a colorless oil.

^{1}H NMR (600 MHz, $CDCl_3$) δ: 7.33–7.24 (m, 5H), 5.90–5.82 (m, 1H), 5.30 (qd, *J* = 1.5, 17.0 Hz, 1H), 5.21 (qd, *J* = 1.1, 10.4 Hz, 1H), 4.61 (tdd, *J* = 1.3, 6.0, 13.0 Hz, 1H), 4.46 (tdd, *J* = 1.3, 6.0, 13.0 Hz, 1H), 4.42 (d, *J* = 11.4 Hz, 1H), 4.37 (d, *J* = 11.1 Hz, 1H), 4.28 (dd, *J* = 7.3, 13.5 Hz, 1H), 3.13 (d, *J* = 9.1 Hz, 1H), 2.62 (dd, *J* = 7.2, 9.2 Hz, 1H), 2.41–2.25 (m, 4H), 2.12–2.00 (m, 1H), 1.94–1.80 (m, 3H), 0.97 (t, *J* = 7.6 Hz, 3H). **^{13}C NMR** (126 MHz, $CDCl_3$) δ: 208.1, 170.1, 138.2, 131.7, 128.3,

127.6, 127.5, 119.0, 95.6, 89.2, 80.2, 71.9, 65.4, 55.3, 51.6, 47.5, 32.5, 25.6, 21.2, 8.8. **FTIR** (thin film) cm^{-1}: 2938, 1761, 1733, 1455, 1354, 1184, 1152, 698. **HRMS** (ESI) (*m/z*) calc'd for $C_{22}H_{26}NaO_5$ $[M+Na]^+$: 393.1673, found 393.1657. **TLC** (2:1 hexanes:EtOAc), R_f: 0.66 (Anis).

1D NOESY (600 MHz, $CDCl_3$):

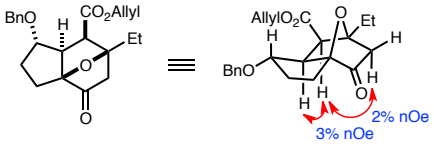

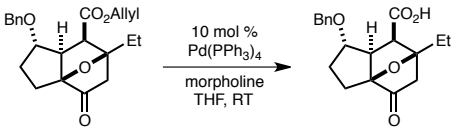

138 **139**

Carboxylic acid 139:

$Pd(PPh_3)_4$ (2.67 g, 2.28 mmol, 0.10 equiv) in THF (85 mL) was added via cannula to a stirred solution of oxanorbornanone allyl ester **138** (8.43 g, 22.8 mmol, 1.00 equiv) in THF (191 mL). Morpholine (19.9 mL, 228 mmol, 10.0 equiv) was then added via syringe to the reaction mixture. After 4 h, the reaction was concentrated under reduced pressure. The resultant residue was then dissolved in CH_2Cl_2 (100 mL) and washed with saturated aqueous $NaHCO_3$ solution (5 × 75 mL). The aqueous layers were combined and acidified by careful dropwise addition of 10% aqueous HCl until the pH reached 2. The aqueous layers were then extracted with CH_2Cl_2 (5 × 120 mL). The organic layers were combined, dried over anhydrous $MgSO_4$, and concentrated under reduced pressure to afford crude carboxylic acid **139** as a white solid (6.44 g, 86% mass recovery). The crude product was carried forward to the next step without further purification.

^{1}H NMR (500 MHz, $CDCl_3$) δ: 7.35–7.27 (m, 5H), 4.43 (d, J = 11.5 Hz, 1H), 4.38 (d, J = 11.2 Hz, 1H), 4.24 (q, J = 6.8 Hz, 1H), 3.17 (d, J = 9.0 Hz, 1H), 2.67 (dd, J = 6.8, 9.0 Hz, 1H), 2.43–2.27 (m, 4H), 2.17–2.06 (m, 1H), 2.00–1.83 (m, 3H), 1.00 (t, J = 7.7 Hz, 3H). **^{13}C NMR** (126 MHz, $CDCl_3$) δ: 207.4, 173.9, 138.0, 128.4, 127.74, 127.68, 95.8, 89.3, 80.3, 71.8, 55.4, 51.7, 47.2, 32.6, 25.7, 21.3, 8.9. **FTIR** (thin film) cm^{-1}: 2972, 2942, 1762, 1706, 1358, 1160, 1119, 1099, 965, 740, 699. **HRMS** (ESI) (*m/z*) calc'd for $C_{19}H_{22}NaO_5$ $[M+Na]^+$: 353.1359, found 353.1363. **TLC** (1:1 hexanes:EtOAc and 1 drop of AcOH), R_f: 0.36 (Anis).

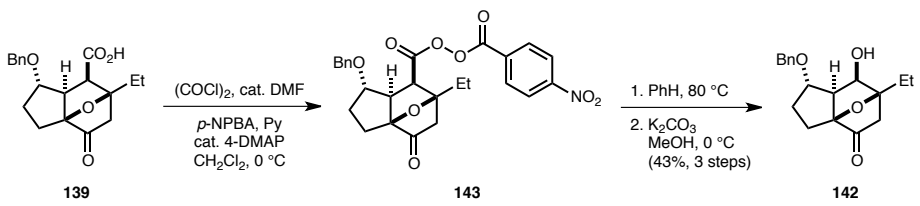

Alcohol 142:

A solution of carboxylic acid **139** (50.0 mg, 0.151 mmol, 1.00 equiv), which was azeotropically dried with benzene (3 × 0.5 mL) in CH_2Cl_2 (1.5 mL) was cooled to 0 °C. Oxalyl chloride (16.0 μL, 0.189 mmol, 1.25 equiv) and a single drop of DMF were then sequentially added via syringe to the stirred solution, which was subsequently allowed to warm to room temperature after 10 min. After 3 h, the reaction mixture was recooled to 0 °C. *p*-Nitroperbenzoic acid[77] (37.0 mg, 0.197 mmol, 1.30 equiv), pyridine (28.0 μL, 0.348 mmol, 2.30 equiv), and a single crystal of 4-DMAP were then added sequentially to the stirred reaction mixture. After 1 h, CH_2Cl_2 (1 mL) and 10% aqueous HCl (1 mL) were sequentially added to the reaction. The mixture was further diluted with CH_2Cl_2 (1 mL) and the layers were separated. The aqueous layer was extracted with CH_2Cl_2 (3 × 1 mL). The organic layers were combined, washed with a saturated aqueous $NaHCO_3$ solution (3 × 1 mL), then dried over anhydrous $MgSO_4$ and concentrated under reduced pressure to afford crude diacyl peroxide **143**, which was carried forward immediately to the next step without further purification.

A pressure tube was charged with crude **143** and benzene (5 mL), sealed, and heated to 80 °C. After 5.5 h, the reaction was allowed to cool to room temperature and was subsequently concentrated under reduced pressure. The crude residue was then suspended in methanol (3 mL) and the resultant mixture was cooled to 0 °C. K_2CO_3 (22.0 mg, 0.159 mmol, 1.05 equiv) was then added in a single portion. After 1 h, the reaction mixture was filtered and concentrated under reduced pressure. The residue was dissolved in EtOAc (3 mL) and washed with a saturated aqueous $NaHCO_3$

[77] Vilkas, M. *Bull. Soc. Chim. Fr.* **1959**, 1401.

solution (2 mL) and brine (2 mL), dried over anhydrous $MgSO_4$, and concentrated under reduced pressure. The resulting crude residue was then purified by flash column chromatography (silica gel, eluent: gradient, 8:1 → 6:1 → 4:1 → 3:1 → 2:1 hexanes:EtOAc) to afford alcohol **142** (19.6 mg, 43% over 3 steps) as a pale yellow solid.

^{1}H NMR (500 MHz, $CDCl_3$) δ: 7.38–7.27 (m, 5H), 4.56 (d, *J* = 12.0 Hz, 1H), 4.48 (d, *J* = 11.7 Hz, 1H), 4.29 (dd, *J* = 6.8, 13.2 Hz, 1H), 4.20 (d, *J* = 6.8 Hz, 1H), 2.42 (t, *J* = 7.0 Hz, 1H), 2.37–2.30 (m, 2H), 2.27 (d, *J* = 17.8 Hz, 1H), 2.17 (d, *J* = 18.1 Hz, 1H), 2.08–1.92 (m, 2H), 1.89–1.75 (m, 2H), 1.01 (t, *J* = 7.6 Hz, 3H). **^{13}C NMR** (126 MHz, $CDCl_3$) δ: 207.9, 138.3, 128.5, 127.8, 127.7, 95.7, 90.1, 77.8, 74.5, 71.7, 56.7, 42.9, 33.2, 23.7, 21.4, 8.5. **FTIR** (thin film) cm^{-1}: 3482, 2970, 2938, 1760, 1454, 1358, 1115, 1065, 739, 698. **HRMS** (ESI) (*m/z*) calc'd for $C_{18}H_{22}NaO_4$ $[M+Na]^+$: 325.1410, found 325.1405. **TLC** (2:1 hexanes:EtOAc), R_f: 0.36 (Anis). **$[\alpha]_D^{25}$**: –4.1 (*c* = 1.41, CH_2Cl_2).

1D NOESY (600 MHz, $CDCl_3$):

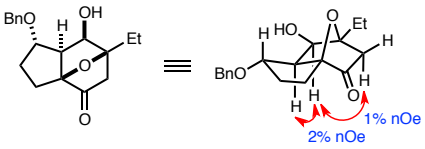

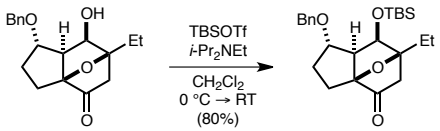

142 144

Oxanorbornanone dimerization precursor 144:

A solution of alcohol **142** (517 mg, 1.71 mmol, 1.00 equiv), which was azeotropically dried with benzene (5 × 2 mL) in CH_2Cl_2 (19 mL) was cooled to 0 °C. *i*-Pr_2NEt (1.19 mL, 6.85 mmol, 4.00 equiv) and TBSOTf (590 μL, 2.56 mmol, 1.50 equiv) were then added dropwise sequentially via syringe to the stirred reaction, which was subsequently allowed to warm slowly to room temperature. After 11 h, additional *i*-Pr_2NEt (306 μL, 1.71 mmol, 1.00 equiv) and TBSOTf (152 μL, 0.684 mmol, 0.40 equiv) were added dropwise sequentially via syringe to the reaction. After an additional 16 h, saturated aqueous NH_4Cl solution (10 mL) was added and the resultant mixture was diluted with EtOAc (25 mL). The layers were separated and the aqueous layer was extracted with EtOAc (3 × 15 mL). The organic layers were combined, washed with brine (15 mL), dried over anhydrous $MgSO_4$, and concentrated under reduced pressure. The resulting crude residue was then purified by flash column chromatography (silica gel, eluent: gradient, 20:1 → 17:1 → 15:1 → 12:1 → 9:1 → 7:1 hexanes:EtOAc) to afford oxanorbornanone dimerization precursor **144** (570 mg, 80%) as a clear oil.

^{1}H NMR (500 MHz, $CDCl_3$) δ: 7.36–7.24 (m, 5H), 4.47 (d, *J* = 11.2 Hz, 1H), 4.39 (d, *J* = 11.2 Hz, 1H), 4.32 (td, *J* = 4.2, 6.0 Hz, 1H), 4.15 (d, *J* = 7.1 Hz, 1H), 2.47 (dd, *J* = 4.4, 7.1 Hz, 1H), 2.36 (d, *J* = 17.8 Hz, 1H), 2.33–2.19 (m, 1H), 2.10–1.94 (m, 2H), 1.92–1.84 (m, 1H), 1.76 (qd, *J* = 7.4, 14.4 Hz, 1H), 0.99 (t, *J* = 7.6 Hz, 3H), 0.94 (s, 9H), 0.09 (s, 3H), 0.06 (s, 3H). **^{13}C NMR** (126 MHz, $CDCl_3$) δ: 209.0, 138.5, 128.32, 128.30, 127.4, 96.3, 89.8, 78.6, 76.4, 71.1, 58.0, 42.2, 32.1, 25.9, 25.8, 22.6, 18.3, 8.4, –4.6, –4.7. **FTIR** (thin film) cm^{-1}: 2956, 2929, 2856, 1763, 1463, 1254, 1122, 837, 776. **HRMS** (ESI) (*m/z*) calc'd for $C_{24}H_{37}O_4Si$ $[M+Na]^+$: 417.2456, found 417.2454. **TLC** (2:1 hexanes:EtOAc), R_f: 0.77 (Anis).

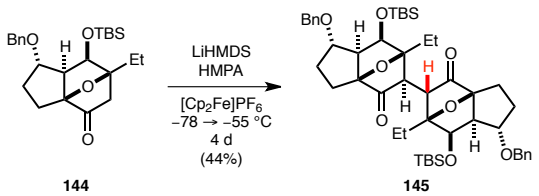

***Exo-endo* dimer 145**:

A two-neck flask was equipped with a solid addition adaptor containing ferrocenium hexafluorophosphate $[Cp_2Fe]PF_6$ (661 mg, 2.00 mmol, 5.00 equiv). HMDS (150 μL, 0.719 mmol, 1.80 equiv) and THF (1.35 mL) were then added sequentially to the two-neck flask and the resultant solution was cooled to −78 °C. A solution of *n*-butyllithium in hexanes (2.56 M, 265 μL, 0.679 mmol, 1.70 equiv) was then added dropwise via syringe to the stirred solution. After 1 h, HMPA (140 μL, 0.799 mmol, 2.00 equiv) was added dropwise via syringe to the solution of LiHMDS. After an additional 1 h, a solution of oxanorbornanone monomer **144** (166 mg, 0.399 mmol, 1.00 equiv) in THF (1.35 mL) was slowly added down the vessel wall via syringe to the reaction mixture. After an additional 2 h, $[Cp_2Fe]PF_6$ was added to the reaction via the solid addition adaptor, yielding a deep blue suspension that turned green in color within 30 min. The reaction mixture was allowed to warm to −55 °C. After 4 d, a saturated aqueous NH_4Cl solution (2 mL) was added to the reaction, which was then allowed to warm to room temperature. The mixture was diluted with Et_2O (2 mL), EtOAc (2 mL), and water (2 mL). The layers were separated and the aqueous layer was extracted with EtOAc (3 × 2 mL). The organic layers were combined, dried over anhydrous $MgSO_4$, and concentrated under reduced pressure. The crude product was then purified by flash column chromatography (silica gel, eluent: gradient, 20:1 → 9:1 hexanes:EtOAc) to afford *exo-endo* dimer **145** (72.6 mg, 44%) as a white flocculent solid.

^{1}H NMR (600 MHz, $CDCl_3$) δ: 7.35–7.28 (m, 10H), 4.61 (d, J = 7.6 Hz, 1H), 4.48–4.43 (m, 2H), 4.41–4.36 (m, 2H), 4.36–4.30 (m, 2H), 4.22 (d, J = 7.6 Hz, 1H), 2.91 (d, J = 7.6 Hz, 1H), 2.39 (dt, J = 4.8, 7.5 Hz, 2H), 2.36–2.27 (m, 3H), 2.26–2.18 (m, 2H), 2.14–2.00 (m, 4H), 1.99–1.83 (m, 3H),

1.40 (dd, J = 7.8, 15.1 Hz, 1H), 1.05 (t, J = 7.6 Hz, 3H), 0.98 (t, J = 7.5 Hz, 3H), 0.94 (s, 9H), 0.91 (s, 9H), 0.17 (s, 3H), 0.13 (s, 3H), 0.06 (s, 3H), 0.05 (s, 3H). **^{13}C NMR** (126 MHz, $CDCl_3$) δ: 211.9, 211.7, 138.6, 138.5, 128.30, 128.25, 128.1, 127.39, 127.35, 127.3, 96.5, 96.3, 94.3, 92.8, 78.9, 78.83, 78.76, 74.1, 71.3, 70.8, 59.7, 58.3, 52.0, 51.0, 32.4, 31.7, 26.1, 25.9, 23.9, 23.7, 22.1, 21.1, 18.2, 18.2, 8.8, 8.1, –4.5, –4.6, –4.8, –4.9. **FTIR** (thin film) cm^{-1}: 2929, 2856, 1753, 1462, 1359, 1253, 1109, 836, 776, 733, 696. **HRMS** (ESI) (*m/z*) calc'd for $C_{48}H_{70}NaO_8Si_2$ $[M+Na]^+$: 853.4501, found 853.4508. **TLC** (4:1 hexanes:EtOAc), R_f: 0.62 (UV, Anis).

1D NOESY (500 MHz, $CDCl_3$):

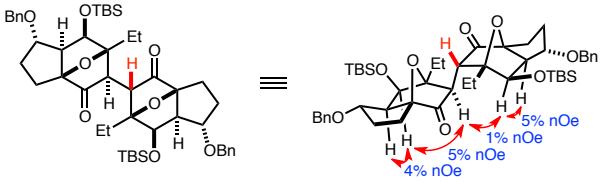

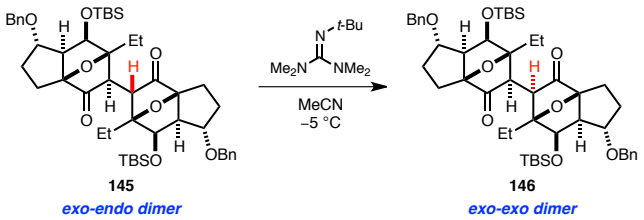

145 *exo-endo dimer* → **146** *exo-exo dimer*

***Exo-exo* dimer 146**:

A solution of *exo-endo* dimer **145** (102 mg, 0.123 mmol, 1.00 equiv), which was azeotropically dried with benzene (5 × 1 mL), in MeCN (7.2 mL) was cooled to –5 °C. Two drops of 2-*tert*-butyl-1,1,3,3-tetramethylguanidine (Barton's base) was then added via syringe to the solution. After 24 h, saturated aqueous NH_4Cl solution (5 mL) was added to the reaction, which was then allowed to warm to room temperature. The resultant mixture was diluted with CH_2Cl_2 (15 mL) and the layers were separated. The aqueous layer was extracted with CH_2Cl_2 (3 × 5 mL) and the organic layers were combined, washed with saturated aqueous NH_4Cl solution (3 × 5 mL), dried over anhydrous $MgSO_4$, and concentrated under reduced pressure. The resulting crude *exo-exo* dimer **146** was then carried forward to the next step without further purification.

^{1}H NMR (500 MHz, $CDCl_3$) δ: 7.35–7.29 (m, 8H), 7.26–7.22 (m, 2H), 4.46 (d, J = 11.5 Hz, 2H), 4.43 (d, J = 11.5 Hz, 2H), 4.41–4.36 (m, 4H), 2.97 (dd, J = 5.7, 7.4 Hz, 2H), 2.38–2.26 (m, 6H), 2.24 (s, 2H), 2.02–1.93 (m, 2H), 1.92–1.83 (m, 2H), 1.43 (qd, J = 7.4, 15.1 Hz, 2H), 1.03 (t, J = 7.4 Hz, 6H), 0.91 (s, 18H), 0.05 (s, 6H), 0.04 (s, 6H). **^{13}C NMR** (126 MHz, $CDCl_3$) δ: 209.1, 138.7, 128.1, 127.3, 127.2, 97.8, 92.1, 78.8, 74.4, 71.1, 58.2, 47.8, 31.8, 25.9, 23.4, 20.9, 18.3, 7.9, –4.8, –5.0. **FTIR** (thin film) cm^{-1}: 2954, 2929, 2857, 1757, 1462, 1357, 1252, 1123, 963, 837, 776, 697. **HRMS** (ESI) (*m/z*) calc'd for $C_{48}H_{70}NaO_8Si_2$ $[M+Na]^+$: 853.4501, found 853.4516. **TLC** (4:1 hexanes:EtOAc), R_f: 0.60 (UV, Anis). **$[\alpha]_D^{25}$**: –48.3 (c = 0.43, CH_2Cl_2).

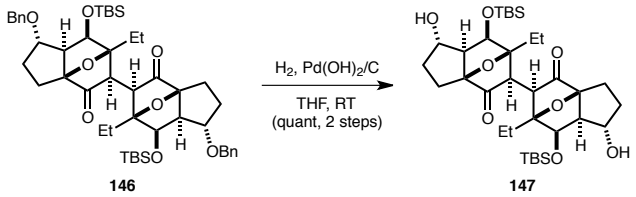

Diol dimer 147:

$Pd(OH)_2$ on carbon (20 wt%, 79.4 mg, 0.113 mmol, 1.00 equiv) was added in a single portion to a stirred solution of *exo-exo* dimer **146** (94.0 mg, 0.113 mmol, 1.00 equiv) in THF (5.65 mL). The reaction vessel was purged with H_2 and placed under an atmosphere of H_2. After 4 h, celite was poured into the stirred reaction mixture and the resultant slurry was filtered through a pad of celite. The solution was concentrated under reduced pressure and the residue was then purified by flash column chromatography (silica gel, eluent: gradient, 3:1 → 2:1 hexanes:EtOAc) to afford diol dimer **147** (73.6 mg, quant. over 2 steps) as a white crystalline solid.

^{1}H NMR (600 MHz, C_6D_6) δ: 4.69 (d, J = 7.3 Hz, 2H), 4.65 (app. t, J = 7.0 Hz, 2H), 2.90 (t, J = 7.5 Hz, 2H), 2.54–2.45 (m, 4H), 2.30 (ddd, J = 4.4, 10.8, 15.3 Hz, 2H), 2.07–2.00 (m, 2H), 1.78–1.68 (m, 2H), 1.58–1.48 (m, 2H), 1.43–1.33 (m, 2H), 1.09 (t, J = 7.5 Hz, 6H), 0.98 (s, 18H), 0.68 (d, J = 7.0 Hz, 2H), 0.19 (s, 6H), 0.04 (s, 6H). **^{13}C NMR** (126 MHz, C_6D_6) δ: 209.8, 98.5, 92.7, 75.0, 72.5, 60.1, 48.8, 36.1, 26.4, 22.7, 21.9, 18.8, 8.4, –4.3, –4.6. **FTIR** (thin film) cm^{-1}: 2951, 2930, 2858, 1757, 1462, 1254, 1126, 1065, 840, 776. **HRMS** (ESI) (*m/z*) calc'd for $C_{34}H_{58}NaO_8Si_2$ $[M+Na]^+$: 673.3562, found 673.3550. **TLC** (4:1 hexanes:EtOAc), R_f: 0.15 (Anis).

Tetracarbonyl oxanorbornanone dimer 148:

A solution of diol dimer **147** (73.2 mg, 0.112 mmol, 1.00 equiv), which was azeotropically dried with benzene (3 × 0.5 mL) in CH_2Cl_2 (2.8 mL) was cooled to −10 °C. DMSO (160 μL, 2.25 mmol, 20.0 equiv), *i*-Pr_2NEt (196 μL, 1.12 mmol, 10.0 equiv), and SO_3•Py (107 mg, 0.675 mmol, 6.00 equiv) were then added sequentially to the solution, which was then allowed to warm slowly to room temperature after stirring at 0 °C for 30 min. After an additional 90 min, water (3 mL), Et_2O (2 mL), and EtOAc (2 mL) were added sequentially to the reaction. The layers were separated and the aqueous layer was extracted with EtOAc (3 × 2 mL). The organic layers were combined and washed with 10% aqueous HCl solution (3 × 5 mL), saturated aqueous $NaHCO_3$ solution (5 mL), and brine (5 mL). The organic layers were dried over anhydrous $MgSO_4$ and concentrated under reduced pressure to afford crude tetracarbonyl oxanorbornanone dimer **148** as a flocculent white solid (68.4 mg, crude mass).

^{1}H NMR (500 MHz, C_6D_6) δ: 4.77 (d, *J* = 7.6 Hz, 2H), 3.14 (d, *J* = 7.6 Hz, 2H), 2.62–2.47 (m, 4H), 2.40–2.26 (m, 2H), 1.90–1.80 (m, 4H), 1.74 (dd, *J* = 9.5, 12.7 Hz, 2H), 1.53 (qd, *J* = 7.4, 15.2 Hz, 2H), 1.06 (t, *J* = 7.4 Hz, 6H), 1.00 (s, 18H), 0.41 (s, 6H), 0.16 (s, 6H). **^{13}C NMR** (126 MHz, C_6D_6) δ: 208.9, 207.5, 96.3, 93.2, 77.5, 58.6, 48.6, 39.0, 26.5, 21.8, 20.8, 19.0, 8.4, –4.3, –5.0. **FTIR** (thin film) cm^{-1}: 2951, 2928, 2856, 1749, 1472, 1257, 1119, 886, 837. **HRMS** (ESI) (*m/z*) calc'd for $C_{34}H_{55}O_8Si_2$ $[M+H]^+$: 647.3430, found 647.3434. **TLC** (2:1 hexanes:EtOAc), R_f: 0.69 (Anis).

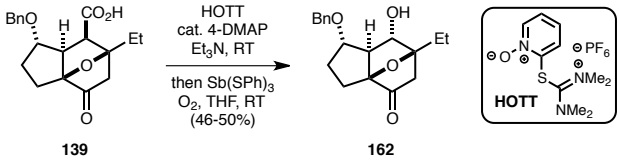

Alcohol 162:

Carboxylic acid **139** (300 mg, 0.908 mmol, 1.00 equiv) was azeotropically dried with $CHCl_3$ (4 × 2 mL) and benzene (5 × 2 mL) before THF (11.2 mL) was added. Et_3N (507 μL, 3.63 mmol, 4.00 equiv) was then added to the solution. The resultant solution of **139** and Et_3N in THF was added dropwise via cannula to a stirred solution of *S*-(1-oxido-2-pyridinyl) 1,1,3,3-tetramethylthiouronium hexafluorophosphate (HOTT)[54] (674 mg, 1.82 mmol, 2.00 equiv) and 4-DMAP (11.1 mg, 0.0910 mmol, 0.10 equiv) in THF (7.1 mL) at room temperature. After 5 h, additional THF (27.6 mL) was added to the reaction mixture. The reaction was then saturated with O_2 before $Sb(SPh)_3$[55] (1.22 g, 2.72 mmol, 3.00 equiv) was added in a single portion. The reaction flask was protected from light with aluminum foil. After 2 h, water (0.25 mL) was added to the reaction. After an additional 45 min, the mixture was filtered through celite and concentrated under reduced pressure. The resulting crude product was then purified by flash column chromatography (silica gel, eluent: gradient, 4:1 → 3:1 → 2:1 hexanes:EtOAc) to afford alcohol **162** (131.8 mg, 48%) as a yellow oil.

^{1}H NMR (500 MHz, $CDCl_3$) δ: 7.39–7.33 (m, 4H), 7.33–7.29 (m, 1H), 4.62 (d, *J* = 12.0 Hz, 1H), 4.47 (d, *J* = 12.0 Hz, 1H), 3.97 (app. q, *J* = 6.8 Hz, 1H), 3.94 (app. t, *J* = 2.9 Hz, 1H), 2.74 (d, *J* = 17.8 Hz, 1H), 2.36–2.25 (m, 2H), 2.14 (dd, *J* = 1.0, 17.8 Hz, 1H), 1.99 (dd, *J* = 2.7, 6.8 Hz, 1H), 1.93–1.85 (m, 1H), 1.83 (dq, *J* = 1.6, 7.5 Hz, 2H), 1.78 (d, *J* = 3.7 Hz, 1H), 1.76–1.68 (m, 1H), 1.00 (t, *J* = 7.6 Hz, 3H). **^{13}C NMR** (126 MHz, $CDCl_3$) δ: 208.8, 138.4, 128.6, 127.9, 127.7, 97.0, 88.4, 84.7, 80.1, 72.1, 62.0, 40.5, 32.3, 26.4, 21.9, 8.0. **FTIR** (thin film) cm^{-1}: 3441, 2969, 2933, 1758, 1574, 1453, 1418, 1097, 1060, 738, 699. **HRMS** (ESI) (*m/z*) calc'd for $C_{18}H_{22}NaO_4$ $[M+Na]^+$: 325.1410, found 325.1407. **TLC** (2:1 hexanes:EtOAc and 1 drop of AcOH), R_f: 0.24 (Anis).

1D NOESY (500 MHz, C_6D_6):

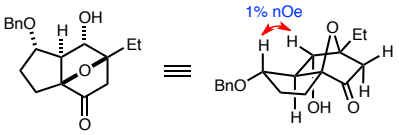
BnO
H
OH
Et
O
O
1% nOe
H
H
O
Et
H
BnO
H
OH
O
H

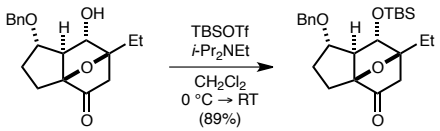

162 **163**

Oxanorbornanone dimerization precursor 163:

A solution of alcohol **162** (150 mg, 0.496 mmol, 1.00 equiv), which was azeotropically dried with benzene (5 × 0.5 mL), in CH_2Cl_2 (5.5 mL) was cooled to 0 °C. *i*-Pr_2NEt (475 μL, 2.73 mmol, 5.50 equiv) and TBSOTf (233 μL, 0.992 mmol, 2.00 equiv) were then added dropwise sequentially via syringe to the stirred solution, which was subsequently allowed to warm slowly to room temperature. After 1.5 h, saturated aqueous NH_4Cl solution (5 mL) was added to the reaction. The resultant mixture was diluted with EtOAc (5 mL) and the layers were separated. The aqueous layer was extracted with EtOAc (3 × 3 mL). The organic layers were combined, washed with brine (5 mL), dried over anhydrous $MgSO_4$, and concentrated under reduced pressure. The crude residue was then purified by flash column chromatography (silica gel, eluent: 16:1 hexanes:EtOAc) to afford oxanorbornanone dimerization precursor **163** (185 mg, 89%) as a pale yellow solid.

^{1}H NMR (500 MHz, C_6D_6) δ: 7.24 (d, *J* = 7.8 Hz, 2H), 7.19 (t, *J* = 7.6 Hz, 2H), 7.10 (t, *J* = 7.3 Hz, 1H), 4.27 (d, *J* = 11.7 Hz, 1H), 4.13 (d, *J* = 11.7 Hz, 1H), 3.95 (d, *J* = 2.0 Hz, 1H), 3.79 (app. q, *J* = 6.5 Hz, 1H), 2.78 (d, *J* = 17.6 Hz, 1H), 2.40 (ddd, *J* = 6.1, 10.0, 14.6 Hz, 1H), 2.18 (dd, *J* = 2.7, 6.6 Hz, 1H), 2.00 (dd, *J* = 1.0, 17.6 Hz, 1H), 1.91 (tdd, *J* = 6.3, 8.2, 12.8 Hz, 1H), 1.71 (ddd, *J* = 6.2, 8.2, 14.6 Hz, 1H), 1.64 (q, *J* = 7.4 Hz, 2H), 1.61–1.52 (m, 1H), 0.89 (t, *J* = 7.4 Hz, 3H), 0.84 (s, 9H), 0.06 (s, 3H), 0.00 (s, 3H). **^{13}C NMR** (126 MHz, $CDCl_3$) δ: 209.5, 137.9, 128.3, 127.8, 127.6, 96.8, 88.6, 84.3, 80.3, 71.8, 62.1, 40.8, 31.3, 25.9, 25.7, 22.4, 17.8, 7.9, –4.6, –5.2. **FTIR** (thin film) cm^{-1}: 2955, 2929, 2857, 1764, 1252, 1117, 1062, 863, 838, 778. **HRMS** (ESI) (*m/z*) calc'd for $C_{24}H_{36}NaO_4Si$ $[M+Na]^+$: 439.2275, found 439.2291. **TLC** (4:1 hexanes:EtOAc), R_f: 0.63 (Anis). **$[\alpha]_D^{25}$**: +28.3 (*c* = 0.12, CH_2Cl_2).

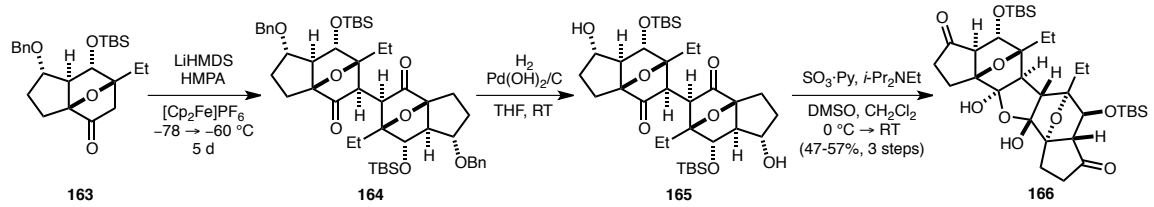

Cyclic hydrate 166:

A two-neck flask was equipped with a solid addition adaptor containing ferrocenium hexafluorophosphate $[Cp_2Fe]PF_6$ (199 mg, 0.600 mmol, 5.00 equiv). HMDS (48.0 μL, 0.228 mmol, 1.90 equiv) and THF (477 μL) were added to the two-neck flask and the resultant stirred solution was cooled to −78 °C. A solution of *n*-butyllithium in hexanes (2.56 M, 80.0 μL, 0.204 mmol, 1.70 equiv) was then added dropwise via syringe to the solution. After 30 min, HMPA (105 μL, 0.600 mmol, 5.00 equiv) was added dropwise via syringe to the solution of LiHMDS. After an additional 1 h, a solution of oxanorbornanone monomer **163** (50.0 mg, 0.120 mmol, 1.00 equiv) in THF (293 μL) was then slowly added down the vessel wall to the reaction. After another 2 h, $[Cp_2Fe]PF_6$ was added from the solid addition adaptor. The initially deep blue suspension turned green within 30 min and was allowed to stir at –60 °C. After 5 d, saturated aqueous NH_4Cl solution (1 mL) was added to the stirred reaction mixture, which was allowed to warm to room temperature. The mixture was diluted with Et_2O (1 mL), EtOAc (1 mL), and water (0.5 mL). The layers were separated and the aqueous layer was extracted with EtOAc (3 × 1 mL). The organic layers were combined, dried over anhydrous $MgSO_4$, and concentrated under reduced pressure. Due to the high instability of crude dimer **164** to silica gel column chromatography, the crude product was quickly plugged through silica gel using 20:1 hexanes:EtOAc (removes ferrocene) and 2:1 hexanes:EtOAc (elutes product) within 10 min to afford crude dimer **164**, which was carried forward without further purification.

$Pd(OH)_2$ on carbon (20 wt.%, 253 mg, 0.360 mmol, 3.00 equiv) was added in a single portion to a stirred solution of crude dimer **164** in THF (4 mL). The reaction vessel was purged with H_2 and placed under an atmosphere of H_2. After 4 h, celite (100 mg) was poured into the reaction,

and the resultant slurry was filtered through a pad of celite and concentrated under reduced pressure to afford crude diol **165**, which was carried forward without further purification.

A solution of crude diol **165**, which was azeotropically dried with benzene (5 × 0.5 mL), in CH_2Cl_2 (3 mL) was cooled to 0 °C. DMSO (228 μL, 3.20 mmol, 26.7 equiv), *i*-Pr_2NEt (278 μL, 1.60 mmol, 13.3 equiv), and SO_3•Py (153 mg, 0.960 mmol, 8.00 equiv) were then added sequentially to the reaction, which was allowed to warm slowly to room temperature after 30 min. After an additional 90 min, water (3 mL), Et_2O (2 mL), and EtOAc (2 mL) were added sequentially to the reaction mixture. The layers were separated and the aqueous layer was extracted with EtOAc (3 × 2 mL). The organic layers were combined and washed with 10% aqueous HCl solution (3 × 5 mL), saturated aqueous $NaHCO_3$ solution (5 mL), and brine (5 mL). The organic layers were dried over anhydrous $MgSO_4$ and concentrated under reduced pressure. The resulting crude product was then purified by flash column chromatography (silica gel, eluent: gradient, 4:1 → 3:1 → 2:1 hexanes:EtOAc) to afford cyclic hydrate **166** (22.7 mg, 57% over 3 steps) as a white solid.

^{1}H NMR (600 MHz, C_6D_6) δ: 4.32 (d, *J* = 2.6 Hz, 2H), 3.21 (s, 2H), 3.18 (s, 2H), 2.71 (d, *J* = 2.6 Hz, 2H), 2.20–2.12 (m, 2H), 2.11–1.98 (m, 4H), 1.95–1.88 (m, 2H), 1.85–1.79 (m, 2H), 1.79–1.70 (m, 2H), 0.96 (t, *J* = 7.6 Hz, 6H), 0.94 (s, 18H), 0.33 (s, 6H), 0.19 (s, 6H). **^{13}C NMR** (126 MHz, C_6D_6) δ: 215.0, 115.6, 94.4, 90.5, 79.5, 61.0, 49.9, 36.9, 26.2, 24.8, 21.4, 18.2, 8.6, –4.3, –4.9. **FTIR** (thin film) cm^{-1}: 3397, 2928, 2856, 1743, 1463, 1251, 1109, 1060, 839, 778. **HRMS** (ESI) (*m/z*) calc'd for $C_{34}H_{56}NaO_9Si_2$ $[M+Na]^+$: 687.3355, found 687.3399. **TLC** (2:1 hexanes:EtOAc), R_f: 0.28 (Anis). **$[\alpha]_D^{25}$**: +61.4 (*c* = 0.14, CH_2Cl_2).

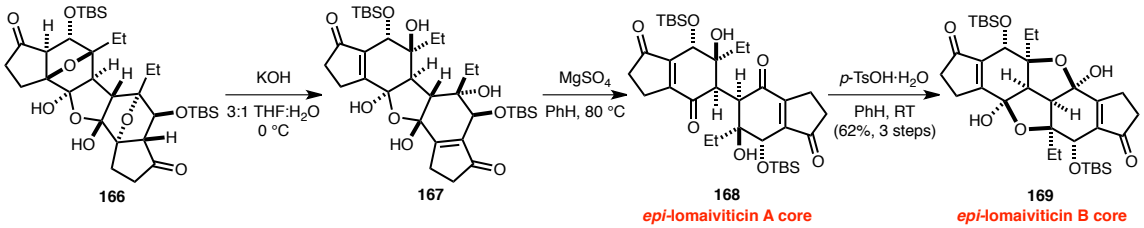

***Epi*-lomaiviticin B core 169**:

A 1 M solution of KOH in water (339 μL, 0.339 mmol, 7.00 equiv) was added dropwise via syringe to a solution of cyclic hydrate **166** (32.2 mg, 0.0480 mmol, 1.00 equiv) in 3:1 THF/water (4.85 mL) at 0 °C. After 24 h, saturated aqueous NH_4Cl solution (1 mL) was added to the stirred reaction mixture, which was then allowed to warm to room temperature. The resultant mixture was diluted with EtOAc (3 mL) and the layers were separated. The aqueous layer was extracted with EtOAc (3 × 3 mL). The organic layers were combined and washed with brine (5 mL), dried over anhydrous $MgSO_4$, and concentrated under reduced pressure to afford crude bisenone cyclic hydrate product **167**, which was carried forward to the next step without further purification.

$MgSO_4$ (70.0 mg, 0.581 mmol, 12.0 equiv) was added in a single portion to a stirred solution of crude **167** in benzene (6.9 mL), and the resultant slurry was heated to 80 °C. After 24 h, the slurry was filtered and concentrated under reduced pressure to afford crude *epi*-lomaiviticin A core **168**, which was carried forward to the next step without further purification.

p-TsOH·H_2O (1.9 mg, 0.010 mmol, 0.20 equiv) was added in a single portion to a stirred solution of crude **168** in benzene (6.9 mL). After 24 h, saturated aqueous $NaHCO_3$ solution was added to the stirred reaction mixture. The resultant mixture was diluted with EtOAc (4 mL) and the layers were separated. The aqueous layer was extracted with EtOAc (3 × 4 mL) and the organic layers were combined, washed with brine (6 mL), dried over anhydrous $MgSO_4$, and concentrated under reduced pressure. The crude residue was then purified by flash column chromatography (silica gel, eluent: gradient, 4:1 → 3:1 → 2:1 hexanes:EtOAc) to afford *epi*-lomaiviticin B core **169** (19.4 mg, 62% over 3 steps) as a white solid.

^{1}H NMR (600 MHz, C_6D_6) δ: 4.73 (s, 2H), 3.18 (s, 2H), 2.17–2.07 (m, 2H), 2.00–1.91 (m, 4H), 1.90–1.78 (m, 6H), 1.08 (t, J = 7.3 Hz, 6H), 0.93 (s, 18H), 0.26 (s, 6H), 0.08 (s, 6H). **^{13}C NMR** (126 MHz, C_6D_6) δ: 206.4, 170.2, 139.8, 102.9, 90.3, 61.6, 60.6, 35.5, 30.4, 26.3, 23.1, 18.6, 7.7, –4.0, –4.9. **FTIR** (thin film) cm^{-1}: 3400, 2956, 2929, 2856, 1690, 1658, 1253, 1097, 1041, 838, 777. **HRMS** (ESI) (*m/z*) calc'd for $C_{34}H_{54}NaO_8Si_2$ $[M+Na]^+$: 669.3249, found 669.3262. **TLC** (2:1 hexanes:EtOAc), R_f: 0.27 (UV, Anis). **$[\alpha]_D^{25}$**: +35.0 (c = 0.53, CH_2Cl_2).

II. A Biomimetic Unified Strategy for the Synthesis of 7-Membered Ring-Containing *Lycopodium* Alkaloids

Chapter 3

Introduction to the *Lycopodium* Alkaloids

Introduction

The *Lycopodium* alkaloids, isolated from the *Lycopodium* club mosses, are a diverse family of complex polycyclic natural products that have long attracted interest in synthetic chemistry due to their fascinating structures and interesting biological activity.[78] Since the isolation of the first *Lycopodium* alkaloid, lycopodine[79] (**1**, Figure 3.1), by Bödeker from *Lycopodium complanatum* in 1881, over 250 *Lycopodium* alkaloids have been isolated and characterized to date.[78] Not only have the *Lycopodium* alkaloids served as challenging targets for total synthesis, but their complex structures have also provided ample opportunities for new synthetic methodology development.

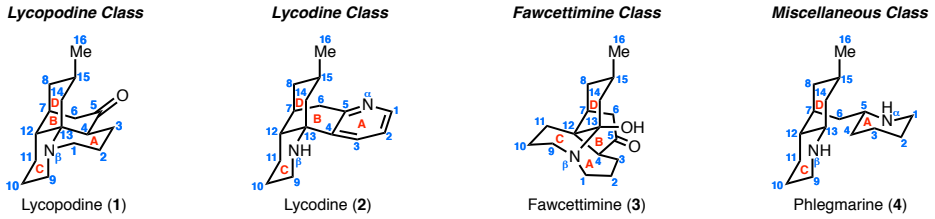

Figure 3.1. Representative members of the four *Lycopodium* alkaloid structural classes.[80]

The *Lycopodium* alkaloids have been categorized into four general structural classes, comprising the lycopodine, lycodine, fawcettimine, and the miscellaneous classes,[78] representative members of which are shown in Figure 3.1 The lycopodine structural class (**1**) is characterized by four fused six-membered rings, two of which (A- and C-rings) form a quinolizidine. In the lycodine class (**2**), members characteristically contain four rings, with the B-, C-, and D-rings being the same as in the lycopodine class. However, the A-ring is rearranged (no Nβ–C1 connectivity) and typically

---

[78] For reviews on the *Lycopodium* alkaloids, see: (a) Kobayashi, J.; Morita, H. In *The Alkaloids*; Cordell, G. A., Ed.; Academic Press: New York, 2005; Vol. 61, pp 1–57. (b) Ma, X.; Gang, D. R. *Nat. Prod. Rep.* **2004**, *21*, 752–772. (c) Ayer, W. A.; Trifonov, L. S. In *The Alkaloids*; Cordell, G. A., Brossi, A., Ed.; Academic Press: New York, 1994; Vol. 45, pp 233–266.

[79] Bödeker, K. *Justus Liebigs Ann. Chem.* **1881**, *208*, 363–367.

[80] The positional numbering system is represented in accordance with Conroy's original proposed biosynthesis. Please see: Conroy, H. *Tetrahedron Lett.* **1960**, *1*, 34–37.

exists as a pyridine or pyridone ring. Thus far, all of the *Lycopodium* alkaloids, notably huperzine A,[81] with biological activity associated with acetylcholinesterase inhibition belong to the lycopodine class. The fawcettimine class (**3**) can be derived from the lycopodine class via C4–C13 to C4–C12 bond migration. Lastly, the miscellaneous class (**4**) encompasses all of the *Lycopodium* alkaloids that do not fall into the category of the three aforementioned classes. In particular, members of the miscellaneous class do not contain either C4–C13 or C4–C12 connectivity.

Since Conroy's original biosynthetic hypothesis, a revised biosynthesis of the *Lycopodium* alkaloids based on ^{14}C- and ^{13}C-feeding studies has been proposed.[82] Lysine could initially undergo decarboxylation and subsequent oxidative cyclization to afford Δ^1-piperideine (**7**, Figure 3.2). Next, a Mannich reaction between **7** and 3-oxoglutaric acid, followed by decarboxylation, could provide pelleterine (**9**). **9** may then undergo dimerization via an intermolecular aldol reaction to furnish dimer **10**. Phlegmarine carbon skeleton **12** could then arise from **10** via oxidation and a subsequent intramolecular aldol reaction to form the C7–C12 bond. An intramolecular Mannich reaction could then establish the C4–C13 bond, resulting in tetracycle **13**, from which the lycodine structural class may arise. Alternatively, the lycopodine class (**1**) could be derived from **13** via: (1) hydrolysis of the Nα–C5 imine, (2) deamination, and (3) formation of the Nβ–C1 bond. Subsequent oxidation of **1** at C12 could then result in the formation of lycodoline (**14**). The fawcettimine class may be accessed from **14** via migration of C4 from C13 to C12.[83] Further rearrangement and oxidation of members of each structural class could then engender the vast and diverse *Lycopodium* alkaloid natural products.

---

[81] (a) Tang, X. C.; Han, Y. F.; Chen, X. P.; Zhu, X. D. *Acta Pharmacol. Sin.* **1986**, *7*, 507–510. (b) Tang, X. C.; Sarno, P. D.; Sugaya, K.; Giacobini, E. *J. Neurosci. Res.* **1989**, *24*, 276–285. (c) Liu, J. S.; Yu, C. M.; Zhou, Y. Z.; Han, Y. Y.; Wu, F. W.; Qi, B. F.; Zhu, Y. L. *Acta Chim. Sin. Eng. Ed.* **1986**, *44*, 1035–1040. (d) Liu, J. S.; Zhu, Y. L.; Yu, C. M.; Zhou, Y. Z.; Han, Y. Y.; Wu, F. W.; Qi, B. F. *Can. J. Chem.* **1986**, *64*, 837–839.

[82] (a) Hemscheidt, T.; Spenser, I. D. *J. Am. Chem. Soc.* **1996**, *118,* 1799–1800. (b) Hemscheidt, T.; Spenser, I. D. *J. Am. Chem. Soc.* **1993**, *115,* 3020–3021, and references therein.

[83] Blumenkopf, T. A.; Heathcock, C. H. In *Alkaloids: Chemical and Biological Perspectives*; Pelletier, S. W., Ed.; John Wiley and Sons: New York, 1983; Chapter 5.

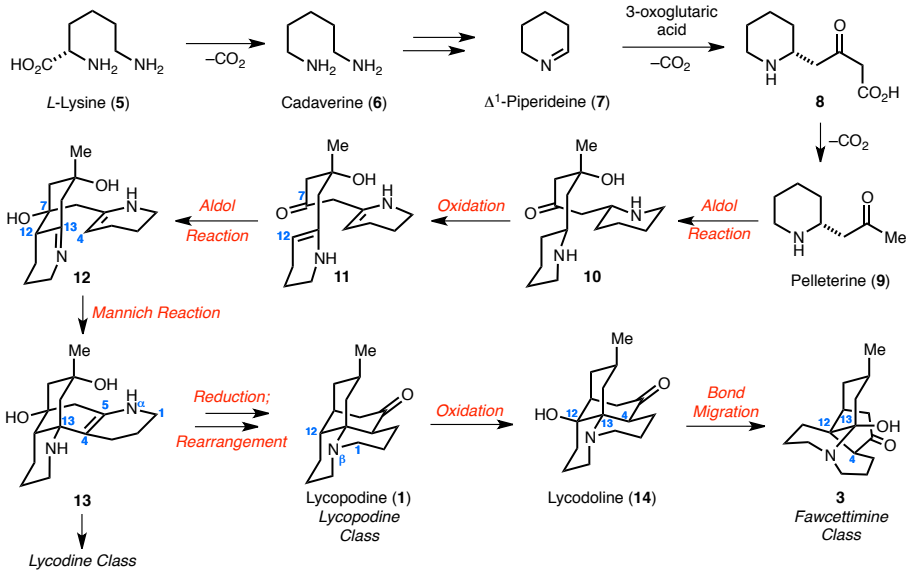

Figure 3.2. Proposal for the biosynthesis of the *Lycopodium* alkaloids.

Selected Total Syntheses of the *Lycopodium* Alkaloids

The structurally diverse *Lycopodium* alkaloids have had an established history in the field of organic synthesis ever since the foundational syntheses of lycopodine (**1**) by Stork[84] and Ayer[85] in 1968; they continue to attract widespread interest due to their fascinating and complex polycyclic structures and promising bioactivity. A survey of relevant total syntheses of various *Lycopodium* alkaloids will be presented.

Highlights from the inaugural synthesis of (±)-lycopodine (**1**) by Stork and coworkers will first be discussed. The synthesis commenced with the diastereoselective 1,4-conjugate addition of methylcuprate, generated from MeMgI and CuCl, to cyclohexenone **15**, furnishing cyclohexanone **16** (Scheme 3.1).[86] The diastereoselectivity of this reaction was controlled through stereoelectronically favored axial attack by the methylcuprate *anti* to the pseudoequatorial C7-substituent. Condensation of **16** with pyrrolidine in the presence of *p*-TsOH resulted in formation of the corresponding pyrrolidinenamine. Treatment with acrylamide then yielded two separable regioisomeric quinolones. Upon exposure to H_3PO_4/HCO_2H, desired quinolone **17** underwent an intramolecular Friedel–Crafts alkylation to afford tetracycle **20** as a single diastereomer. This transformation occurred via initial formation of *N*-acyliminium ions **18** and **19**, which could then undergo an intramolecular Friedel–Crafts reaction to establish the C4–C13 bond by trapping with the pendant *p*-methoxybenzyl group, leading to two possible epimeric products at C12, **21** and **20**, respectively. Stork and coworkers postulated that a Curtin-Hammett situation could be operative and if initial protonation of enamide **17** was reversible and faster than the ensuing intramolecular Friedel–Crafts reaction, then only the desired C12-epimer **20** would be obtained from *N*-acyliminium **19**, since the reactive conformation of **18** is unfavorable. A total synthesis of lycopodine (**1**) was then accomplished from **20**.

---

[84] Stork, G.; Kretchmer, R. H.; Schlessinger, J. *J. Am. Chem. Soc.* **1968**, *90*, 1647–1648.

[85] Ayer, W. A.; Bowman, W. R.; Joseph, T. C.; Smith, P. *J. Am. Chem. Soc.* **1968**, *90*, 1648–1650.

[86] Allinger, N. L.; Riew, C. K. *Tetrahedron Lett.* **1966**, *12*, 1269–1272.

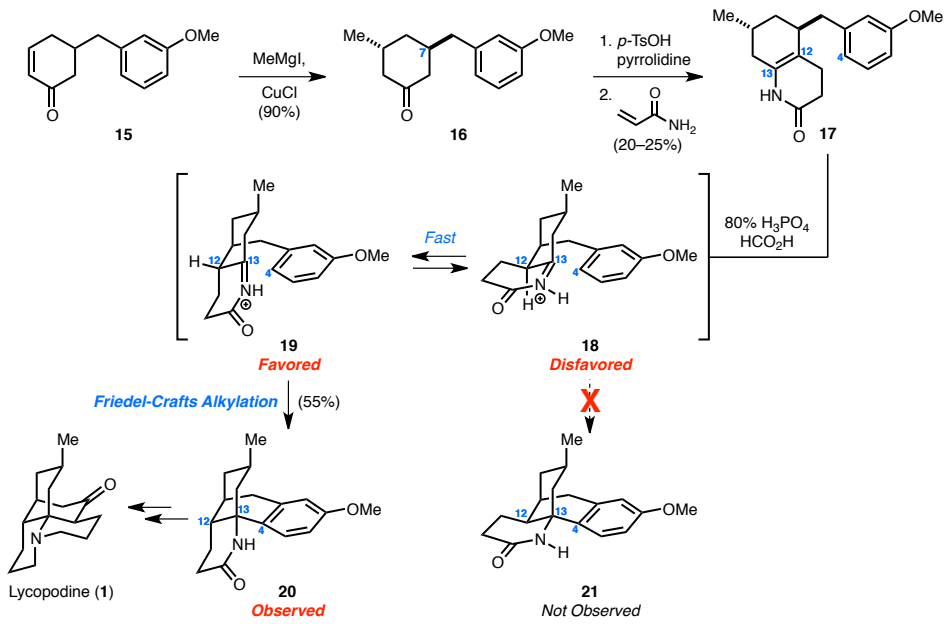

Scheme 3.1. Stork's total synthesis of (±)-lycopodine (**1**).

In 1978, Heathcock and coworkers also achieved a synthesis of (±)-lycopodine (**1**).[87] The synthesis commenced with stereoelectronically favored 1,4-conjugate addition of the lithium anion of *N,N*-dimethylhydrazone **23** to cyclohexenone **22** *anti* to the C16-methyl group,[86] furnishing cyclohexanone **24** upon hydrolysis of the hydrazone (Scheme 3.2). A ~1:1 mixture of inconsequential C12-epimers (vide infra) was obtained as a result of unselective protonation of the copper enolate intermediate. Ketal-protection of the carbonyl groups followed by nitrile reduction afforded primary amine **25**. Heating **25** in the presence of HCl then furnished tricycle **26** as a single diastereomer via a cascade set of reactions. This cascade occurred via: (1) cleavage of the ketal groups, (2) condensation of the primary amine with the C13-ketone to form the corresponding iminium ion intermediate, and (3) an intramolecular Mannich reaction to establish the C4–C13 bond. Although **25** existed as a ~1:1 mixture of C12-epimers, Heathcock postulated that rapid interconversion of the C12-epimers of the C13-iminium ion intermediate could occur via the Nβ–

---

[87] (a) Heathcock, C. H.; Kleinman, E.; Binkley, E. S. *J. Am. Chem. Soc.* **1978**, *100*, 8036–8037; (b) Heathcock, C. H.; Kleinman, E.; Binkley, E. S. *J. Am. Chem. Soc.* **1982**, *104*, 1054–1068.

C13–C12 enamine tautomer. However, only one C12-epimer of the C13-iminium ion could undergo a favorable intramolecular Mannich cyclization reaction.[84] Tricycle **26** was then converted to (±)-lycopodine (**1**) in two steps.

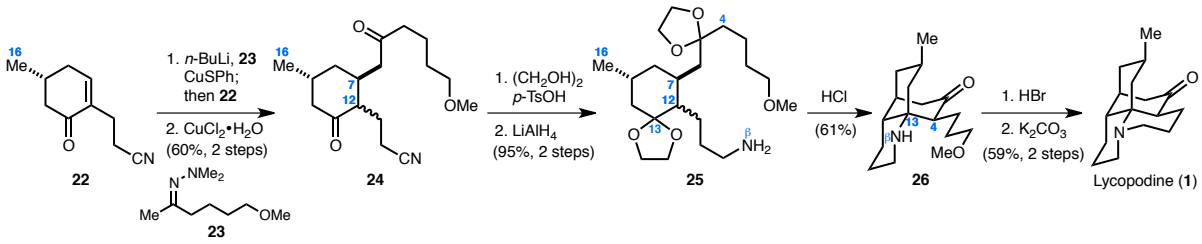

Scheme 3.2. Heathcock's total synthesis of (±)-lycopodine (**1**).

More recently, Smith and Beshore achieved the total syntheses of (+)-lyconadin A (**31**) and (–)-lyconadin B (**32**),[88] members of the miscellaneous class (Scheme 3.3). The lyconadins contain an additional C4–C10 linkage, resulting in a 7-membered ring. The key transformation involved exposure of ketoaldehyde **27** to HCl to afford tricycle **30** as a single diastereomer (84% yield) via: (1) a Robinson annulation to construct cyclohexenone intermediate **28**, (2) intramoleculer *7-endo-trig* 1,4-conjugate addition to form the C6–C7 bond via stereoelectronically favored axial attack[89] *anti* to the C16-methyl group, and (3) protonation of the resultant enol intermediate **29** to provide the incorrect C12-stereocenter. Unfortunately, the C12-stereocenter could not be directly epimerized, and several synthetic operations were required to invert the configuration of this stereocenter.

---

[88] (a) Beshore, D. C.; Smith, A. B., III. *J. Am. Chem. Soc.* **2007**, *129*, 4148–4149; (b) Beshore, D. C.; Smith, A. B., III. *J. Am. Chem. Soc.* **2008**, *130*, 13778–13789.

[89] Pseudoequatorial attack of cyclohexenone intermediate **28** is disfavored due to a developing 1,2-allylic strain between the C7- and C12-substituents in the transition state. This rationale likely accounts for the stereoselectivity of the conjugate addition in the key step of Heathcock's synthesis of lycopodine (**22** to **24**).

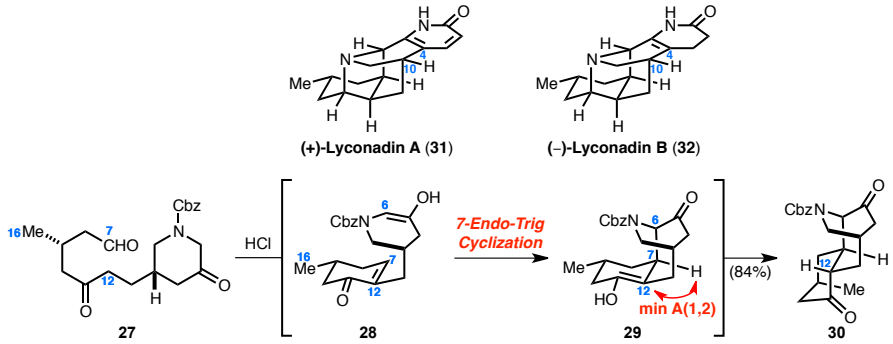

Scheme 3.3. Key step from Smith's syntheses of (+)-lyconadin A (**31**) and (–)-lyconadin B (**32**).

In 2009, Sarpong and coworkers also completed a total synthesis of (+)-lyconadin A (**31**) (Scheme 3.4).[90] Hydrogenolysis of advanced intermediate **33**, followed by addition of $NaBH_4$, delivered secondary amine **34** via: (1) cleavage of the Cbz group, (2) condensation of the resultant amine with the ketone to form the corresponding imine, and (3) reduction of the imine intermediate. Treatment of **34** with *n*-BuLi resulted in deprotonation of the amine and the pseudobenzylic position to form the corresponding dianion, which upon addition of I_2, furnished desired pentacycle **36**. Alternatively, **36** could also be accessed via a two-step protocol involving: (1) addition of NIS to the dianion generated from *n*-BuLi at −78 °C to afford iodide **35**, and (2) heating **35** with *t*-BuOK to yield the tertiary amine with the desired C6–N connectivity. Finally, cleavage of the methyl ether in **36** with NaSEt delivered (+)-lyconadin A (**31**).

---

[90] (a) Bisai, A.; West, S. W.; Sarpong, R. *J. Am. Chem. Soc.* **2008**, *130*, 7222–7223. (b) West, S. P.; Bisai, A.; Lim, A. D.; Narayan, R. R.; Sarpong, R. *J. Am. Chem. Soc.* **2009**, *131*, 11187–11194.

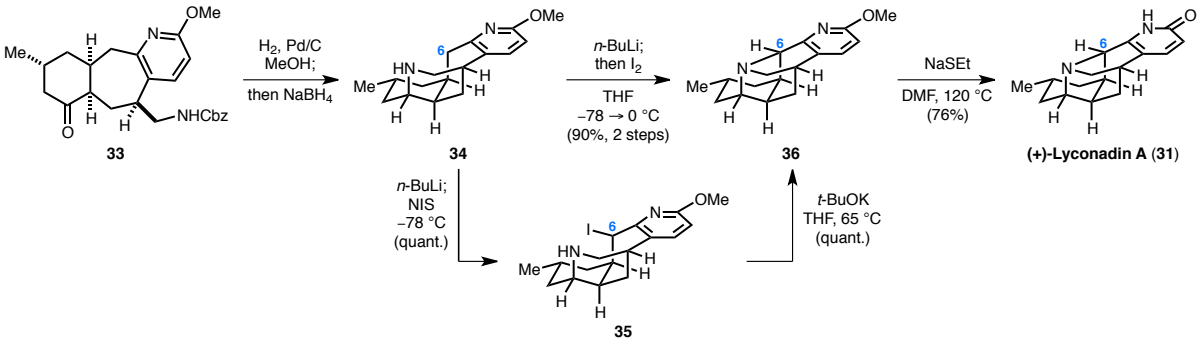

Scheme 3.4. Key transformations from Sarpong's synthesis of (+)-lyconadin A (**31**).

To summarize this chapter, a brief introduction and background for the *Lycopodium* alkaloid family of natural products was presented. Selected relevant syntheses, including Stork and Heathcock's respective total syntheses of (±)-lycopodine (**1**) and Smith and Sarpong's respective syntheses of lyconadins A and B (**31** and **32**, respectively), were reviewed. Key lessons learned from the syntheses presented, which are relevant to our own syntheses of himeradine A (**38**), lycopecurine (**39**), and lyconadins A (**31**) and B (**32**), include: (1) introduction of the C6–C7 bond *anti* to the C16-methyl group could be accomplished stereoselectively, (2) the C4–C13 bond could be established via a biomimetic Mannich reaction, and (3) the C6–N bond of the lyconadins could be introduced at a late-stage through an oxidative amination reaction.

II. A Biomimetic Unified Strategy for the Synthesis of 7-Membered Ring-Containing *Lycopodium* Alkaloids

Chapter 4

Total Synthesis of the Proposed Structure of (–)-Himeradine A

Introduction

A unique subset of the lycodine structural class, including (+)-fastigiatine (**37**)[91] and (–)-himeradine A (**38**),[92] contains an unprecedented pentacyclic core with a C4–C10 or C14–C3 bond, respectively, in contrast to lycodine (**2**) (Figure 4.1). The C4–C10 or C14–C3 linkage introduces significant strain and complexity to these structures, resulting in five contiguous stereocenters and a densely functionalized pyrrolidine ring. From a synthetic perspective, (–)-himeradine A (**38**) is arguably the most challenging *Lycopodium* alkaloid and contains seven rings, three potentially basic nitrogens, ten stereocenters, and a quinolizidine subunit appended to the pentacyclic core via a methylene linker.

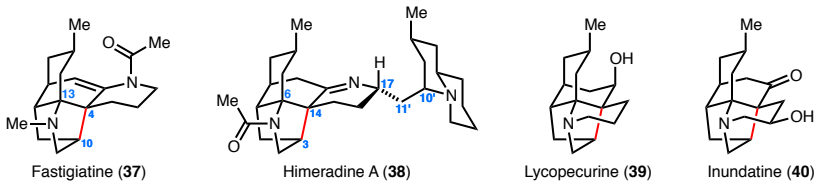

Figure 4.1. Examples of *Lycopodium* alkaloids containing an unprecedented pentacyclic core.

Although the relative stereochemistry of fastigiatine (**37**) was unambiguously established by single crystal X-ray diffraction analysis,[91] the structure and relative stereochemistry of each individual subunit of himeradine A (**38**), the pentacyclic core and the quinolizidine, were elucidated by ^{1}H, ^{13}C, COSY, HMQC, HMBC, and NOESY NMR experiments in addition to IR and FABMS/MS data.[92] However, the relative stereochemistry between the pentacyclic core and the quinolizidine remains ambiguous due to their relative isolation from one another. The large vicinal coupling constants observed between H11'b/H17 and H11'b/H10' suggest that the relative conformation between the two individual subunits is rigidly locked through H11'. Furthermore, a

---

[91] (a) Gerard, R. V.; MacLean, D. B.; Fagianni, R.; Lock, C. J. *Can. J. Chem.* **1986**, *64*, 943–949; (b) Gerard, R. V.; MacLean D. B. *Phytochemistry* **1986**, *25*, 1143–1150.

[92] Morita, H.; Hirasawa, Y.; Kobayashi, J. *J. Org. Chem.* **2003**, *68*, 4563–4566.

Monte Carlo simulation followed by minimization was consistent with the observed NOESY data and proton vicinal coupling constants. Thus, the relative stereochemistry of himeradine A (**38**) was assigned as illustrated in Figure 4.1.

MacLean and coworkers originally proposed a biosynthesis of the pentacyclic core of fastigiatine (**37**) and himeradine A (**38**)[91a] (Figure 4.2). Iminium ion intermediate **41** was postulated to undergo an intramolecular Mannich reaction,[82,83] forming the C4–C13 bond to afford lycodane skeleton **42**. **42** could then undergo oxidative functionalization at C10 to yield tetracycle **43**. Next, it was proposed that an enamine S_N2 cyclization to form the key C4–C10 bond occurs, furnishing the desired pentacyclic core **44**. We speculated, however, that this proposed S_N2 alkylation requires accessing an unfavorable, strained boat-like conformation in order to achieve requisite orbital overlap. Furthermore, **43** is not a particularly reactive electrophile.

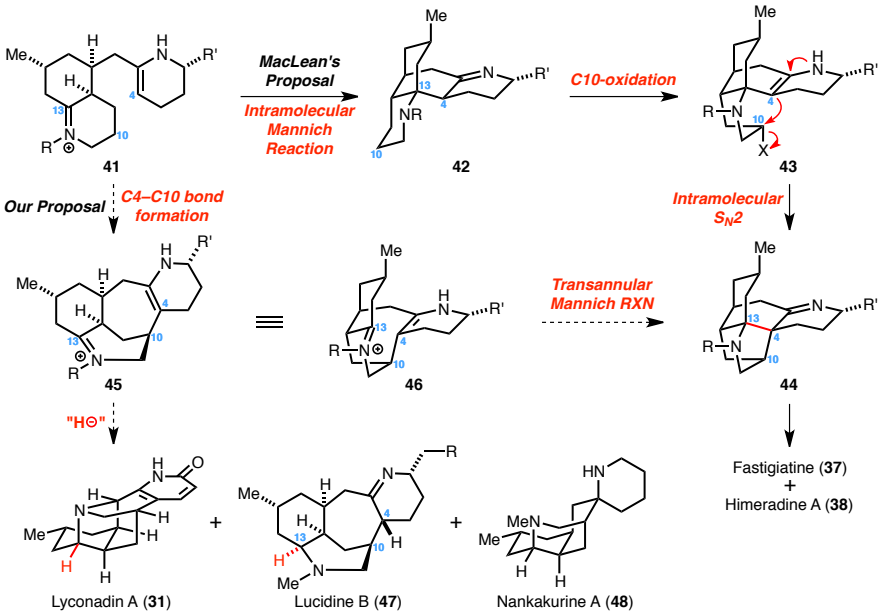

Figure 4.2. MacLean's proposal for the biosynthesis of the pentacyclic core of fastigiatine (**37**) and himeradine A (**38**) and our revised biosynthesis.

Hence, we proposed an alternative biosynthetic pathway for accessing the strained pentacyclic core of **37** and **38**. We speculated that the C4–C10 bond of **41** is installed prior to the formation of the C4–C13 bond, potentially via an intramolecular enamine S_N2 reaction of an

oxidatively functionalized derivative of **41** at C10. The proposed reactive conformation for this intramolecular S_N2 reaction to occur is less strained than that required for **43**. Drawing analogy to MacLean's proposed biosynthesis, tetracycle **45** (redrawn in 3D as **46**) could now undergo a key intramolecular transannular Mannich reaction to construct the pentacyclic core of fastigiatine (**37**) and himeradine A (**38**). Other *Lycopodium* alkaloids could also be accessed from intermediate **45**, including lyconadin A (**31**), lucidine B (**47**), and nankakurine A (**48**) via reduction of the C13-iminium ion. Our proposed biosynthetic hypothesis straightforwardly illuminates both the common origin and divergence of 7-membered ring-containing *Lycopodium* alkaloids. MacLean's biosynthetic proposal, however, would require **44** to undergo a retro-Mannich reaction to **46**, which although plausible, seems circuitous.

We were attracted to a synthesis of fastigiatine (**37**) and himeradine A (**38**) not only because of their structural complexity and unprecedented pentacyclic cores, but we also wanted to address our proposed biosynthetic hypothesis and whether a transannular Mannich reaction could be employed. Furthermore, due to their low abundance from natural sources, extensive biological testing of **37** and **38** has not been conducted. Himeradine A (**38**) has been demonstrated to exhibit cytotoxicity against murine lymphoma L1210 cells in vitro with IC_{50} = 10 μg/mL,[92] and related members have shown promising neurological bioactivity. At the outset of this project, a synthesis of fastigiatine (**37**) and himeradine A (**38**) had not yet been achieved in the literature. In 2010, Dr. Brian B. Liau[93] in the Shair group accomplished the first total synthesis of (+)-fastigiatine, which will be discussed in the next section.

---

[93] Liau, B. B.; Shair, M. D. *J. Am. Chem. Soc.* **2010**, *132*, 9594–9595

Total Synthesis of (+)-Fastigiatine

Dr. Brian B. Liau's proposed cascade sequence[94] for the synthesis of (+)-fastigiatine (**37**) is illustrated in Scheme 4.1. As discussed previously, we envisioned installing the C4–C13 bond in tetracycle **57** via a biomimetic transannular Mannich reaction to afford the strained pentacyclic core **58**. Tetracycle **57** could be accessed from enone **49** via initial condensation of Nα with the C5-ketone to form imine **50**, followed by tautomerization to the exocyclic Nα–C5–C6 enamine,[95,96] which is now poised to undergo a 7-*endo-trig* intramolecular cyclization[88] to form the C6–C7 bond. Two possible reactive conformations exist, **51** and **52**, which result from either stereoelectronically favored pseudoaxial[97] 1,4-conjugate addition *syn* or *anti* to the C16-methyl group, respectively. Based on a steric argument, addition *anti* to the C16-methyl group should be favored.[88] Next, stereoelectronically favored axial protonation of the resultant enol **53** (redrawn as **54**) at C12 could then afford tricycle **55**. At this stage of synthetic planning, the exact order of bond-forming events was considered flexible and hence, numerous strategies could be possible depending on a judicious selection of nitrogen protecting groups.

Tricycle **55** could either exist as the keto-enamine form or undergo a subsequent transannular aldol reaction to afford tetracycle **56**. However, if the C13-ketone is kinetically accessible from **56**, then condensation of Nβ with the C13-ketone could occur to provide iminium ion intermediate **57**, which could then undergo the key biomimetic transannular Mannich reaction to furnish the desired pentacyclic core **58**. This cascade sequence, which constitutes a formal [3+3]-

---

[94] Liau, B. B. Ph.D. Thesis, Harvard University, 2013.

[95] Although the endocyclic enamine tautomer is thermodynamically favored over the exocyclic tautomer in related systems, the exocyclic enamine tautomer can be accessed. Please see: Movassaghi, M.; Chen, B. *Angew. Chem. Int. Ed.* **2007**, *46*, 565–568.

[96] This would render the C4-stereocenter inconsequential to the cascade reaction.

[97] Pseudo-equatorial attack would result in an intermediate that suffers 1,2-allylic strain.

cycloaddition,[98] could potentially occur in a one-pot operation to generate up to two σ C–C bonds, two σ C–N bonds, and one σ C–H bond. (+)-Fastigiatine (**37**) could then be synthesized from pentacycle **58** in a few straightforward steps.

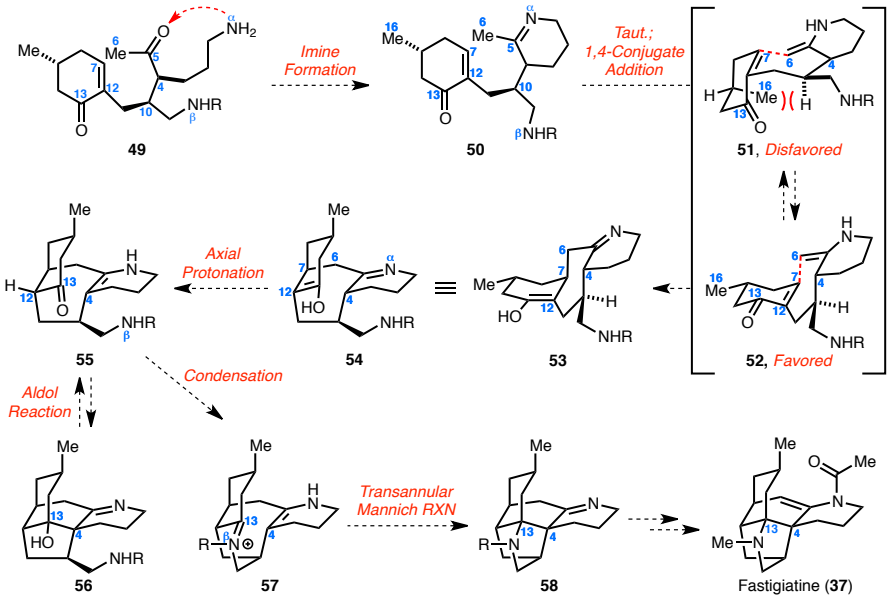

Scheme 4.1. Proposed cascade sequence for the total synthesis of (+)-fastigiatine (**37**).

Our retrosynthetic analysis of the cascade precursor **59** is shown in Scheme 4.2. Diamine **59** could be accessed from a pyrrolidinone precursor such as **60**, which could be assembled in a highly convergent fashion from three building blocks via nucleophilic opening of cyclopropane[99] **62** by organometallic **61** to form the C12–C11 bond, followed by alkylation of the resultant dicarbonyl anion intermediate with electrophile **63**.

---

[98] Schumann, D.; Naumann, A. *Liebigs Ann. Chem.* **1983**, 220–225.

[99] For a review on electrophilic cyclopropanes, see: Danishefsky, S. *Acc. Chem. Res.* **1979**, *12*, 66–72.

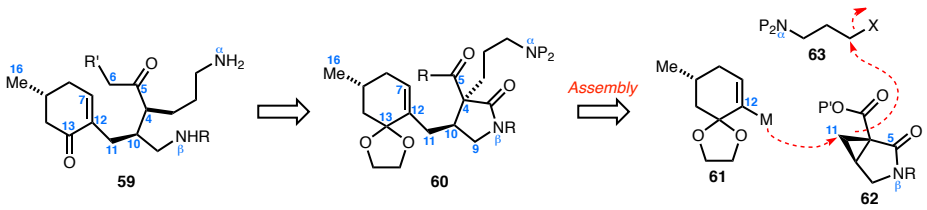

Scheme 4.2. Retrosynthetic analysis of cascade precursor **59**.

In beautiful work by Dr. Brian B. Liau, the synthesis commenced with the nucleophilic opening of cyclopropane **64**, which was prepared in six steps from (*S*)-epichlorohydrin, by organometallic **65** (Scheme 4.3).[93,100] Upon treatment with mixed dioorganocuprate **65**, cyclopropane **64** underwent regioselective opening at C11 to afford carboxyimide **66** in excellent yield (93%). This convergent coupling could be conducted on greater than 5-g scale. Carboxyimide **66** underwent efficient alkylation with 1-chloro-3-iodopropane and the resultant primary chloride was then displaced with NaN_3 to yield azide **67**. Exposure of **67** to TBAF in the presence of DBU resulted in cleavage of the 2-(trimethylsilyl)ethyl (TMSE) ester with concomitant decarboxylation,[101] followed by in situ base-catalyzed epimerization at C4. Next, the C6-carbon was introduced by addition of MeMgBr to the C5-carbonyl, affording hemiaminal **69** as a mixture of diastereomers. Dehydration and ketal deprotection of **69** with CSA occurred smoothly to furnish the corresponding dihydropyrrole. Staudinger reduction of the azide then yielded primary amine **70**.

---

[100] Majetich, G.; Leigh, A. J.; Condon, S. *Tetrahedron Lett*. **1991**, *32*, 605–608.

[101] Knobloch, E.; Brückner, R. *Synlett* **2008**, *12*, 1865–1869.

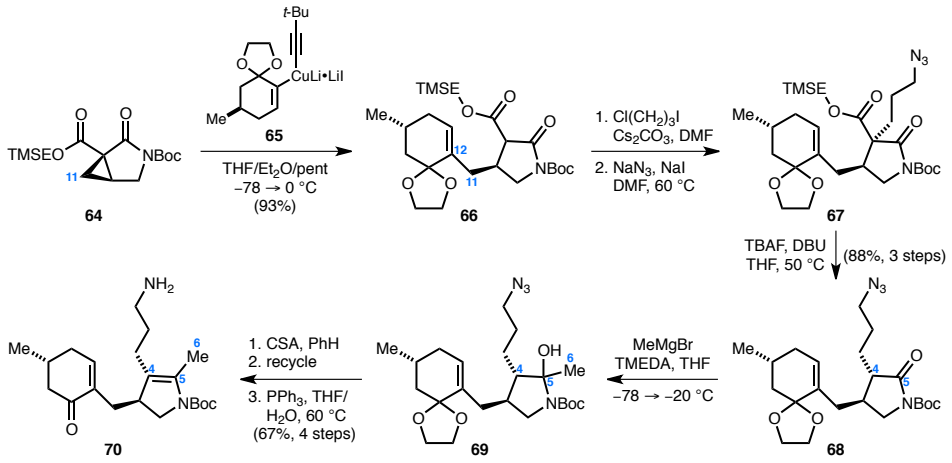

Scheme 4.3. Synthesis of cascade precursor dihydropyrrole **70**.

Although the C–N bond connectivity was incorrect, **70** could still potentially serve as a cascade substrate since the more nucleophilic Nα-amine could theoretically exchange with the Nβ-carbamate to provide imine **74** (Scheme 4.4). At the time, we assumed that **70** could not undergo 5-*endo-trig* cyclization to form the undesired C4–C7 bond since this would be in violation of Baldwin's rules.[102] Imine **74** could then undergo 7-*endo-trig* cyclization to afford tricycle **75**, which, after a subsequent transannular aldol reaction, should result in the formation of tetracycle **71** or **72**. Heating **70** with PPTS in EtOH resulted in the formation of a single new product. However, instead of obtaining desired tetracycle **71** or **72**, constitutional isomer **73** was isolated instead.

[102] (a) Baldwin, J. E. *J. Chem. Soc., Chem. Commun.*, **1976**, 734–736. (b) Johnson, C. D. *Acc. Chem. Res.* **1993**, *26*, 476–482.

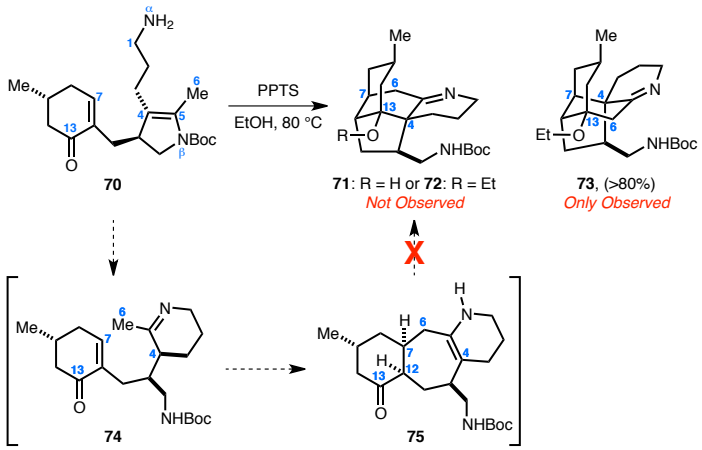

Scheme 4.4. Attempted cascade with dihydropyrrole **70**.

Our proposed mechanism for the formation of **73** is illustrated in Scheme 4.5. Formation of the corresponding oxocarbenium from dihydropyrrole **70** resulted in a 5-*endo-trig* cyclization to establish the undesired C4–C7 bond *anti* to the C16-methyl group in the *cis*-5,5-bicyclic iminium ion intermediate **76**. The highly charged oxocarbenium intermediate most likely allowed an exception to Baldwin's rules, which generally disfavors 5-*endo-trig* cyclizations. Nα and Nβ could then undergo transamination to provide imine **77**, which upon tautomerization to the corresponding exocyclic enamine, could undergo cyclization via a transannular aldol reaction to yield **73**. Two important lessons were learned from such a disappointing result: (1) the correct C–N bond connectivity was required for the cascade reaction because (2) the 5-*endo-trig* cyclization was facile.

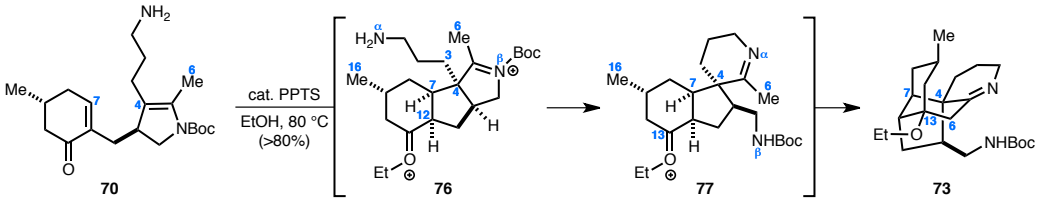

Scheme 4.5. 5-*Endo-trig* cyclization to form tetracycle **73**.

To this end, we next focused our attention on installing the correct C–N bond connectivity (Scheme 4.6). Unfortunately, however, efforts to form the 6-membered imine **78** with the correct

C5–Nα bond connectivity from **69** proved unsuccessful (Eq. 1). We speculate that these results were suggestive of a strong thermodynamic preference for the 5-membered ring system containing the incorrect C5–Nβ bond.[103] Hydrolysis of the C5–Nβ bond or formation of the corresponding Weinreb amide from **68** (Eq. 2) were also explored. Unsurprisingly, recyclization back to **68** was a recurring problem. Eventually we discovered that Staudinger reduction of the azide in **68** resulted in formation of valerolactam **79**, which possessed the desired C5–Nα bond connectivity.

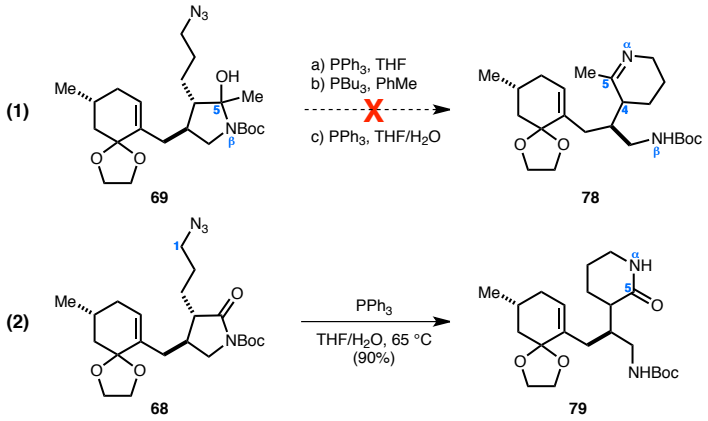

Scheme 4.6. Efforts to install the correct C5–Nα bond connectivity.

Attempted introduction of the C6-carbon unit proved challenging (Scheme 4.7). We initially planned to synthesize the corresponding thioamide of **79**, followed by a subsequent Eschenmoser coupling reaction. However, thioamide formation proved unsuccessful. Efforts to synthesize the exocyclic enamide [104] of Boc-protected lactam **80** with Petasis reagent [105] resulted in translactamization to **81**.

---

[103] A very similar thermodynamic preference to form the 5-membered ring system was also observed with the butyrolactone series. See ref. 94.

[104] Langlois, N. *Org. Lett.* **2002**, *4*, 185–187.

[105] Petasis, N. A.; Bzowej, E. I. *J. Am. Chem. Soc.* **1990**, *112*, 6392–6394.

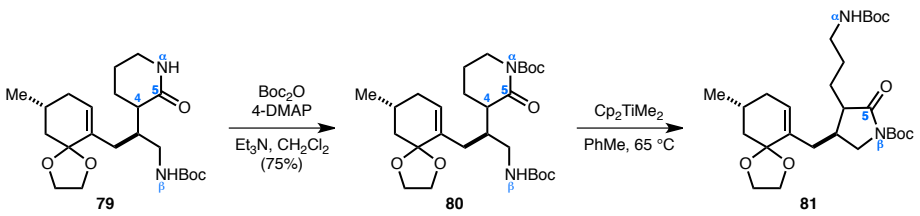

Scheme 4.7. Attempted incorporation of the C6-carbon unit.

At this point, it became apparent that a revised protecting group strategy was necessary in order to reduce the propensity of our system to form the cyclic 5-membered ring with the incorrect C5–Nβ bond connectivity. We postulated that such a solution could be realized by replacing the Nβ-Boc group with a 2-nitrobenzenesulfonyl (Ns) group,[106] which should inductively deactivate the nitrogen atom. To this end, chemoselective cleavage of the *N*-Boc group of **68** with $Mg(ClO_4)_2$ in the presence of the C13-ketal occurred smoothly (Scheme 4.8).[107] Protection of the resultant pyrrolidinone with a Ns group afforded *N*-Ns-2-pyrrolidinone **82**. Gratifyingly, addition of the lithium enolate of *t*-butylacetate to the C5-carbonyl occurred smoothly to furnish β-keto ester **83**, with Nβ completely disengaged from C5. Heating **83** with PPh_3 resulted in a Staudinger reaction[108] to provide vinylogous urethane **84** as an inconsequential ~3:2 mixture of C4-epimers. The C6-*t*-butyloxycarbonyl serves two crucial functions, one of which was to induce preferential formation of the exocyclic Nα–C5–C6 enamine in order to suppress undesired 5-*endo-trig* cyclization. Secondly, vinylogous urethanes are easier to handle in comparison to their enamine counterparts because they are stable, non-basic, and can be readily purified.

All that remained in order to test the key cascade sequence included: (1) deprotection of the Nβ-Ns group, (2) cleavage of the C13-ketal, and (3) condensation of Nβ with the C13-carbonyl to

---

[106] Fukuyama, T.; Jow, C.-K.; Cheung, M. *Tetrahedron Lett*. **1995**, *35*, 6373–6374.

[107] Stafford, J. A.; Brackeen, M. F.; Karanewsky, D. S.; Valvano, N. L. *Tetrahedron Lett*. **1993**, *34*, 7873–7876.

[108] Lambert, P. H.; Vaultier, M.; Carrié, R. *J. Org. Chem*. **1985**, *50*, 5352–5356.

form the corresponding iminium ion intermediate. Attempted cleavage of the Nβ-Ns group, however, resulted in the formation of 5-membered vinylogous urethane **85**, the product of a facile transamination reaction. Hence, it was clear from these results that the Nβ-Ns group would have to be removed at a later stage.

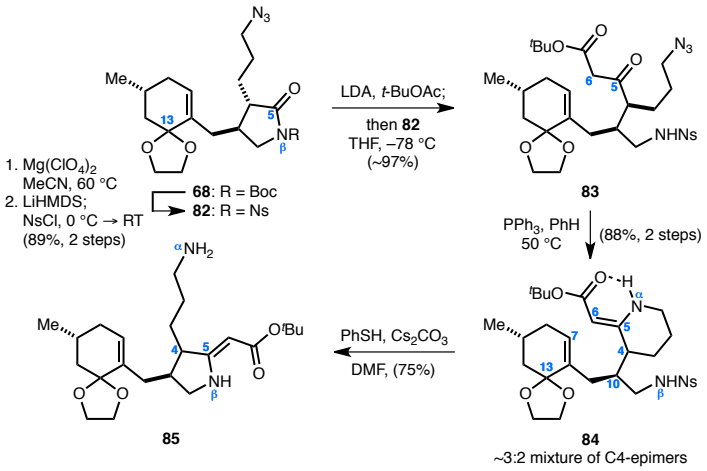

Scheme 4.8. Installation of the correct C5–Nα connectivity via inductive deactivation of Nβ.

Instead, vinylogous urethane **84** was directly exposed to aqueous HCl (Scheme 4.9), which furnished tetracycle **92** as a single diastereomer in 92% yield via: (1) initial C13-dioxolane cleavage, (2) 7-*endo-trig* intramolecular 1,4-conjugate addition[88] to form the C6–C7 bond via stereoelectronically favored axial attack *anti* to the C16-methyl group, (3) tautomerization to secure the C12-stereocenter via stereoelectronically favored axial protonation, and (4) a transannular aldol reaction to form the C4–C13 bond. This transformation constitutes a formal [3+3]-cycloaddition.[109]

---

[109] (a) Gosh, S. K.; Buchanan, G. S.; Long, Q. A.; Wei, Y.; Al-Rashid, Z. F.; Sklenicka, H. M.; Hsung, R. P. *Tetrahedron* **2008**, *64*, 883–893, and references therein. (b) See ref 95.

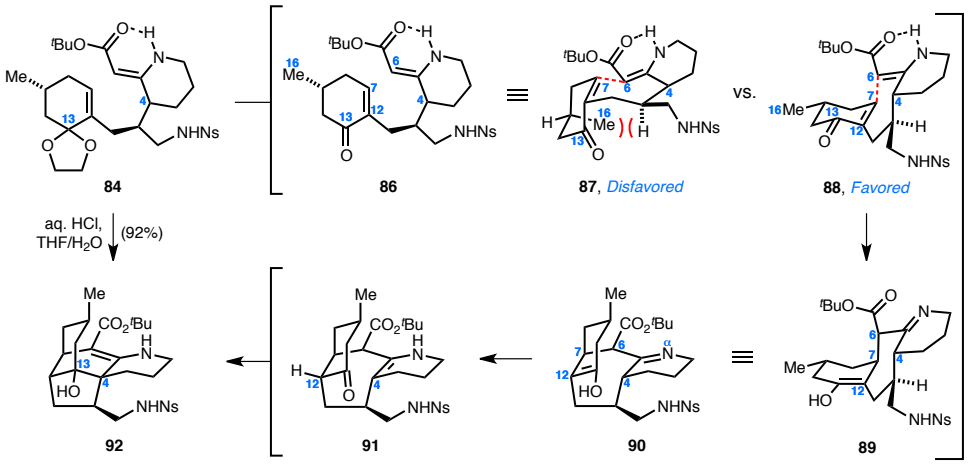

Scheme 4.9. A formal [3+3]-cycloaddition reaction to construct tetracycle **92**.

All that remained in order to complete a synthesis of the pentacyclic core of fastigiatine (**37**) was to formally exchange the C13-hydroxyl with Nβ (Scheme 4.10). This was accomplished via initial alkylation of **92** with MeI in the presence of K_2CO_3, followed by addition of PhSH, to yield *N*-methylamine **93**. Heating **93** in 2,2,2-trifluoroethanol (TFEOH) cleanly delivered pentacycle **96** in 85% yield via: (1) an initial retro-aldol reaction, (2) condensation of Nβ with the C13-ketone to form the corresponding iminium ion, and (3) the pivotal biomimetic transannular Mannich reaction. Use of TFEOH, a strong hydrogen-bond donor but not a strong acid, as solvent was crucial to the success of this reaction. We speculated that under acidic conditions, protonation of Nβ would occur, thus disfavoring the formation of the positively charged intermediates involved in the retro-aldol reaction. Next, heating **96** in the presence of *p*-TsOH induced *t*-butyloxycarbonyl removal to afford the corresponding imine. Finally, exposure of the resultant imine to Ac_2O in the presence of Et_3N cleanly delivered (+)-fastigiatine (**37**). The structure of **37** was unambiguously confirmed by single crystal X-ray diffraction analysis.

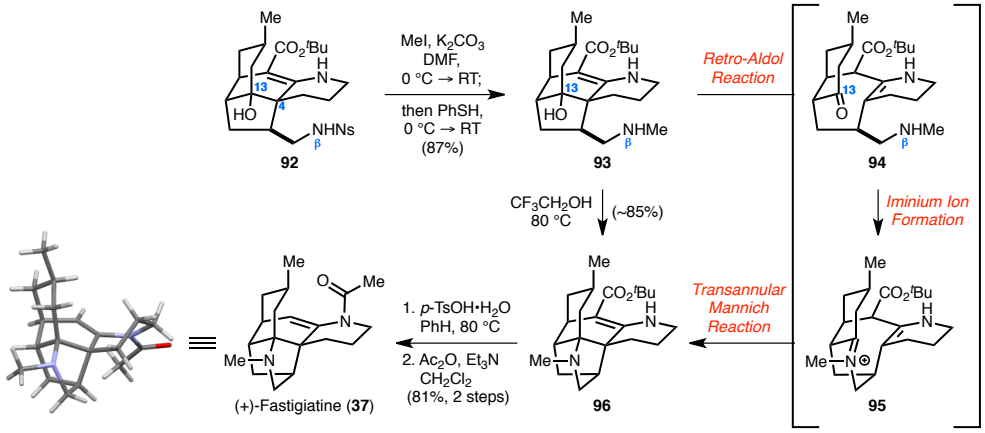

Scheme 4.10. Completed total synthesis of (+)-fastigiatine (**37**).

Key lessons learned from Dr. Brian B. Liau's synthesis of fastigiatine (**37**), which would subsequently be applied to a successful synthesis of the proposed structure of (–)-himeradine A (**38**), include a highly convergent fragment coupling via a nucleophilic cyclopropane opening, a diastereoselective formal [3+3]-cycloaddition reaction, and a transannular Mannich reaction to construct the pentacyclic core common to both **37** and **38**. However, the ultimate goal we hoped to achieve in a total synthesis of himeradine A (**38**), which was not realized in our synthesis of fastigiatine (**37**), was a one-pot cascade reaction to construct the strained core system that would obviate the need to formally exchange the C13-hydroxyl with Nβ. Furthermore, we envisioned we could program the new cascade sequence order such that we could potentially access all 7-membered ring-containing *Lycopodium* alkaloids via a unified, biomimetic, convergent strategy.

Total Synthesis of the Proposed Structure of (–)-Himeradine A

(–)-Himeradine A (**38**) is arguably the most synthetically challenging *Lycopodium* alkaloid and contains, in addition to the aforementioned unprecedented pentacyclic core with a C3–C14 linkage, seven rings, three potentially basic nitrogens, ten stereocenters, and a quinolizidine subunit appended to the core via a methylene linker. A synthesis of himeradine A (**38**) has not yet been reported in the literature. Our retrosynthetic analysis of **38** is outlined in Scheme 4.11. Analogous to our synthesis of fastigiatine (**37**), we envisioned constructing the C6–C14 bond in **38** from hexacyclic intermediate **97** via a biomimetic transannular Mannich reaction to afford the strained core skeleton. Intermediate **97** (redrawn in 2D as **98**) could arise from a 7-*endo-trig* intramolecular 1,4-conjugate addition of the β-keto ester to the cyclohexenone in **99**, and condensation of Nα and Nβ with the C13- and C6-carbonyls, respectively. As discussed previously, the ultimate objective was to accomplish a one-pot cascade reaction to construct the strained core in **38** from β-keto ester **99** in a single operation, a goal not realized in our synthesis of fastigiatine (**37**). **99** could be synthesized in a highly convergent fashion from three building blocks via alkylation of β-carboxyimide **100** with quinolizidine iodide **101** or related derivatives, followed by subsequent addition of the lithium enolate of *t*-butylacetate **102** to the C13-carbonyl.

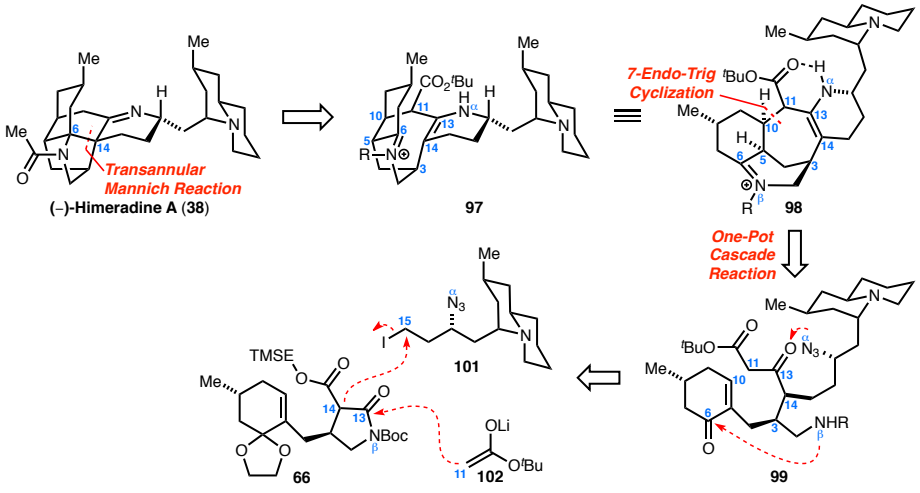

Scheme 4.11. Retrosynthetic analysis of (–)-himeradine A (**38**).

Our first-generation retrosynthesis of the quinolizidine subunit is outlined in Scheme 4.12. The desired carboxyimide alkylation electrophile **101** could potentially be synthesized from quinolizidine **103** via a few straightforward manipulations, including a Mitsunobu displacement of the C17-hydroxyl group by azide. Quinolizidine **103** could be constructed from allyl *N*-Boc-piperidine **104**. The C6'-stereocenter in **104** could be installed via a diastereotopic deprotonation at C6' in *N*-Boc piperidine **105**, followed by alkylation. Furthermore, we envisioned installing the C10'- and C17-stereocenters by relaying the stereochemical information of the single C8'-stereocenter in *N*,*O*-methoxyacetal **106** to first introduce the C10'- followed by the C17-stereocenter.

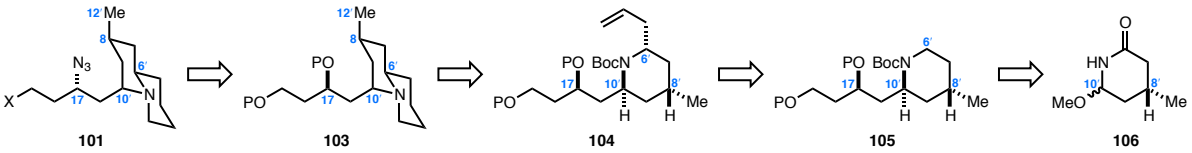

Scheme 4.12. First-generation retrosynthesis of the quinolizidine subunit.

The synthesis commenced with the lipase-mediated desymmetrization of 3-methylglutaric anhydride with *n*-PrOH to afford carboxylic acid **107** (93% ee) (Scheme 4.13).[110] Chemoselective reduction of the carboxylic acid with BH_3•SMe_2 occurred smoothly to provide the corresponding carbinol, which underwent Parikh-Doering oxidation to yield aldehyde **108**. Heating **108** in NH_3/MeOH afforded a mixture of *N*,*O*-hydroxy- and *N*,*O*-methoxyacetals. Exposure of this crude product mixture to *p*-TsOH in MeOH[111] at 50 °C resulted in complete conversion to the desired *N*,*O*-methoxyacetal **106** as a mixture of diastereomers.

---

[110] Marcoux, D.; Bindschädler, P.; Speed, A. W. H.; Chiu, A.; Pero, J. E.; Borg, G. A.; Evans, D. A. *Org. Lett.* **2011**, *13*, 3758–3761.

[111] Han, M. J.; Yoo, K. S.; Kim, Y. H.; Chang, J. Y. *Org. Biomol. Chem.* **2003**, *1*, 2276–2282.

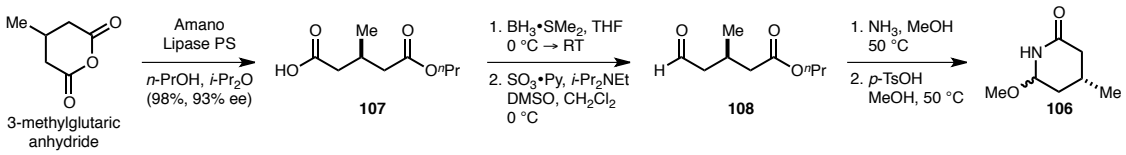

Scheme 4.13. Synthesis of *N*,*O*-methoxyacetal **106**.

Exposure of *N*,*O*-methoxyacetal **106** to BF_3•OEt_2 in the presence of silyl enol ether **109** afforded lactam **110** as a single diastereomer via an *N*-acyliminium ion Mannich reaction (Scheme 4.14).[112] The diastereoselectivity of this reaction was controlled through stereoelectronically favored axial attack by silyl enol ether **109** at C10' of the intermediate *N*-acyliminium ion *anti* to the C12'-methyl group. Chelate-controlled 1,3-*syn* reduction[113] of the ketone in **110** with DIBAL-H afforded alcohol **111** as a single diastereomer. TBS-protection of the C17-hydroxyl, followed by *N*-Boc protection of the lactam, provided imide **112**. Next, reduction of the carbonyl in **112** with DIBAL-H and subsequent exposure to BF_3•OEt_2 in the presence of Et_3SiH,[114] delivered *N*-Boc-piperidine **114**. With **114** in hand, we could next investigate the introduction of the C6'-stereocenter.

---

[112] (a) Vink, M. K. S.; Schortinghuis, C. A.; Luten, J.; Maarseveen, J. H.; Schoemaker, H. E.; Hiemstra, H.; Rutjes, F. P. J. T. *J. Org. Chem.* **2002**, *67*, 7869–7871. (b) Suzuki, H.; Aoyagi, S.; Kibayashi, C. *Tetrahedron Lett.* **1995**, *36*, 935–936.

[113] Josephsohn, N. S.; Snapper, M. L.; Hoveyda, A. H. *J. Am. Chem. Soc.* **2004**, *126*, 3734–3735.

[114] Liang, N.; Datta, A. *J. Org. Chem.* **2005**, *70*, 10182–10185.

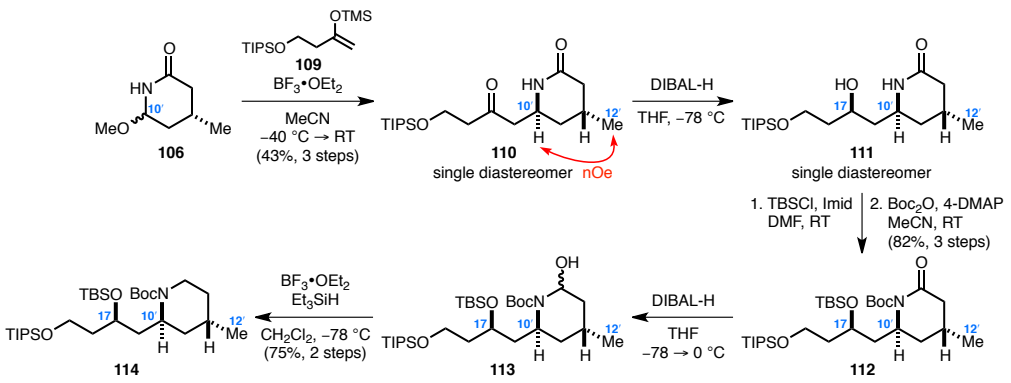

Scheme 4.14. Synthesis of *N*-Boc piperidine **114** as a single diastereomer.

We envisioned installing the C6'-stereocenter via a diastereotopic deprotonation at C6', followed by addition of a suitable electrophile.[115] A diastereotopic deprotonation of **114** at C6' was performed with *sec*-BuLi in the presence of TMEDA (Scheme 4.15). The conformation of lithiated *N*-Boc piperidine **115** is rigidly locked due to 1,3-allylic strain minimization between the *N*-Boc group and the C10'-stereocenter, which is further reinforced by equatorial positioning of the C12'-methyl group. Equatorial organolithium **115** was favored due to chelation with the *N*-Boc group. Transmetallation with Cu(I), followed by alkylation with allyl bromide, furnished the desired allylated piperidine **116** (redrawn as **117**) as a single diastereomer in 50% yield (97% brsm).

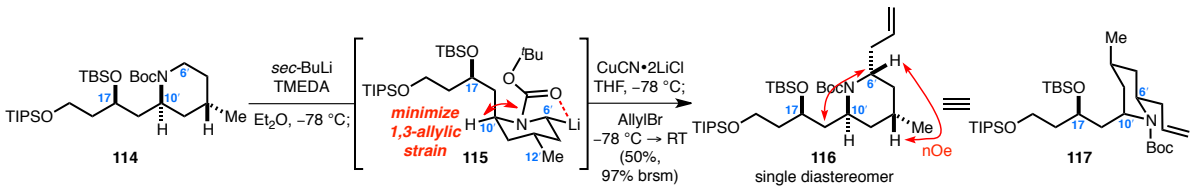

Scheme 4.15. Successful introduction of the C6'-stereocenter.

Attempts to improve the yield of the allylated product **116** beyond 50% proved challenging. Transmetallation with Cu(I) was essential or else only trace quantities of **116** were obtained. Varying

---

[115] (a) Beak, P.; Lee, W. K. *J. Org. Chem.* **1990**, *55*, 2578–2580. (b) Beak, P.; Lee, W. K. *J. Org. Chem.* **1993**, *58*, 1109–1117. (c) Guerrero, C. A.; Sorensen, E. J. *Org. Lett.* **2011**, *13*, 5164–5167.

the temperature, concentration, and time allotted for deprotonation, as well as the amount of *sec*-BuLi (from 1.3 to 3.0 equiv), TMEDA (from 1.3 to 3.0 equiv), CuCN•2LiCl (from 0.6 to 1.8 equiv), and AllylBr (from 1.5 to 3.6 equiv) used all resulted in similar or diminished yields. We suspected that complete deprotonation of sterically encumbered C6' was challenging. However, warming of the deprotonation with *sec*-BuLi (up to 0 °C) resulted in partial cleavage of the *N*-Boc protecting group. Alkylation with various electrophiles, which could potentially result in fewer downstream step manipulations, was also explored (Figure 4.3). However, in all cases, either trace quantities of the corresponding product or complete recovery of starting material **114** was observed.

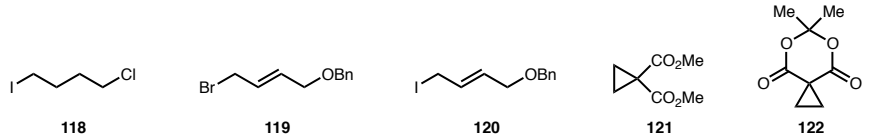

118 **119** **120** **121** **122**

Figure 4.3. Attempted introduction of other electrophiles to the C6' position.

Next, allyl *N*-Boc-piperidine **117** was converted to the desired quinolizidine **127** (Scheme 4.16). Exposure of **117** to TMSOTf in the presence of 2,6-lutidine afforded the corresponding Boc-cleaved piperidine, which underwent subsequent allylation with AllylBr and K_2CO_3 to provide tertiary amine **123**. A Grubbs II-catalyzed ring-closing metathesis[116] with *p*-TsOH protonation of the tertiary amine cleanly delivered cyclized product **124**. Hydrogenation of the alkene in **124** in the presence of AcOH furnished quinolizidine **125**. Global silyl deprotection upon heating with HCl in MeOH, followed by selective monosilylation of the primary hydroxyl group, afforded TBS-ether **126**. Finally, Mitsunobu displacement of the secondary hydroxyl group in **126** with azide, followed by cleavage of the primary TBS ether, occurred smoothly to yield alcohol **127**.

---

[116] (a) Compain, P. *Adv*. *Synth*. *Catal*. **2007**, *349*, 1829–1846. (b) Srivastava, A. K.; Das, S. K.; Panda, G. *Tetrahedron* **2009**, *65*, 5322–5327.

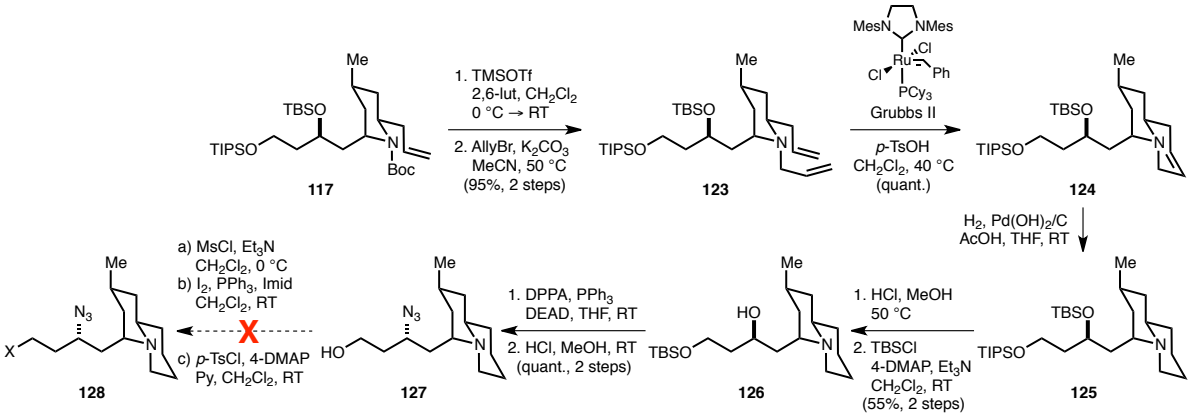

Scheme 4.16. Synthesis of quinolizidine **127**.

Unfortunately, efforts to synthesize a suitable alkylation electrophile for carboxyimide **66** from alcohol **127** were unsuccessful. Attempted synthesis of the corresponding mesylate, tosylate, and iodide from **127** resulted in decomposition in all cases. We speculate that the observed decomposition could be attributed to facile intra- and intermolecular alkylation of the desired product by the tertiary amine. Nonetheless, we demonstrated, as a proof-of-principle, that successful construction of the quinolizidine subunit from *N*-Boc-piperidine **117** was possible. In the global scheme, the quinolizidine would either have to be constructed after alkylation with imide **66** or introduced in a protected form.

To this end, we decided to synthesize the quinolizidone, a protected form of the quinolizidine (Scheme 4.17). Cleavage of the *N*-Boc protecting group, followed by condensation of the resultant secondary amine with acryloyl choride, yielded amide **129**. A Grubbs II-catalyzed ring-closing metathesis cleanly provided cyclized amide **130**. Hydrogenation of the alkene in **130** yielded quinolizidone **131**, which was converted in six steps to the desired alkylation electrophile, iodide **132**.

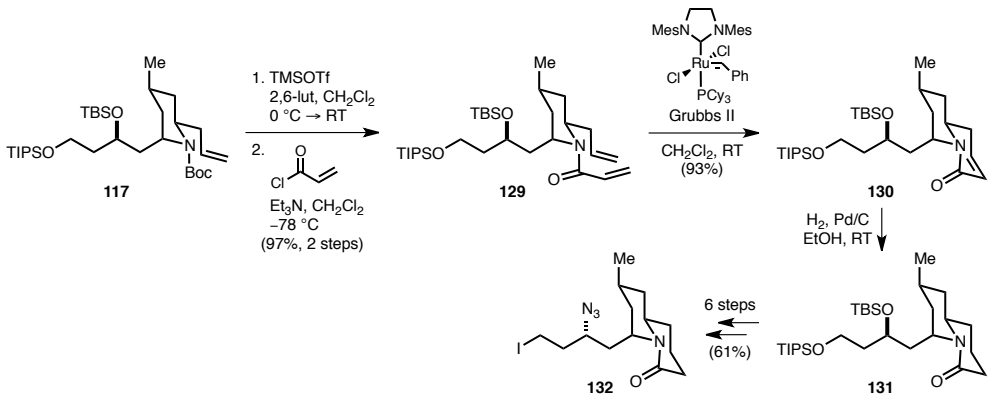

Scheme 4.17. Synthesis of quinolizidone iodide **132**.

Imide **66** underwent efficient alkylation with iodide **132** to furnish the desired alkylated product **133** in excellent yield (Scheme 4.18). **133** was converted to vinylogous urethane **134** in five steps, analogous to the sequence used in our synthesis of fastigiatine (**37**). At the outset, as a proof-of-concept, we decided to replicate the cascade utilized in our synthesis of fastigiatine (**37**) to construct the strained pentacyclic core of himeradine A (**38**). To this end, exposure of **134** to aqueous HCl resulted in a formal [3+3]-cycloaddition to afford hexacycle **136** as a single diastereomer. Next, in order to conduct a formal exchange between the C6-hydroxyl group with Nβ, the *N*-Ns protecting group must be cleaved. Surprisingly, attempted cleavage of the Ns group of **136**, or alkylated derivatives **137** and **138**, by treatment with PhSH in the presence of K_2CO_3 resulted in decomposition. We rationalized that milder deprotection conditions could be employed if a more readily cleaved Nβ-protecting group was utilized. Instead of a 2-nitrobenzenesulfonyl group, we were able to protect Nβ with a 2,4-dinitrobenzenesulfonyl group, which, unfortunately, was immediately cleaved upon addition of lithiated *t*-butylacetate during attempted formation of the desired β-ketoester analogue precursor to **134**.

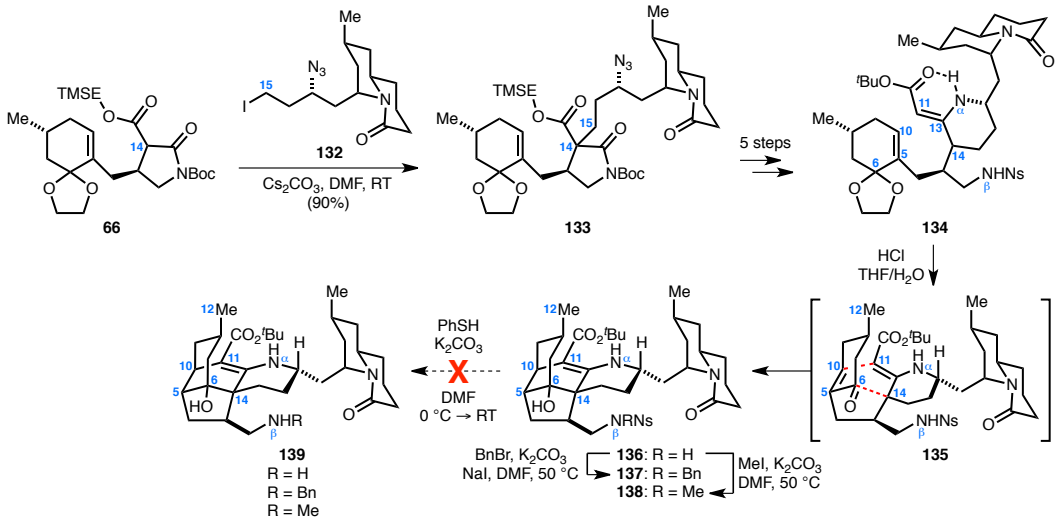

Scheme 4.18. Successful formal [3+3]-cycloaddition to afford hexacycle **136**.

A new cascade order was subsequently developed in order to circumvent the need for the C6-hydroxyl and Nβ exchange as well as to potentially permit the one-pot construction of the strained core structure in a single operation, which was not realized in our synthesis of fastigiatine (**37**) (Scheme 4.19). To this end, our strategy was revised and instead of forming vinylogous urethane **134**, **140** was directly exposed to aqueous HCl, which resulted in facile cleavage of the C6-dioxolane, affording enone **141**. Treatment of **141** with Barton's base cleanly delivered ketone **143** via: (1) a 7-*endo-trig* intramolecular 1,4-conjugate addition to form the C10–C11 bond via stereoelectronically favored axial attack *anti* to the C12-methyl group, and (2) tautomerization of the ensuing C5–C6 enol to secure the C5-stereocenter through stereoelectronically favored axial protonation. Next, cleavage of the *N*-Ns protecting group by treatment with PhSH in the presence of K_2CO_3 cleanly provided the tricyclic core of imine **144**. By forming the C10–C11 bond in **143** prior to Ns deprotection, we avoided problems associated with C13–Nβ bond formation and 5-*endo*-trig cyclizations that plagued our first-generation synthesis of fastigiatine (**37**). Furthermore, we believed that under the appropriate conditions, we could perform all of the aforementioned events in a single one-pot operation (**141** → **144**).

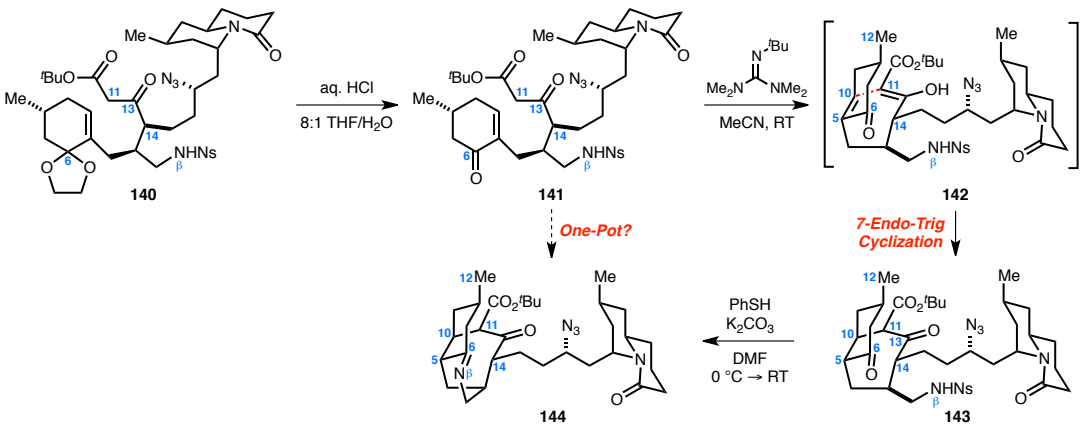

Scheme 4.19. Successful execution of a new sequence to construct tricyclic imine **144**.

While developing this novel, revised cascade sequence, we also concurrently investigated conversion of the quinolizidone moiety to the corresponding quinolizidine on a model system. Due to sensitive functionalities present in the molecule, only limited methods for converting the quinolizidone to the desired quinolizidine subunit were available. These methods include treatment of the amide with Meerwein's salt (Me_3OBF_4)[117] and subsequent reduction ($NaBH_4$), triflation of the tertiary amide followed by reduction, and formation of the corresponding thioamide and subsequent reduction.[118] Unfortunately, however, all of these methods failed to provide any desired product on our simpler model systems. Hence, another revision in our strategy was necessary.

Instead of preforming the quinolizidine or quinolizidone from **116**, we decided to carry the *N*-Boc allyl piperidine **116** forward and construct the quinolizidine bicyclic structure at a later stage (Scheme 4.20). Global silyl deprotection of *N*-Boc-piperidine **116**, followed by selective protection of the resultant primary hydroxyl, afforded TBS ether **145**. Following the same reaction sequence

---

[117] (a) Ishikawa, H.; Elliott, G. I.; Velcicky, J.; Choi, Y.; Boger, D. L. *J. Am. Chem. Soc.* **2006**, *128*, 10596–10612. (b) Martin, S. F.; Clark, C. W.; Ito, M.; Mortimore, M. *J. Am. Chem. Soc.* **1996**, *118*, 9804–9805. (c) Bonazzi, S.; Cheng, B.; Wzorek, J. S.; Evans, D. A. *J. Am. Chem. Soc.* **2013**, *135*, 9338–9341.

[118] (a) Kurasaki, H.; Okamoto, I.; Morita, N.; Tamura, O. *Org. Lett.* **2009**, *11*, 1179–1181. (b) Sirasani, G.; Paul, T.; Dougherty, W.; Kassel, S.; Andrade, R. B. *J. Org. Chem.* **2010**, *75*, 3529–3532. (c) Campbell, E. L.; Zuhl, A. M.; Liu, C. M.; Boger, D. L. *J. Am. Chem. Soc.* **2010**, *132*, 3009–3012.

utilized previously, Mitsunobu displacement of the secondary hydroxyl group in **145** with azide, followed by cleavage of the TBS ether, and formation of the corresponding iodide, occurred smoothly to yield the desired alkylation partner, iodide **147**.

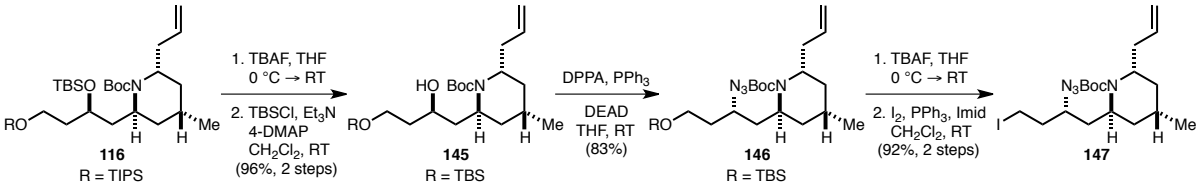

Scheme 4.20. Synthesis of *N*-Boc-piperidine iodide **147**.

Imide **66** underwent efficient alkylation with iodide **147** to provide the desired alkylated product **148** in excellent yield (94%) (Scheme 4.21). Cleavage of the TMSE ester with concomitant decarboxylation upon treatment with TBAF, followed by chemoselective cleavage of the *N*-Boc group of **149** with $Mg(ClO_4)_2$, occurred smoothly to afford pyrrolidinone **150**. Protection of **150** with a Ns group then delivered *N*-Ns-2-pyrrolidinone **151**.[119] Next, addition of the lithium enolate of *t*-butylacetate to the C13-carbonyl of **151** furnished β-ketoester **152**.

[119] Unfortunately, performing an exchange of protecting groups from Boc to Ns was necessary because attempted nucleophilic cyclopropane opening of the corresponding Ns-protected derivative of cyclopropane **64** did not yield any desired product. The Ns group appeared to have been compromised.

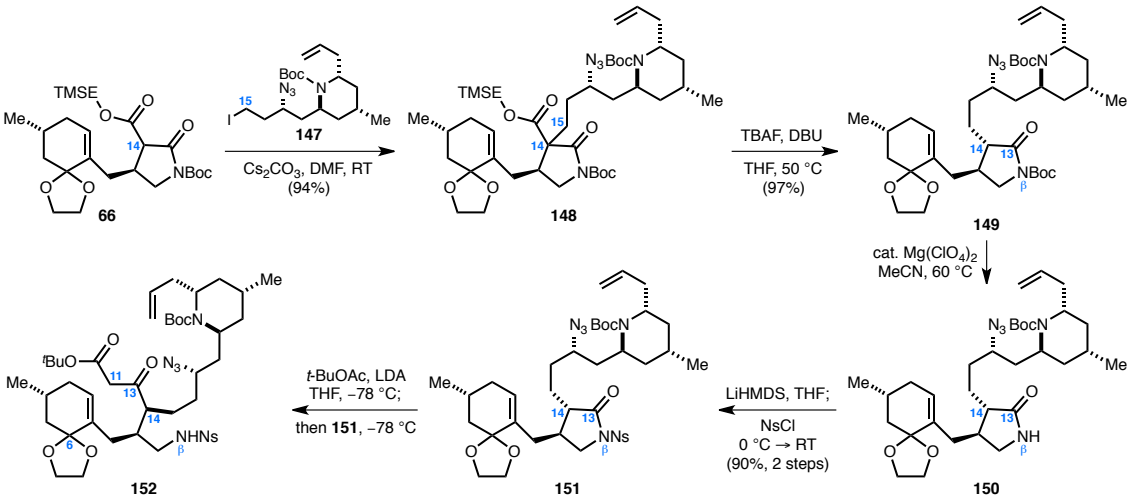

Scheme 4.21. Successful imide alkylation and synthesis of β-ketoester **152**.

Next, the C6-dioxolane of **152** was directly cleaved upon treatment with *p*-TsOH to provide enone **153** (Scheme 4.22). Next, we discovered that in a one-pot sequence involving initial exposure of **153** to Barton's base in MeCN, followed by subsequent addition of PhSH in the presence of K_2CO_3, **153** was converted to imine **156** (84%, 3 steps) via: (1) 7-*endo-trig* intramolecular conjugate addition to form the C10–C11 bond, (2) tautomerization of the ensuing C5–C6 enol to secure the C5 stereocenter, (3) cleavage of the *N*-Ns protecting group upon addition of PhSH in the presence of K_2CO_3, and (4) in situ condensation of Nβ with the C6-ketone to form the corresponding imine. Isolation of imine **156** was exciting; we believe **156** lends credence to our biosynthetic hypothesis (Figure 4.2), and this type of intermediate could potentially allow us to access other 7-membered ring-containing *Lycopodium* alkaloids, including lyconadins A-C, nankakurines A-B,[120] and lucidines A-B,[121] via reduction of the imine. Alternatively, if imine **156** undergoes the key

---

[120] For isolation and revised structural assignment, see: (a) Hirasawa, Y.; Morita, H.; Kobayashi, J. *Org. Lett.* **2004**, *6*, 3389–3391. (b) Ayer, W. A.; Ball, L. F.; Browne, L. M.; Tori, M.; Delbaere, L. T. J.; Silverberg, A. *Can. J. Chem.* **1984**, *62*, 298–302. (c) Hirasawa, Y.; Kobayashi, J.; Obara, Y.; Nakahata, N.; Kawahara, N.; Goda, Y.; Morita, H. *Heterocycles* **2006**, *68*, 2357–2364.

[121] Tori, M.; Shimoji, T.; Shimura, E.; Takaoka, S.; Nakashima, K.; Sono, M.; Ayer, W. A. *Phytochemistry* **2000**, *53*, 503–509.

biomimetic transannular Mannich reaction, not only could himeradine A (**38**) be accessed, but also lycopecurine (**39**) and inundatine (**40**). In accord with our proposed biosynthetic hypothesis, a diverse set of *Lycopodium* alkaloids could arise from a common precursor derivative such as **156**.

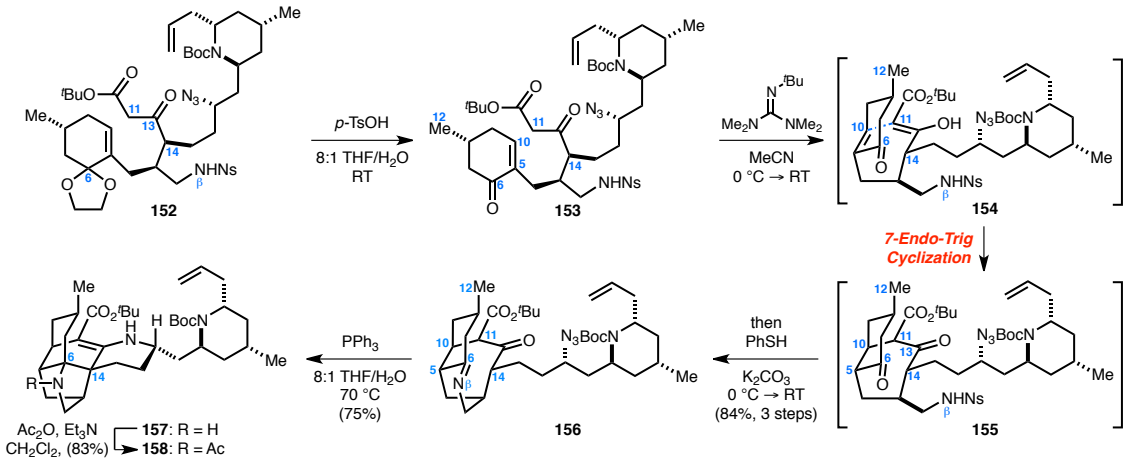

Scheme 4.22. Successful one-pot sequence to construct imine **156**, containing the strained core of himeradine A (**38**).

Next, exposure of azide **156** to PPh_3 in the presence of water afforded hexacyclic vinylogous urethane **157** in 75% yield via: (1) Staudinger reduction of the azide to the corresponding amine, (2) condensation of the resultant amine with the neighboring β-ketoester to form the vinylogous urethane, and (3) the key pivotal transannular Mannich reaction to construct the C6–C14 bond. Acetylation of the secondary amine in **157** with Ac_2O and Et_3N provided hexacycle **158** in 83% yield.

With **158** in hand, all that remained in order to complete a total synthesis of himeradine A (**38**) was to convert the *N*-Boc allyl piperidine moiety in **158** to the corresponding quinolizidine and cleave the *t*-butyl ester. As described previously (Scheme 4.16), a reaction sequence had already been developed for the construction of the quinolizidine subunit. To this end, formation of the corresponding silyloxy carbamate from *N*-Boc piperidine **158** occurred smoothly upon exposure to TBSOTf and 2,6-lutidine (Scheme 4.23). Treatment with TBAF resulted in cleavage of the silyloxy

carbamate with concomitant decarboxylation, furnishing piperidine **159**. Alkylation of **159** with AllylBr in the presence of K_2CO_3 afforded allylated product **160**. However, increasing the scale of this allylation reaction resulted in a complex product mixture, including byproducts in which the vinylogous urethane nitrogen was allylated. A new strategy for installing the quinolizidine subunit was necessary.

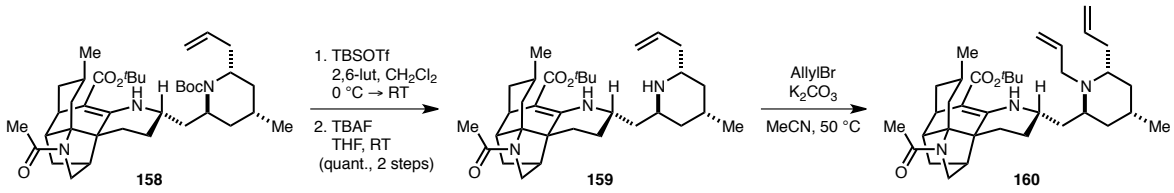

Scheme 4.23. Attempted construction of the quinolizidine subunit.

To this end, cross-metathesis[122] of the allyl group in **158** with acrolein was accomplished with Hoveyda–Grubbs catalyst II, which furnished enal **161** (Scheme 4.24). Hydrogenation of **161**, followed by reduction of the resultant aldehyde and tosylation of the corresponding hydroxyl group, afforded tosylate **162** (70%, 3 steps). Exposure of **162** to TBSOTf resulted in formation of the silyloxy carbamate, which was cleaved upon treatment with TBAF. In situ cyclization via S_N2 displacement of the tosylate group with the resultant secondary amine delivered heptacycle **163** (48%, 2 steps), which now contains the quinolizidine subunit.

[122] (a) Chatterjee, A. K.; Choi, T. L.; Sanders, D. P.; Grubbs, R. H. *J. Am. Chem. Soc.* **2003**, *125*, 11360–11370. (b) Movassaghi, M; Tjandra, M.; Qi, J. *J. Am. Chem. Soc.* **2009**, *131*, 9648–9650.

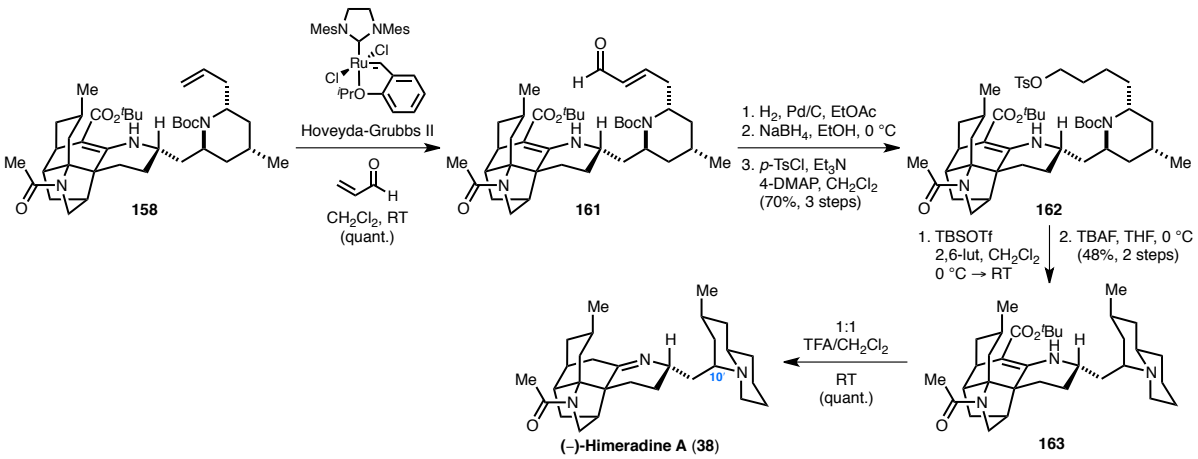

Scheme 4.24. Synthesis of the proposed structure of (−)-himeradine A (**38**).

Finally, treatment of **163** with TFA resulted in facile removal of the *t*-butyloxycarbonyl group to yield the proposed structure of (−)-himeradine A (**38**) as the double TFA salt (quant., $[\alpha]_D^{24}$ = −19 (*c* 0.3, MeOH)). Except for the chemical shift of H10', which is shifted upfield by $\Delta\delta$ = 0.14 ppm (Figure 4.4), the ^{1}H NMR, ^{13}C NMR, COSY, NOESY, HSQC, and HMBC spectra for synthetic (−)-himeradine A (**38**) are in good agreement with the values reported for the natural product ($[\alpha]_D^{25}$ = −23 (*c* 0.3, MeOH)).

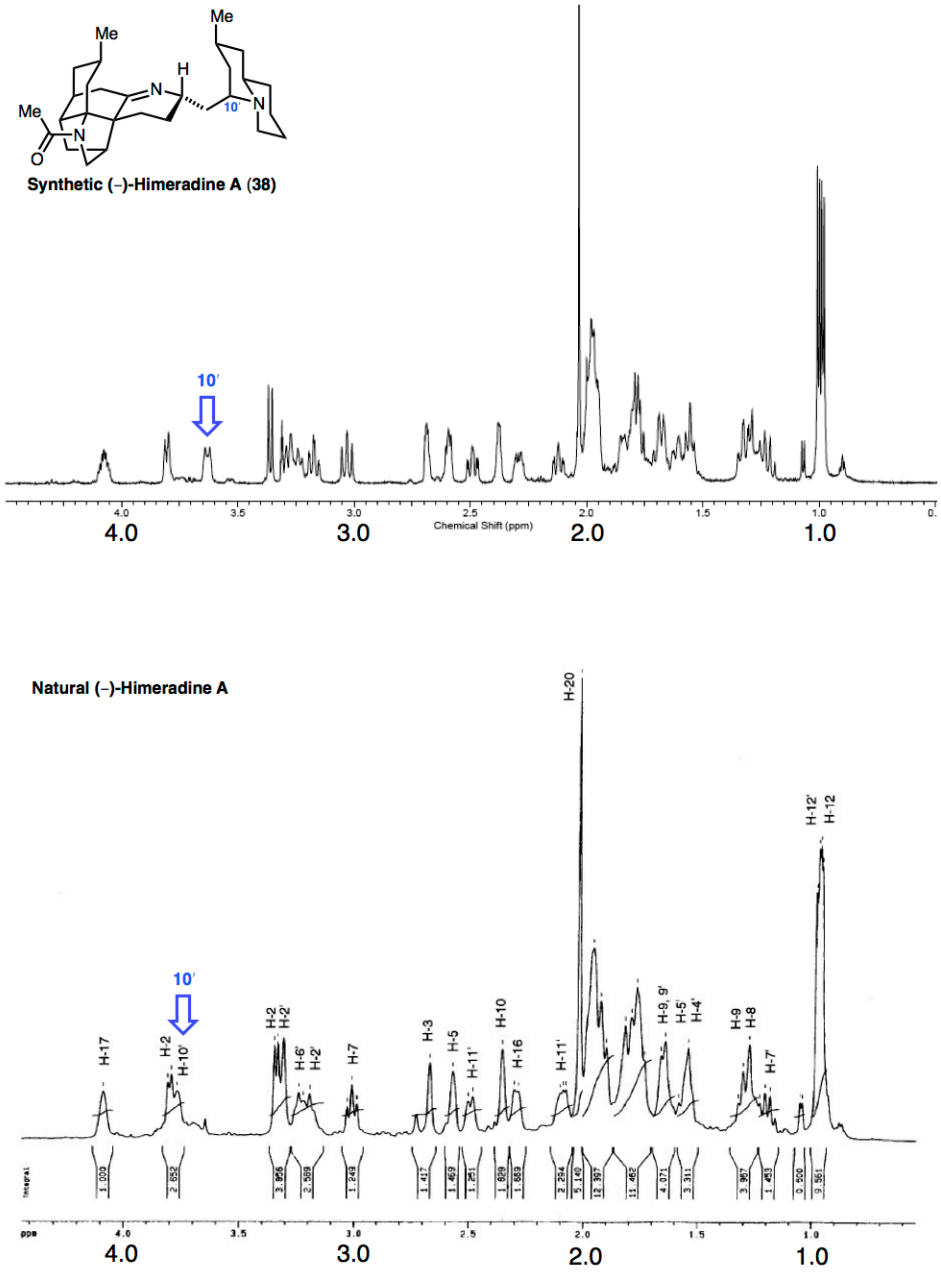

Figure 4.4. Comparison of ^{1}H NMR spectra of synthetic (**38**) and natural (–)-himeradine A as the double TFA salt in CD_3OD.

Because the protonation state of basic nitrogen atoms can have a significant impact on proton chemical shifts,[123] we carefully titrated the double TFA salt of himeradine A (**38**) with a solution of $NaOCD_3$ in CD_3OD until the free base was obtained, and then incrementally titrated known aliquots of TFA in CD_3OD until the double TFA salt was reisolated. At no point during the titration experiments were we able to identically replicate the ^1H NMR spectrum of natural himeradine A (**38**). Variable concentration and temperature effects were also investigated and found not to have an effect on H10' proton chemical shift.

We were able to obtain the ^1H NMR spectrum of the free base of natural himeradine A in CD_3OD via private communication with Professor Hiroshi Morita (Figure 4.5). While the ^1H NMR spectra of the free base of natural and synthetic himeradine A (**38**) appeared to correspond, we suspected that a structural misassignment of natural himeradine A in the original isolation report may have occurred. Several misassignment possibilities existed (Figure 4.6), including (1) the C10'-stereocenter, (2) the C6'-stereocenter, (3) the C17-stereocenter, (4) the absolute stereochemistry of the quinolizidine subunit, and (5) permutations thereof.

---

[123] (a) Altman, R. A.; Nilsson, B. K.; Overman, L. E.; Alaniz, J. R.; Rohde, J. M.; Taupin, V. *J. Org. Chem.* **2010**, *75*, 7519–7534. (b) Martin, C. L.; Overman, L. E.; Rohde, J. M. *J. Am. Chem. Soc.* **2008**, *130*, 7568–7569.

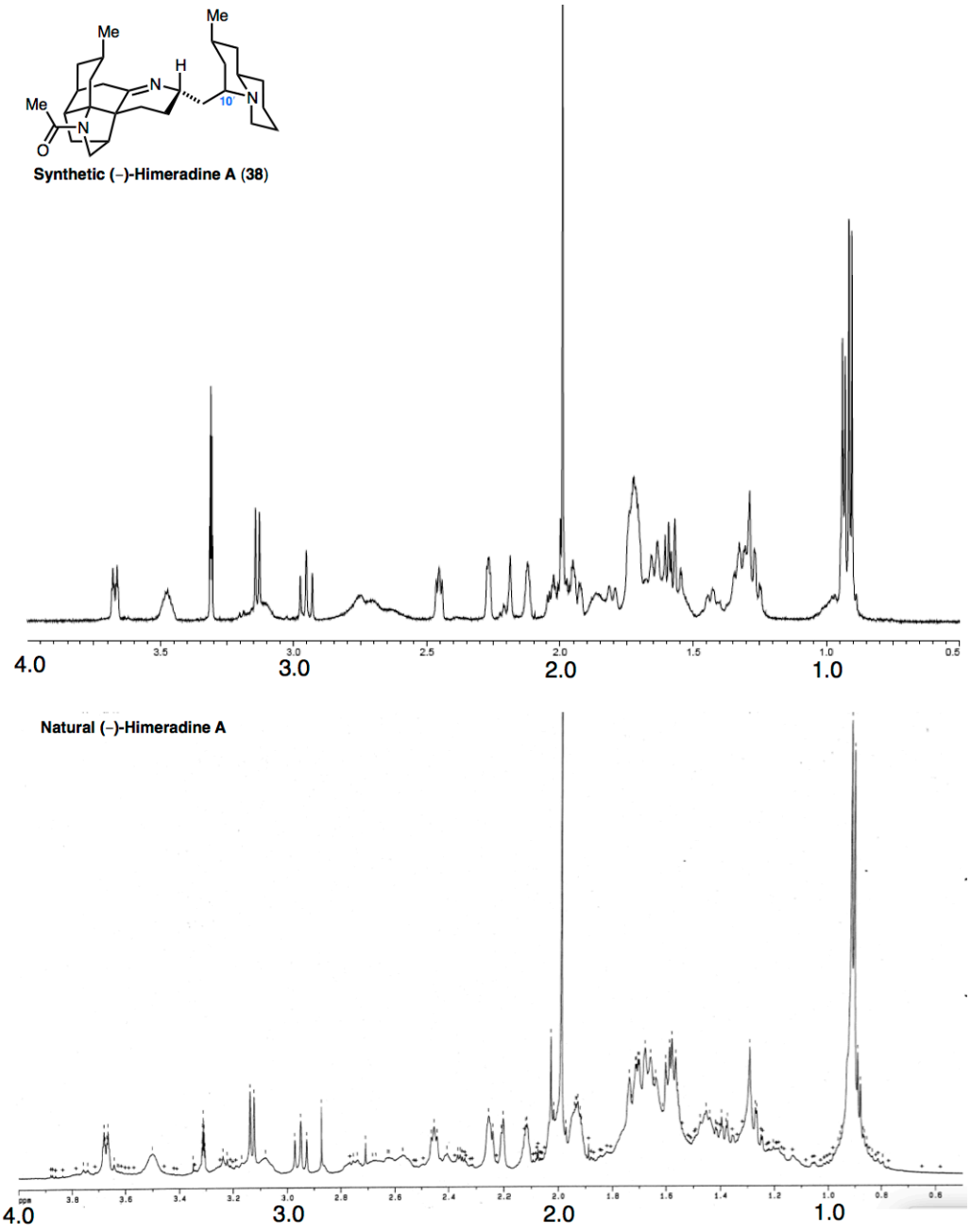

Figure 4.5. Comparison of ^{1}H NMR spectra of synthetic (**38**) and natural (–)-himeradine A as the free base in CD_3OD.

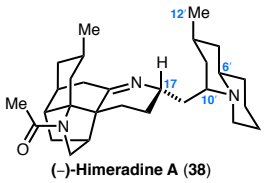

Figure 4.6. Possible candidates for the structural misassignment of himeradine A (**38**).

Since other related *Lycopodium* alkaloids[124] containing a quinolizidine subunit all possess the same absolute stereochemistry at the C12'-methyl group position, we believed it was unlikely that the absolute stereochemistry of the quinolizidine was misassigned (Figure 4.7). Additionally, we hypothesized that the stereochemical assignment of the C17-stereocenter was correct since the chemical shift of H17 for synthetic (**38**) and natural himeradine A are in good agreement. Furthermore, we believed at the time that if H17 was equatorial instead of axial, there would be a significant perturbation to the chemical shift, especially due to the adjacent imine π-system.

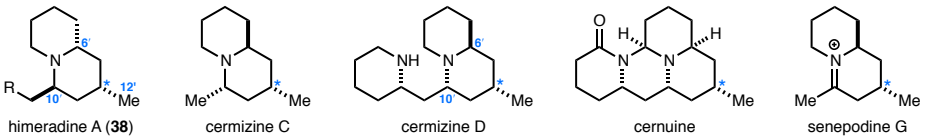

Figure 4.7. Examples of *Lycopodium* alkaloids possessing a quinolizidine subunit with the same absolute stereochemistry (denoted by *) as the C12'-methyl group in himeradine A (**38**).

Due to the aforementioned discussion, we suspected that a stereochemical misassignment of the quinolizidine subunit (C10' or C6') may have occurred, resulting in four possible stereoisomers. In the original isolation report by Kobayashi and coworkers, the stereochemical assignment of the quinolizidine subunit was made based on the putative observation of several key NOESY

---

[124] (a) Morita, H; Hirasawa, Y.; Shinzato, T.; Kobayashi, J. *Tetrahedron* **2004**, *60*, 7015–7023. (b) Ayer, W. A.; Jenkins, J. K.; Valverde-Lopez, S. *Can. J. Chem.* **1967**, *45*, 433–443. (c) Ayer, W. A.; Jenkins, J. K.; Piers, K.; Valverde-Lopez, S. *Can. J. Chem.* **1967**, *45*, 445–450. (d) Ayer, W. A.; Piers, K. *Can. J. Chem.* **1967**, *45*, 451–459.

correlations (Figure 4.8). However, in the 2D NOESY spectrum provided in the isolation report, NOESY correlations between H6' and H8', and H6' and H2' are not readily apparent. Furthermore, we were skeptical of the assignment of H8' to δ = 1.92 ppm in CD_3OD, since in the published ^1H NMR spectrum, this region encompassed one broad nondescript and undefined cluster of twelve protons.

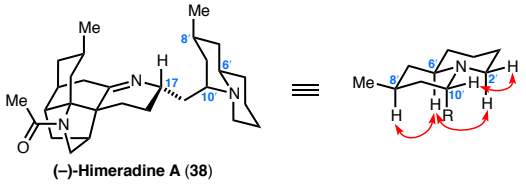

Figure 4.8. Putative NOESY correlations observed in the original isolation report of himeradine A (**38**).

Based on ^1H NMR spectra comparisons between the TFA salts of natural himeradine A (**38**) and cermizine D,[125] a *Lycopodium* alkaloid in which both C10' and C6' have the opposite configuration to the proposed structure (see Figure 4.7), we ruled out the possibility that both C10' and C6' in the proposed structure of himeradine A were misassigned. Hence, we embarked on a new synthetic effort to independently invert the C10'- and C6'-stereocenters.

Since the quinolizidine is relatively remote from the pentacyclic core of himeradine A (**38**), we believed that we could synthesize only the quinolizidine subunit with either C10' or C6' inverted as a model to predict the ^1H NMR chemical shifts of the final natural product. As a control, we synthesized the TFA salt of only the quinolizidine subunit of the proposed structure of himeradine A (**38**) and were pleased to discover that the ^1H NMR chemical shifts of H10', H6', and H2' were in excellent agreement with synthetic himeradine A (**38**) (Figure 4.9).

---

[125] Veerasamy, N.; Carlson, E. C.; Carter, R. G. *Org. Lett.* **2012**, *14*, 1596–1599.

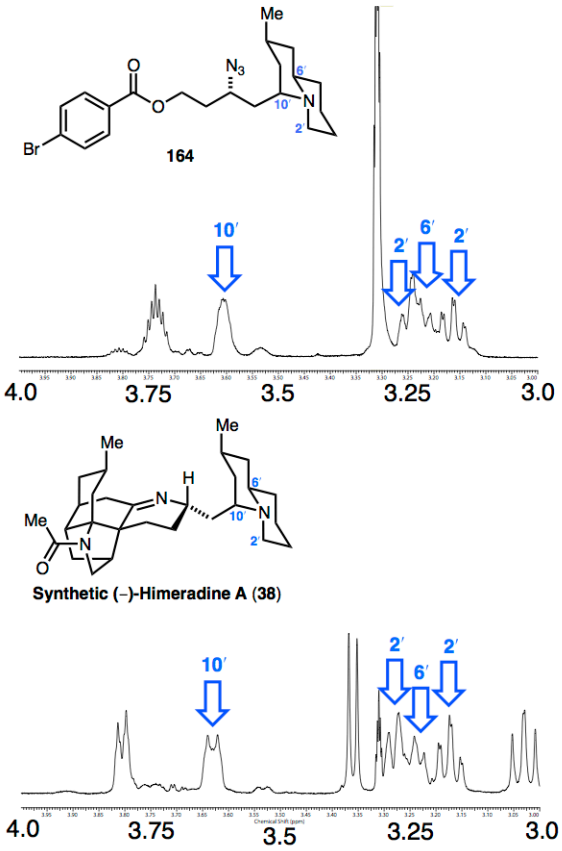

Figure 4.9. Comparison of ^{1}H NMR spectra of quinolizidine subunit model **164** and synthetic himeradine A (**38**) as the TFA salts in CD_3OD.

We decided to first embark on a synthesis of a quinolizidine subunit model in which the C6'-stereocenter is inverted relative to the proposed structure of himeradine A (**38**). This can be readily accomplished with the synthetic route we have previously developed and discussed, with minor modifications (Scheme 4.25). The C6'-stereocenter was introduced via exposure of intermediate **113** to $AllylSnBu_3$ in the presence of BF_3•OEt_2, delivering allyl *N*-Boc piperidine **165** as a single diastereomer. The diastereoselectivity of this reaction is controlled through stereoelectronically favored axial attack of the corresponding *N*-acyliminium ion intermediate by $AllylSnBu_3$ *anti* to the C12'-methyl group. Cleavage of the *N*-Boc protecting group in **165**, followed by allylation of the resultant piperidine, occurred smoothly to afford tertiary amine **166**. **166** was transformed to quinolizidine **168** in four steps via: (1) ring-closing metathesis to provide alkene **167**, (2)

hydrogenation of the resultant alkene, (3) global silyl deprotection, and (4) selective protection of the resultant primary hydroxyl group. Finally, Mitsunobu displacement of the secondary hydroxyl group in **168** with azide, followed by cleavage of the primary TBS ether, yielded quinolizidine **169**, our desired model substrate.

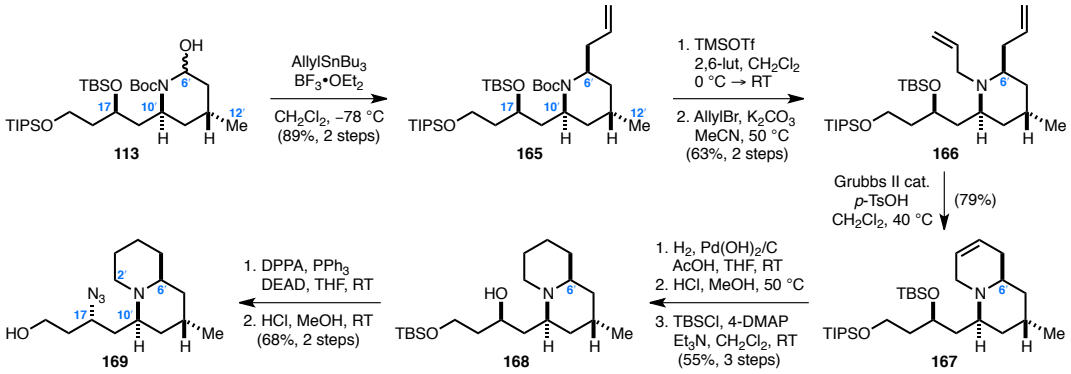

Scheme 4.25. Synthesis of a model of the quinolizidine subunit **169** in which the C6'-stereocenter is inverted relative to the proposed structure of himeradine A (**38**).

Treatment of **169** with TFA cleanly provided the corresponding TFA salt, the ^{1}H NMR spectrum of which was directly compared with that of natural himeradine A (Figure 4.10). As is readily apparent, the ^{1}H NMR spectrum of the TFA salt of **169** is noticeably different from natural himeradine A. We were originally concerned about the accuracy of our quinolizidine model system in which C17 is connected to an azide (**169**), versus an imine functionality in himeradine A, in predicting the chemical shift of the H10'-proton. However, it is evident that the chemical shifts of the H2'-protons in **169** (δ = 3.82 and 2.89 ppm (the latter is not shown in Figure 4.10)) were remarkably different from that in natural himeradine A (δ = 3.33 and 3.19 ppm). Hence, we concluded that it was unlikely that the C6'-stereocenter in the proposed structure of himeradine A (**38**) was misassigned.

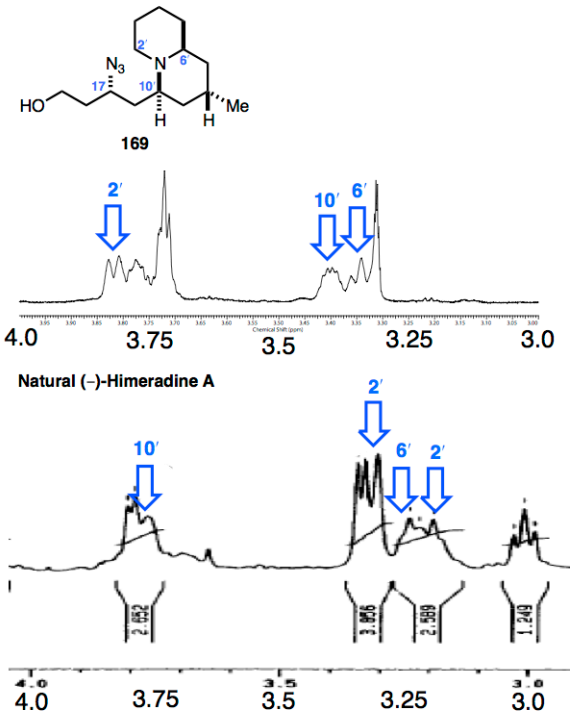

Figure 4.10. Comparison of ^{1}H NMR spectra of quinolizidine subunit model **169**, in which the C6'-stereocenter has been inverted, and natural himeradine A as the TFA salts in CD_3OD.

Next, we turned our focus to inverting the C10'-stereocenter, which unfortunately could not be accomplished with the previously developed synthetic route. A new strategy was devised (Scheme 4.26). Utilizing the enantioselective transfer aminoallylation reaction developed by Kobayashi et al,[126] aldehyde **108** and α-aminoketone **170**, derived from (1*R*)-(–)-camphorquinone, were stirred together in the presence of catalytic CSA, furnishing lactam **171** as a single diastereomer via: (1) condensation of aldehyde **108** with the amine in **170**, (2) a 2-aza-Cope rearrangement of the resultant imine, (3) cleavage of the newly formed imine under acidic conditions with the use of $HONH_2$•AcOH to reveal the homoallylamine product, and (4) in situ lactam formation.

---

[126] (a) Sugiura, M.; Mori, C.; Kobayashi, S. *J. Am. Chem. Soc.* **2006**, *128*, 11038–11039. For an example of the use of **170** in a synthesis, see: (b) Nishikawa, Y.; Kitajima, M.; Kogure, N.; Takayama, H. *Tetrahedron* **2009**, *65*, 1608–1617.

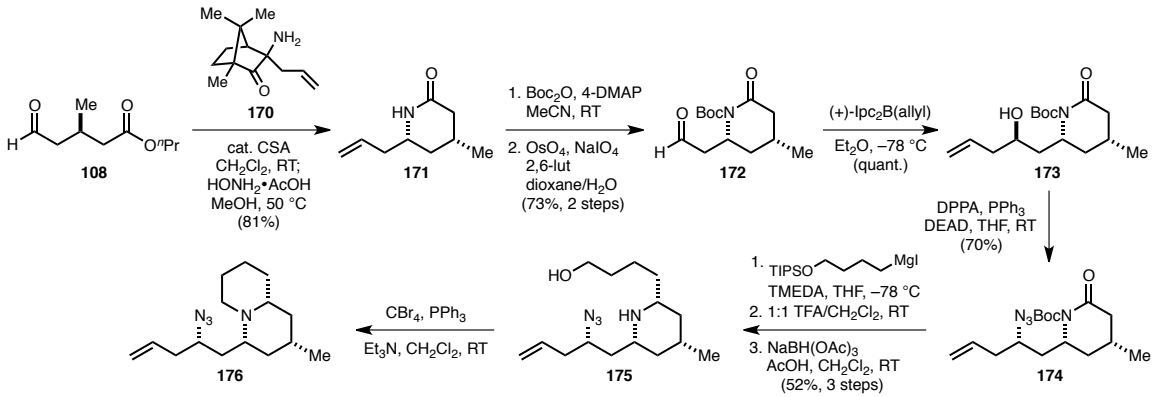

Scheme 4.26. Synthesis of a model of the quinolizidine subunit **176** in which the C10'-stereocenter is inverted relative to the proposed structure of himeradine A (**38**).

Protection of lactam **171** as the corresponding Boc-imide, followed by exposure to OsO_4 and $NaIO_4$ in the presence of 2,6-lutidine,[127] yielded aldehyde **172** via oxidative cleavage of the terminal olefin. An asymmetric allylboration of **172** with Brown's chiral (+)-Ipc_2B(allyl) allylborane reagent[128] provided alcohol **173** as a single diastereomer. Mitsunobu displacement of the secondary hydroxyl group in **173** with azide occurred smoothly to afford azide **174**. **174** was converted to amine **175** as a single diastereomer via a three-step protocol involving: (1) addition of Grignard reagent $TIPSO(CH_2)_4MgI$ to the imide functionality, (2) subsequent exposure to TFA to cleave the *N*-Boc group and form the corresponding imine with concomitant cleavage of the TIPS ether group, and (3) reductive amination with $NaBH(OAc)_3$ in the presence of AcOH. Finally, **175** underwent an Appel reaction with CBr_4 and PPh_3 in the presence of Et_3N, resulting in the formation of the corresponding bromide and in situ intramolecular S_N2 cyclization to deliver quinolizidine **176**, the desired model.

Treatment of **176** with TFA cleanly provided the corresponding TFA salt, the ^1H NMR

---

[127] Yu, W.; Mei, Y.; Kang, Y.; Hua, Z.; Jin, Z. *Org. Lett.* **2004**, *6*, 3217–3219.

[128] (a) Racherla, U. S.; Brown, H. C. *J. Org. Chem.* **1991**, *56*, 401–404. (b) Jadhav, P. K.; Bhat, K. S.; Perumal, P. T.; Brown, H. C. *J. Org. Chem.* **1967**, *32*, 404–407. (c) Nicolaou, K. C.; Ninkovic, S.; Sarabia, F.; Vourloumis, D.; He, Y.; Vallberg, H.; Finlay, M. R. V.; Yang, Z. *J. Am. Chem. Soc.* **1997**, *119*, 7974–7991.

spectrum of which was directly compared with that of natural himeradine A (Figure 4.11). Once again, the ^{1}H NMR spectrum of the TFA salt of **176** was distinctively different from natural himeradine A. Not only was the chemical shift of H10' considerably different (δ = 3.22 ppm versus 3.77 ppm in natural himeradine A), but also the chemical shifts of the H2'-protons in **176** (δ = 3.86 and 2.75 ppm (the latter is not shown in Figure 4.11) versus 3.33 and 3.19 ppm in natural himeradine A). Hence, we concluded that it was unlikely that the C10'-stereocenter in the proposed structure of himeradine A (**38**) was misassigned.

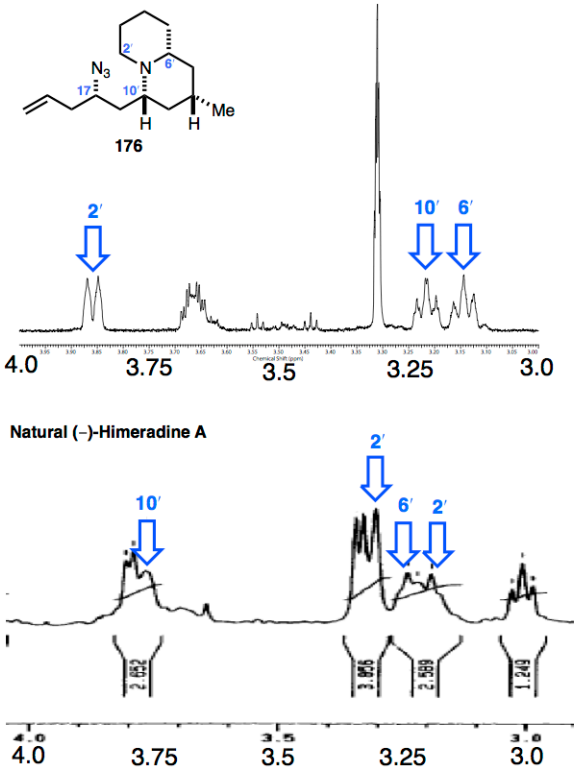

Figure 4.11. Comparison of ^{1}H NMR spectra of quinolizidine subunit model **176**, in which the C10'-stereocenter has been inverted, and natural himeradine A as the TFA salts in CD_3OD.

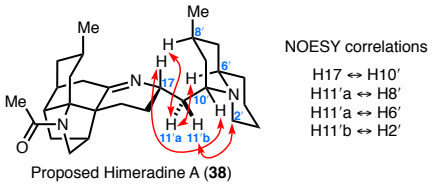

Figure 4.12. Selected NOESY correlations observed for the proposed structure of himeradine A (**38**).

Although these results were discouraging, we turned our attention to the most probable remaining candidate for stereochemical misassignment—the C17-stereocenter. In the original isolation report by Kobayashi and coworkers, the stereochemical assignment of H17 as the axial configuration was based on observed NOESY correlations (Figure 4.12) between H17 and H10', 11'a and H8', H11'a and H6', and H11'b and H2'. However, both the axial and equatorial configurations of H17 would result in these observed NOESY correlations. Hence, we believed the proposed C17 stereochemical assignment was ambiguous. Furthermore, both epimers of C17 exist in related *Lycopodium* alkaloids, lucidines A and B,[121] suggesting that the opposite C17 configuration to the proposed structure of himeradine A (**38**) was plausible (Figure 4.13).

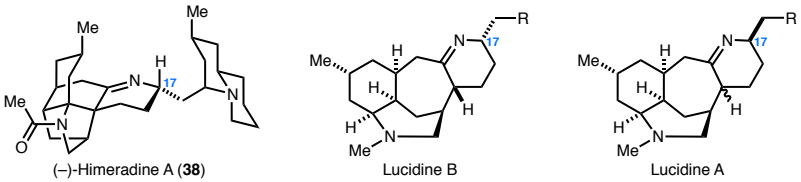

Figure 4.13. Lucidine A and B are epimeric at the C17-stereocenter.

Candidate for the Structural Reassignment of (–)-Himeradine A

As discussed in the previous section, we next embarked on a synthesis of the C17-epimer of the proposed structure of himeradine A (**38**). This could readily be accomplished with the synthetic route we originally developed with minor modifications (Scheme 4.27). In order to introduce the C17-stereocenter, a double inversion of the secondary hydroxyl group in intermediate **145** is required. Mitsunobu displacement of the C17-hydroxyl with *p*-nitrobenzoic acid,[129] followed by cleavage of the resultant ester, afforded inverted alcohol **177**. A second Mitsunobu displacement with azide then yielded azide **178**. Cleavage of the TBS-ether, followed by iodide formation, furnished alkyl iodide **179**, the desired alkylation electrophile. β-carboxyimide **66** underwent efficient alkylation with **179** in the presence of Cs_2CO_3 to provide alkylated product **180** in 77% yield.

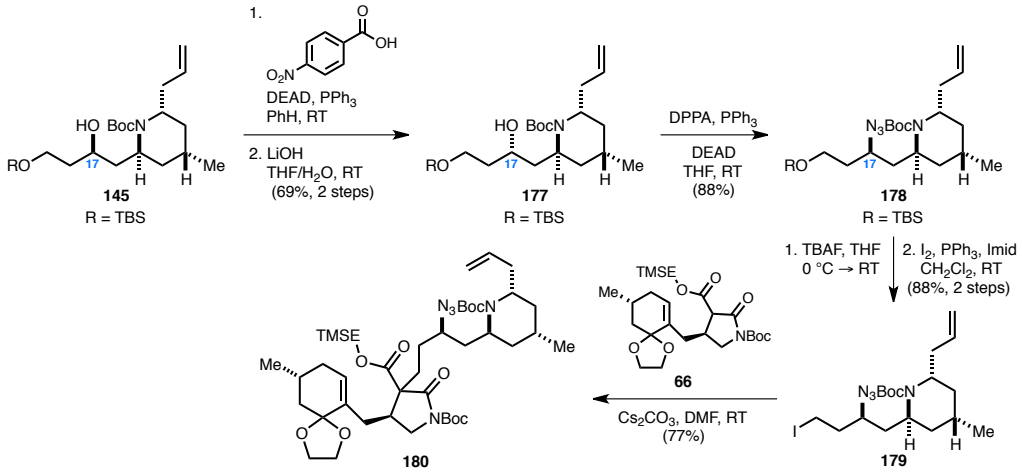

Scheme 4.27. Double inversion of the C17-stereocenter.

Following the same reaction sequence utilized in the synthesis of the proposed structure of himeradine A (**38**), **180** was converted to *N*-Ns-2-pyrrolidinone **181** in three steps via: (1) cleavage of the TMSE ester with concomitant decarboxylation, (2) cleavage of the *N*-Boc group with

---

[129] Martin, S. F.; Dodge, J. A. *Tetrahedron Lett*. **1991**, *32*, 3017–3020.

$Mg(ClO_4)_2$, and (3) protection of the resultant pyrrolidinone with a Ns group (Scheme 4.28). Addition of the lithium enolate of *t*-butylacetate to C13 of **181** and subsequent cleavage of the C6-dioxolane yielded enone **182**. Utilizing our optimized one-pot protocol, exposure of **182** to Barton's base, followed by addition of PhSH in the presence of K_2CO_3, furnished imine **183**. Next, a Staudinger reduction of the azide in **183** and condensation of the resultant amine with the neighboring β-ketoester, provided the corresponding vinylogous urethane product, which underwent subsequent acetylation to afford amide **184** (50%, 2 steps). Next, a cross-metathesis of the allyl group in **184** with acrolein in the presence of Hoveyda–Grubbs II catalyst occurred smoothly to yield enal **185** (88%).

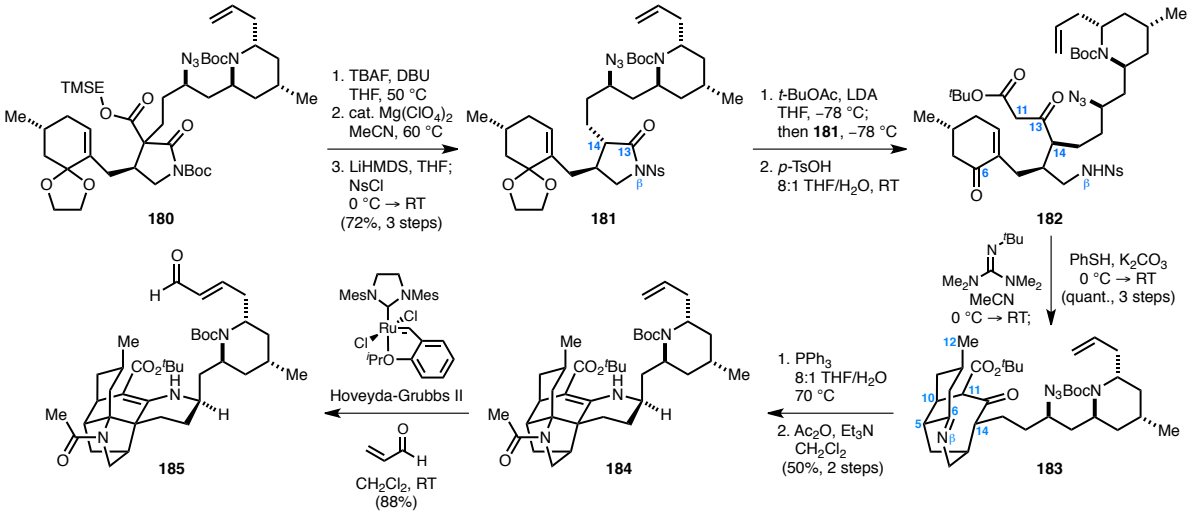

Scheme 4.28. Successful application of our one-pot sequence protocol toward the synthesis of himeradine A candidate structure **188**.

Hydrogenation of **185**, reduction of the corresponding aldehyde with $NaBH_4$, and tosylation of the resultant hydroxyl group provided tosylate **186** (73%, 3 steps) (Scheme 4.29). **186** was converted to quinolizidine **187** (59%, 2 steps) via: (1) initial formation of the silyloxy carbamate by exposure to TBSOTf and 2,6-lutidine, (2) subsequent cleavage of the carbamate with concomitant decarboxylation upon treatment with TBAF, and (3) in situ cyclization via S_N2 displacement of the tosylate group with the resultant secondary amine. Exposure of **187** to TFA then yielded our

candidate structure for (–)-himeradine A (**188**) as the double TFA salt ($[\alpha]_D^{22}$ = –56 (*c* 0.3, MeOH)).

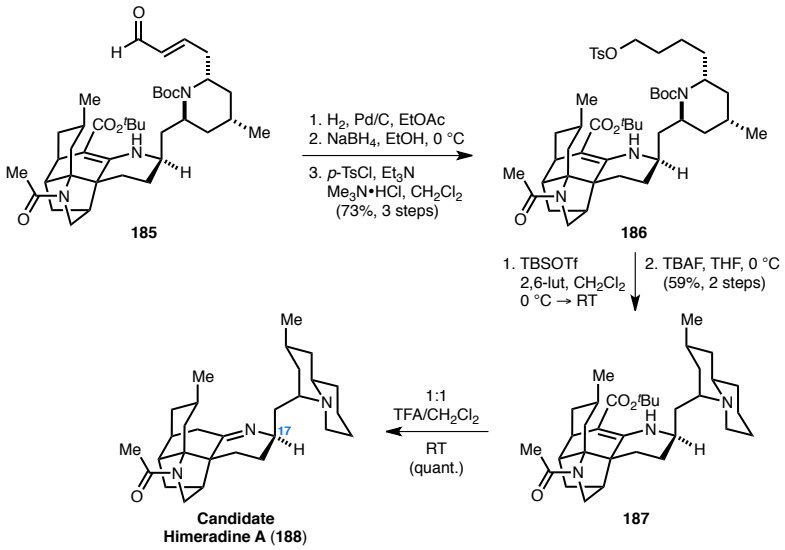

Scheme 4.29. Synthesis of our candidate structure for himeradine A (**188**).

We were excited to discover that the chemical shift of H10' (δ = 3.79–3.74 ppm) in our candidate structure for himeradine A (**188**) was in excellent agreement with that for natural himeradine A (δ = 3.77 ppm) (Figure 4.14). In fact, the chemical shifts of the key protons of the quinolizidine subunit (H6', H10', and H2') are all in good agreement with the values reported for natural himeradine A. Unfortunately, however, several protons corresponding to the pentacyclic core of **188** (boxed in red) no longer match the reported values. Additionally, as expected, H17 is shifted upfield relative to the chemical shift in natural himeradine A.

Based on the combined results of our quinolizidine model systems (**169** and **176**) and our candidate structure for himeradine A (**188**), we speculated that it could indeed be the absolute stereochemistry of the quinolizidine subunit, and not the relative configuration of the C17-, C6'-, or C10'-stereocenters, of himeradine A (**38**) that may have been misassigned. The synthesis of the opposite absolute stereochemistry of the quinolizidine subunit of **38** should be readily feasible with our developed route due to the latent C_2-symmetry of starting material **107**. However, embarking on a new route without further information—in particular, an authentic sample of himeradine A—would

be impractical. Despite our educated hypothesis based on our model studies, there are still theoretically a total of sixteen possible stereoisomers. Furthermore, we cannot definitively rule out the possibility that we have successfully synthesized the correct structure of himeradine A (**38**) without an authentic sample of the natural product. Nonetheless, we have demonstrated that all sixteen possible stereoisomers could theoretically be accessed from the chemistry that we have developed.

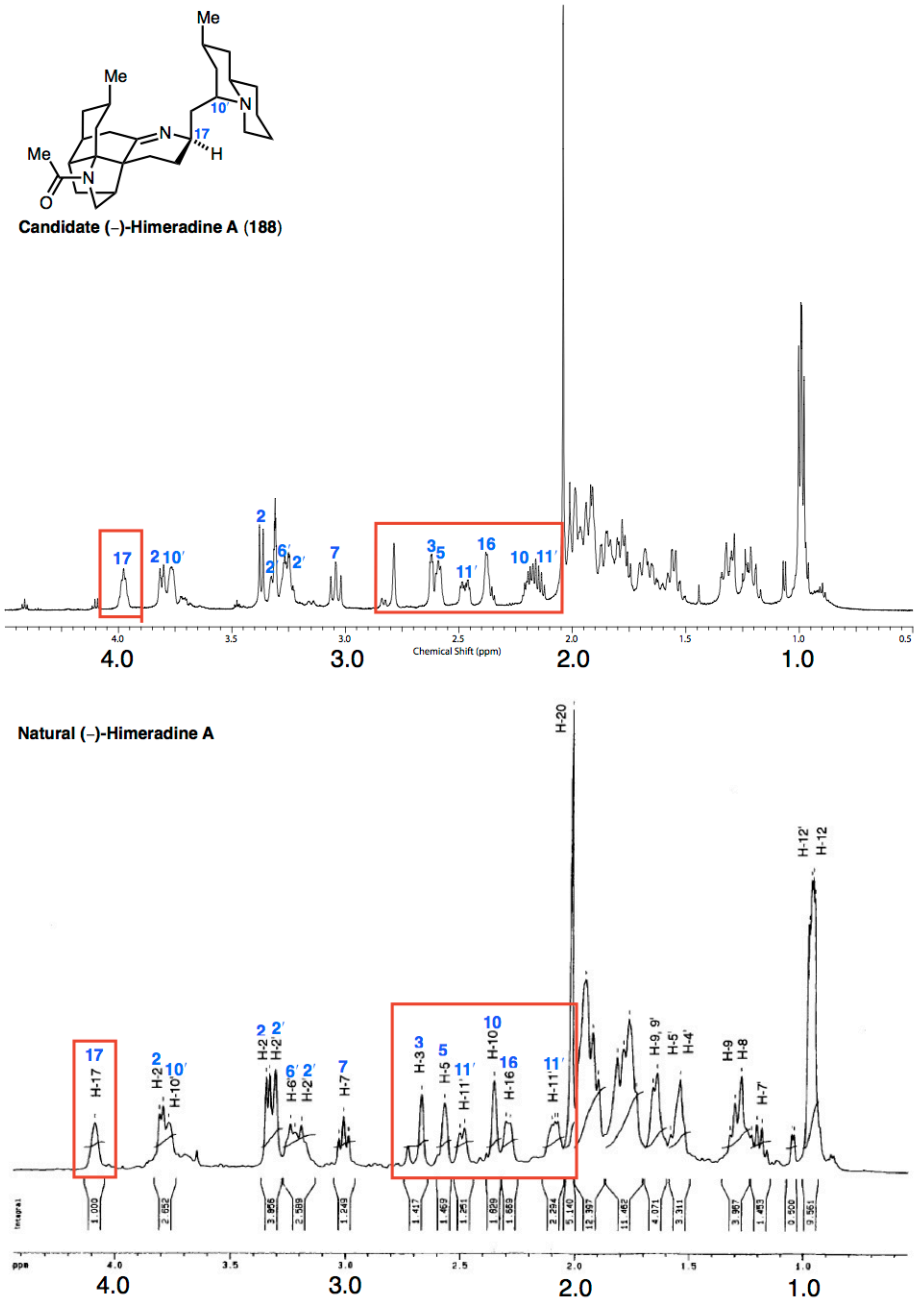

Figure 4.14. Comparison of ^{1}H NMR spectra of candidate (**188**) and natural (–)-himeradine A as the double TFA salt in CD_3OD.

In summary, this constitutes the first reported total synthesis of the proposed structure of (–)-himeradine A (**38**). Noteworthy transformations include a biosynthetically inspired, diastereoselective, one-pot sequence for constructing the strained core common to himeradine A (**38**)

and other *Lycopodium* alkaloids, and a key biomimetic transannular Mannich reaction. This highly convergent and unifying strategy can now be applied towards the streamlined synthesis of other 7-membered ring-containing *Lycopodium* alkaloids, which will be the subject of the next chapter.

II. A Biomimetic Unified Strategy for the Synthesis of 7-Membered Ring-Containing *Lycopodium* Alkaloids

Chapter 5

Total Syntheses of 7-Membered Ring-Containing *Lycopodium* Alkaloids

Introduction

In the previous chapter, we presented the development of a biosynthetically inspired one-pot cascade sequence for the construction of the strained core system common to a variety of 7-membered ring-containing *Lycopodium* alkaloids, including himeradine A (**38**) and fastigiatine (**37**). This unifying and highly convergent strategy supports our biosynthetic hypothesis (Figure 4.2) and can be applied towards the synthesis of a diverse set of *Lycopodium* alkaloids (Scheme 5.1).

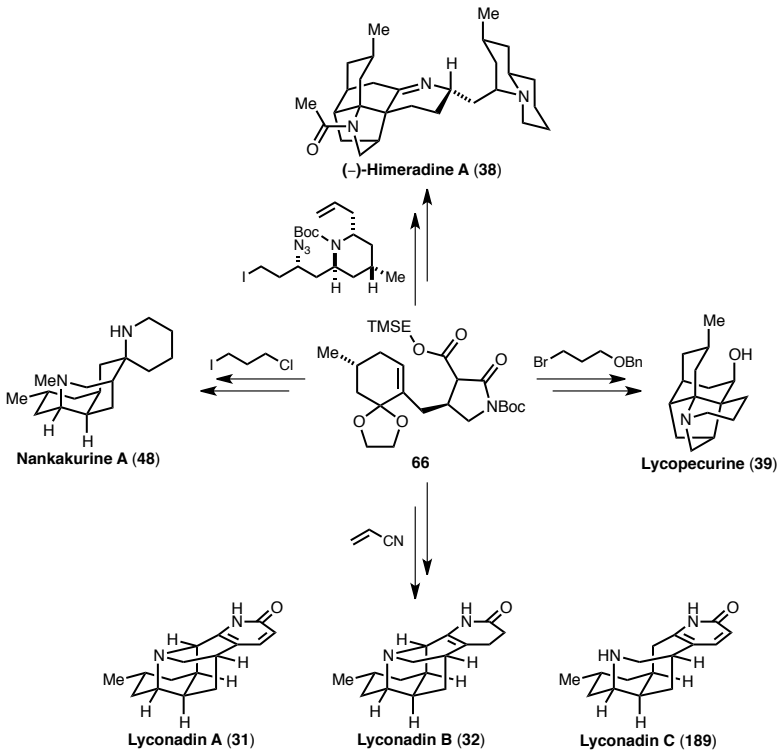

Scheme 5.1. A biomimetic and unified strategy for the total syntheses of structurally diverse *Lycopodium* alkaloids.

As illustrated in Scheme 5.2, a variety of structurally diverse *Lycopodium* alkaloids can be accessed with our strategy by varying the alkylation electrophile partner of carboxyimide **66**. Examples of such alkaloids include not only himeradine A (**38**) and fastigiatine (**37**), but also lycopecurine (**39**), lyconadins A (**31**), B (**32**), and C (**189**), and nankakurine (**48**). General precursor imine **190** can be accessed from the one-pot reaction sequence that we have developed. A subsequent

biomimetic transannular Mannich reaction would deliver himeradine A (**38**), fastigiatine (**37**), and lycopecurine (**39**). Alternatively, reduction of **190** by hydride could give rise to the lyconadin group of alkaloids, such as lyconadin B (**32**) and lyconadin C (**189**), or nankakurine A (**48**), which has undergone a subsequent rearrangement.

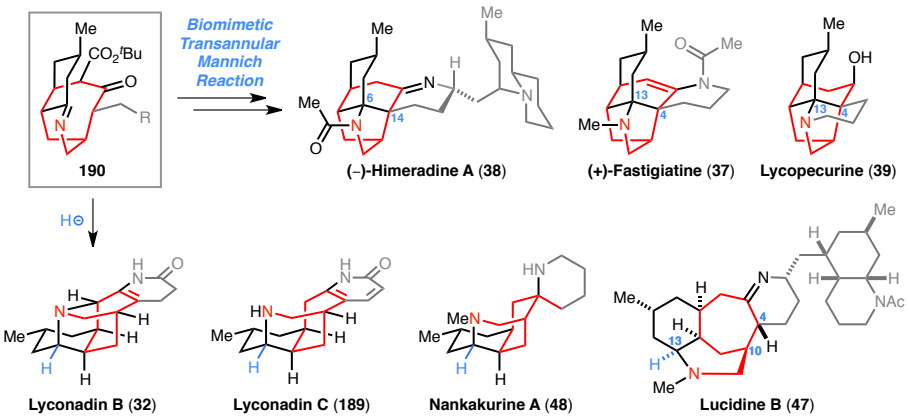

Scheme 5.2. Proposed unified strategy for the synthesis of a variety of *Lycopodium* alkaloids. Highlighted in red is the common 7-membered ring structural motif. Highlighted in gray is the variable alkyl chain.

A structurally diverse set of *Lycopodium* alkaloids could potentially be accessed from our biosynthetically inspired unifying strategy. The successful application of our unifying approach to the total syntheses of other *Lycopodium* alkaloids would lend credence to our biosynthetic hypothesis and showcase the utility of the one-pot reaction sequence that we have developed.

Total Synthesis of Dehydrolycopecurine and Lycopecurine

Lycopecurine (**39**), isolated in 1969 from *Lycopodium alopecuroides*,[130] contains the strained tetracyclic core common to himeradine A (**38**) and fastigiatine (**37**). Although no NMR spectra were provided, the structure was unambiguously determined by single crystal X-ray crystallography of the hydrobromide salt of lycopecurine (**39**). To date, a synthesis of lycopecurine has not yet been achieved. We envisioned that we could achieve the first total synthesis of lycopecurine with our biosynthetically inspired, unifying strategy to construct the strained core system.

To this end, alkylation of β-carboxyimide **66** with benzyl 3-bromopropylether occurred smoothly to provide alkylated product **191** (Scheme 5.3). Employing the same reaction sequence used in the synthesis of himeradine A (**38**), **191** was converted in five steps to enone **194**. In a one-pot reaction sequence involving initial exposure to K_2CO_3 and subsequent addition of PhSH, **194** underwent a cascade reaction to afford imine **195** (84%, 3 steps) via: (1) 7-*endo-trig* intramolecular conjugate addition and (2) in situ condensation of Nβ with the C13-ketone.

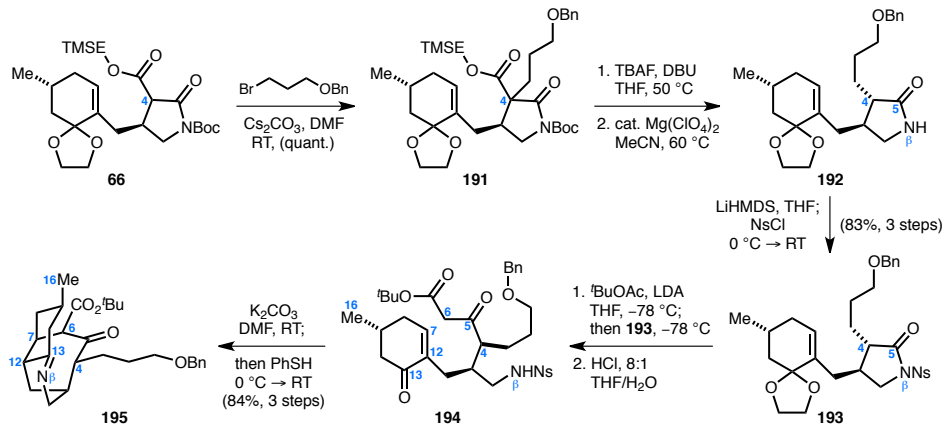

Scheme 5.3. Synthesis of imine **195**.

---

[130] (a) Ayer, W. A.; Altenkirk, B.; Masaki, N.; Valverde-Lopez, S. *Can. J. Chem.* **1969**, *47*, 2449–2455. (b) Ayer, W. A.; Masaki, N. *Can. J. Chem.* **1971**, *49*, 524–527.

Next, treatment of **195** with TFA resulted in loss of the *t*-butyloxycarbonyl group to afford the corresponding ketone, which then underwent the key biomimetic transannular Mannich reaction upon heating with HCl in MeOH[87] to construct the C4–C13 bond in tetracycle **197** (95%, 2 steps) (Scheme 5.4). Hydrogenolysis of the benzyl group in **197**, followed by exposure of the resultant alcohol **198** to 25% HBr in glacial AcOH[87] resulted in bromination of the hydroxyl group and formation of the ammonium bromide salt. Upon treatment with K_2CO_3, this intermediate underwent cyclization to yield dehydrolycopecurine[131] (**199**) in 59% yield over 2 steps ($[\alpha]_D^{22}$ = –69 (*c* 0.34, MeOH)). Finally, reduction of the ketone with $LiEt_3BH$ delivered lycopecurine (**39**) in 66% yield ($[\alpha]_D^{22}$ = –19 (*c* 0.14, MeOH)), constituting the first total syntheses of *Lycopodium* alkaloids **39** and **199**. The structure of **39** was unambiguously established via single crystal X-ray diffraction analysis of the hydrobromide salt of **39**.

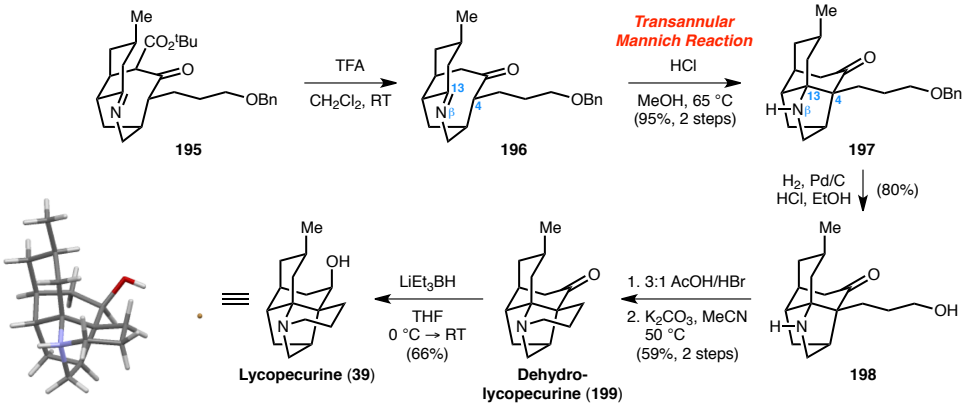

Scheme 5.4. Total synthesis of dehydrolycopecurine (**199**) and lycopecurine (**39**).

By varying the alkylation electrophile partner with carboxyimide **66**, we were able to accomplish the first total syntheses of dehydrolycopecurine (**199**) and lycopecurine (**39**) using our biosynthetically inspired, unifying strategy. Our one-pot cascade sequence was employed in the construction of the tricyclic core of **199** and **39**. A key biomimetic transannular Mannich reaction

---

[131] Braekman, J. C.; Hootele, C.; Ayer, W. A. *Bull. Soc. Chim. Belges* **1971**, *80*, 83–90.

then established the C4–C13 bond, furnishing the tetracyclic core common to himeradine A (**38**) and fastigiatine (**37**).

Total Synthesis of (+)-Lyconadin A and (–)-Lyconadin B

In 2001, Kobayashi and coworkers isolated (+)-lyconadin A (**31**) from the club moss *Lycopodium complanatum.*[132a] The structure of lyconadin A (**31**) was revealed to contain a pentacyclic core, including a 2-pyridone ring, six stereocenters, and a tertiary amine. **31** exhibits modest cytotoxicity against murine lymphoma L1210 cells (IC_{50} = 0.46 μg/mL) and human epidermoid carcinoma KB cells (IC_{50} = 1.7 μg/mL). Four syntheses of **31** have been accomplished to date.[88,90,133] (–)-Lyconadin B (**32**),[132b] which differs from **31** in that it contains a dihydropyridone instead of a pyridone moiety, was isolated in 2006. To date, two total syntheses[88,134] of lyconadin B (**32**) have been achieved. Both **31** and **32** demonstrate enhanced mRNA expression for nerve growth factor in 1321N1 human astrocytoma cells. We envisioned that a synthesis of lyconadin A (**31**) and B (**32**) could be realized by utilizing our unifying strategy to construct the core system via our one-pot reaction sequence.

To this end, alkylation of β-carboxyimide **66** with acrylonitrile proceeded smoothly to afford alkylated product **200** (Scheme 5.5). Utilizing the same reaction sequence employed in the synthesis of himeradine A (**38**) and lycopecurine (**39**), **200** was converted to enone **203** in five steps. A one-pot reaction sequence involving initial exposure to K_2CO_3 followed by addition of PhSH then delivered tricyclic imine **204** (63%, 3 steps).

---

[132] (a) Kobayashi, J.; Hirasawa, Y.; Yoshida, N.; Morita, H. *J. Org. Chem.* **2001**, *66*, 5901–5904. (b) Ishiuchi, K.; Kubota, T.; Hoshino, T.; Obara, Y.; Nakahata, N.; Kobayashi, J. *Bioorg. Med. Chem.* **2006**, *14*, 5996–6000.

[133] (a) Nishimura, T.; Unni, A. K.; Yokoshima, S.; Fukuyama, T. *J. Am. Chem. Soc.* **2011**, *133*, 418–419. (b) Yang, Y.; Haskins, C. W.; Zhang, W.; Low, P. L.; Dai, M. *Angew. Chem. Int. Ed.* **2014**, *53*, 3922–3925.

[134] Nishimura, T.; Unni, A. K.; Yokoshima, S.; Fukuyama, T. *J. Am. Chem. Soc.* **2013**, *135*, 3243–3247.

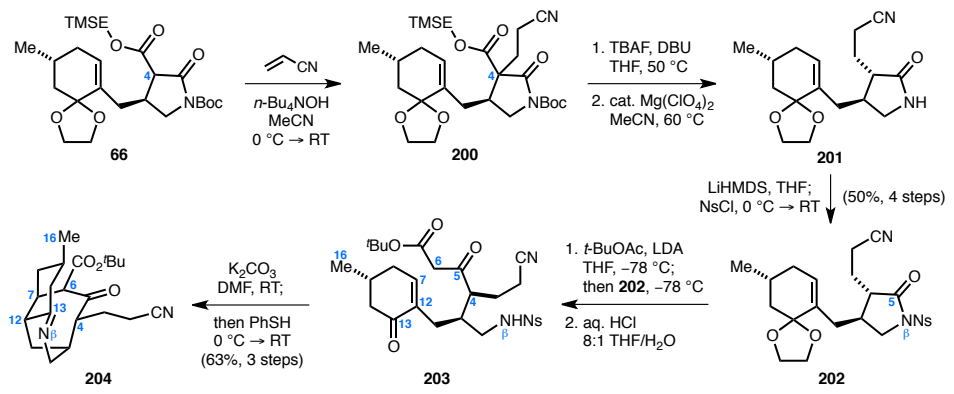

Scheme 5.5. Synthesis of imine **204**.

Unlike himeradine A (**38**) and lycopecurine (**39**), which underwent a subsequent transannular Mannich reaction, a synthesis of the lyconadins would require reduction of the imine functionality (Scheme 5.6). Treatment of **204** (redrawn as **205**) with $NaBH(OAc)_3$ and AcOH resulted in chemoselective reduction of the imine to furnish amine **206**. Next, treatment of **206** with TFA resulted in removal of the *t*-butyloxycarbonyl group to afford ketone **207** (59%, 2 steps).

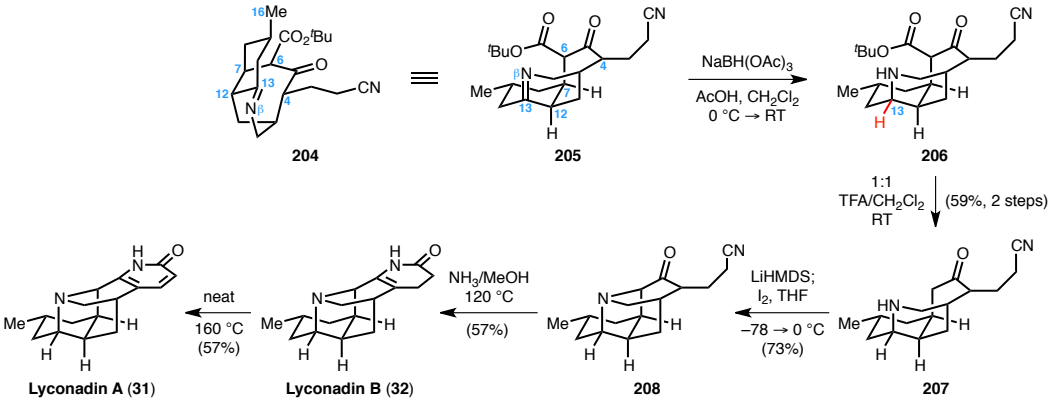

Scheme 5.6. Total synthesis of (+)-lyconadin A (**31**) and (−)-lyconadin B (**32**).

Deprotonation of **207** with LiHMDS, followed by trapping with I_2,[90] directly delivered amine **208** (73%); this presumably occurred via one of two possible mechanisms, including: (1) initial α-iodination of the ketone from the convex face, followed by intramolecular S_N2 displacement of the iodide by the secondary amine, or (2) oxidative enolate amination via a radical pathway.

Finally, heating nitrile **208** in a 7.0 M NH_3/MeOH[135] solution in a sealed vessel at 120 °C furnished (−)-lyconadin B (**32**) in 57% yield ($[\alpha]_D^{21} = -102$ (*c* 0.5, MeOH)). The ^{1}H NMR (Figure 5.1) and ^{13}C NMR spectra for synthetic (−)-lyconadin B (**32**) are in good agreement with the spectra reported for the natural product. During our studies to convert **208** to lyconadin B (**32**), we discovered a trace byproduct in the crude ^{1}H NMR corresponding to lyconadin A (**31**) after heating the reaction in NH_3/MeOH for two days.[136] Lyconadin A (**31**) presumably formed by autoxidation in the presence of trace oxygen. Gratifyingly, heating lyconadin B (**32**) neat at 160 °C under an atmosphere of air afforded lyconadin A (**31**) in 57% yield ($[\alpha]_D^{22} = +37$ (*c* 0.12, MeOH)). The ^{1}H NMR and ^{13}C NMR spectra for synthetic and natural (+)-lyconadin A (**31**) are in good agreement (Figure 5.2)

---

[135] Högenauer, K.; Baumann, K.; Mulzer, J. *Tetrahedron Lett*. **2000**, *41*, 9229–9232.

[136] A similar observation was made by Fukuyama and coworkers: See ref. 134.

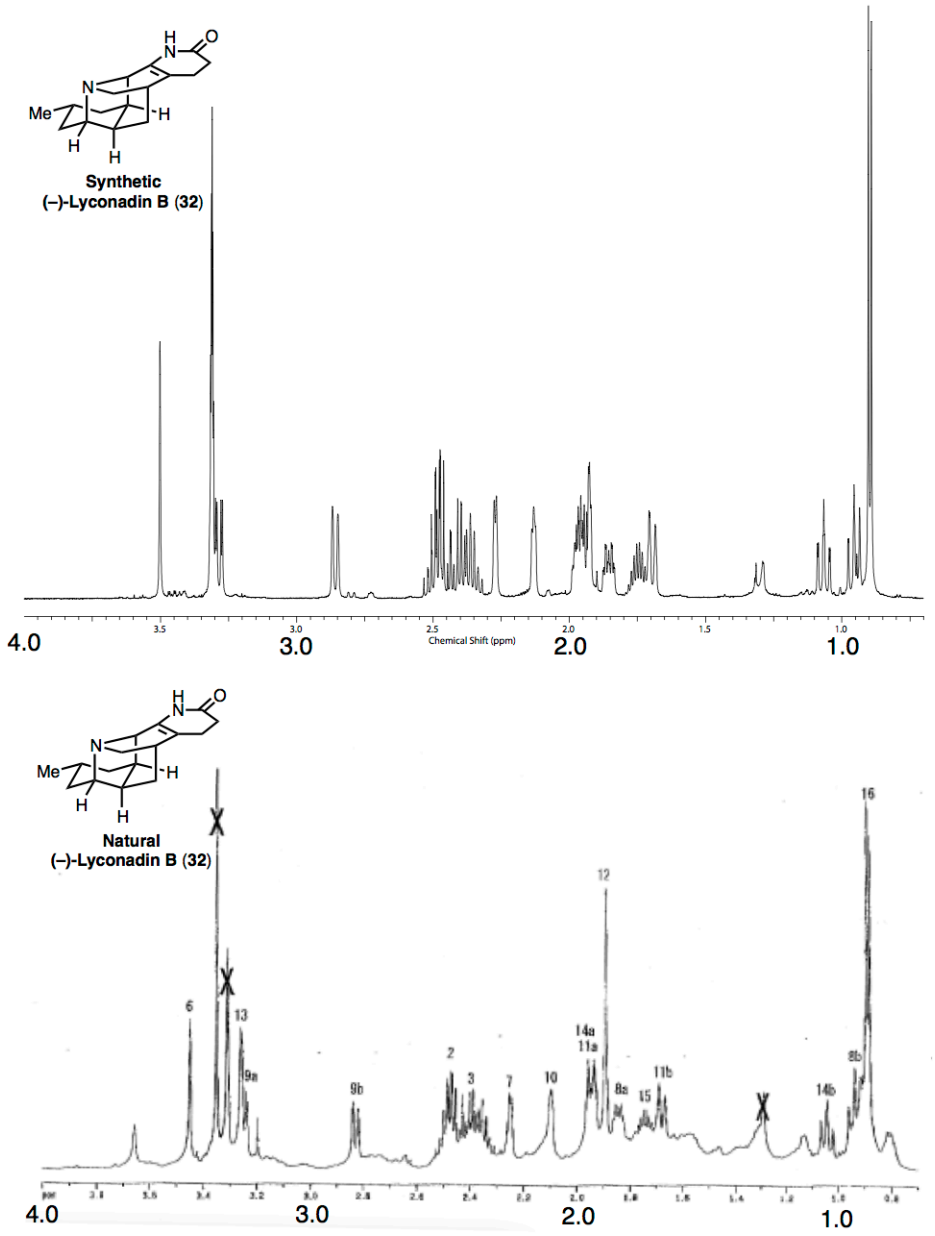

Figure 5.1. Comparison of ^{1}H NMR spectra of natural and synthetic (–)-lyconadin B (**32**) in CD_3OD.

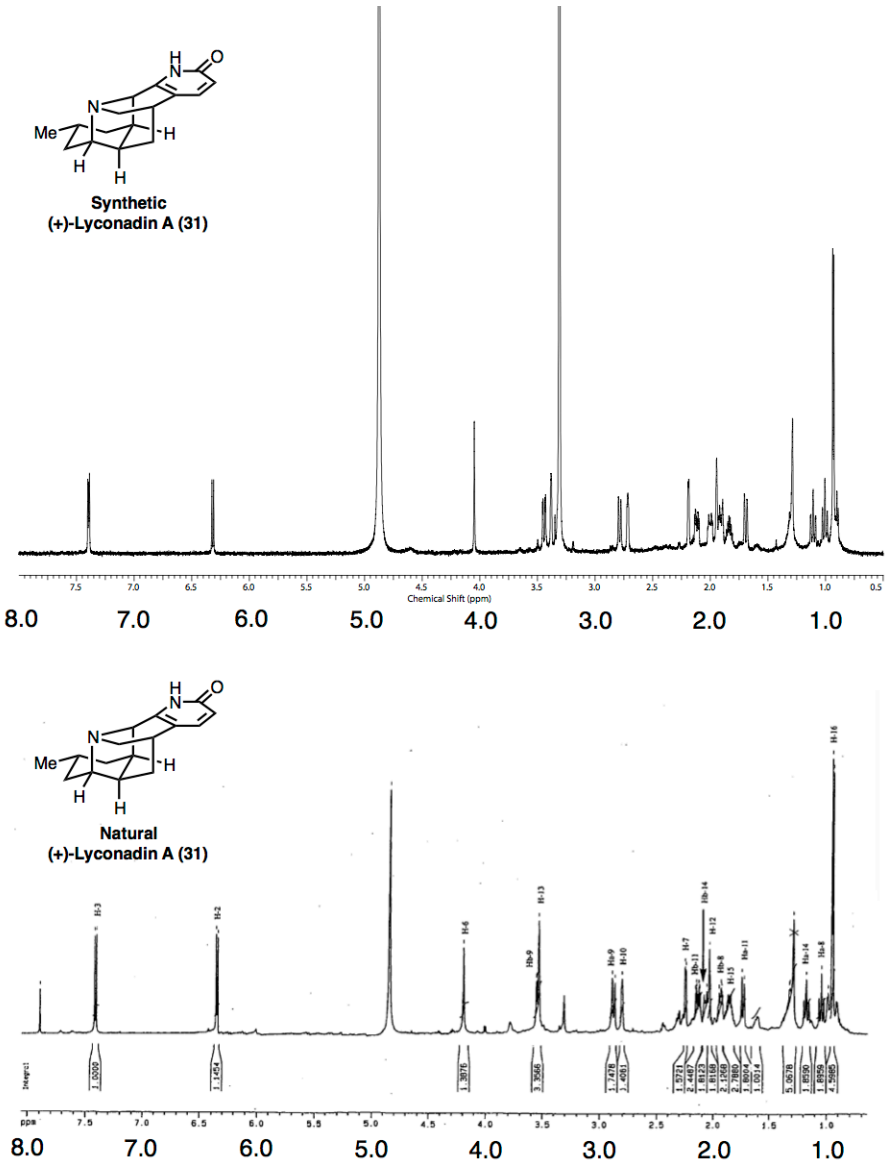

Figure 5.2. Comparison of ^{1}H NMR spectra of natural and synthetic (+)-lyconadin A (**31**) in CD_3OD.

The successful total syntheses of lyconadin A (**31**) and lyconadin B (**32**) further lend support to our biosynthetic hypothesis that 7-membered ring-containing *Lycopodium* alkaloids arise from a common imine precursor, which can then undergo either a transannular Mannich reaction or imine reduction to generate a large diverse group of alkaloid natural products. Our biomimetic and unifying strategy has allowed us to readily and efficiently access a variety of structurally diverse *Lycopodium* alkaloids by simply varying the carboxyimide alkylation electrophile partner. The application of our

strategy enabled the successful total syntheses of himeradine A (**38**), lycopecurine (**39**), dehydrolycopecurine (**199**), lyconadin A (**31**), and lyconadin B (**32**), and can potentially be used to synthesize all other 7-membered ring-containing *Lycopodium* alkaloids.

Concluding Remarks

In conclusion, the first total synthesis of the proposed structure of himeradine A (**38**), arguably the most complex and synthetically challenging *Lycopodium* alkaloid, was achieved. A biosynthetically inspired, diastereoselective, one-pot reaction sequence for constructing the strained core common to 7-membered ring-containing *Lycopodium* alkaloids was developed. A key biomimetic transannular Mannich reaction was successfully executed in the synthesis of the pentacyclic core of **38**.

This biosynthetically inspired reaction sequence was further applied towards the first total syntheses of lycopecurine (**39**) and dehydrolycopecurine (**199**), which also featured a key biomimetic intramolecular Mannich reaction. Our one-pot cascade sequence was also successfully utilized in a concise and streamlined synthesis of (+)-lyconadin A (**31**) and (–)-lyconadin B (**32**), which involved reduction of an imine intermediate instead of a transannular Mannich reaction to construct the core system. Our results constitute a unified strategy towards the synthesis of a structurally diverse set of 7-membered ring-containing *Lycopodium* alkaloids, lending support to our proposed revised biosynthetic hypothesis of these natural products.

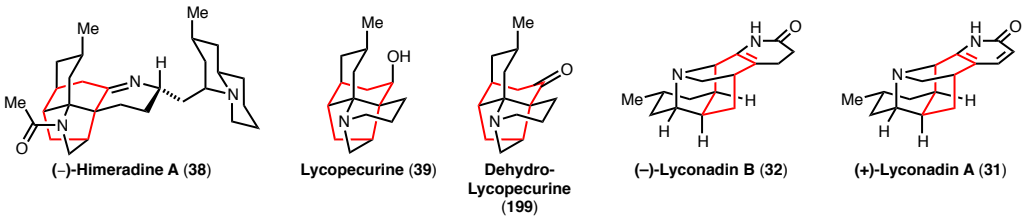

Scheme 5.7. Successful synthesis of a diverse set of 7-membered ring-containing *Lycopodium* alkaloids by employing our biomimetic unifying strategy.

Experimental Section

General Procedures. All reactions were performed in flame-dried glassware under a positive pressure of argon unless otherwise noted. Flash column chromatography was performed as described by Still et al. employing silica gel 60 (40-63 μm, Whatman).[72] Where necessary (so specified), silica gel was neutralized by treatment of the silica gel prior to chromatography with the eluent containing triethylamine or 5 M aqueous NH_4OH. Analytical thin-layer chromatography (TLC) was performed using 0.25 mm silica gel 60 F_{254} plates purchased from EMD Chemicals. TLC plates were visualized by exposure to ultraviolet light (UV) and/or exposure to an acidic solution of *p*-anisaldehyde (Anis) or an aqueous solution of potassium permanganate ($KMnO_4$), followed by heating on a hot plate.

Materials. Commercial reagents and solvents were used as received with the following exceptions: tetrahydrofuran (THF), diethyl ether (Et_2O), dichloromethane (CH_2Cl_2), acetonitrile (MeCN), hexamethyldisilazane (HMDS), benzene (PhH), and *N,N*-dimethylformamide (DMF) were degassed with argon and passed through a solvent purification system (designed by J. C. Meyer of Glass Contour) utilizing alumina columns as described by Grubbs et al.[73] Triethylamine, diisopropylamine, and pyridine were distilled over calcium hydride before use. TMSOTf was distilled before use. *N,N,N′N′*-Tetramethylethylenediamine was distilled over potassium hydroxide immediately before use. The celite used was Celite® 545, purchased from J.T. Baker. The molarities of *n*-butyllithium and *sec*-butyllithium solutions were determined by titration using 1,10-phenanthroline as an indicator (average of three determinations).

Instrumentation. ^1H NMR spectra were recorded with a Varian INOVA-600 or Varian INOVA-500 spectrometer. Proton chemical shifts are reported in parts per million (δ scale) and are calibrated using residual undeuterated solvent as an internal reference ($CDCl_3$: δ 7.26 ($CHCl_3$),

CD_3OD: δ 3.31 (CD_2HOD), C_6D_6: δ 7.15 (C_6D_5H)). Data for ^1H NMR spectra are reported as follows: chemical shift (δ ppm) (multiplicity, coupling constant (Hz), integration). Multiplicities are reported as follows: s = singlet, d = doublet, t = triplet, q = quartet, m = multiplet, br = broad, app = apparent, or combinations thereof. ^{13}C NMR spectra were recorded with a Varian INOVA-500 spectrometer. Carbon chemical shifts are reported in parts per million (δ scale) and are referenced from the carbon resonances of the solvent ($CDCl_3$: δ 77.00, CD_3OD: δ 49.00, C_6D_6: δ 128.39). Infrared (FTIR) spectra were recorded on a Bruker Alpha FT-IR spectrophotometer referenced to a polystyrene standard. FTIR data is reported in frequency of absorption (cm^{-1}). High-resolution mass spectra (HRMS) were obtained from the Harvard University Mass Spectrometry Laboratory where electrospray ionization (ESI) mass spectroscopy (MS) experiments were performed on an Agilent 6210 TOF LC/MS instrument. Optical rotations were measured on a Jasco P-2000 digital polarimeter with a sodium lamp. Reported readings are the average of five measurements for each sample. The structure of (–)-lycopecurine (**39**) was obtained with the assistance of Dr. Shao-Liang Zheng at the X-ray diffraction facility of the Department of Chemistry and Chemical Biology, Harvard University.

*(For clarity, intermediates that have not been assigned numbers in the text are numbered sequentially in the experimental section beginning with **S1**).*

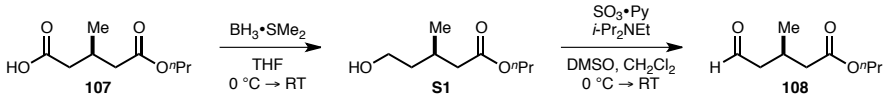

(*R*)-Propyl 3-methyl-5-oxopentanoate (108):

Borane dimethyl sulfide complex (4.54 mL, 46.3 mmol, 1.20 equiv) was added dropwise via syringe to a stirred solution of (*R*)-3-methyl-5-oxo-5-propoxypentanoic acid (**107**)[110,137] (7.26 g, 38.6 mmol, 1.00 equiv), which was azeotropically dried with benzene (5 × 10 mL), in THF (103 mL) at 0 °C, which was subsequently allowed to warm naturally to room temperature. After stirring for an additional 21 h, the reaction mixture was recooled to 0 °C and water (40 mL) was added. The resultant mixture was stirred vigorously and allowed to warm to room temperature. All volatiles were subsequently removed *in vacuo* and the resultant solution was partitioned between Et_2O (150 mL) and water (60 mL). The layers were separated and the aqueous layers were further extracted with Et_2O (3 × 50 mL). The organic layers were combined, washed with saturated aqueous $NaHCO_3$ solution (100 mL) and brine (100 mL), then dried over anhydrous $MgSO_4$, filtered, and concentrated under reduced pressure to afford the corresponding alcohol **S1** as a colorless oil, which was carried forward to the next step without further purification.

A solution of alcohol **S1**, which was azeotropically dried with benzene (5 × 50 mL), in CH_2Cl_2 (193 mL) was cooled to 0 °C. DMSO (27.4 mL, 386 mmol, 10.0 equiv), *i*-Pr_2NEt (33.6 mL, 193 mmol, 5.00 equiv), and SO_3•Py (18.4 g, 116 mmol, 3.00 equiv) were then added sequentially to the solution, which was then allowed to warm to room temperature. After stirring for 1 h, water (200 mL) and Et_2O (400 mL) were added to the reaction mixture. The layers were separated and the aqueous layer was extracted with Et_2O (3 × 150 mL). The organic layers were combined and washed with 10% aqueous HCl solution (3 × 150 mL), saturated aqueous $NaHCO_3$ solution (200 mL), and

---

[137] Synthesized in one step from 3-methylglutaric anhydride. The enantiopurity of **107** was determined to be 93% ee by chiral HPLC using authentic (±)-**107**.

brine (200 mL). The organic layers were dried over anhydrous $MgSO_4$ and concentrated under reduced pressure to afford crude (*R*)-propyl 3-methyl-5-oxopentanoate **108** as a pale yellow oil, which was carried forward to the next step without further purification.

^{1}H NMR (500 MHz, $CDCl_3$) δ: 9.76 (t, *J* = 2.2 Hz, 1H), 4.04 (t, *J* = 6.7 Hz, 2H), 2.64–2.48 (m, 2H), 2.39–2.32 (m, 2H), 2.28 (dd, *J* = 7.1, 15.1 Hz, 1H), 1.65 (sxt, *J* = 7.1 Hz, 2H), 1.04 (d, *J* = 6.6 Hz, 3H), 0.94 (t, *J* = 7.4 Hz, 3H). **^{13}C NMR** (126 MHz, $CDCl_3$) δ: 201.5, 172.3, 66.0, 50.1, 40.9, 25.2, 21.9, 20.1, 10.4. **FTIR** (thin film) cm^{-1}: 2966, 2880, 1724, 1460, 1263, 1213, 1170, 1088. **HRMS** (ESI) (*m/z*) calc'd for $C_9H_{16}NaO_3$ $[M+Na]^+$: 195.0992, found 195.0995. **TLC** (1:1 hexanes:EtOAc), R_f: 0.84 ($KMnO_4$).

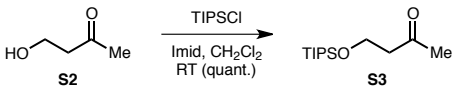

4-((Triisopropylsilyl)oxy)butan-2-one (S3):

Imidazole (39.5 g, 581 mmol, 2.50 equiv) and TIPSCl (55.0 mL, 279 mmol, 1.10 equiv) were added successively to a solution of 4-hydroxy-2-butanone (**S2**) (20.0 mL, 232 mmol, 1.00 equiv) in DMF (42 mL) at room temperature. The resultant solution was allowed to stir for 19.5 h, at which point water (150 mL), Et_2O (100 mL), and EtOAc (100 mL) were added. The layers were separated and the aqueous layer was extracted with Et_2O (3 × 200 mL). The organic layers were combined, washed with brine (300 mL), dried over anhydrous $MgSO_4$, filtered, and concentrated under reduced pressure. The resulting oil was then purified by flash column chromatography (silica gel, eluent: 12:1 hexanes:EtOAc) to afford 4-(triisopropylsilyl)oxy)butan-2-one (**S3**) (56.8 g, quant.) as a clear colorless oil.

^{1}H NMR (500 MHz, $CDCl_3$) δ: 3.98 (t, *J* = 6.3 Hz, 2H), 2.64 (t, *J* = 6.3 Hz, 2H), 2.20 (s, 3H), 1.12–1.02 (m, 21 H). **^{13}C NMR** (126 MHz, $CDCl_3$) δ: 208.3, 59.3, 46.7, 30.9, 17.9, 11.9. **FTIR** (thin film) cm^{-1}: 2942, 2866, 1716, 1463, 1356, 1105, 882, 680. **HRMS** (ESI) (*m/z*) calc'd for $C_{13}H_{28}NaO_2Si$ $[M+Na]^+$: 267.1751, found 267.1755. **TLC** (4:1 hexanes:EtOAc), R_f: 0.62 ($KMnO_4$).

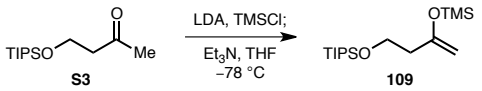

Silyl enol ether 109:

To a solution of diisopropylamine (21.5 mL, 153 mmol, 1.50 equiv) in THF (255 mL) at 0 °C was added dropwise a solution of *n*-butyllithium in hexanes (2.60 M, 57.0 mL, 148 mmol, 1.45 equiv). After 10 min, the reaction was recooled to −78 °C and TMSCl (65.0 mL, 511 mmol, 5.00 equiv) was added dropwise via syringe. After stirring the resultant mixture for 20 min, a solution of 4-(triisopropylsilyl)oxy)butan-2-one (**S3**) (25.0 g, 102 mmol, 1.00 equiv) in THF (255 mL), which was azeotropically dried with benzene (5 × 50 mL), was added dropwise via cannula to the stirred reaction at –78 °C. After 15 min, Et_3N (47.0 mL, 338 mmol, 3.30 equiv) was added dropwise via syringe to the reaction. The reaction was stirred for an additional 1.5 h at −78 °C, at which point a saturated aqueous $NaHCO_3$ solution (400 mL) was added. The resultant mixture was allowed to warm to room temperature and Et_2O (200 mL), EtOAc (200 mL), and water (100 mL) were subsequently added. The layers were separated and the aqueous layer was extracted with Et_2O (3 × 300 mL). The organic layers were combined, washed with brine (300 mL), dried over anhydrous $MgSO_4$, filtered, and concentrated under reduced pressure to afford crude silyl enol ether **109** as a pale yellow oil and as a 2:1 mixture of regioisomers, favoring the indicated **109**. The crude silyl enol ether was carried forward to the next step without further purification.

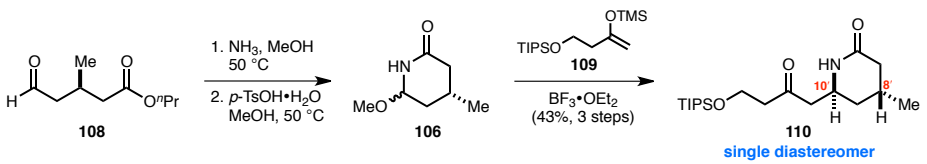

Lactam 110:

Aldehyde **108** (800 mg, 4.65 mmol, 1.00 equiv), which was azeotropically dried with benzene (3 × 5 mL), was dissolved in a solution of NH_3 in MeOH (2.00 M, 24.0 mL) and heated at 50 °C for 8 h. The reaction mixture was subsequently concentrated under reduced pressure to afford a mixture of *N,O*-hydroxy- and *N,O*-methoxyacetals, and uncyclized (3*R*)-propyl 5-amino-5-hydroxy-3-methylpentanoate. The crude product mixture was carried forward to the next step without further purification.

p-TsOH•H_2O (177 mg, 0.930 mmol, 0.20 equiv) was added as a single portion to a stirred solution of the crude product mixture in MeOH (46.5 mL), which was subsequently heated at 50 °C for 2 days, during which additional *p*-TsOH•H_2O (40.0 mg, 0.210 mmol, 0.05 equiv) was added. The reaction was then allowed to cool to room temperature and a saturated aqueous $NaHCO_3$ solution (50 mL) was added. The mixture was subsequently concentrated under reduced pressure to remove all volatiles. The resultant aqueous layer was diluted with $CHCl_3$ (100 mL), water (50 mL), and brine (50 mL), and the layers were separated. The aqueous layer was further extracted with $CHCl_3$ (5 × 50 mL) and the organic layers were combined, washed with brine (100 mL), dried over anhydrous $MgSO_4$, and concentrated under reduced pressure to afford a diastereomeric mixture of *N,O*-methoxyacetals **106** as a crude white solid, which was carried forward to the next step without further purification.

BF_3•OEt_2 (922 μL, 7.47 mmol, 2.00 equiv) was added dropwise to a solution of crude **106** and silyl enol ether **109** (7.10 g, 22.4 mmol, 6.00 equiv), which were azeotropically dried with benzene (5 × 15 mL), in MeCN (37.5 mL) at –40 °C. The reaction was allowed to warm gradually to room temperature. After 2.5 h, water (100 mL), Et_2O (50 mL), and EtOAc (50 mL) were added to

the reaction mixture. The layers were separated and the aqueous layer was extracted with EtOAc (3 × 50 mL). The organic layers were combined, washed with brine (200 mL), dried over anhydrous $MgSO_4$, and concentrated under reduced pressure. The resulting oil was then purified by flash column chromatography (silica gel, eluent: gradient: EtOAc → 15:1 EtOAc:MeOH) to afford lactam **110** (709 mg, 43% over 3 steps) as a single diastereomer and as a pale yellow oil.

^{1}H NMR (500 MHz, $CDCl_3$) δ: 6.26 (s, 1H), 4.06–3.89 (m, 3H), 2.78 (dd, *J* = 9.5, 18.3 Hz, 1H), 2.69 (dd, *J* = 3.2, 18.3 Hz, 1H), 2.66–2.51 (m, 2H), 2.41 (dd, *J* = 4.2, 17.8 Hz, 1H), 1.98 (dd, *J* = 8.3, 16.8 Hz, 1H), 1.68–1.60 (m, 1H), 1.15–0.97 (m, 23H). **^{13}C NMR** (126 MHz, $CDCl_3$) δ: 208.9, 171.3, 59.3, 50.8, 46.1, 45.8, 39.3, 34.8, 24.3, 20.4, 17.9, 11.8. **FTIR** (thin film) cm^{-1}: 2942, 2866, 1712, 1662, 1462, 1364, 1101, 882, 681. **HRMS** (ESI) (*m/z*) calc'd for $C_{19}H_{37}NNaO_3Si$ $[M+Na]^+$: 378.2435, found 378.2448. **$[\alpha]_D^{22}$**: –52 (*c* = 0.94, CH_2Cl_2). **TLC** (9:1 EtOAc:MeOH), R_f: 0.50 ($KMnO_4$,UV).

1D NOESY (500 MHz, $CDCl_3$):

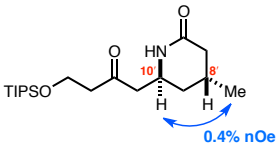

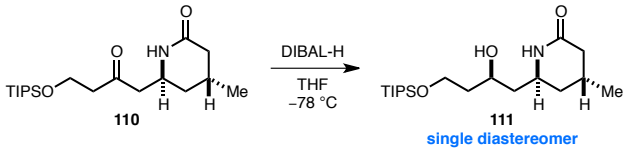

Alcohol 111:

Diisobutylaluminum hydride (3.80 mL, 21.3 mmol, 8.00 equiv) was added to a stirred solution of lactam **110** (945 mg, 2.66 mmol, 1.00 equiv), which was azeotropically dried with benzene (5 × 5 mL), in THF (53 mL) at −78 °C. After stirring the resultant reaction for 4 h at −78 °C, a saturated aqueous solution of Rochelle's salt (200 mL) was carefully added at a slow rate. The resultant mixture was allowed to warm to room temperature and was subsequently diluted with Et_2O (150 mL) and EtOAc (150 mL), and stirred vigorously for 12 h. The layers were separated and the aqueous layer was extracted with EtOAc (3 × 150 mL). The organic layers were combined, washed with brine (200 mL), dried over anhydrous $MgSO_4$, and concentrated under reduced pressure to afford crude alcohol **111** as a single diastereomer and as a pale yellow oil, which was carried forward to the next step without further purification.

^{1}H NMR (600 MHz, $CDCl_3$) δ: 76.83 (br. s, 1H), 4.10–3.97 (m, 3H), 3.93 (dt, *J* = 2.7, 10.3 Hz, 1H), 3.77–3.68 (m, 1H), 2.43 (dd, *J* = 5.5, 17.2 Hz, 1H), 2.18–2.09 (m, 1H), 2.04 (dd, *J* = 5.5, 17.2 Hz, 1H), 1.81–1.71 (m, 1H), 1.71–1.57 (m, 4H), 1.49 (d, *J* = 13.7 Hz, 1H), 1.17–1.01 (m, 24H). **^{13}C NMR** (126 MHz, $CDCl_3$) δ: 171.2, 73.0, 63.6, 49.2, 44.0, 38.7, 38.6, 35.4, 24.6, 19.8, 17.9, 11.7. **FTIR** (thin film) cm^{-1}: 2941, 2865, 1650, 1462, 1316, 1095, 882, 679. **HRMS** (ESI) (*m/z*) calc'd for $C_{19}H_{39}NNaO_3Si$ $[M+Na]^+$: 380.2591, found 380.2588. **TLC** (9:1 EtOAc:MeOH), R_f: 0.42 ($KMnO_4$).

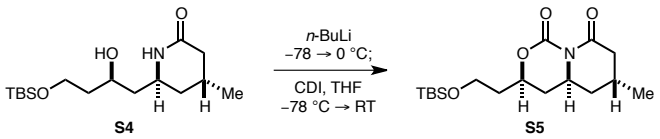

Cyclic imide S5:

A solution of *n*-butyllithium in hexanes (2.56 M, 15.5 μL, 0.0396 mmol, 2.50 equiv) was added to a stirred solution of alcohol **S4**[138] (5.0 mg, 0.016 mmol, 1.0 equiv), which was azeotropically dried with benzene (5 × 1 mL), in THF (200 μL) at −78 °C. After 20 min, the reaction was allowed to warm to 0 °C and stirred for an additional 10 min, at which point the solution was recooled to −78 °C. A solution of 1,1'-carbonyldiimidazole (9.0 mg, 0.055 mmol, 3.5 equiv) in THF (200 μL) was added to the stirred reaction mixture, which was subsequently allowed to warm gradually to room temperature over 30 min. A solution of saturated aqueous NH_4Cl (1 mL) and EtOAc (1 mL) were added sequentially to the reaction mixture. The layers were separated and the aqueous layer was extracted with EtOAc (3 × 1 mL). The organic layers were combined, washed with brine (2 mL), dried over anhydrous $MgSO_4$, and concentrated under reduced pressure. The resultant residue was purified by flash column chromatography (silica gel, eluent: 2:1 EtOAc:hexanes) to afford cyclic imide **S5** as a white solid.

^{1}H NMR (600 MHz, $CDCl_3$) δ: 4.54–4.47 (m, 1H), 3.99 (tt, *J* = 4.4, 11.4 Hz, 1H), 3.85–3.78 (m, 1H), 3.73 (td, *J* = 5.2, 10.3 Hz, 1H), 2.64 (dd, *J* = 5.1, 15.4 Hz, 1H), 2.34–2.26 (m, 1H), 2.19 (ddd, *J* = 2.0, 4.8, 14.0 Hz, 1H), 1.94–1.84 (m, 2H), 1.82–1.63 (m, 4H), 1.10 (d, *J* = 6.6 Hz, 3H), 0.88 (s, 9H), 0.05 (s, 6H). **^{13}C NMR** (126 MHz, $CDCl_3$) δ: 171.9, 148.1, 74.1, 58.2, 52.7, 42.1, 37.9, 37.3, 35.1, 25.9, 24.3, 21.6, 18.2, –5.4, –5.4. **FTIR** (thin film) cm^{-1}: 2957, 2927, 2855, 1762, 1313, 1101, 837, 773. **HRMS** (ESI) (*m/z*) calc'd for $C_{17}H_{31}NNaO_4Si$ $[M+Na]^+$: 364.1915, found 364.1931. **TLC** (9:1 EtOAc:MeOH), R_f: 0.68 ($KMnO_4$, UV).

---

[138] **S4** was synthesized according to the sequence utilized in the synthesis of **111**.

1D NOESY (500 MHz, $CDCl_3$):

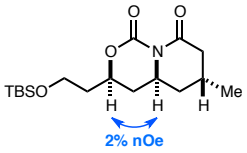

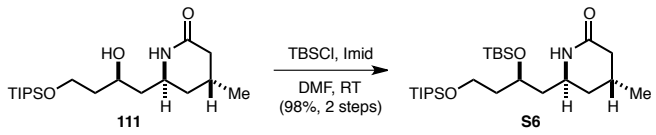

Silyl ether S6:

Imidazole (905 mg, 13.3 mmol, 5.00 equiv) and TBSCl (962 mg, 6.38 mmol, 2.40 equiv) were added successively to a stirred solution of crude alcohol **111**, which was azeotropically dried with benzene (3 × 3 mL), in DMF (26 mL) at room temperature. After 15.5 h, water (50 mL), Et_2O (30 mL), and EtOAc (30 mL) were added. The layers were separated and the aqueous layer was extracted with EtOAc (3 × 50 mL). The organic layers were combined, washed with brine (100 mL), dried over anhydrous $MgSO_4$, and concentrated under reduced pressure. The resulting oil was then purified by flash column chromatography (silica gel, eluent: EtOAc) to afford silyl ether **S6** (1.23 g, 98%) as a clear colorless oil.

^{1}H NMR (500 MHz, $CDCl_3$) δ: 5.94 (br. s., 1H), 4.04–3.97 (m, 1H), 3.76–3.70 (m, 2H), 3.67–3.61 (m, 1H), 2.42 (dd, *J* = 5.5, 17.2 Hz, 1H), 2.15–2.05 (m, 1H), 2.00 (dd, *J* = 7.1, 17.3 Hz, 1H), 1.86–1.78 (m, 1H), 1.77–1.71 (m, 1H), 1.68–1.57 (m, 4H), 1.13–1.01 (m, 24H), 0.90 (s, 9H), 0.09 (s, 3H), 0.08 (s, 3H). **^{13}C NMR** (126 MHz, C_6D_6) δ: 171.3, 68.4, 60.8, 47.8, 44.9, 41.6, 39.9, 35.5, 26.5, 24.9, 20.6, 18.7, 18.6, 12.7, –3.7, –3.9. **FTIR** (thin film) cm^{-1}: 3202, 3090, 2941, 2928, 2864, 1663, 1462, 1252, 1100, 1070, 835, 774. **HRMS** (ESI) (*m/z*) calc'd for $C_{25}H_{53}NNaO_3Si_2$ $[M+Na]^+$: 494.3456, found 494.3465. **$[\alpha]_D^{22}$**: –4.2 (*c* = 1.4, CH_2Cl_2). **TLC** (EtOAc), R_f: 0.45 ($KMnO_4$).

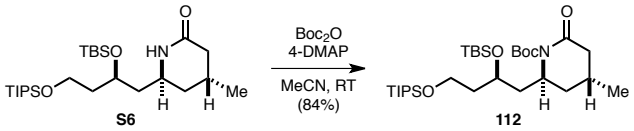

Imide 112:

Boc_2O (5.82 g, 25.9 mmol, 2.00 equiv) and 4-DMAP (1.90 g, 15.5 mmol, 1.20 equiv) were added successively to a solution of silyl ether **S6** (6.10 g, 12.9 mmol, 1.00 equiv), which was azeotropically dried with benzene (5 × 10 mL), in MeCN (120 mL) at room temperature. The resultant solution was stirred for 96 h, during which additional Boc_2O (23.3 g, 103 mmol, 8.00 equiv) and 4-DMAP (7.60 g, 62.0 mmol, 4.80 equiv) were added in four portions. Water (100 mL), Et_2O (150 mL), and EtOAc (100 mL) were added to the reaction mixture. The layers were separated and the aqueous layer was extracted with EtOAc (3 × 100 mL). The organic layers were combined, washed with brine (200 mL), dried over anhydrous $MgSO_4$, and concentrated under reduced pressure. The resulting oil was then purified by flash column chromatography (silica gel, eluent: gradient: 12:1 → 7:1 hexanes:EtOAc) to afford imide **112** (6.24 g, 84%) as a pale yellow oil.

^{1}H NMR (600 MHz, $CDCl_3$) δ: 4.44–4.37 (m, 1H), 4.04–3.95 (m, 1H), 3.80–3.68 (m, 2H), 2.59 (dd, *J* = 3.9, 17.3 Hz, 1H), 2.17–2.09 (m, 1H), 2.08–1.97 (m, 2H), 1.87–1.72 (m, 3H), 1.64 (dt, *J* = 5.7, 13.0 Hz, 1H), 1.53–1.49 (m, 10H), 1.14–1.01 (m, 21H), 0.98 (d, *J* = 6.3 Hz, 3H), 0.89 (s, 9H), 0.08 (s, 3H), 0.06 (s, 3H). **^{13}C NMR** (126 MHz, C_6D_6) δ: 170.9, 154.9, 82.3, 67.9, 60.8, 52.9, 43.5, 41.3, 41.1, 34.7, 28.5, 26.5, 24.6, 21.9, 18.7, 12.7, –3.8, –3.9. **FTIR** (thin film) cm^{-1}: 2941, 2929, 2865, 1715, 1367, 1291, 1249, 1158, 1100, 836, 775. **HRMS** (ESI) (*m/z*) calc'd for $C_{30}H_{61}NNaO_5Si_2$ $[M+Na]^+$: 594.3971, found 594.3980. **TLC** (12:1 hexanes:EtOAc), R_f: 0.58 ($KMnO_4$).

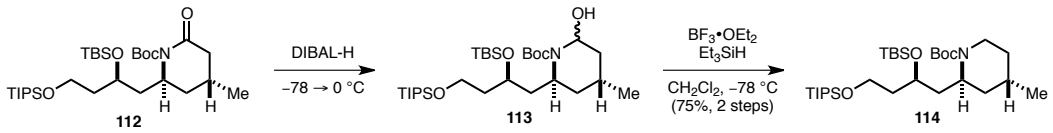

***N*-Boc piperidine 114:**

Diisobutylaluminum hydride (887 μL, 4.97 mmol, 4.00 equiv) was added to a stirred solution of imide **112** (711 mg, 1.24 mmol, 1.00 equiv), which was azeotropically dried with benzene (5 × 5 mL), in THF (12.4 mL) at −78 °C. The reaction was allowed to warm gradually to room temperature over 2 h, at which point a saturated aqueous solution of Rochelle's salt (50 mL) was carefully added at a slow rate. The resultant mixture was subsequently diluted with Et_2O (50 mL) and EtOAc (50 mL), and stirred vigorously for 5 h. The layers were separated and the aqueous layer was extracted with EtOAc (3 × 50 mL). The organic layers were combined, washed with brine (100 mL), dried over anhydrous $MgSO_4$, and concentrated under reduced pressure to afford crude *N,O*-hemiaminal **113** as a pale yellow flocculent solid and as a 1:1 mixture of diastereomers, which was carried forward to the next step without further purification.

BF_3•OEt_2 (1.53 mL, 12.4 mmol, 10.0 equiv) was added dropwise to a solution of crude **113**, which was azeotropically dried with benzene (5 × 5 mL), and Et_3SiH (1.99 mL, 12.4 mmol, 10.0 equiv) in CH_2Cl_2 (62 mL) at −78 °C. After 2 h, saturated aqueous $NaHCO_3$ solution (50 mL), Et_2O (50 mL), and EtOAc (50 mL) were added successively to the reaction. The resultant mixture was allowed to warm to room temperature. The layers were separated and the aqueous layer was extracted with EtOAc (3 × 50 mL). The organic layers were combined, washed with brine (100 mL), dried over anhydrous $MgSO_4$, and concentrated under reduced pressure. The resulting oil was then purified by flash column chromatography (silica gel, eluent: gradient: 20:1 → 7:1 hexanes:EtOAc) to afford *N*-Boc piperidine **114** (522 mg, 75% over 2 steps) as a clear colorless oil.

^{1}H NMR (600 MHz, $CDCl_3$, 50 °C) δ: 4.45–4.31 (m, 1H), 4.17–3.93 (m, 1H), 3.86–3.78 (m, 2H), 3.77–3.70 (m, 1H), 2.78 (t, *J* = 13.6 Hz, 1H), 1.85–1.76 (m, 3H), 1.76–1.65 (m, 3H), 1.63–1.54 (m,

2H), 1.46 (s, 9H), 1.24–1.16 (m, 1H), 1.12–1.02 (m, 24H), 0.89 (s, 9H), 0.06 (s, 3H), 0.05 (s, 3H). **^{13}C NMR** (126 MHz, C_6D_6, 70 °C) δ: 155.1, 79.3, 68.8, 61.5, 48.4, 41.0, 40.1, 39.1, 38.4, 35.0, 29.1, 26.6, 26.2, 22.7, 18.7, 13.0, –3.7, –3.9. **FTIR** (thin film) cm^{-1}: 2946, 2927, 2865, 1693, 1413, 1364, 1251, 1164, 1095, 1070, 836, 773. **HRMS** (ESI) (*m/z*) calc'd for $C_{30}H_{63}NNaO_4Si_2$ $[M+Na]^+$: 580.4188, found 580.4165. **$[\alpha]_D^{22}$**: –5.6 (*c* = 0.67, CH_2Cl_2). **TLC** (6:1 hexanes:EtOAc), R_f: 0.45 ($KMnO_4$).

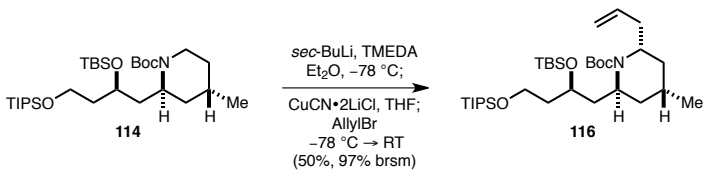

Allyl *N*-Boc piperidine 116:

A solution of *sec*-butyllithium in cyclohexane (1.45 M, 968 μL, 1.40 mmol, 1.50 equiv) was added to a stirred solution of *N*-Boc piperidine **114** (522 mg, 0.935 mmol, 1.00 equiv), which was azeotropically dried with benzene (5 × 5 mL), and TMEDA (210 μL, 1.40 mmol 1.50 equiv) in Et_2O (11 mL) at −78 °C. The reaction was stirred for 7 h at −78 °C.

During this period, a separate 0.10 M stock solution of CuCN•2LiCl in THF was prepared according to the following protocol: CuCN (100 mg, 1.12 mmol, 1.00 equiv) and LiCl (94.6 mg, 2.24 mmol, 2.00 equiv) in THF (11.1 mL) were stirred vigorously for 20 min at room temperature prior to use.

After the 7 h deprotonation period of **114**, a solution of CuCN•2LiCl in THF (0.10 M, 5.60 mL, 0.60 equiv) was added slowly via syringe down the walls of the reaction vessel. The resultant reaction was stirred vigorously for 1 h, at which point allyl bromide (151 μL, 1.68 mmol, 1.80 equiv) was added dropwise via syringe to the reaction mixture, which immediately turned bright yellow. After stirring for 1 h at −78 °C, the reaction was gradually allowed to warm to room temperature over 3 h. After stirring for an additional 1 h at room temperature, the reaction was cooled to 0 °C and an aqueous solution of 5 M NH_4OH (3 mL) was added. The resultant mixture was allowed to warm to room temperature and was stirred vigorously for 30 min, at which point the mixture was filtered through Celite. The Celite filter cake was washed with Et_2O (50 mL) and water (10 mL). The layers were separated and the aqueous layer was extracted with Et_2O (3 × 50 mL). The organic layers were combined, washed with water (100 mL), then brine (100 mL), and dried over anhydrous $MgSO_4$ and concentrated under reduced pressure. The resulting oil was then purified by flash column

chromatography (silica gel, eluent: gradient: 30:1 → 7:1 → 4:1 hexanes:EtOAc) to afford allyl *N*-Boc piperidine **116** (277 mg, 50%, 97% brsm) as a single diastereomer as a clear colorless oil.

^{1}H NMR (600 MHz, C_6D_6) δ: 6.00–5.91 (m, 1H), 5.17 (d, *J* = 17.1 Hz, 1H), 5.09 (d, *J* = 10.3 Hz, 1H), 4.51–4.42 (m, 1H), 4.08–4.02 (m, 1H), 3.98–3.92 (m, 1H), 3.87 (td, *J* = 6.5, 9.6 Hz, 1H), 3.43–3.31 (m, 1H), 3.09–2.96 (m, 1H), 2.53–2.39 (m, 1H), 2.13 (ddd, *J* = 5.4, 8.3, 13.9 Hz, 1H), 2.04–1.88 (m, 2H), 1.75–1.63 (m, 2H), 1.61–1.52 (m, 1H), 1.49 (s, 9H), 1.31–1.22 (m, 2H), 1.19 (d, *J* = 13.2 Hz, 1H), 1.17–1.09 (m, 21H), 1.04 (s, 9H), 0.79 (d, *J* = 6.6 Hz, 3H), 0.18 (s, 3H), 0.18 (s, 3H). **^{13}C NMR** (126 MHz, C_6D_6) δ: 156.1, 137.6, 116.86, 79.3, 68.1, 61.2, 54.3, 51.0, 40.5, 40.3, 39.5, 37.1, 36.9, 28.9, 26.6, 26.5, 23.0, 18.7, 18.6, 12.7, –3.6, –4.0. **FTIR** (thin film) cm^{-1}: 2927, 2865, 1702, 1365, 1251, 1171, 1097, 836, 774. **HRMS** (ESI) (*m/z*) calc'd for $C_{33}H_{67}NNaO_4Si_2$ $[M+Na]^+$: 620.4501, found 620.4526. **TLC** (6:1 hexanes:EtOAc), R_f: 0.71 ($KMnO_4$).

1D NOESY (500 MHz, C_6D_6):

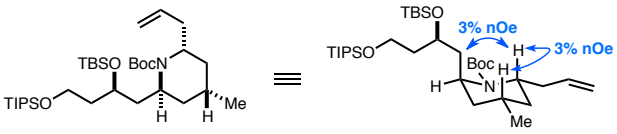

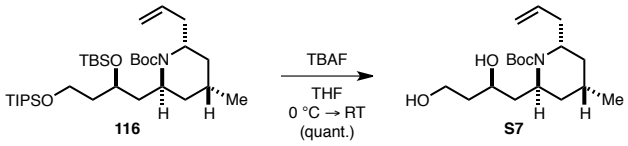

Diol S7:

A solution of TBAF in THF (1.00 M, 8.10 mL, 8.06 mmol, 6.00 equiv) was added to a solution of allyl *N*-Boc piperidine **116** (803 mg, 1.34 mmol, 1.00 equiv) in THF (13.4 mL) at 0 °C. After 5 min, the reaction was allowed to warm to room temperature and was stirred for an additional 3.5 h, at which point saturated aqueous NH_4Cl solution (25 mL), water (10 mL), Et_2O (20 mL), and EtOAc (20 mL) were added successively. The layers were separated and the aqueous layer was extracted with EtOAc (3 × 20 mL). The organic layers were combined, washed with brine (50 mL), then dried over anhydrous $MgSO_4$ and concentrated under reduced pressure. The resultant oil was purified by flash column chromatography (silica gel, eluent: gradient: 2:1 EtOAc:hexanes → EtOAc) to afford diol **S7** (439 mg, quant.) as a pale yellow oil.

^{1}H NMR (500 MHz, $CDCl_3$) δ: 5.80–5.70 (m, 1H), 5.12–5.02 (m, 2H), 4.16–4.09 (m, 1H), 4.07 (br. s., 1H), 3.92 (tt, *J* = 3.8, 8.2 Hz, 2H), 3.83 (t, *J* = 5.5 Hz, 2H), 3.56 (dt, *J* = 5.9, 9.9 Hz, 1H), 3.00 (br. s., 1H), 2.59 (td, *J* = 6.0, 13.5 Hz, 1H), 2.30 (td, *J* = 8.5, 13.7 Hz, 1H), 1.90 (td, *J* = 6.4, 12.4 Hz, 1H), 1.87–1.77 (m, 2H), 1.73–1.63 (m, 4H), 1.51–1.43 (m, 10H), 1.33 (td, *J* = 6.1, 13.9 Hz, 1H), 1.01 (d, *J* = 6.8 Hz, 3H). **^{13}C NMR** (126 MHz, $CDCl_3$) δ: 156.3, 135.8, 117.1, 110.7, 80.2, 71.4, 61.8, 52.8, 51.2, 41.9, 40.2, 38.7, 35.8, 33.0, 28.5, 23.2. **FTIR** (thin film) cm^{-1}: 3401, 2950, 2928, 2871, 1661, 1399, 1365, 1168, 1115, 1069. **HRMS** (ESI) (*m/z*) calc'd for $C_{18}H_{33}KNO_4$ $[M+K]^+$: 366.2041, found 366.2056. **$[\alpha]_D^{22}$**: –4.4 (*c* = 0.50, CH_2Cl_2). **TLC** (2:1 EtOAc:hexanes), R_f: 0.14 ($KMnO_4$).

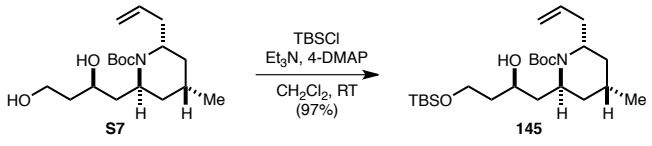

Silyl ether 145:

Et_3N (220 μL, 1.57 mmol, 1.20 equiv), TBSCl (217 mg, 1.44 mmol, 1.10 equiv), and 4-DMAP (16.0 mg, 0.131 mmol, 0.10 equiv) were added sequentially to a stirred solution of diol **S7** (428 mg, 1.31 mmol, 1.00 equiv), which was azeotropically dried with benzene (5 × 1.5 mL), in CH_2Cl_2 (13 mL) at room temperature. After 17 h, saturated aqueous NH_4Cl solution (15 mL) was added and the resultant mixture was diluted with EtOAc (15 mL), Et_2O (20 mL), and water (10 mL). The layers were separated and the aqueous layer was extracted with EtOAc (3 × 20 mL). The organic layers were combined, washed with brine (50 mL), dried over anhydrous $MgSO_4$, and concentrated under reduced pressure. The resulting crude residue was then purified by flash column chromatography (silica gel, eluent: gradient: 12:1 → 6:1 hexanes:EtOAc) to afford silyl ether **145** (560 mg, 97%) as a clear colorless oil.

^{1}H NMR (500 MHz, $CDCl_3$) δ: 5.82–5.71 (m, 1H), 5.07 (d, *J* = 16.8 Hz, 1H), 5.02 (d, *J* = 10.0 Hz, 1H), 4.23–4.16 (m, 1H), 3.91–3.75 (m, 3H), 3.64 (br. s., 1H), 3.50–3.42 (m, 1H), 2.70–2.60 (m, 1H), 2.37–2.27 (m, 1H), 1.95–1.88 (m, 1H), 1.88–1.81 (m, 1H), 1.78–1.55 (m, 5H), 1.49–1.41 (m, 9H), 1.39–1.31 (m, 1H), 1.24 (td, *J* = 7.7, 13.9 Hz, 1H), 0.96 (d, *J* = 6.6 Hz, 3H), 0.89 (s, 9H), 0.07 (s, 6H). **^{13}C NMR** (126 MHz, $CDCl_3$) δ: 155.9, 136.3, 116.7, 79.5, 69.4, 62.1, 52.9, 50.6, 39.9, 39.9, 38.5, 35.9, 34.5, 28.5, 25.9, 24.5, 22.9, 18.2, –5.5, –5.5. **FTIR** (thin film) cm^{-1}: 3419, 2952, 2928, 2857, 1686, 1662, 1392, 1365, 1251, 1171, 1090, 836, 775. **HRMS** (ESI) (*m/z*) calc'd for $C_{24}H_{47}NNaO_4Si$ $[M+Na]^+$: 464.3167, found 464.3195. **$[\alpha]_D^{23}$**: –2.2 (*c* = 0.72, CH_2Cl_2). **TLC** (2:1 EtOAc: hexanes), R_f: 0.82 ($KMnO_4$).

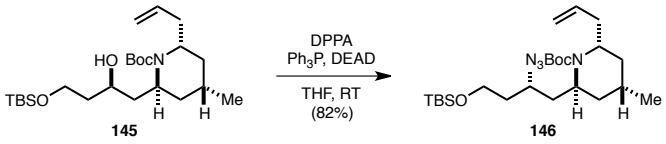

Azide 146:

Triphenylphosphine (1.32 g, 5.02 mmol, 4.00 equiv), diethyl azodicarboxylate (806 μL, 5.02 mmol, 4.00 equiv), and diphenyl phosphoryl azide (1.11 mL, 5.02 mmol, 4.00 equiv) were added sequentially to a stirred solution of silyl ether **145** (554 mg, 1.25 mmol, 1.00 equiv), which was azeotropically dried with benzene (5 × 1 mL), in THF (20 mL) at room temperature. After 1 h, the reaction was concentrated under reduced pressure. The resultant residue was then purified by flash column chromatography (silica gel, eluent: 16:1 hexanes:EtOAc) to afford alkyl azide **146** (479 mg, 82%) as a pale yellow oil.

^{1}H NMR (500 MHz, $CDCl_3$) δ: 5.82–5.72 (m, 1H), 5.08 (qd, *J* = 1.6, 17.1 Hz, 1H), 5.02 (td, *J* = 1.0, 10.2 Hz, 1H), 4.26–4.15 (m, 1H), 3.79–3.69 (m, 2H), 3.59–3.51 (m, 1H), 3.38–3.31 (m, 1H), 2.71 (td, *J* = 6.6, 13.5 Hz, 1H), 2.39–2.29 (m, 1H), 2.03 (ddd, *J* = 3.8, 9.8, 14.0 Hz, 1H), 1.82–1.73 (m, 2H), 1.72–1.61 (m, 3H), 1.52–1.43 (m, 10H), 1.34–1.15 (m, 2H), 0.94 (d, *J* = 6.6 Hz, 3H), 0.89 (s, 9H), 0.06 (s, 3H), 0.06 (s, 3H). **^{13}C NMR** (126 MHz, $CDCl_3$) δ: 155.9, 136.4, 116.5, 79.5, 59.5, 57.7, 53.5, 50.8, 39.4, 38.2, 36.8, 36.2, 35.7, 28.5, 25.9, 25.8, 22.5, 18.3, –5.4, –5.5. **FTIR** (thin film) cm^{-1}: 2953, 2928, 2857, 2104, 1694, 1365, 1322, 1252, 1167, 1109, 835, 776. **HRMS** (ESI) (*m/z*) calc'd for $C_{24}H_{47}N_4O_3Si$ $[M+H]^+$: 467.3412, found 467.3417. **$[\alpha]_D^{23}$**: –13 (*c* = 0.39, CH_2Cl_2). **TLC** (12:1 hexanes:EtOAc), R_f: 0.69 ($KMnO_4$).

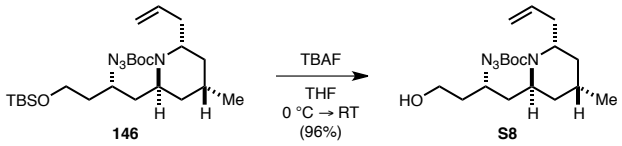

Alcohol S8:

A solution of TBAF in THF (1.00 M, 2.00 mL, 2.02 mmol, 2.00 equiv) was added to a solution of alkyl azide **146** (472 mg, 1.01 mmol, 1.00 equiv) in THF (20 mL) at 0 °C. After 5 min, the reaction was allowed to warm to room temperature and was stirred for an additional 1 h, at which point saturated aqueous NH_4Cl solution (10 mL), water (10 mL), Et_2O (15 mL), and EtOAc (15 mL) were added successively. The layers were separated and the aqueous layer was extracted with EtOAc (3 × 15 mL). The organic layers were combined, washed with brine (30 mL), then dried over anhydrous $MgSO_4$ and concentrated under reduced pressure. The resultant oil was purified by flash column chromatography (silica gel, eluent: gradient: 4:1 → 2:1 hexanes:EtOAc) to afford alcohol **S8** (340 mg, 96%) as a pale yellow oil.

^{1}H NMR (500 MHz, $CDCl_3$) δ: 5.79 (tdd, *J* = 7.1, 10.1, 17.2 Hz, 1H), 5.08 (dd, *J* = 1.3, 17.2 Hz, 1H), 5.03 (td, *J* = 1.0, 10.3 Hz, 1H), 3.97 (dd, *J* = 4.9, 8.8 Hz, 1H), 3.84–3.73 (m, 2H), 3.62–3.50 (m, 2H), 2.61 (td, *J* = 6.8, 13.5 Hz, 1H), 2.32–2.22 (m, 2H), 1.93–1.84 (m, 1H), 1.79–1.66 (m, 4H), 1.48–1.39 (m, 10H), 1.31–1.22 (m, 1H), 1.19 (td, *J* = 9.4, 13.2 Hz, 1H), 0.95 (d, *J* = 6.1 Hz, 3H). **^{13}C NMR** (126 MHz, $CDCl_3$) δ: 156.1, 136.2, 116.6, 79.7, 59.4, 57.8, 54.1, 50.0, 39.3, 37.1, 36.5, 36.1, 35.5, 28.5, 25.7, 22.3. **FTIR** (thin film) cm^{-1}: 3432, 2951, 2929, 2873, 2102, 1685, 1366, 1323, 1253, 1166, 1117. **HRMS** (ESI) (*m/z*) calc'd for $C_{18}H_{33}N_4O_3$ $[M+H]^+$: 353.2547, found 353.2549. **$[\alpha]_D^{23}$**: –2.0 (*c* = 0.59, CH_2Cl_2). **TLC** (2:1 hexanes:EtOAc), R_f: 0.22 ($KMnO_4$).

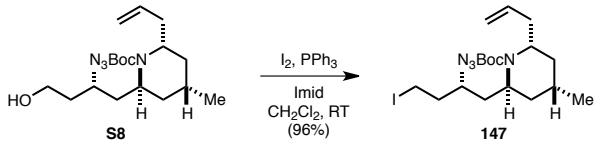

Alkyl iodide 147:

Triphenylphosphine (671 mg, 2.56 mmol, 2.70 equiv) and iodine (722 mg, 2.84 mmol, 3.00 equiv) were added sequentially as single portions to a stirred solution of imidazole (387 mg, 5.69 mmol, 6.00 equiv) in CH_2Cl_2 (9.5 mL). After 20 min, a solution of alcohol **S8** (334 mg, 0.948 mmol, 1.00 equiv), which was azeotropically dried with benzene (5 × 1 mL), in CH_2Cl_2 (9.5 mL) was added dropwise via syringe to the reaction mixture. After 30 min, saturated aqueous $Na_2S_2O_3$ solution (20 mL), EtOAc (15 mL), and Et_2O (15 mL) were added sequentially to the reaction. The layers were separated and the aqueous layer was extracted with EtOAc (3 × 15 mL). The organic layers were combined, washed with brine (50 mL), dried over anhydrous $MgSO_4$, and concentrated under reduced pressure. The resulting residue was then purified by flash column chromatography (silica gel, eluent: 12:1 hexanes:EtOAc) to afford alkyl iodide **147** (419 mg, 96%) as a pale yellow oil.

^{1}H NMR (500 MHz, $CDCl_3$) δ: 5.81 (dddd, *J* = 6.2, 8.0, 10.3, 16.9 Hz, 1H), 5.10 (qd, *J* = 1.5, 17.2 Hz, 1H), 5.05 (td, *J* = 1.1, 10.1 Hz, 1H), 4.24–4.16 (m, 1H), 3.51 (tt, *J* = 4.2, 9.1 Hz, 1H), 3.38–3.32 (m, 1H), 3.32–3.19 (m, 2H), 2.74 (td, *J* = 6.5, 13.6 Hz, 1H), 2.37–2.26 (m, 1H), 2.09–1.92 (m, 3H), 1.82–1.73 (m, 1H), 1.72–1.67 (m, 1H), 1.63 (td, *J* = 4.5, 13.6 Hz, 1H), 1.55–1.49 (m, 1H), 1.47 (s, 9H), 1.31 (ddd, *J* = 5.5, 11.7, 13.6 Hz, 1H), 1.26–1.17 (m, 1H), 0.95 (d, *J* = 6.6 Hz, 3H). **^{13}C NMR** (126 MHz, $CDCl_3$) δ: 155.9, 136.4, 116.8, 79.7, 60.8, 53.7, 50.5, 39.4, 39.0, 36.2, 36.0, 35.7, 28.5, 25.8, 22.5, 1.7. **FTIR** (thin film) cm^{-1}: 2952, 2927, 2118, 2100, 1690, 1365, 1322, 1252, 1167, 1111. **HRMS** (ESI) (*m/z*) calc'd for $C_{18}H_{31}IN_4NaO_2$ $[M+Na]^+$: 485.1384, found 485.1388. **TLC** (1:1 hexanes:EtOAc), R_f: 0.68 ($KMnO_4$, UV).

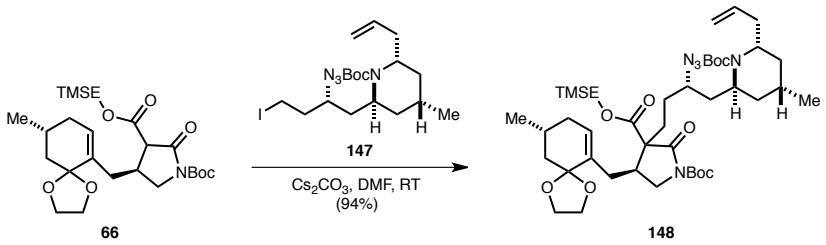

Alkylated imide 148:

A solution of alkyl iodide **147** (419 mg, 0.906 mmol, 1.00 equiv), which was azeotropically dried with benzene (5 × 1 mL), in DMF (5 mL) was added dropwise to a stirred solution of β-carboxyimide **66**[93] (584 mg, 1.18 mmol, 1.30 equiv) and Cs_2CO_3 (886 mg, 2.72 mmol, 3.00 equiv) in DMF (4 mL). After 12.5 h, Et_2O (20 mL) and saturated aqueous NH_4Cl solution (15 mL) were added sequentially to the reaction mixture. The layers were separated and the aqueous layer was extracted with EtOAc (3 × 10 mL). The organic layers were combined and washed with brine (20 mL), dried over anhydrous $MgSO_4$, and concentrated under reduced pressure. The resultant residue was purified by flash column chromatography (silica gel, eluent: gradient: 9:1 → 7:1 → 4:1 hexanes:EtOAc, 1% Et_3N) to afford alkylated imide **148** (708 mg, 94%) as a white flocculent solid.

^{1}H NMR (500 MHz, C_6D_6) δ: 6.05–5.93 (m, 1H), 5.60 (d, *J* = 3.9 Hz, 1H), 5.23 (d, *J* = 18.3 Hz, 1H), 5.14 (d, *J* = 10.3 Hz, 1H), 4.44–4.36 (m, 1H), 4.28–4.19 (m, 1H), 4.18–4.09 (m, 1H), 4.09–4.01 (m, 1H), 3.84–3.74 (m, 3H), 3.73–3.68 (m, 1H), 3.57–3.48 (m, 2H), 3.06 (br. s., 2H), 2.89–2.76 (m, 2H), 2.51–2.41 (m, 1H), 2.32 (dt, *J* = 4.4, 13.2 Hz, 1H), 2.26–2.18 (m, 1H), 2.06–1.88 (m, 4H), 1.84–1.72 (m, 3H), 1.49 (s, 9H), 1.44 (s, 9H), 1.40–1.25 (m, 5H), 1.24–1.04 (m, 3H), 0.89–0.84 (m, 2H), 0.80 (d, *J* = 6.6 Hz, 3H), 0.71 (d, *J* = 6.3 Hz, 3H), –0.17 (s, 9H). **^{13}C NMR** (126 MHz, C_6D_6) δ: 171.4, 170.5, 156.3, 151.6, 137.7, 134.9, 132.3, 117.1, 108.8, 83.1, 79.5, 65.8, 64.5, 64.2, 62.2, 61.4, 54.5, 51.6, 50.6, 42.5, 39.8, 38.4, 37.3, 37.1, 36.6, 34.6, 31.2, 30.8, 29.8, 28.9, 28.4, 28.1, 26.8, 22.8, 21.9, 18.1, –1.4. **FTIR** (thin film) cm^{-1}: 2952, 2106, 1719, 1701, 1367, 1314, 1251, 1171, 839. **HRMS** (ESI) (*m/z*) calc'd for $C_{43}H_{71}N_5NaO_9Si$ $[M+Na]^+$: 852.4918, found 852.4913. **TLC** (4:1 hexanes:EtOAc), R_f: 0.65 (Anis, $KMnO_4$, UV).

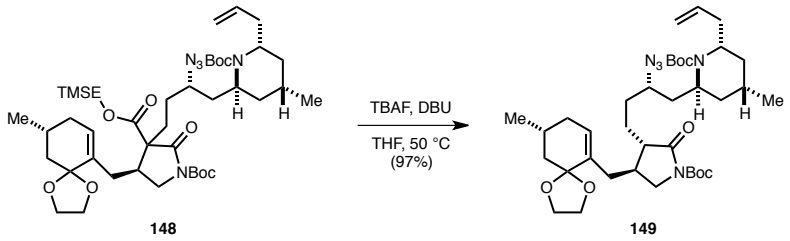

***N*-Boc-2-pyrrolidinone 149**:

A solution of TBAF in THF (1.00 M, 843 μL, 0.843 mmol, 1.00 equiv) was added to a solution of alkylated imide **148** (700 mg, 0.843 mmol, 1.00 equiv) and DBU (32.0 μL, 0.211 mmol, 0.25 equiv) in THF (17 mL) at room temperature. After 5 min, the reaction was heated to 50 °C and was stirred for 16 h, at which point water (20 mL), Et_2O (15 mL), and EtOAc (15 mL) were added successively. The layers were separated and the aqueous layer was extracted with EtOAc (3 × 15 mL). The organic layers were combined, washed with brine (30 mL), then dried over anhydrous $MgSO_4$ and concentrated under reduced pressure. The resultant residue was purified by flash column chromatography (silica gel, eluent: gradient: 8:1 → 6:1 → 4:1 → 2:1 hexanes:EtOAc, 1% Et_3N) to afford *N*-Boc-2-pyrrolidinone **149** (562 mg, 97%) as a white flocculent solid.

^{1}H NMR (500 MHz, C_6D_6) δ: 6.05–5.88 (m, 1H), 5.44 (d, *J* = 3.4 Hz, 1H), 5.20 (d, *J* = 17.1 Hz, 1H), 5.12 (dd, *J* = 2.0, 10.3 Hz, 1H), 4.42–4.36 (m, *J* = 4.6 Hz, 1H), 3.97–3.88 (m, 1H), 3.68–3.53 (m, 4H), 3.51–3.39 (m, 3H), 3.05 (dd, *J* = 8.8, 10.7 Hz, 3H), 2.36 (dd, *J* = 4.5, 13.8 Hz, 1H), 2.29–2.22 (m, 1H), 2.20–2.12 (m, 1H), 1.98–1.89 (m, 2H), 1.88–1.81 (m, 1H), 1.81–1.68 (m, 5H), 1.49 (s, 9H), 1.47 (s, 9H), 1.45–1.27 (m, 5H), 1.27–1.04 (m, 3H), 0.82 (d, *J* = 6.6 Hz, 3H), 0.73 (d, *J* = 6.3 Hz, 3H). **^{13}C NMR** (126 MHz, C_6D_6) δ: 174.2, 156.3, 151.6, 137.8, 135.7, 131.3, 117.0, 108.7, 82.4, 79.5, 65.8, 64.4, 61.5, 54.4, 51.6, 50.7, 49.5, 42.6, 39.9, 37.2, 37.2, 36.6, 35.8, 35.0, 34.6, 32.6, 28.9, 28.5, 28.1, 26.8, 26.1, 22.8, 22.0. **FTIR** (thin film) cm^{-1}: 2950, 2925, 2074, 1784, 1712, 1367, 1316, 1160. **HRMS** (ESI) (*m/z*) calc'd for $C_{37}H_{59}N_5NaO_7$ $[M+Na]^+$: 708.4307, found 708.4306. **TLC** (1:1 hexanes:EtOAc), R_f: 0.61 (Anis, $KMnO_4$, UV).

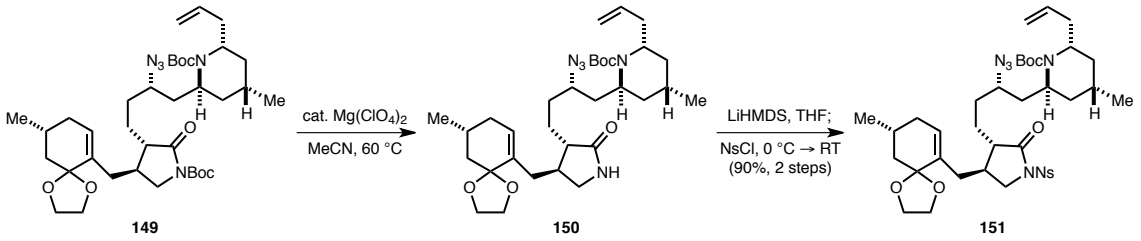

***N*-2-Nitrobenzenesulfonyl-2-pyrrolidinone 151**:

$Mg(ClO_4)_2$ (36.5 mg, 0.164 mmol, 0.20 equiv) was added as a single portion to a stirred solution of *N*-Boc-2-pyrrolidinone **149** (561 mg, 0.818 mmol, 1.00 equiv), which was azeotropically dried with benzene (5 × 1 mL), in MeCN (13.6 mL) at room temperature. The resultant mixture was heated to 60 °C and stirred for 2 h, at which point it was cooled to room temperature and Et_2O (25 mL) and saturated aqueous NH_4Cl solution (15 mL) were added sequentially. The layers were separated and the aqueous layer was extracted with EtOAc (3 × 15 mL). The organic layers were combined, washed with brine (30 mL), then dried over anhydrous $MgSO_4$ and concentrated under reduced pressure to afford crude 2-pyrrolidinone **150** as a white flocculent solid, which was carried forward to the next step without further purification.

A freshly prepared solution of LiHMDS in THF (1.00 M, 982 μL, 0.982 mmol, 1.20 equiv) was added dropwise to a solution of **150**, which was azeotropically dried with benzene (5 × 1 mL), in THF (4.25 mL) at room temperature. After 1 h, the reaction was cooled to 0 °C and a solution of NsCl in THF (1.00 M, 1.06 mL, 1.06 mmol, 1.30 equiv) was added. After 5 min, the reaction was warmed to room temperature and stirred for 1 h. Saturated aqueous NH_4Cl solution (10 mL), and then Et_2O (10 mL), were added. The layers were separated and the aqueous layer was extracted with EtOAc (3 × 10 mL). The organic layers were combined, washed with brine (20 mL), dried over anhydrous $MgSO_4$, and concentrated *in vacuo*. The residue was purified by flash column chromatography (silica gel, eluent: gradient: 7:1 → 4:1 → 2:1 hexanes:EtOAc, 1% Et_3N) to afford *N*-2-nitrobenzenesulfonyl-2-pyrrolidinone **151** (566 mg, 90% over 2 steps) as a white flocculent solid.

^{1}H NMR (500 MHz, C_6D_6) δ: 8.45 (dd, *J* = 1.3, 7.9 Hz, 1H), 6.76–6.71 (m, 1H), 6.66–6.60 (m, 1H), 6.49–6.41 (m, 1H), 5.99–5.84 (m, 1H), 5.52 (d, *J* = 3.7 Hz, 1H), 5.14 (d, *J* = 17.1 Hz, 1H), 5.07 (dd, *J* = 2.0, 10.0 Hz, 1H), 4.33–4.23 (m, 2H), 3.69 (dd, *J* = 4.5, 7.4 Hz, 1H), 3.66 (d, *J* = 6.8 Hz, 2H), 3.56–3.46 (m, 2H), 3.40–3.31 (m, 1H), 3.07–2.96 (m, 1H), 2.55–2.43 (m, 1H), 2.36 (dd, *J* = 5.7, 14.0 Hz, 1H), 2.25–2.14 (m, 1H), 1.98–1.79 (m, 4H), 1.78–1.63 (m, 3H), 1.60–1.50 (m, 1H), 1.47–1.42 (m, 11H), 1.40–1.23 (m, 6H), 1.18–1.02 (m, 3H), 0.82 (d, *J* = 6.6 Hz, 3H), 0.71 (d, *J* = 6.3 Hz, 3H). **^{13}C NMR** (126 MHz, C_6D_6) δ: 175.6, 156.3, 148.7, 137.7, 135.2, 135.0, 134.6, 132.5, 132.1, 131.7, 124.1, 116.9, 108.7, 79.6, 65.7, 64.5, 61.2, 54.4, 51.6, 51.5, 48.9, 42.5, 39.9, 37.8, 37.1, 36.5, 34.9, 34.5, 32.5, 29.0, 28.0, 26.7, 25.8, 22.7, 21.9. **FTIR** (thin film) cm^{-1}: 2952, 2926, 2102, 1737, 1691, 1545, 1366, 1174, 1128, 594. **HRMS** (ESI) (*m/z*) calc'd for $C_{38}H_{55}N_6O_9S$ $[M+H]^+$: 771.3746, found 771.3738. **TLC** (2:1 hexanes:EtOAc), R_f: 0.39 (Anis, $KMnO_4$, UV).

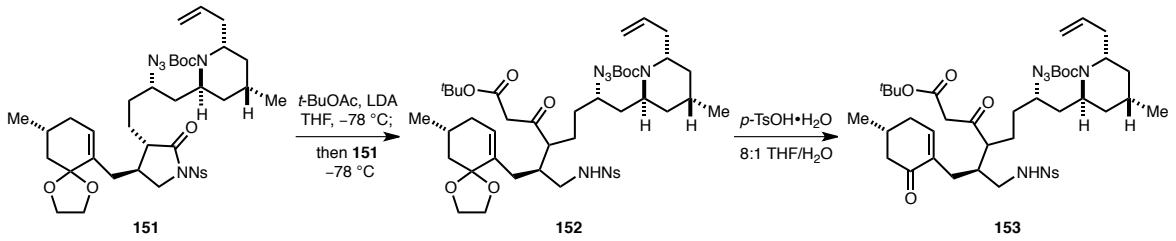

Enone 153:

A solution of *n*-butyllithium in hexanes (2.53 M, 869 µL, 2.20 mmol, 3.00 equiv) was added dropwise to a stirred solution of diisopropylamine (339 µL, 2.42 mmol, 3.30 equiv) in THF (4.2 mL) at −78 °C. The reaction was stirred for 10 min, at which point it was warmed to 0 °C. After 10 min, the reaction was warmed to room temperature. The solution was recooled to −78 °C after 5 min. *t*-Butylacetate (295 µL, 2.20 mmol, 3.00 equiv) was then added dropwise to the reaction mixture. After 1 h, a solution of **151** (565 mg, 0.733 mmol, 1.00 equiv), which was azeotropically dried with benzene (5 × 2 mL), in THF (9.3 mL) was added dropwise down the walls of the reaction vessel. After stirring at −78 °C for 1.5 h, saturated aqueous NH_4Cl solution (15 mL) was added to the deep red reaction mixture at −78 °C. The resultant mixture was then allowed to warm to room temperature. Et_2O (15 mL) and EtOAc (15 mL) were added and the layers were separated. The aqueous layer was extracted with EtOAc (3 × 10 mL). The organic layers were combined, washed with brine (30 mL), then dried over anhydrous $MgSO_4$ and concentrated under reduced pressure to afford crude β-ketoester **152** as a white flocculent solid, which was carried forward to the next step without further purification.

p-TsOH•H_2O (70.0 mg, 0.366 mmol, 0.50 equiv) was added as a single portion to a stirred solution of crude **152** in THF (13 mL) and water (1.6 mL) at room temperature. After 3 h, a saturated aqueous $NaHCO_3$ solution (20 mL) was added, followed by Et_2O (10 mL), EtOAc (10 mL), and water (5 mL). The layers were separated and the aqueous layer was extracted with EtOAc (3 × 10 mL). The organic layers were combined, washed with brine (30 mL), then dried over anhydrous

$MgSO_4$ and concentrated under reduced pressure to afford crude enone **153** as a white flocculent solid, which was carried forward to the next step without further purification.

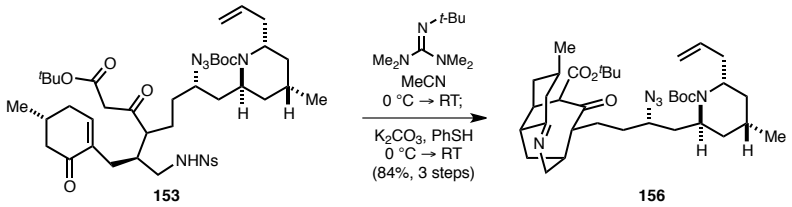

Imine 156:

2-*t*-Butyl-1,1,3,3-tetramethylguanidine (591 μL, 2.90 mmol, 5.00 equiv) was added dropwise to a solution of crude enone **153**, which was azeotropically dried with benzene (5 × 2 mL), in MeCN (29 mL) at 0 °C. After 15 min, the reaction mixture was warmed to room temperature and stirred for 18 h, at which point K_2CO_3 (401 mg, 2.90 mmol, 5.00 equiv) was added as a single portion. The suspension was then cooled to 0 °C and PhSH (298 μL, 2.90 mmol, 5.00 equiv) was added dropwise via syringe. After 10 min, the reaction was warmed to room temperature and stirred for an additional 4.5 h, at which point water (100 mL), Et_2O (100 mL), and EtOAc (100 mL) were added sequentially. The layers were separated and the aqueous layer was extracted with EtOAc (3 × 50 mL). The organic layers were combined, washed with brine (100 mL), dried over anhydrous $MgSO_4$, and concentrated under reduced pressure. The crude residue was then purified by flash column chromatography (silica gel, eluent: gradient: 2:1 → 1:1 → 0:1 hexanes:EtOAc, 1% Et_3N) to afford imine **156** (312 mg, 84% over 3 steps) as a pale yellow flocculent solid.

^{1}H NMR (500 MHz, C_6D_6) δ: 6.06–5.89 (m, 1H), 5.17 (d, *J* = 16.6 Hz, 1H), 5.08 (d, *J* = 9.8 Hz, 1H), 4.37–4.25 (m, 1H), 4.03 (d, *J* = 18.3 Hz, 1H), 3.57–3.52 (m, *J* = 7.8 Hz, 1H), 3.49 (d, *J* = 3.2 Hz, 1H), 3.23 (d, *J* = 19.5 Hz, 1H), 3.20–3.14 (m, 1H), 3.09–2.97 (m, *J* = 5.9 Hz, 1H), 2.87 (br. s., 1H), 2.64–2.56 (m, 1H), 2.51 (d, *J* = 12.0 Hz, 1H), 2.34–2.20 (m, 2H), 2.05 (t, *J* = 11.8 Hz, 1H), 1.95 (br. s., 1H), 1.86 (br. s., 1H), 1.82–1.71 (m, 2H), 1.66 (br. s., 1H), 1.58–1.50 (m, 4H), 1.48 (s, 9H), 1.46–1.40 (m, *J* = 12.2 Hz, 2H), 1.37 (s, 9H), 1.36–1.32 (m, 3H), 1.19–1.02 (m, 3H), 0.73 (d, *J* = 6.1 Hz, 3H), 0.62 (d, *J* = 6.1 Hz, 3H). **^{13}C NMR** (126 MHz, $CDCl_3$) δ: 205.1, 170.5, 169.0, 156.3, 137.7, 116.9, 82.2, 79.5, 66.2, 61.4, 55.3, 54.6, 51.5, 49.2, 48.4, 43.4, 39.9, 39.0, 38.3, 37.3, 37.1, 36.1,

34.4, 33.1, 30.2, 29.8, 28.9, 28.3, 26.9, 26.7, 22.7, 22.6. **FTIR** (thin film) cm^{-1}: 2951, 2926, 2101, 1699, 1455, 1366, 1253, 1154. **HRMS** (ESI) (*m/z*) calc'd for $C_{36}H_{58}N_5O_5$ $[M+H]^+$: 640.4432, found 640.4418. **TLC** (90:9:1 $CHCl_3$:MeOH:NH_4OH), R_f: 0.38 ($KMnO_4$, UV).

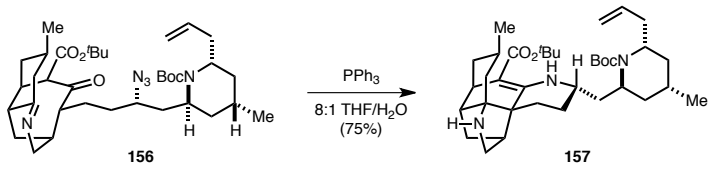

Vinylogous Urethane 157:

Triphenylphosphine (84.0 mg, 0.321 mmol, 1.50 equiv) was added as a single portion to a stirred solution of imine **156** (137 mg, 0.214 mmol, 1.00 equiv) in THF (6.2 mL) and water (780 μL) at room temperature. The reaction was heated to 70 °C and stirred for 23 h, at which point the reaction was cooled to room temperature and concentrated. The resultant residue was azeotropically dried with MeOH (5 × 3 mL), then benzene (3 × 3 mL), and stirred with silica gel (200 mg) in CH_2Cl_2 (5 mL) for 2 h. The slurry was subsequently filtered and washed with 90:9:1 $CHCl_3$:MeOH:NH_4OH (10 × 5 mL) and concentrated *in vacuo*. The crude residue was then purified by flash column chromatography (silica gel, eluent: gradient: 1:1 → 0:1 hexanes:EtOAc, 1% Et_3N → 90:9:1 $CHCl_3$:MeOH:NH_4OH) to afford vinylogous urethane **157** (95.4 mg, 75%) as a pale yellow flocculent solid.

^{1}H NMR (500 MHz, C_6D_6) δ: 9.73 (s, 1 H), 6.03–5.83 (m, 1H), 5.17 (d, *J* = 16.1 Hz, 1H), 5.07 (d, *J* = 12.5 Hz, 1H), 4.21–4.07 (m, 1H), 3.59–3.48 (m, 1H), 3.31–3.22 (m, *J* = 6.2, 11.8 Hz, 1H), 2.95 (d, *J* = 3.7 Hz, 1H), 2.90 (dd, *J* = 6.6, 12.5 Hz, 1H), 2.76 (d, *J* = 7.8 Hz, 1H), 2.48–2.36 (m, 1H), 2.17 (br. s., 1H), 2.08–2.01 (m, 2H), 2.01–1.90 (m, 1H), 1.88–1.81 (m, *J* = 6.1 Hz, 1H), 1.80–1.73 (m, 1H), 1.71–1.61 (m, *J* = 8.5 Hz, 2H), 1.57–1.52 (m, *J* = 6.3 Hz, 2H), 1.51 (s, 9H), 1.47 (s, 9H), 1.40–1.29 (m, 4H), 1.21 (t, *J* = 13.9 Hz, 1H), 1.16–1.07 (m, *J* = 10.3 Hz, 3H), 1.07–0.98 (m, 2H), 0.95 (d, *J* = 6.1 Hz, 3H), 0.79 (d, *J* = 5.9 Hz, 3H). **^{13}C NMR** (126 MHz, $CDCl_3$) δ: 170.9, 162.8, 156.2, 137.6, 116.7, 90.5, 79.3, 78.0, 63.9, 54.2, 51.7, 51.3, 50.4, 50.3, 47.6, 47.0, 41.4, 40.5, 40.5, 39.9, 38.1, 36.3, 35.7, 34.0, 29.2, 29.0, 27.9, 25.6, 25.5, 23.1, 23.1, 21.5. **FTIR** (thin film) cm^{-1}: 2948, 2926, 2868, 1686, 1635, 1594, 1453, 1364, 1249, 1155, 1114. **HRMS** (ESI) (*m/z*) calc'd for

$C_{36}H_{58}N_3O_4$ $[M+H]^+$: 596.4422, found 596.4416. $\mathbf{[\alpha]_D^{23}}$: –69 (*c* = 0.55, CH_2Cl_2). **TLC** (90:9:1 $CHCl_3$:MeOH:NH_4OH), R_f: 0.20 ($KMnO_4$, UV).

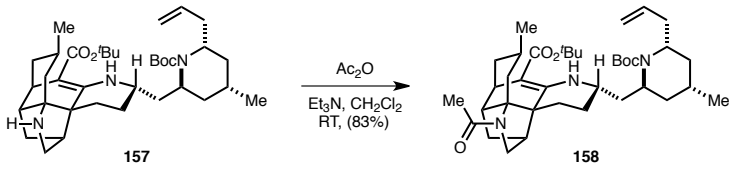

Amide 158:

Acetic anhydride (562 μL, 5.95 mmol, 20.0 equiv) was added dropwise to a stirred solution of vinylogous urethane **157** (177 mg, 0.297 mmol, 1.00 equiv), which was azeotropically dried with benzene (5 × 3 mL), and Et_3N (830 μL, 5.95 mmol, 20.0 equiv) in CH_2Cl_2 (6 mL) at room temperature. After stirring for 30 h, the reaction was concentrated under reduced pressure. The resultant residue was then directly purified by flash column chromatography (silica gel, eluent: gradient: 2:1 → 1:1 → 0:1 hexanes:EtOAc) to afford amide **158** (158 mg, 83%) as a white flocculent solid.

^{1}H NMR (600 MHz, C_6D_6) δ: 9.58 (s, 1H), 5.97–5.86 (m, 1H), 5.17 (d, *J* = 17.0 Hz, 1H), 5.08 (d, *J* = 10.3 Hz, 1H), 4.21–4.09 (m, *J* = 5.0 Hz, 1H), 3.66 (t, *J* = 13.1 Hz, 1H), 3.60–3.49 (m, 1H), 3.28–3.16 (m, 1H), 3.00 (br. s., 1H), 2.93–2.81 (m, 2H), 2.70–2.59 (m, 1H), 2.46–2.32 (m, 2H), 2.08 (dd, *J* = 6.9, 13.1 Hz, 1H), 2.02 (br. s., 1H), 1.95 (d, *J* = 11.2 Hz, 1H), 1.80–1.73 (m, 2H), 1.73–1.71 (m, 1H), 1.70 (s, 3H), 1.67–1.60 (m, 1H), 1.59–1.51 (m, 2H), 1.50–1.45 (m, 18H), 1.42–1.25 (m, 5H), 1.18–1.09 (m, 2H), 1.08–1.05 (m, 1H), 1.03 (d, *J* = 6.2 Hz, 3H), 0.80 (d, *J* = 6.2 Hz, 3H). **^{13}C NMR** (126 MHz, C_6D_6) δ: 170.8, 170.7, 161.2, 156.1, 137.5, 116.8, 90.9, 79.4, 78.4, 70.5, 54.5, 54.1, 52.7, 51.8, 50.3, 43.3, 42.9, 41.2, 40.7, 40.0, 39.2, 36.1, 35.5, 34.5, 33.8, 29.1, 29.0, 27.5, 25.6, 25.3, 24.9, 23.1, 23.0, 22.1. **FTIR** (thin film) cm^{-1}: 2972, 2948, 2928, 2870, 1686, 1655, 1641, 1596, 1389, 1365, 1251, 1166, 1155. **HRMS** (ESI) (*m/z*) calc'd for $C_{38}H_{59}N_3NaO_5$ $[M+Na]^+$: 660.4347, found 660.4374. **$[\alpha]_D^{23}$**: –156 (*c* = 0.23, CH_2Cl_2). **TLC** (90:9:1 $CHCl_3$:MeOH:NH_4OH), R_f: 0.79 ($KMnO_4$, UV).

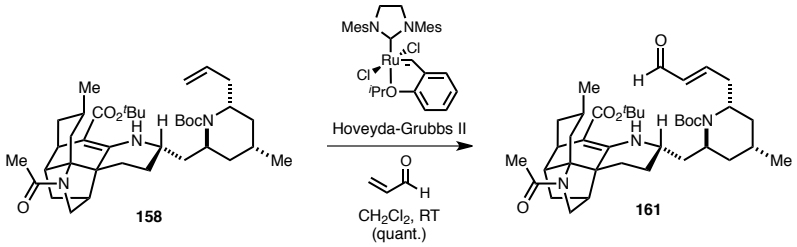

Enal 161:

Hoveyda-Grubbs 2nd generation catalyst (20.0 mg, 0.0322 mmol, 0.50 equiv) was added as a single portion to a solution of amide **158** (41.4 mg, 0.0644 mmol, 1.00 equiv), which was azeotropically dried with benzene (5 × 1 mL), and acrolein (50.0 μL, 0.644 mmol, 10.0 equiv) in CH_2Cl_2 (1.8 mL) at room temperature. The reaction was stirred for 21 h, at which point additional acrolein (25.0 μL, 0.322 mmol, 5.00 equiv) and Hoveyda-Grubbs catalyst (10.0 mg, 0.0161 mmol, 0.25 equiv) were added. After stirring for a further 12 h, the reaction was concentrated under reduced pressure. The resultant residue was then directly purified by flash column chromatography (silica gel, eluent: gradient: 4:1 → 2:1 → 1:1 hexanes:EtOAc) to afford enal **161** (43.0 mg, quant.) as a yellow solid.

^{1}H NMR (500 MHz, C_6D_6) δ: 9.56 (s, 1H), 9.42 (d, *J* = 7.8 Hz, 1H), 6.53–6.44 (m, 1H), 6.14 (dd, *J* = 7.7, 15.7 Hz, 1H), 4.01 (br. s., 1H), 3.66 (t, *J* = 13.5 Hz, 1H), 3.43 (br. s., 1H), 3.25–3.12 (m, 1H), 3.03–2.85 (m, 3H), 2.64 (br. s., 1H), 2.43 (d, *J* = 8.8 Hz, 1H), 2.26 (td, *J* = 7.0, 14.6 Hz, 1H), 2.04 (br. s., 1H), 2.02–1.90 (m, 3H), 1.80 (d, *J* = 12.4 Hz, 1H), 1.75–1.68 (m, 4H), 1.65–1.59 (m, 1H), 1.53–1.48 (m, *J* = 5.9 Hz, 1H), 1.45 (s, 9H), 1.42 (s, 9H), 1.37–1.23 (m, 6H), 1.06 (d, *J* = 6.3 Hz, 4H), 1.04–0.97 (m, 1H), 0.97–0.93 (m, 1H), 0.89–0.86 (m, 1H), 0.73 (d, *J* = 6.3 Hz, 3H). **^{13}C NMR** (126 MHz, C_6D_6) δ: 193.3, 171.1, 161.2, 156.1, 155.3, 134.9, 128.9, 91.4, 79.9, 78.3, 70.3, 54.5, 53.5, 52.6, 51.7, 50.4, 43.4, 42.8, 41.1, 40.0, 39.2, 38.6, 36.8, 36.5, 34.5, 33.7, 29.1, 28.9, 27.7, 25.8, 25.5, 24.9, 23.0, 22.8, 22.1. **FTIR** (thin film) cm^{-1}: 2949, 2927, 2869, 1691, 1653, 1639, 1596, 1390, 1365, 1166, 1154. **HRMS** (ESI) (*m/z*) calc'd for $C_{39}H_{59}N_3NaO_6$ $[M+Na]^+$: 688.4296, found 688.4289. **$[\alpha]_D^{23}$**: –86 (*c* = 0.35, CH_2Cl_2). **TLC** (EtOAc), R_f: 0.43 ($KMnO_4$, UV).

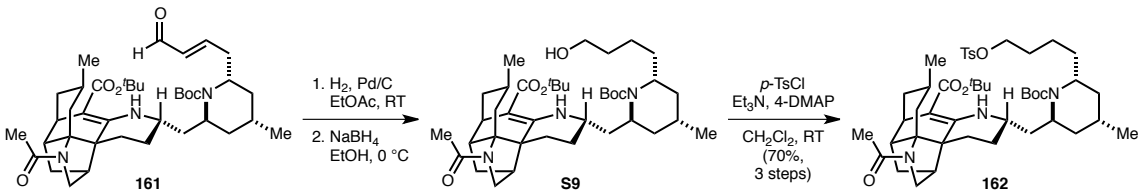

Tosylate 162:

Palladium on carbon (10 wt%, 14.0 mg, 0.0130 mmol, 0.20 equiv) was added as a single portion to a stirred solution of enal **161** (43.0 mg, 0.0650 mmol, 1.00 equiv) in EtOAc (3.2 mL). The reaction vessel was purged with H_2 and placed under an atmosphere of H_2. After 2 h, Celite was poured into the stirred reaction mixture and the resultant slurry was then filtered through a pad of Celite. The solution was concentrated under reduced pressure to afford the corresponding aldehyde, which was carried forward to the next step without further purification.

$NaBH_4$ (5.0 mg, 0.13 mmol, 2.0 equiv) was added as a single portion to a stirred solution of the crude aldehyde, which was azeotropically dried with benzene (5 × 1 mL), in EtOH (1.5 mL) at 0 °C. The reaction was stirred for 40 min, at which point saturated aqueous NH_4Cl solution (0.5 mL) was added and all volatiles were removed *in vacuo*. Water (2 mL), Et_2O (2 mL), and EtOAc (2 mL) were added sequentially to the crude residue. The layers were separated and the aqueous layer was extracted with EtOAc (3 × 2 mL). The organic layers were combined, washed with brine (5 mL), dried over anhydrous $MgSO_4$, and concentrated under reduced pressure to provide alcohol **S9**, which was carried forward to the next step without further purification.

Next, Et_3N (75.0 μL, 0.520 mmol, 8.00 equiv), 4-DMAP (8.0 mg, 0.065 mmol, 1.0 equiv), and *p*-TsCl (50.0 mg, 0.260 mmol, 4.00 equiv) were added sequentially to a stirred solution of crude alcohol **S9**, which was azeotropically dried with benzene (5 × 1 mL), in CH_2Cl_2 (1.3 mL) at room temperature. After stirring for 12 h, a saturated aqueous $NaHCO_3$ solution (2 mL) and brine (2 mL) were added sequentially, followed by Et_2O (2 mL), and EtOAc (2 mL). The layers were separated and the aqueous layer was extracted with EtOAc (3 × 2 mL). The organic layers were combined, dried over anhydrous $MgSO_4$, and concentrated under reduced pressure. The residue was purified by

flash column chromatography (silica gel, eluent: gradient: 2:1 → 1:1 → 0:1 hexanes:EtOAc) to afford tosylate **162** (37.5 mg, 70% over 3 steps) as a yellow solid.

^{1}H NMR (500 MHz, C_6D_6) δ: 9.57 (s, 1H), 7.77 (d, *J* = 7.8 Hz, 2H), 6.73 (d, *J* = 8.1 Hz, 2H), 4.13 (br. s., 1H), 3.97–3.84 (m, 2H), 3.66 (t, *J* = 12.9 Hz, 1H), 3.27 (br. s., 1H), 3.25–3.19 (m, 1H), 2.98 (d, *J* = 2.9 Hz, 1H), 2.93 (d, *J* = 8.1 Hz, 1H), 2.64 (t, *J* = 5.4 Hz, 1H), 2.44 (d, *J* = 8.5 Hz, 1H), 2.07 (dd, *J* = 3.0, 4.3 Hz, 1H), 2.05–2.00 (m, 2H), 1.93 (d, *J* = 11.5 Hz, 2H), 1.84 (s, 3H), 1.82–1.76 (m, 2H), 1.73 (s, 3H), 1.68–1.62 (m, 1H), 1.58–1.51 (m, 3H), 1.48 (s, 9H), 1.46 (s, 9H), 1.41–1.32 (m, 7H), 1.31–1.24 (m, 3H), 1.18–1.05 (m, 3H), 1.01 (d, *J* = 5.6 Hz, 3H), 0.79 (d, *J* = 6.1 Hz, 3H). **^{13}C NMR** (126 MHz, C_6D_6) δ: 170.8, 170.7, 161.2, 156.3, 144.4, 135.0, 130.2, 128.0, 90.9, 79.5, 78.4, 70.7, 70.5, 54.5, 54.3, 52.7, 51.9, 50.6, 43.3, 42.9, 41.3, 40.0, 39.2, 36.9, 36.7, 35.0, 34.4, 33.8, 29.7, 29.1, 29.0, 27.7, 26.0, 25.6, 24.9, 23.7, 23.0, 23.0, 22.1, 21.5. **FTIR** (thin film) cm^{-1}: 2946, 2928, 1685, 1654, 1638, 1595, 1389, 1364, 1175, 1166, 1154. **HRMS** (ESI) (*m/z*) calc'd for $C_{46}H_{69}N_3NaO_8S$ $[M+Na]^+$: 846.4698, found 846.4716. **TLC** (EtOAc), R_f: 0.56 ($KMnO_4$, UV).

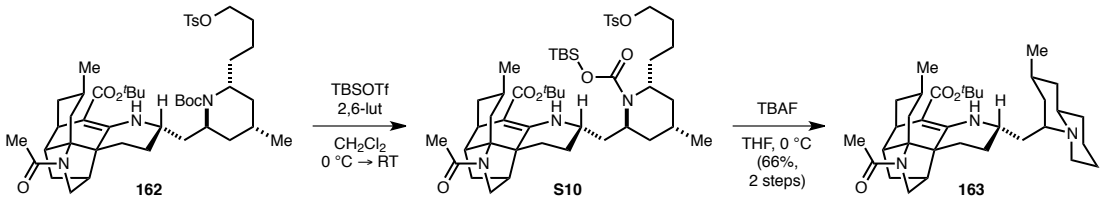

Quinolizidine 163:

2,6-Lutidine (13.5 μL, 0.115 mmol, 10.0 equiv) was added dropwise to a stirred solution of tosylate **162** (9.5 mg, 0.012 mmol, 1.0 equiv), which was azeotropically dried with benzene (5 × 0.5 mL) in CH_2Cl_2 (1 mL) at 0 °C, followed by TBSOTf (21.0 μL, 0.0922 mmol, 8.00 equiv). After stirring for 5 min at 0 °C, the reaction mixture was allowed to warm to room temperature and was stirred for an additional 16.5 h, at which point a saturated aqueous $NaHCO_3$ solution (0.5 mL) was added, followed by Et_2O (1 mL) and EtOAc (1 mL). The layers were separated and the aqueous layer was extracted with EtOAc (3 × 1 mL). The organic layers were combined, washed with brine (2 mL), dried over anhydrous $MgSO_4$, and concentrated under reduced pressure to afford the corresponding silyloxy carbamate **S10**, which was carried forward to the next step without further purification.

A solution of TBAF in THF (1.00 M, 23.0 μL, 0.0230 mmol, 2.00 equiv) was added to a solution of crude silyloxy carbamate **S10** in THF (1 mL) at 0 °C. After stirring for 0.5 h at 0 °C, 8 drops of AcOH were added and the reaction was concentrated under reduced pressure. The resultant residue was then directly purified by flash column chromatography (silica gel, eluent, gradient: 2:1 → 1:1 → 0:1 hexanes:EtOAc, 1% Et_3N → 9:1 CH_2Cl_2:MeOH, 1% Et_3N) to afford quinolizidine **163**. **163** was further purified by preparatory thin-layer chromatography (PTLC) using 90:9:1 $CHCl_3$:MeOH:NH_4OH, furnishing quinolizidine **163** (4.2 mg, 66% over 2 steps) as a white solid.

^{1}H NMR (600 MHz, C_6D_6) δ: 9.57 (br. s., 1H), 3.67 (t, *J* = 13.2 Hz, 1H), 3.11 (dt, *J* = 5.4, 11.6 Hz, 1H), 3.01 (br. s., 1H), 2.92 (d, *J* = 5.1 Hz, 1H), 2.88 (d, *J* = 6.8 Hz, 1H), 2.70–2.63 (m, 1H), 2.58 (d, *J* = 10.8 Hz, 1H), 2.41 (d, *J* = 8.3 Hz, 2H), 2.15–2.06 (m, 1H), 2.05–1.92 (m, 3H), 1.80 (d, *J* = 13.4

Hz, 1H), 1.72 (s, 3H), 1.70–1.62 (m, 3H), 1.61–1.50 (m, 6H), 1.46 (s, 9H), 1.38 (d, J = 14.2 Hz, 1H), 1.34–1.19 (m, 6H), 1.18–1.06 (m, 2H), 1.03 (d, J = 6.1 Hz, 3H), 1.00–0.94 (m, 1H), 0.93–0.87 (m, 1H), 0.84 (d, J = 5.6 Hz, 3H). **^{13}C NMR** (126 MHz, C_6D_6) δ: 170.7, 170.6, 161.1, 90.9, 78.4, 70.4, 57.3, 54.4, 53.2, 52.7, 52.3, 52.0, 43.3, 42.9, 42.0, 40.0, 39.2, 37.5, 34.8, 34.5, 33.8, 33.3, 29.1, 27.5, 27.4, 25.6, 25.6, 24.9, 24.7, 23.2, 23.1, 22.1. **FTIR** (thin film) cm^{-1}: 2926, 2866, 1655, 1641, 1596, 1388, 1154. **HRMS** (ESI) (*m/z*) calc'd for $C_{34}H_{54}N_3O_3$ $[M+H]^+$: 552.4160, found 552.4173. **$[\alpha]_D^{23}$**: –91 (c = 0.22, CH_2Cl_2). **TLC** (90:9:1 $CHCl_3$:MeOH:NH_4OH), R_f: 0.16 ($KMnO_4$, UV).

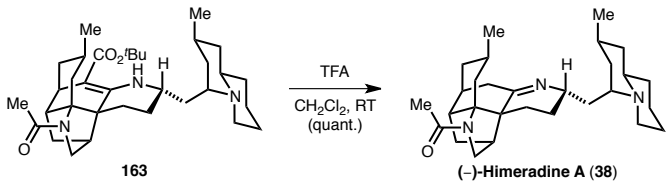

Proposed structure of (–)-himeradine A (38):

Trifluoroacetic acid (500 μL) was added to a stirred solution of quinolizidine **163** (9.4 mg, 0.017 mmol, 1.0 equiv) in CH_2Cl_2 (500 μL) at room temperature. After stirring for 13 h, the reaction was concentrated *in vacuo* to afford (–)-himeradine A (**38**) as the double TFA salt (11.6 mg, quant.) and as a white solid.

^{1}H NMR (600 MHz, CD_3OD) δ: 4.08 (tt, *J* = 5.0, 9.9 Hz, 1H), 3.81 (d, *J* = 9.4 Hz, 1H), 3.63 (d, *J* = 11.7 Hz, 1H), 3.36 (d, *J* = 9.4 Hz, 1H), 3.28 (d, *J* = 11.2 Hz, 1H), 3.26–3.21 (m, 1H), 3.17 (dt, *J* = 2.3, 12.5 Hz, 1H), 3.03 (dd, *J* = 12.6, 14.1 Hz, 1H), 2.69 (dd, *J* = 2.9, 4.7 Hz, 1H), 2.62–2.56 (m, 1H), 2.53–2.46 (m, 1H), 2.38 (d, *J* = 4.4 Hz, 1H), 2.32–2.26 (m, 1H), 2.16–2.09 (m, 1H), 2.03 (s, 3H), 2.01–1.93 (m, 7H), 1.87–1.75 (m, 5H), 1.74–1.64 (m, 3H), 1.64–1.58 (m, 1H), 1.55 (t, *J* = 11.2 Hz, 2H), 1.37–1.26 (m, 3H), 1.22 (q, *J* = 12.3 Hz, 1H), 1.00 (d, *J* = 6.2 Hz, 3H), 0.98 (d, *J* = 5.9 Hz, 3H). **^{13}C NMR** (126 MHz, C_6D_6) δ: 196.5, 174.3, 75.9, 59.7, 58.7, 57.4, 57.1, 55.9, 53.1, 45.1, 43.0, 40.7, 40.6, 40.5, 35.4, 35.3, 35.0, 32.6, 31.5, 29.6, 27.7, 24.6, 24.6, 24.4, 24.1, 23.0, 22.8, 21.4, 20.3. **FTIR** (thin film) cm^{-1}: 3430, 2955, 2931, 2875, 1667, 1400, 1199, 1132. **HRMS** (ESI) (*m/z*) calc'd for $C_{29}H_{46}N_3O$ $[M+H]^+$: 452.3635, found 452.3637. **$[\alpha]_D^{23}$**: –19 (*c* = 0.3, MeOH).[139] **TLC** (80:18:2 $CHCl_3$:MeOH:NH_4OH), R_f: 0.62 ($KMnO_4$).

[139] The reported specific rotation for (–)-himeradine A (**38**) is $[\alpha]_D^{25}$: –23 (*c* = 0.3, MeOH).

Table S1. ^{1}H NMR Data Comparison Between Natural and Synthetic Proposed Structure of (−)-Himeradine A (**38**) as the Double TFA Salt in CD_3OD.

Isolation Report[92] (^{1}H, 600 MHz, CD_3OD)	Synthetic (−)-Himeradine A (**38**) (^{1}H, 600 MHz, CD_3OD)
0.96 (d, *J* = 4.6 Hz, 3H)	0.98 (d, *J* = 5.9 Hz, 3H)
0.98 (d, *J* = 5.9 Hz, 3H)	1.00 (d, *J* = 6.2 Hz, 3H)
1.19 (br. q, *J* = 13.2 Hz, 1H)	1.22 (q, *J* = 12.3 Hz, 1H)
1.23–1.32 (m, 3H)	1.37–1.26 (m, 3H)
1.54–1.58 (m, 3H)	1.55 (t, *J* = 11.2 Hz, 2H)
	1.64–1.58 (m, 1H)
1.64–1.66 (m, 3H)	1.74–1.64 (m, 3H)
1.73–1.82 (m, 5H)	1.87–1.75 (m, 5H)
1.90–1.95 (m, 7H)	2.01–1.93 (m, 7H)
2.02 (s, 3H)	2.03 (s, 3H)
2.10 (m, 1H)	2.16–2.09 (m, 1H)
2.29 (m, 1H)	2.32–2.26 (m, 1H)
2.35 (br. s, 1H)	2.38 (d, *J* = 4.4 Hz, 1H)
2.49 (br. d, *J* = 11.8 Hz, 1H)	2.53–2.46 (m, 1H)
2.57 (br. s, 1H)	2.62–2.56 (m, 1H)
2.70 (br. s, 1H)	2.69 (dd, *J* = 2.9, 4.7 Hz, 1H)
3.01 (br. t, *J* = 12.9 Hz, 1H)	3.03 (dd, *J* = 12.6, 14.1 Hz, 1H)
3.19 (m, 1H)	3.17 (dt, *J* = 2.3, 12.5 Hz, 1H)
3.24 (m, 1H)	3.26–3.21 (m, 1H)
3.33 (m, 1H)	3.28 (d, *J* = 11.2 Hz, 1H)
3.34 (m, 1H)	3.36 (d, *J* = 9.4 Hz, 1H)
3.77 (m, 1H)*	3.63 (d, *J* = 11.7 Hz, 1H)*
3.80 (m, 1H)	3.81 (d, *J* = 9.4 Hz, 1H)
4.09 (m, 1H)	4.08 (tt, *J* = 5.0, 9.9 Hz, 1H)

*The chemical shift of H10' in the synthetic proposed structure of himeradine A (**38**) was shifted upfield by $\Delta\delta$ = 0.14 ppm relative to natural himeradine A.

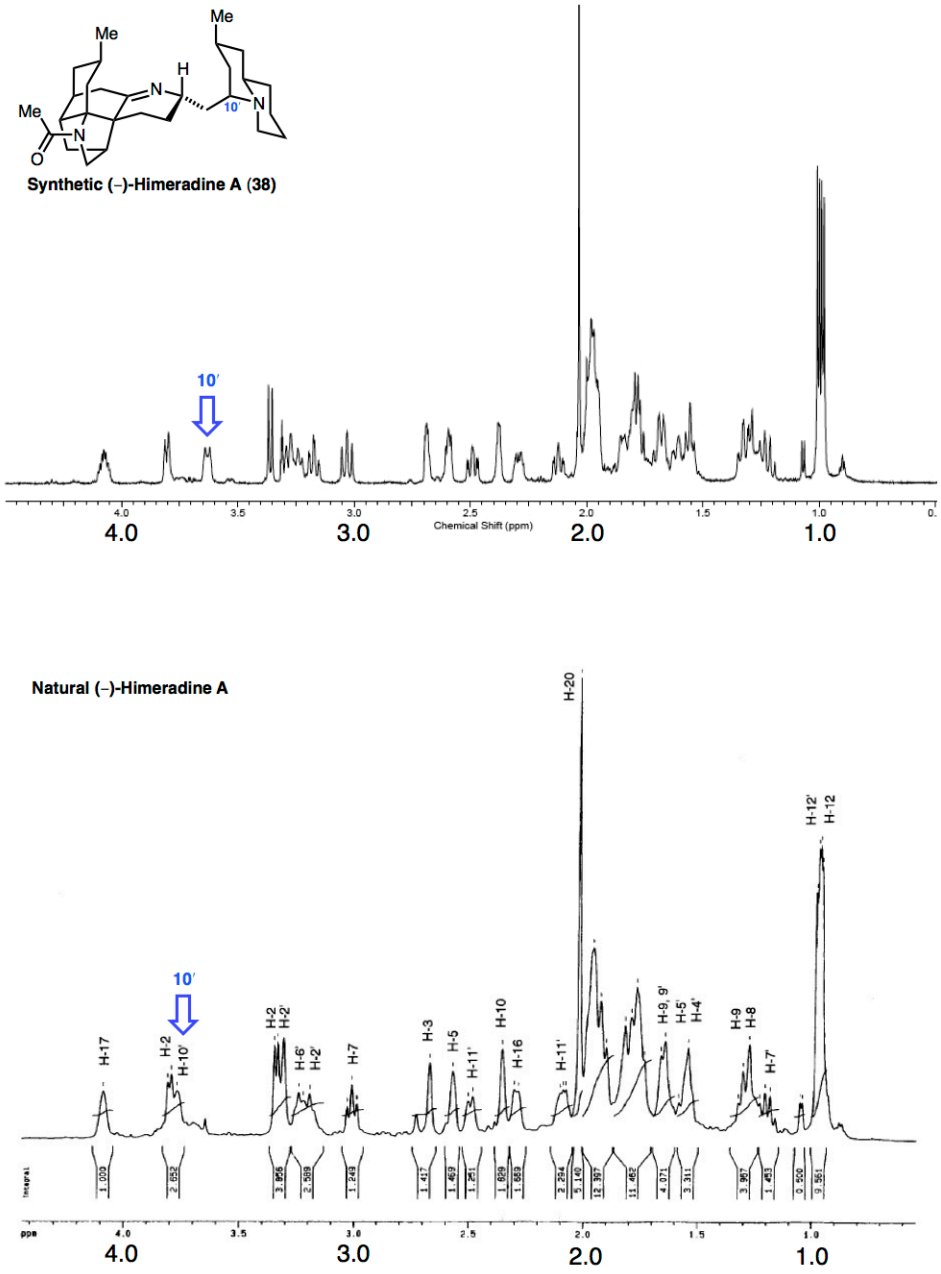

Figure S1. Comparison of ^{1}H NMR Spectra of Natural and Synthetic Proposed Structure of (–)-Himeradine A (**38**) as the Double TFA Salt in CD_3OD.

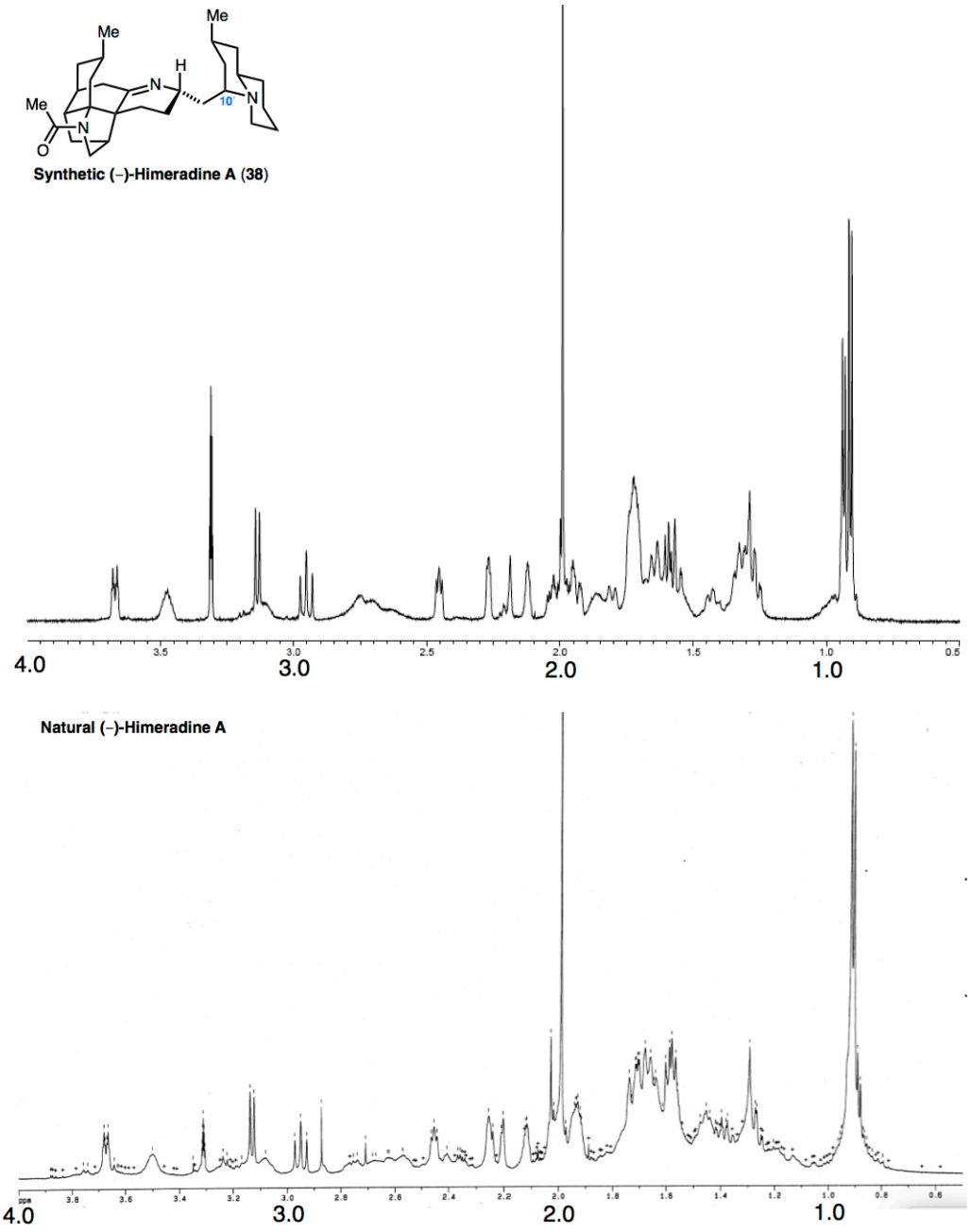

Figure S2. Comparison of ^{1}H NMR Spectra of Natural and Synthetic Proposed Structure of (–)-Himeradine A (**38**) as the Free Base in CD_3OD.[140]

---

[140] The free base ^{1}H NMR spectrum of natural himeradine A (**38**) in CD_3OD was kindly provided by Professor Hiroshi Morita via private communication.

Table S2. ^{13}C NMR Data Comparison Between Natural and Synthetic Proposed Structure of (–)-Himeradine A (**38**) as the Double TFA Salt in CD_3OD.

Isolation Report[92] (^{13}C, 150 MHz, CD_3OD)	Synthetic (–)-Himeradine A (**38**) (^{13}C, 126 MHz, CD_3OD)
20.6	20.3
21.5	21.4
22.8	22.8
22.9	23.0
24.2	24.1
24.4	24.4
24.6	24.6
26.0	24.6
27.7	27.7
31.1	29.6
31.6	31.5
32.5	32.6
35.0	35.0
35.5	35.3
37.0	35.4
39.0[141]	40.5
40.5	40.6
40.7	40.7
43.0	43.0
45.4	45.1
52.9	53.1
56.6	55.9
57.1	57.1
57.5	57.4
58.4	58.7
60.0	59.7
76.1	75.9
174.3	174.3
196.7	196.5

[141] In pyridine-d_5.

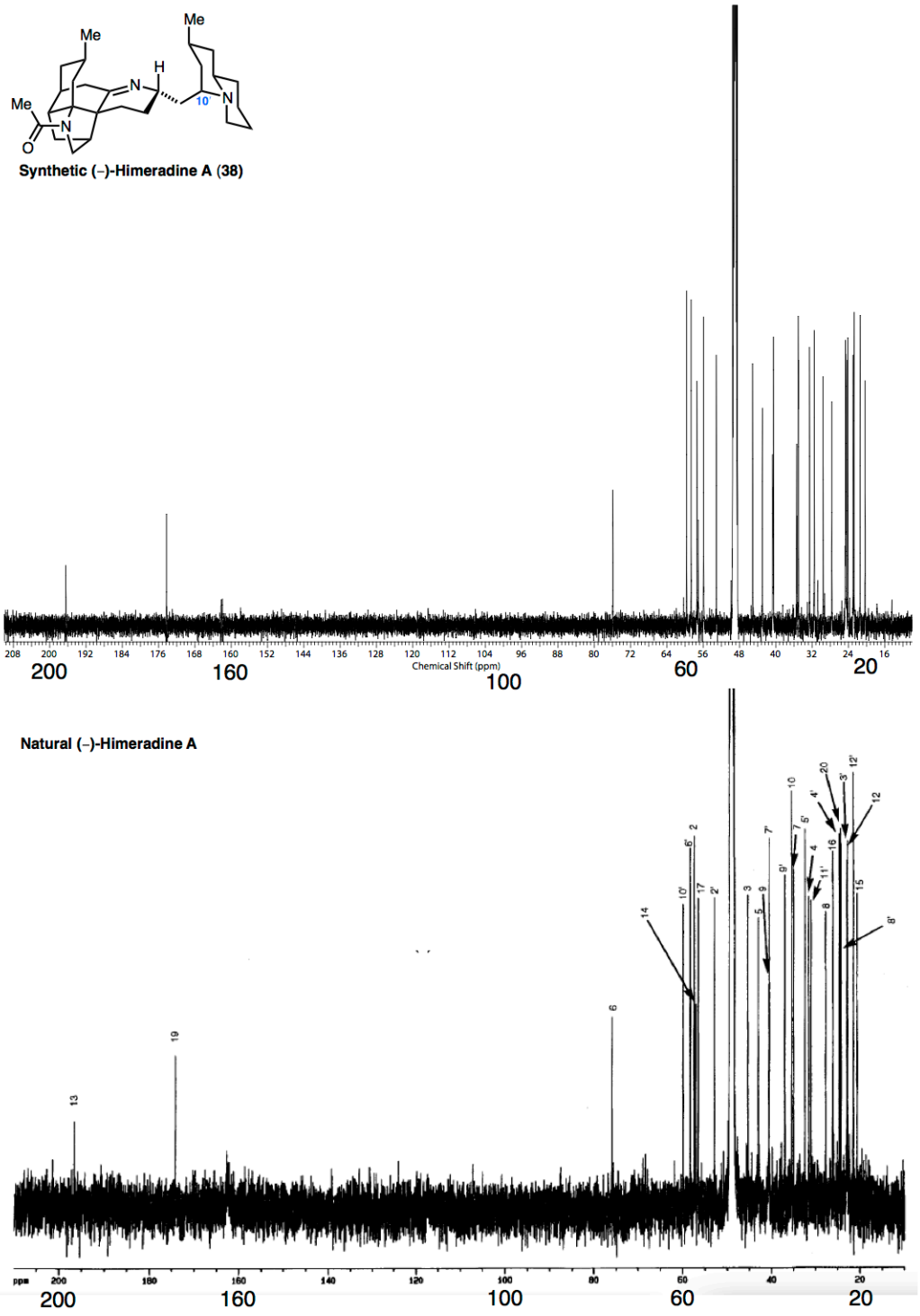

Figure S3. Comparison of ^{13}C NMR Spectra of Synthetic Proposed Structure and Natural (–)-Himeradine A (**38**) as the Double TFA Salt in CD_3OD.

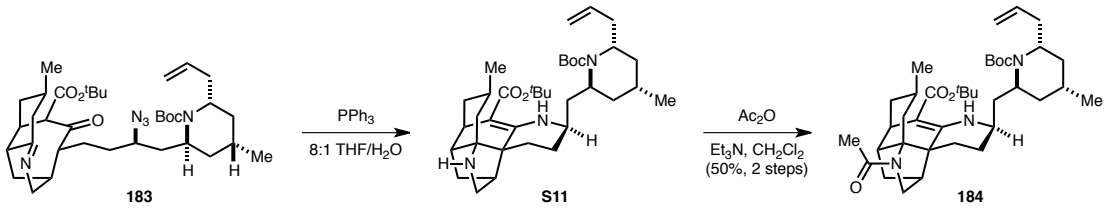

Candidate amide 184:

Triphenylphosphine (31.0 mg, 0.118 mmol, 1.50 equiv) was added as a single portion to a stirred solution of imine **183** (50.2 mg, 0.0785 mmol, 1.00 equiv) in THF (1.4 mL) and water (180 μL) at room temperature. The reaction was heated to 70 °C and stirred for 15.5 h, at which point the reaction was cooled to room temperature and concentrated. The resultant residue was azeotroped with MeOH (5 × 1 mL), followed by benzene (3 × 1 mL), then stirred with silica gel (100 mg) in CH_2Cl_2 (5 mL) for 4 h. The slurry was subsequently filtered and washed with a solution of 80:18:2 $CHCl_3$:MeOH:NH_4OH (10 × 1 mL) and concentrated *in vacuo*. The crude residue was then purified by flash column chromatography (silica gel, eluent: gradient: 1:1 → 0:1 hexanes:EtOAc, 1% Et_3N → 90:9:1 $CHCl_3$:MeOH:NH_4OH) to afford vinylogous urethane **S11** as a pale white flocculent solid. **S11** was contaminated with inseparable Ph_3PO byproduct and was carried forward to the next step without further purification.

Acetic anhydride (150 μL, 1.58 mmol, 20.0 equiv) was added dropwise to a stirred solution of vinylogous urethane **S11**, which was azeotropically dried with benzene (5 × 1 mL), and Et_3N (331 μL, 1.58 mmol, 20.0 equiv) in CH_2Cl_2 (1.6 mL) at room temperature. After stirring for 10 h, the reaction was concentrated under reduced pressure. The resultant residue was then directly purified by flash column chromatography (silica gel, eluent, gradient: 2:1 → 1:1 hexanes:EtOAc) to afford amide **184** (25.0 mg, 50% over 2 steps) as a white flocculent solid.

^{1}H NMR (500 MHz, C_6D_6) δ: 9.60 (s, 1H), 5.92–5.82 (m, 1H), 5.15 (dd, *J* = 1.7, 17.1 Hz, 1H), 5.06 (dd, *J* = 1.8, 10.1 Hz, 1H), 4.32 (br. s., 1H), 3.68 (t, *J* = 12.8 Hz, 1H), 3.39 (br. s., 1H), 3.13 (dd, *J* = 7.8, 17.3 Hz, 1H), 3.04 –2.93 (m, 2H), 2.87 (d, *J* = 9.3 Hz, 1H), 2.65 (br. s., 1H), 2.41 (d, *J* = 8.5 Hz,

1H), 2.27–2.13 (m, 1H), 2.03–1.90 (m, 3H), 1.83 (dd, *J* = 5.4, 15.1 Hz, 1H), 1.80–1.74 (m, 1H), 1.71 (s, 3H), 1.69– 1.63 (m, 1H), 1.61–1.51 (m, 2H), 1.48 (s, 9H), 1.46 (s, 9H), 1.40–1.31 (m, 5H), 1.31–1.24 (m, 2H), 1.18 (dd, *J* = 5.2, 11.8 Hz, 1H), 1.11–1.07 (m, 2H), 1.03 (d, *J* = 6.6 Hz, 3H), 0.74 (d, *J* = 6.3 Hz, 3H). **^{13}C NMR** (126 MHz, C_6D_6) δ: 171.1, 170.6, 161.5, 156.4, 137.5, 116.8, 91.2, 79.6, 78.3, 70.8, 54.8, 54.0, 52.5, 50.9, 47.8, 43.2, 43.0, 39.9, 39.8, 39.5, 39.1, 37.1, 37.1, 34.5, 33.5, 29.2, 28.9, 26.4, 25.8, 24.9, 24.9, 23.1, 22.9, 19.2. **FTIR** (thin film) cm^{-1}: 2949, 2925, 2870, 1686, 1654, 1641, 1597, 1390, 1348, 1250, 1232, 1166, 1153. **HRMS** (ESI) (*m/z*) calc'd for $C_{38}H_{60}N_3O_5$ $[M+H]^+$: 638.4527, found 638.4548. **TLC** (90:9:1 $CHCl_3$:MeOH:NH_4OH), R_f: 0.68 ($KMnO_4$, UV).

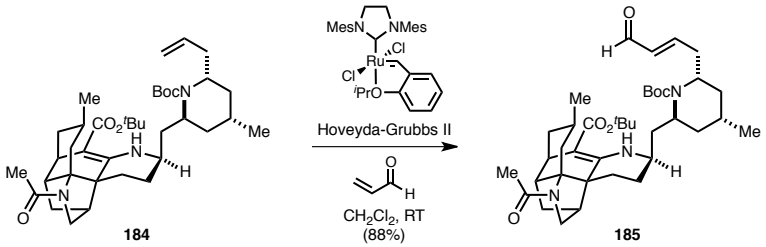

Candidate enal 185:

Hoveyda-Grubbs 2nd generation catalyst (12.3 mg, 0.0200 mmol, 0.50 equiv) was added as a single portion to a solution of amide **184** (25.0 mg, 0.0390 mmol, 1.00 equiv), which was azeotropically dried with benzene (5 × 1 mL), and acrolein (30.0 μL, 0.390 mmol, 10.0 equiv) in CH_2Cl_2 (800 μL) at room temperature. The reaction was stirred for 32.5 h, at which point the reaction was concentrated under reduced pressure. The resultant residue was then directly purified by flash column chromatography (silica gel, eluent: gradient: 4:1 → 2:1 → 1:1 → 1:2 hexanes:EtOAc) to afford enal **185** (22.8 mg, 88%) as a yellow flocculent solid.

^{1}H NMR (500 MHz, C_6D_6) δ: 9.57 (s, 1H), 9.41 (d, *J* = 7.6 Hz, 1H), 6.47–6.33 (m, 1H), 6.13 (dd, *J* = 7.7, 15.5 Hz, 1H), 4.21 (br. s., 1H), 3.67 (t, *J* = 13.2 Hz, 1H), 3.25–3.15 (m, 1H), 3.04–2.93 (m, 3H), 2.64 (t, *J* = 5.4 Hz, 1H), 2.51 (d, *J* = 8.8 Hz, 1H), 2.13–2.02 (m, 1H), 2.01–1.88 (m, 4H), 1.82 (d, *J* = 14.9 Hz, 1H), 1.79–1.74 (m, 1H), 1.73 (s, 3H), 1.68 (d, *J* = 14.4 Hz, 1H), 1.59 (td, *J* = 4.4, 13.7 Hz, 1H), 1.47 (s, 9H), 1.40 (s, 9H), 1.36–1.27 (m, 4H), 1.25–1.15 (m, 2H), 1.14–1.05 (m, 2H), 1.02 (d, *J* = 6.4 Hz, 3H), 0.99–0.82 (m, 3H), 0.69 (d, *J* = 6.4 Hz, 3H). **^{13}C NMR** (126 MHz, C_6D_6) δ: 192.9, 170.9, 170.7, 161.6, 156.2, 155.4, 135.0, 91.7, 80.0, 78.4, 70.8, 55.0, 52.9, 52.4, 51.1, 47.8, 43.6, 43.0, 39.8, 39.5, 38.9, 38.1, 37.7, 37.1, 34.5, 33.5, 29.1, 28.8, 26.4, 25.9, 25.5, 24.9, 23.1, 22.7, 19.8. **FTIR** (thin film) cm^{-1}: 2951, 2907, 2869, 1691, 1637, 1597, 1390, 1167, 1154. **HRMS** (ESI) (*m/z*) calc'd for $C_{39}H_{59}N_3NaO_6$ $[M+Na]^+$: 688.4296, found 688.4314. **TLC** (EtOAc), R_f: 0.58 ($KMnO_4$, UV).

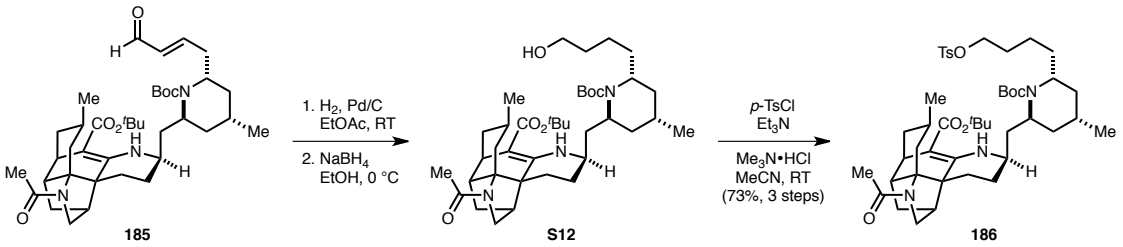

Candidate tosylate 186:

Palladium on carbon (10 wt%, 7.3 mg, 0.0069 mmol, 0.20 equiv) was added as a single portion to a stirred solution of enal **185** (22.8 mg, 0.0342 mmol, 1.00 equiv) in EtOAc (1.7 mL). The reaction vessel was purged with H_2 and placed under an atmosphere of H_2. After 1 h, Celite was poured into the stirred reaction mixture and the resultant slurry was then filtered through a pad of Celite. The solution was concentrated under reduced pressure to afford the corresponding aldehyde, which was carried forward to the next step without further purification.

$NaBH_4$ (2.6 mg, 0.069 mmol, 2.0 equiv) was added as a single portion to a stirred solution of the crude aldehyde, which was azeotropically dried with benzene (5 × 1 mL), in EtOH (850 μL) at 0 °C. The reaction was stirred for 50 min, at which point saturated aqueous NH_4Cl solution (0.5 mL) was added and all volatiles were removed *in vacuo*. Water (1 mL), Et_2O (1 mL), and EtOAc (1 mL) were added sequentially to the crude residue. The layers were separated and the aqueous layer was extracted with EtOAc (3 × 1 mL). The organic layers were combined, washed with brine (4 mL), dried over anhydrous $MgSO_4$, and concentrated under reduced pressure to provide alcohol **S12**, which was carried forward to the next step without further purification.

Next, Et_3N (9.5 μL, 0.068 mmol, 2.0 equiv), Me_3N•HCl (3.3 mg, 0.034 mmol, 1.0 equiv), and *p*-TsCl (7.8 mg, 0.041 mmol, 1.2 equiv) were added sequentially to a stirred solution of crude alcohol **S12**, which was azeotropically dried with benzene (5 × 1 mL), in MeCN (1.1 mL) at room temperature. After stirring for 6.5 h, additional Et_3N (4.8 μL, 0.034 mmol, 1.0 equiv), Me_3N•HCl (1.7 mg, 0.017 mmol, 0.50 equiv), and *p*-TsCl (3.9 mg, 0.021 mmol, 0.60 equiv) were added successively. After stirring for an additional 2 h, water (1 mL), Et_2O (1 mL), and EtOAc (1 mL)

were added to the reaction mixture. The layers were separated and the aqueous layer was extracted with EtOAc (3 × 1 mL). The organic layers were combined, dried over anhydrous $MgSO_4$, and concentrated under reduced pressure. The residue was purified by flash column chromatography (silica gel, eluent: gradient: 2:1 → 1:1 → 1:2 → 0:1 hexanes:EtOAc) to afford tosylate **186** (20.6 mg, 73% over 3 steps) as a pale yellow flocculent solid.

^{1}H NMR (600 MHz, C_6D_6) δ: 9.61 (s, 1H), 7.79 (d, *J* = 8.2 Hz, 2H), 6.77 (d, *J* = 8.5 Hz, 2H), 4.26 (br. s., 1H), 3.94–3.85 (m, 2H), 3.69 (t, *J* = 13.5 Hz, 1H), 3.37 (dd, *J* = 4.7, 9.7 Hz, 1H), 3.04–2.97 (m, 2H), 2.88 (br. s., 1H), 2.66 (t, *J* = 5.9 Hz, 1H), 2.55 (d, *J* = 8.8 Hz, 1H), 2.10 (dd, *J* = 2.6, 4.4 Hz, 1H), 2.06 (d, *J* = 9.4 Hz, 1), 2.03–1.94 (m, 3H), 1.86 (s, 3H), 1.85–1.82 (m, 1H), 1.75 (s, 3H), 1.73–1.69 (m, 1H), 1.63–1.55 (m, 2H), 1.47 (s, 9H), 1.46 (s, 9H), 1.45–1.40 (m, 2H), 1.40–1.29 (m, 5H), 1.29–1.19 (m, 3H), 1.19–1.07 (m, 4H), 1.03 (d, *J* = 6.2 Hz, 3H), 0.98 (q, *J* = 10.6 Hz, 1H), 0.73 (d, *J* = 6.5 Hz, 3H). **^{13}C NMR** (126 MHz, C_6D_6) δ: 170.9, 170.8, 161.9, 156.5, 144.5, 135.0, 130.2, 128.0, 91.4, 79.6, 78.3, 70.7, 55.0, 53.9, 52.6, 50.7, 47.8, 43.4, 43.0, 39.9, 39.5, 38.8, 38.4, 37.5, 34.6, 34.5, 33.6, 29.7, 29.2, 29.1, 28.9, 27.0, 25.9, 24.9, 24.7, 23.8, 23.1, 22.8, 21.5, 19.3. **FTIR** (thin film) cm^{-1}: 2948, 2927, 2870, 1686, 1648, 1596, 1389, 1364, 1175, 1153. **HRMS** (ESI) (*m/z*) calc'd for $C_{46}H_{69}N_3NaO_8S$ $[M+Na]^+$: 846.4698, found 846.4698. **TLC** (EtOAc), R_f: 0.59 ($KMnO_4$, UV).

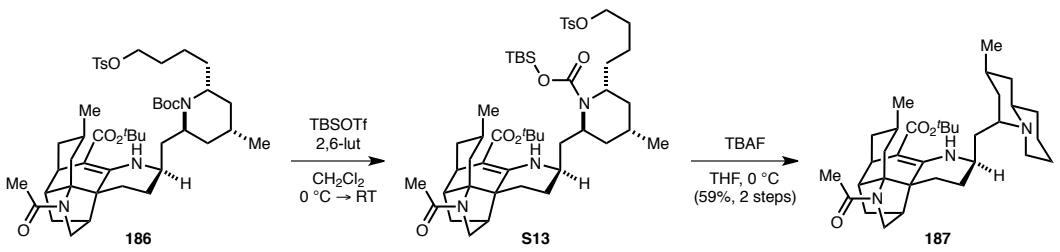

Candidate quinolizidine 187:

2,6-Lutidine (18.0 μL, 0.150 mmol, 10.0 equiv), followed by TBSOTf (28.0 μL, 0.120 mmol, 8.00 equiv), were added dropwise to a stirred solution of tosylate **186** (12.4 mg, 0.0150 mmol, 1.00 equiv), which was azeotropically dried with benzene (5 × 0.5 mL), in CH_2Cl_2 (1.5 mL) at 0 °C. After stirring for 5 min at 0 °C, the reaction mixture was allowed to room temperature and was stirred for an additional 12 h, at which point a saturated aqueous $NaHCO_3$ solution (0.5 mL) was added, followed by Et_2O (1 mL), and EtOAc (1 mL). The layers were separated and the aqueous layer was extracted with EtOAc (3 × 1 mL). The organic layers were combined, washed with brine (2 mL), dried over anhydrous $MgSO_4$, and concentrated under reduced pressure to afford the corresponding silyloxy carbamate **S13**, which was carried forward to the next step without further purification.

A solution of TBAF in THF (1.00 M, 30.0 μL, 0.0301 mmol, 2.00 equiv) was added to a solution of crude silyloxy carbamate **S13** in THF (1.5 mL) at 0 °C. After stirring for 45 min at 0 °C, AcOH (13.0 μL, 0.226 mmol, 15.0 equiv) was added and the reaction was concentrated under reduced pressure. The resultant residue was then directly purified by flash column chromatography (silica gel, eluent: gradient: 2:1 → 1:1 → 0:1 hexanes:EtOAc, 1% Et_3N → 9:1 CH_2Cl_2:MeOH, 1% Et_3N) to afford quinolizidine **187**. **187** was further purified by preparatory thin-layer chromatography (PTLC) using 90:9:1 $CHCl_3$:MeOH:NH_4OH, furnishing quinolizidine **187** (4.9 mg, 59% over 2 steps) as a white solid.

^{1}H NMR (600 MHz, C_6D_6) δ: 9.70 (br. s., 1H), 3.66 (t, *J* = 13.5 Hz, 1H), 3.13 (br. s., 1H), 3.07 (d, *J* = 5.3 Hz, 1H), 2.99 (br. s., 1H), 2.89 (d, *J* = 7.9 Hz, 1H), 2.70 (d, *J* = 10.9 Hz, 1H), 2.63 (t, *J* = 5.6 Hz, 1H), 2.43 (d, *J* = 8.8 Hz, 1H), 2.31 (dt, *J* = 2.1, 11.0 Hz, 1H), 2.06 (t, *J* = 10.3 Hz, 1H), 2.00–1.86 (m, 4H), 1.83 (d, *J* = 11.4 Hz, 1H), 1.73 (s, 3H), 1.66 (td, *J* = 2.6, 12.8 Hz, 1H), 1.63–1.59 (m, 2H), 1.58–1.48 (m, 4H), 1.45 (s, 9H), 1.36–1.29 (m, 3H), 1.28–1.21 (m, 3H), 1.21–1.14 (m, 2H), 1.12–1.05 (m, 2H), 1.01 (d, *J* = 6.2 Hz, 3H), 0.96–0.88 (m, 2H), 0.83 (d, *J* = 5.3 Hz, 3H). **^{13}C NMR** (126 MHz, C_6D_6) δ: 170.7, 170.5, 161.2, 92.3, 78.4, 70.7, 57.6, 54.9, 53.5, 52.5, 52.1, 49.3, 43.3, 43.0, 42.6, 40.0, 39.4, 38.3, 35.0, 34.6, 33.6, 32.5, 29.1, 27.3, 27.1, 25.9, 25.8, 24.9, 24.9, 23.1, 22.9, 19.5. **FTIR** (thin film) cm^{-1}: 2929, 2896, 1643, 1595, 1388, 1232, 1167, 1152. **HRMS** (ESI) (*m/z*) calc'd for $C_{34}H_{54}N_3O_3$ $[M+H]^+$: 552.4160, found 552.4175. **TLC** (90:9:1 $CHCl_3$:MeOH:NH_4OH), R_f : 0.69 ($KMnO_4$, UV).

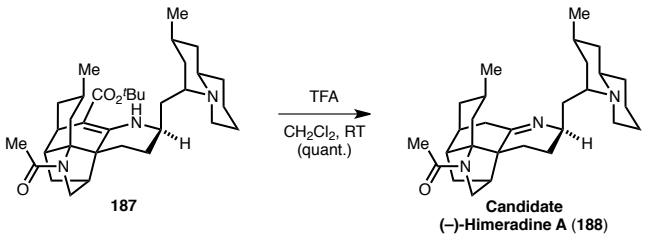

Candidate (–)-himeradine A (188):

Trifluoroacetic acid (300 μL) was added to a stirred solution of quinolizidine **187** (4.9 mg, 0.0089 mmol, 1.0 equiv) in CH_2Cl_2 (300 μL) at room temperature. After stirring for 14 h, the reaction was concentrated *in vacuo* to afford candidate (–)-himeradine A (**188**) as the double TFA salt (6.0 mg, quant.) and as a white solid.

^{1}H NMR (600 MHz, CD_3OD) δ: 4.04–3.94 (m, *J* = 5.0 Hz, 1H), 3.81 (d, *J* = 9.4 Hz, 1H), 3.79–3.74 (m, 1H), 3.37 (d, *J* = 9.4 Hz, 1H), 3.34–3.31 (m, 1H), 3.29–3.22 (m, 2H), 3.04 (t, *J* = 12.9 Hz, 1H), 2.79 (br. s., 1H), 2.62 (dd, *J* = 2.8, 4.8 Hz, 1H), 2.61–2.56 (m, 1H), 2.47 (td, *J* = 4.7, 10.3 Hz, 1H), 2.38 (d, *J* = 3.5 Hz, 1H), 2.23–2.11 (m, 2H), 2.04 (s, 3H), 2.02–1.89 (m, 7H), 1.89–1.74 (m, 5H), 1.72–1.62 (m, 3H), 1.61 –1.50 (m, 2H), 1.36–1.28 (m, 2H), 1.26–1.16 (m, 2H), 1.00 (d, *J* = 6.2 Hz, 3H), 0.98 (d, *J* = 6.2 Hz, 3H). **^{13}C NMR** (126 MHz, CD_3OD) δ: 197.1, 174.3, 76.4, 60.2, 58.4, 57.7, 57.2, 54.9, 52.7, 46.2, 43.2, 40.6, 40.5, 37.1, 35.8, 34.8, 32.5, 31.6, 30.4, 28.3, 25.2, 24.6, 24.4, 24.2, 22.9, 22.7, 21.5, 19.1. **FTIR** (thin film) cm^{-1}: 3367, 2956, 2929, 2876, 1671, 1404, 1200, 1131, 720. **HRMS** (ESI) (*m/z*) calc'd for $C_{29}H_{46}N_3O$ $[M+H]^+$: 452.3635, found 452.3633. **$[\alpha]_D^{22}$**: –56 (*c* = 0.35, MeOH). **TLC** (80:18:2 $CHCl_3$:MeOH:NH_4OH), R_f: 0.50 ($KMnO_4$).

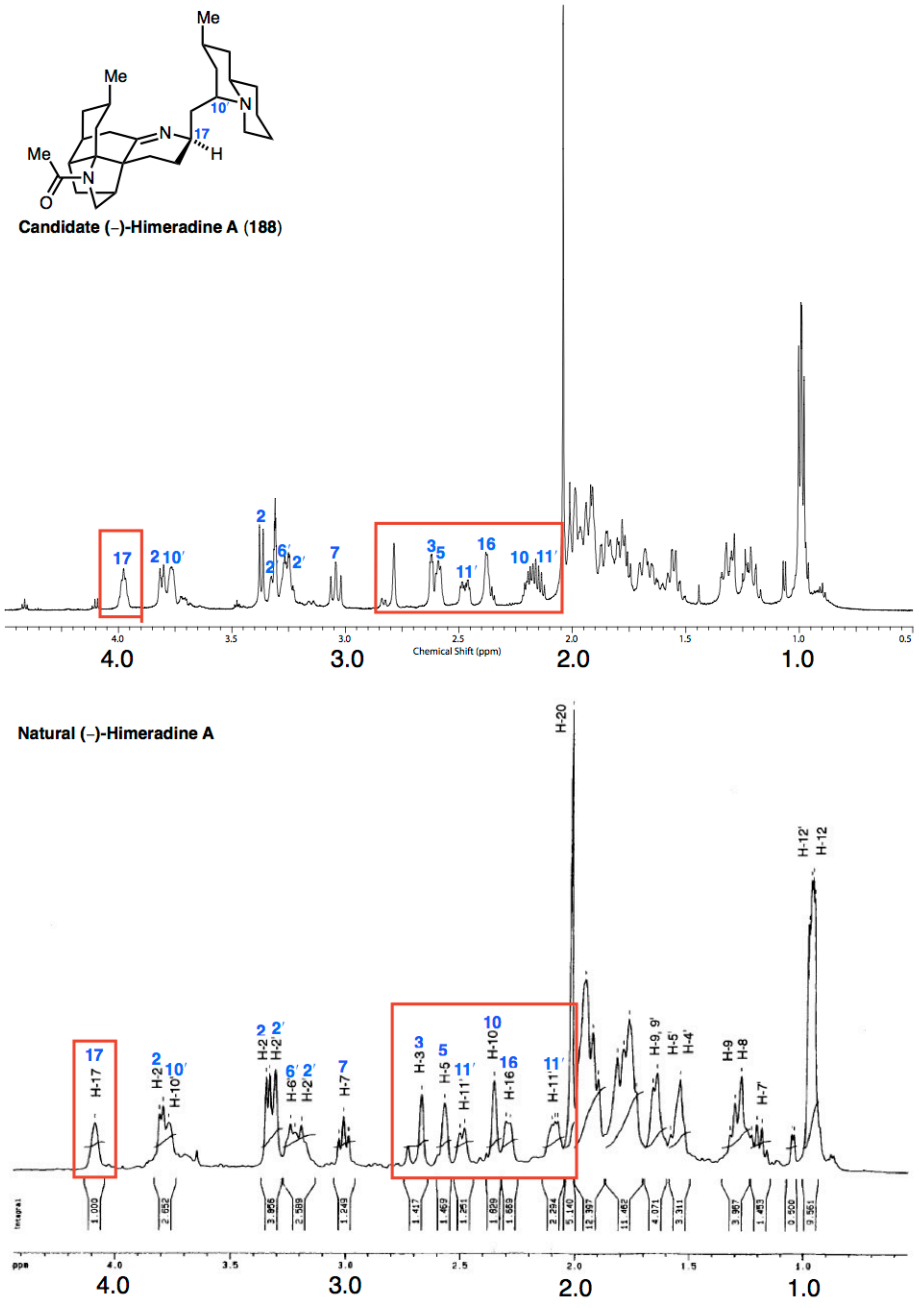

Figure S4. Comparison of ^{1}H NMR Spectra of Natural and Candidate (–)-Himeradine A (**188**) as the Double TFA Salt in CD_3OD.

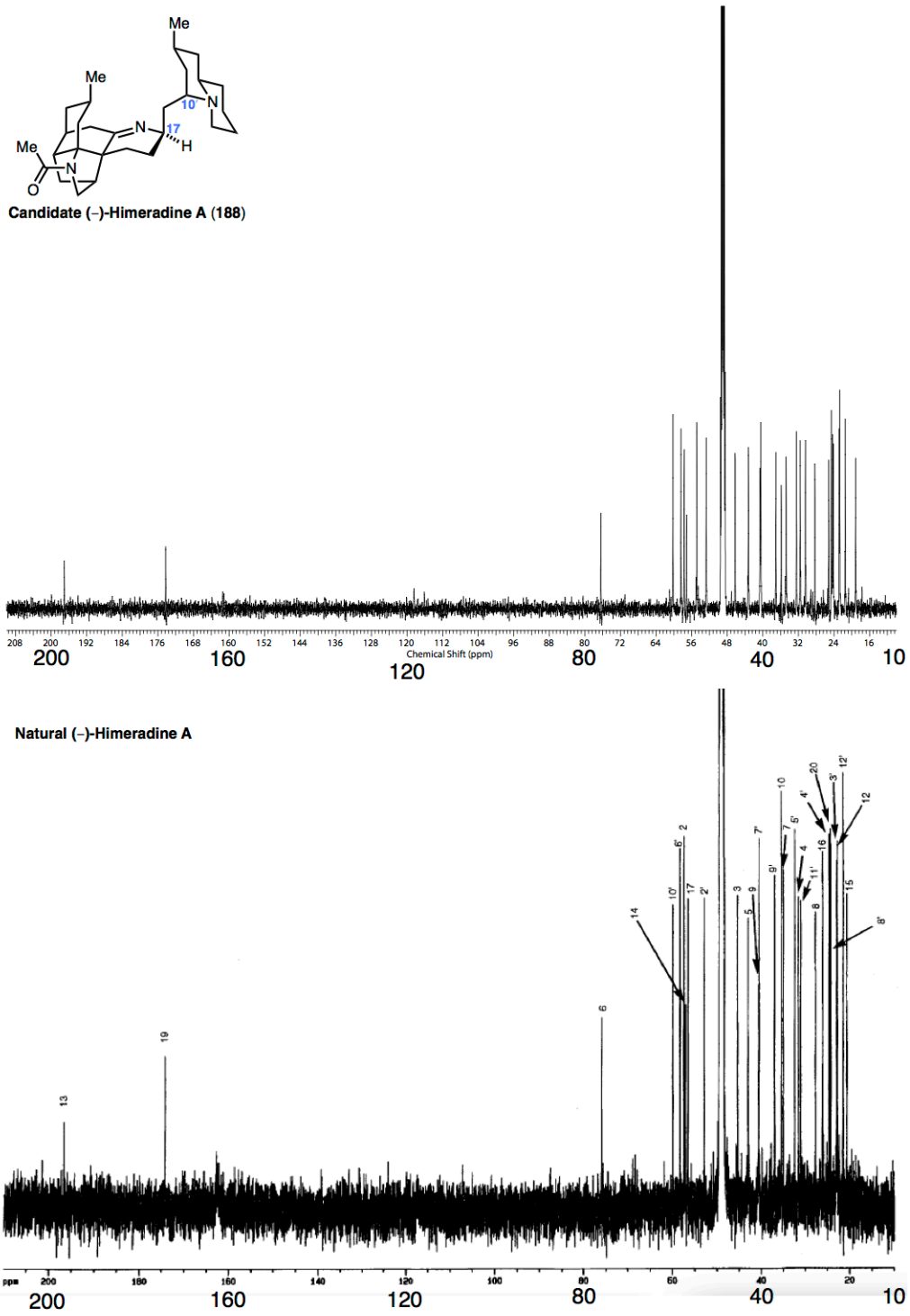

Figure S5. Comparison of ^{13}C NMR Spectra of Natural and Candidate (–)-Himeradine A (**188**) as the Double TFA Salt in CD_3OD.

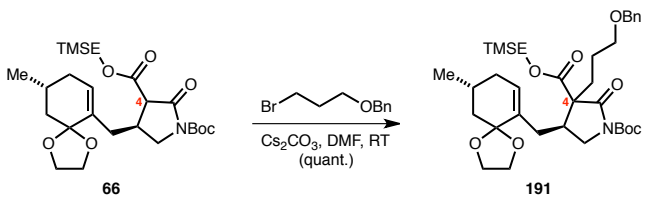

Alkylated imide 191:

Benzyl 3-bromopropyl ether (118 μL, 0.656 mmol, 1.30 equiv) was added dropwise to a stirred solution of β-carboxyimide **66** (250 mg, 0.504 mmol, 1.00 equiv) and Cs_2CO_3 (329 mg, 1.01 mmol, 2.00 equiv) in DMF (3.4 mL). After 17.5 h, Et_2O (5 mL) and saturated aqueous NH_4Cl solution (10 mL) were added sequentially to the reaction mixture. The layers were separated and the aqueous layer was extracted with EtOAc (3 × 10 mL). The organic layers were combined and washed with brine (20 mL), dried over anhydrous $MgSO_4$, and concentrated under reduced pressure. The resultant residue was purified by flash column chromatography (silica gel, eluent: 6:1 hexanes:EtOAc, 1% Et_3N) to afford alkylated imide **191** (325 mg, quant.) as a 9:1 mixture of diastereomers at C4 and as a clear colorless oil.

^{1}H NMR (500 MHz, C_6D_6, major C4-epimer reported) δ: 7.21 (d, *J* = 7.6 Hz, 2H), 7.12 (d, *J* = 7.8 Hz, 2H), 7.06 (t, *J* = 7.1 Hz, 1H), 5.53 (d, *J* = 3.7 Hz, 1H), 4.21 (s, 2H), 4.20–4.17 (m, 1H), 4.17–4.09 (m, 1H), 4.07–3.99 (m, 1H), 3.79 (t, *J* = 10.3 Hz, 1H), 3.68–3.58 (m, 2H), 3.57–3.49 (m, 1H), 3.46–3.37 (m, 1H), 3.36–3.22 (m, 2H), 2.81 (d, *J* = 9.8 Hz, 2H), 2.39 (td, *J* = 4.9, 12.5 Hz, 1H), 2.27 (td, *J* = 4.2, 13.2 Hz, 1H), 2.00 (t, *J* = 13.2 Hz, 1H), 1.96–1.86 (m, 2H), 1.83–1.73 (m, 2H), 1.71 (d, *J* = 12.9 Hz, 1H), 1.45 (s, 9H), 1.40–1.31 (m, 1H), 1.27 (t, *J* = 13.2 Hz, 1H), 0.89–0.82 (m, 2H), 0.77 (d, *J* = 6.8 Hz, 3H), –0.17 (s, 3H), –0.18 (s, 3H). **^{13}C NMR** (126 MHz, C_6D_6, major C4-epimer reported) δ: 171.6, 170.7, 151.7, 139.7, 135.1, 131.8, 128.8, 128.7, 127.9, 108.8, 82.9, 73.3, 71.1, 65.8, 64.3, 64.0, 61.4, 50.6, 42.6, 38.0, 34.6, 30.8, 29.8, 28.4, 28.1, 25.5, 21.9, 18.1, –1.4. **FTIR** (thin film) cm^{-1}: 2952, 2925, 2871, 1753, 1716, 1313, 1250, 1172, 1156, 839. **HRMS** (ESI) (*m/z*) calc'd

for $C_{35}H_{53}NNaO_8Si$ $[M+Na]^+$: 666.3433, found 666.3438. **TLC** (3:1 hexanes:EtOAc), R_f: 0.32 (Anis, UV).

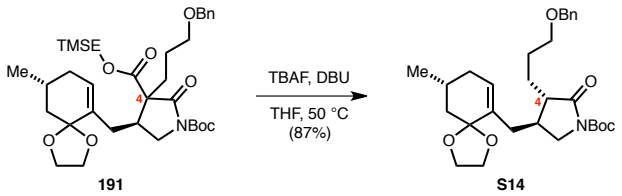

***N*-Boc-2-pyrrolidinone S14**:

A solution of TBAF in THF (1.00 M, 530 µL, 0.530 mmol, 1.00 equiv) was added to a solution of alkylated imide **191** (341 mg, 0.530 mmol, 1.00 equiv) and DBU (20.0 µL, 0.133 mmol, 0.25 equiv) in THF (10 mL) at room temperature. After 5 min, the reaction was heated to 50 °C and was stirred for 19 h, at which point water (15 mL), Et_2O (10 mL), and EtOAc (10 mL) were added successively. The layers were separated and the aqueous layer was extracted with EtOAc (3 × 10 mL). The organic layers were combined, washed with brine (25 mL), then dried over anhydrous $MgSO_4$ and concentrated under reduced pressure. The resultant residue was purified by flash column chromatography (silica gel, eluent: 2:1 hexanes:EtOAc, 1% Et_3N) to afford *N*-Boc-2-pyrrolidinone **S14** (232 mg, 87%) as a >4:1 mixture of diastereomers at C4 and as a clear colorless oil.

^{1}H NMR (500 MHz, C_6D_6, major C4-epimer reported) δ: 7.27 (d, *J* = 7.6 Hz, 2H), 7.18 (d, *J* = 1.7 Hz, 2H), 7.11–7.05 (m, 1H), 5.45–5.34 (m, 1H), 4.28 (s, 2H), 3.90 (dd, *J* = 7.8, 11.0 Hz, 1H), 3.57–3.45 (m, 3H), 3.43–3.35 (m, 1H), 3.32–3.27 (m, 2H), 3.09 (dd, *J* = 8.3, 10.7 Hz, 1H), 2.41 (dd, *J* = 3.4, 14.6 Hz, 1H), 2.18–2.06 (m, 1H), 1.96–1.85 (m, 2H), 1.84–1.60 (m, 6H), 1.48 (s, 9H), 1.42–1.33 (m, 2H), 1.31–1.23 (m, 1H), 0.78 (d, *J* = 6.6 Hz, 3H). **^{13}C NMR** (126 MHz, C_6D_6, major C4-epimer reported) δ: 174.6, 151.8, 139.8, 135.8, 131.1, 128.9, 128.1, 127.9, 108.7, 82.2, 73.3, 70.8, 65.7, 64.3, 50.6, 49.9, 42.7, 36.0, 35.1, 34.5, 28.5, 28.0, 27.6, 26.7, 21.9. **FTIR** (thin film) cm^{-1}: 2949, 2925, 2869, 1783, 1747, 1712, 1367, 1314, 1157, 1124. **HRMS** (ESI) (*m/z*) calc'd for $C_{29}H_{42}NO_6$ $[M+H]^+$: 500.3007, found 500.3016. **TLC** (2:1 hexanes:EtOAc), R_f: 0.34 (Anis, UV).

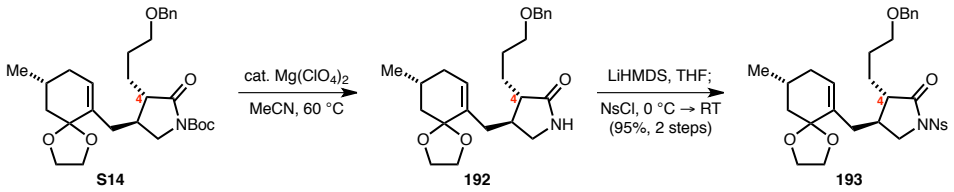

***N*-2-Nitrobenzenesulfonyl-2-pyrrolidinone 193**:

$Mg(ClO_4)_2$ (21.0 mg, 0.0927 mmol, 0.20 equiv) was added as a single portion to a stirred solution of *N*-Boc-2-pyrrolidinone **S14** (232 mg, 0.464 mmol, 1.00 equiv), which was azeotropically dried with benzene (5 × 1 mL), in MeCN (7.7 mL) at room temperature. The resultant mixture was heated to 60 °C and stirred for 5.5 h, at which point it was cooled to room temperature and Et_2O (10 mL) and saturated aqueous NH_4Cl solution (10 mL) were added sequentially. The layers were separated and the aqueous layer was extracted with EtOAc (3 × 10 mL). The organic layers were combined, washed with brine (20 mL), then dried over anhydrous $MgSO_4$ and concentrated under reduced pressure to afford crude 2-pyrrolidinone **192** as a white flocculent solid, which was carried forward to the next step without further purification.

A solution of freshly prepared LiHMDS in THF (1.00 M, 478 μL, 0.478 mmol, 1.20 equiv) was added to a solution of **192**, which was azeotropically dried with benzene (5 × 1 mL), in THF (4 mL) at room temperature. After 1 h, the reaction was cooled to 0 °C and a solution of NsCl in THF (1.00 M, 518 μL, 0.518 mmol, 1.30 equiv) was added dropwise. After 5 min, the reaction was allowed to warm to room temperature and stirred for 2 h, at which point saturated aqueous NH_4Cl solution (5 mL) and Et_2O (5 mL) were added sequentially. The layers were separated and the aqueous layer was extracted with EtOAc (3 × 5 mL). The organic layers were combined, washed with brine (15 mL), then dried over anhydrous $MgSO_4$ and concentrated under reduced pressure. The residue was purified by flash column chromatography (silica gel, eluent: gradient: 6:1 → 4:1 → 2:1 hexanes:EtOAc, 1% Et_3N) to afford *N*-2-nitrobenzenesulfonyl-2-pyrrolidinone **193** (585 mg, 95% over 2 steps) as a 5:1 mixture of diastereomers at C4 and as a white flocculent solid.

^{1}H NMR (500 MHz, C_6D_6, major C4-epimer reported) δ: 8.48 (dd, *J* = 1.3, 7.9 Hz, 1H), 7.22–7.19 (m, 2H), 7.14–7.11 (m, 2H), 7.10–7.04 (m, 1H), 6.72 (dd, *J* = 1.2, 7.8 Hz, 1H), 6.64 (dt, *J* = 1.2, 7.8 Hz, 1H), 6.44 (dt, *J* = 1.3, 7.8 Hz, 1H), 5.48 (d, *J* = 3.4 Hz, 1H), 4.28 (dd, *J* = 7.7, 9.9 Hz, 1H), 4.20 (s, 2H), 3.67–3.59 (m, 1H), 3.58–3.54 (m, 2H), 3.51 (dd, *J* = 8.1, 9.8 Hz, 1H), 3.48–3.40 (m, 1H), 3.20–3.12 (m, 2H), 2.50–2.35 (m, 2H), 1.98–1.84 (m, 2H), 1.83–1.67 (m, 4H), 1.65–1.52 (m, 2H), 1.45–1.31 (m, 2H), 1.26 (t, *J* = 13.2 Hz, 1H), 0.78 (d, *J* = 6.6 Hz, 3H). **^{13}C NMR** (126 MHz, C_6D_6, major C4-epimer reported) δ: 175.9, 148.6, 139.6, 135.2, 135.0, 134.5, 132.6, 132.3, 131.9, 131.6, 128.9, 128.1, 124.0, 108.7, 73.2, 70.4, 65.7, 64.3, 51.5, 49.1, 42.5, 37.9, 34.9, 34.5, 28.0, 27.4, 26.4, 21.9. **FTIR** (thin film) cm^{-1}: 2951, 2923, 2854, 1735, 1543, 1366, 1173, 1126, 1096, 966, 738, 594. **HRMS** (ESI) (*m/z*) calc'd for $C_{30}H_{37}N_2O_8S$ $[M+H]^+$: 585.2265, found 585.2272. **TLC** (1:1 hexanes:EtOAc), R_f: 0.72 (Anis, UV).

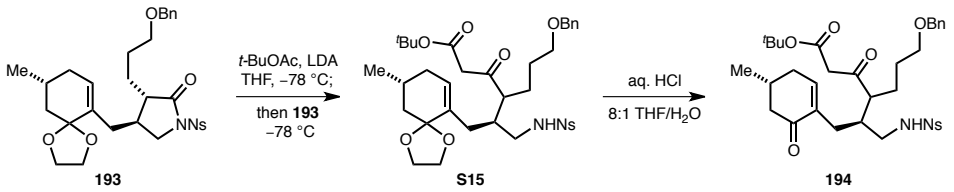

Enone 194:

A solution of *n*-butyllithium in hexanes (2.55 M, 445 µL, 1.14 mmol, 3.00 equiv) was added dropwise to a stirred solution of diisopropylamine (175 µL, 1.25 mmol, 3.30 equiv) in THF (2.1 mL) at −78 °C. The reaction was allowed to stir for 10 min, at which point it was warmed to 0 °C. After 10 min, the reaction was warmed to room temperature. The solution was recooled to −78 °C after 10 min. *t*-Butylacetate (152 µL, 1.14 mmol, 3.00 equiv) was then added dropwise to the reaction mixture. After 1.5 h, a solution of **193** (221 mg, 0.379 mmol, 1.00 equiv), which was azeotropically dried with benzene (5 × 1 mL), in THF (4.7 mL) was added dropwise down the walls of the reaction vessel. After stirring at −78 °C for 2.5 h, saturated aqueous NH_4Cl solution (10 mL) was added to the deep red reaction mixture at −78 °C. The resultant mixture was then allowed to warm to room temperature. Et_2O (10 mL) and EtOAc (10 mL) were added and the layers were separated. The aqueous layer was extracted with EtOAc (3 × 10 mL). The organic layers were combined, washed with brine (30 mL), then dried over anhydrous $MgSO_4$ and concentrated under reduced pressure to afford crude β-ketoester **S15** as a pale yellow flocculent solid, which was carried forward to the next step without further purification.

10% aqueous HCl (680 µL) was added dropwise to a stirred solution of crude **S15** in THF (5.5 mL) at room temperature. After 4 h, a saturated aqueous $NaHCO_3$ solution (10 mL) was added, followed by Et_2O (10 mL), EtOAc (10 mL), and water (5 mL). The layers were separated and the aqueous layer was extracted with EtOAc (3 × 10 mL). The organic layers were combined, washed with brine (30 mL), then dried over anhydrous $MgSO_4$ and concentrated under reduced pressure to afford crude enone **194** as a yellow flocculent solid, which was carried forward to the next step without further purification.

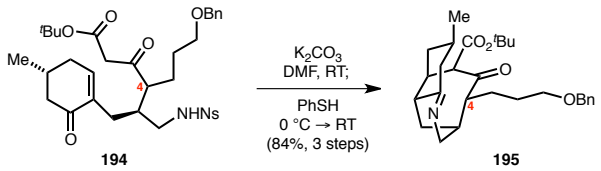

Imine 195:

K_2CO_3 (262 mg, 1.90 mmol, 5.00 equiv) was added in a single portion to a stirred solution of crude enone **194**, which was azeotropically dried with benzene (5 × 1 mL), in DMF (5.4 mL) at room temperature. After 18.5 h, the suspension was cooled to 0 °C and PhSH (97.0 μL, 0.948 mmol, 2.50 equiv) was added dropwise via syringe. After 5 min, the reaction was warmed to room temperature and stirred for an additional 6.5 h, at which point water (10 mL), Et_2O (10 mL), and EtOAc (10 mL) were added sequentially. The layers were separated and the aqueous layer was extracted with EtOAc (3 × 10 mL). The organic layers were combined, washed with brine (30 mL), dried over anhydrous $MgSO_4$, and concentrated under reduced pressure. The crude residue was then purified by flash column chromatography (silica gel, eluent: gradient: 1:1 → 0:1 hexanes:EtOAc, 1% Et_3N → 90:9:1 $CHCl_3$:MeOH:NH_4OH) to afford imine **195** (145 mg, 84% over 3 steps) as a >4:1 mixture of diastereomers at C4 and as a pale yellow oil.

^{1}H NMR (500 MHz, C_6D_6, major C4-epimer reported) δ: 7.30 (d, *J* = 7.6 Hz, 2H), 7.18 (t, *J* = 7.6 Hz, 2H), 7.10 (t, *J* = 7.1 Hz, 1H), 4.31 (s, 2H), 3.98 (d, *J* = 18.1 Hz, 1H), 3.47 (d, *J* = 3.4 Hz, 1H), 3.32 (dd, *J* = 6.1, 8.8 Hz, 1H), 3.27 (td, *J* = 2.9, 9.3 Hz, 1H), 3.21 (d, *J* = 15.6 Hz, 1H), 2.92–2.86 (m, 1H), 2.61–2.53 (m, 2H), 2.19–2.07 (m, 1H), 2.01–1.92 (m, 1H), 1.89 (t, *J* = 6.1 Hz, 1H), 1.79–1.61 (m, 3H), 1.60–1.46 (m, 3H), 1.38–1.34 (m, 2H), 1.32 (s, 9H), 1.10 (td, *J* = 3.7, 12.9 Hz, 1H), 0.61 (d, *J* = 6.6 Hz, 3H). **^{13}C NMR** (126 MHz, C_6D_6, major C4-epimer reported) δ: 205.2, 170.5, 169.2, 139.8, 128.9, 128.1, 127.9, 82.1, 73.4, 71.0, 66.2, 55.2, 49.1, 48.2, 43.4, 38.8, 38.3, 32.9, 30.1, 29.8, 29.3, 28.3, 27.5, 22.6. **FTIR** (thin film) cm^{-1}: 2949, 2924, 2862, 1737, 1701, 1668, 1455, 1368, 1154, 1110, 734. **HRMS** (ESI) (*m/z*) calc'd for $C_{28}H_{39}NNaO_4$ $[M+Na]^+$: 476.2781, found 476.2771. **TLC** (90:9:1 $CHCl_3$:MeOH:NH_4OH), R_f: 0.40 ($KMnO_4$, UV).

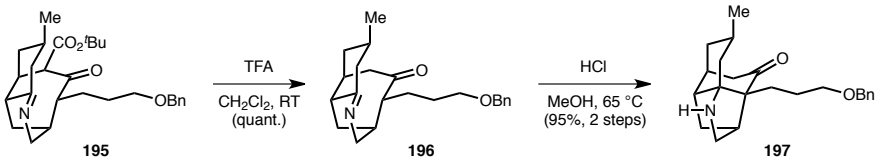

Amine 197:

Trifluoroacetic acid (2.1 mL) was added to a stirred solution of imine **195** (43.4 mg, 0.0957 mmol, 1.00 equiv) in CH_2Cl_2 (2.1 mL) at room temperature. After stirring for 19 h, the reaction was concentrated *in vacuo* to afford ketone **196**, which was carried forward to the next step without further purification.

A solution of HCl in Et_2O (2.00 M, 144 µL, 0.287 mmol, 3.00 equiv) was added to a stirred solution of crude ketone **196** in MeOH (1.9 mL). The resultant mixture was heated to 65 °C and stirred for 3 d, at which point it was cooled to room temperature and concentrated under reduced pressure. The crude residue was then purified by flash column chromatography (silica gel, eluent: 90:9:1 $CHCl_3$:MeOH:NH_4OH) to afford amine **197** (32.3 mg, 95% over 2 steps) as a pale yellow oil.

^{1}H NMR (500 MHz, C_6D_6) δ: 7.36–7.33 (m, 2H), 7.17 (t, *J* = 7.6 Hz, 2H), 7.08 (t, *J* = 7.3 Hz, 1H), 4.41 (s, 2H), 3.54 (td, *J* = 5.9, 9.0 Hz, 1H), 3.47 (ddd, *J* = 6.0, 7.5, 9.1 Hz, 1H), 2.84 (td, *J* = 2.6, 9.2 Hz, 1H), 2.36 (d, *J* = 8.8 Hz, 1H), 2.35–2.31 (m, 1H), 2.29 (dd, *J* = 8.5, 18.8 Hz, 1H), 1.99 (d, *J* = 19.1 Hz, 1H), 1.88 (t, *J* = 3.8 Hz, 1H), 1.75 (td, *J* = 4.1, 12.0 Hz, 1H), 1.71 (dd, *J* = 2.8, 7.5 Hz, 1H), 1.65 (q, *J* = 1.0 Hz, 2H), 1.45 (ddd, *J* = 1.6, 4.0, 13.4 Hz, 1H), 1.40–1.34 (m, 1H), 1.33 (dt, *J* = 2.3, 4.8 Hz, 1H), 1.30 (d, *J* = 7.9 Hz, 1H), 1.29–1.26 (m, 1H), 1.25–1.21 (m, 1H), 0.90 (t, *J* = 12.6 Hz, 1H), 0.81 (dt, *J* = 3.2, 12.6 Hz, 1H), 0.67 (d, *J* = 6.5 Hz, 3H). **^{13}C NMR** (126 MHz, C_6D_6) δ: 214.2, 140.0, 128.9, 128.7, 127.9, 73.3, 72.0, 69.5, 64.8, 53.2, 47.4, 44.8, 43.0, 41.5, 36.9, 33.8, 32.0, 27.4, 26.2, 23.7, 23.0. **FTIR** (thin film) cm^{-1}: 3340, 2949, 2909, 2869,1685, 1453, 1099, 735, 698. **HRMS** (ESI) (*m/z*) calc'd for $C_{23}H_{31}NNaO_2$ $[M+Na]^+$: 376.2247, found 376.2250. **$[\alpha]_D^{23}$**: –41 (*c* = 0.56, CH_2Cl_2). **TLC** (80:18:2 $CHCl_3$:MeOH:NH_4OH), R_f: 0.58 ($KMnO_4$, UV).

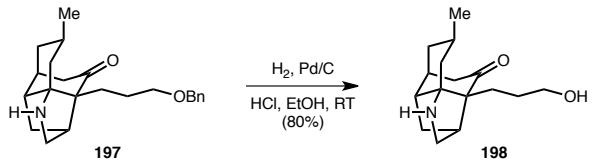

Alcohol 198:

Palladium on carbon (10 wt%, 146 mg, 0.137 mmol, 1.50 equiv) was added as a single portion to a stirred solution of amine **197** (32.3 mg, 0.0914 mmol, 1.00 equiv) and aqueous HCl (3.00 M, 46.0 μL, 0.137 mmol, 1.50 equiv) in EtOH (3 mL). The reaction vessel was purged with H_2 and placed under an atmosphere of H_2. After 1.5 h, Celite was poured into the stirred reaction mixture and the resultant slurry was then filtered through a pad of Celite and washed with $CHCl_3$ (10 mL). The filtrate was concentrated under reduced pressure and the resultant crude residue was then purified by flash column chromatography (silica gel, eluent: gradient: 90:9:1 → 80:18:2 $CHCl_3$:MeOH:NH_4OH) to afford alcohol **198** (19.3 mg, 80%) as a pale yellow oil.

^{1}H NMR (500 MHz, $CDCl_3$) δ: 3.73–3.61 (m, 2H), 3.09 (td, *J* = 2.9, 9.4 Hz, 1H), 2.72 (d, *J* = 9.3 Hz, 1H), 2.64 (dd, *J* = 8.6, 19.1 Hz, 1H), 2.26 (t, *J* = 4.2 Hz, 1H), 2.20–2.11 (m, 3H), 2.07–2.02 (m, 1H), 1.95–1.85 (m, 1H), 1.79 (tdd, *J* = 2.4, 4.8, 13.5 Hz, 1H), 1.75–1.65 (m, 3H), 1.63–1.54 (m, 2H), 1.40–1.30 (m, 2H), 1.21–1.12 (m, 2H), 0.89 (d, *J* = 6.4 Hz, 3H). **^{13}C NMR** (126 MHz, $CDCl_3$) δ: 213.8, 71.4, 64.2, 63.0, 51.7, 44.0, 43.6, 42.1, 40.3, 35.2, 33.0, 30.8, 29.1, 25.6, 22.4, 22.2. **FTIR** (thin film) cm^{-1}: 3341, 2951, 2913, 1687, 1456, 1059, 731. **HRMS** (ESI) (*m/z*) calc'd for $C_{16}H_{26}NO_2$ $[M+H]^+$: 264.1958, found 264.1972. **TLC** (80:18:2 $CHCl_3$:MeOH:NH_4OH), R_f: 0.18 ($KMnO_4$).

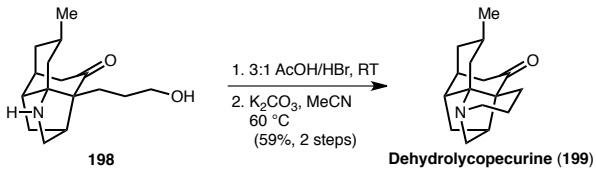

Dehydrolycopecurine (199):

An aqueous solution of HBr (48 wt%, 800 μL) was added to a stirred solution of alcohol **198** (19.3 mg, 0.0736 mmol, 1.00 equiv) in AcOH (2.4 mL). After 14 h, all volatiles were removed *in vacuo* and the resultant residue was azeotropically dried with MeOH (5 × 2 mL), then benzene (5 × 2 mL), and carried forward to the next step without further purification.

K_2CO_3 (152 mg, 1.10 mmol, 15.0 equiv) was added as a single portion to a stirred solution of the crude product, which was azeotropically dried with benzene (5 × 1 mL), in MeCN (3.6 mL). The reaction was heated to 60 °C and stirred for 18.5 h, at which point it was cooled to room temperature and diluted with Et_2O (1 mL). The resultant slurry was then filtered through a pad of Celite and washed with Et_2O (6 mL). The filtrate was concentrated under reduced pressure and the resultant crude residue was then purified by flash column chromatography (silica gel, eluent: gradient: 90:9:1 → 80:18:2 $CHCl_3$:MeOH:NH_4OH) to afford dehydrolycopecurine (**199**) (10.7 mg, 59% over 2 steps) as a white solid.

^{1}H NMR (600 MHz, $CDCl_3$) δ: 3.18 (td, *J* = 7.9, 14.4 Hz, 1H), 3.12 (td, *J* = 4.2, 10.9 Hz, 1H), 2.74 (d, *J* = 10.9 Hz, 1H), 2.65 (dd, *J* = 8.8, 19.7 Hz, 1H), 2.61–2.55 (m, 1H), 2.27 (t, *J* = 4.5 Hz, 1H), 2.25–2.22 (m, 1H), 2.17–2.14 (m, 1H), 2.12 (d, *J* = 20.0 Hz, 1H), 2.04 (br. s., 1H), 1.98–1.86 (m, 3H), 1.76–1.71 (m, 1H), 1.63–1.59 (m, 1H), 1.57 (dd, *J* = 8.4, 13.1 Hz, 1H), 1.53–1.46 (m, 1H), 1.42 (dtd, *J* = 2.3, 6.2, 10.2 Hz, 1H), 1.30 (t, *J* = 13.2 Hz, 1H), 1.20 (dt, *J* = 2.9, 12.6 Hz, 1H), 0.95 (d, *J* = 6.5 Hz, 3H). **^{13}C NMR** (126 MHz, $CDCl_3$) δ: 215.2, 68.4, 59.7, 58.8, 47.8, 46.5, 43.7, 42.2, 40.8, 35.4, 34.9, 34.3, 25.4, 22.8, 19.2, 15.6. **FTIR** (thin film) cm^{-1}: 3382, 2950, 2912, 1687, 1455, 1216, 1124, 1099, 830. **HRMS** (ESI) (*m/z*) calc'd for $C_{16}H_{23}NO$ $[M+H]^+$: 246.1852, found 246.1863. **$[\alpha]_D^{22}$**: –69 (*c* = 0.34, MeOH). **TLC** (80:18:2 $CHCl_3$:MeOH:NH_4OH), R_f: 0.33 ($KMnO_4$).

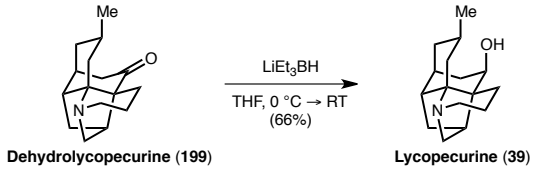

Dehydrolycopecurine (**199**) Lycopecurine (**39**)

Lycopecurine (39):

A solution of $LiEt_3BH$ in THF (1.00 M, 21.0 μL, 0.0210 mmol, 2.50 equiv) was added dropwise to a stirred solution of dehydrolycopecurine (**199**) (2.1 mg, 0.0086 mmol, 1.0 equiv) in THF (400 μL) at 0 °C. The reaction was allowed to warm naturally to room temperature and was stirred for 3 h, at which point saturated aqueous NH_4Cl solution (100 μL), followed by a 1 M NaOH aqueous solution (until pH>10), were added. $CHCl_3$ (1 mL) was added and the layers were separated. The aqueous layer was further extracted with $CHCl_3$ (3 × 1 mL). The organic layers were combined, dried over anhydrous $MgSO_4$, and concentrated under reduced pressure. The resultant crude residue was then purified by flash column chromatography (silica gel, eluent: gradient: 90:9:1 → 80:18:2 $CHCl_3$:MeOH:NH_4OH) to afford lycopecurine (**39**) (1.4 mg, 66%) as a white crystalline solid. The structure of **39** was unambiguously established via single crystal X-ray diffraction analysis. Crystals suitable for X-ray diffraction were obtained by recrystallization of the hydrobromide salt of **39**[142] from MeOH and acetone.

^{1}H NMR (600 MHz, $CDCl_3$) δ: 3.99 (dd, *J* = 1.0, 8.8 Hz, 1H), 3.47 (ddd, *J* = 7.3, 9.8, 13.6 Hz, 1H), 3.26 (td, *J* = 4.1, 11.7 Hz, 1H), 3.09 (d, *J* = 10.9 Hz, 1H), 2.92 (dd, *J* = 9.5, 13.1 Hz, 1H), 2.55 (td, *J* = 9.0, 16.4 Hz, 1H), 2.49–2.39 (m, 2H), 2.31 (dq, *J* = 5.4, 11.8 Hz, 1H), 2.20 (t, *J* = 4.3 Hz, 1H), 2.17 (dd, *J* = 4.4, 12.9 Hz, 1H), 2.14–2.09 (m, 1H), 2.05–1.94 (m, 1H), 1.92–1.83 (m, 1H), 1.70–1.63 (m, 1H), 1.62–1.50 (m, 4H), 1.31 (d, *J* = 16.1 Hz, 1H), 1.20 (td, *J* = 3.2, 13.2 Hz, 1H), 0.99 (d, *J* =

---

[142] The hydrobromide salt of **39** was prepared from **39** via the following procedure: two drops of HBr (48 wt% in water) was added to a solution of **39** (1.4 mg) in CH_2Cl_2. The resulting suspension was concentrated *in vacuo* and the resultant solid was recrystallized from MeOH (single drop) and acetone (300 μL). This protocol provided crystals of the hydrobromide salt of **39** that were suitable for X-ray diffraction analysis.

6.7 Hz, 3H). **^{13}C NMR** (126 MHz, $CDCl_3$) δ: 67.8, 56.4, 52.0, 45.4, 45.4, 41.1, 39.9, 36.0, 35.8, 34.3, 33.2, 29.7, 24.6, 22.6, 19.9, 15.7. **FTIR** (thin film) cm^{-1}: 3349, 2951, 2924, 2581, 1579, 1456, 1399, 1062, 1052. **HRMS** (ESI) (*m/z*) calc'd for $C_{16}H_{26}NO$ $[M+H]^+$: 248.2009, found 248.2021. **$[\alpha]_D^{22}$**: –19 (*c* = 0.14, MeOH). **M.p.:** 236–238 °C.[143] **TLC** (80:18:2 $CHCl_3$:MeOH:NH_4OH), R_f: 0.18 ($KMnO_4$).

[143] The reported melting point for lycopecurine (**39**) is 239–241 °C.

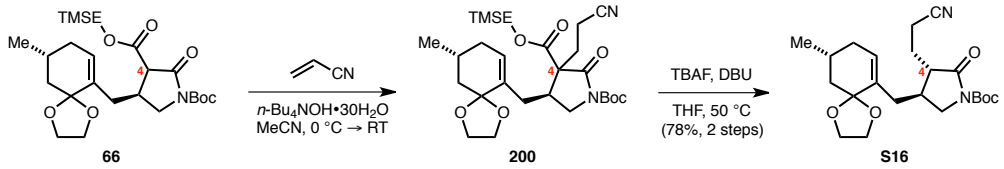

***N*-Boc-2-pyrrolidinone S16:**

Acrylonitrile (150 μL, 2.27 mmol, 3.00 equiv) and *n*-$Bu_4NOH•30H_2O$ (61.0 mg, 0.0757 mmol, 0.10 equiv) were added sequentially to a stirred solution of β-carboxyimide **66** (375 mg, 0.757 mmol, 1.00 equiv) in MeCN (19 mL) at 0 °C. After 5 min, the reaction was allowed to warm to room temperature and was stirred for 2 h, at which point water (10 mL), Et_2O (15 mL), and EtOAc (10 mL) were added sequentially. The layers were separated and the aqueous layer was extracted with EtOAc (3 × 10 mL). The organic layers were combined, washed with brine (50 mL), dried over anhydrous $MgSO_4$, and concentrated under reduced pressure to afford alkylated imide **200**, which was carried forward to the next step without further purification.

A solution of TBAF in THF (1.00 M, 757 μL, 0.757 mmol, 1.00 equiv) was added to a solution of crude **200** and DBU (28.0 μL, 0.189 mmol, 0.25 equiv) in THF (15 mL) at room temperature. After 5 min, the reaction was heated to 50 °C and was stirred for 15 h, at which point water (10 mL), Et_2O (15 mL), and EtOAc (10 mL) were added successively. The layers were separated and the aqueous layer was extracted with EtOAc (3 × 10 mL). The organic layers were combined, washed with brine (30 mL), then dried over anhydrous $MgSO_4$ and concentrated under reduced pressure. The resultant residue was purified by flash column chromatography (silica gel, eluent: gradient: 2:1 → 1:1 hexanes:EtOAc, 1% Et_3N) to afford *N*-Boc-2-pyrrolidinone **S16** (239 mg, 78% over 2 steps) as a >14:1 mixture of diastereomers at C4 and as a white flocculent solid.

^{1}H NMR (600 MHz, C_6D_6, major C4-epimer reported) δ: 5.38 (d, *J* = 4.1 Hz, 1H), 3.74 (dd, *J* = 7.6, 10.9 Hz, 1H), 3.56–3.51 (m, 1 H), 3.49–3.45 (m, 1H), 3.44–3.37 (m, 2H), 2.85 (dd, *J* = 8.8, 10.9 Hz, 1H), 2.20 (td, *J* = 8.1, 16.7 Hz, 1H), 2.11 (dd, *J* = 4.7, 14.1 Hz, 1H), 1.97 (td, *J* = 6.4, 16.9 Hz, 1H), 1.92–1.86 (m, 1H), 1.82 (td, *J* = 5.3, 10.3 Hz, 1H), 1.78–1.63 (m, 4H), 1.47 (s, 9H), 1.46–1.40 (m,

1H), 1.39–1.29 (m, 2H), 1.25 (t, J = 12.9 Hz, 1H), 0.79 (d, J = 6.7 Hz, 3H). **^{13}C NMR** (126 MHz, C_6D_6, major C4-epimer reported) δ: 173.7, 151.3, 135.3, 131.6, 119.7, 108.6, 82.5, 65.6, 64.4, 50.4, 48.0, 42.5, 36.2, 34.5, 34.4, 28.5, 28.0, 26.2, 21.9, 14.9. **FTIR** (thin film) cm^{-1}: 2951, 2930, 1782, 1744, 1714, 1368, 1314, 1157, 1125, 967. **HRMS** (ESI) (*m/z*) calc'd for $C_{22}H_{32}N_2NaO_5$ $[M+Na]^+$: 427.2203, found 427.2203. **TLC** (1:1 hexanes:EtOAc), R_f: 0.48 (Anis).

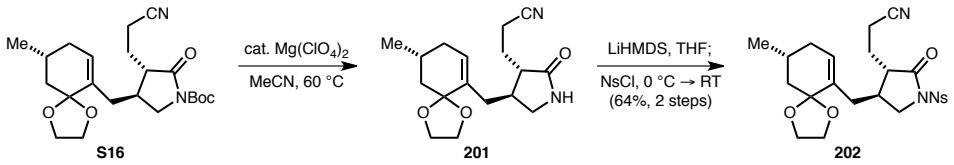

***N*-2-Nitrobenzenesulfonyl-2-pyrrolidinone 202**:

$Mg(ClO_4)_2$ (18.5 mg, 0.0830 mmol, 0.20 equiv) was added as a single portion to a stirred solution of *N*-Boc-2-pyrrolidinone **S16** (168 mg, 0.415 mmol, 1.00 equiv), which was azeotropically dried with benzene (5 × 1 mL), in MeCN (6.9 mL) at room temperature. The resultant mixture was heated to 60 °C and stirred for 4 h, at which point it was cooled to room temperature and Et_2O (10 mL) and saturated aqueous NH_4Cl solution (10 mL) were added sequentially. The layers were separated and the aqueous layer was extracted with EtOAc (3 × 10 mL). The organic layers were combined, washed with brine (20 mL), then dried over anhydrous $MgSO_4$ and concentrated under reduced pressure to afford crude 2-pyrrolidinone **201** as a white flocculent solid, which was carried forward to the next step without further purification.

A solution of freshly prepared LiHMDS in THF (1.00 M, 610 µL, 0.610 mmol, 1.20 equiv) was added to a solution of **201**, which was azeotropically dried with benzene (5 × 1 mL), in THF (5 mL) at room temperature. After 1 h, the reaction was cooled to 0 °C and a solution of NsCl in THF (1.00 M, 661 µL, 0.661 mmol, 1.30 equiv) was added dropwise. After 5 min, the reaction was allowed to warm to room temperature and stirred for 2 h, at which point saturated aqueous NH_4Cl solution (5 mL) and Et_2O (5 mL) were added sequentially. The layers were separated and the aqueous layer was extracted with EtOAc (3 × 5 mL). The organic layers were combined, washed with brine (15 mL), then dried over anhydrous $MgSO_4$ and concentrated under reduced pressure. The residue was purified by flash column chromatography (silica gel, eluent: gradient: 4:1 → 2:1 → 1:1 hexanes:EtOAc, 1% Et_3N) to afford *N*-2-nitrobenzenesulfonyl-2-pyrrolidinone **202** (158 mg, 64% over 2 steps) as a white flocculent solid.

^{1}H NMR (600 MHz, C_6D_6) δ: 8.41 (dd, *J* = 1.3, 8.1 Hz, 1H), 6.72 (dd, *J* = 1.2, 7.9 Hz, 1H), 6.64 (dt, *J* = 1.2, 7.8 Hz, 1H), 6.44 (dt, *J* = 1.3, 7.7 Hz, 1H), 5.45 (d, *J* = 3.2 Hz, 1H), 4.16 (dd, *J* = 7.9, 10.0 Hz, 1H), 3.63–3.58 (m, 1H), 3.57–3.52 (m, 1H), 3.49–3.43 (m, 2H), 3.32 (dd, *J* = 8.5, 10.0 Hz, 1H), 2.20–2.13 (m, 1H), 2.12–2.05 (m, 1H), 1.94–1.87 (m, 2H), 1.85 (dd, *J* = 5.6, 7.9 Hz, 1H), 1.83–1.78 (m, 1H), 1.75 (dd, *J* = 8.7, 13.9 Hz, 1H), 1.73–1.68 (m, 2H), 1.46–1.39 (m, 1H), 1.33–1.26 (m, 1H), 1.23 (t, *J* = 12.9 Hz, 1H), 1.20–1.14 (m, 1H), 0.79 (d, *J* = 6.7 Hz, 3H). **^{13}C NMR** (126 MHz, C_6D_6) δ: 175.0, 134.9, 134.8, 134.7, 132.5, 131.8, 127.9, 127.7, 124.1, 119.2, 108.5, 65.6, 64.4, 51.4, 47.4, 42.4, 38.0, 34.5, 34.3, 28.0, 25.8, 21.9, 14.6. **FTIR** (thin film) cm^{-1}: 2952, 2910, 1733, 1543, 1367, 1174, 1128, 1046, 966, 594. **HRMS** (ESI) (*m/z*) calc'd for $C_{23}H_{27}N_3NaO_7S$ $[M+Na]^+$: 512.1462, found 512.1463. **TLC** (1:1 hexanes:EtOAc), R_f: 0.38 (Anis).

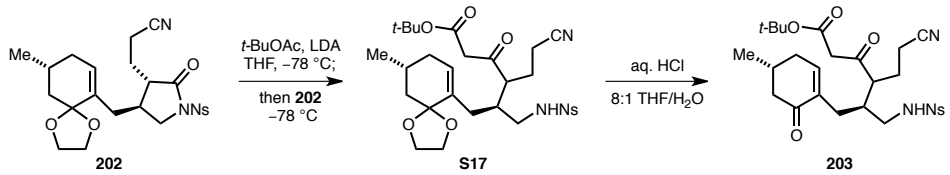

Enone 203:

A solution of *n*-butyllithium in hexanes (2.53 M, 414 μL, 1.05 mmol, 3.00 equiv) was added dropwise to a stirred solution of diisopropylamine (161 μL, 1.15 mmol, 3.30 equiv) in THF (2 mL) at −78 °C. The reaction was allowed to stir for 10 min, at which point it was warmed to 0 °C. After 10 min, the reaction was warmed to room temperature. The solution was recooled to −78 °C after 10 min. *t*-Butylacetate (140 μL, 1.05 mmol, 3.00 equiv) was then added dropwise to the reaction mixture. After 1 h, a solution of **202** (171 mg, 0.349 mmol, 1.00 equiv), which was azeotropically dried with benzene (5 × 1 mL), in THF (4.3 mL) was added dropwise down the walls of the reaction vessel. After stirring at −78 °C for 3 h, saturated aqueous NH_4Cl solution (10 mL) was added to the deep red reaction mixture at −78 °C. The resultant mixture was then allowed to warm to room temperature. Et_2O (10 mL) and EtOAc (10 mL) were added and the layers were separated. The aqueous layer was extracted with EtOAc (3 × 10 mL). The organic layers were combined, washed with brine (30 mL), then dried over anhydrous $MgSO_4$ and concentrated under reduced pressure to afford crude β-ketoester **S17** as a pale yellow flocculent solid, which was carried forward to the next step without further purification.

10% aqueous HCl (775 μL) was added dropwise to a stirred solution of crude **S17** in THF (6.2 mL) at room temperature. After 1 h, a saturated aqueous $NaHCO_3$ solution (10 mL) was added, followed by Et_2O (10 mL), EtOAc (10 mL), and water (5 mL). The layers were separated and the aqueous layer was extracted with EtOAc (3 × 10 mL). The organic layers were combined, washed with brine (30 mL), then dried over anhydrous $MgSO_4$ and concentrated under reduced pressure to afford crude enone **203** as a yellow flocculent solid, which was carried forward to the next step without further purification.

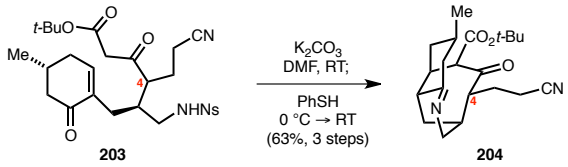

Imine 204:

K_2CO_3 (241 mg, 1.75 mmol, 5.00 equiv) was added as a single portion to a stirred solution of crude enone **203**, which was azeotropically dried with benzene (5 × 1 mL), in DMF (5.8 mL) at room temperature and stirred for 13 h, at which point the suspension was then cooled to 0 °C and PhSH (90.0 μL, 0.873 mmol, 2.50 equiv) was added dropwise via syringe. After 5 min, the reaction was warmed to room temperature and stirred for an additional 10 h, at which point water (10 mL), Et_2O (10 mL), and EtOAc (10 mL) were added sequentially. The layers were separated and the aqueous layer was extracted with EtOAc (3 × 10 mL). The organic layers were combined, washed with brine (30 mL), dried over anhydrous $MgSO_4$, and concentrated under reduced pressure. The crude residue was then purified by flash column chromatography (silica gel, eluent: gradient: 2:1 → 1:1 → 0:1 hexanes:EtOAc, 1% Et_3N → 90:9:1 $CHCl_3$:MeOH:NH_4OH) to afford imine **204** (79.5 mg, 63% over 3 steps) as a >3:1 mixture of diastereomers at C4 and as a pale yellow flocculent solid.

^{1}H NMR (600 MHz, C_6D_6, major C4-epimer reported) δ: 3.62 (dd, *J* = 2.3, 17.9 Hz, 1H), 3.40 (d, *J* = 3.5 Hz, 1H), 3.06– 3.00 (m, 1H), 2.83 (td, *J* = 3.8, 8.0 Hz, 1H), 2.61 (td, *J* = 4.7, 9.2 Hz, 1H), 2.46 (ddd, *J* = 2.2, 4.0, 12.8 Hz, 1H), 2.02 (tdd, *J* = 6.6, 9.2, 13.7 Hz, 1H), 1.92–1.83 (m, 1H), 1.77 (ddd, *J* = 2.1, 5.2, 7.4 Hz, 1H), 1.68–1.63 (m, 2H), 1.61–1.57 (m, 1H), 1.52–1.46 (m, 2H), 1.36 (s, 9H), 1.35–1.32 (m, 1H), 1.25–1.21 (m, 1H), 1.13–1.04 (m, 2H), 0.60 (d, *J* = 6.5 Hz, 3H). **^{13}C NMR** (126 MHz, C_6D_6, major C4-epimer reported) δ: 204.7, 170.1, 169.5, 119.9, 83.0, 66.3, 53.2, 48.8, 48.2, 43.5, 39.0, 38.0, 32.7, 29.9, 29.7, 28.4, 28.2, 26.4, 22.5, 15.4. **FTIR** (thin film) cm^{-1}: 2947, 2927, 2869, 1735, 1670, 1368, 1249, 1152. **HRMS** (ESI) (*m/z*) calc'd for $C_{21}H_{30}N_2NaO_3$ $[M+Na]^+$: 381.2149, found 381.2150. **TLC** (90:9:1 $CHCl_3$:MeOH:NH_4OH), R_f: 0.45 ($KMnO_4$).

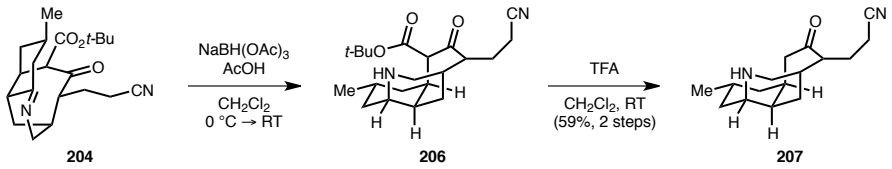

Amine 207:

$NaBH(OAc)_3$ (99.0 mg, 0.444 mmol, 2.00 equiv) was added as a single portion to a stirred solution of imine **204**, which was azeotropically dried with benzene (5 × 0.5 mL), and AcOH (15.2 μL, 0.266 mmol, 1.20 equiv) in CH_2Cl_2 (4.4 mL) at 0 °C. After 5 min, the reaction was warmed to room temperature and stirred for 3.5 h. Additional $NaBH(OAc)_3$ (50.0 mg, 0.222 mmol, 1.00 equiv) and AcOH (7.6 μL, 0.13 mmol, 0.60 equiv) were added and the reaction was stirred for 5 h, at which point a 1 M NaOH aqueous solution (5 mL) and $CHCl_3$ (10 mL) were added sequentially. The layers were separated and the aqueous layer was extracted with $CHCl_3$ (3 × 5 mL). The organic layers were combined, dried over anhydrous $MgSO_4$, and concentrated under reduced pressure to afford crude amine **206**, which was carried forward to the next step without further purification.

Trifluoroacetic acid (3.7 mL) was added to a stirred solution of crude amine **206** in CH_2Cl_2 (3.7 mL) at room temperature. After stirring for 17 h, the reaction was concentrated *in vacuo*. The crude residue was then purified by flash column chromatography (silica gel, eluent: 90:9:1 $CHCl_3$:MeOH:NH_4OH) to afford amine **207** (34.1 mg, 59% over 2 steps) as a pale yellow solid.

^{1}H NMR (500 MHz, C_6D_6) δ: 3.46 (dd, *J* = 10.0, 12.2 Hz, 1H), 2.47 (d, *J* = 12.0 Hz, 1H), 2.38–2.30 (m, 1H), 2.21 (td, *J* = 5.3, 10.7 Hz, 1H), 2.14 (dd, *J* = 3.5, 12.1 Hz, 1H), 2.10–2.03 (m, 1H), 1.80–1.69 (m, 3H), 1.69–1.63 (m, 2H), 1.51 (td, *J* = 5.9, 14.1 Hz, 1H), 1.40–1.31 (m, 2H), 1.24– 1.18 (m, 1H), 1.18–1.12 (m, 2H), 1.11–1.02 (m, 1H), 0.91 (dtd, *J* = 4.1, 12.8, 16.4 Hz, 2H), 0.74 (d, *J* = 6.6 Hz, 3H). **^{13}C NMR** (126 MHz, C_6D_6) δ: 211.1, 119.7, 57.6, 56.4, 49.4, 48.4, 48.3, 43.5, 42.7, 37.3, 35.6, 32.2, 26.5, 23.0, 21.7, 15.8. **FTIR** (thin film) cm^{-1}: 3335, 2946, 2912, 2870, 1691, 1454, 1445, 1430, 1085. **HRMS** (ESI) (*m/z*) calc'd for $C_{16}H_{25}N_2O$ $[M+H]^+$: 261.1961, found 261.1963. **TLC** (80:18:2 $CHCl_3$:MeOH:NH_4OH), R_f: 0.70 ($KMnO_4$, UV).

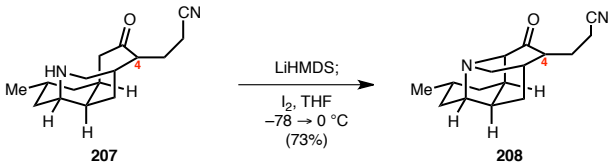

Tertiary amine 208:

A solution of freshly prepared LiHMDS in THF (1.00 M, 170 µL, 0.171 mmol, 3.00 equiv) was added to a solution of **207** (14.8 mg, 0.0568 mmol, 1.00 equiv), which was azeotropically dried with benzene (5 × 1 mL), in THF (1.5 mL) at –78 °C. After 2 h, a freshly prepared solution of iodine in THF (1.00 M, 170 µL, 0.171 mmol, 3.00 equiv) was added dropwise to the stirred reaction mixture. After stirring for 1 h at –78 °C, the reaction was allowed to warm to 0 °C and was stirred for an additional 2 h, at which point water (0.5 mL), a saturated aqueous $NaHSO_3$ solution (1 mL), a 1 M NaOH aqueous solution (until pH>10), and $CHCl_3$ (2 mL) were added sequentially. The layers were separated and the aqueous layer was extracted with $CHCl_3$ (3 × 2 mL). The organic layers were combined, dried over anhydrous $MgSO_4$, and concentrated under reduced pressure. The residue was purified by flash column chromatography (silica gel, eluent: gradient: 2:1 → 1:1 → 0:1 hexanes:EtOAc, 1% Et_3N → 90:9:1 $CHCl_3$:MeOH:NH_4OH) to afford tertiary amine **208** (10.7 mg, 73%) as a >9:1 mixture of diastereomers at C4 and as a pale yellow oil.

^{1}H NMR (500 MHz, C_6D_6, major C4-epimer reported) δ: 3.58 (s, 1H), 2.65 (d, *J* = 1.7 Hz, 1H), 2.56 (s, 1H), 1.99 (t, *J* = 6.7 Hz, 1H), 1.90 (d, *J* = 4.1 Hz, 1H), 1.85–1.79 (m, 1H), 1.79–1.76 (m, 1H), 1.77–1.72 (m, 1H), 1.66–1.59 (m, 3H), 1.59–1.52 (m, 2H), 1.34–1.29 (m, 1H), 1.28 (t, *J* = 3.0 Hz, 1H), 1.23 (d, *J* = 2.7 Hz, 1H), 1.21–1.18 (m, 1H), 0.96 (dd, *J* = 2.1, 4.0 Hz, 1H), 0.71 (d, *J* = 0.7 Hz, 1H), 0.68 (d, *J* = 6.6 Hz, 3H). **^{13}C NMR** (126 MHz, C_6D_6, major C4-epimer reported) δ: 213.1, 119.5, 73.8, 70.8, 56.7, 51.2, 46.8, 46.0, 41.0, 39.9, 38.3, 33.3, 26.9, 25.2, 22.4, 15.5. **FTIR** (thin film) cm^{-1}: 2924, 2880, 2007, 1705, 1453. **HRMS** (ESI) (*m/z*) calc'd for $C_{16}H_{22}N_2NaO$ $[M+Na]^+$: 281.1624, found 281.1624. **TLC** (90:9:1 $CHCl_3$:MeOH:NH_4OH), R_f: 0.22 ($KMnO_4$).

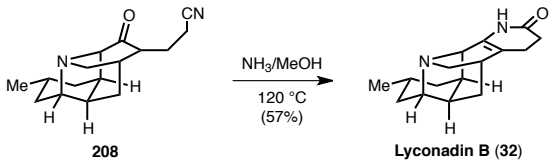

(–)-Lyconadin B (32):

A solution of NH_3 in MeOH (7.00 M, 2 mL) was added to tertiary amine **208** (10.7 mg, 0.0414 mmol, 1.00 equiv). The resultant solution was heated to 120 °C and stirred for 3 d, at which point it was cooled to room temperature and concentrated under reduced pressure. The crude residue was then purified by preparatory thin-layer chromatography (silica gel, eluent: 85:13.5:1.5 $CHCl_3$:MeOH:NH_4OH) to afford (–)-lyconadin B (**32**) (6.1 mg, 57%) as a white solid.

^{1}H NMR (600 MHz, CD_3OD) δ: 3.50 (s, 1H), 3.31 (s, 1H), 3.29 (dd, *J* = 3.2, 12.0 Hz, 1H), 2.86 (d, *J* = 12.3 Hz, 1H), 2.54–2.43 (m, 2H), 2.43–2.32 (m, 2H), 2.27 (d, *J* = 5.0 Hz, 1H), 2.15–2.11 (m, 1H), 2.00–1.94 (m, 2H), 1.93 (dd, *J* = 3.7, 5.7 Hz, 1H), 1.89–1.82 (m, 1H), 1.79–1.72 (m, 1H), 1.70 (d, *J* = 13.5 Hz, 1H), 1.07 (ddd, *J* = 2.1, 12.1, 13.7 Hz, 1H), 0.95 (t, *J* = 13.2 Hz, 1H), 0.90 (d, *J* = 6.5 Hz, 3H). **^{13}C NMR** (126 MHz, CD_3OD) δ: 173.2, 135.2, 120.7, 73.0, 63.9, 61.6, 49.5, 48.5, 40.6, 40.4, 34.3, 33.0, 31.4, 26.1, 24.9, 22.0. **FTIR** (thin film) cm^{-1}: 3403, 3205, 2946, 2923, 2849, 1672, 1372. **HRMS** (ESI) (*m/z*) calc'd for $C_{16}H_{23}N_2O$ $[M+H]^+$: 259.1805, found 259.1810. **$[\alpha]_D^{21}$**: –102 (*c* = 0.5, MeOH).[144] **TLC** (80:18:2 $CHCl_3$:MeOH:NH_4OH), R_f: 0.33 ($KMnO_4$, UV).

[144] The specific rotation reported for (–)-lyconadin B (**32**), which is contaminated with impurities, is $[\alpha]_D^{23}$: –66 (*c* = 0.5, MeOH).

Table S3. ^{1}H NMR Data Comparison Between Natural and Synthetic (–)-Lyconadin B (**32**) in CD_3OD.

Isolation Report[132b] (^{1}H, 600 MHz, CD_3OD)	Synthetic (–)-Lyconadin B (**32**) (^{1}H, 600 MHz, CD_3OD)
0.89 (d, *J* = 6.5 Hz, 3H)	0.90 (d, *J* = 6.5 Hz, 3H)
0.94 (t, *J* = 13.2 Hz, 1H)	0.95 (t, *J* = 13.2 Hz, 1H
1.04 (ddd, *J* = 2.4, 12.6, 12.6 Hz, 1H)	1.07 (ddd, *J* = 2.1, 12.1, 13.7 Hz, 1H)
1.68 (d, *J* = 13.5 Hz, 1H)	1.70 (d, *J* = 13.5 Hz, 1H)
1.74 (m, 1H)	1.79–1.72 (m, 1H)
1.84 (m, 1H)	1.89–1.82 (m, 1H)
1.89 (s, 1H)	1.93 (dd, *J* = 3.7, 5.7 Hz, 1H)
1.95 (m, 2H)	2.00–1.94 (m, 2H)
2.10 (m, 1H)	2.15–2.11 (m, 1H)
2.25 (d, *J* = 4.8 Hz, 1H)	2.27 (d, *J* = 5.0 Hz, 1H)
2.37 (m, 2H)	2.43–2.32 (m, 2H)
2.47 (m, 2H)	2.54–2.43 (m, 2H)
2.83 (d, *J* = 12.0 Hz, 1H)	2.86 (d, *J* = 12.3 Hz, 1H)
3.25 (m, 1H)	3.29 (dd, *J* = 3.2, 12.0 Hz, 1H)
3.26 (d, *J* = 3.1 Hz, 1H)	3.31 (s, 1H)
3.45 (s, 1H)	3.50 (s, 1H)

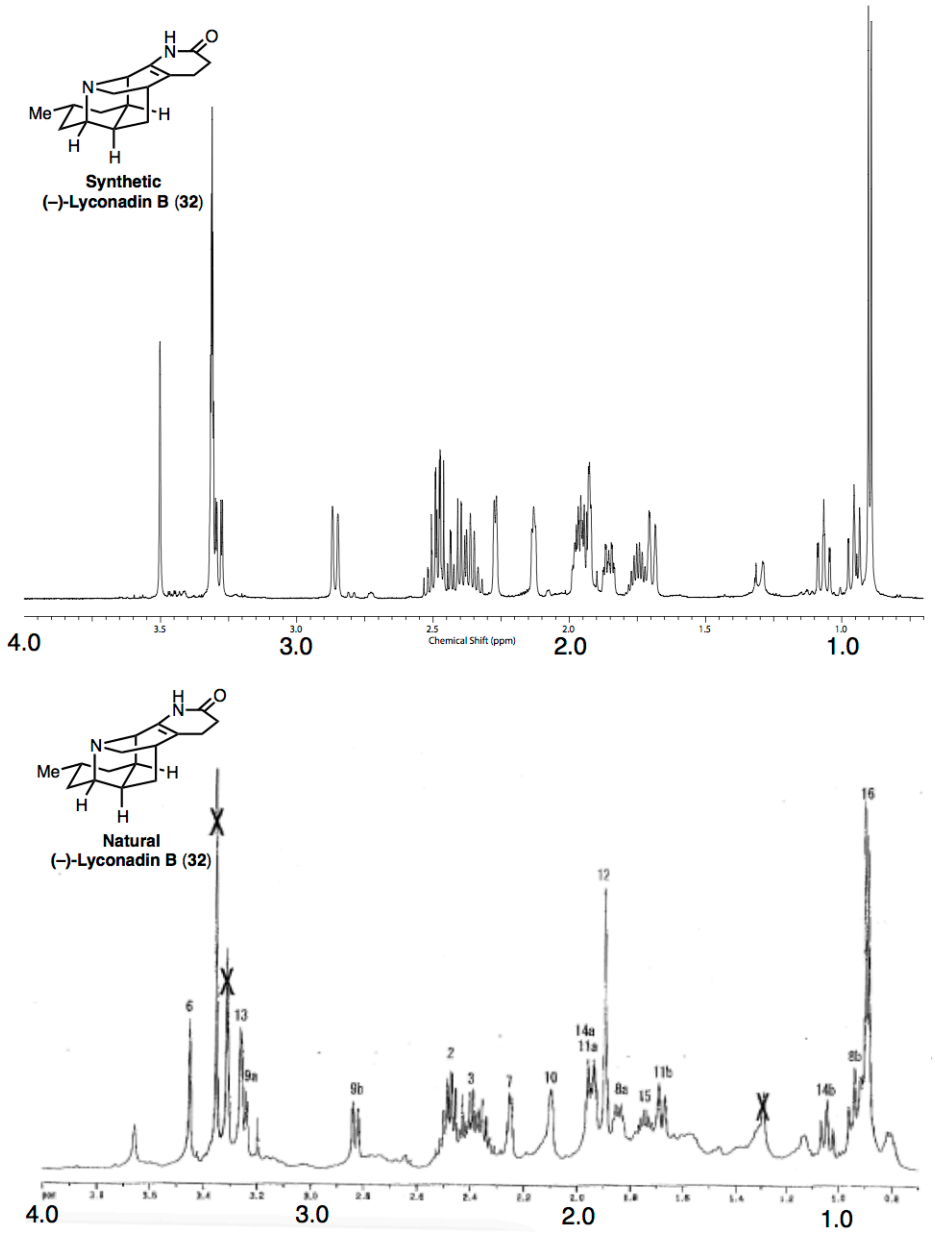

Figure S6. Comparison of ^{1}H NMR Spectra of Natural and Synthetic (–)-Lyconadin B (**32**) in CD_3OD.

Table S4. ^{13}C NMR Data Comparison Between Natural and Synthetic (–)-Lyconadin B (**32**) in CD_3OD.

Isolation Report[132b] (^{13}C, 126 MHz, CD_3OD)	Synthetic (–)-Lyconadin B (**32**) (^{13}C, 126 MHz, CD_3OD)
22.1	22.0
24.0	24.9
26.2	26.1
31.5	31.4
33.4	33.0
34.6	34.3
40.9	40.4
41.2	40.6
48.2	48.5
49.9	49.5
61.9	61.6
63.6	63.9
72.5	73.0
120.7	120.7
135.8	135.2
173.3	173.2

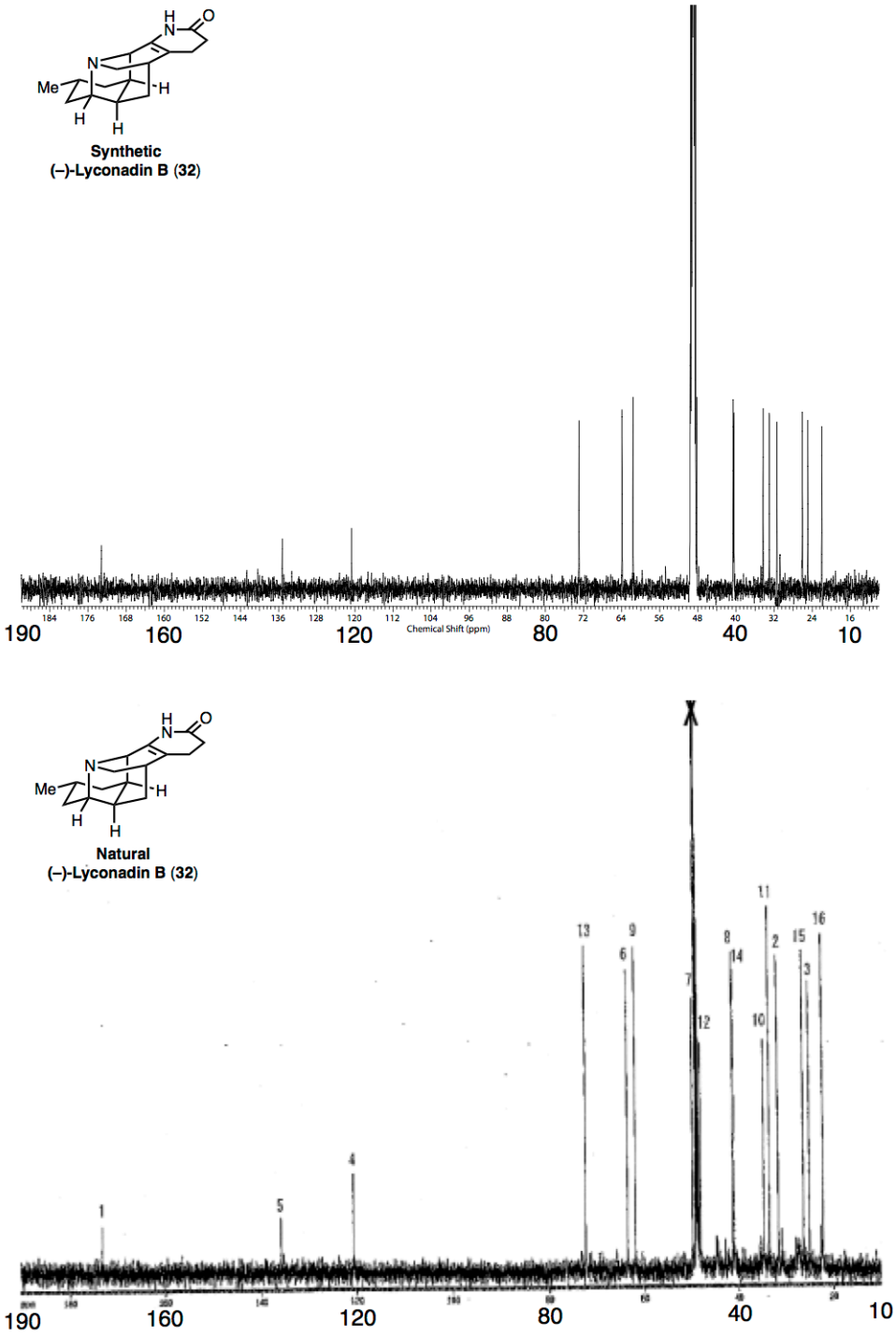

Figure S7. Comparison of ^{13}C NMR Spectra of Natural and Synthetic (–)-Lyconadin B (**32**) in CD_3OD.

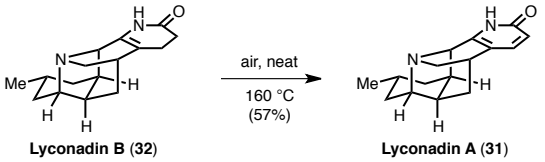

(+)-Lyconadin A (31):

Lyconadin B (**32**) was heated neat under an atmosphere of air at 160 °C for 25 h. The crude residue was then purified by flash column chromatography (silica gel, eluent: gradient: 90:9:1 → 80:18:2 $CHCl_3$:MeOH:NH_4OH) to afford (+)-lyconadin A (**31**) (1.8 mg, 57%) as a white solid.

^{1}H NMR (600 MHz, CD_3OD) δ: 7.39 (d, *J* = 9.1 Hz, 1H), 6.32 (d, *J* = 8.8 Hz, 1H), 4.05 (s, 1H), 3.44 (dd, *J* = 2.9, 12.6 Hz, 1H), 3.38 (br. s., 1H), 2.79 (d, *J* = 12.3 Hz, 1H), 2.72 (br. s., 1H), 2.19 (d, *J* = 4.4 Hz, 1H), 2.12 (ddd, *J* = 3.5, 5.3, 13.5 Hz, 1 H), 2.03–1.97 (m, 1H), 1.95 (br. s., 1H), 1.93–1.88 (m, 1H), 1.83 (dt, *J* = 6.0, 12.0 Hz, 1H), 1.69 (d, *J* = 14.1 Hz, 1H), 1.11 (t, *J* = 12.2 Hz, 1H), 1.01 (t, *J* = 12.5 Hz, 1H), 0.93 (d, *J* = 6.5 Hz, 3H). **^{13}C NMR** (126 MHz, CD_3OD) δ: 165.4, 149.3, 141.8, 126.3, 116.6, 72.6, 64.0, 61.7, 50.8, 48.1, 41.0, 40.5, 34.3, 33.8, 26.2, 22.0. **FTIR** (thin film) cm^{-1}: 3197, 2922, 2850, 1655, 1611, 1457, 947. **HRMS** (ESI) (*m/z*) calc'd for $C_{16}H_{21}N_2O$ $[M+H]^+$: 257.1648, found 257.1660. **$[\alpha]_D^{22}$**: +37 (*c* = 0.12, MeOH). **TLC** (80:18:2 $CHCl_3$:MeOH:NH_4OH), R_f : 0.33 ($KMnO_4$).

Table S5. ^{1}H NMR Data Comparison Between Natural and Synthetic (+)-Lyconadin A (**31**) in CD_3OD.

Isolation Report[132a] (^{1}H, 600 MHz, CD_3OD)	Synthetic (+)-Lyconadin A (**31**) (^{1}H, 600 MHz, CD_3OD)
0.95 (d, *J* = 6.4 Hz, 3H)	0.93 (d, *J* = 6.5 Hz, 3H)
1.05 (t, *J* = 13.0 Hz, 1H)	1.01 (t, *J* = 12.5 Hz, 1H)
1.18 (t, *J* = 12.1 Hz, 1H)	1.11 (t, *J* = 12.2 Hz, 1H)
1.74 (br. d., *J* = 13.9 Hz, 1H)	1.69 (d, *J* = 14.1 Hz, 1H)
1.86 (m, 1H)	1.83 (dt, *J* = 6.0, 12.0 Hz, 1H)
1.94 (m, 1H)	1.93–1.88 (m, 1H)
2.04 (m, 1H)	1.95 (br. s., 1H)
2.07 (m, 1H)	2.03–1.97 (m, 1H)
2.14 (ddd, *J* = 3.9, 5.6, 13.9 Hz, 1H)	2.12 (ddd, *J* = 3.5, 5.3, 13.5 Hz, 1 H)
2.25 (br. d., *J* = 4.4 Hz, 1H)	2.19 (d, *J* = 4.4 Hz, 1H)
2.81 (m, 1H)	2.72 (br. s., 1H)
2.88 (d, *J* = 13.7 Hz, 1H)	2.79 (d, *J* = 12.3 Hz, 1H)
3.54 (d, *J* = 2.7 Hz, 1H)	3.38 (br. s., 1H)
3.55 (dd, *J* = 3.1, 13.7 Hz, 1H)	3.44 (dd, *J* = 2.9, 12.6 Hz, 1H)
4.19 (br. s., 1H)	4.05 (s, 1H)
6.35 (d, *J* = 8.9 Hz, 1H)	6.32 (d, *J* = 8.8 Hz, 1H)
7.42 (d, *J* = 8.9 Hz, 1H)	7.39 (d, *J* = 9.1 Hz, 1H)

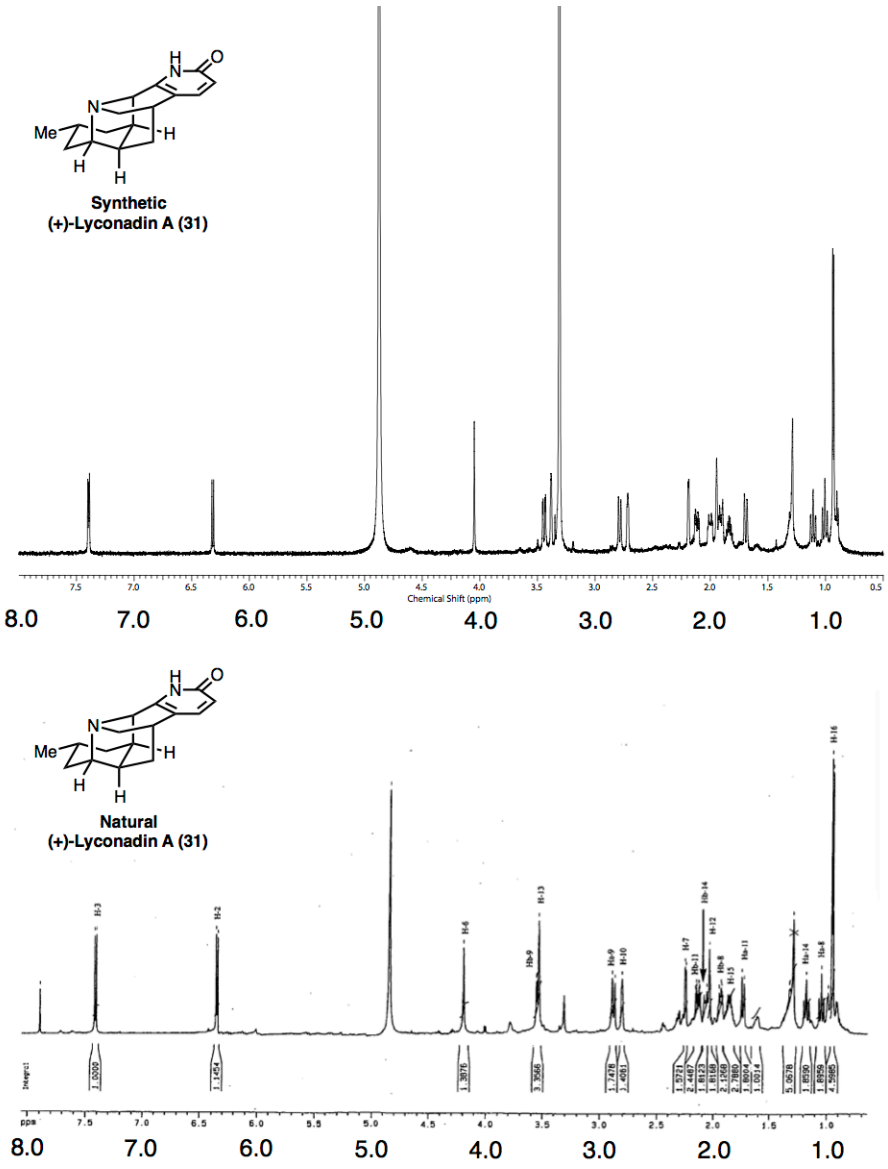

Figure S8. Comparison of ^{1}H NMR Spectra of Natural and Synthetic (+)-Lyconadin A (**31**) in CD_3OD.

Table S6. ^{13}C NMR Data Comparison Between Natural and Synthetic (+)-Lyconadin A (**31**) in CD_3OD.

Isolation Report[132a] (^{13}C, 126 MHz, CD_3OD)	Synthetic (+)-Lyconadin A (**31**) (^{13}C, 126 MHz, CD_3OD)
21.9	22.0
26.1	26.2
33.6	33.8
34.0	34.3
40.2	40.5
40.2	41.0
48.1	48.1
50.4	50.8
61.4	61.7
64.6	64.0
73.1	72.6
116.6	116.6
126.2	126.3
141.6	141.8
148.8	149.3
165.3	165.4

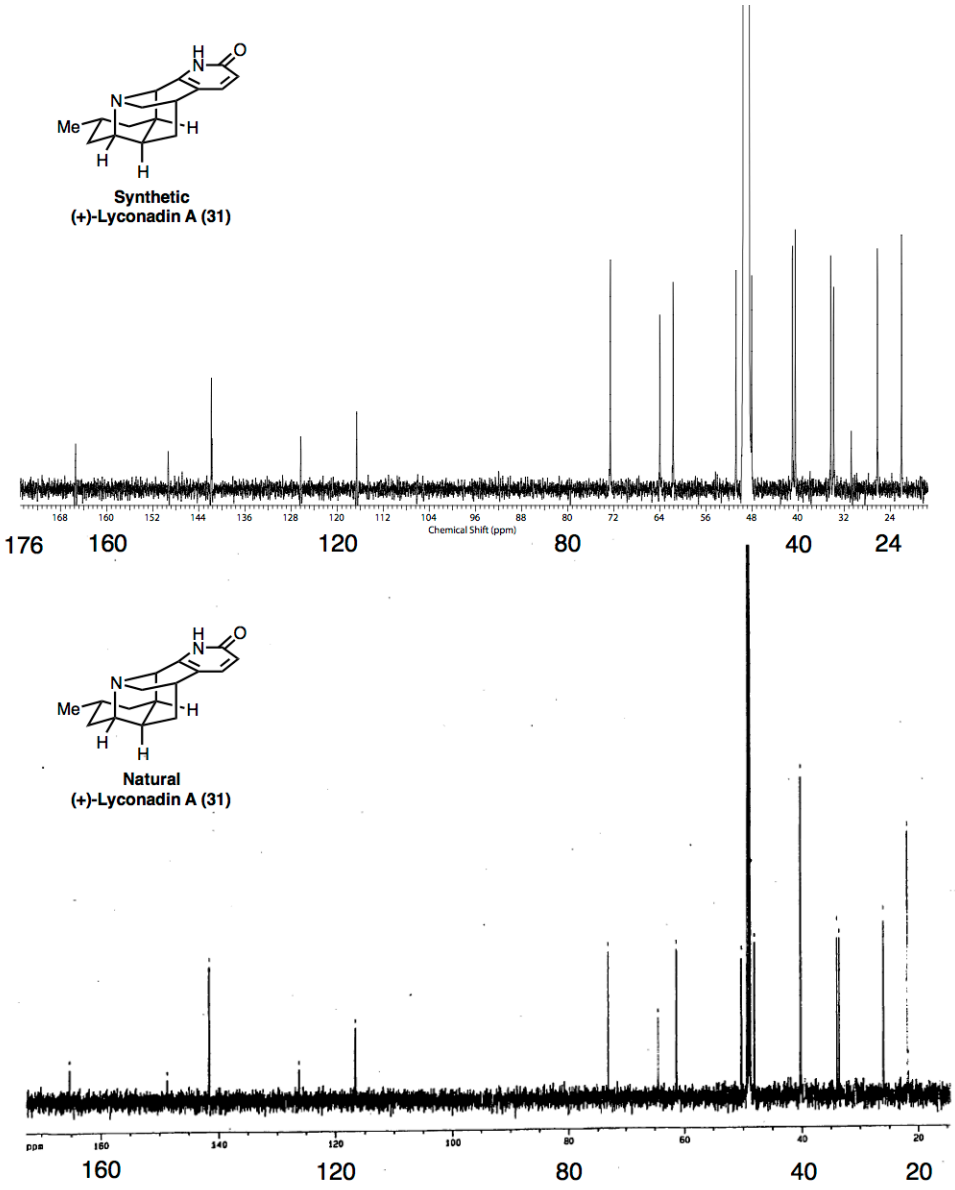

Figure S9. Comparison of ^{13}C NMR Spectra of Natural and Synthetic (+)-Lyconadin A (**31**) in CD_3OD.

Appendix A

Chapter Two Catalog of ^{1}H and ^{13}C NMR Spectra

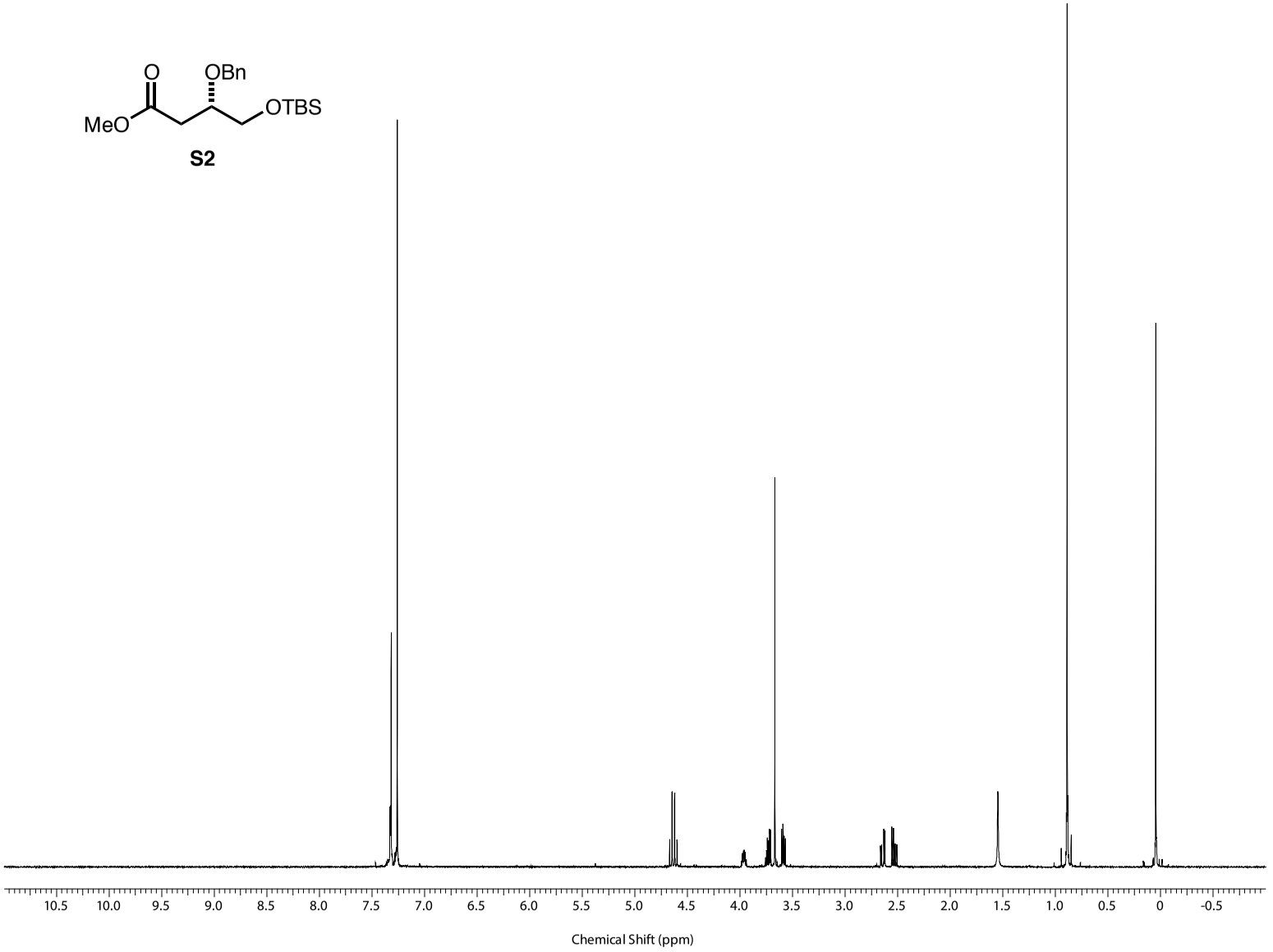
O
OBn
MeO
OTBS
S2
10.5
10.0
9.5
9.0
8.5
8.0
7.5
7.0
6.5
6.0
5.5
5.0
4.5
4.0
3.5
3.0
2.5
2.0
1.5
1.0
0.5
0
-0.5
Chemical Shift (ppm)

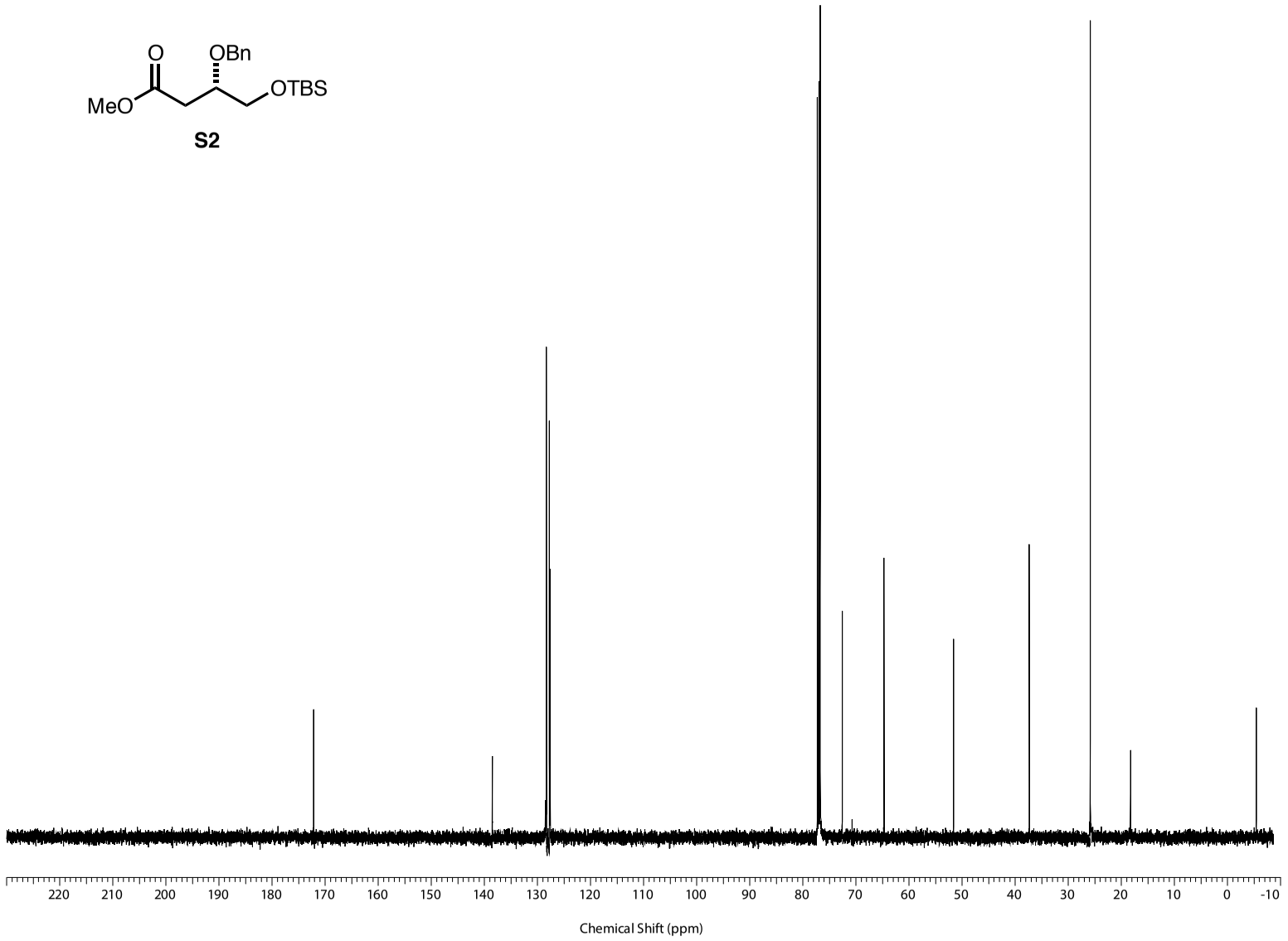
O
OBn
MeO
OTBS
S2
220
210
200
190
180
170
160
150
140
130
120
110
100
90
80
70
60
50
40
30
20
10
0
-10
Chemical Shift (ppm)

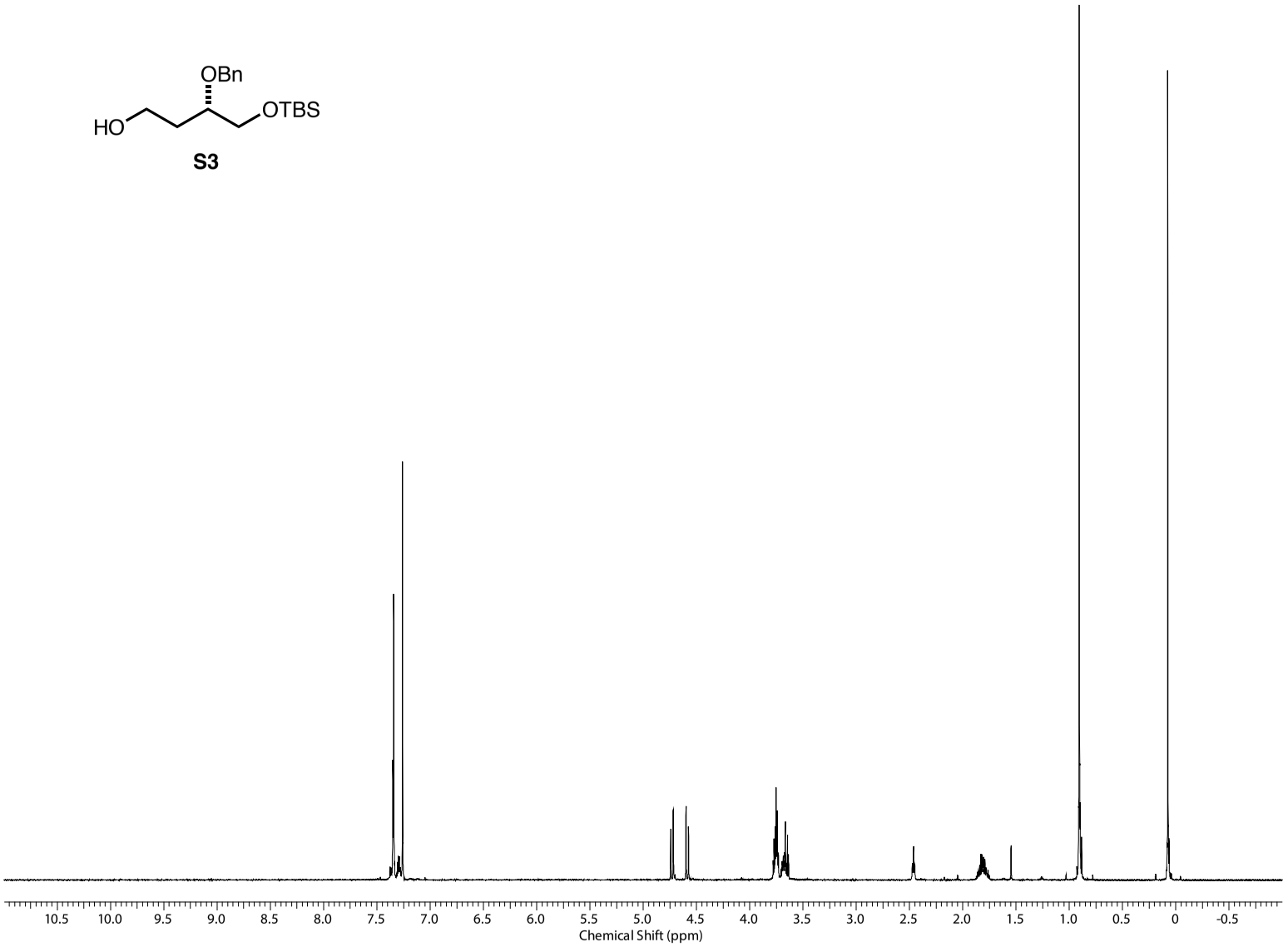
OBn
HO
OTBS
S3
10.5
10.0
9.5
9.0
8.5
8.0
7.5
7.0
6.5
6.0
5.5
5.0
4.5
4.0
3.5
3.0
2.5
2.0
1.5
1.0
0.5
0
-0.5
Chemical Shift (ppm)

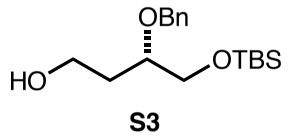
OBn
HO
OTBS

S3

210
200
190
180
170
160
150
140
130
120
110
100
90
80
70
60
50
40
30
20
10
0
-10
Chemical Shift (ppm)

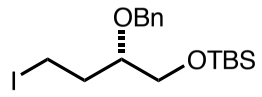
OBn
OTBS
I

134

10.5
10.0
9.5
9.0
8.5
8.0
7.5
7.0
6.5
6.0
5.5
5.0
4.5
4.0
3.5
3.0
2.5
2.0
1.5
1.0
0.5
0
-0.5
Chemical Shift (ppm)

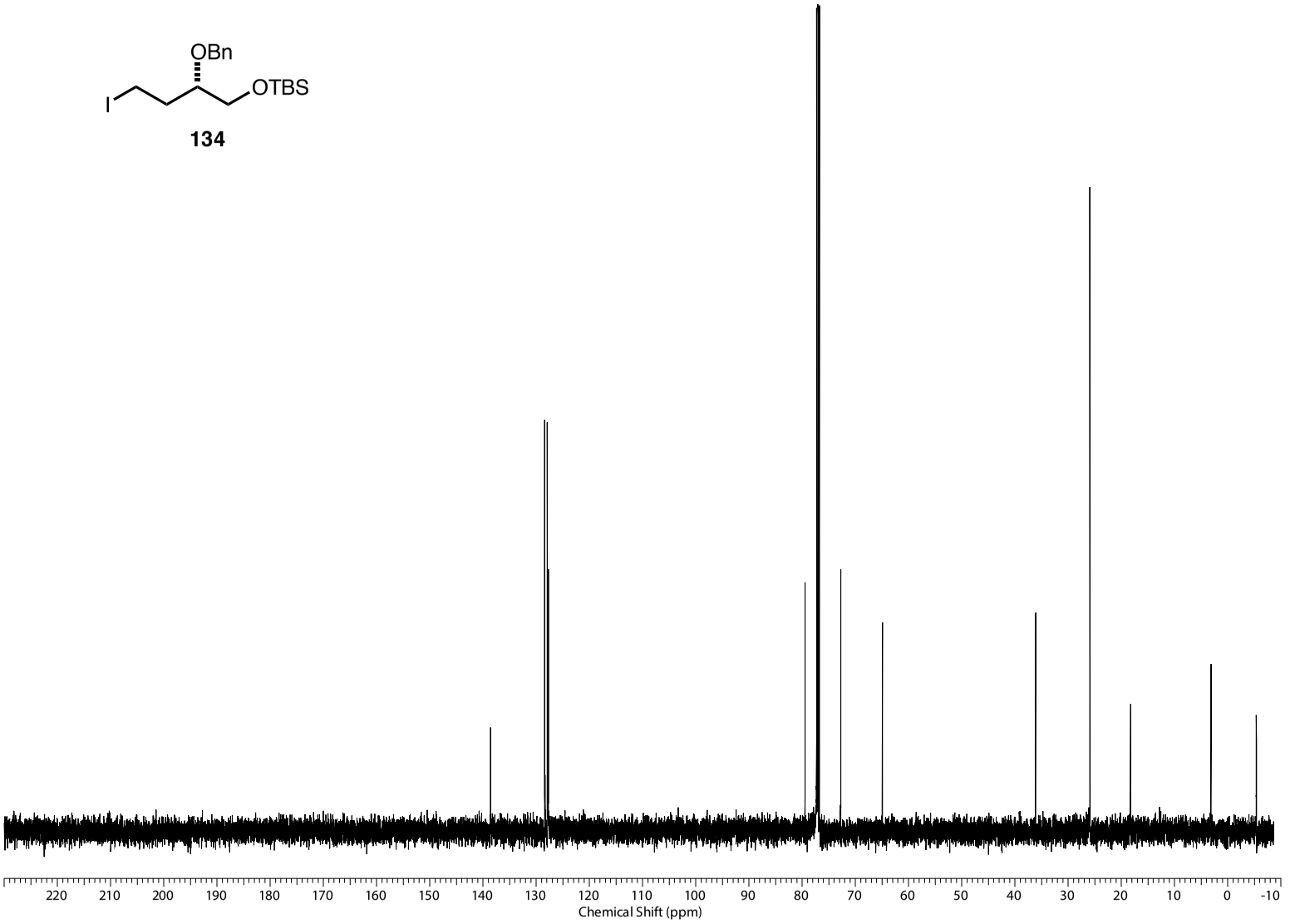
OBn
OTBS
I
134
220
210
200
190
180
170
160
150
140
130
120
110
100
90
80
70
60
50
40
30
20
10
0
-10
Chemical Shift (ppm)

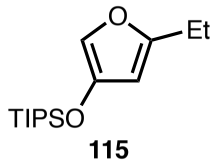
O
Et
TIPSO

115

10.5
10.0
9.5
9.0
8.5
8.0
7.5
7.0
6.5
6.0
5.5
5.0
4.5
4.0
3.5
3.0
2.5
2.0
1.5
1.0
0.5
0
-0.5
-1.0
Chemical Shift (ppm)

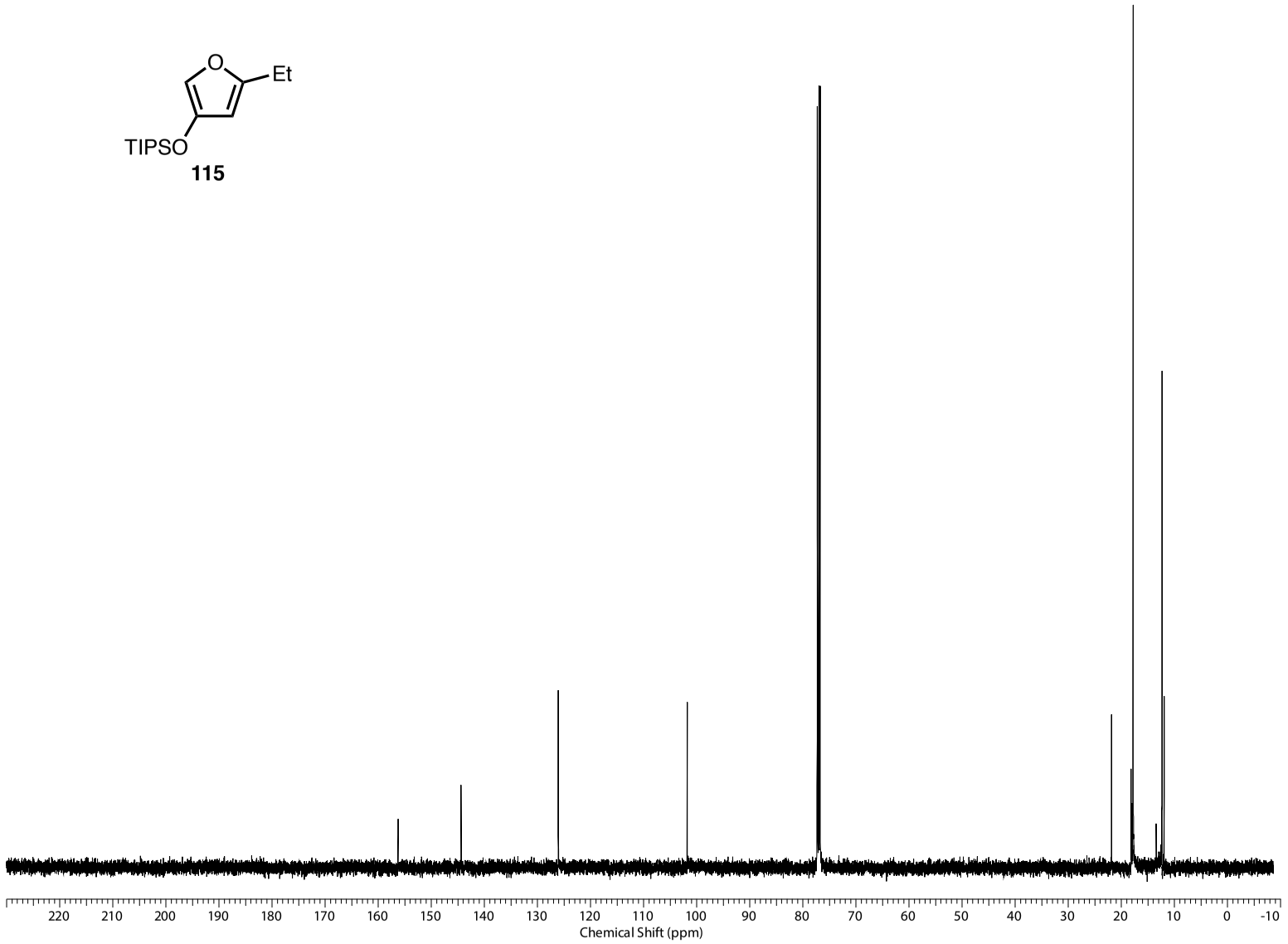
O
Et
TIPSO
115
220 210 200 190 180 170 160 150 140 130 120 110 100 90 80 70 60 50 40 30 20 10 0 -10
Chemical Shift (ppm)

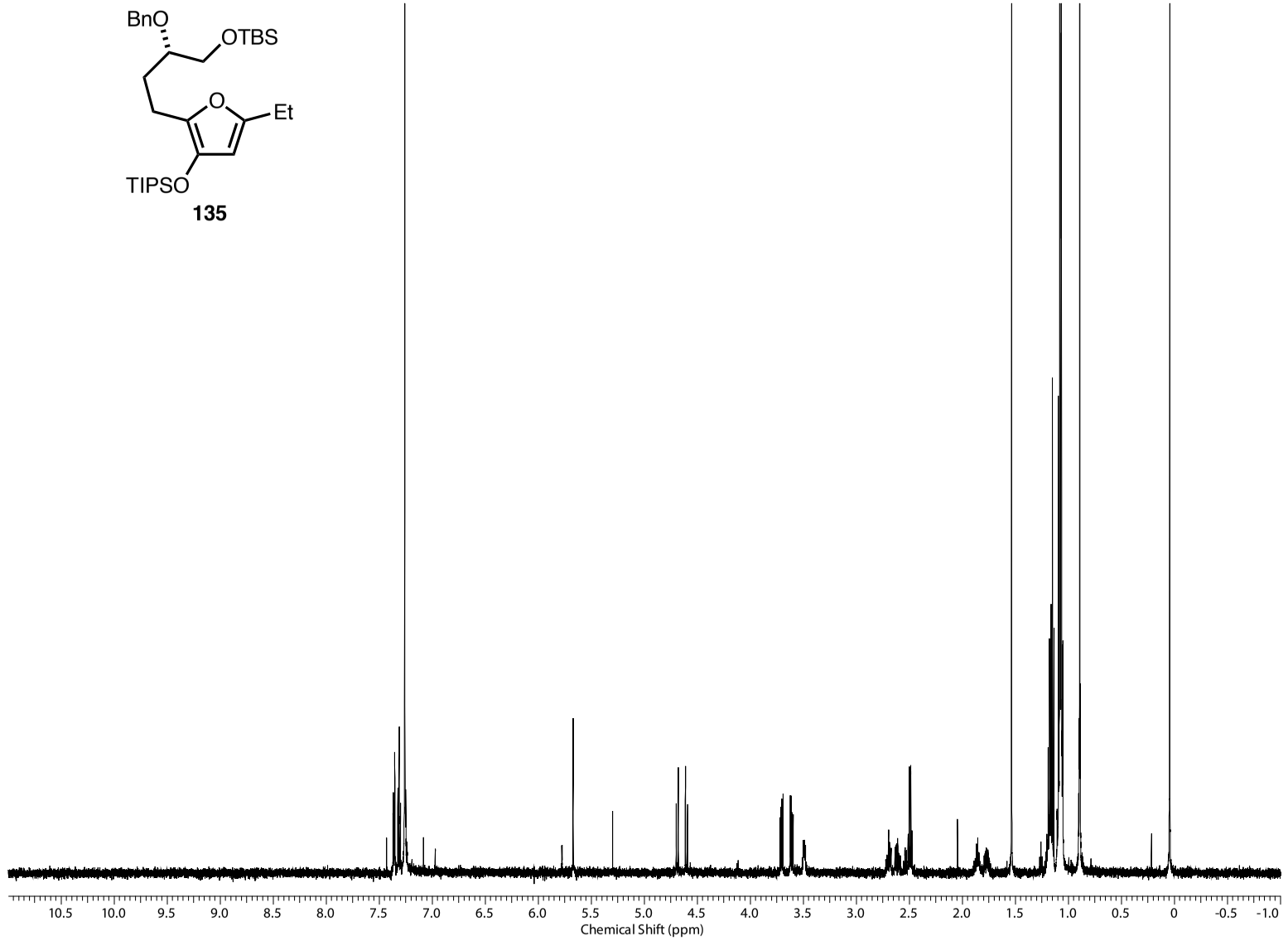
BnO
OTBS
O
Et
TIPSO
135
10.5 10.0 9.5 9.0 8.5 8.0 7.5 7.0 6.5 6.0 5.5 5.0 4.5 4.0 3.5 3.0 2.5 2.0 1.5 1.0 0.5 0 -0.5 -1.0
Chemical Shift (ppm)

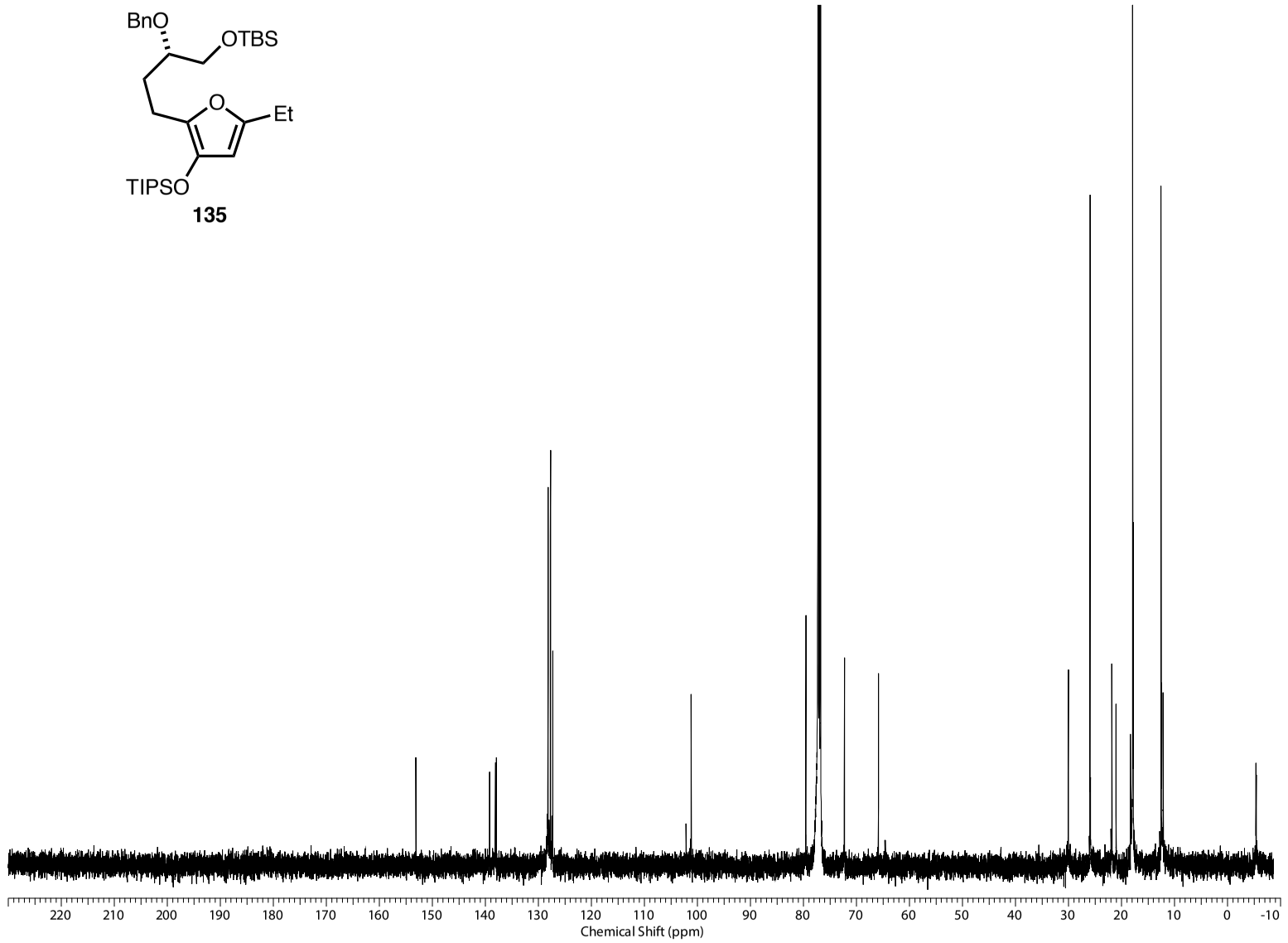
BnO
OTBS
O
Et
TIPSO
135
220 210 200 190 180 170 160 150 140 130 120 110 100 90 80 70 60 50 40 30 20 10 0 -10
Chemical Shift (ppm)

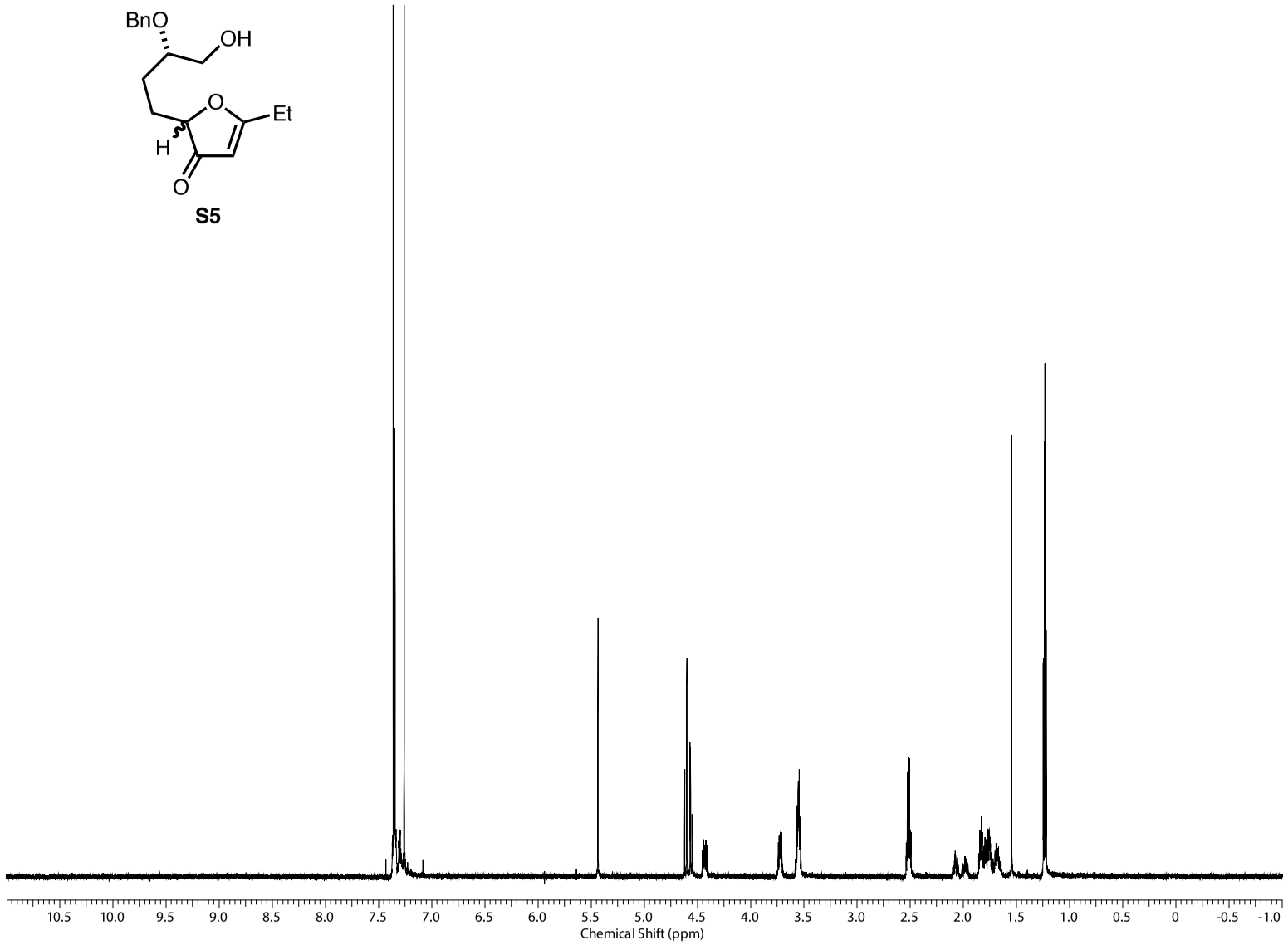
BnO
OH
O
Et
H
O
S5
10.5
10.0
9.5
9.0
8.5
8.0
7.5
7.0
6.5
6.0
5.5
5.0
4.5
4.0
3.5
3.0
2.5
2.0
1.5
1.0
0.5
0
-0.5
-1.0
Chemical Shift (ppm)

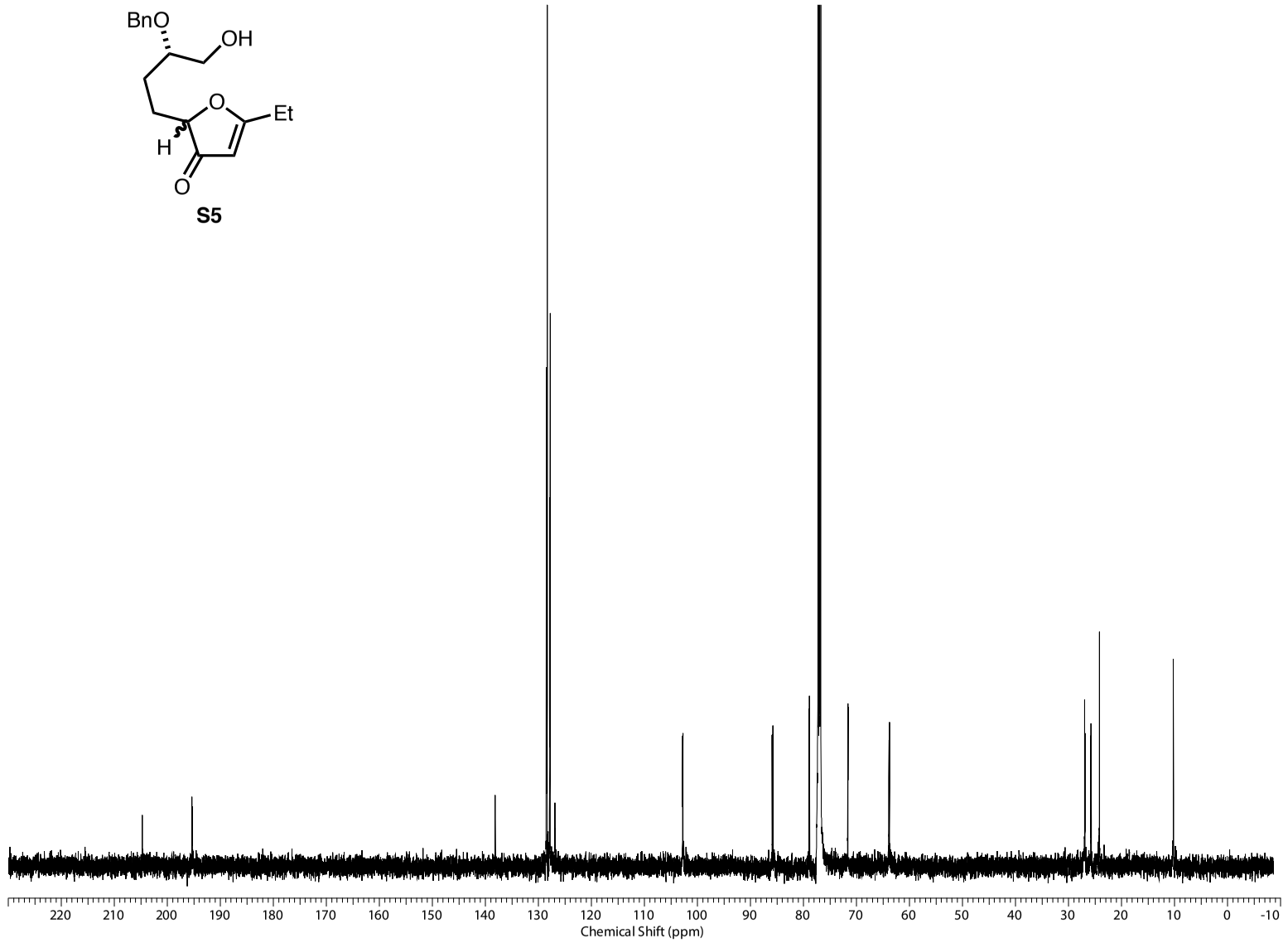
BnO
OH
O
Et
H
O
S5
220 210 200 190 180 170 160 150 140 130 120 110 100 90 80 70 60 50 40 30 20 10 0 -10
Chemical Shift (ppm)

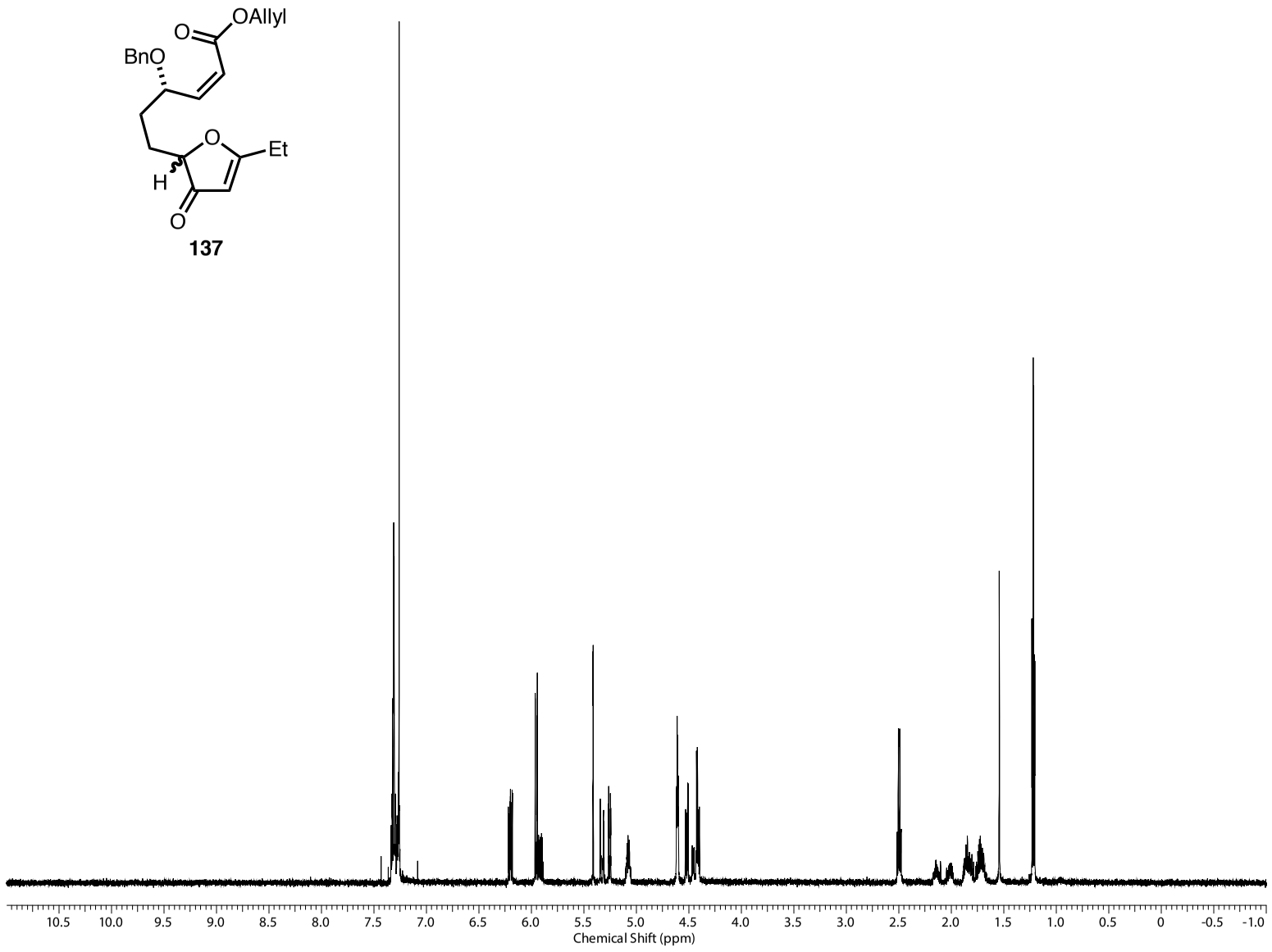
OAllyl
O
BnO
O
Et
H
O
137
10.5
10.0
9.5
9.0
8.5
8.0
7.5
7.0
6.5
6.0
5.5
5.0
4.5
4.0
3.5
3.0
2.5
2.0
1.5
1.0
0.5
0
-0.5
-1.0
Chemical Shift (ppm)

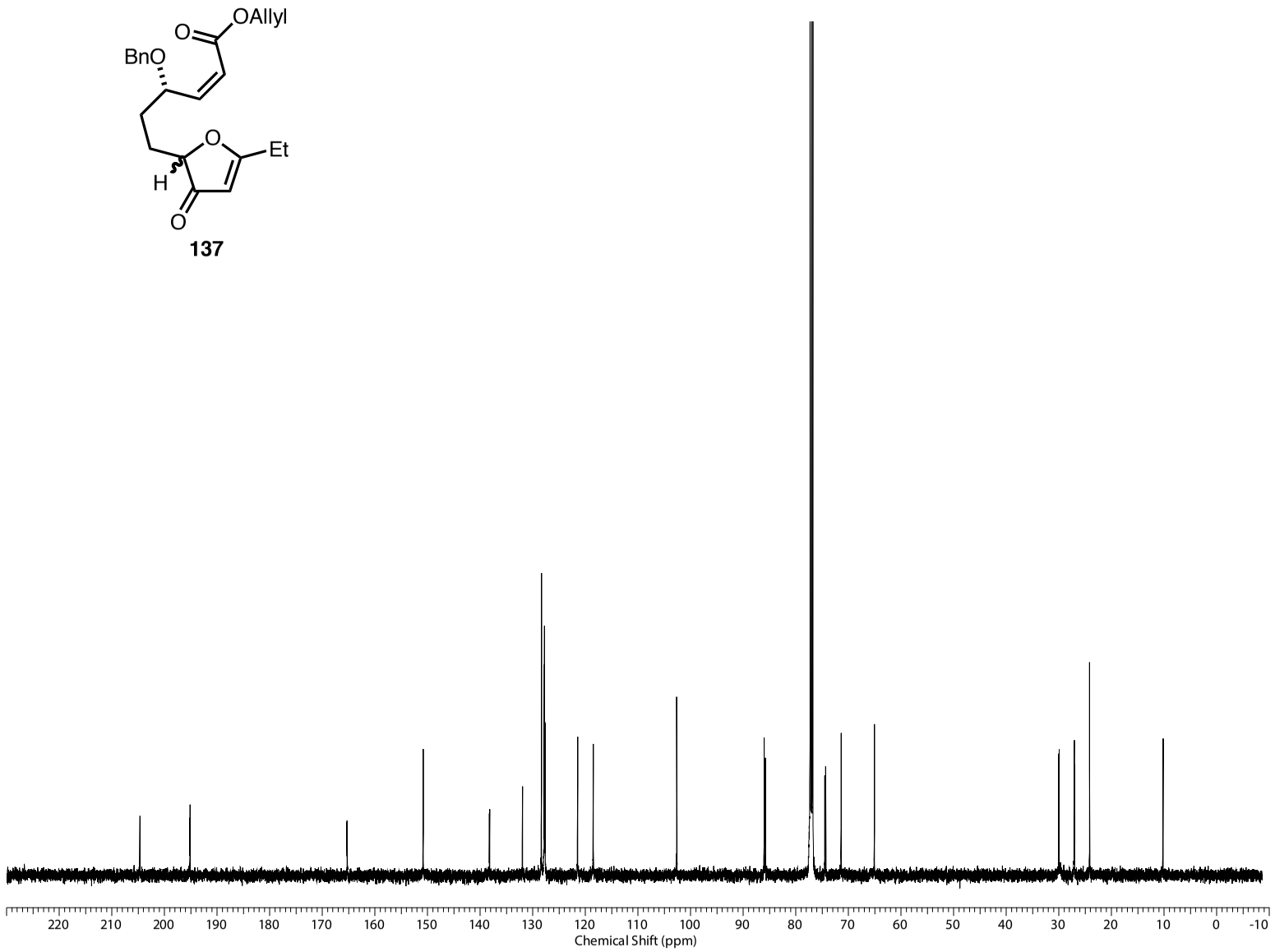
OAllyl
O
BnO
O
Et
H
O
137
220 210 200 190 180 170 160 150 140 130 120 110 100 90 80 70 60 50 40 30 20 10 0 -10
Chemical Shift (ppm)

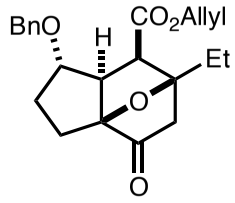
BnO
H
CO2Allyl
Et
O
O

138

10.5
10.0
9.5
9.0
8.5
8.0
7.5
7.0
6.5
6.0
5.5
5.0
4.5
4.0
3.5
3.0
2.5
2.0
1.5
1.0
0.5
0
-0.5
-1.0
Chemical Shift (ppm)

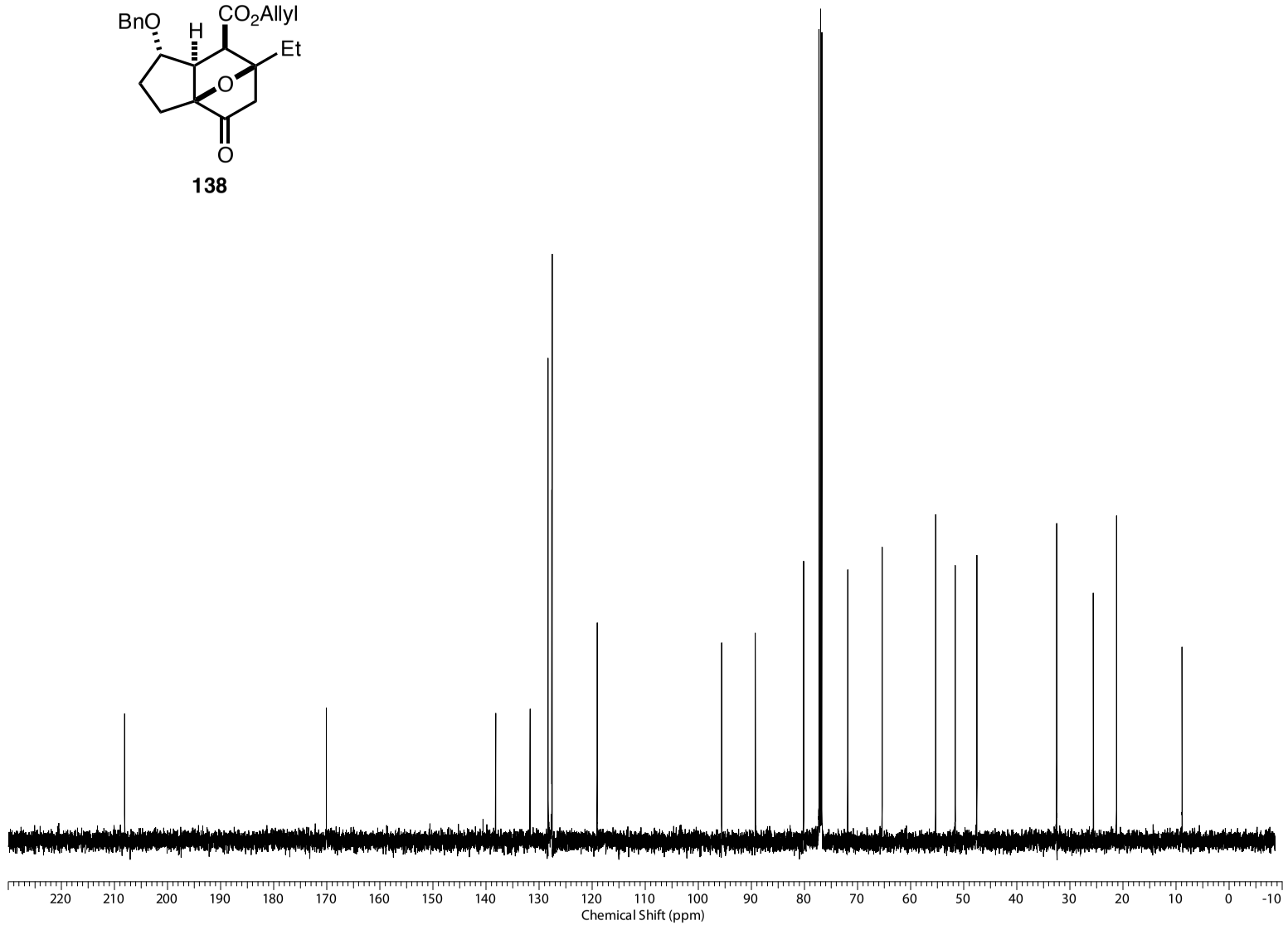
BnO
H
CO2Allyl
Et
O
O
138
220 210 200 190 180 170 160 150 140 130 120 110 100 90 80 70 60 50 40 30 20 10 0 -10
Chemical Shift (ppm)

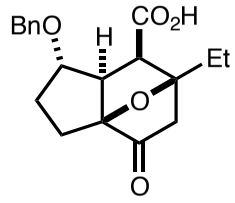
BnO
H
CO2H
Et
O
O

139

10.5
10.0
9.5
9.0
8.5
8.0
7.5
7.0
6.5
6.0
5.5
5.0
4.5
4.0
3.5
3.0
2.5
2.0
1.5
1.0
0.5
0
-0.5
-1.0
Chemical Shift (ppm)

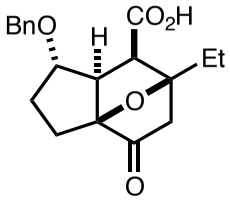
BnO
H
CO2H
Et
O
O

139

220
210
200
190
180
170
160
150
140
130
120
110
100
90
80
70
60
50
40
30
20
10
0
-10
Chemical Shift (ppm)

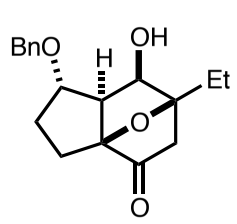
BnO
H
OH
Et
O
O

142

10.5
10.0
9.5
9.0
8.5
8.0
7.5
7.0
6.5
6.0
5.5
5.0
4.5
4.0
3.5
3.0
2.5
2.0
1.5
1.0
0.5
0
-0.5
Chemical Shift (ppm)

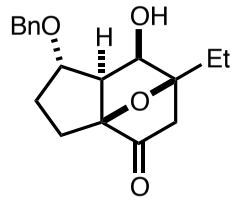
BnO
H
OH
Et
O
O

142

220
210
200
190
180
170
160
150
140
130
120
110
100
90
80
70
60
50
40
30
20
10
0
-10
Chemical Shift (ppm)

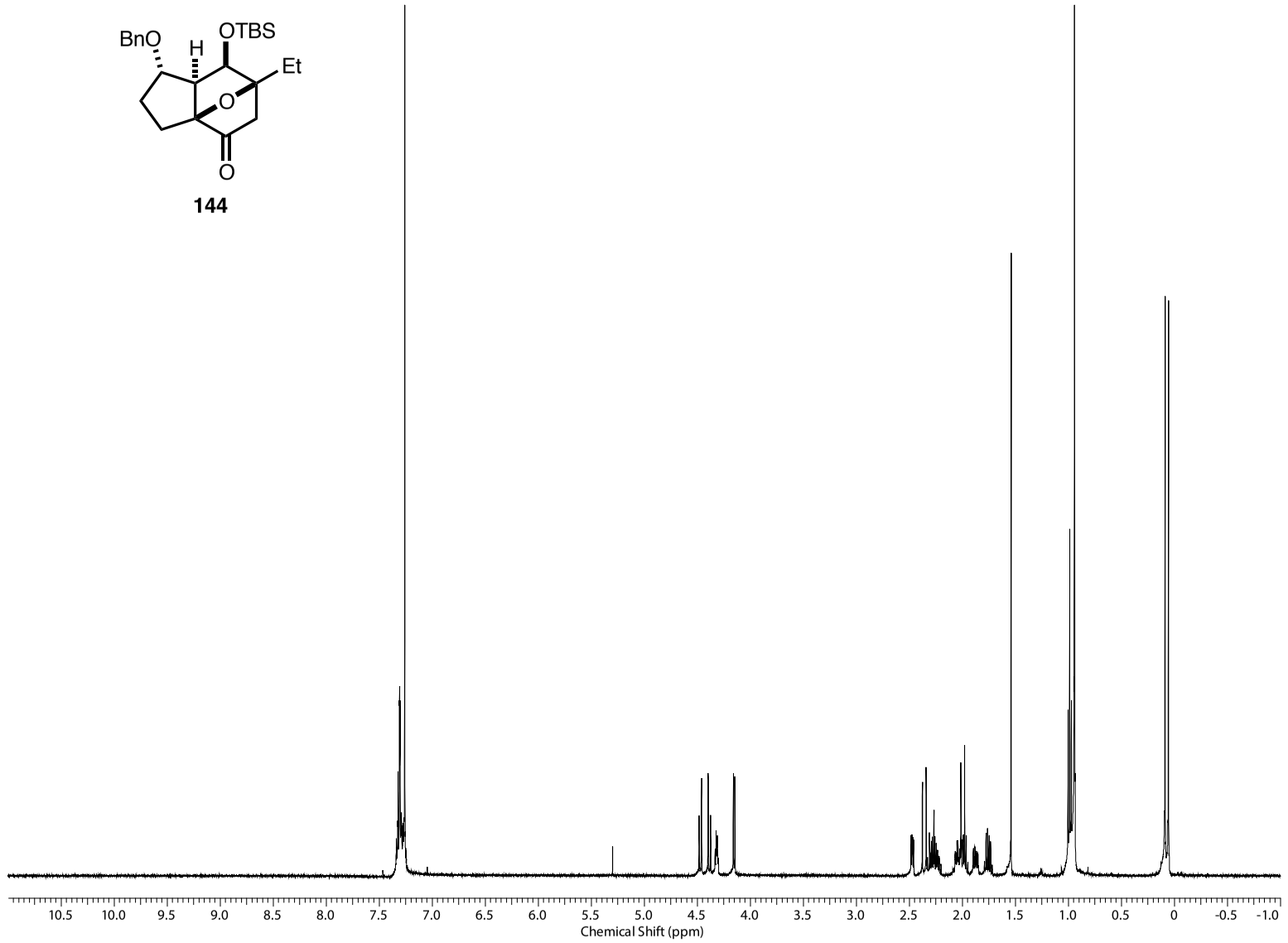
BnO
H
OTBS
Et
O
O
144
10.5
10.0
9.5
9.0
8.5
8.0
7.5
7.0
6.5
6.0
5.5
5.0
4.5
4.0
3.5
3.0
2.5
2.0
1.5
1.0
0.5
0
-0.5
-1.0
Chemical Shift (ppm)

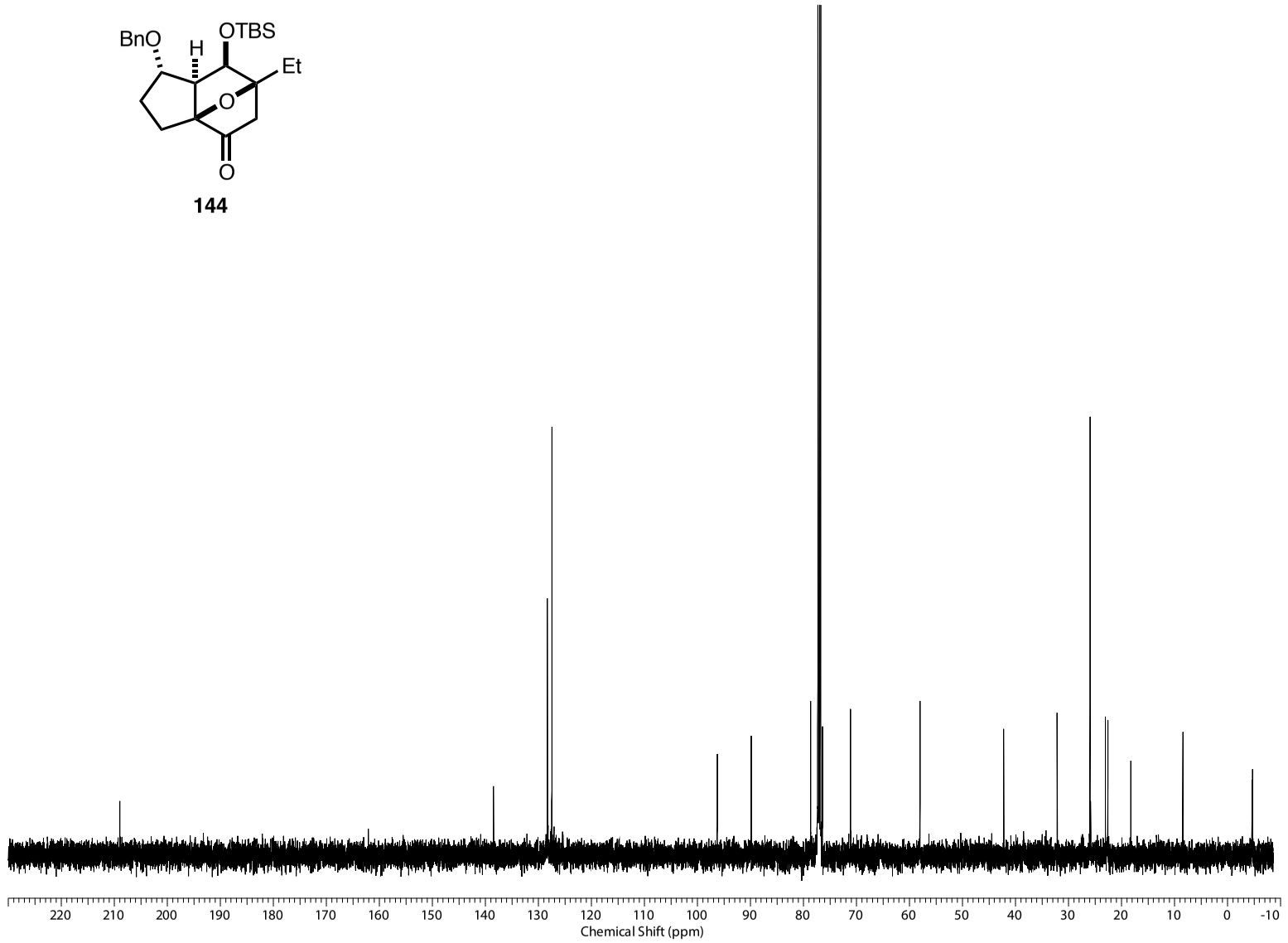
BnO
H
OTBS
Et
O
O
144
220
210
200
190
180
170
160
150
140
130
120
110
100
90
80
70
60
50
40
30
20
10
0
-10
Chemical Shift (ppm)

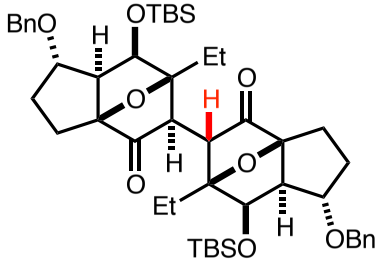
BnO
H
OTBS
Et
O
H
O
H
O
O
Et
TBSO
H
OBn

145

10.5
10.0
9.5
9.0
8.5
8.0
7.5
7.0
6.5
6.0
5.5
5.0
4.5
4.0
3.5
3.0
2.5
2.0
1.5
1.0
0.5
0
-0.5
-1.0
Chemical Shift (ppm)

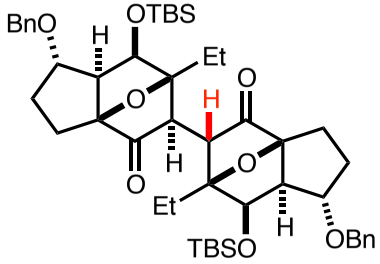
BnO
H
OTBS
Et
O
O
H
H
O
O
Et
TBSO
H
OBn

145

220
210
200
190
180
170
160
150
140
130
120
110
100
90
80
70
60
50
40
30
20
10
0
-10
Chemical Shift (ppm)

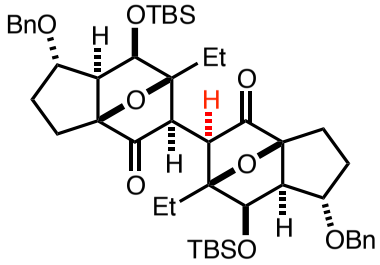
BnO
H
OTBS
Et
O
O
H
H
O
O
Et
TBSO
H
OBn

146

10.5
10.0
9.5
9.0
8.5
8.0
7.5
7.0
6.5
6.0
5.5
5.0
4.5
4.0
3.5
3.0
2.5
2.0
1.5
1.0
0.5
0
-0.5
Chemical Shift (ppm)

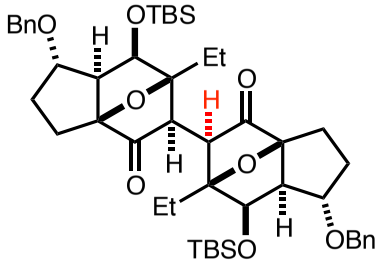
BnO
H
OTBS
Et
O
O
H
H
O
O
Et
TBSO
H
OBn

146

220
210
200
190
180
170
160
150
140
130
120
110
100
90
80
70
60
50
40
30
20
10
0
-10
Chemical Shift (ppm)

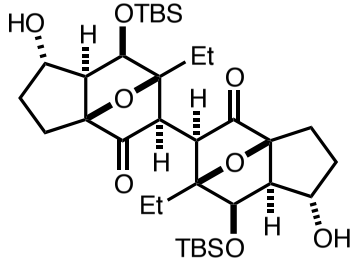
HO
H
OTBS
Et
O
O
H
H
O
O
Et
TBSO
H
OH

147

10.5
10.0
9.5
9.0
8.5
8.0
7.5
7.0
6.5
6.0
5.5
5.0
4.5
4.0
3.5
3.0
2.5
2.0
1.5
1.0
0.5
0
-0.5
Chemical Shift (ppm)

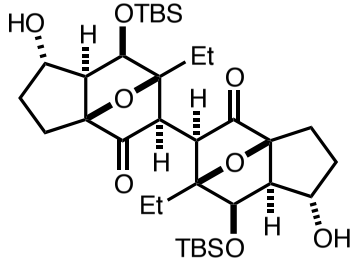
HO
H
OTBS
Et
O
O
H
H
O
O
Et
TBSO
H
OH

147

220
210
200
190
180
170
160
150
140
130
120
110
100
90
80
70
60
50
40
30
20
10
0
-10
Chemical Shift (ppm)

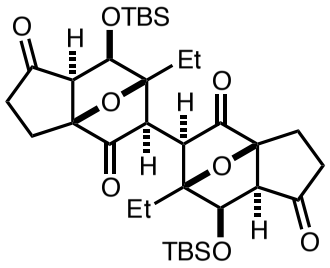
O
H
OTBS
Et
O
O
H
H
O
O
Et
TBSO
H
O

148

10.5
10.0
9.5
9.0
8.5
8.0
7.5
7.0
6.5
6.0
5.5
5.0
4.5
4.0
3.5
3.0
2.5
2.0
1.5
1.0
0.5
0
-0.5
Chemical Shift (ppm)

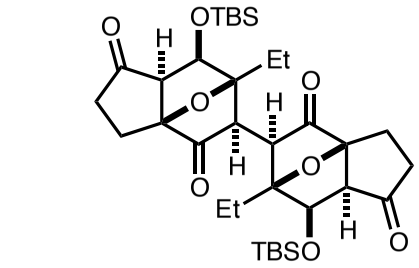
O
H
OTBS
Et
O
O
H
H
O
O
Et
TBSO
H
O

148

220
210
200
190
180
170
160
150
140
130
120
110
100
90
80
70
60
50
40
30
20
10
0
-10
Chemical Shift (ppm)

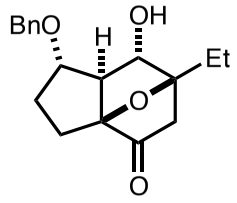
BnO
H
OH
Et
O
O

162

10.5
10.0
9.5
9.0
8.5
8.0
7.5
7.0
6.5
6.0
5.5
5.0
4.5
4.0
3.5
3.0
2.5
2.0
1.5
1.0
0.5
0
-0.5
Chemical Shift (ppm)

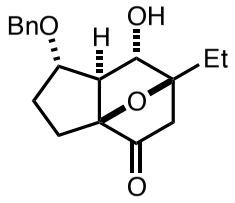
BnO
H
OH
Et
O
O

162

220
210
200
190
180
170
160
150
140
130
120
110
100
90
80
70
60
50
40
30
20
10
0
-10
Chemical Shift (ppm)

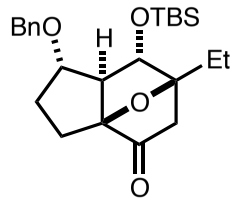
BnO
H
OTBS
Et
O
O

163

10.5
10.0
9.5
9.0
8.5
8.0
7.5
7.0
6.5
6.0
5.5
5.0
4.5
4.0
3.5
3.0
2.5
2.0
1.5
1.0
0.5
0
-0.5
Chemical Shift (ppm)

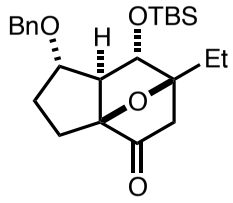
BnO
H
OTBS
Et
O
O

163

220
210
200
190
180
170
160
150
140
130
120
110
100
90
80
70
60
50
40
30
20
10
0
-10
Chemical Shift (ppm)

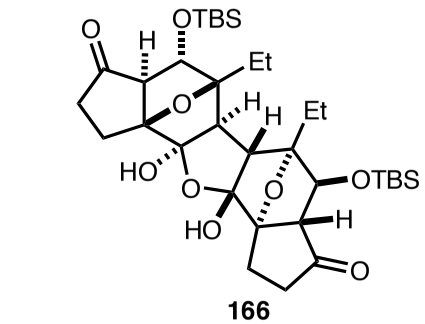
O
H
OTBS
Et
O
H
H
Et
HO
O
O
OTBS
HO
H
O

166

10.5
10.0
9.5
9.0
8.5
8.0
7.5
7.0
6.5
6.0
5.5
5.0
4.5
4.0
3.5
3.0
2.5
2.0
1.5
1.0
0.5
0
-0.5
Chemical Shift (ppm)

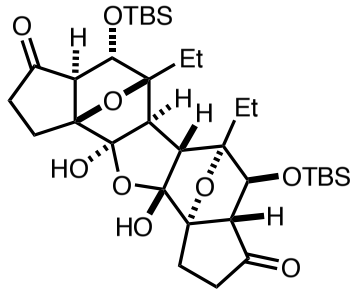
O
H
OTBS
Et
O
H
H
Et
HO
O
O
OTBS
HO
H
O

166

220 210 200 190 180 170 160 150 140 130 120 110 100 90 80 70 60 50 40 30 20 10 0 -10
Chemical Shift (ppm)

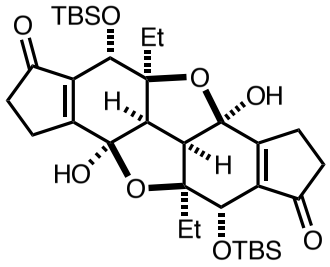

169

***epi*-lomaiviticin B core**

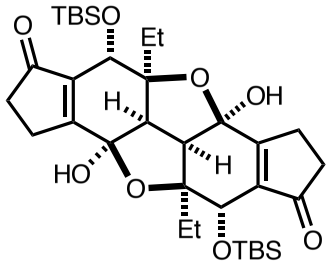

169

***epi*-lomaiviticin B core**

Appendix B

Chapter Four Catalog of ^{1}H and ^{13}C NMR Spectra

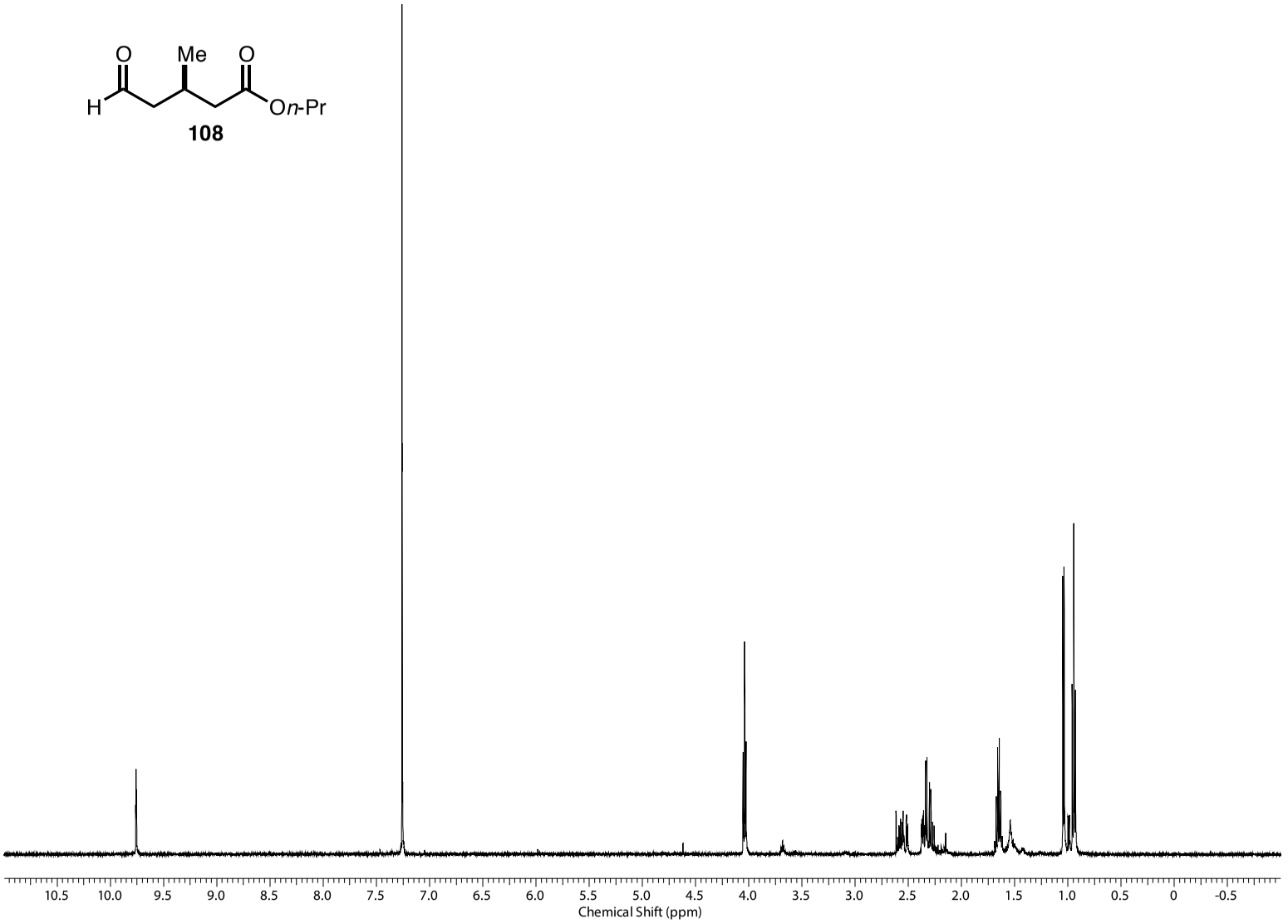
O
Me
O
H
O*n*-Pr
108
10.5
10.0
9.5
9.0
8.5
8.0
7.5
7.0
6.5
6.0
5.5
5.0
4.5
4.0
3.5
3.0
2.5
2.0
1.5
1.0
0.5
0
-0.5
Chemical Shift (ppm)

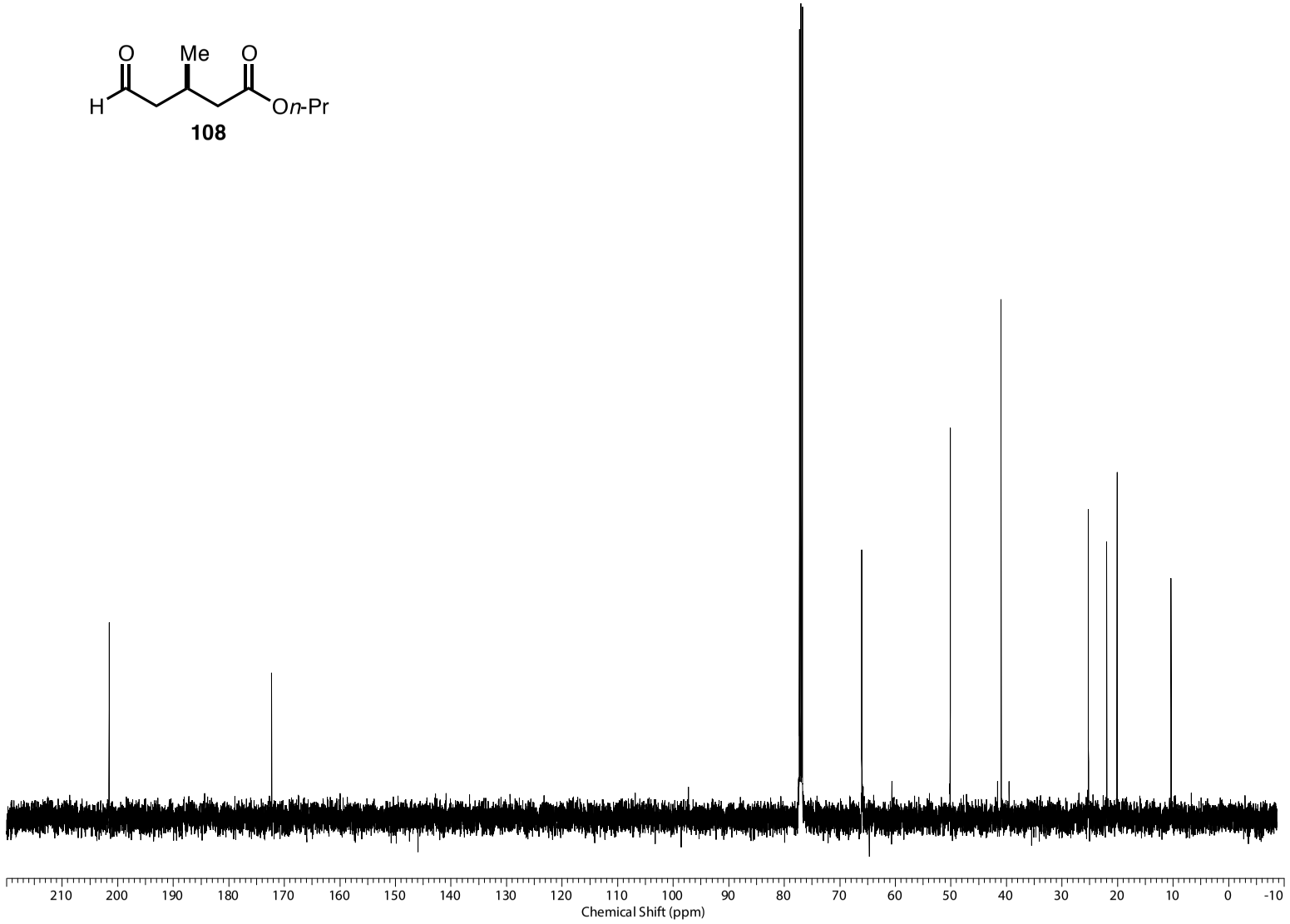
O
Me
O
H
On-Pr
108
210
200
190
180
170
160
150
140
130
120
110
100
90
80
70
60
50
40
30
20
10
0
-10
Chemical Shift (ppm)

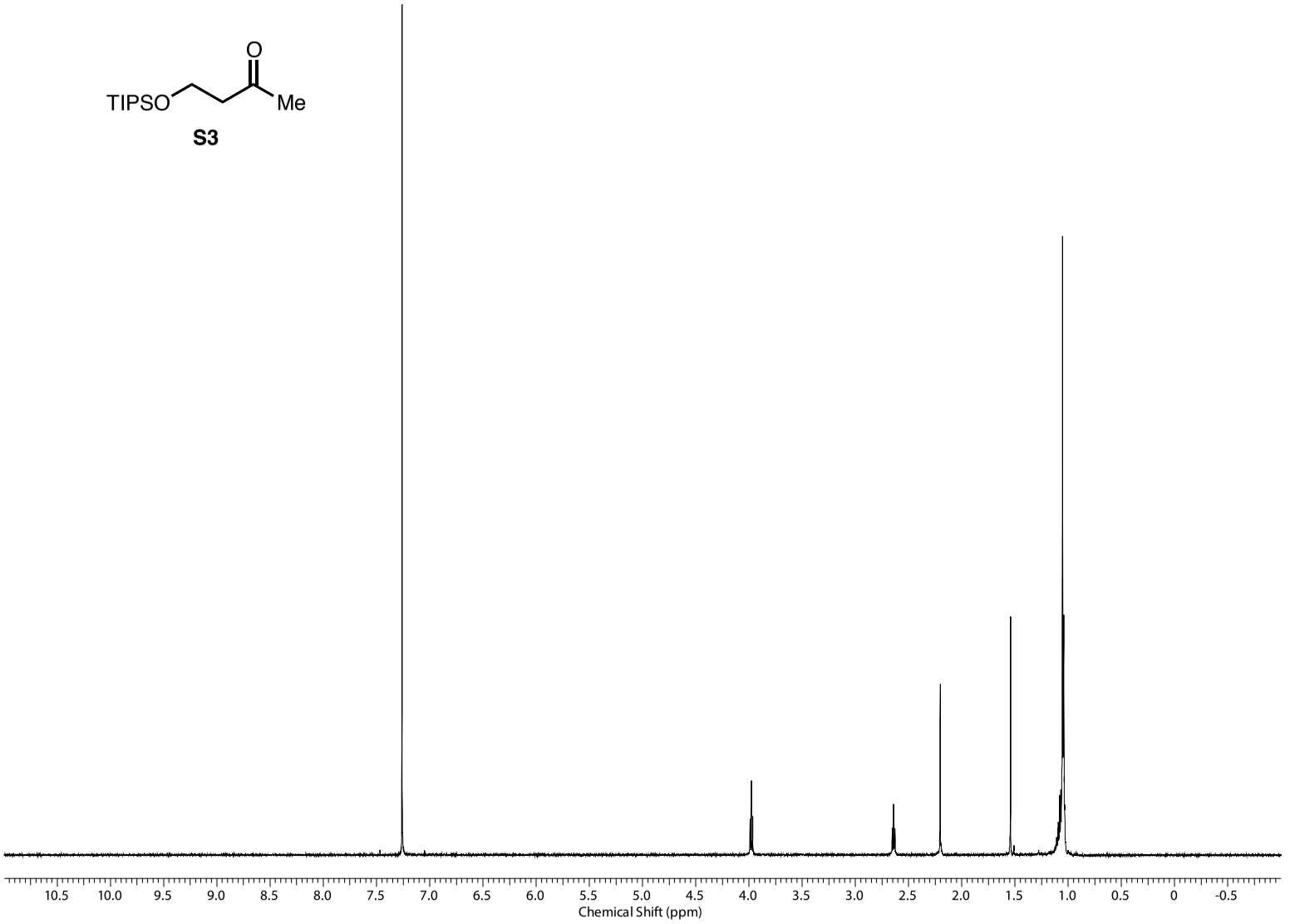
O
TIPSO
Me
S3
10.5
10.0
9.5
9.0
8.5
8.0
7.5
7.0
6.5
6.0
5.5
5.0
4.5
4.0
3.5
3.0
2.5
2.0
1.5
1.0
0.5
0
-0.5
Chemical Shift (ppm)

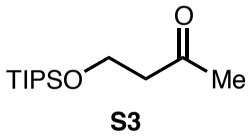
O
TIPSO
Me

S3

210
200
190
180
170
160
150
140
130
120
110
100
90
80
70
60
50
40
30
20
10
0
-10
Chemical Shift (ppm)

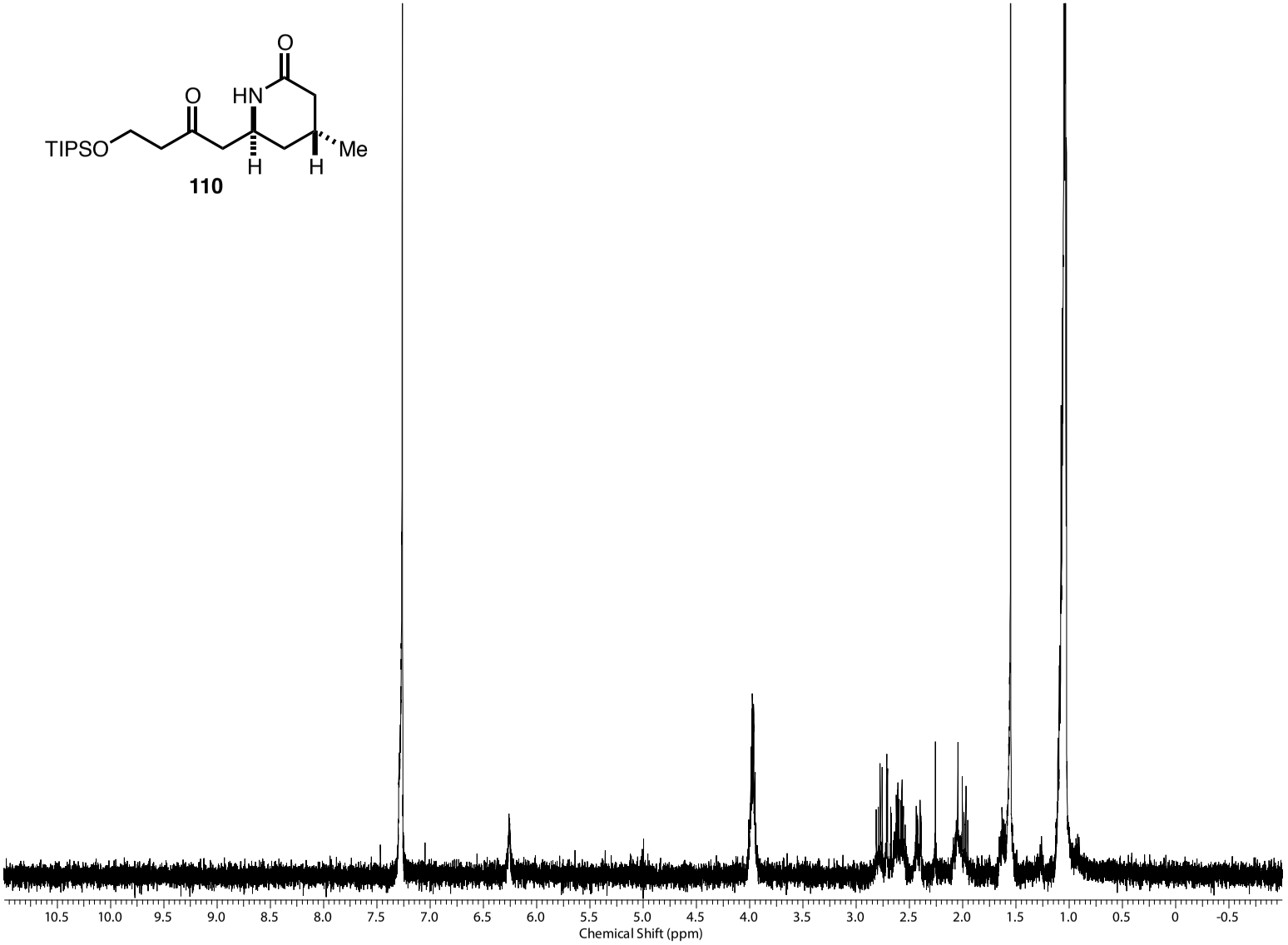
O
HN
O
TIPSO
Me
H
H
110
10.5
10.0
9.5
9.0
8.5
8.0
7.5
7.0
6.5
6.0
5.5
5.0
4.5
4.0
3.5
3.0
2.5
2.0
1.5
1.0
0.5
0
-0.5
Chemical Shift (ppm)

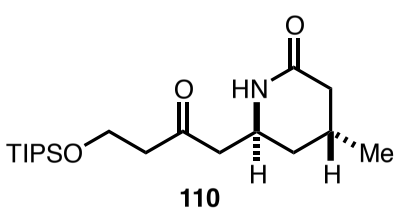
O
HN
O
TIPSO
H
H
Me

110

210
200
190
180
170
160
150
140
130
120
110
100
90
80
70
60
50
40
30
20
10
0
-10
Chemical Shift (ppm)

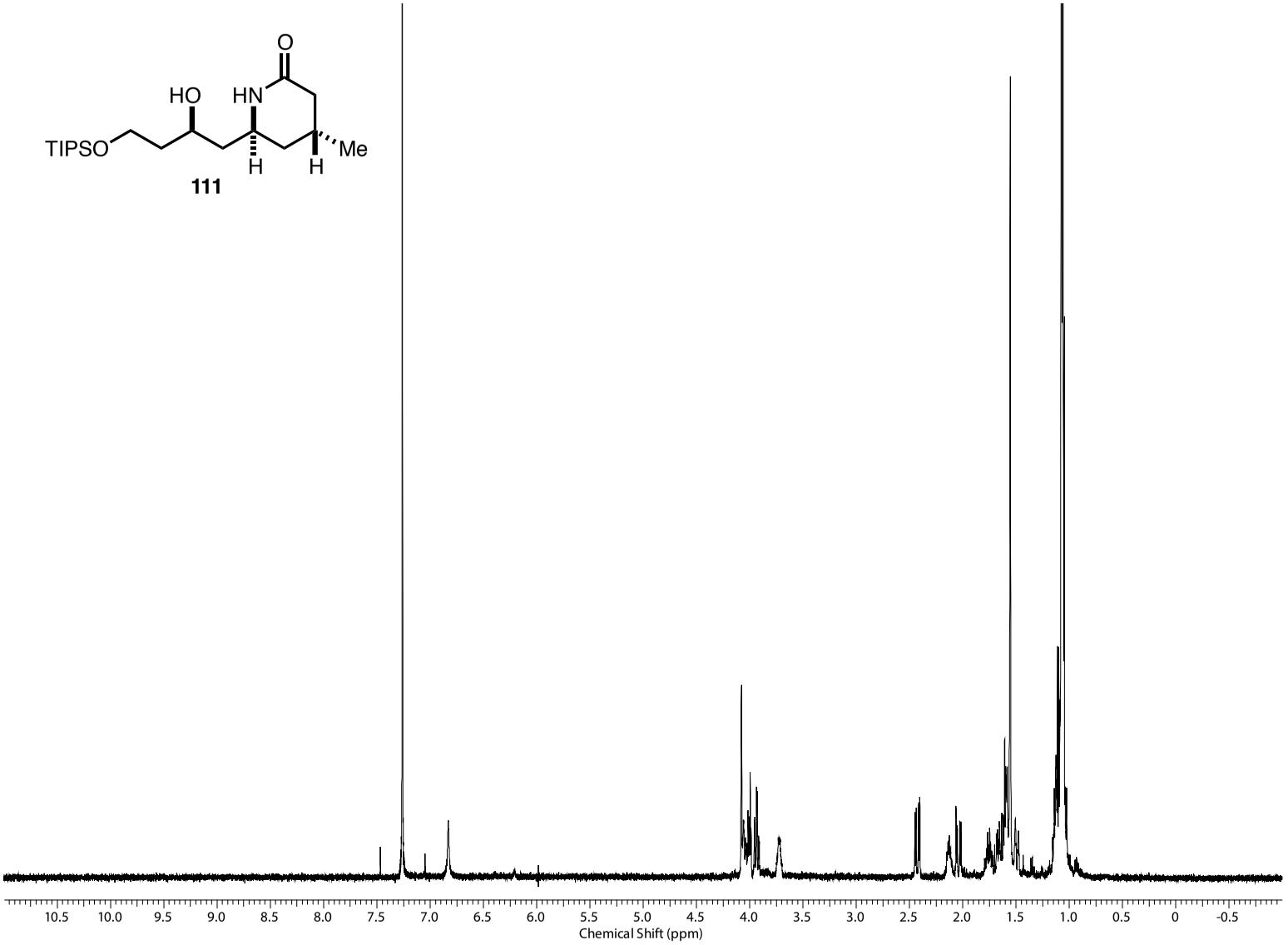
O
HO
HN
TIPSO
Me
H
H
111
10.5
10.0
9.5
9.0
8.5
8.0
7.5
7.0
6.5
6.0
5.5
5.0
4.5
4.0
3.5
3.0
2.5
2.0
1.5
1.0
0.5
0
-0.5
Chemical Shift (ppm)

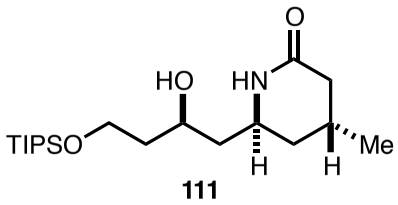
O
HO
HN
TIPSO
Me
H
H

111

210
200
190
180
170
160
150
140
130
120
110
100
90
80
70
60
50
40
30
20
10
0
-10
Chemical Shift (ppm)

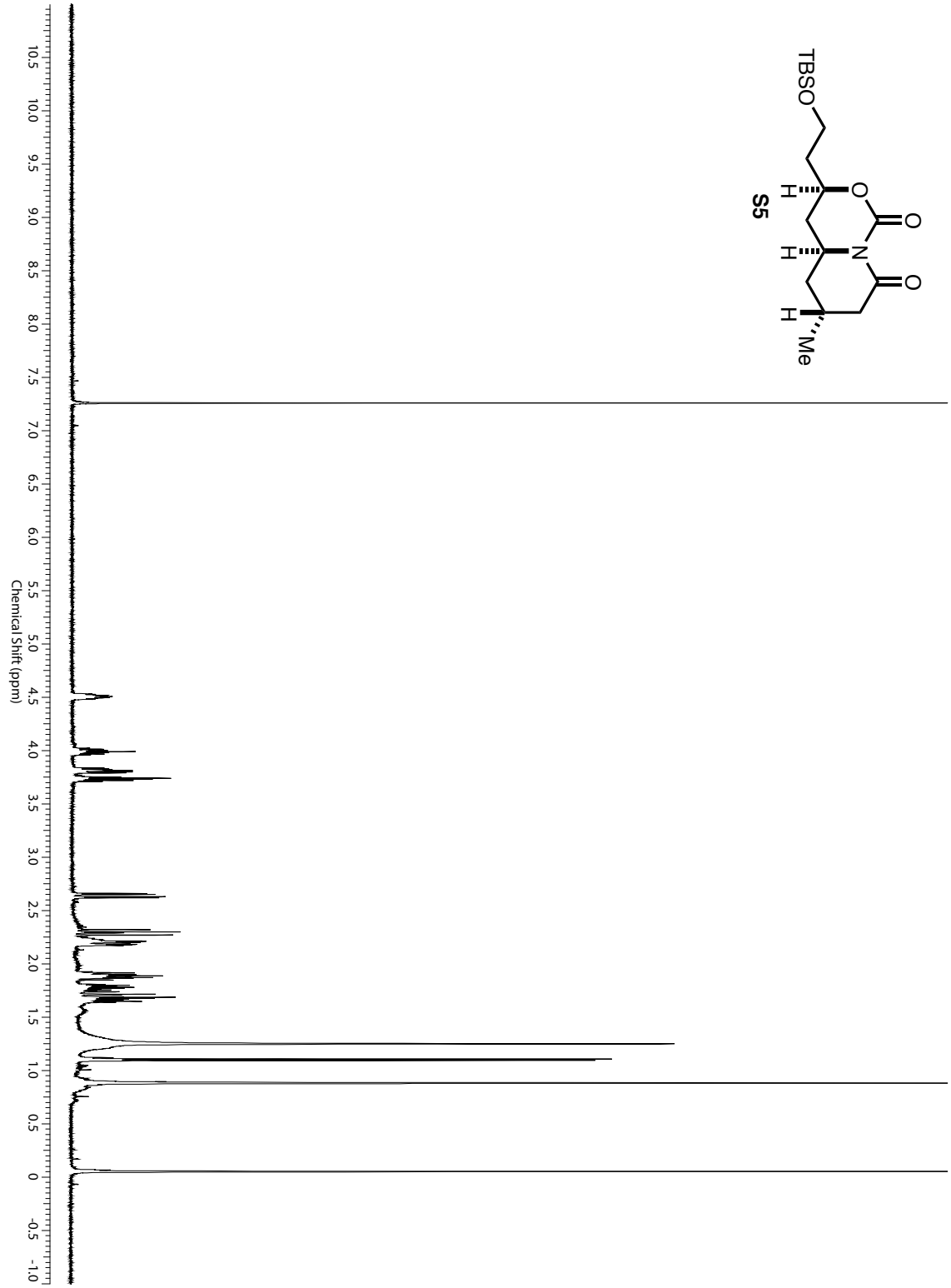
TBSO
H
H
H
Me
O
O
N
O
O
S5
10.5
10.0
9.5
9.0
8.5
8.0
7.5
7.0
6.5
6.0
5.5
5.0
4.5
4.0
3.5
3.0
2.5
2.0
1.5
1.0
0.5
0
-0.5
-1.0
Chemical Shift (ppm)

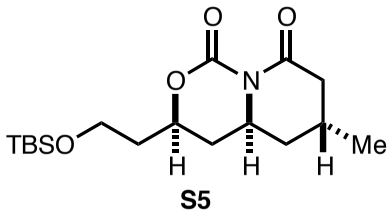
O
O
O
N
TBSO
Me
H
H
H

S5

210
200
190
180
170
160
150
140
130
120
110
100
90
80
70
60
50
40
30
20
10
0
-10
Chemical Shift (ppm)

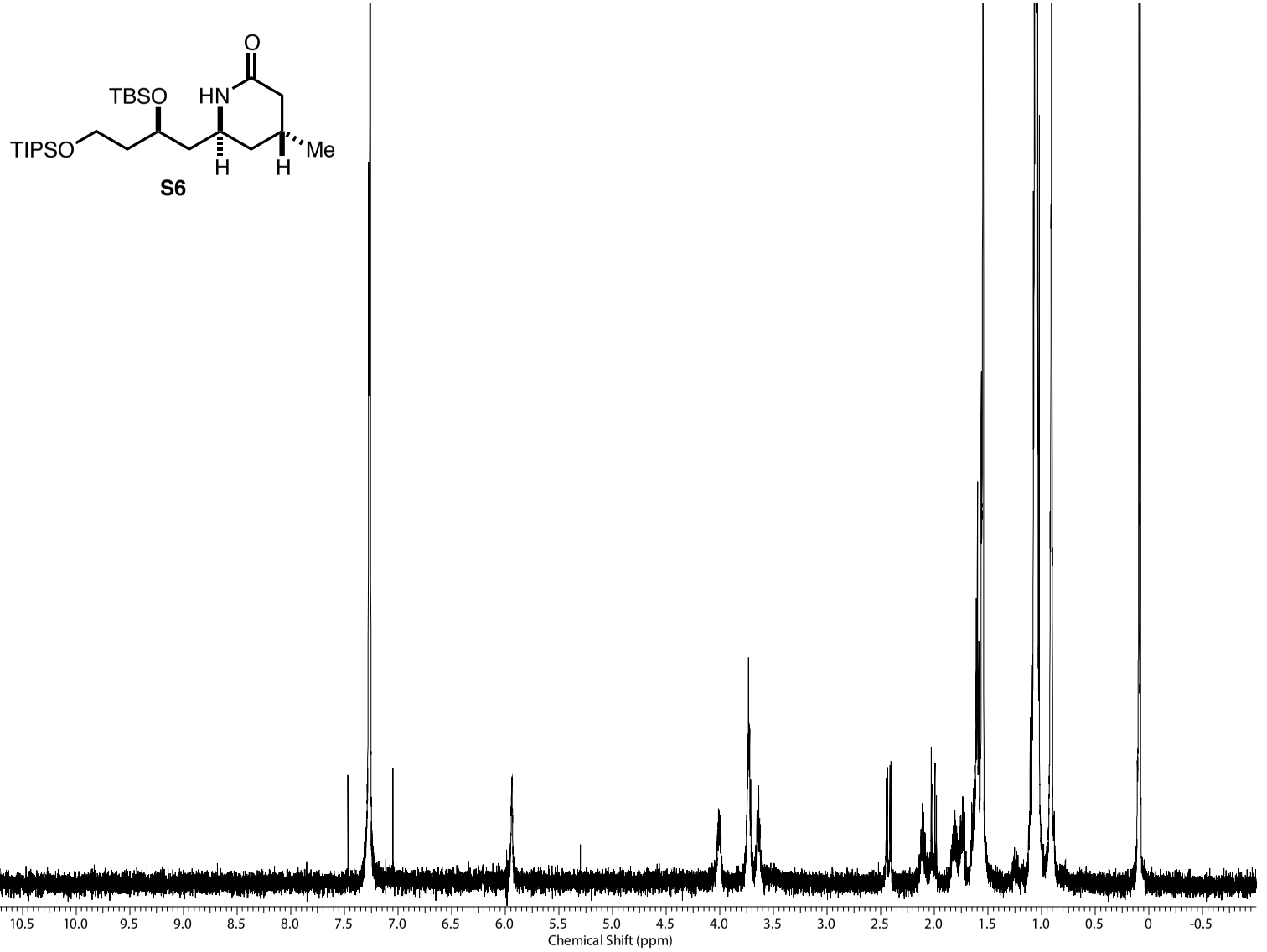
TBSO
HN
O
TIPSO
Me
H
H
S6
10.5
10.0
9.5
9.0
8.5
8.0
7.5
7.0
6.5
6.0
5.5
5.0
4.5
4.0
3.5
3.0
2.5
2.0
1.5
1.0
0.5
0
-0.5
Chemical Shift (ppm)

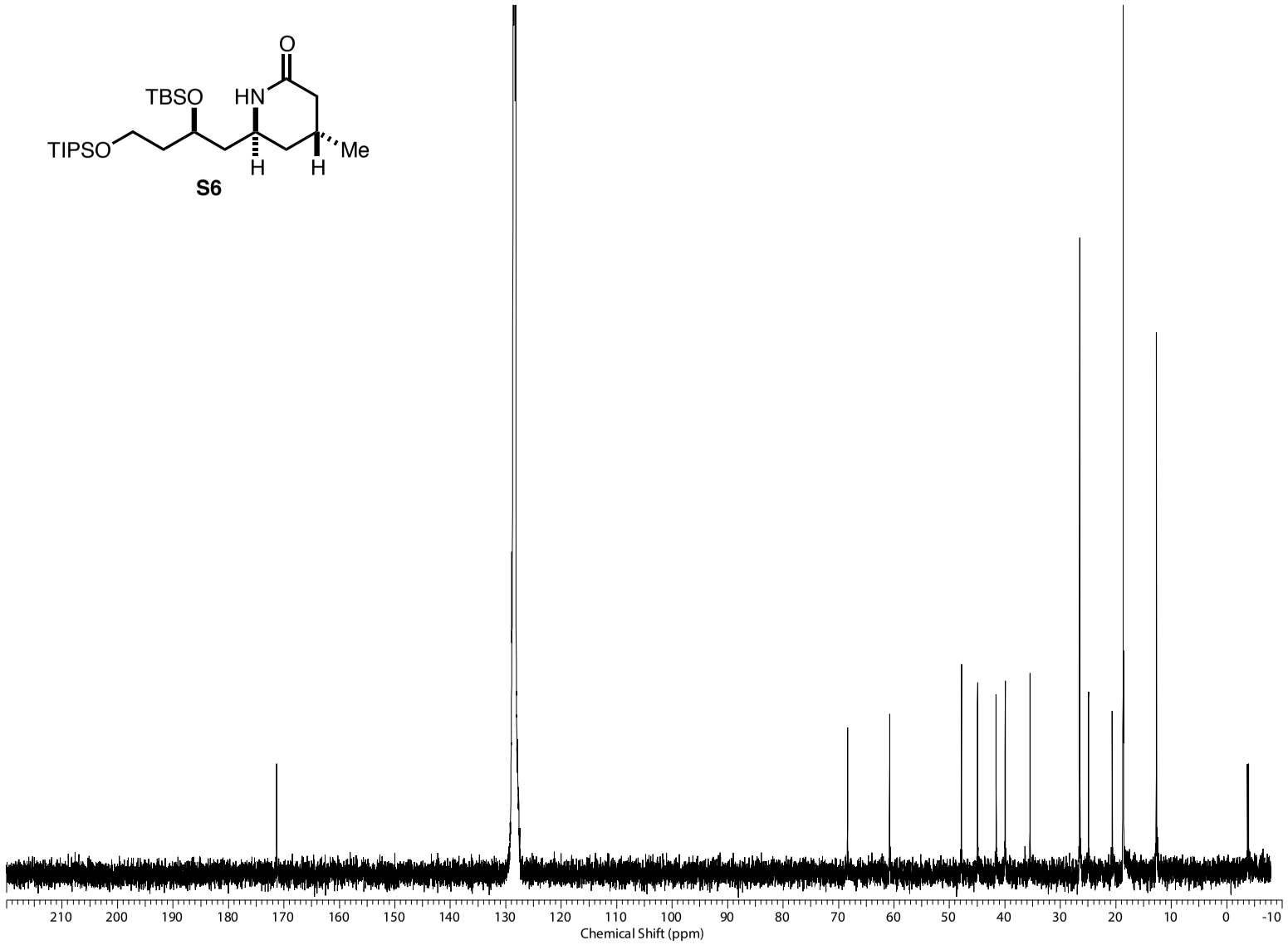
TBSO
HN
O
TIPSO
Me
H
H
S6
210
200
190
180
170
160
150
140
130
120
110
100
90
80
70
60
50
40
30
20
10
0
-10
Chemical Shift (ppm)

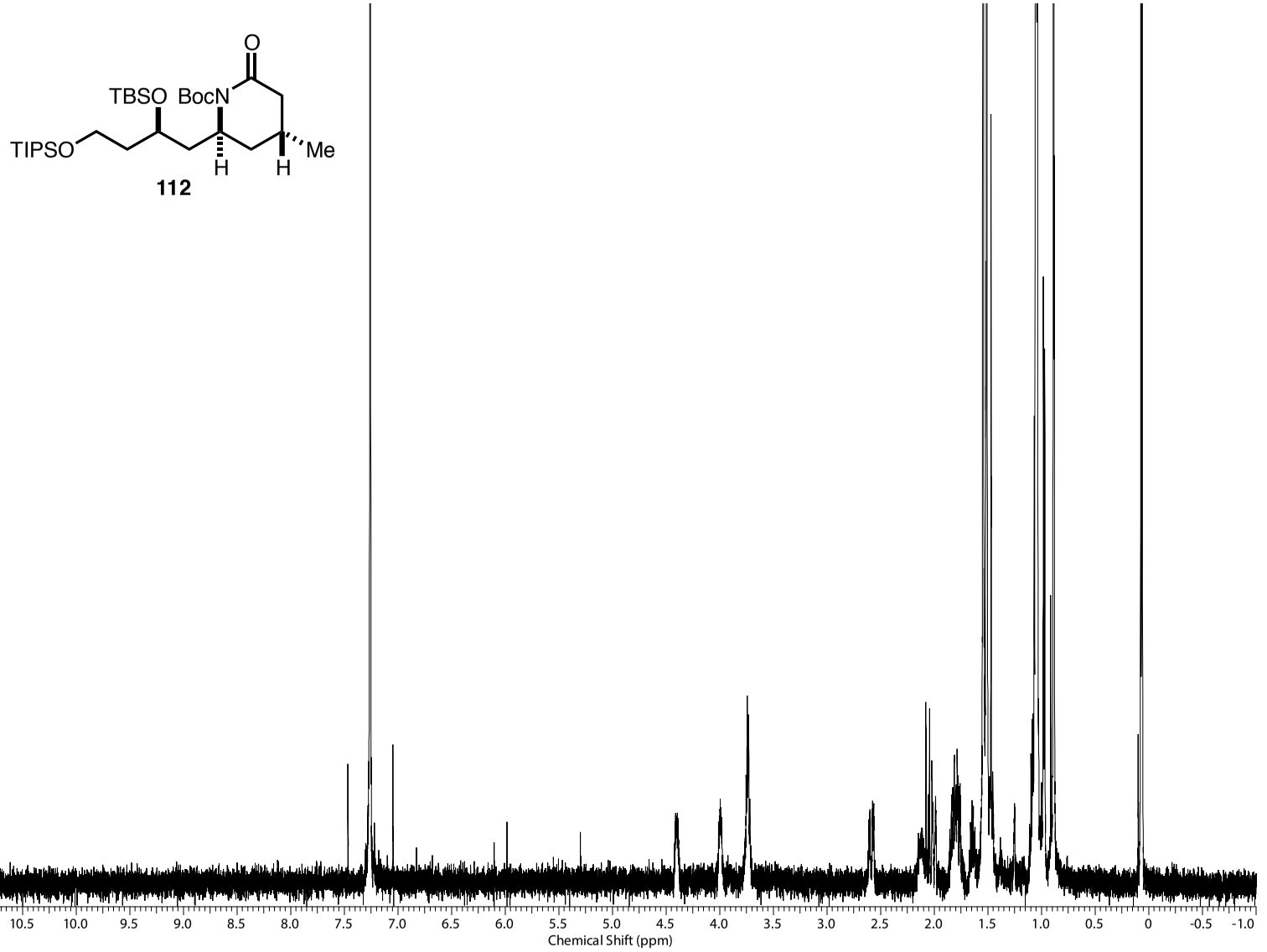
TBSO
BocN
O
TIPSO
Me
H
H
112
10.5
10.0
9.5
9.0
8.5
8.0
7.5
7.0
6.5
6.0
5.5
5.0
4.5
4.0
3.5
3.0
2.5
2.0
1.5
1.0
0.5
0
-0.5
-1.0
Chemical Shift (ppm)

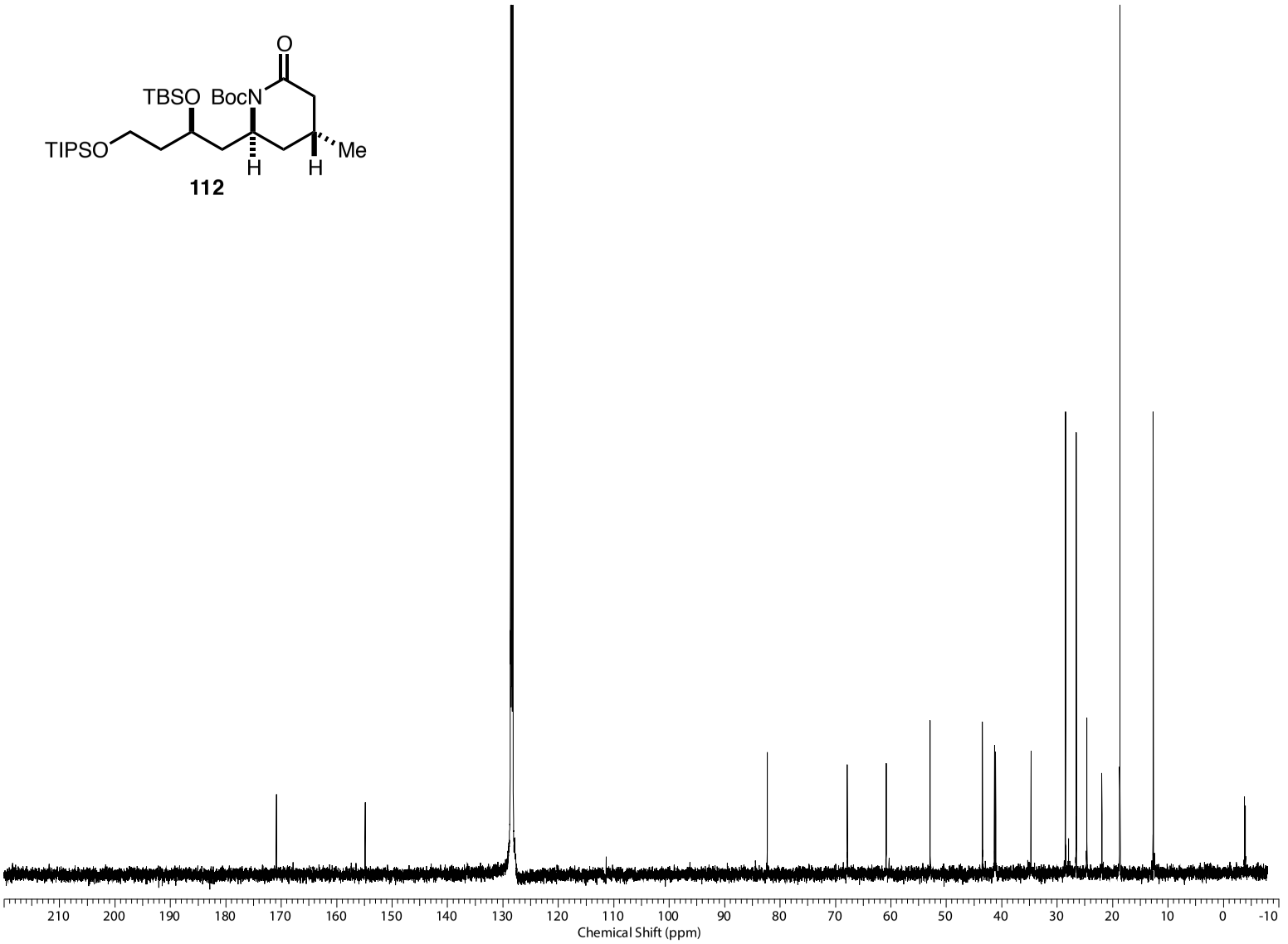
O
TBSO
BocN
TIPSO
Me
H
H
112
210
200
190
180
170
160
150
140
130
120
110
100
90
80
70
60
50
40
30
20
10
0
-10
Chemical Shift (ppm)

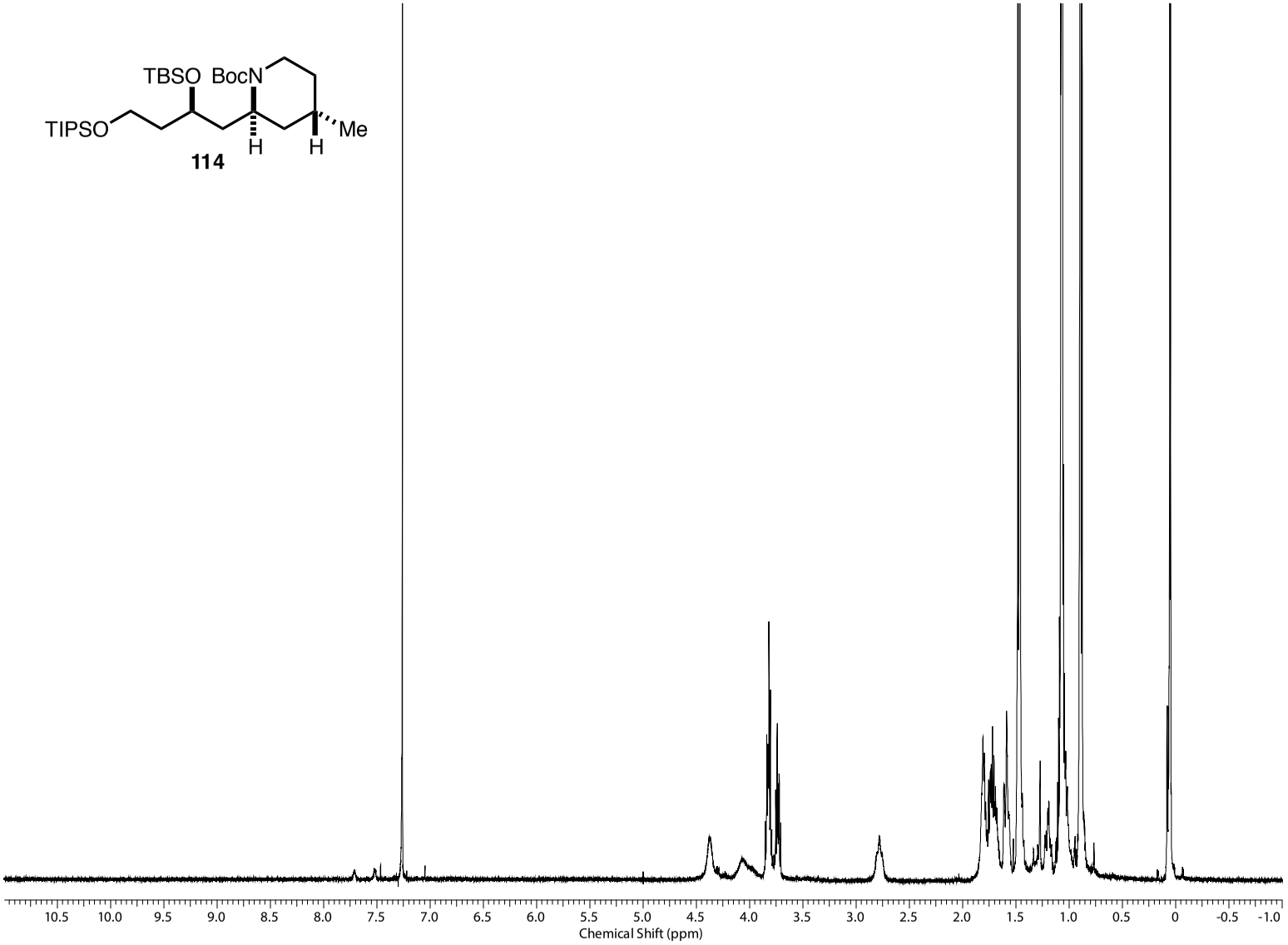
TBSO
BocN
TIPSO
Me
H
H
114
10.5
10.0
9.5
9.0
8.5
8.0
7.5
7.0
6.5
6.0
5.5
5.0
4.5
4.0
3.5
3.0
2.5
2.0
1.5
1.0
0.5
0
-0.5
-1.0
Chemical Shift (ppm)

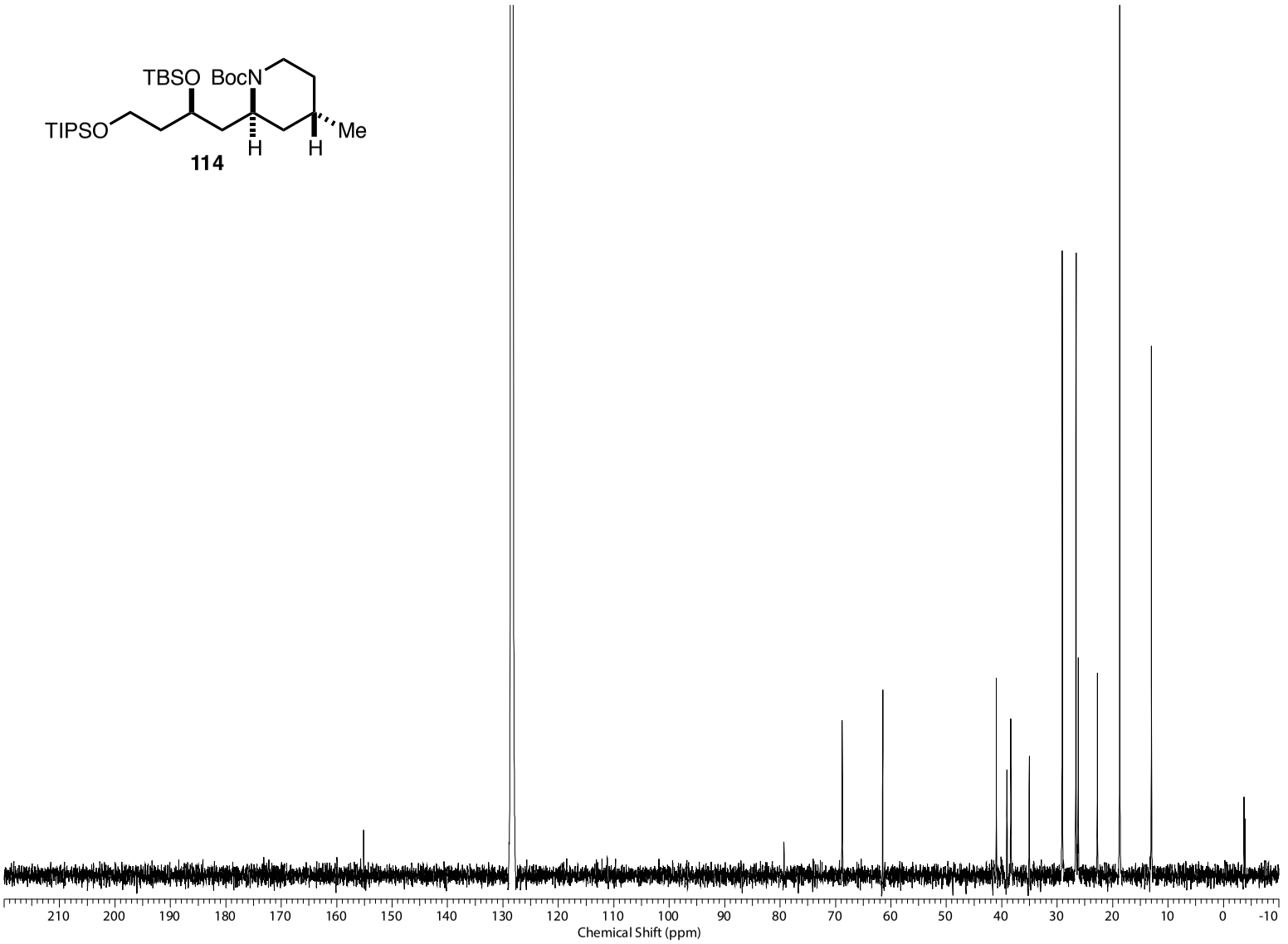
TBSO
BocN
TIPSO
Me
H
H
114
210
200
190
180
170
160
150
140
130
120
110
100
90
80
70
60
50
40
30
20
10
0
-10
Chemical Shift (ppm)

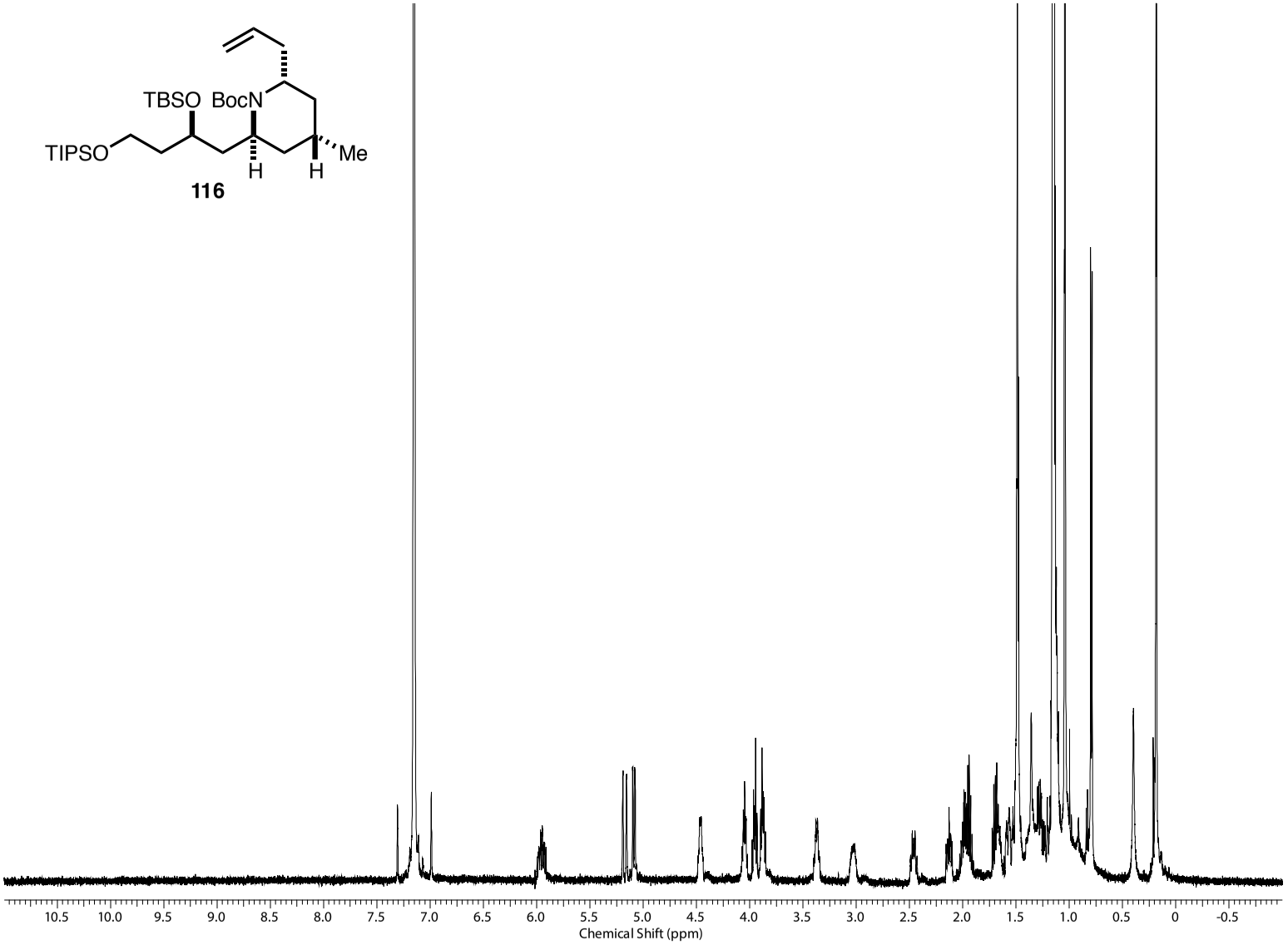
TBSO
BocN
TIPSO
Me
H
H
116
10.5
10.0
9.5
9.0
8.5
8.0
7.5
7.0
6.5
6.0
5.5
5.0
4.5
4.0
3.5
3.0
2.5
2.0
1.5
1.0
0.5
0
-0.5
Chemical Shift (ppm)

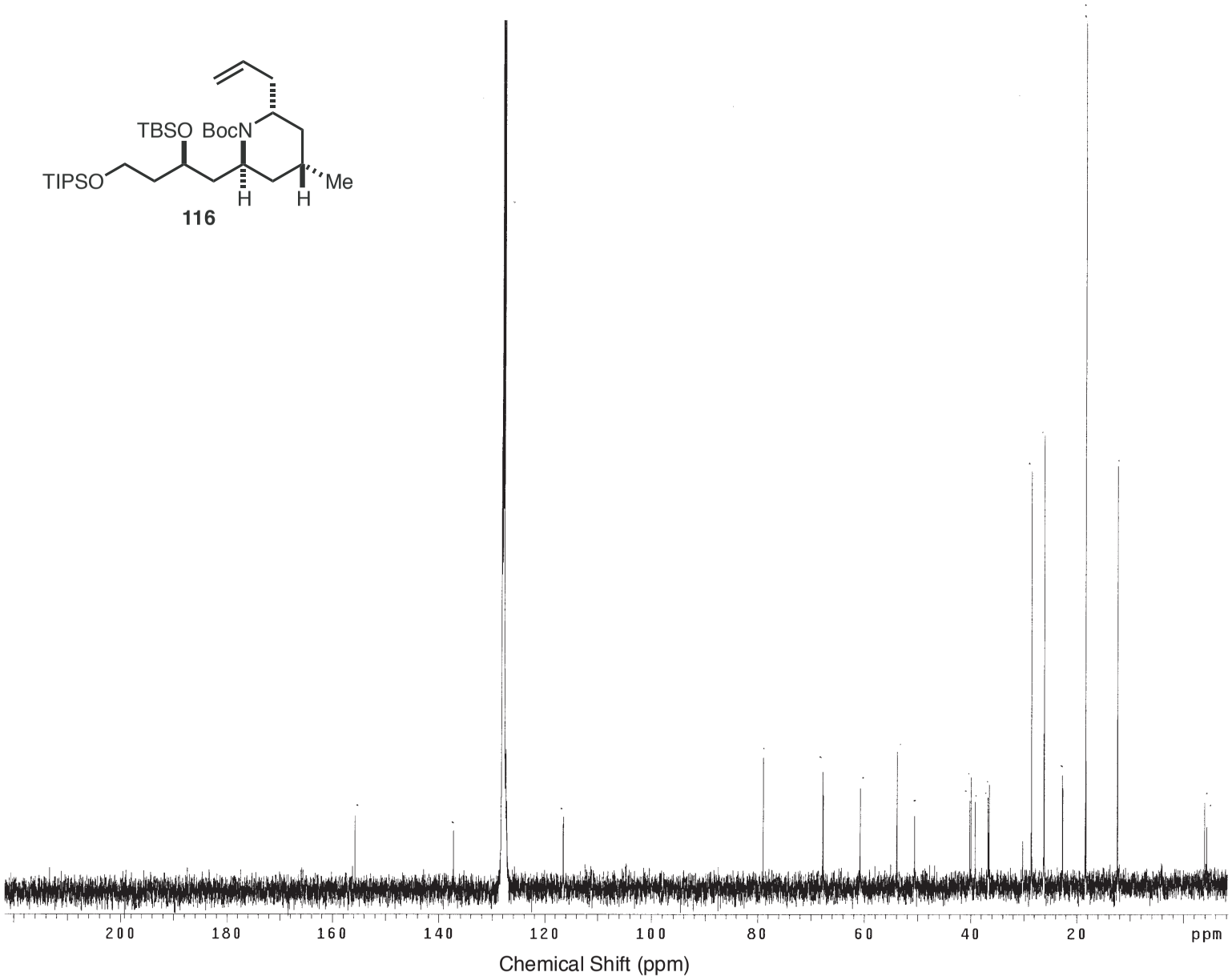
TBSO
BocN
TIPSO
Me
H
H
116
200
180
160
140
120
100
80
60
40
20
ppm
Chemical Shift (ppm)

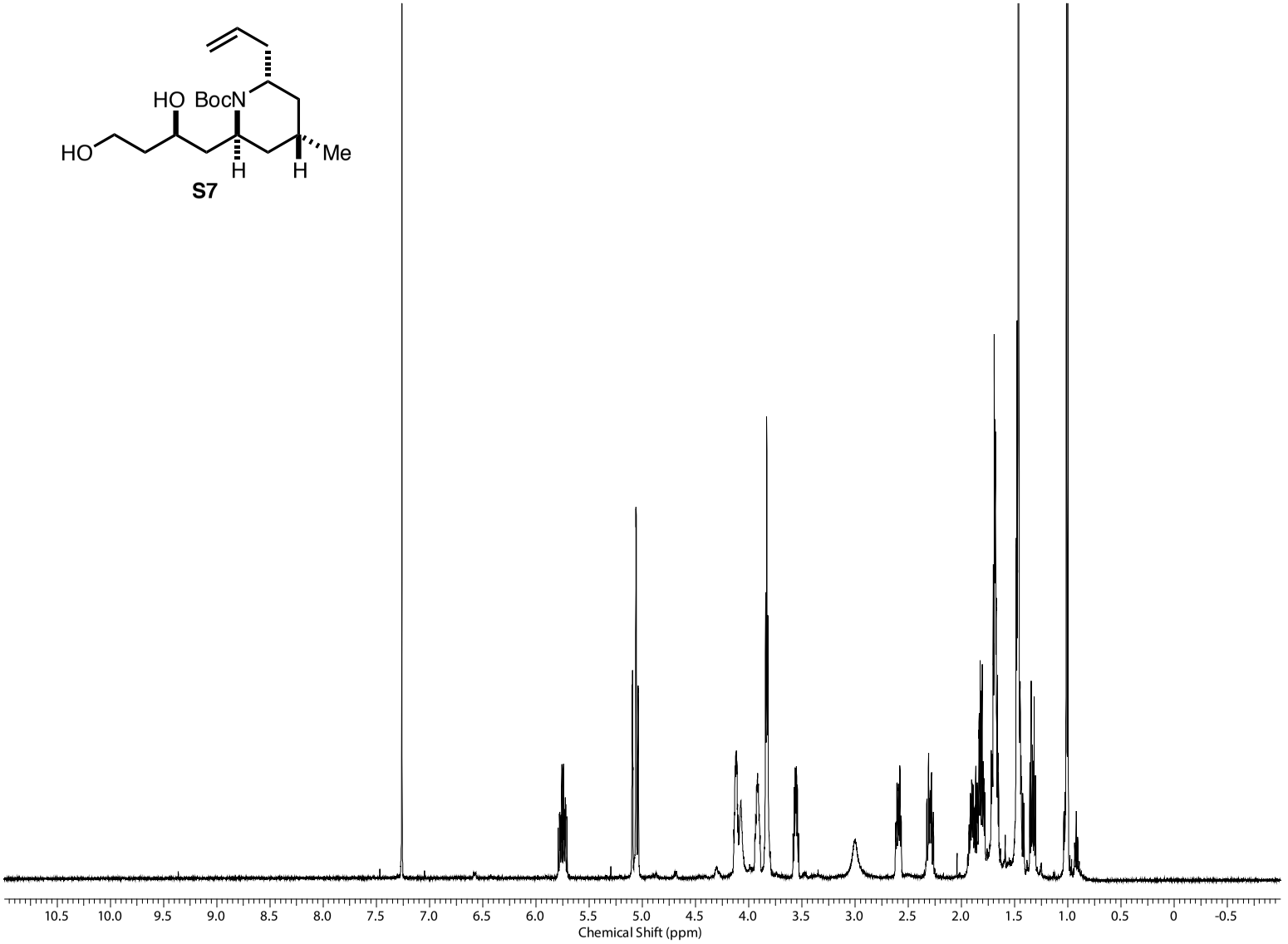
HO
BocN
HO
Me
H
H
S7
10.5
10.0
9.5
9.0
8.5
8.0
7.5
7.0
6.5
6.0
5.5
5.0
4.5
4.0
3.5
3.0
2.5
2.0
1.5
1.0
0.5
0
-0.5
Chemical Shift (ppm)

HO
HO
BocN
H
H
Me
S7
Chemical Shift (ppm)
210
200
190
180
170
160
150
140
130
120
110
100
90
80
70
60
50
40
30
20
10
0
-10

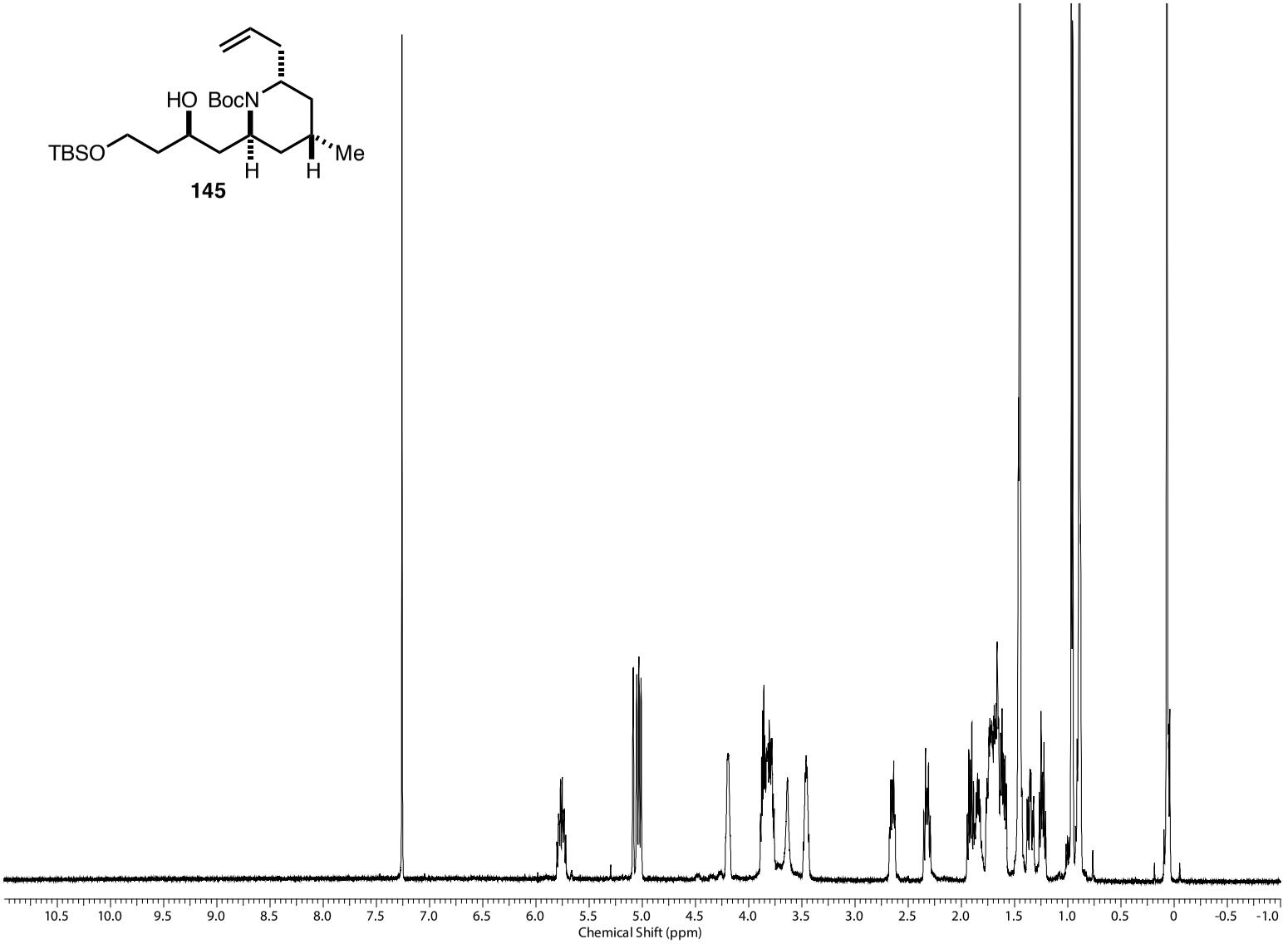
HO
BocN
TBSO
H
H
Me
145
10.5
10.0
9.5
9.0
8.5
8.0
7.5
7.0
6.5
6.0
5.5
5.0
4.5
4.0
3.5
3.0
2.5
2.0
1.5
1.0
0.5
0
-0.5
-1.0
Chemical Shift (ppm)

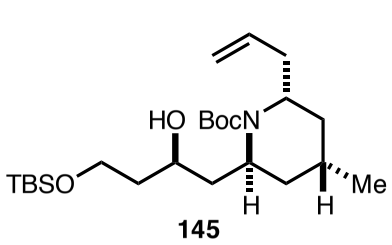
HO
BocN
TBSO
Me
H
H

145

210
200
190
180
170
160
150
140
130
120
110
100
90
80
70
60
50
40
30
20
10
0
-10
Chemical Shift (ppm)

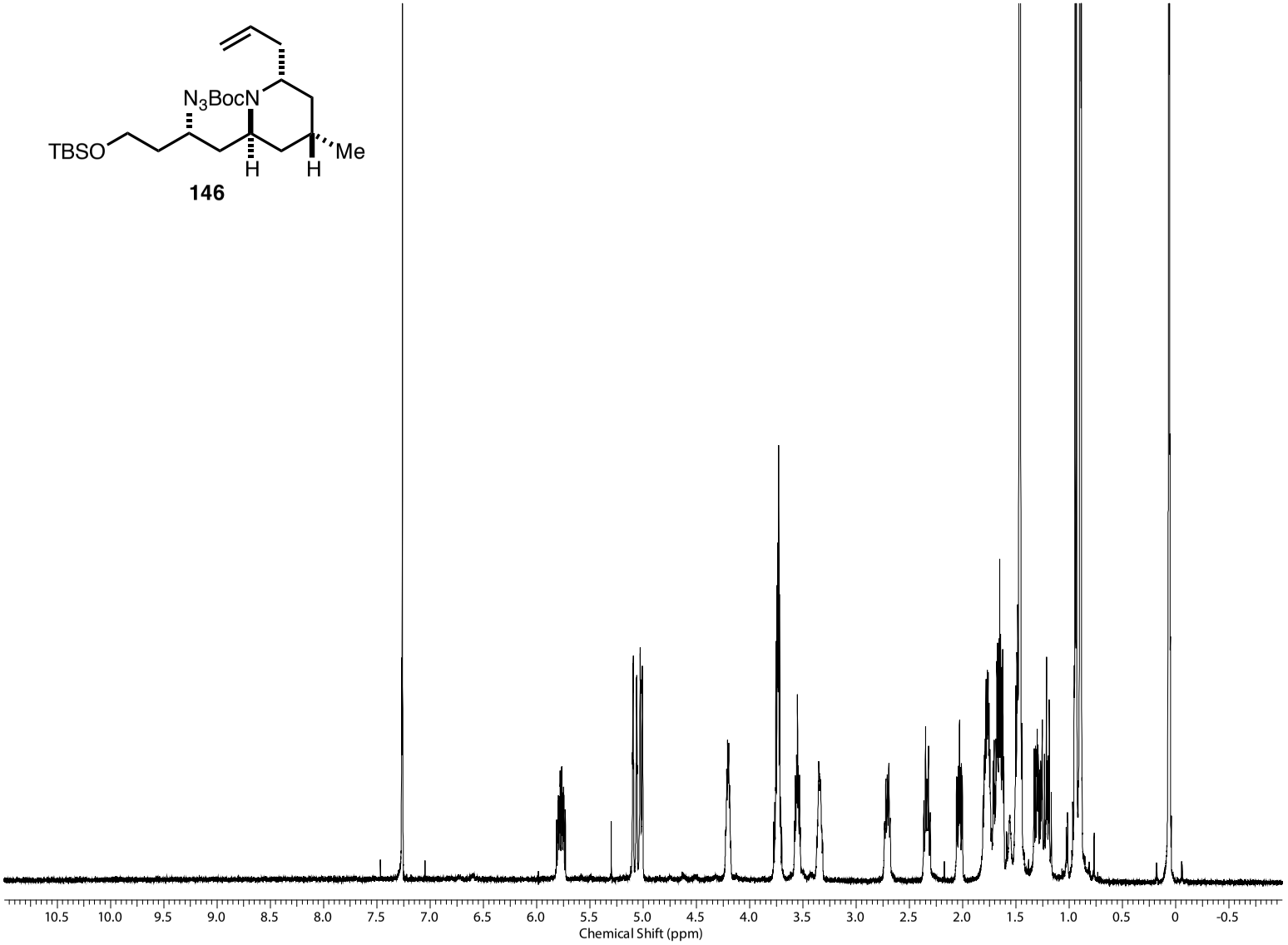
N3BocN
TBSO
Me
H
H
146
10.5
10.0
9.5
9.0
8.5
8.0
7.5
7.0
6.5
6.0
5.5
5.0
4.5
4.0
3.5
3.0
2.5
2.0
1.5
1.0
0.5
0
-0.5
Chemical Shift (ppm)

TBSO
N3BocN
H
H
Me
146
Chemical Shift (ppm)
210
200
190
180
170
160
150
140
130
120
110
100
90
80
70
60
50
40
30
20
10
0
-10

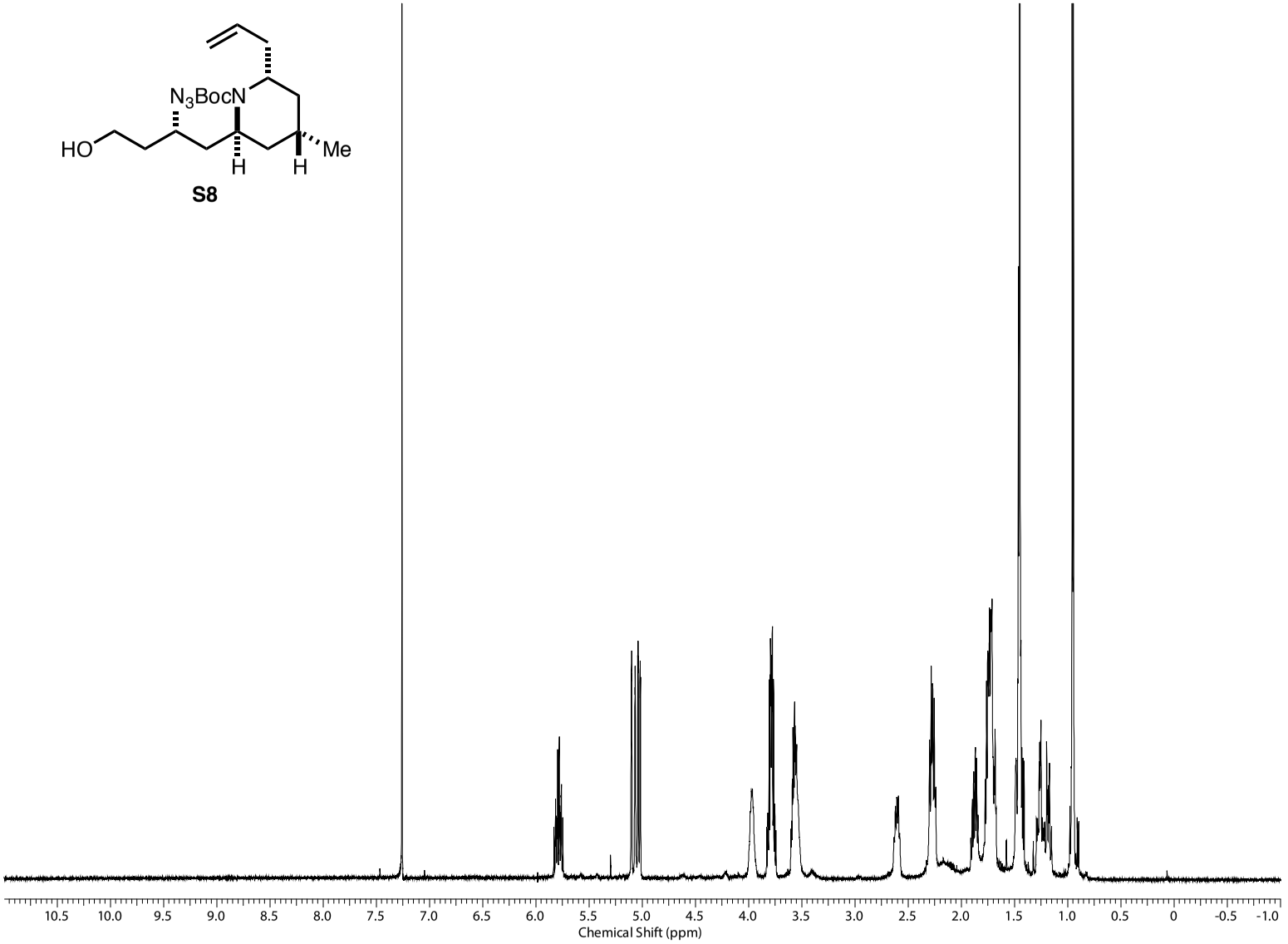
N3BocN
HO
H
H
Me
S8
10.5
10.0
9.5
9.0
8.5
8.0
7.5
7.0
6.5
6.0
5.5
5.0
4.5
4.0
3.5
3.0
2.5
2.0
1.5
1.0
0.5
0
-0.5
-1.0
Chemical Shift (ppm)

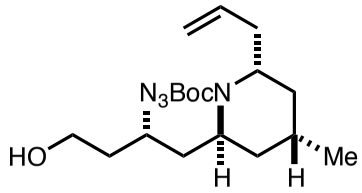
N3BocN
HO
H
H
Me

S8

210
200
190
180
170
160
150
140
130
120
110
100
90
80
70
60
50
40
30
20
10
0
-10
Chemical Shift (ppm)

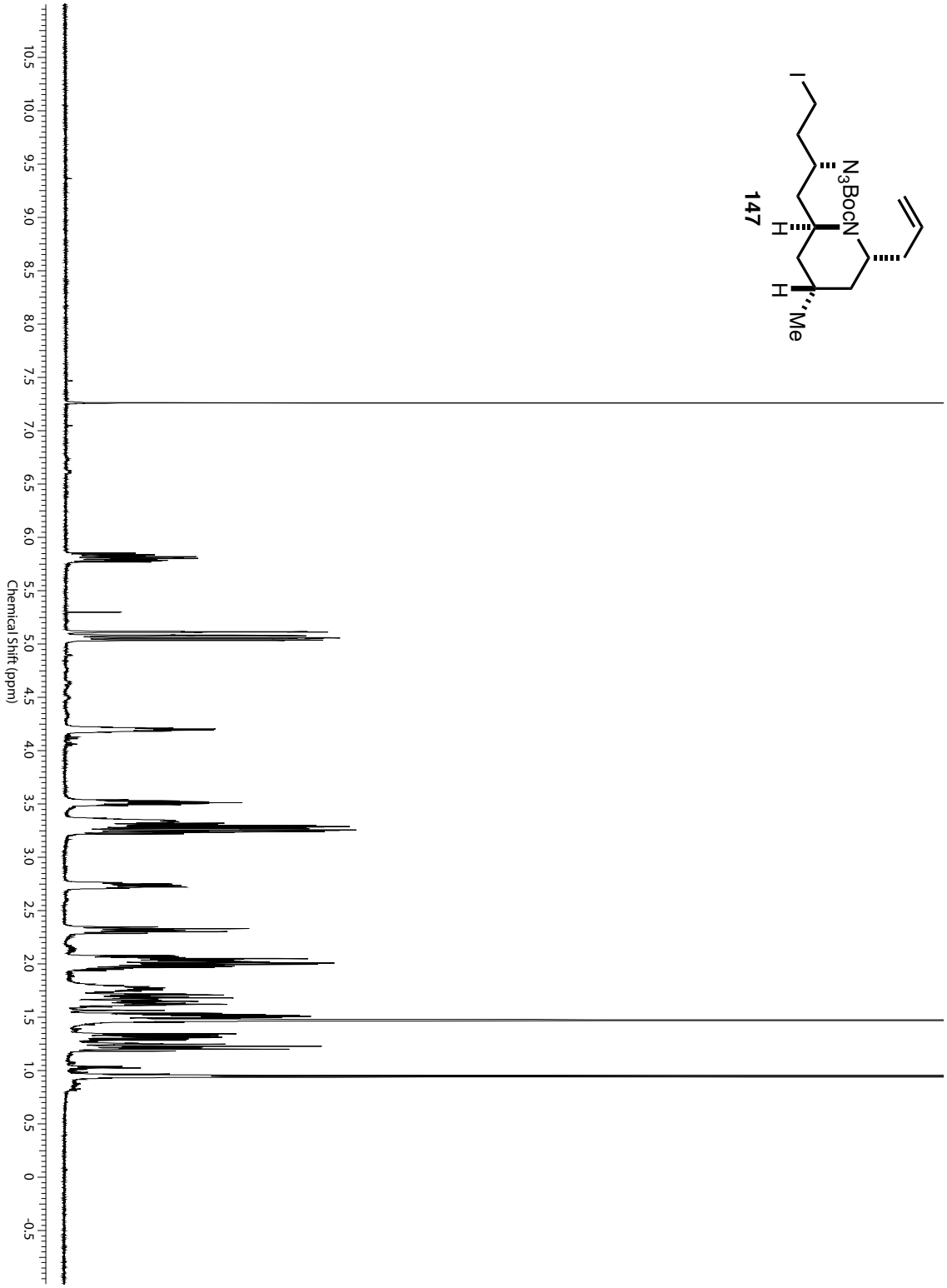
I
N3BocN
H
H
Me
147
Chemical Shift (ppm)
10.5
10.0
9.5
9.0
8.5
8.0
7.5
7.0
6.5
6.0
5.5
5.0
4.5
4.0
3.5
3.0
2.5
2.0
1.5
1.0
0.5
0
-0.5

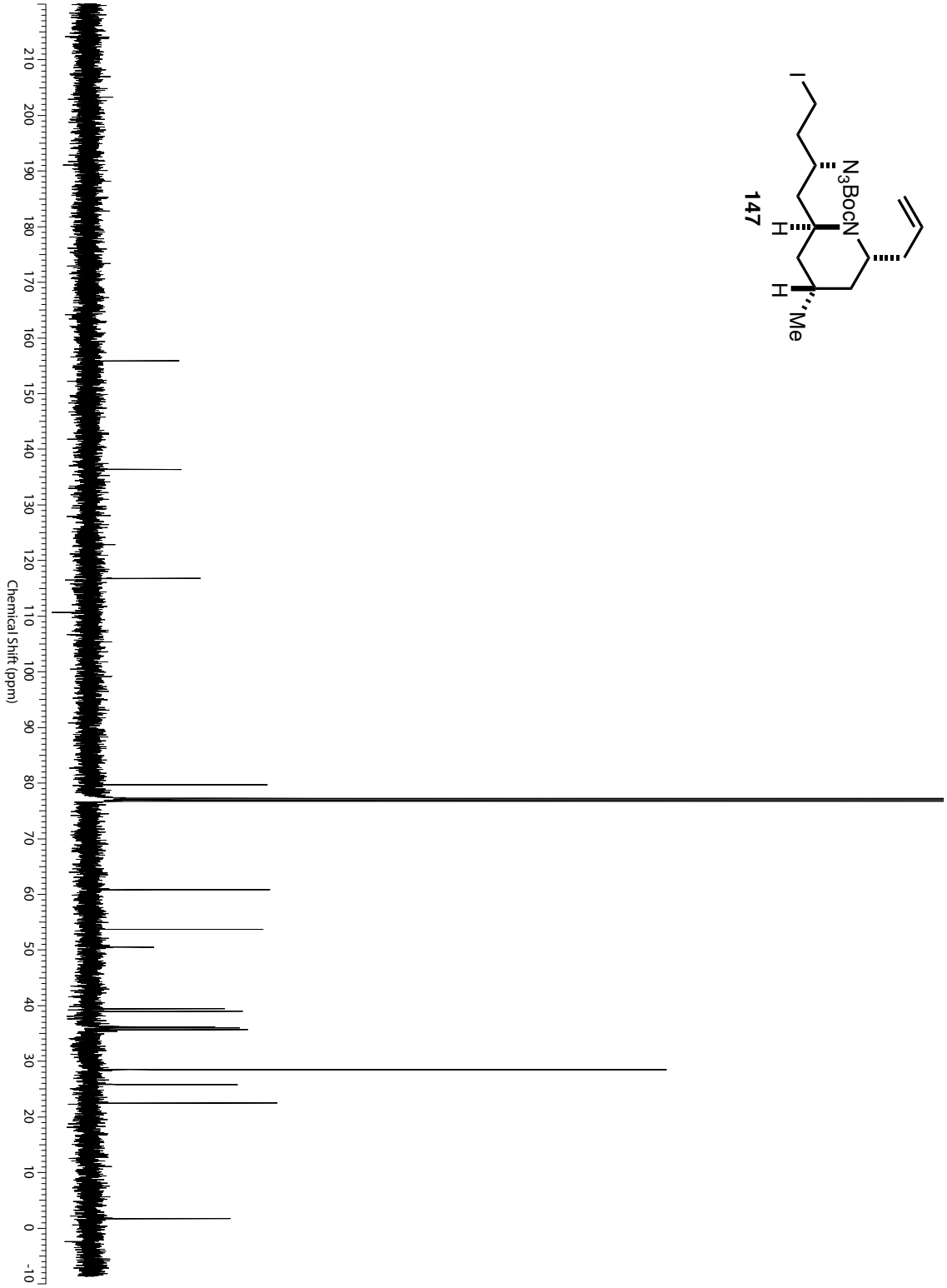
I
N3BocN
H
H
Me
147
Chemical Shift (ppm)
210
200
190
180
170
160
150
140
130
120
110
100
90
80
70
60
50
40
30
20
10
0
-10

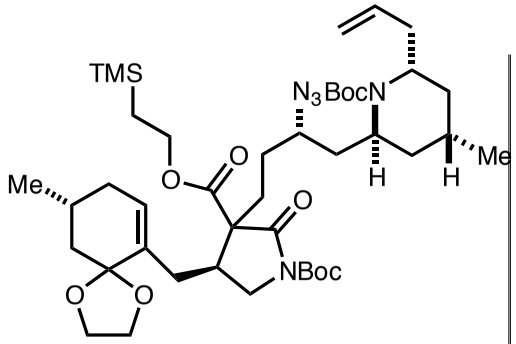
TMS
O
O
Me
O
O
O
O
N3BocN
H
H
Me
NBoc

148

10.5
10.0
9.5
9.0
8.5
8.0
7.5
7.0
6.5
6.0
5.5
5.0
4.5
4.0
3.5
3.0
2.5
2.0
1.5
1.0
0.5
0
-0.5
Chemical Shift (ppm)

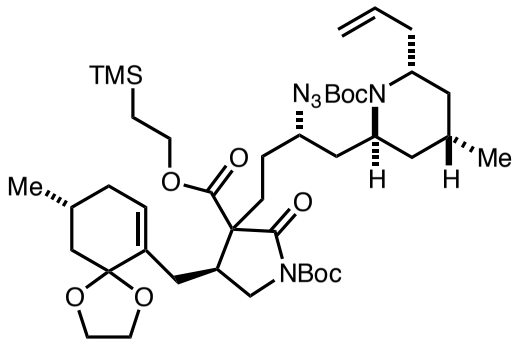
TMS
O
O
Me
O
O
O
N3BocN
H
H
Me
NBoc

148

210
200
190
180
170
160
150
140
130
120
110
100
90
80
70
60
50
40
30
20
10
0
-10
Chemical Shift (ppm)

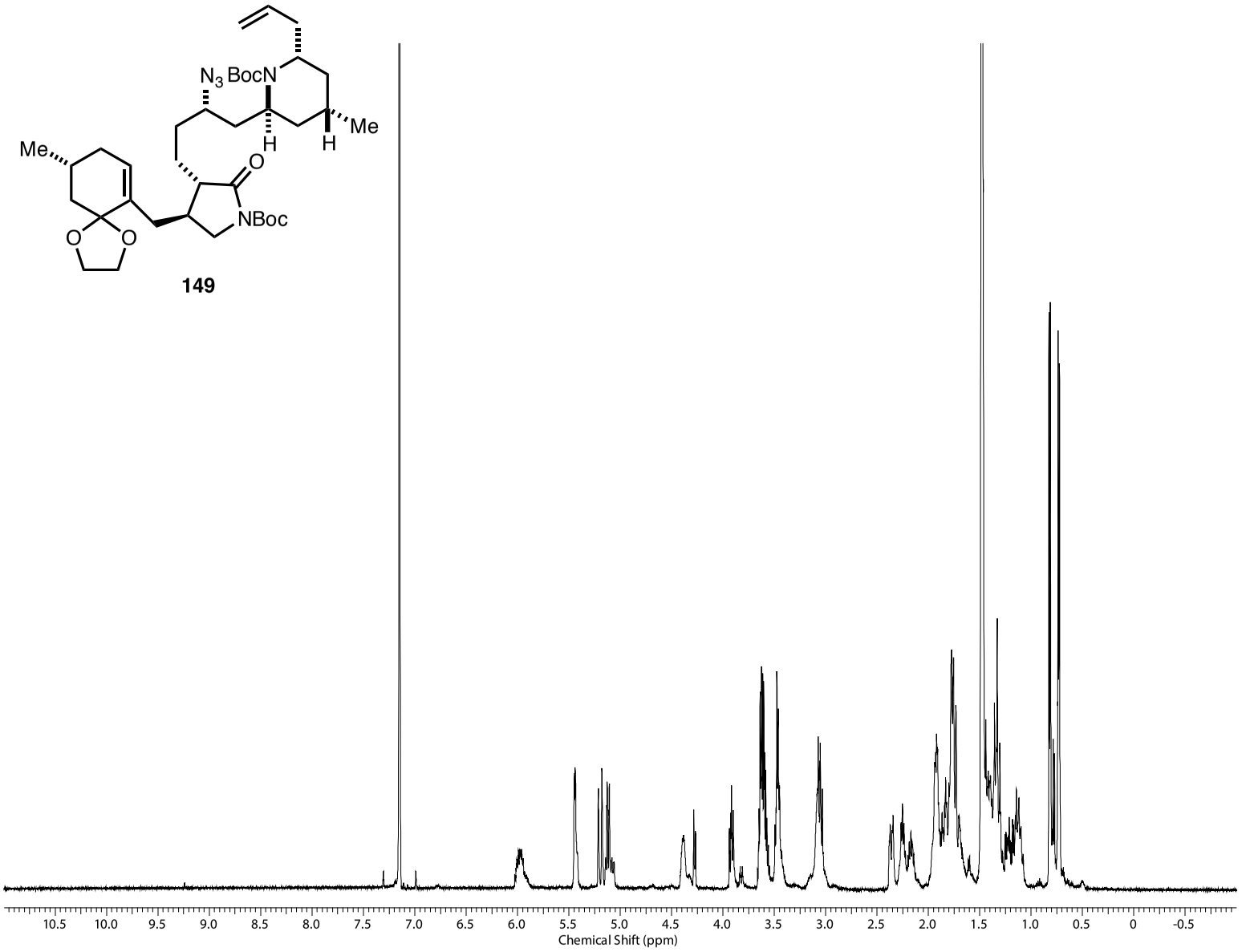
N3 BocN
Me
H
H
Me
O
NBoc
O
O
149
10.5
10.0
9.5
9.0
8.5
8.0
7.5
7.0
6.5
6.0
5.5
5.0
4.5
4.0
3.5
3.0
2.5
2.0
1.5
1.0
0.5
0
-0.5
Chemical Shift (ppm)

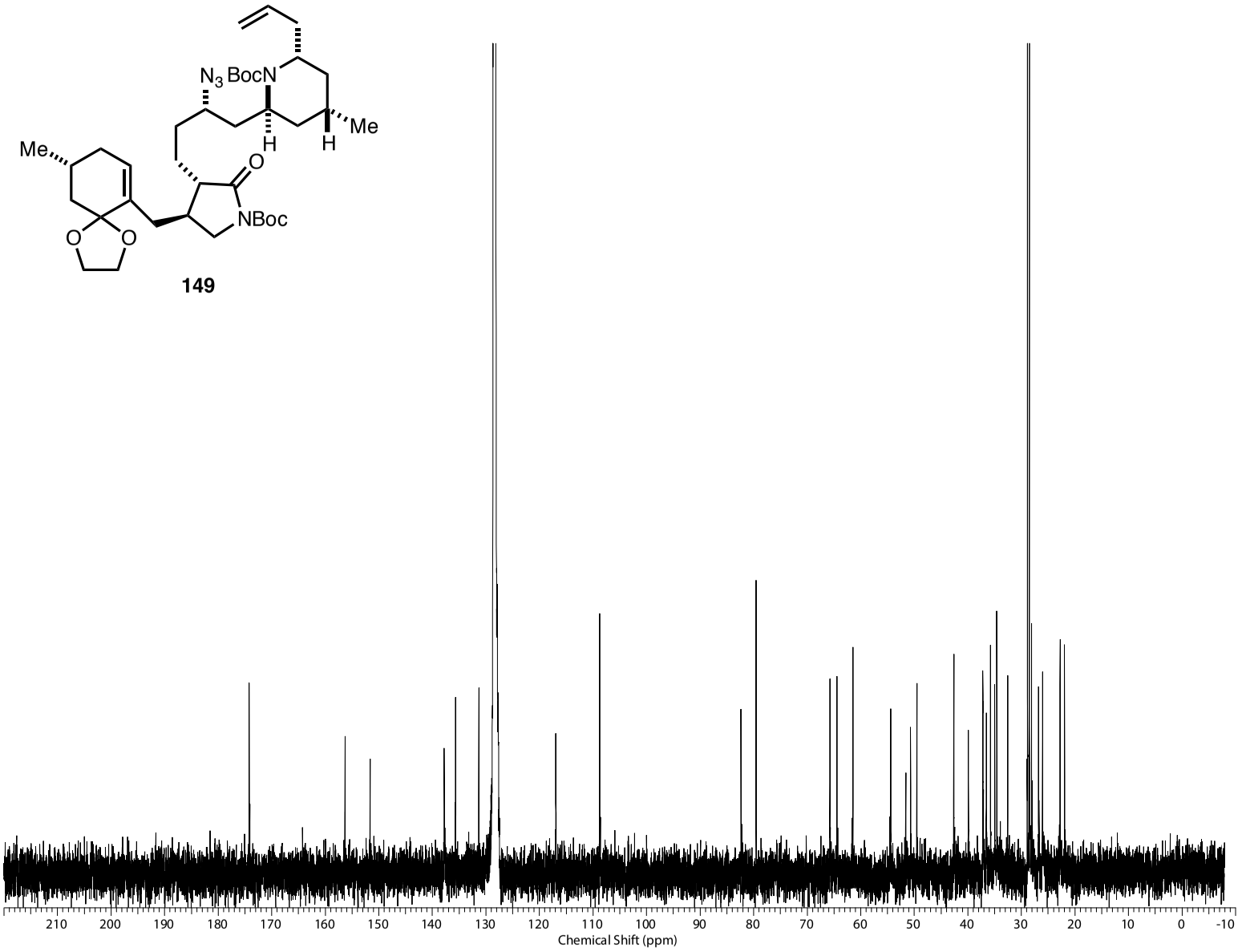
N3 BocN
Me
H
H
Me
O
NBoc
O
O
210
200
190
180
170
160
150
140
130
120
110
100
90
80
70
60
50
40
30
20
10
0
-10
Chemical Shift (ppm)

149

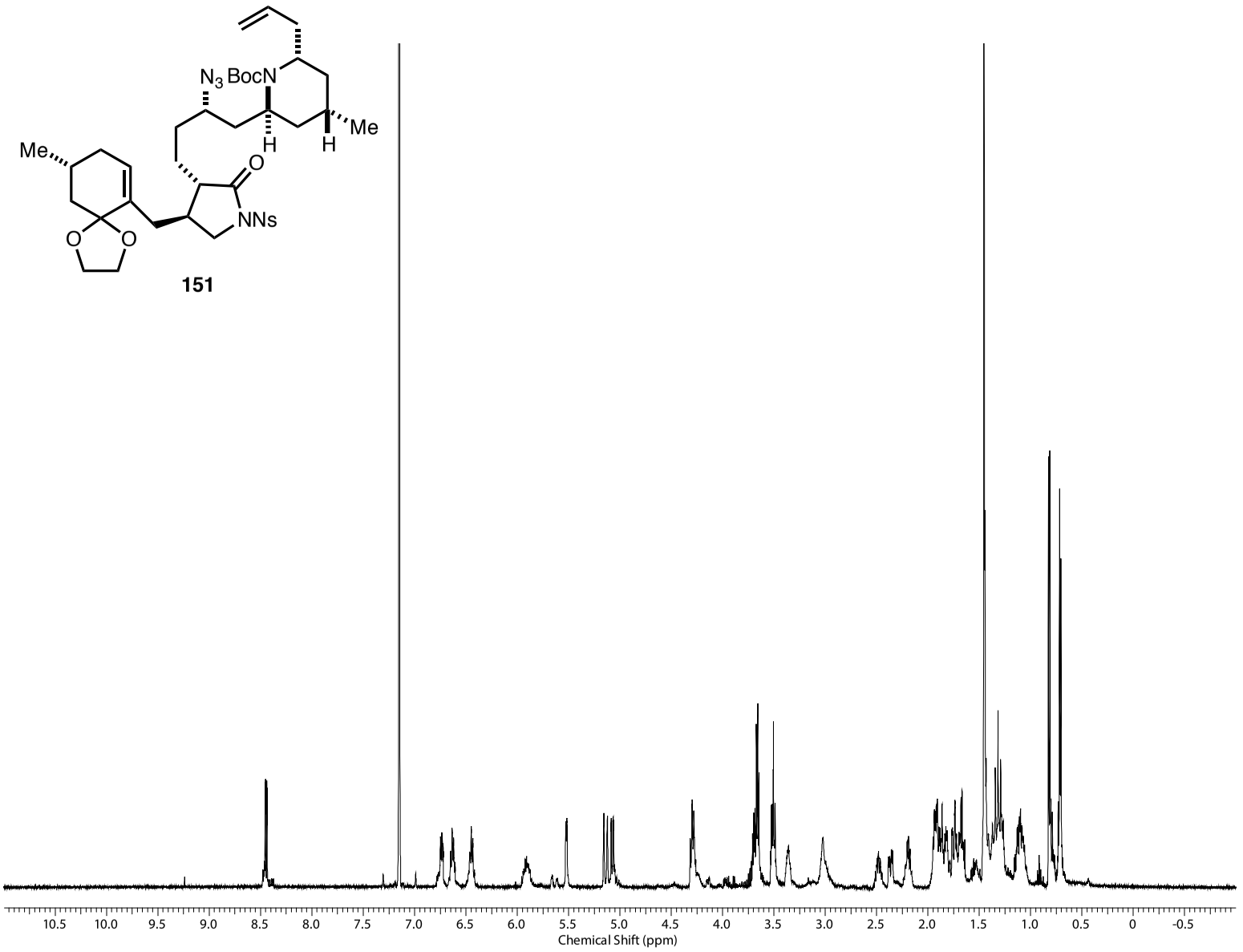
N3 BocN
Me
H
H
Me
O
NNs
O
O
151
10.5
10.0
9.5
9.0
8.5
8.0
7.5
7.0
6.5
6.0
5.5
5.0
4.5
4.0
3.5
3.0
2.5
2.0
1.5
1.0
0.5
0
-0.5
Chemical Shift (ppm)

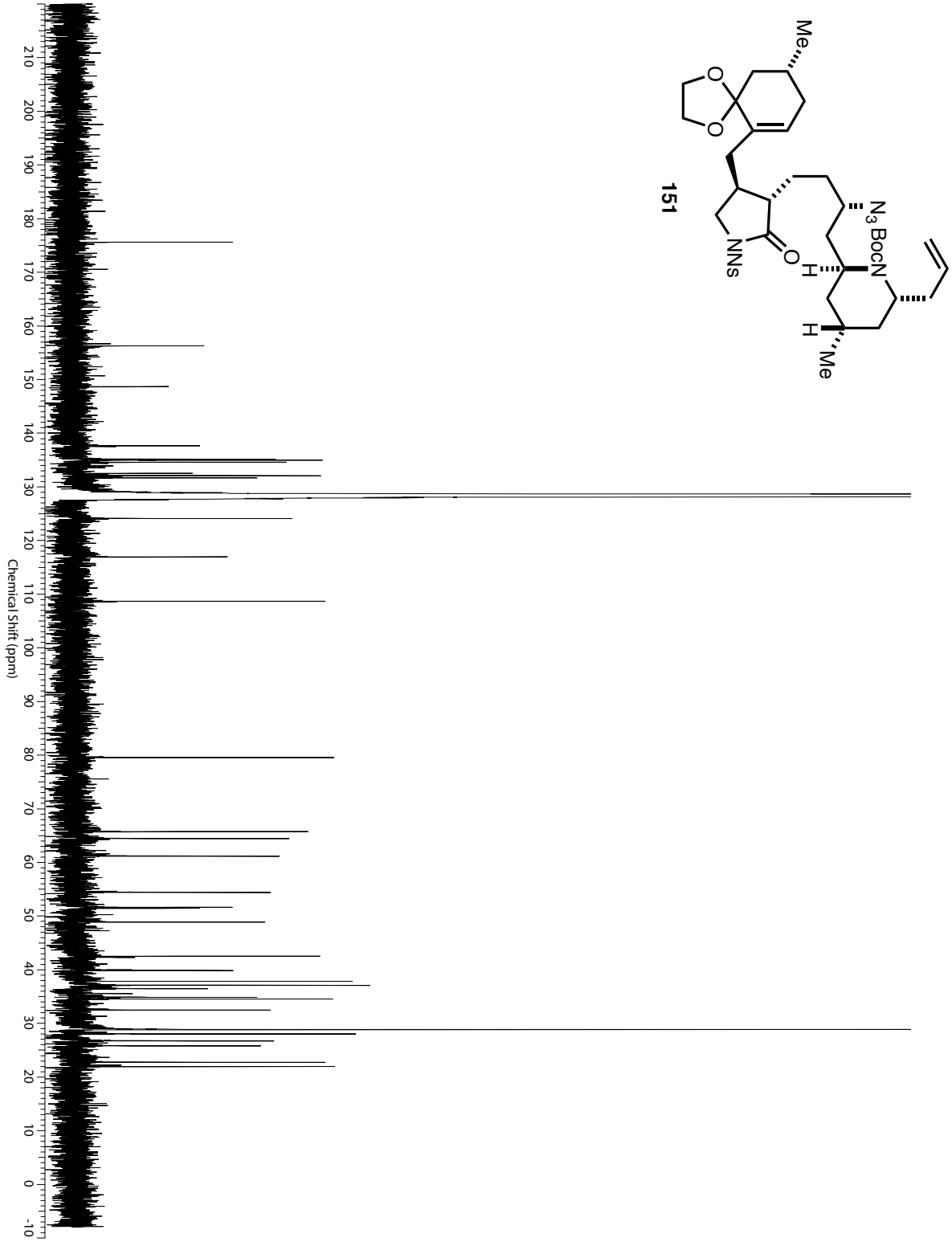
Me
O
O
N3 BocN
NNs
O
H
H
Me
151
Chemical Shift (ppm)
210
200
190
180
170
160
150
140
130
120
110
100
90
80
70
60
50
40
30
20
10
0
-10

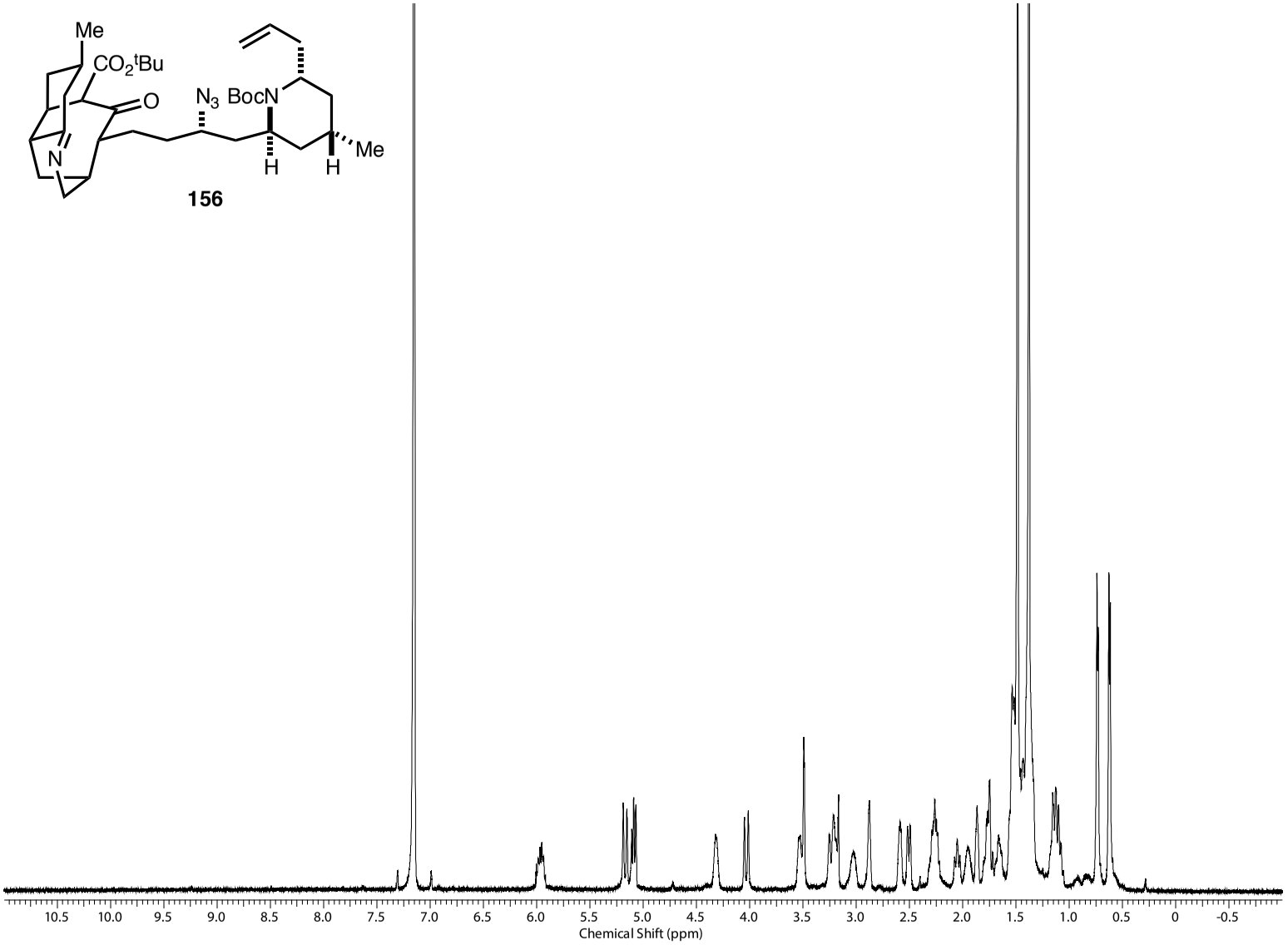
Me
CO2tBu
O
N3 BocN
N
H
H
Me
156
10.5 10.0 9.5 9.0 8.5 8.0 7.5 7.0 6.5 6.0 5.5 5.0 4.5 4.0 3.5 3.0 2.5 2.0 1.5 1.0 0.5 0 -0.5
Chemical Shift (ppm)

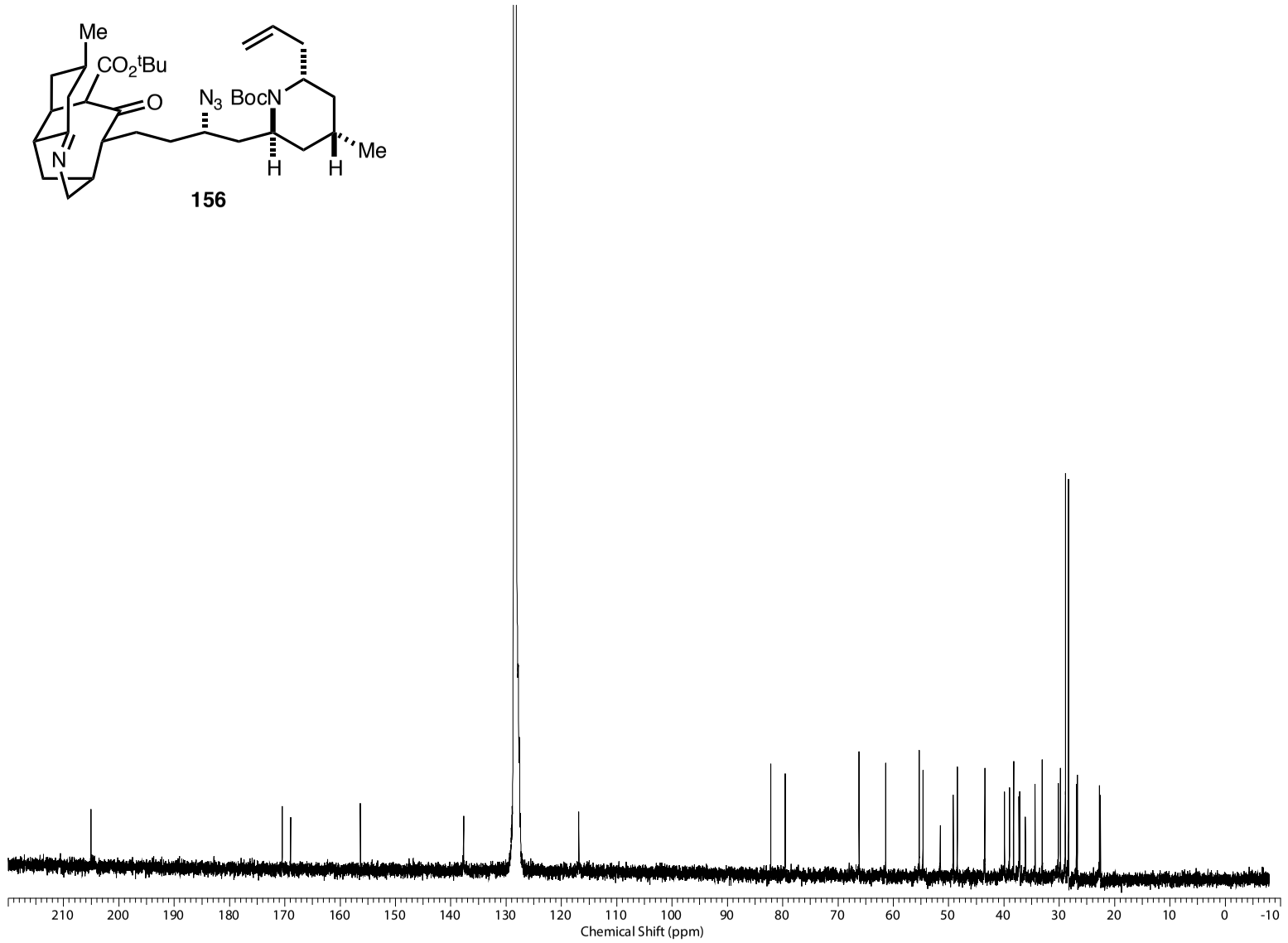
Me
CO2tBu
O
N3
BocN
N
H
H
Me
156
210
200
190
180
170
160
150
140
130
120
110
100
90
80
70
60
50
40
30
20
10
0
-10
Chemical Shift (ppm)

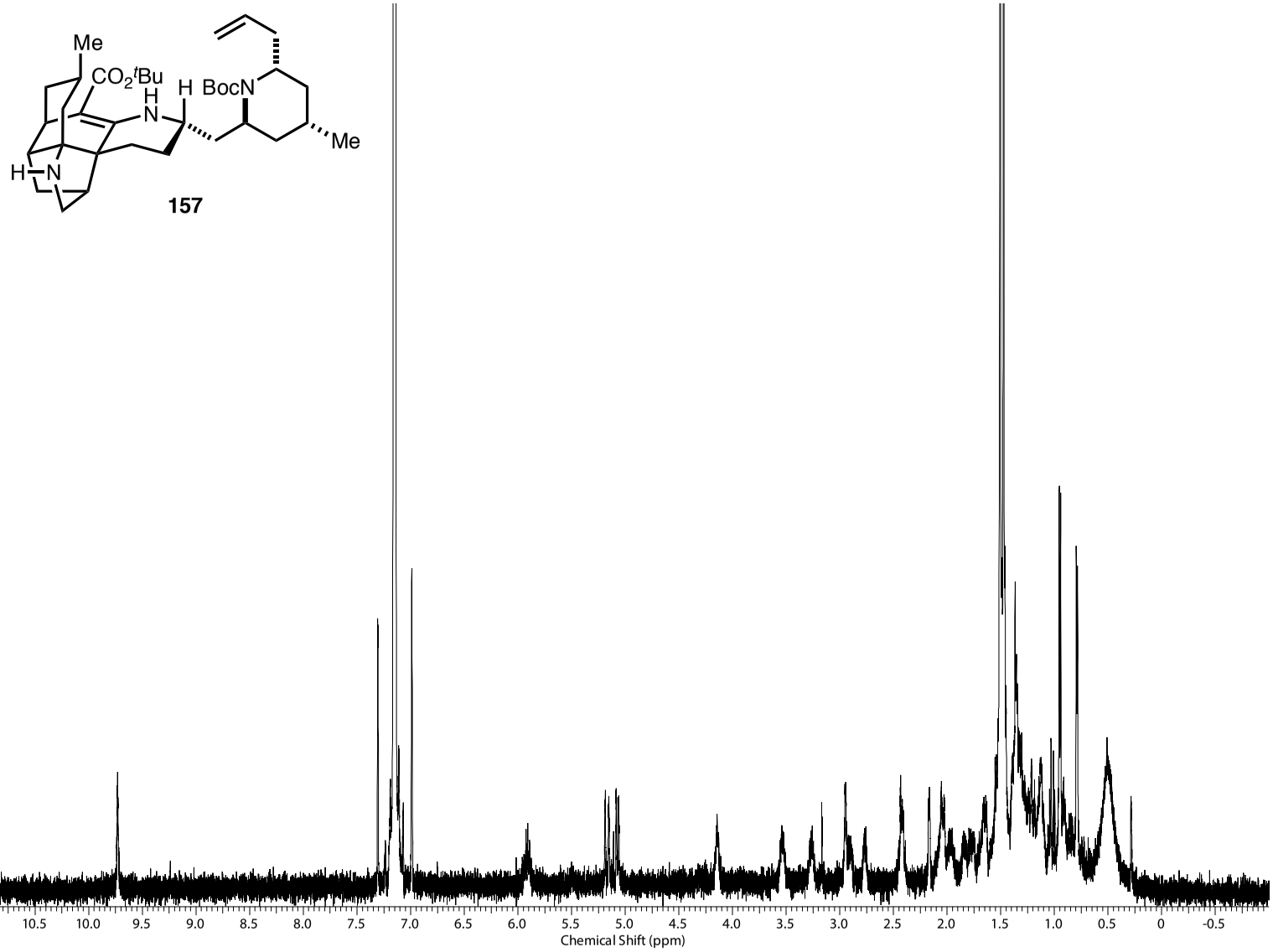
Me
CO2tBu
H
N
H BocN
Me
H
N
157
10.5
10.0
9.5
9.0
8.5
8.0
7.5
7.0
6.5
6.0
5.5
5.0
4.5
4.0
3.5
3.0
2.5
2.0
1.5
1.0
0.5
0
-0.5
Chemical Shift (ppm)

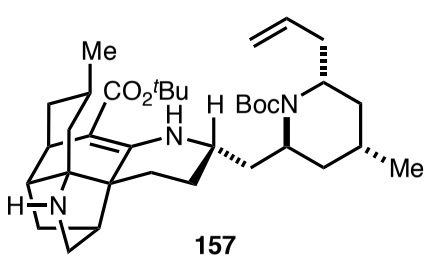
Me
CO2tBu
H
N
H BocN
Me
H
N

157

210
200
190
180
170
160
150
140
130
120
110
100
90
80
70
60
50
40
30
20
10
0
-10
Chemical Shift (ppm)

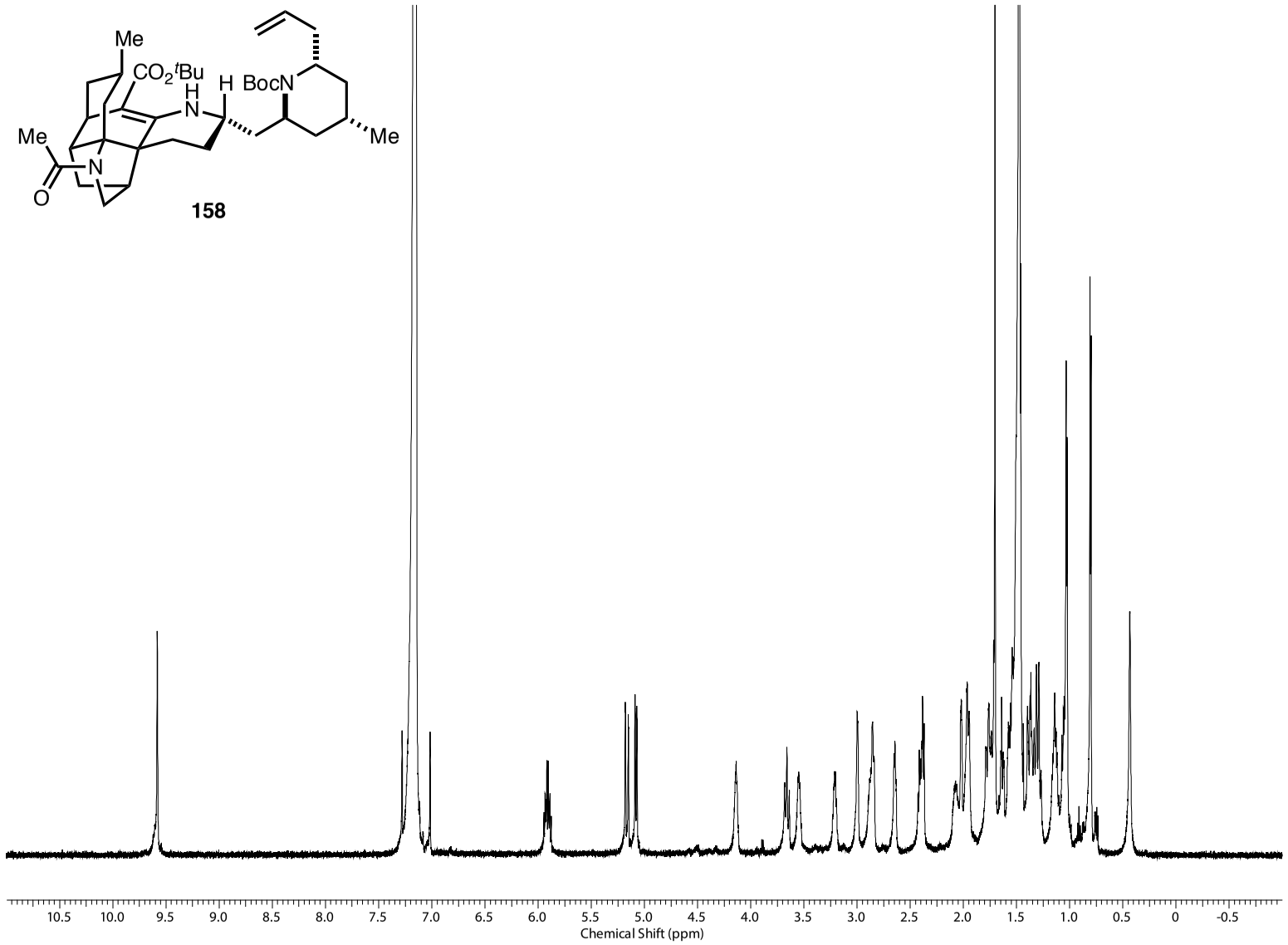
Me
CO2tBu
H
N
H BocN
Me
Me
N
O
158
10.5
10.0
9.5
9.0
8.5
8.0
7.5
7.0
6.5
6.0
5.5
5.0
4.5
4.0
3.5
3.0
2.5
2.0
1.5
1.0
0.5
0
-0.5
Chemical Shift (ppm)

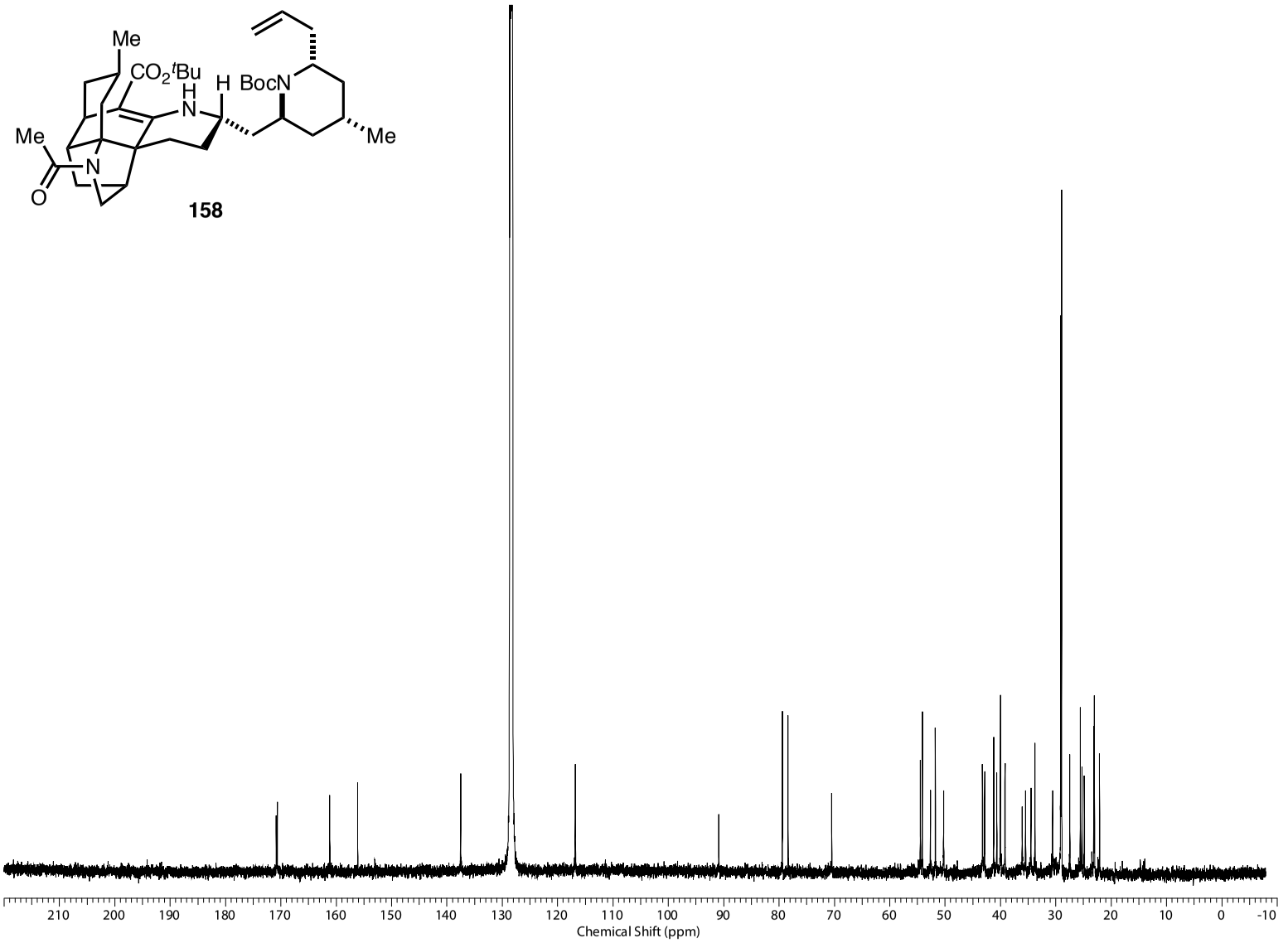
Me
CO2tBu
H
N
H BocN
Me
Me
N
O
158
210 200 190 180 170 160 150 140 130 120 110 100 90 80 70 60 50 40 30 20 10 0 -10
Chemical Shift (ppm)

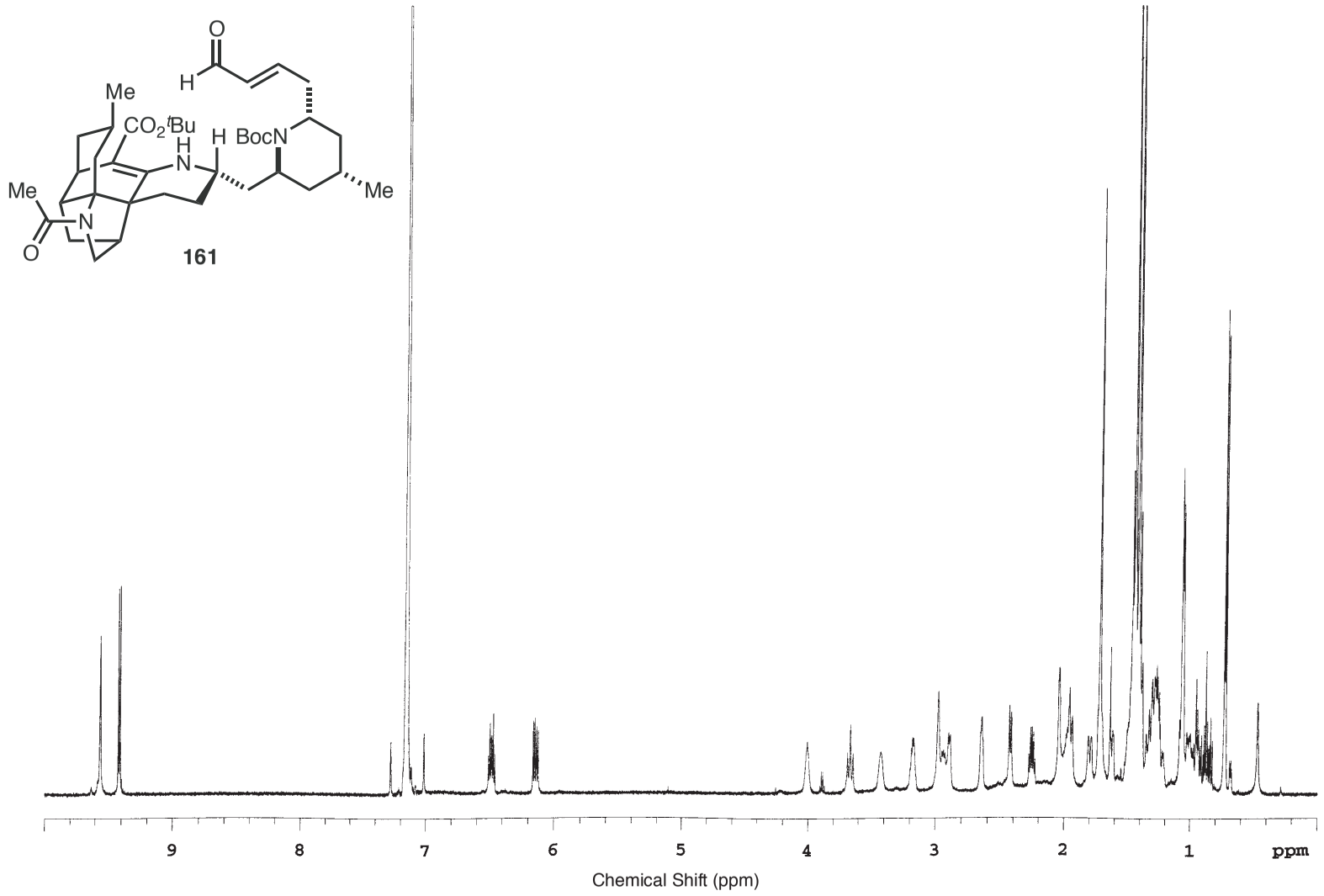
O
H
Me
CO2tBu
H
N
H BocN
Me
Me
N
O
161
9
8
7
6
5
4
3
2
1
ppm
Chemical Shift (ppm)

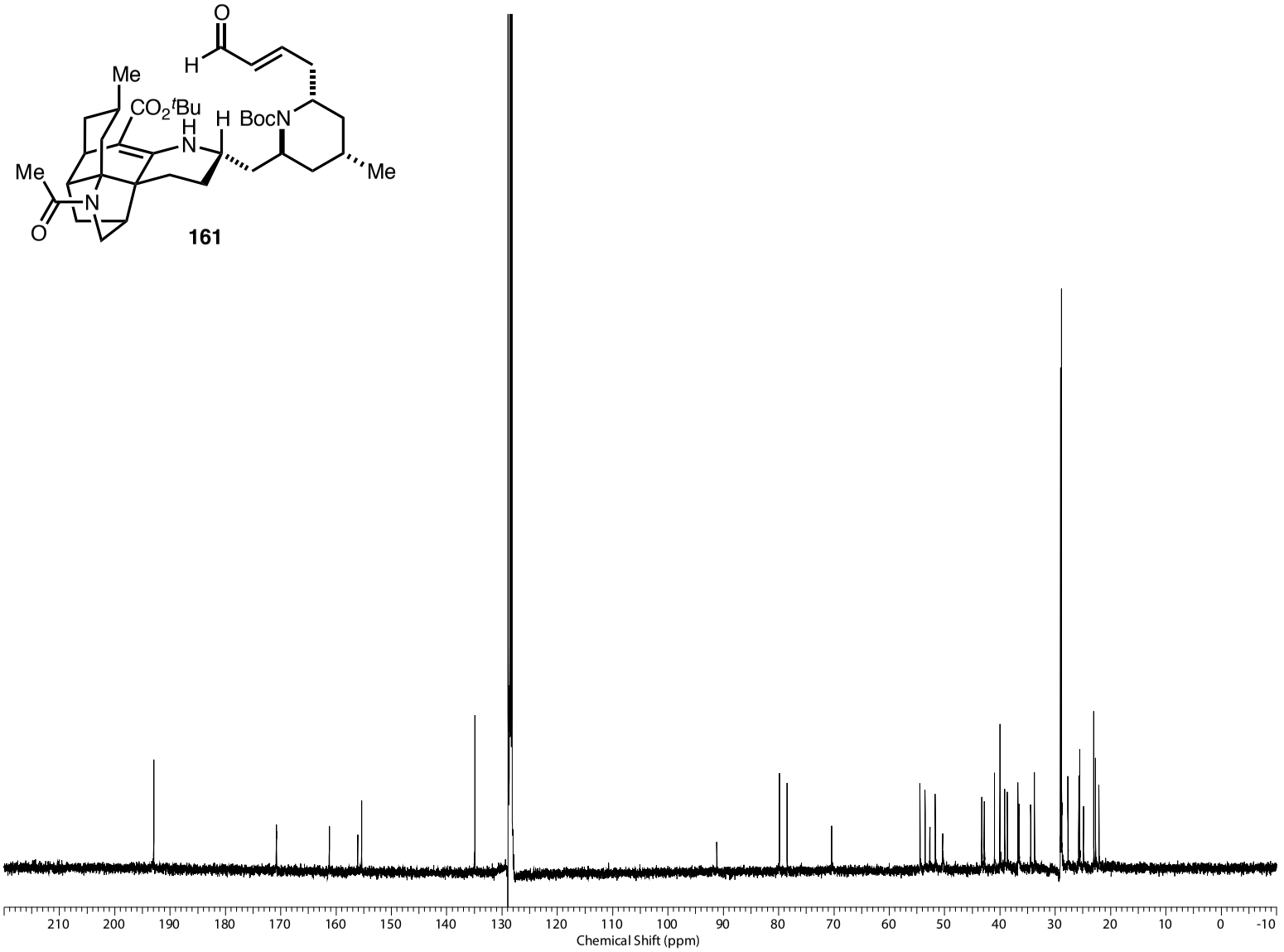
O
H
Me
CO2tBu
H
N
H
BocN
Me
Me
N
O
161
210
200
190
180
170
160
150
140
130
120
110
100
90
80
70
60
50
40
30
20
10
0
-10
Chemical Shift (ppm)

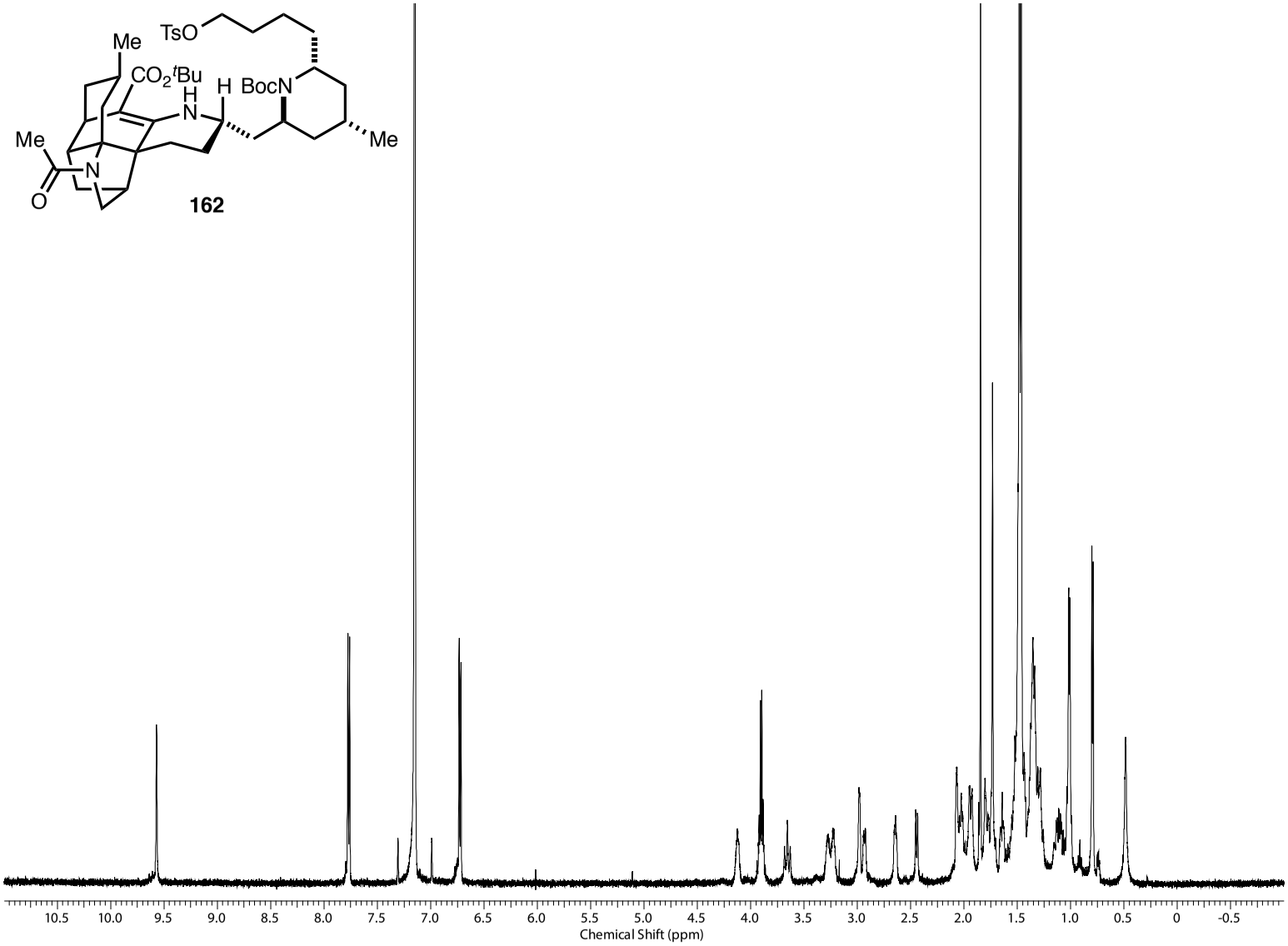
TsO
Me
CO2tBu
H
N
H
BocN
Me
Me
N
O
162
10.5
10.0
9.5
9.0
8.5
8.0
7.5
7.0
6.5
6.0
5.5
5.0
4.5
4.0
3.5
3.0
2.5
2.0
1.5
1.0
0.5
0
-0.5
Chemical Shift (ppm)

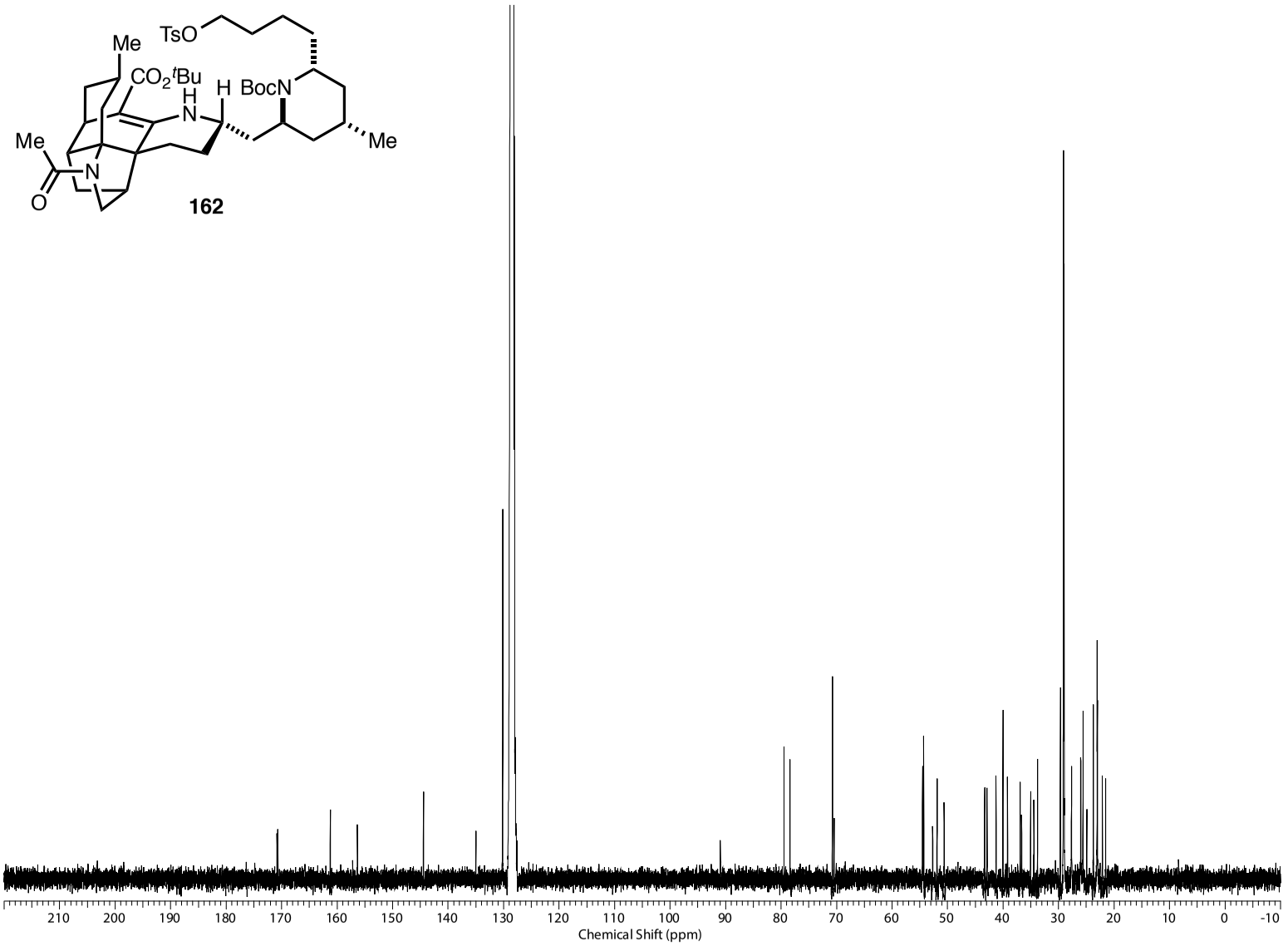
TsO
Me
CO2tBu
H
N
H
BocN
Me
Me
N
O
162
210
200
190
180
170
160
150
140
130
120
110
100
90
80
70
60
50
40
30
20
10
0
-10
Chemical Shift (ppm)

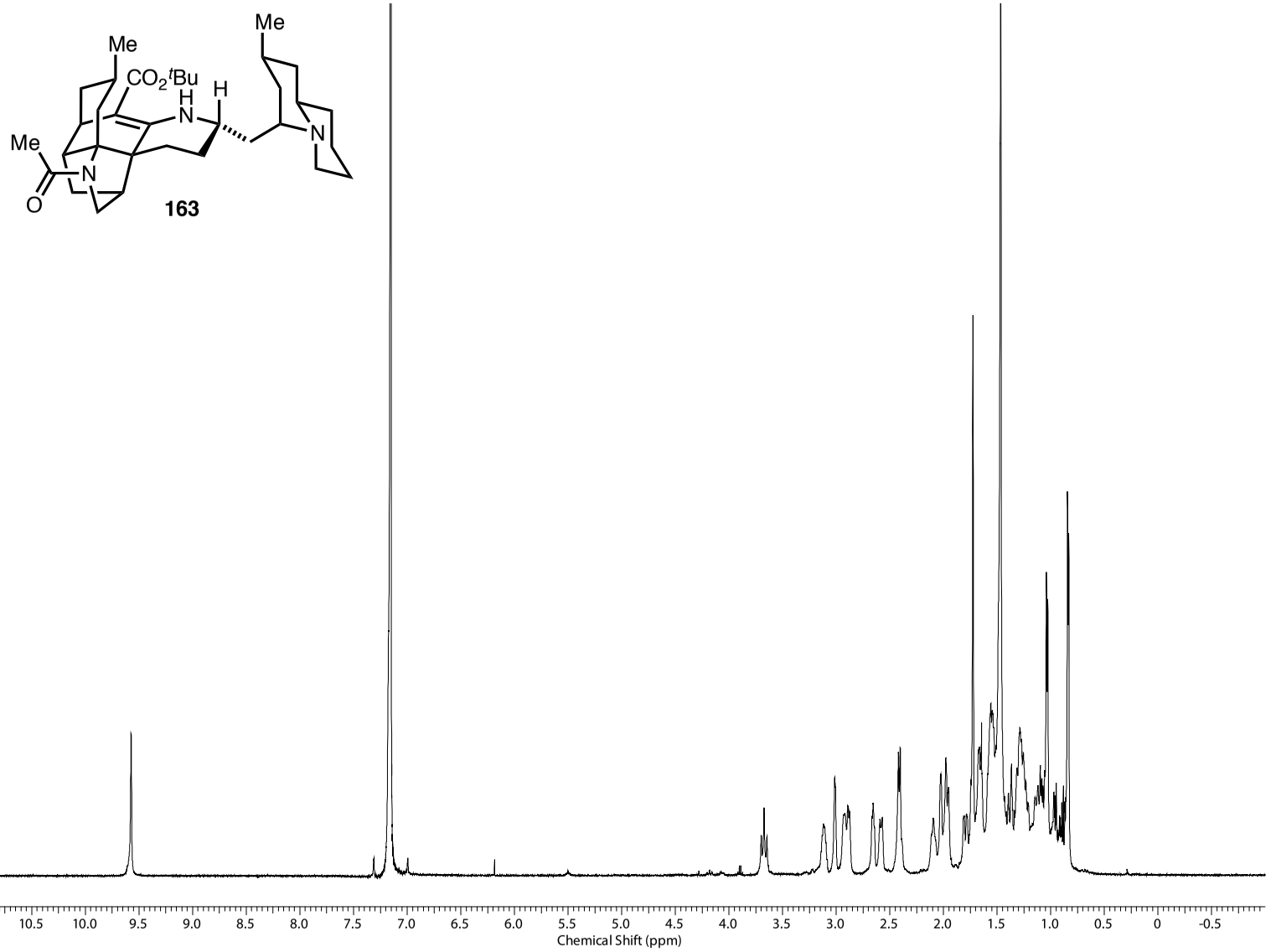
Me
Me
CO2tBu
H
H
N
Me
N
N
O
163
10.5
10.0
9.5
9.0
8.5
8.0
7.5
7.0
6.5
6.0
5.5
5.0
4.5
4.0
3.5
3.0
2.5
2.0
1.5
1.0
0.5
0
-0.5
Chemical Shift (ppm)

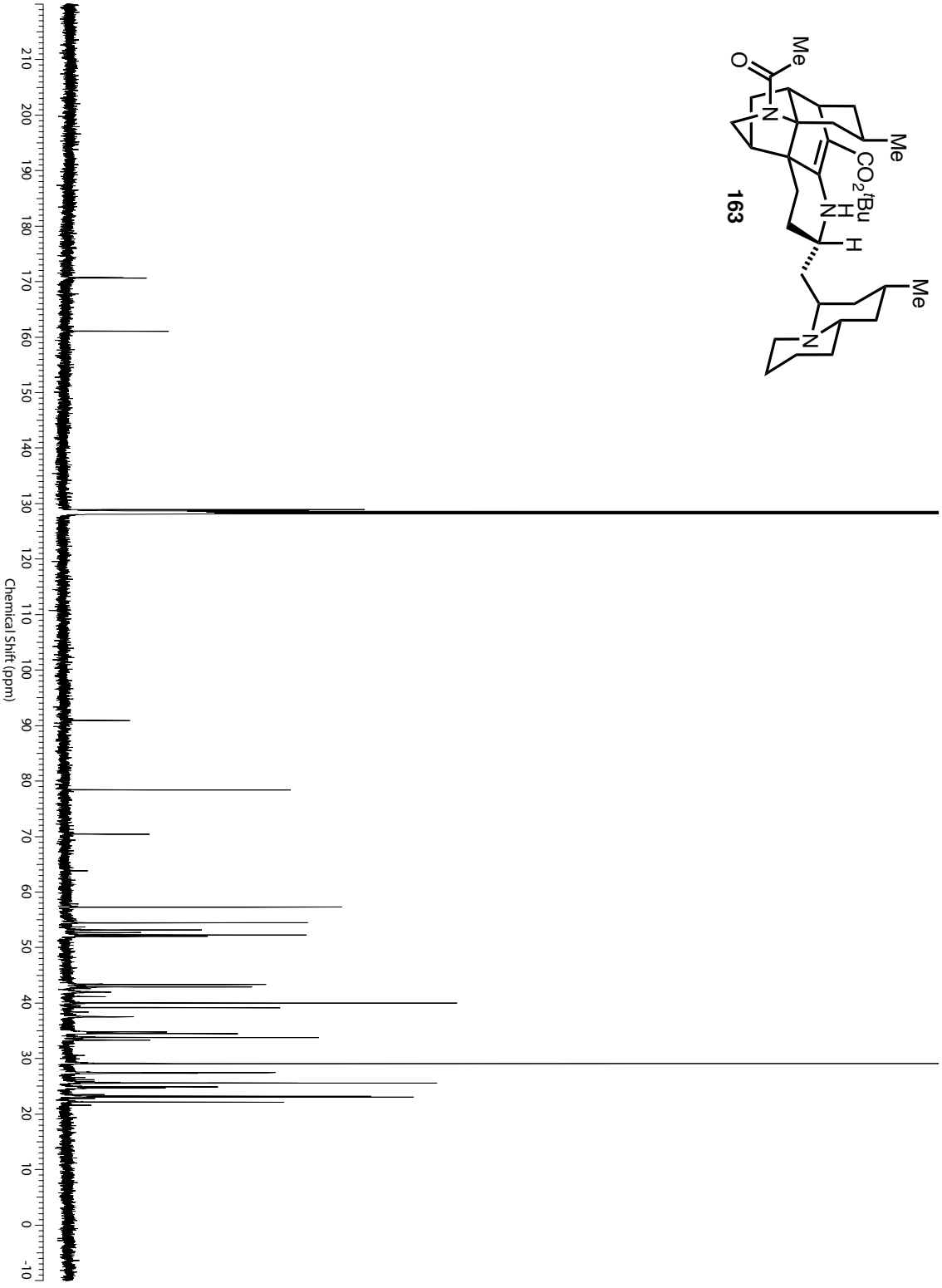
Me
O
N
Me
CO2tBu
H
N
H
163
Me
N
210
200
190
180
170
160
150
140
130
120
110
100
90
80
70
60
50
40
30
20
10
0
-10
Chemical Shift (ppm)

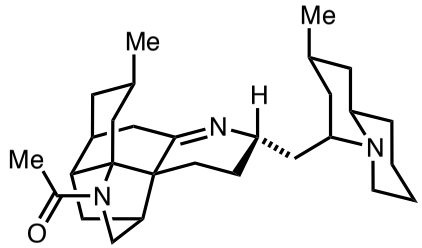

(–)-Himeradine A (**38**)

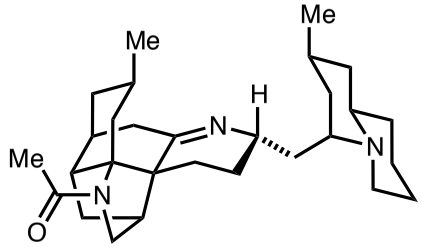

(–)-Himeradine A (**38**)

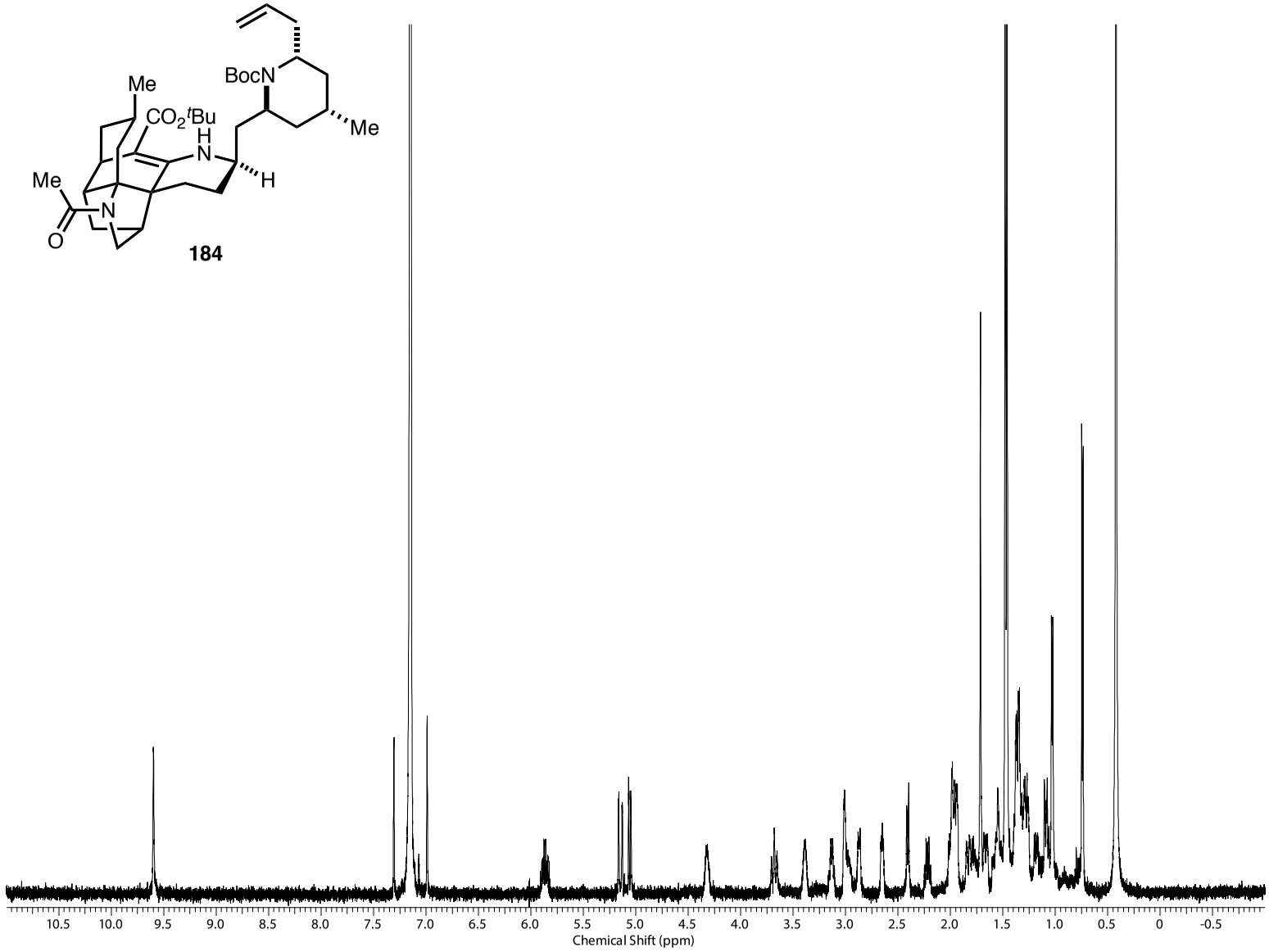
Me
CO2tBu
BocN
Me
H
N
Me
H
N
O
184
10.5
10.0
9.5
9.0
8.5
8.0
7.5
7.0
6.5
6.0
5.5
5.0
4.5
4.0
3.5
3.0
2.5
2.0
1.5
1.0
0.5
0
-0.5
Chemical Shift (ppm)

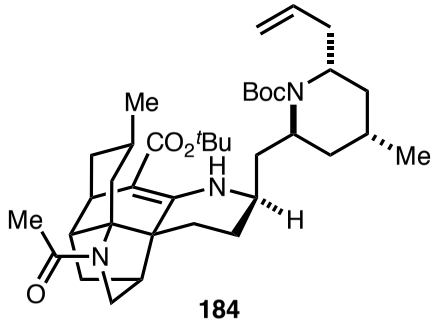
Me
BocN
CO2tBu
H
N
Me
Me
H
N
O

184

210
200
190
180
170
160
150
140
130
120
110
100
90
80
70
60
50
40
30
20
10
0
-10
Chemical Shift (ppm)

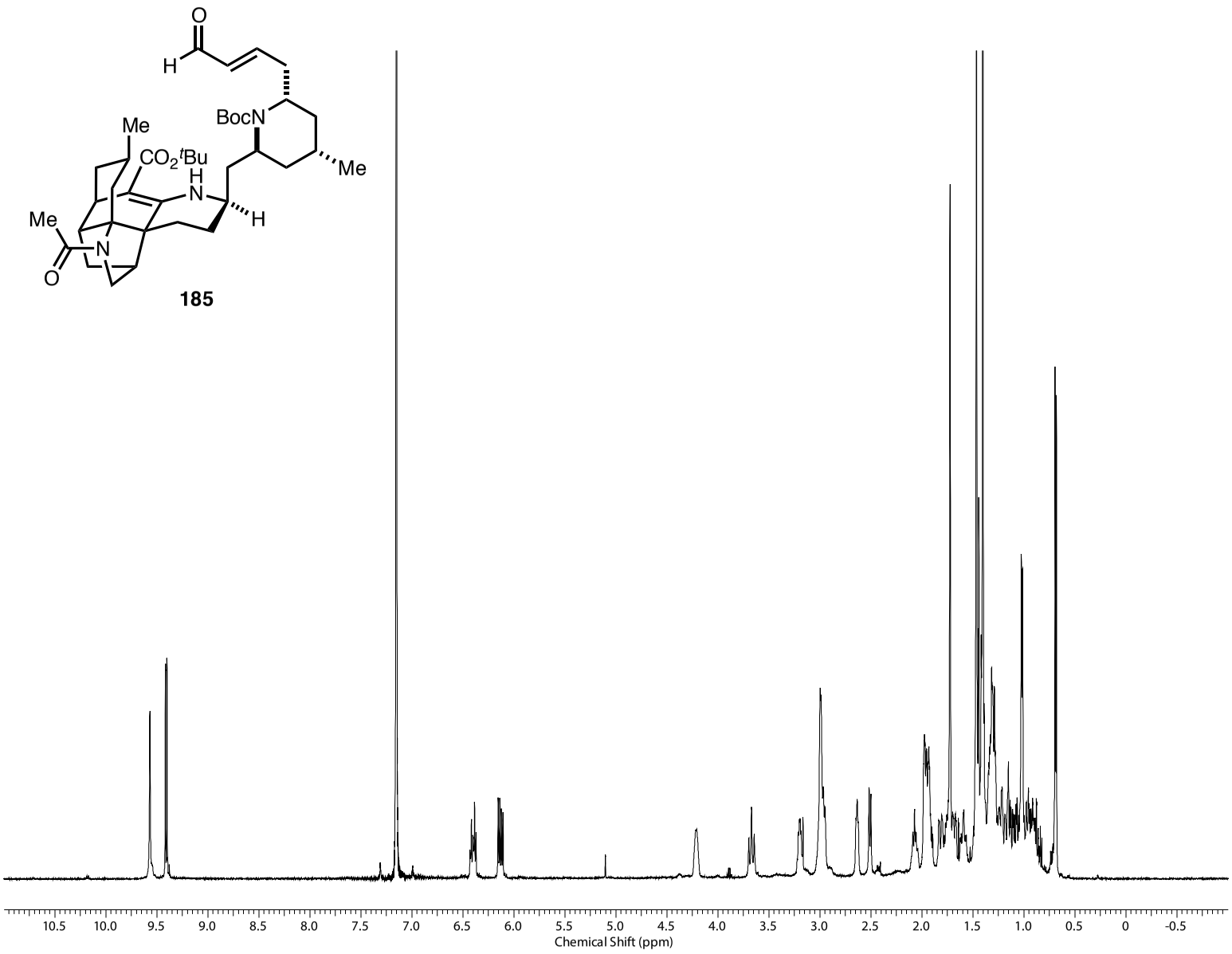
O
H
BocN
Me
CO2tBu
H
N
Me
Me
H
N
O
10.5
10.0
9.5
9.0
8.5
8.0
7.5
7.0
6.5
6.0
5.5
5.0
4.5
4.0
3.5
3.0
2.5
2.0
1.5
1.0
0.5
0
-0.5
Chemical Shift (ppm)

185

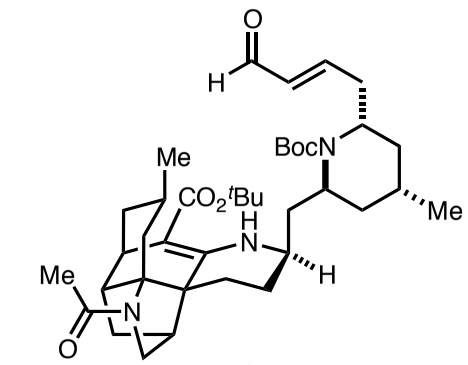
O
H
BocN
Me
CO2tBu
H
N
Me
Me
H
N
O

185

210
200
190
180
170
160
150
140
130
120
110
100
90
80
70
60
50
40
30
20
10
0
-10
Chemical Shift (ppm)

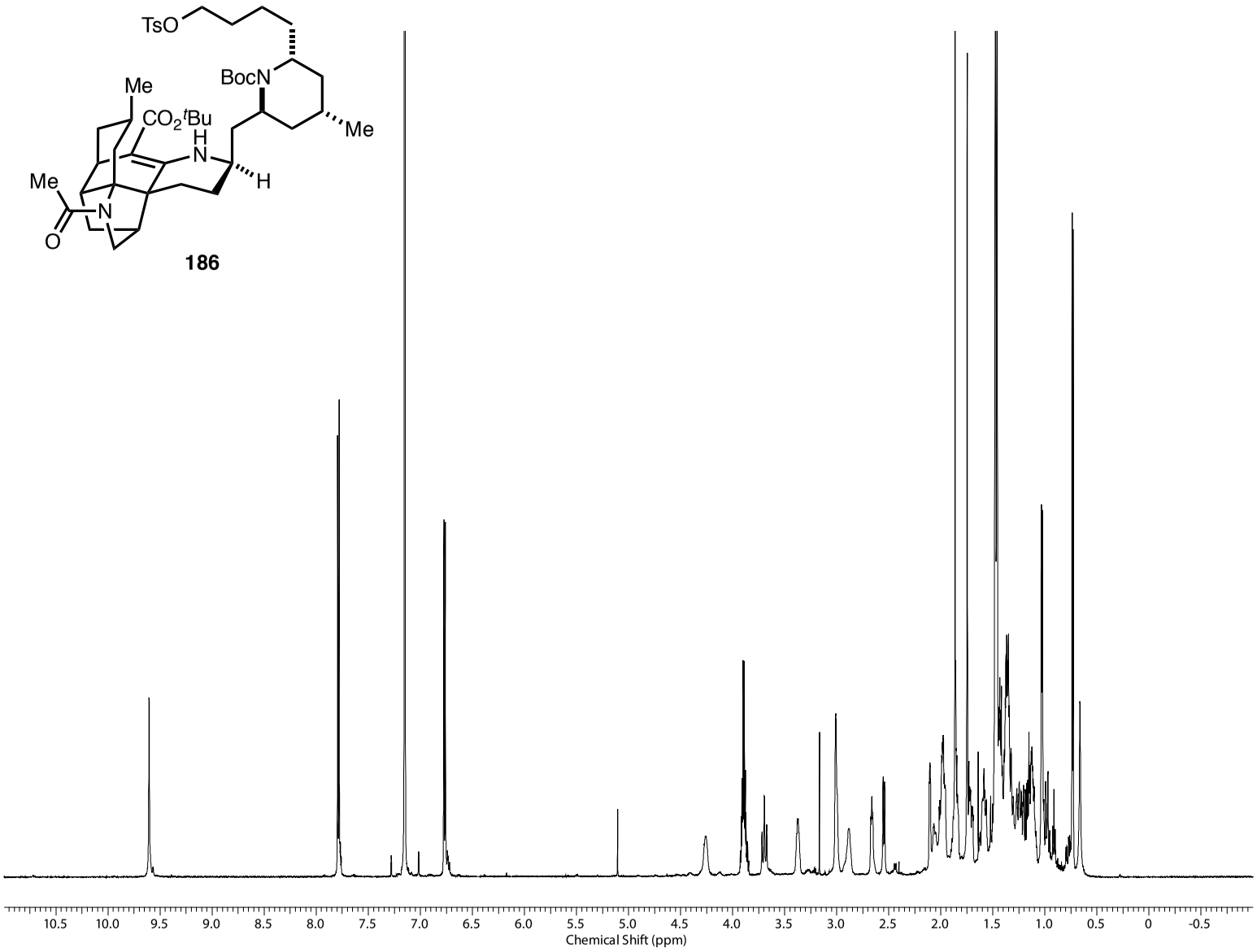
TsO
BocN
Me
CO2tBu
H
N
Me
Me
N
H
O
186
10.5
10.0
9.5
9.0
8.5
8.0
7.5
7.0
6.5
6.0
5.5
5.0
4.5
4.0
3.5
3.0
2.5
2.0
1.5
1.0
0.5
0
-0.5
Chemical Shift (ppm)

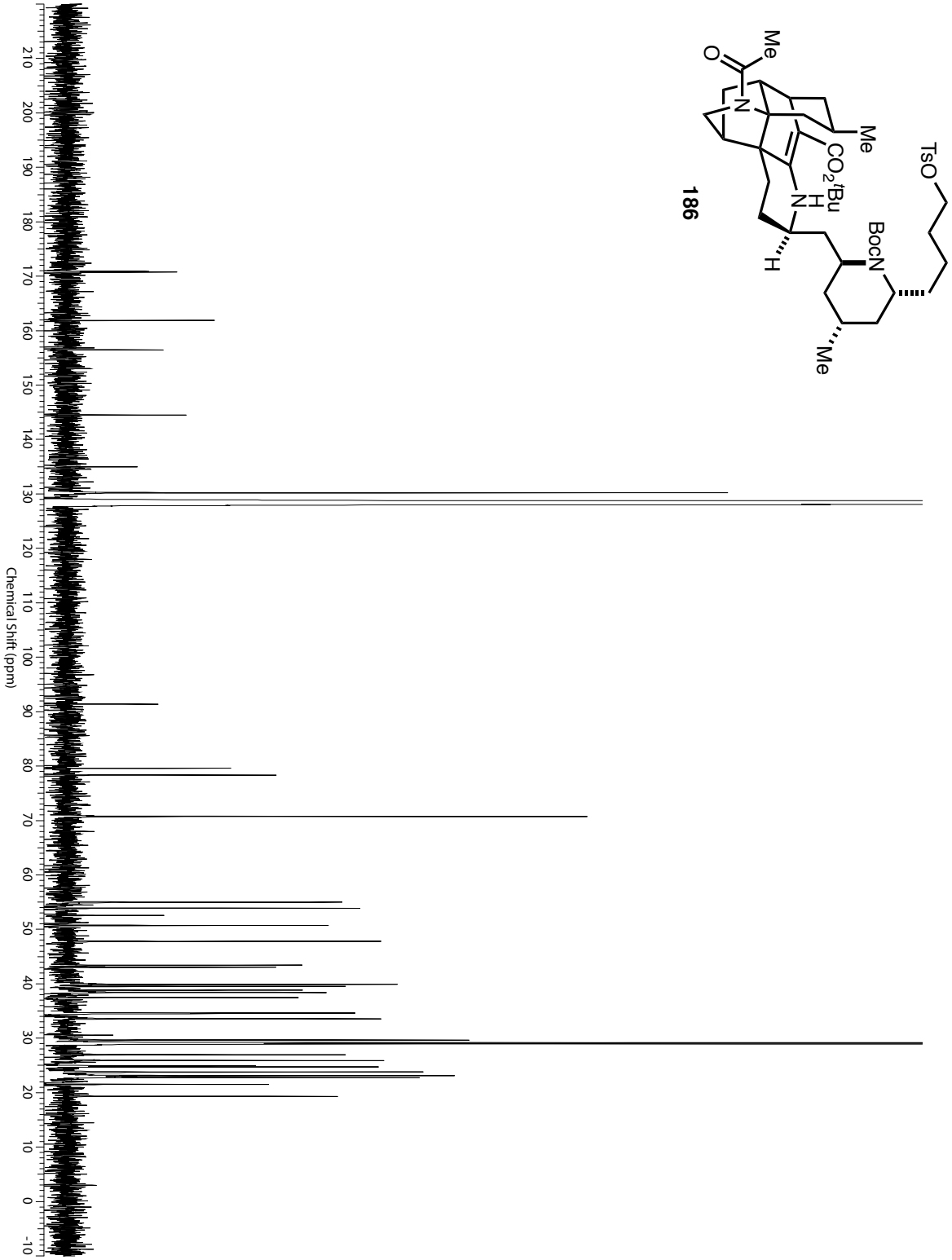
Me
O
N
Me
CO2tBu
H
N
H
BocN
TsO
Me
186
Chemical Shift (ppm)
210
200
190
180
170
160
150
140
130
120
110
100
90
80
70
60
50
40
30
20
10
0
-10

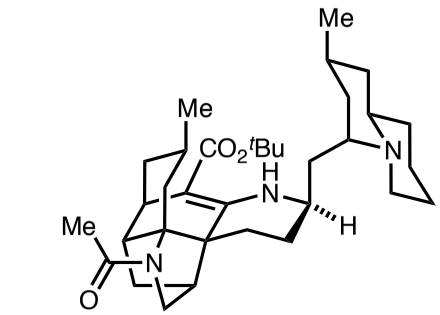
Me
Me
CO2tBu
H
N
N
H
Me
N
O

187

10.5
10.0
9.5
9.0
8.5
8.0
7.5
7.0
6.5
6.0
5.5
5.0
4.5
4.0
3.5
3.0
2.5
2.0
1.5
1.0
0.5
0
-0.5
Chemical Shift (ppm)

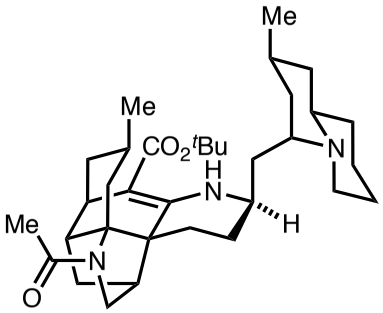
Me
Me
CO2tBu
H
N
N
H
Me
N
O

187

210
200
190
180
170
160
150
140
130
120
110
100
90
80
70
60
50
40
30
20
10
0
-10
Chemical Shift (ppm)

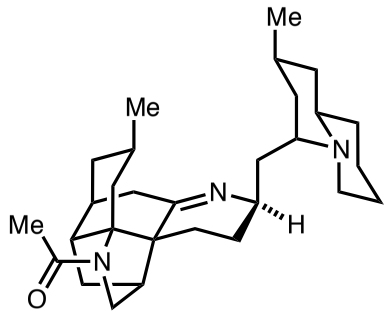

Candidate
(–)-Himeradine A (**188**)

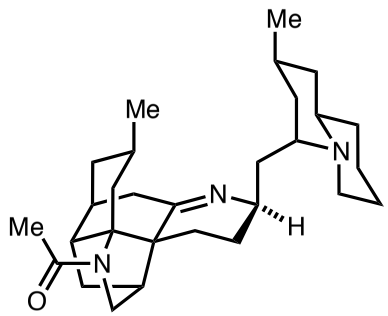

Candidate
(–)-Himeradine A (**188**)

Appendix C

Chapter Five Supplementary Figures

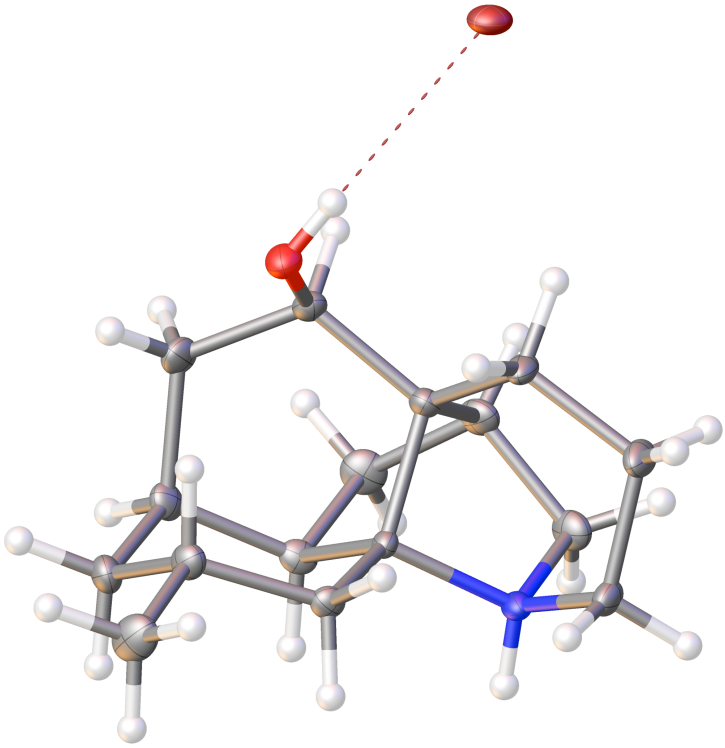

Figure S10. X-Ray Crystal Structure of (–)-Lycopecurine (**39**).

X-Ray Crystallography: A crystal mounted on a diffractometer was collected data at 100 K. The intensities of the reflections were collected by means of a Bruker APEX II DUO CCD diffractometer ($Cu_{K\alpha}$ radiation, λ=1.54178 Å), and equipped with an Oxford Cryosystems nitrogen flow apparatus. The collection method involved 1.0° scans in *ω* at 30°, 55°, 80° and 115° in *2θ*. Data integration down to 0.84 Å resolution was carried out using SAINT V7.46 A (Bruker diffractometer, 2009) with reflection spot size optimisation. Absorption corrections were made with the program SADABS (Bruker diffractometer, 2009). The structure was solved by the direct methods procedure and refined by least-squares methods again F^2 using SHELXS-97 and SHELXL-97 (Sheldrick, 2008) with OLEX 2 interface (Dolomanov, et al., 2009). Non-hydrogen atoms were refined anisotropically, and hydrogen atoms were allowed to ride on the respective atoms. Crystal data as well as details of data collection and refinement are summarized in Table 1, geometric parameters are shown in Table 2 and hydrogen-bond parameters are listed in Table 3. The Ortep plots produced with SHELXL-97 program, and the other drawings were produced with Accelrys DS Visualizer 2.0 (Accelrys, 2007).

Table S7. Experimental Details.

Crystal data	
Chemical formula	$C_{16}H_{26}BrNO$
M_r	328.29
Crystal system, space group	Orthorhombic, $P2_12_12_1$
Temperature (K)	100
a, *b*, *c* (Å)	9.1763 (3), 9.5392 (3), 17.2775 (7)
V (Å^3)	1512.38 (9)
Z	4
Radiation type	Cu *K*α
μ (mm^{-1})	3.63
Crystal size (mm)	0.16 × 0.14 × 0.12
Data collection	
Diffractometer	Bruker D8 goniometer with CCD area detector diffractometer
Absorption correction	Multi-scan *SADABS*
T_{min}, T_{max}	0.594, 0.670
No. of measured, independent and observed [$I > 2\sigma(I)$] reflections	30629, 2677, 2676

R_{int}	0.039
$(\sin \theta/\lambda)_{max}$ (Å^{-1})	0.595
Refinement	
$R[F^2 > 2\sigma(F^2)]$, $wR(F^2)$, S	0.016, 0.043, 1.09
No. of reflections	2677
No. of parameters	181
H-atom treatment	H atoms treated by a mixture of independent and constrained refinement
$\Delta\rho_{max}$, $\Delta\rho_{min}$ (e Å^{-3})	0.23, -0.30
Absolute structure	Flack H D (1983), Acta Cryst. A39, 876-881
Absolute structure parameter	-0.013 (12)

Computer programs: *APEX2* v2009.3.0 (Bruker-AXS, 2009), *SAINT* 7.46A (Bruker-AXS, 2009), *SHELXS97* (Sheldrick, 2008), *SHELXL97* (Sheldrick, 2008), Bruker *SHELXTL* (Sheldrick, 2008).

Table S8. Geometric parameters (Å, º).

C1—N21	1.498 (2)	C8—H8B	0.9900
C1—C2	1.528 (2)	C9—C16	1.521 (2)
C1—H1A	0.9900	C9—C10	1.530 (2)
C1—H1B	0.9900	C9—H9	1.0000
C2—C3	1.539 (2)	C10—C11	1.520 (2)
C2—H2A	0.9900	C10—H10A	0.9900
C2—H2B	0.9900	C10—H10B	0.9900
C3—C4	1.533 (2)	C11—N21	1.5385 (18)
C3—H3A	0.9900	C11—C12	1.540 (2)
C3—H3B	0.9900	C12—C13	1.550 (2)
C4—C11	1.5387 (19)	C12—H12	1.0000
C4—C5	1.5671 (19)	C13—C14	1.537 (2)
C4—C14	1.578 (2)	C13—H13A	0.9900
C5—O1	1.431 (2)	C13—H13B	0.9900
C5—C6	1.557 (2)	C14—C15	1.531 (2)
C5—H5	1.0000	C14—H14	1.0000
C6—C7	1.555 (2)	C15—N21	1.519 (2)
C6—H6A	0.9900	C15—H15A	0.9900
C6—H6B	0.9900	C15—H15B	0.9900
C7—C8	1.523 (2)	C16—H16A	0.9800
C7—C12	1.528 (2)	C16—H16B	0.9800

C7—H7	1.0000	C16—H16C	0.9800
C8—C9	1.523 (2)	N21—H21	0.88 (2)
C8—H8A	0.9900	O1—H1	0.80 (2)
N21—C1—C2	109.63 (13)	C8—C9—H9	108.0
N21—C1—H1A	109.7	C10—C9—H9	108.0
C2—C1—H1A	109.7	C11—C10—C9	114.10 (13)
N21—C1—H1B	109.7	C11—C10—H10A	108.7
C2—C1—H1B	109.7	C9—C10—H10A	108.7
H1A—C1—H1B	108.2	C11—C10—H10B	108.7
C1—C2—C3	113.07 (13)	C9—C10—H10B	108.7
C1—C2—H2A	109.0	H10A—C10—H10B	107.6
C3—C2—H2A	109.0	C10—C11—N21	109.62 (12)
C1—C2—H2B	109.0	C10—C11—C4	122.13 (14)
C3—C2—H2B	109.0	N21—C11—C4	98.99 (11)
H2A—C2—H2B	107.8	C10—C11—C12	113.92 (12)
C4—C3—C2	116.30 (13)	N21—C11—C12	109.19 (12)
C4—C3—H3A	108.2	C4—C11—C12	101.57 (12)
C2—C3—H3A	108.2	C7—C12—C11	107.39 (12)
C4—C3—H3B	108.2	C7—C12—C13	109.81 (13)
C2—C3—H3B	108.2	C11—C12—C13	104.71 (12)
H3A—C3—H3B	107.4	C7—C12—H12	111.5
C3—C4—C11	111.28 (13)	C11—C12—H12	111.5
C3—C4—C5	109.82 (12)	C13—C12—H12	111.5
C11—C4—C5	114.36 (12)	C14—C13—C12	101.96 (13)
C3—C4—C14	117.04 (13)	C14—C13—H13A	111.4
C11—C4—C14	92.93 (11)	C12—C13—H13A	111.4
C5—C4—C14	110.68 (13)	C14—C13—H13B	111.4
O1—C5—C6	106.46 (13)	C12—C13—H13B	111.4
O1—C5—C4	112.07 (13)	H13A—C13—H13B	109.2
C6—C5—C4	116.25 (12)	C15—C14—C13	103.15 (14)
O1—C5—H5	107.2	C15—C14—C4	104.07 (12)
C6—C5—H5	107.2	C13—C14—C4	103.06 (12)
C4—C5—H5	107.2	C15—C14—H14	115.0
C7—C6—C5	117.58 (13)	C13—C14—H14	115.0
C7—C6—H6A	107.9	C4—C14—H14	115.0
C5—C6—H6A	107.9	N21—C15—C14	102.18 (12)

C7—C6—H6B	107.9	N21—C15—H15A	111.3
C5—C6—H6B	107.9	C14—C15—H15A	111.3
H6A—C6—H6B	107.2	N21—C15—H15B	111.3
C8—C7—C12	110.82 (13)	C14—C15—H15B	111.3
C8—C7—C6	113.05 (14)	H15A—C15—H15B	109.2
C12—C7—C6	109.78 (13)	C9—C16—H16A	109.5
C8—C7—H7	107.7	C9—C16—H16B	109.5
C12—C7—H7	107.7	H16A—C16—H16B	109.5
C6—C7—H7	107.7	C9—C16—H16C	109.5
C7—C8—C9	111.01 (13)	H16A—C16—H16C	109.5
C7—C8—H8A	109.4	H16B—C16—H16C	109.5
C9—C8—H8A	109.4	C1—N21—C15	109.19 (12)
C7—C8—H8B	109.4	C1—N21—C11	112.76 (12)
C9—C8—H8B	109.4	C15—N21—C11	105.13 (11)
H8A—C8—H8B	108.0	C1—N21—H21	111.8 (13)
C16—C9—C8	112.64 (14)	C15—N21—H21	108.8 (15)
C16—C9—C10	109.62 (13)	C11—N21—H21	108.9 (13)
C8—C9—C10	110.55 (13)	C5—O1—H1	105.8 (15)
C16—C9—H9	108.0		
N21—C1—C2—C3	40.1 (2)	C8—C7—C12—C11	-60.35 (16)
C1—C2—C3—C4	-35.4 (2)	C6—C7—C12—C11	65.24 (16)
C2—C3—C4—C11	50.1 (2)	C8—C7—C12—C13	-173.65 (13)
C2—C3—C4—C5	177.78 (14)	C6—C7—C12—C13	-48.07 (17)
C2—C3—C4—C14	-55.0 (2)	C10—C11—C12—C7	53.76 (16)
C3—C4—C5—O1	-31.50 (18)	N21—C11—C12—C7	176.66 (12)
C11—C4—C5—O1	94.41 (15)	C4—C11—C12—C7	-79.45 (14)
C14—C4—C5—O1	-162.23 (12)	C10—C11—C12—C13	170.46 (13)
C3—C4—C5—C6	-154.25 (15)	N21—C11—C12—C13	-66.64 (15)
C11—C4—C5—C6	-28.3 (2)	C4—C11—C12—C13	37.25 (15)
C14—C4—C5—C6	75.02 (17)	C7—C12—C13—C14	113.42 (14)
O1—C5—C6—C7	-113.45 (15)	C11—C12—C13—C14	-1.61 (16)
C4—C5—C6—C7	12.2 (2)	C12—C13—C14—C15	74.38 (14)
C5—C6—C7—C8	94.35 (18)	C12—C13—C14—C4	-33.71 (15)
C5—C6—C7—C12	-30.0 (2)	C3—C4—C14—C15	63.42 (17)
C12—C7—C8—C9	62.88 (17)	C11—C4—C14—C15	-52.31 (14)
C6—C7—C8—C9	-60.85 (18)	C5—C4—C14—C15	-169.75 (12)

C7—C8—C9—C16	-177.37 (14)	C3—C4—C14—C13	170.81 (14)
C7—C8—C9—C10	-54.35 (17)	C11—C4—C14—C13	55.08 (13)
C16—C9—C10—C11	172.64 (14)	C5—C4—C14—C13	-62.35 (15)
C8—C9—C10—C11	47.88 (17)	C13—C14—C15—N21	-80.85 (14)
C9—C10—C11—N21	-171.87 (12)	C4—C14—C15—N21	26.48 (15)
C9—C10—C11—C4	73.32 (18)	C2—C1—N21—C15	52.05 (17)
C9—C10—C11—C12	-49.20 (18)	C2—C1—N21—C11	-64.42 (17)
C3—C4—C11—C10	56.32 (18)	C14—C15—N21—C1	-110.75 (14)
C5—C4—C11—C10	-68.83 (19)	C14—C15—N21—C11	10.47 (15)
C14—C4—C11—C10	176.88 (13)	C10—C11—N21—C1	-54.47 (16)
C3—C4—C11—N21	-63.73 (15)	C4—C11—N21—C1	74.43 (14)
C5—C4—C11—N21	171.13 (13)	C12—C11—N21—C1	-179.91 (12)
C14—C4—C11—N21	56.83 (12)	C10—C11—N21—C15	-173.34 (13)
C3—C4—C11—C12	-175.57 (13)	C4—C11—N21—C15	-44.44 (14)
C5—C4—C11—C12	59.29 (16)	C12—C11—N21—C15	61.23 (14)
C14—C4—C11—C12	-55.01 (12)		

Table S9. Hydrogen-Bond Parameters.

D—H···*A*	*D*—H (Å)	H···*A* (Å)	*D*···*A* (Å)	*D*—H···*A* (°)
N21—H21···Br1^{i}	0.88 (2)	2.29 (2)	3.1728 (12)	178.3 (18)
O1—H1···Br1	0.80 (2)	2.52 (2)	3.3162 (13)	174 (2)

Symmetry code(s): (i) *x*, *y*+1, *z*.

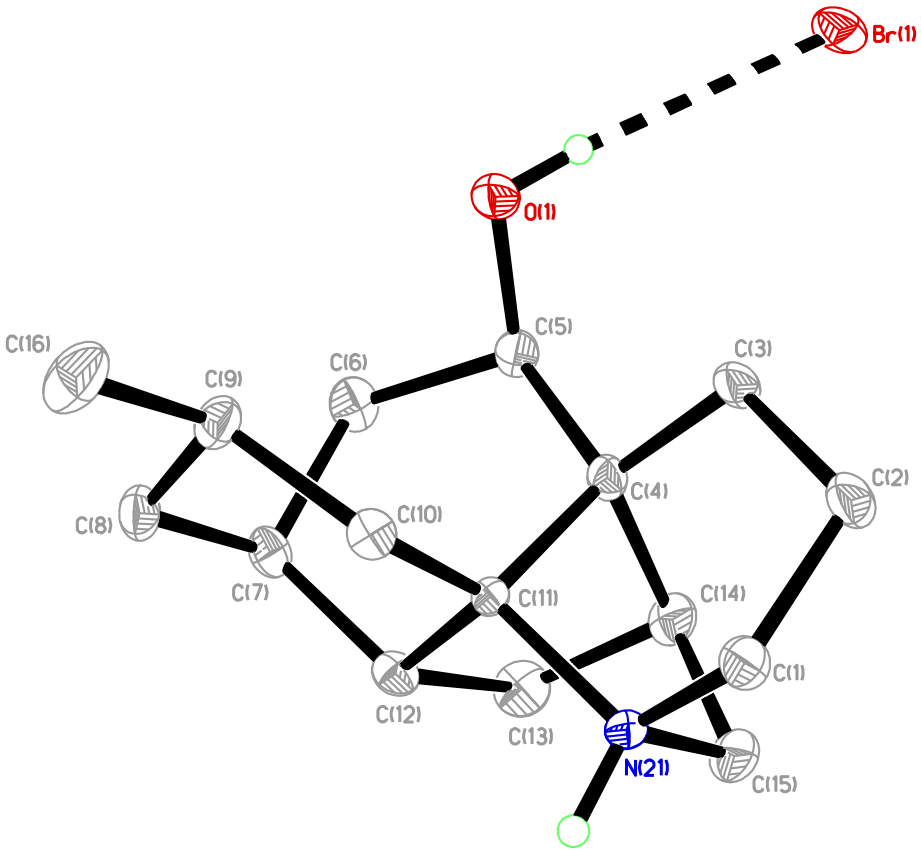

Figure S11. Perspective views showing 50% probability displacement.

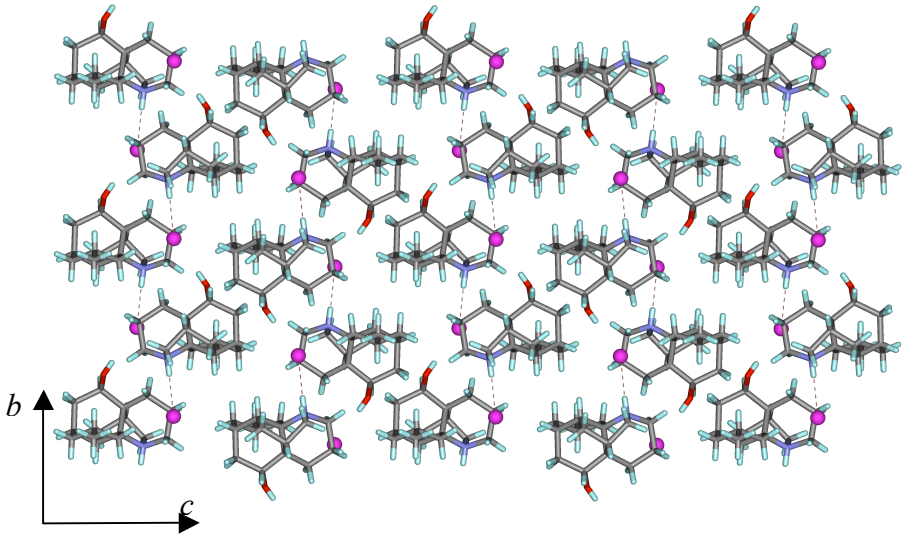

Figure S12. Three-dimensional supramolecular architecture viewed along the *a*-axis direction.

Appendix D

Chapter Five Catalog of ^{1}H and ^{13}C NMR Spectra

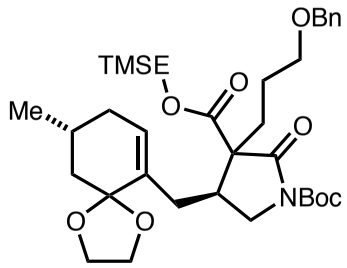
OBn
TMSE
O
O
Me
O
NBoc
O
O

191

10.5
10.0
9.5
9.0
8.5
8.0
7.5
7.0
6.5
6.0
5.5
5.0
4.5
4.0
3.5
3.0
2.5
2.0
1.5
1.0
0.5
0
-0.5
Chemical Shift (ppm)

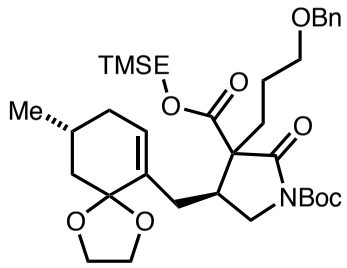
OBn
TMSE
O
O
Me
O
NBoc
O
O

191

210
200
190
180
170
160
150
140
130
120
110
100
90
80
70
60
50
40
30
20
10
0
-10
Chemical Shift (ppm)

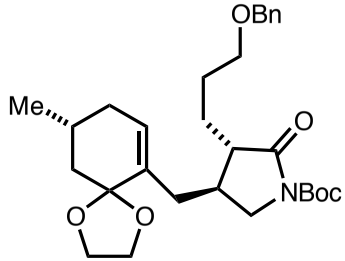
OBn
Me
O
NBoc
O
O

S14

10.5
10.0
9.5
9.0
8.5
8.0
7.5
7.0
6.5
6.0
5.5
5.0
4.5
4.0
3.5
3.0
2.5
2.0
1.5
1.0
0.5
0
-0.5
Chemical Shift (ppm)

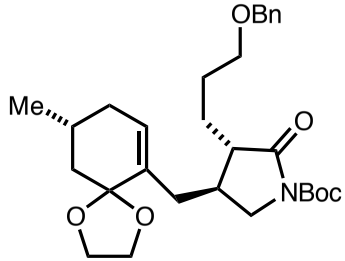
OBn
Me
O
NBoc
O
O

S14

210
200
190
180
170
160
150
140
130
120
110
100
90
80
70
60
50
40
30
20
10
0
-10
Chemical Shift (ppm)

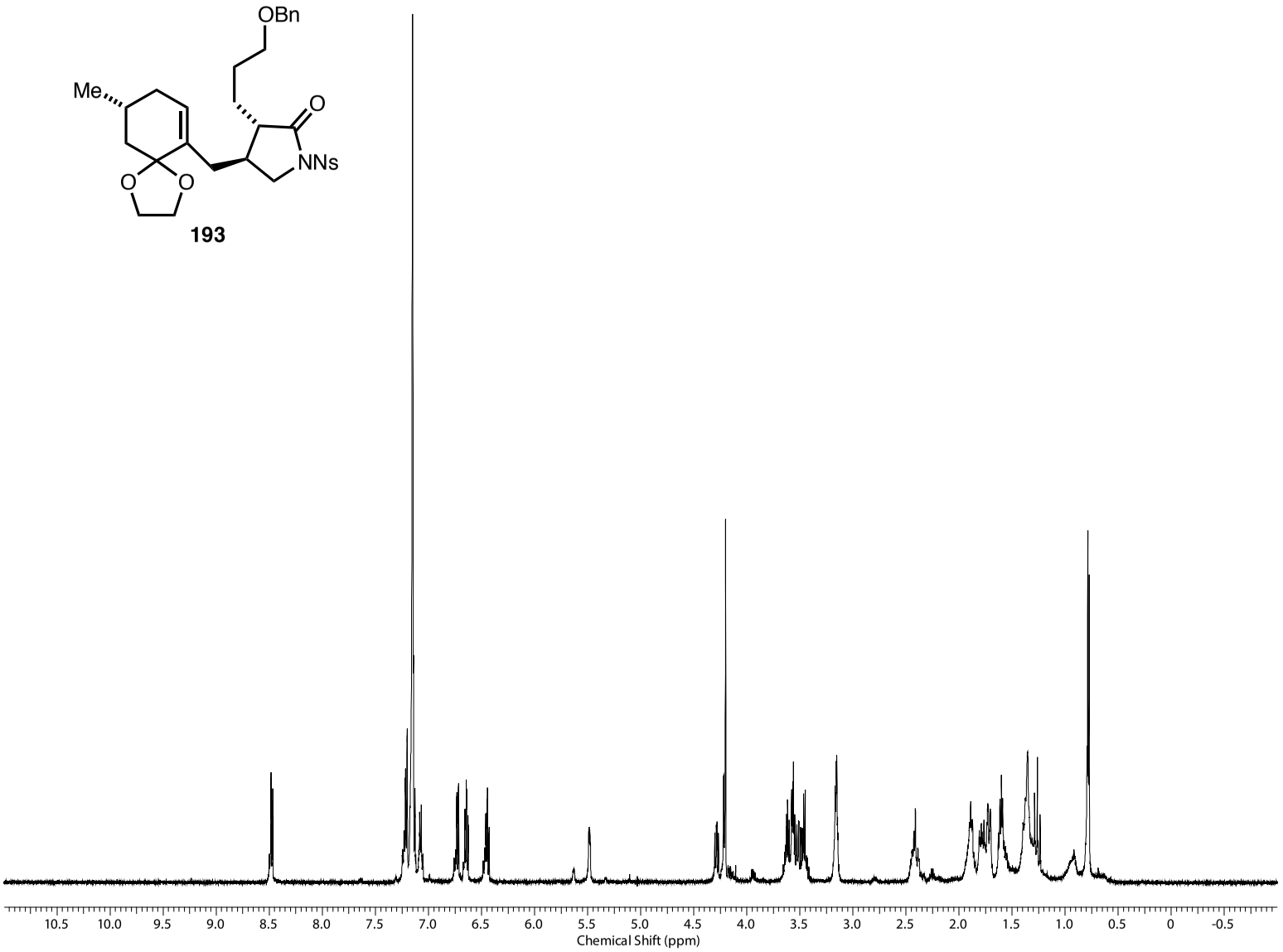
OBn
Me
O
NNs
O
O
193
10.5
10.0
9.5
9.0
8.5
8.0
7.5
7.0
6.5
6.0
5.5
5.0
4.5
4.0
3.5
3.0
2.5
2.0
1.5
1.0
0.5
0
-0.5
Chemical Shift (ppm)

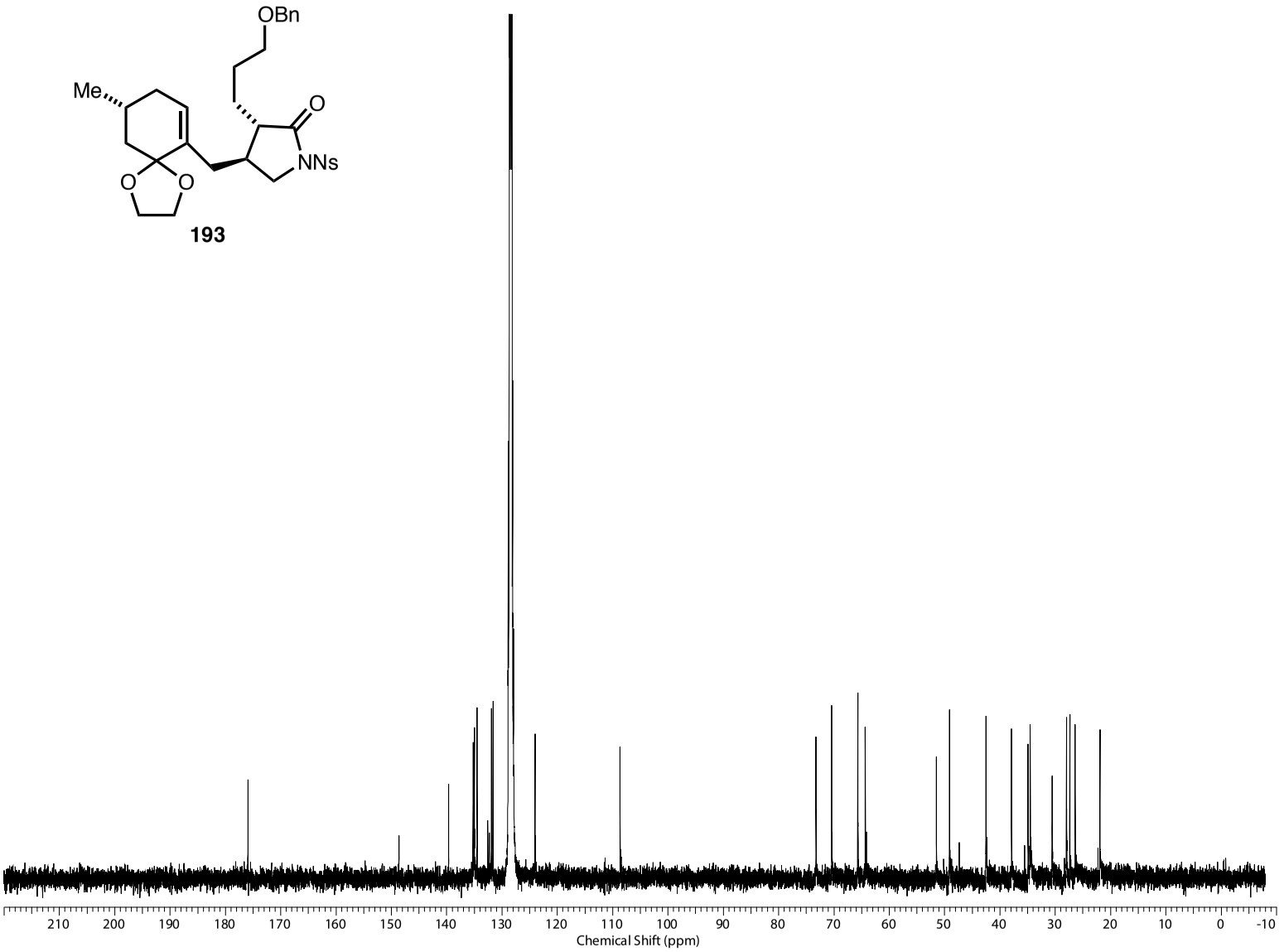
OBn
Me
O
NNs
O
O
193
210
200
190
180
170
160
150
140
130
120
110
100
90
80
70
60
50
40
30
20
10
0
-10
Chemical Shift (ppm)

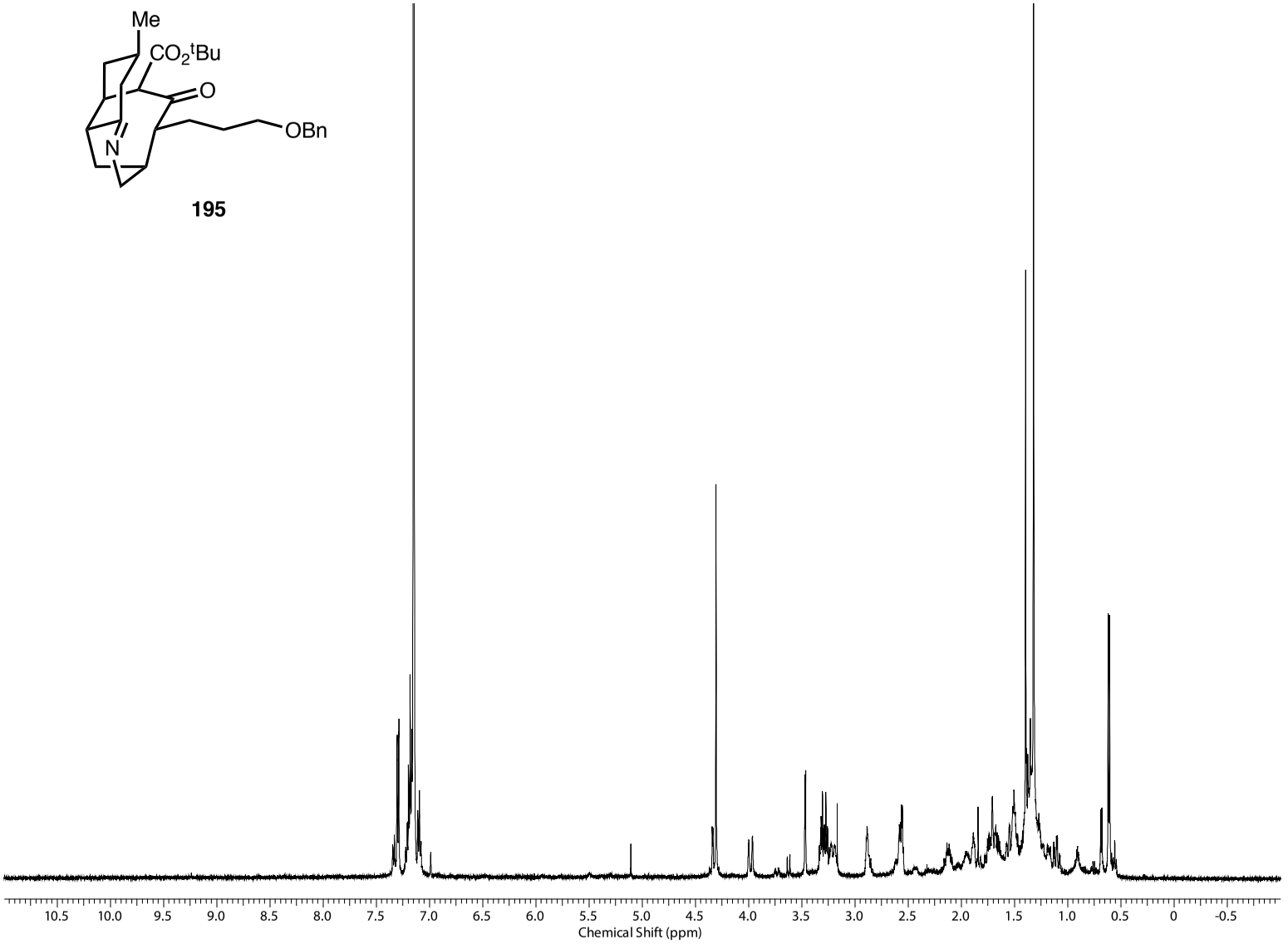
Me
CO2tBu
O
OBn
N
195
10.5
10.0
9.5
9.0
8.5
8.0
7.5
7.0
6.5
6.0
5.5
5.0
4.5
4.0
3.5
3.0
2.5
2.0
1.5
1.0
0.5
0
-0.5
Chemical Shift (ppm)

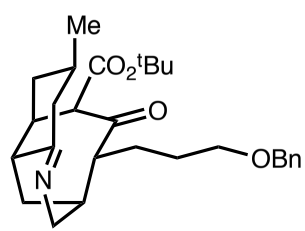
Me
CO2tBu
O
OBn
N

195

210
200
190
180
170
160
150
140
130
120
110
100
90
80
70
60
50
40
30
20
10
0
-10
Chemical Shift (ppm)

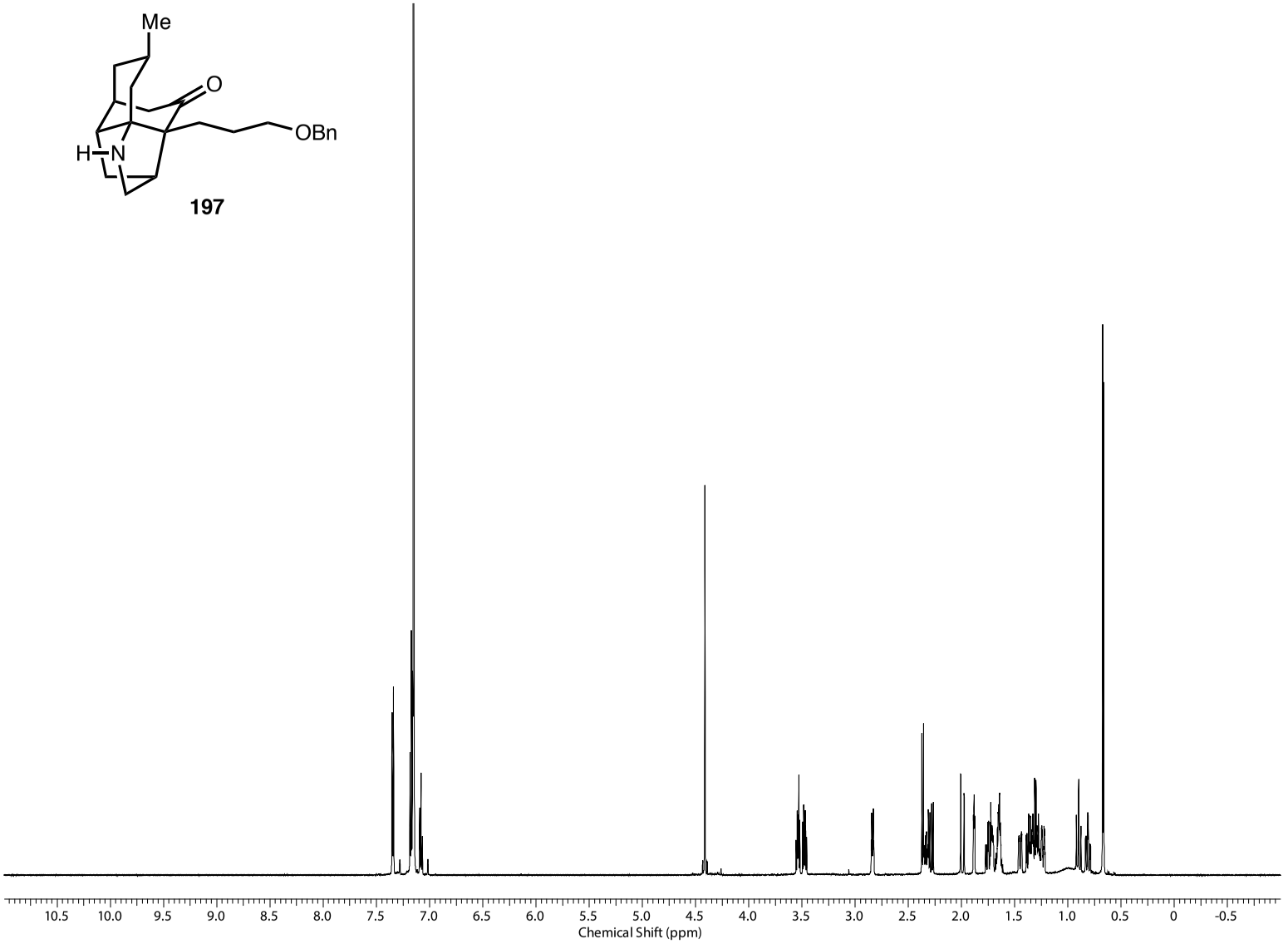
Me
O
OBn
H
N
197
10.5
10.0
9.5
9.0
8.5
8.0
7.5
7.0
6.5
6.0
5.5
5.0
4.5
4.0
3.5
3.0
2.5
2.0
1.5
1.0
0.5
0
-0.5
Chemical Shift (ppm)

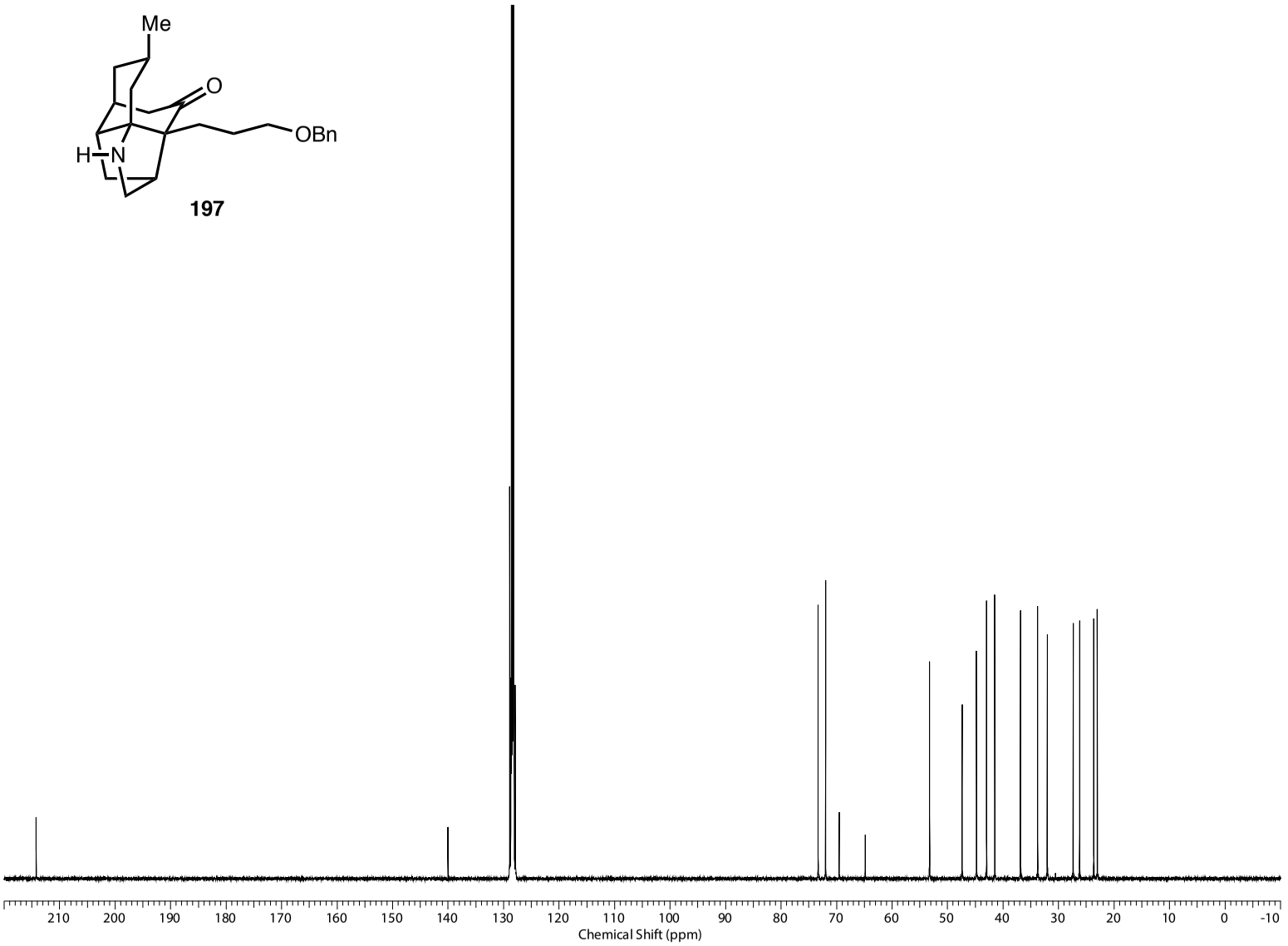
Me
O
OBn
H
N
197
210
200
190
180
170
160
150
140
130
120
110
100
90
80
70
60
50
40
30
20
10
0
-10
Chemical Shift (ppm)

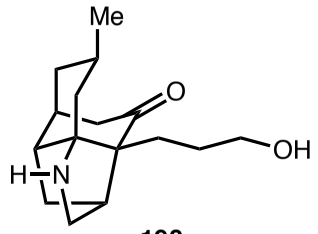
Me
O
OH
H
N

198

10.5
10.0
9.5
9.0
8.5
8.0
7.5
7.0
6.5
6.0
5.5
5.0
4.5
4.0
3.5
3.0
2.5
2.0
1.5
1.0
0.5
0
-0.5
Chemical Shift (ppm)

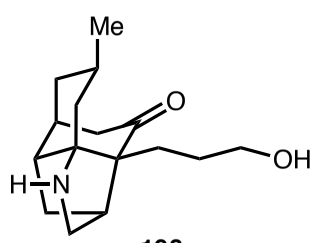
Me
O
OH
H
N

198

210
200
190
180
170
160
150
140
130
120
110
100
90
80
70
60
50
40
30
20
10
0
-10
Chemical Shift (ppm)

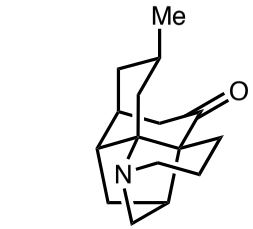

Dehydrolycopecurine (199)

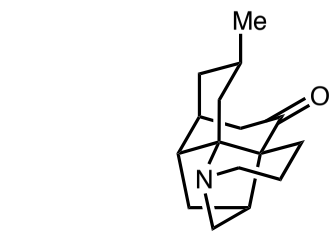

Dehydrolycopecurine (199)

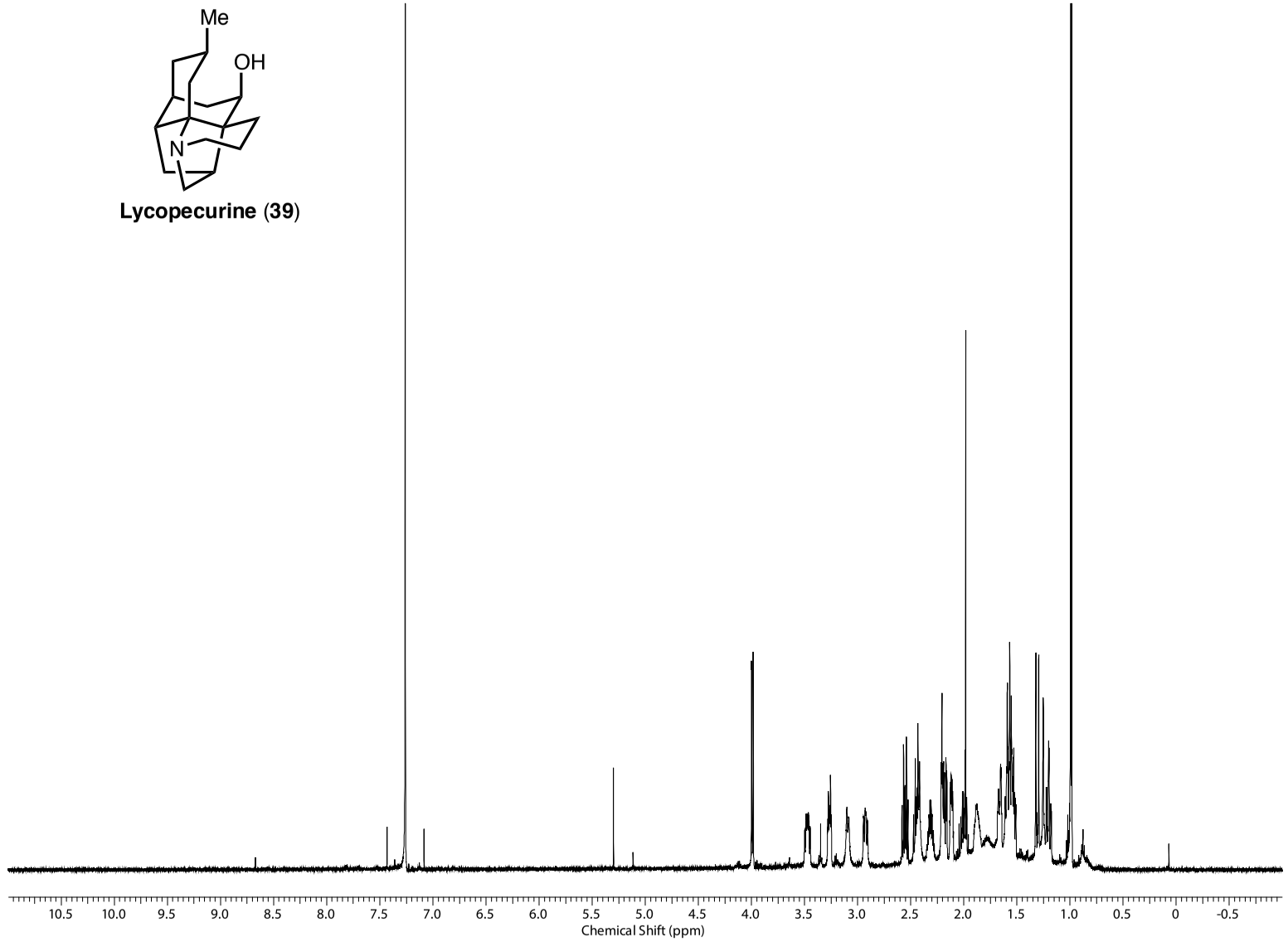

Lycopecurine (39)

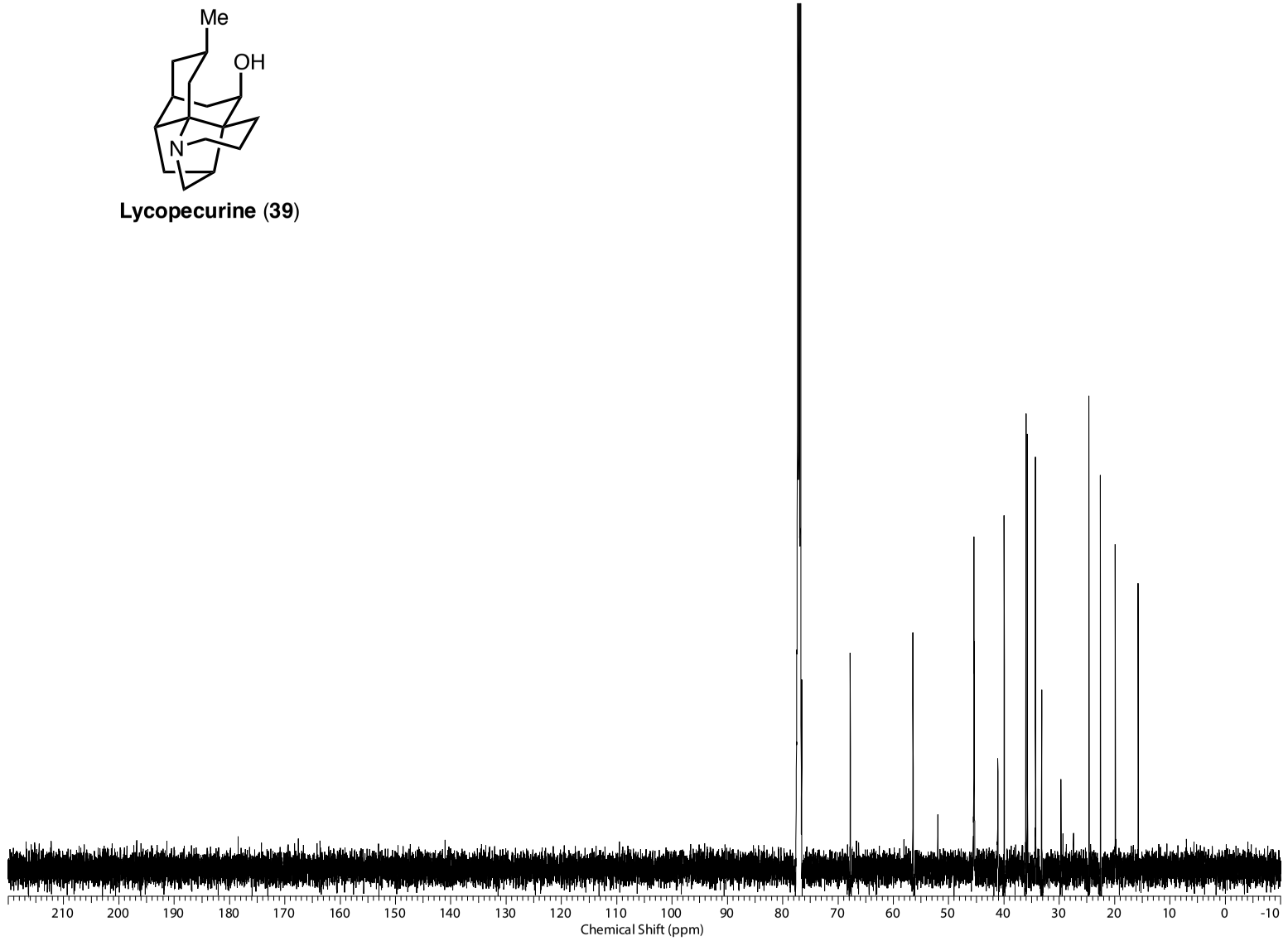

Lycopecurine (39)

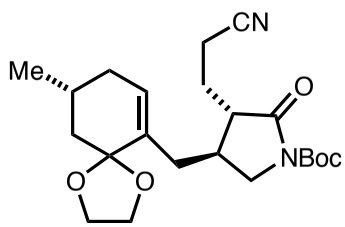
CN
Me
O
NBoc
O
O

S16

10.5
10.0
9.5
9.0
8.5
8.0
7.5
7.0
6.5
6.0
5.5
5.0
4.5
4.0
3.5
3.0
2.5
2.0
1.5
1.0
0.5
0
-0.5
Chemical Shift (ppm)

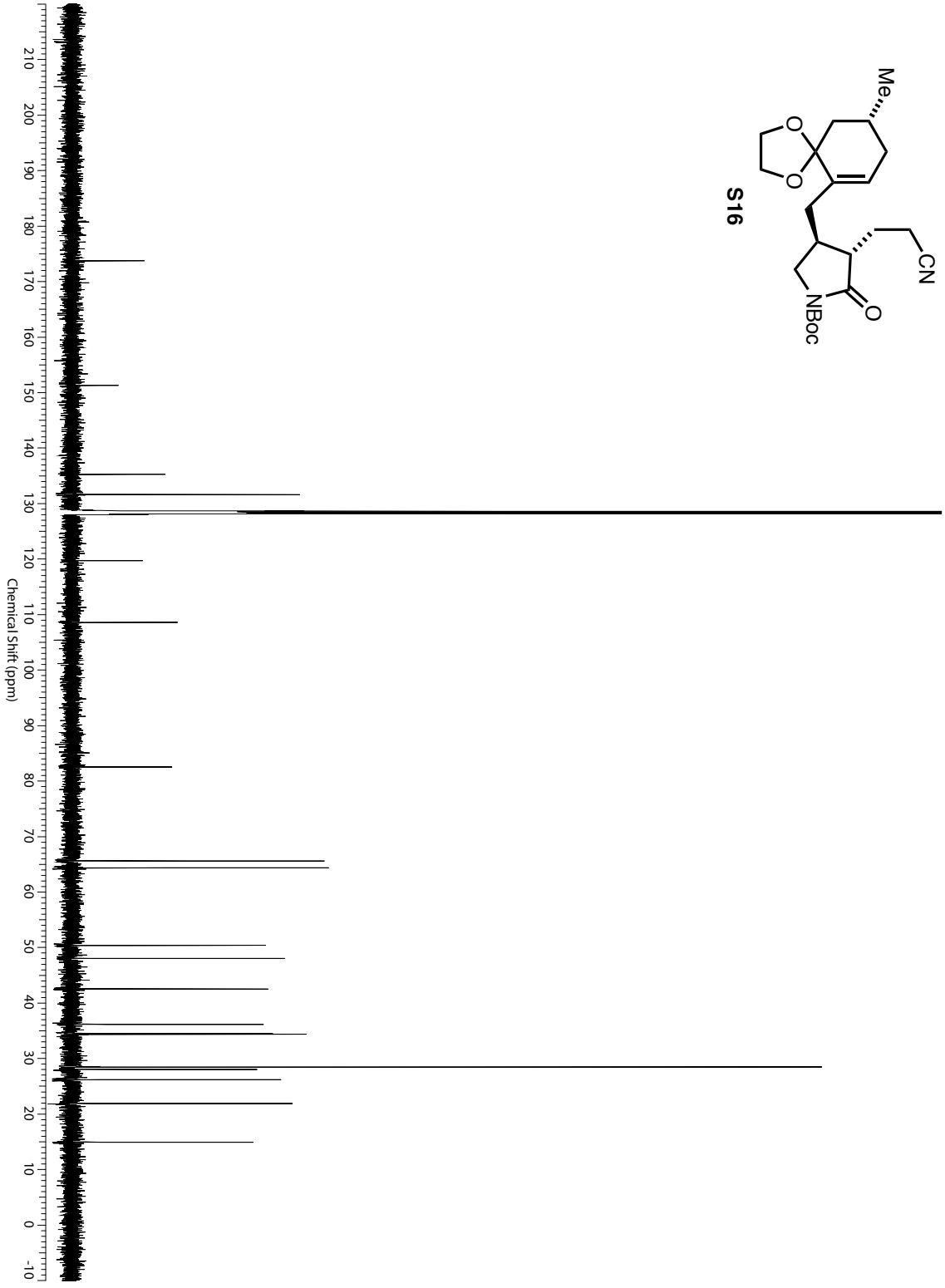
Me
O
O
CN
O
NBoc
S16
Chemical Shift (ppm)
210
200
190
180
170
160
150
140
130
120
110
100
90
80
70
60
50
40
30
20
10
0
-10

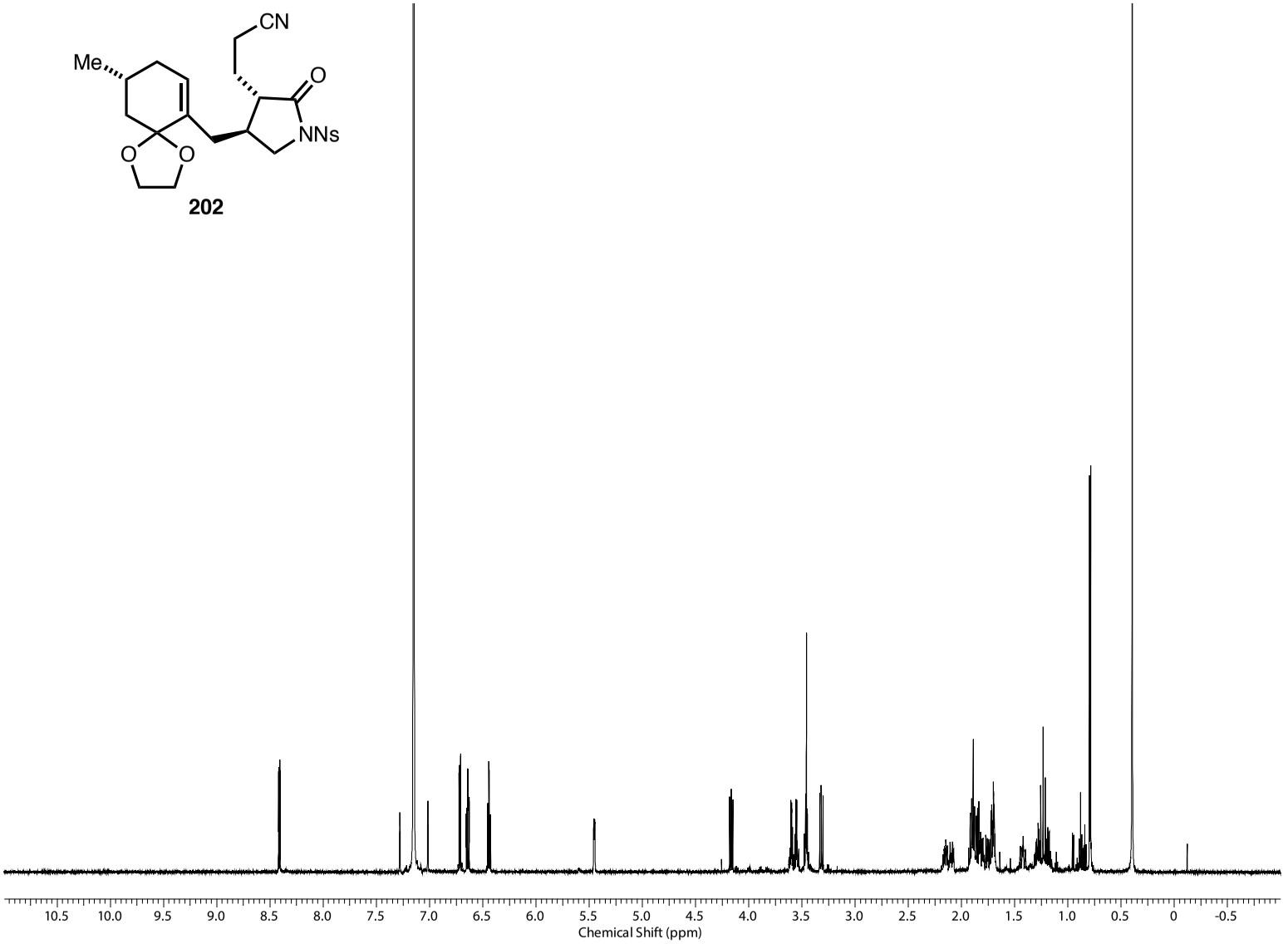
CN
Me
O
NNs
O
O
202
10.5
10.0
9.5
9.0
8.5
8.0
7.5
7.0
6.5
6.0
5.5
5.0
4.5
4.0
3.5
3.0
2.5
2.0
1.5
1.0
0.5
0
-0.5
Chemical Shift (ppm)

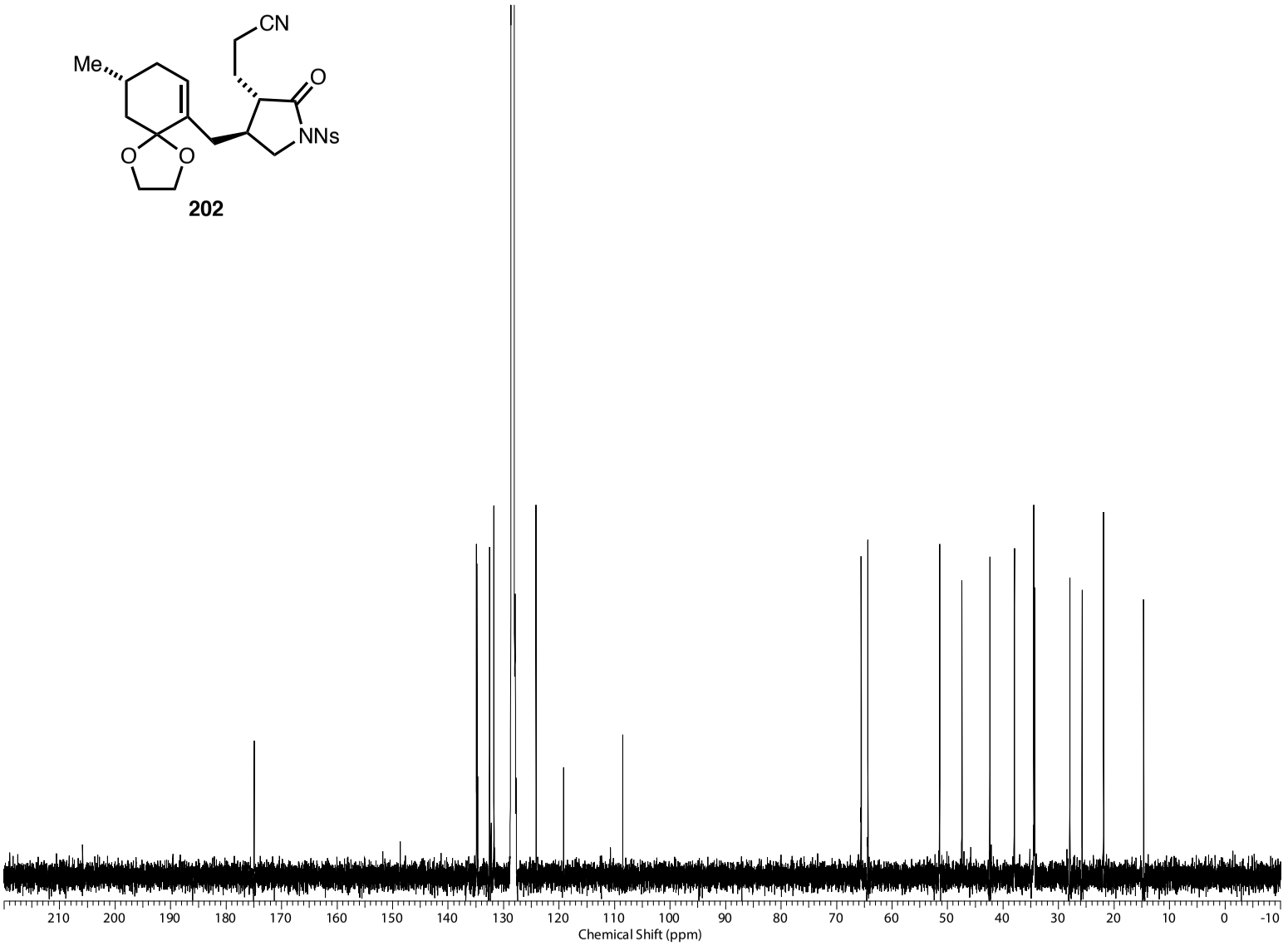
CN
Me
O
NNs
O
O
202
210
200
190
180
170
160
150
140
130
120
110
100
90
80
70
60
50
40
30
20
10
0
-10
Chemical Shift (ppm)

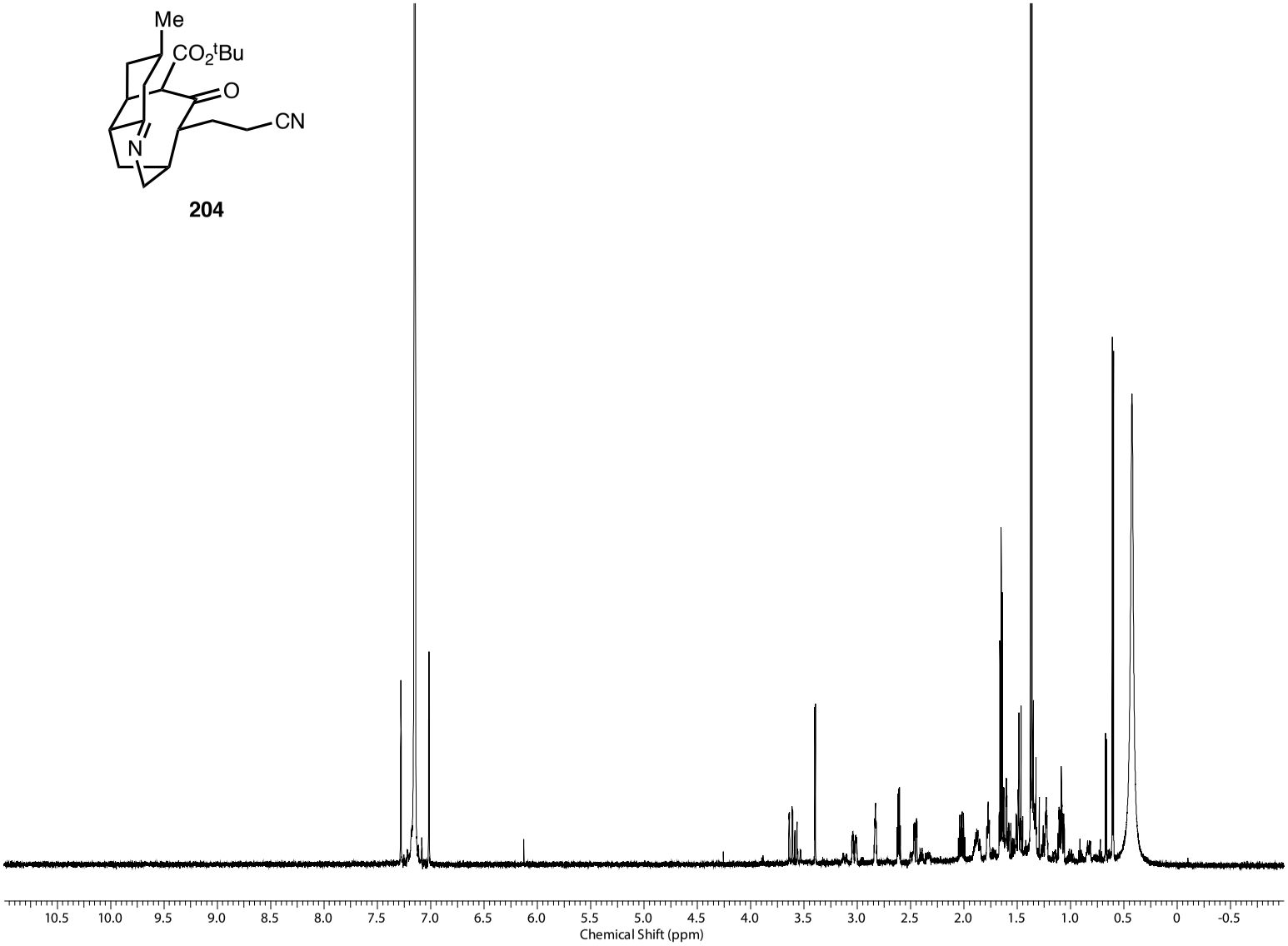
Me
CO2tBu
O
CN
N
204
10.5
10.0
9.5
9.0
8.5
8.0
7.5
7.0
6.5
6.0
5.5
5.0
4.5
4.0
3.5
3.0
2.5
2.0
1.5
1.0
0.5
0
-0.5
Chemical Shift (ppm)

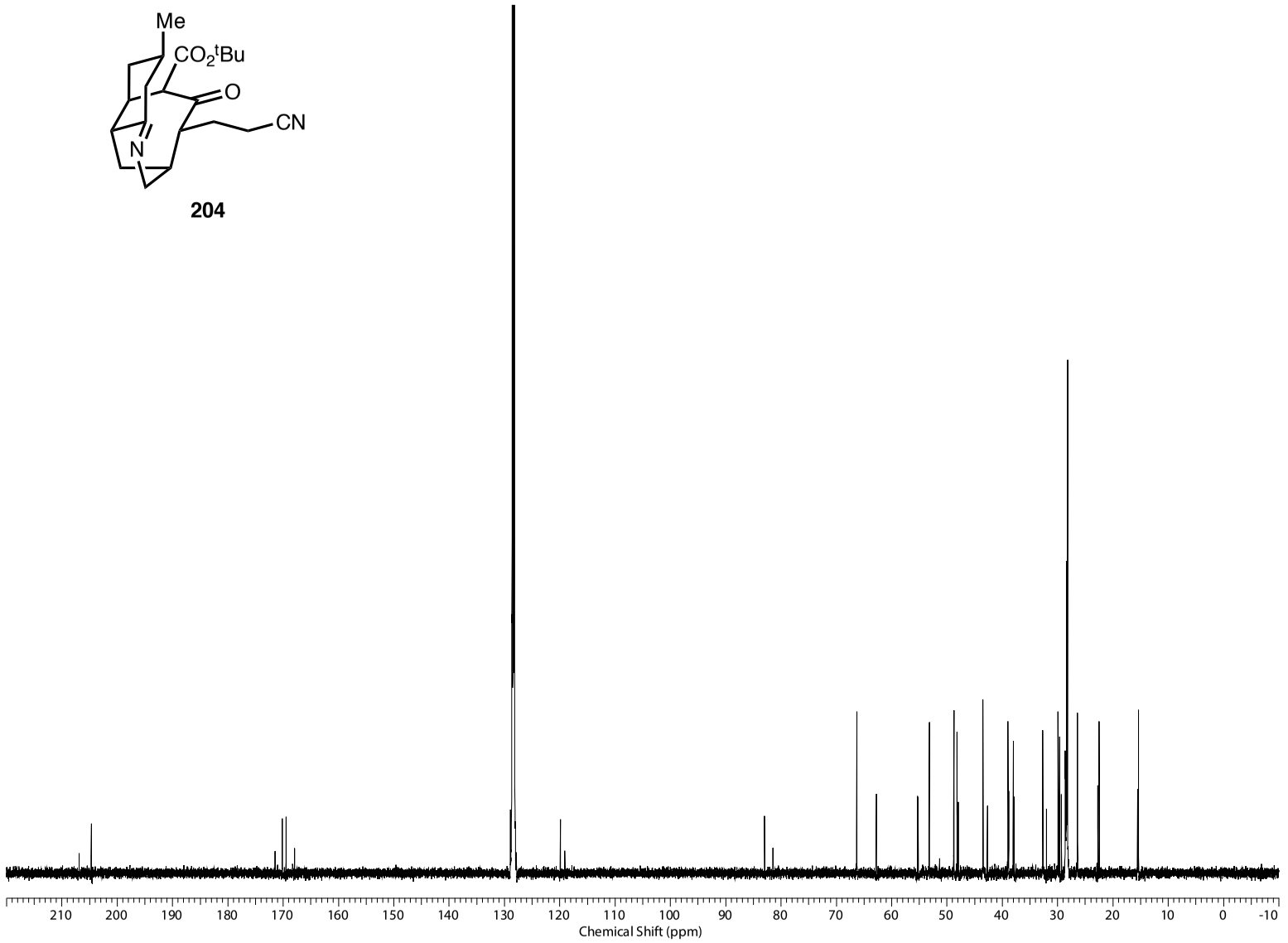
Me
CO2tBu
O
CN
N
204
210
200
190
180
170
160
150
140
130
120
110
100
90
80
70
60
50
40
30
20
10
0
-10
Chemical Shift (ppm)

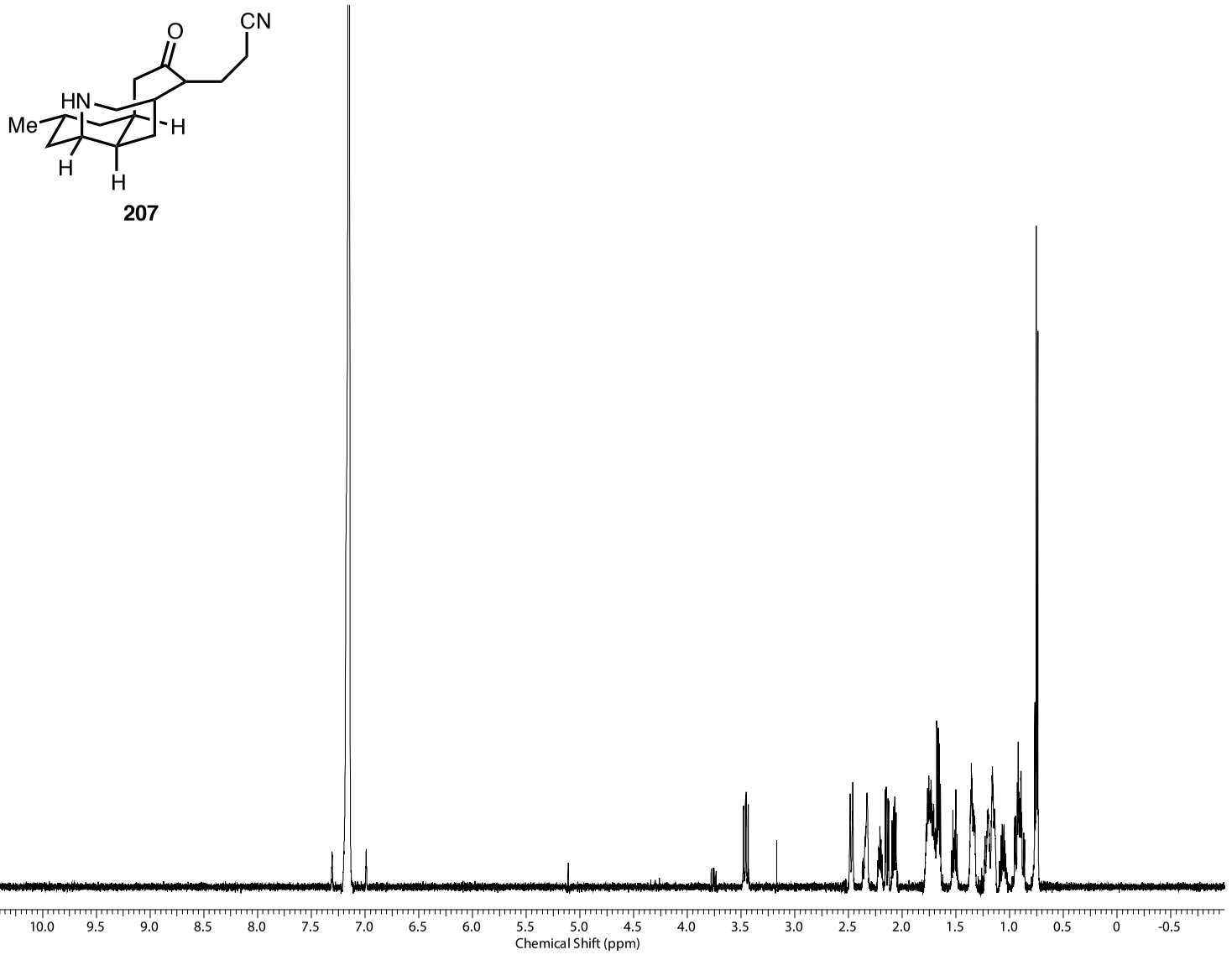
O
CN
HN
Me
H
H
H
207
10.5
10.0
9.5
9.0
8.5
8.0
7.5
7.0
6.5
6.0
5.5
5.0
4.5
4.0
3.5
3.0
2.5
2.0
1.5
1.0
0.5
0
-0.5
Chemical Shift (ppm)

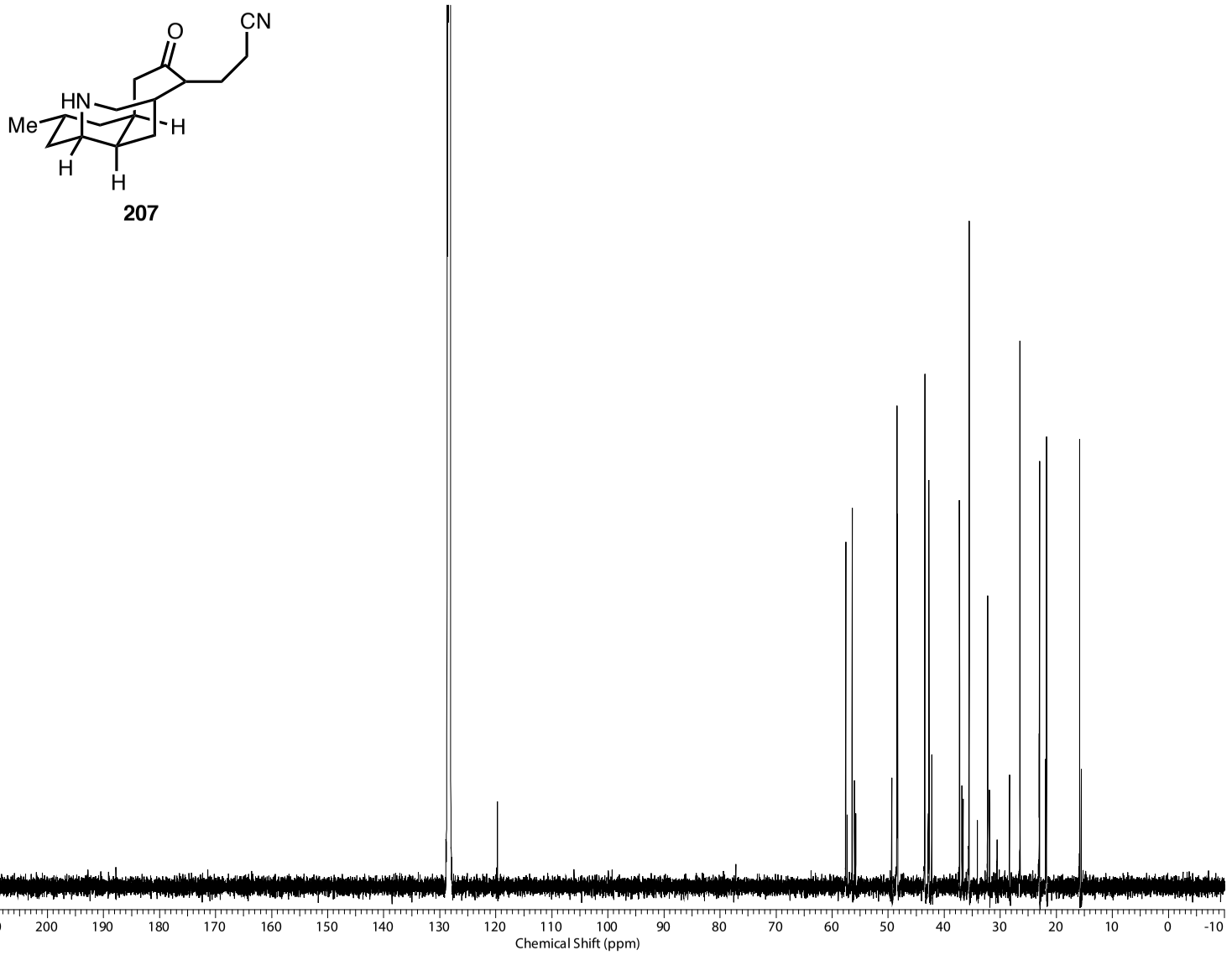
O
CN
HN
Me
H
H
H
207
210 200 190 180 170 160 150 140 130 120 110 100 90 80 70 60 50 40 30 20 10 0 -10
Chemical Shift (ppm)

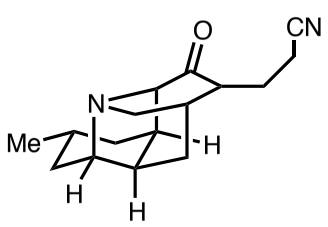
O
CN
N
Me
H
H
H

208

10.5
10.0
9.5
9.0
8.5
8.0
7.5
7.0
6.5
6.0
5.5
5.0
4.5
4.0
3.5
3.0
2.5
2.0
1.5
1.0
0.5
0
-0.5
Chemical Shift (ppm)

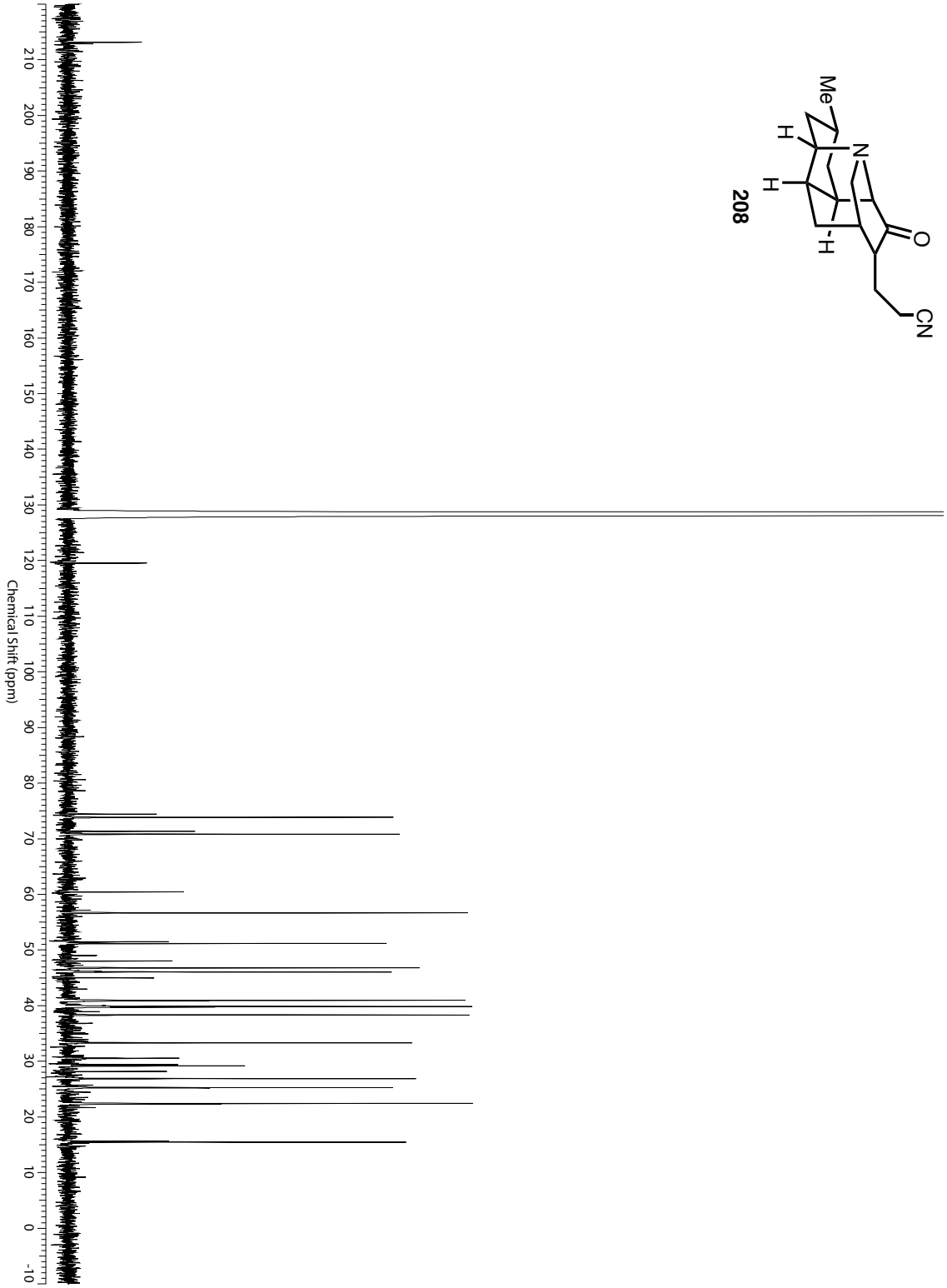
Me
H
H
H
N
O
CN
208
Chemical Shift (ppm)
210
200
190
180
170
160
150
140
130
120
110
100
90
80
70
60
50
40
30
20
10
0
-10

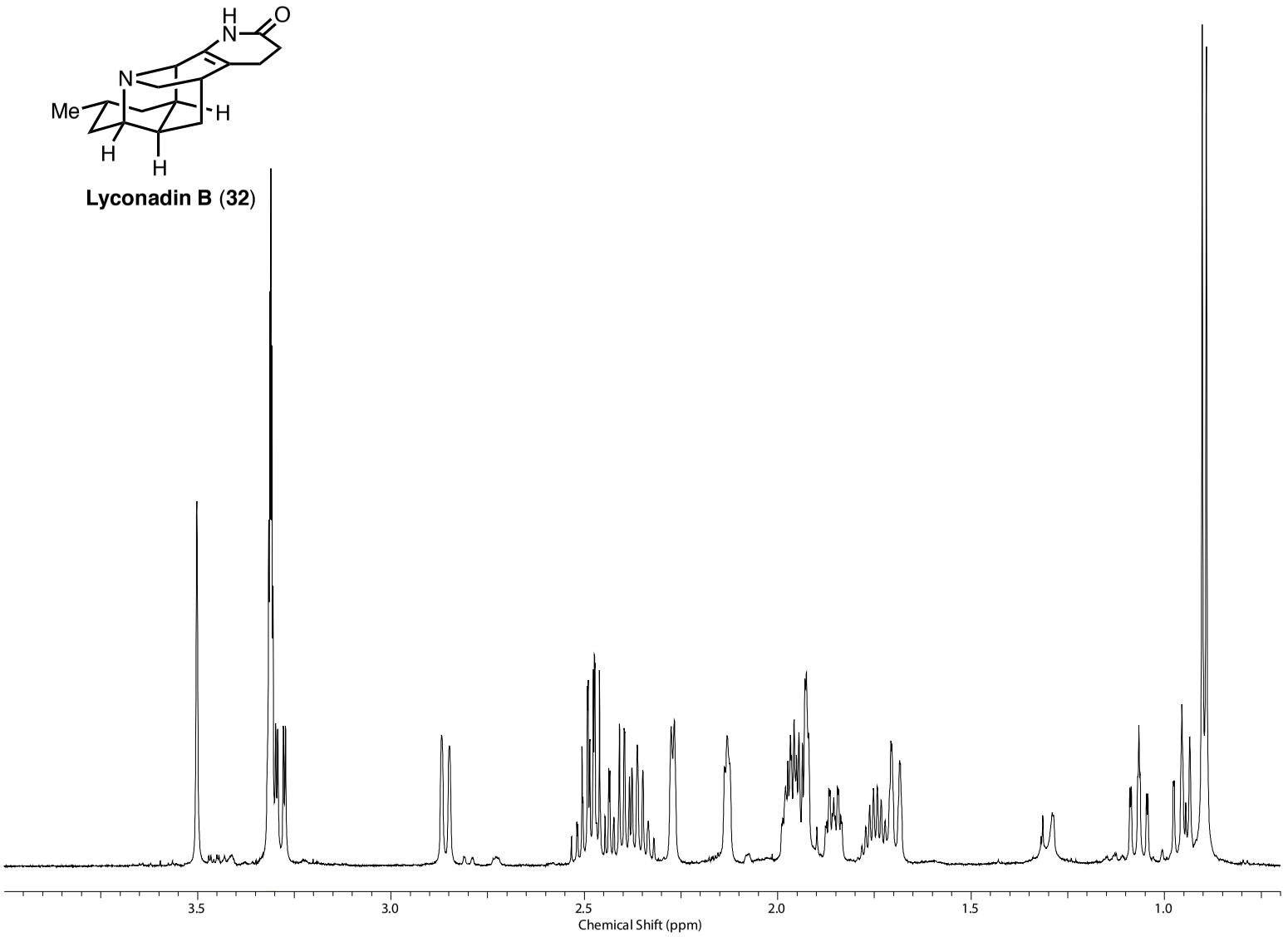
H
N
O
N
Me
H
H
H
Lyconadin B (32)
3.5
3.0
2.5
2.0
1.5
1.0
Chemical Shift (ppm)

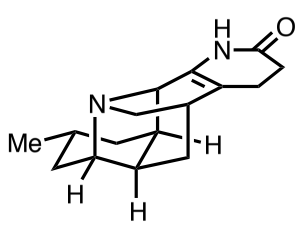

Lyconadin B (32)

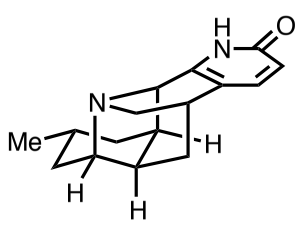

(+)-Lyconadin A (31)

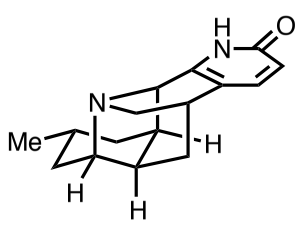

(+)-Lyconadin A (31)